Multi-sensor platforms for the geophysical evaluation of sensitive archaeological landscapes.

Evaluation of and improvement to the MSP40 mobile sensor device for rapid multi-technique and low impact measurements on archaeological sites with vulnerable soil.

Andrew Keith PARKYN

Submitted for the degree of

Doctor of Philosophy

Archaeological, Geographical and Environmental Sciences

School of Life Sciences

University of Bradford

2012

Andrew Parkyn

Multi-sensor platforms for the geophysical evaluation of sensitive archaeological landscapes.

Key Words

MSP40, Archaeology, Geophysics, mobile platform, multi-sensor, low impact, electrical resistance.

Abstract

Mobile platforms for archaeological purposes have increased in use over the last 20 years with many of the developments coming from Continental Europe. Mobile platform developments have mainly focused on one type of instrumentation, offering multiple sensors, depths of detection or frequencies. This development of mobile platforms has focused on data acquisition rates but has not considered the physical impact on the soil.

The Geoscan Research Mobile Sensor Platform (MSP40) was intended to improve survey efficiency and remain a lightweight system. The platform can collect two earth resistance configurations that show directional variation of the current flow through soil. Additional sensors were integrated on to the square frame of the hand-pulled cart to record simultaneous fluxgate gradiometer data and a microtopographic surveys.

Ground based geophysical investigation will always have a physical impact on a site. The MSP40 is no exception but careful selection of wheel types and the lightweight frame limit the damage compared to many mobile arrays.

The MSP40 has been tested on a number of different soils at various times of the year with encouraging results; however issues with overcoming the contact resistance of electrodes remain.

The continuous collection rate and combination of techniques means a slight drop in data quality is inevitable. However the increased data density, multiple-sensors and improved rate of collection offset reductions in data quality.

The research has shown that the MSP40 can perform low impact rapid site assessments on 'vulnerable' sites, whilst maximising the information gained from a single traverse.

Contents

List of tables

1.1.0 Introduction

Archaeological investigations of sites can take many different forms ranging from excavation and desk based assessments to remote sensing and ground based archaeological geophysics. Archaeological excavation often represents the final form of site investigation as it is a destructive process, which cannot be repeated. It is therefore only undertaken after all other appropriate modes of investigation have been considered.

Archaeological prospection / geophysics however can be seen as a non-destructive means of investigating the buried archaeological remains of a site. A variety of techniques can be used to investigate sites ranging from ground penetrating radar (GPR), electro-magnetic systems (EM), to earth resistance and magnetometery. Each technique has its benefits and limitations that must be considered when proposing a geophysical investigation based on the soil and geology type, the time of year, site location and the depth and type of archaeology amongst others. It is important to acknowledge that no single instrument or technique will ever give the 'correct' or definitive answer and only by combining multiple techniques it is possible to get a better understanding of the buried archaeology. Previously this has only been achieved through the repeated surveying of the same survey area with each individual instrument. However, due to recent technological developments by Geoscan Research two of these techniques have been combined into a lightweight cart system. This mobile sensor platform incorporates earth resistance and gradiometer instruments to allow simultaneous surveys. The earth resistance array is configured as a square array because its geometry made it ideal for development as a wheeled cart system.

The square array was initially tested in the UK during the 1960s by Anthony Clark. Clark (1968 ; 1996 46-47) focused on the potential archaeological applications of the square array.

The square array was also the focus of research in a geological context with multiple publications focusing on the theoretical understanding of the square array by Habberjam and Watkins (1967). However, since the development of the twin probe system, the square array has been seldom used in the UK in archaeological geophysics, although greater use has been reported elsewhere, especially in France (Panissod *et al.* 1998a ; Panissod *et al.* 1998b).

Recent developments in archaeological geophysics have focused on improving rates of data acquisition and higher resolution survey through the use of mobile arrays. Many of the mobile arrays currently available have focused on a single survey technique (earth resistance or magnetometery). This has led to the development of a variety of instrumentation that offers multiple sensors, channels or frequencies often designed to be towed behind a vehicle, to decrease data acquisition time.

However, the increasing focus on improving survey speeds has failed to consider the potential damage to archaeological sites that heavy towed arrays may have on vulnerable soils. This must be considered as archaeological geophysics is a form of remote sensing intended to provide a means of non-invasive site investigation. The closest assessment of physical impact comes from agricultural research and has focused on the impact of heavy machinery on the soil and the implications it has on soil structure and future productivity of the soil. Therefore it is necessary to attempt to quantify the physical impact mobile arrays (only the MSP40 is considered in this study) may have on the soil surface.

The main thrust of the research was in quantifying and understanding the physical impact of the MSP40 and how to reduce the impact for use on a variety of 'vulnerable' archaeological sites.

The research sought to encourage the use of appropriate geophysical survey equipment to minimize the physical impact on soil whilst increasing survey speed and data density with multiple types of survey instruments. This should protect even the most vulnerable of archaeological sites but allow for maximum information to be recorded with minimal impact.

Primarily the research is linked to surveys over thin or otherwise vulnerable soils that have a high archaeological potential. Such sites may be prone to erosion or damage from agricultural practices (ploughing) where heavy geophysics equipment or repeated trampling during surveys may cause further damage.

A number of archaeological sites were identified for study due to their vulnerability brought about by modern agricultural practices (ploughing) on thin soil or were deemed to be 'sensitive' or vulnerable soils for other reasons. This research focused on improving our understanding of mobile sensor platforms and the square array so that appropriate strategies can be employed for future site investigations. In order to gain a greater understanding of the MSP40, a number of aims and objectives were investigated with comparisons made with other array types where appropriate.

The Geoscan Research MSP40 (mobile sensor platform) is a hand-pulled wheeled earth resistance array. The framework can be modified to integrate a single fluxgate gradiometer (Geoscan Research FM18, 36 or 256) for simultaneous earth resistance and magnetic surveys. The MSP40 is a lightweight system constructed of aluminium, stainless steel and plastic components which can be pulled by a single operator.

The two wheel pairings have independent suspension to enable continuous contact with the ground surface even on variable terrain. The platform has two mounted handles to quickly reposition the array between and at the end of traverses. This also means the array orientation is kept constant throughout the survey as there is no need to rotate the array between traverses.

The MSP40 currently requires an RM15 resistance meter, DL256 data logger and a MPX40 multiplexer (see figure 1.1). The MSP40 is usually configured as a square array as the wheels are located 0.75m apart. The square geometry of the array enables perpendicular measurements to be recorded consecutively offering directional information about the current flow through the soil.

The near continuous collection rate of the MSP40 means that the survey time for a 20m x 20m grid can be reduced to approximately 8 minutes and the instrumentation allows for up to 8 samples per meter (for both Alpha and Beta configurations).

The MSP40 can log data using two different techniques. The first method uses a time based collection / triggering and works the same as the Geoscan Research FM 256 where a measurement is recorded at a designated time interval regardless of position. The second method uses an optical encoder that triggers at a calibrated distance along a traverse. Both methods also trigger the gradiometer (if in use).
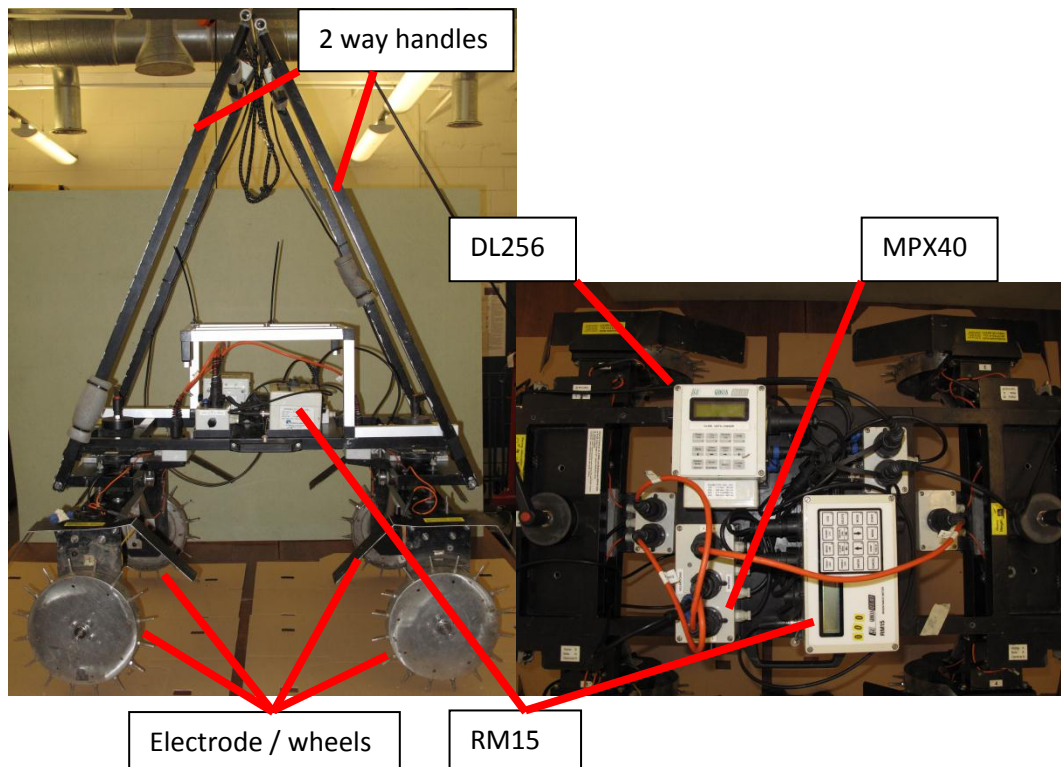
Figure 1.1 The MSP40 prototype used for the PhD research viewed from the side and top view of the platform with highlighted annotations (Sparrow 2013).

1.2.0 Aim.

The aim of the project is to investigate how the MSP40 can be used for rapid assessment of archaeological sites, whilst maximizing the information gained from a single traverse and minimizing the physical impact on the soil.

1.3.0 Objectives.

- Compare 'traditional' geophysical survey instrument collection rates with the MSP40 and develop ways to further improve survey time of the MSP40.

- Assess the data sets collected by the MSP40 with 'traditional' geophysics instruments considering responses and 'noise' in the data.

- Increase knowledge of square arrays and cart-based systems and the potential advantages and disadvantages.

- Aid further development of a lightweight mobile sensor platform through additional sensor testing and integration whilst increasing our understanding of the MSP40's potential applications.

- Increase efficiency in data collection rates, to encourage the use of earth resistance data in the wider archaeological geophysics community.

- Perform monthly testing of the MSP40 earth resistance array to investigate the seasonal effects of soil moisture on the recorded earth resistance values and the appropriateness of using the MSP40 during drier periods. This will include other earth resistance arrays for comparison purposes.

- Assess the level of physical impact the MSP40 has on the soil surface. In order to identify and quantify the potential damage to archaeological sites and where appropriate reduce this impact.

Chapter 2 discusses earth resistance measurement theory in detail, focused on the square array and other relevant themes. The Alpha and Beta configurations are discussed and defined; these definitions apply to all data sets and topics throughout the research. Other concepts associated with the square array from previous research are also reported including Azimuthal Inhomogeneity Ratio (A.I.R.) calculations.

Chapter 3 introduces the early developments of the square array and its practitioners, with additional discussion of mobile arrays in general before describing the MSP40 in detail. The chapter also includes a description of the hardware with a brief outline of the various functions and settings. This is followed by discussion of the modifications made to the mobile sensor platform during the research and the testing of additional sensors (GPS and fluxgate gradiometer). The final section is a suggested schedule for examining the cart for signs of wear and the replacement of parts based on experiences gained during the research that are linked to the modifications made during the research.

Chapter 4 examines the data from a number of practical trials intended to test the applications of the MSP40. In light of discussion from chapter two the testing included an investigation of Alpha, Beta, calculated Gamma and A.I.R. measurements, a seasonality test, wheel type and general configuration testing. This chapter culminates in an attempt to quantify the physical impact the MSP40 may have on an archaeological site.

Chapter 5 focuses on data processing and considers the effects of reduced data quality when faults develop with the MSP40. The chapter discusses the different methods of combining the Alpha and Beta data sets before examining a theoretical data set with different percentages of errors and what can be done to remove many of the errors.

Chapter 6 forms the discussion chapter that draws on practical examples (where appropriate) to highlight the salient points identified during the previous chapters in greater detail.

Chapter 7 draws together the conclusion of the research and relates the advantages and disadvantages of mobile sensor platforms back to the aim and objectives of the project. Future research objectives are then discussed, relating to the further development of the MSP40

Examples of fieldwork are discussed throughout the PhD to highlight issues and support arguments where appropriate. Archaeological sites were chosen for their archaeological potential or for the 'vulnerability' of the site.

The 'vulnerability' of a site was often determined by thin top and subsoil over limestone or chalk bedrocks that were generally used for agriculture (Eining and Pförring, Germany and Towthorpe, UK). Other 'sensitive' or 'vulnerable' sites included a World War II artillery range on Bingley Moor.

The thin soils were chosen as they were at greatest risk from damage through agriculture and from heavy mobile arrays or repeated surveying with different techniques. The MSP40 is usually configured as a square array which has a shallower depth of detection compared too many linear arrays again making it suitable for this type of site investigation.

.

2.0.0 Resistance measurements theory and the square array

2.1.0 Introduction

Before a more in-depth discussion of the main protagonists of the square and mobile arrays in general are considered it is first important to understand the theory behind earth resistance measurements specifically related to the square array. The square array requires special consideration as it one of only a few arrays that has a symmetrical two dimensional geometry.

2.2.0 Resistance measurement theory

Resistance measurements require a known current (I) which passes through an object before recording of the potential (V).

Therefore

(2.1) $R = \frac{V}{I}$

In the simplified case of a wire, the current and voltmeter can be linked with two connectors attached to the ends of the wire. However, when taking earth resistance measurements the 'contact resistance' needs to be overcome (the resistance between the electrodes and the soil medium as the current flows from the electrode). This can be achieved by using four electrodes; two current probes inject the current a constant current (DC) with alternating polarity and two potential electrodes record the potential drop through the soil medium.

A high impedance voltmeter is required to record earth resistance measurements. Gaffney and Gater (2003 28) discuss how current probes have a finite (and unknown) contact resistance. The potential probes also have a contact resistance but this is usually considerably smaller than the high input impedance from the voltmeter thus not significantly affecting readings. Constant currents (DC) with alternating polarity are used for earth resistance measurements. Non alternating DC currents would lead to polarisation of the soil; polarisation can take place around the probes due to electrolytic action.

The polarisation eventually impeding the current flow completely as the charged ions are attracted to the correspondingly charged electrode.

The square array has four electrodes located on each corner and due to the two dimensional nature of the array it is possible to collect multiple configurations at each sampling location. As a result it is possible to collect longitudinal and broadside traverses concurrently, often referred to in the literature as Alpha and Beta measurements respectively. The individual data will show a directional bias (see figure 2.1) but it is possible to combine the data sets to create a new data set which is free from anisotropy (requires multiple orientations of survey / angle of strike to the anomaly). The square array has also been identified as being more directionally stable than longitudinal and broadside traverses with collinear arrays due to the array's symmetry.

Littlemoor Castle Alpha

6.95   16.16 ohms

Littlemoor Castle Beta

7.39   16.63 ohms
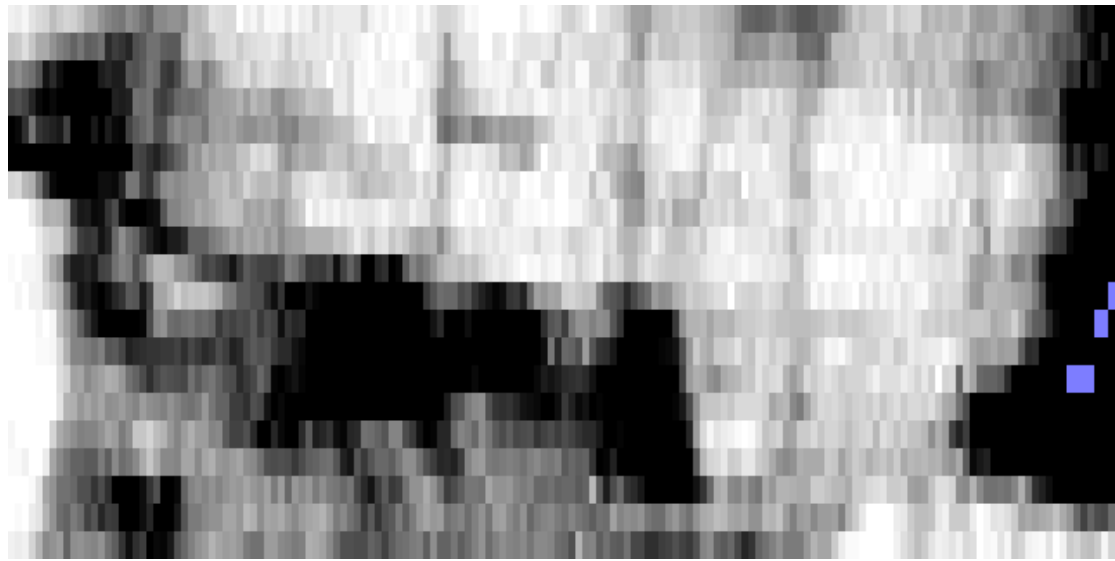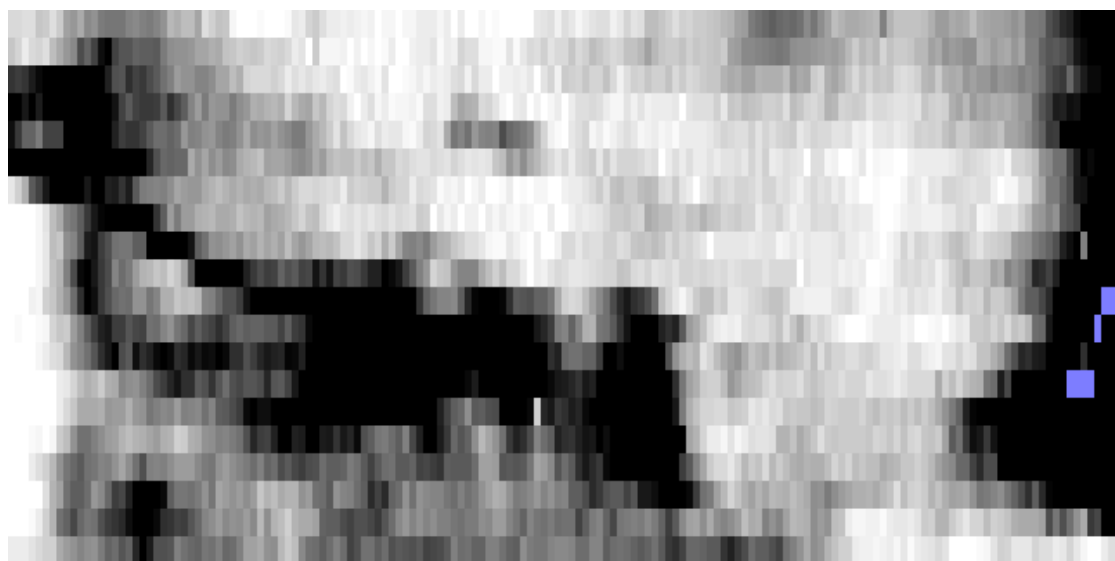
Figure 2.1   Directional variation of Alpha and Beta earth resistance measurements, from Littlemoor Castle (Victorian pond), West Yorkshire, UK. Raw data provided by Geoscan Research (Walker 2005).

An additional measurement can also be taken when the current electrodes are positioned on the diagonal corners; this is referred to as a Gamma measurement. As the potential electrodes are positioned perpendicularly to the current electrodes, the recorded potential measurement is along the lines of equipotential. Therefore in a theoretical homogenous half space the measurement would always be zero. As archaeological sites are inhomogeneous media the readings are based around a common zero point and can have both positive and negative values. The Gamma readings can be used to define edges of features, areas of significant disturbance and where there is a strong directional bias in the Alpha or Beta measurements. When a Gamma measurement has not been recorded it can be calculated by subtracting one measurement from the other (Alpha – Beta or vice versa) (see figure 2.2-2.4).
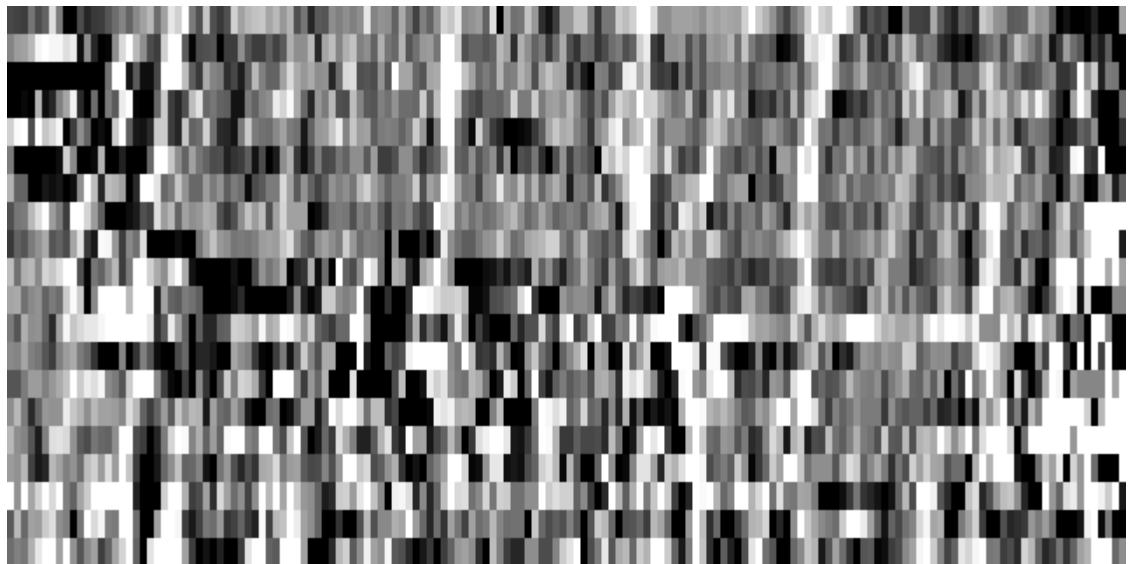
Figure 2.2   Littlemoor Castle Beta minus Alpha data

± 1 STD

-1   + 1 ohms
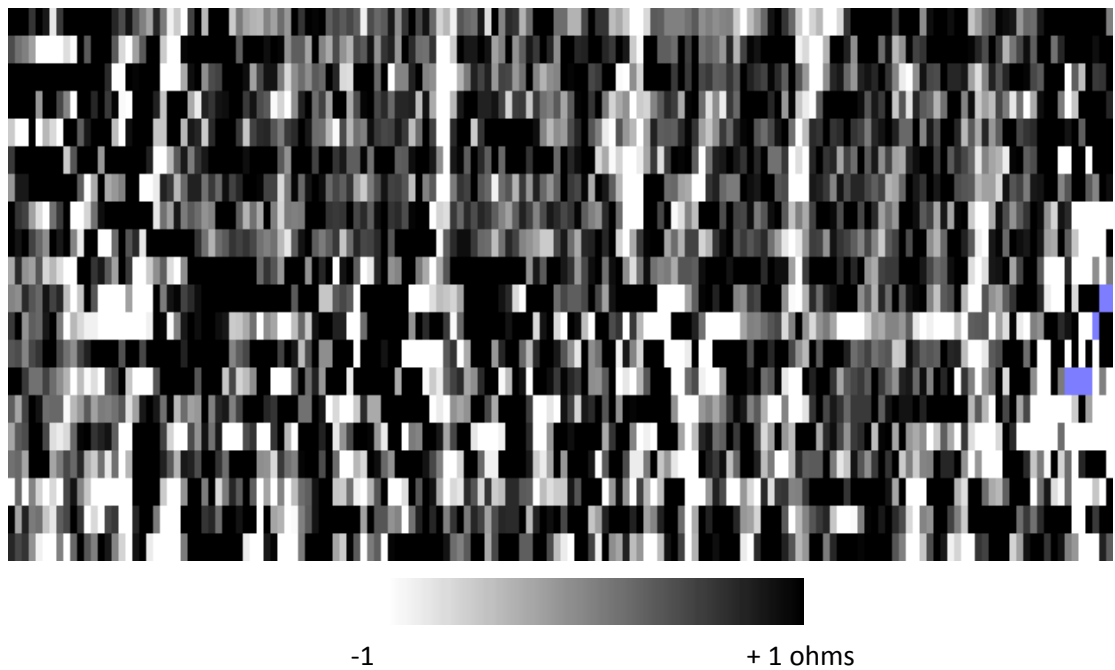
Figure 2.3   Littlemoor Castle Beta minus Alpha data, displayed as absolute values to increase display contrast.
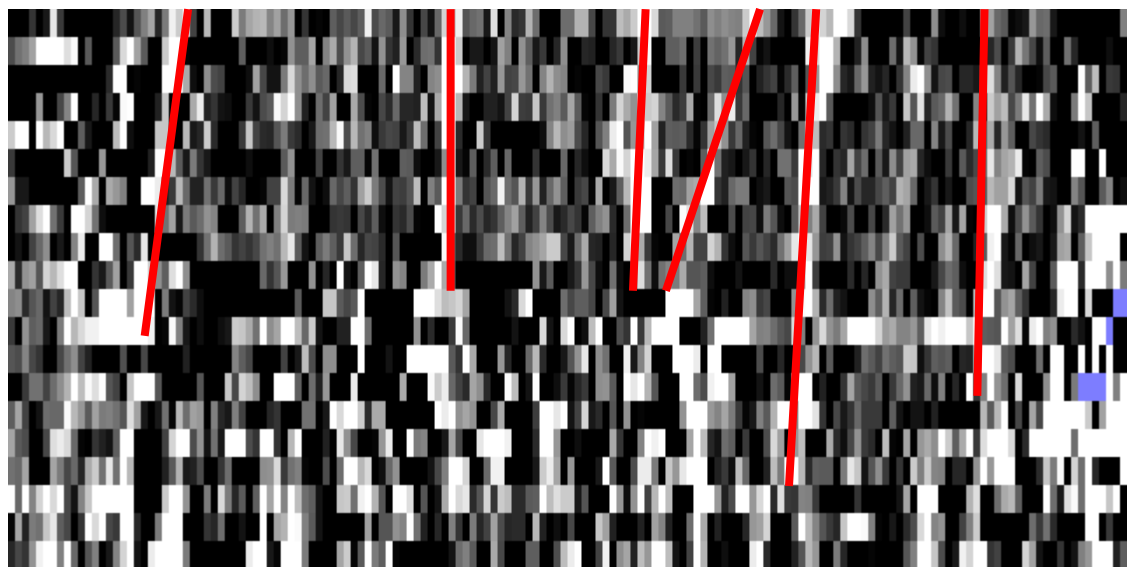
Figure 2.4   Beta minus Alpha data, displayed as absolute values with linear anomalies from the Alpha linear anomalies highlighted in red.

See chapter 4.1 for further detailed discussion of practical Alpha, Beta and Gamma tests.

2.3.0 Alpha, Beta & Gamma definitions

As the literature contains no consensus on which definition is the Alpha and Beta measurement then the terms are often used interchangeably between authors. However, the same general relationships can be highlighted.

Array configurations defined in the literature by Aspinall and Saunders (2005),
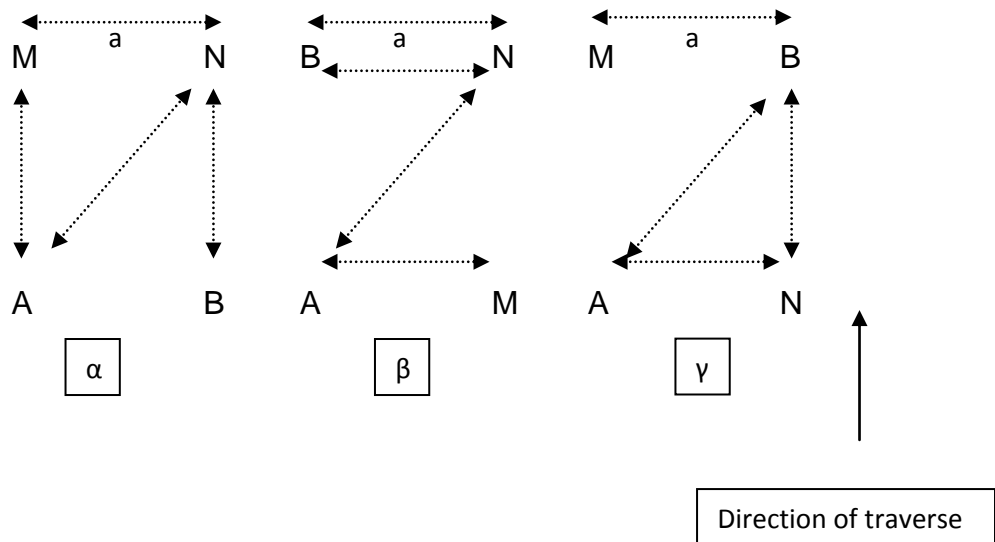
Key

a= probe separation

A, B, M & N = Current and potential probes respectively.

The array configurations defined in the literature by Tsokas (1997) has the Alpha and Beta configurations switched around. For the purposes of the research it was decided to follow the definitions used by Aspinall and Saunders (2005), this configuration was being used for the MSP40 and manual square arrays.

a

M   N

B   N

Direction of traverse

A   B

α Alpha

A   M

β Beta
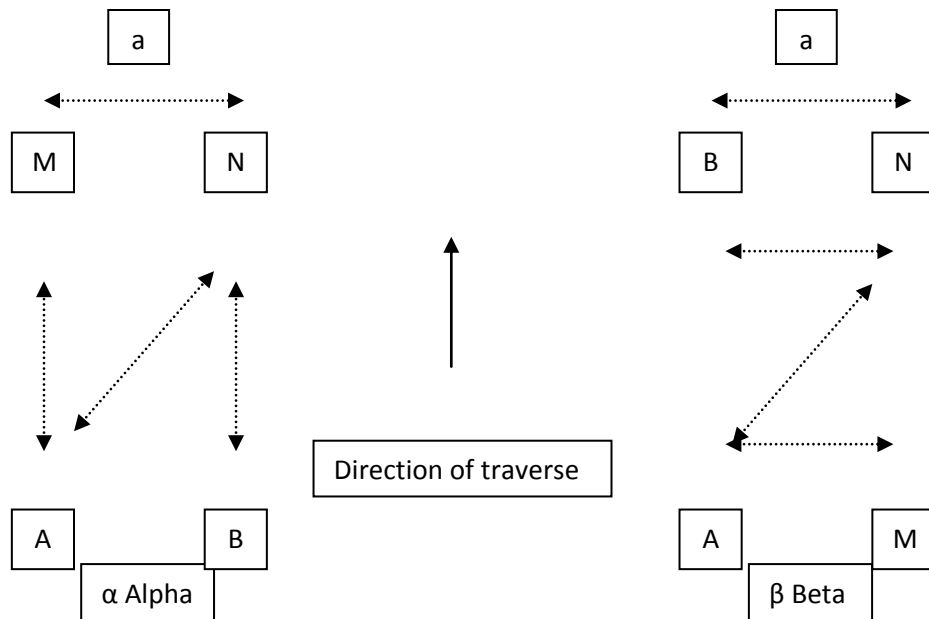
Due to the logging speed restrictions of the current hardware for the MSP40 only the pre-programmed Alpha and Beta measurements can be recorded. Future hardware developments for the MSP40 will allow for programmable array configurations (see chapter 7.2).

2.4.0 Theory of Reciprocity

Habberjam (1979) and Carpenter & Habberjam (1956) argued that an earth resistance measurement by a four electrode array is based on the sum of the potential measured between a pair of electrodes.

If the resistances measured at the potential electrodes are combined the resistance of a four probe array can be

(2.2) $$R = R_M - R_N$$

$$= (R_{AM} - R_{MB}) - (R_{AN} - R_{NB})$$

At the sink (B) current is flowing in the opposite direction to the current source (A) so the value is a negative.

(2.3) $$= R_{AM} - R_{MB} - R_{AN} + R_{NB}$$

Habberjam (1979) discusses that calculating the overall resistance of any array using this method is the Principle of Superposition. The superposition principle states that the net electric field produced at any point in a system of charges is equal to the vector sum of all individual fields.

If the electrodes are assigned a number from 1 - 4 it is possible to use the equation above to calculate the 24 configurations. This reduces equally to values which are equivalent to the Alpha, Beta and Gamma configurations.

Configurations start from bottom left corner in a clockwise direction.

α = A, M, N, B

β = A, B, N, M

γ = A, M, B, N

Or

$R_\alpha = R_{12} - R_{13} + R_{34} - R_{24}$

$R_\beta = R_{14} - R_{13} + R_{23} - R_{24}$

$R_\gamma = R_{12} - R_{14} + R_{34} - R_{23}$

Alpha			Beta			Gamma	
$_2$M	$_3$N		$_2$B	$_3$N		$_2$M	$_3$B
$_1$A	$_4$B		$_1$A	$_4$M		$_1$A	$_4$N

Each of the 24 configurations of a square array will have a resistance equal to combinations listed above due to the Helmholtz's Reciprocal Theorem (Carpenter and Habberjam 1956 ; Habberjam 1979 ; Tsokas *et al.* 1997).

Reciprocal Theorem works on the assumption that the function of an electrode can be interchanged from current to potential or vice versa and will not alter the measured resistance. Keller and Frischknecht (1966 100) proved this was the case in an isotropic homogenous half space.

However, it is also believed to be the case for an anisotropic inhomogeneous half space; for example R_{12} will produce the same resistance values as R_{21} if the A & M electrodes were interchanged. An anisotropic inhomogeneous half space is a directionally dependent mixed medium that is measured on the surface of a plane of a split three dimensional shape (for example the current flowing through a hemisphere, as a spherical current distribution is not possible).

When the resistance measurements have been recorded for the Alpha, Beta and Gamma configurations it is possible to observe the relationships between them. This is referred to by Carpenter and Habberjam (1956) & Habberjam (1979) as the Tripotential Condition.

(2.4) $\qquad R_{\beta} + R_{\gamma} \qquad = R14 - R_{13} - R_{24} + R_{23} + R_{12} - R_{14} - R_{23} + R_{34}$

$$= R_{12} - R_{13} - R_{24} + R_{34}$$

$$= R_{\alpha}$$

$$\therefore R \quad = R_{\beta} + R_{\gamma}$$

In a homogenous half space the Gamma γ resistance readings will always be 0 as the potential probes M & N are perpendicular to current probes A & B so measurements are recorded along the lines of equipotential.

(2.5) If $\qquad\qquad R_{\gamma} = 0$

$$\therefore R_{\alpha} = R_{\beta}$$

Saunders (2002) argues that there are sometimes difficulties achieving equivalent measurement on small-scale arrays on anisotropic inhomogeneous ground, while Parasnis (1986 125) suggests that the following relationship is not always true.

(2.6) $\quad R_\beta + R_\gamma = R_{14} - R_{13} - R_{24} + R_{23} + R_{12} - R_{14} - R_{23} + R_{34}$

$$= R_{12} - R_{13} - R_{24} + R_{34}$$

$$= R_\alpha$$

$$\therefore R_\alpha = R_\beta + R_\gamma$$

Saunders (2002) tested the relationship both in the deep tank and field measurements and found that as a general rule the relationship held.

When errors were found in previous research the errors were simply explained as errors in field measurements or operator error (Carpenter and Habberjam 1956 ; Habberjam 1979 ; Tsokas *et al.* 1997). Much of the work was focused on geological investigation with wide probe separations and may respond slightly differently with smaller probe separations in an archaeological context.

The amount of discrepancy can be calculated by subtracting the Beta (β) & Gamma (γ) measurements from the Alpha (α) values.

(2.7) $$R_e = R_\alpha - R_\beta - R_\gamma$$

The error term can be calculated as

(2.8) $$\varepsilon = \frac{R_e}{|R\alpha| + |R\beta| + |R\gamma|}$$

Saunders (2002) questioned whether such errors could be simply explained away as the result of poor data collection and instrumental errors or if the relationship between the configurations should be challenged. Saunders found that generally the relationship held but some unknown factor meant that it did not hold every time. This may have been due to slight distortion of the array's geometry during survey as it is likely that only small fluctuations may mean the Alpha, Beta and Gamma relationships no longer hold.

2.5.0 Apparent resistivity calculations

Apparent resistivity calculations provide a means of comparing measurements from different arrays by removing geometric and dimensional effects on earth resistance measurements. When surveying over a homogenous medium the resistance measurements are easily converted into apparent resistivity by using the following equation.

(2.9) $$\rho_A = K \cdot R$$

ρ_A = Apparent resistivity measurement, is used as different values for resistivity can be calculated for varying array types and sizes.

K = Geometry factor specific to spatial relationship of the electrodes.

Further definition of this relationship can be gained from the calculated potential of an electrode.

(2.10) $$\rho_A = R \cdot n \cdot 2\pi a$$

n= Geometry index

a = spacing between electrodes

However, as archaeological geophysics surveys are done in an inhomogeneous medium with individual resistance measurements of anomalies then $\rho_A = R \cdot n \cdot 2\pi a$ can no longer be applied. As n & a value remain constant, then an apparent resistivity of the average resistivity of the medium can be calculated. The n value of an array can be calculated by knowing the distances between each electrode and the resistance values between them. To calculate the apparent resistivity of the square arrays Alpha Beta and Gamma configurations the following equation can be used.

(2.11) $$R_{CP} = \frac{\rho_A}{2\pi} \left(\frac{1}{CP} \right)$$

R_{CP} = measured resistance between current and potential electrode

CP = electrode separation

2.6.0 Alpha and Beta configurations

(2.12) $\qquad R = R_{AM} - R_{BM} - R_{AN} + R_{BN}$

$$= 2R_a - 2R_{\sqrt{2}a}$$

$$R = \frac{\rho_A}{2\pi a}\left(2 - \sqrt{2}\right)$$

$$\therefore \rho_A = \frac{2\pi a R}{2 - \sqrt{2}}$$

2.7.0 Gamma configuration

(2.13) $\qquad R = R_a - R_a - R_a + R_a$

$$= \frac{\rho_A}{2\pi a}\left(0\right)$$

The calculation relates to the Gamma values of a theoretical homogenous half space where Gamma will always measure zero as measurements are recorded along the lines of equipotential. An inhomogeneous medium will produce positive or negative readings due to variations between Alpha and Beta readings. When gamma cannot be recorded (on the MSP40) it can still be calculated.

(2.14) $\qquad R_\gamma = R_\alpha - R_\beta$

2.8.0 Azimuthal Inhomogeneity Ratio (A.I.R.)

Directionality is often a factor of any geophysical anomaly, often dominating in one direction. However, the square array can be used to take two readings perpendicular to each other. The two data sets can be used to calculate a mean resistance ($\overline{R}$) or apparent resistivity ($\overline{\rho}_A$) for each anomaly reducing directional effects.

The mean can be calculated by the following calculations.

(2.15) $\qquad \overline{R} = \frac{Ra + Rb}{2}$

Ra = Primary directional variant.

Rb = Secondary reading perpendicular to initial reading.

The apparent resistivity values can be calculated in the same way by combining the two directional variants.

(2.16) $$\overline{\rho}_A = \frac{\rho_A a + \rho_A b}{2}$$

The difference between the two measured resistances can be used to identify the directional bias of an anomaly. Habberjam (1979) describes how the difference between Alpha and Beta measurements can also be used to calculate the Azimuthal Inhomogeneity Ratio (A.I.R.) of an anomaly and show directional bias. Habberjam & Watkins (1967) & Habberjam (1972) calculated the A.I.R. by using the following equation.

(2.17) $$A.I.R = \frac{2R\gamma}{R\alpha + R\beta}$$

Leckebusch (1999) indicated that A.I.R. was a useful way of establishing edges of features as two different resistive mediums were likely to be anisotropic as current was likely to be diverted at the interface between the two media. Habberjam and Watkins (1967) & Tsokas et al. (1997) indicate that A.I.R. calculations are useful when negative Gamma values cannot be recorded by instrumentation.

A.I.R. calculation shows how measurements from the Alpha and Beta configurations are affected by the directionality influences of the medium. However, this can also be affected by the angle of strike of the array to the feature. Therefore multiple measurements may be required with different strike angles to reduce the directional variation.

Sparrow's (2004) MSc. dissertation at the University of Bradford specifically looked at the angle of strike of the square array to a series of anomalies. Sparrow (2004) found that the responses from the square array configurations were altered with changes in the strike angle of the feature. However, the research was not able to measure the angle of strike from the Alpha, Beta & Gamma data sets due to the symmetry of the response repeating every 90°.

2.9.0 Combining Alpha and Beta data sets

Both Clark (1975; 1980) and Habberjam (1967) averaged the perpendicular Alpha and Beta readings to produce a data set free of directional bias. However, the averaging of the data sets smoothes the data which may mean a loss of subtle information. Careful data processing is always required so that errors are reduced / removed before the averaging is performed as this could produce artificial anomalies.

The Geoscan Research commercial software package (Geoplot 3.0) now contains processing options specifically designed to merge the two data sets by applying a series of filters to the data before choosing the data point that best fits the surrounding data points. However, the careful choice of a suitable filter size is important to achieve the best results from the combined data. For practical examples of data combination see chapter 5.

2.10.0 Depth of detection

The depth of detection of an array should form an important part of the decision making process when undertaking geophysical surveys. This is especially true on sites not previously surveyed, where depths of top and sub soil are unknown. An array's geometric arrangement and probe separations have a significant influence on the depth of investigation. Roy and Apparao (1971) state the depth of investigation is defined as the point where a thin buried horizontal layer contributes the greatest potential measurement at the measured surface. However, this does not mean archaeological features cannot be detected above or below this depth.

Roy and Apparao's (1971) research looked at testing various arrays for their optimal depth of investigation. Their work included a Wenner array, twin probe array and a square (referred to in the text as an Equatorial dipole (Roy and Apparao 1971) all of which had a probe separation of a= 0.76m.

The results showed that the twin probe had the greatest optimal depth detection with the square array having the shallowest depth of the greatest current density.

Wenner array

The depth of investigation = 0.33a = 0.25m

Twin probe array

The depth of investigation = 0.35a = 0.26m

Square array

The depth of investigation = 0.25a = 0.19m

> **Key**
>
> a= Depth of investigation related to the probe separation distance.

Other investigations have suggested different depths are achievable. Panissod et al (1998b) indicated that a square array with a probe separation of 1m may detect features down to approximately 1m depth. Clark (1968; 1975) suggested a depth 1.5 times the probe separation is detectable although this is only likely to be on highly conductive or insulating anomaly.

Scollar (1990 321) discusses that the greater the distance between the electrodes, the greater the volume traversed by the current which potentially will increase depth detection. However, this is dependent on the geometry and dimensions of the array and the object being investigated. As a theoretical rule Scollar argues that an anomaly must produce a response of 10% difference above or below background levels to be detectable. The decrease in resistance values with increasing electrode separation is related to

(2.18) $R= \frac{\rho_A}{2\pi a} (2-\sqrt{2})$

Saunder's (2002) dissertation incorporated a series of deep tank measurements looking at both insulating and conducting objects. However, only the two smallest probe separations were likely to show a definitive response to even the greatest length of the cylinder as the probe separation exceeds the size of the anomaly.

Saunders showed many of the trace plots produced little response from either the conducting or insulating spheres even though the anomalies were very close to the array.

This was explained as being the result of the square array's poor depth detection. The results also showed the directional dependence of each array as the Alpha and Beta responses favoured a longitudinal or broadside approach to the anomalies.

The previous research indicated that the square array had a poorer depth of detection than a comparable sized twin probe array. However, this makes the square array more suitable for near-surface measurements and the multiple configurations may make it a more suitable array on certain sites. Therefore the MSP40 is a viable solution to investigate sites with thin top and subsoil's that are more at risk from agricultural damage.

Interest in the square array and its potential applications has increased within the UK in the last ten years with continued interest in Continental Europe since the early research. Chapter 3 considers the historical development of mobile arrays, the square array and specifically the MSP40 with additional consideration of the developments / modifications made during this research project.

3.0.0 Square and mobile array practitioners and MSP40 hardware developments

3.1.1 Introduction

The potential benefits of the square array are considered and the developments of towed mobile arrays are discussed. This is followed by a section on hardware development completed during the research.

3.1.2 Square array and mobile array developments

The square array's initial developments in the 1960s were mainly researched by Clark and Habberjam. Both worked independently of each other and saw different potentials in the square array's application in archaeological geophysics and geological geophysics, respectively.

Clark's goal was to use an easily manoeuvrable array that would not suffer from the double peaking of anomalies as was found to be the case for collinear arrays (four electrodes on a straight line) as seen with the Wenner and double dipole response curves. Double peaking can confuse archaeological interpretations as one anomaly could be misinterpreted as two separate features (Clark 1968; 1986 ; 1996 39). Clark found that by surveying with the square array and averaging the two readings (at right angles) it was possible to remove the double peaking effect (Clark 1996 39-48).

However, Habberjam sought to reduce the collinear array orientation effect on geological area surveys. Previous to this research this had only been achieved by resurveying areas with multiple orientations.

The square array with the Alpha and Beta orientations appeared to negate this need to resurvey multiple times from different orientations (Habberjam and Watkins 1967 ; Habberjam 1979). Geological applications of the square array have been carried out by Matias (2002), Matias and Habberjam (1986) and Habberjam and Watkins (1967) and have focused on a crossed measurements. A crossed measurement involves taking multiple measurements at different angles of strike or orientation.

A.I.R. values were calculated for the multiple array orientations and allowed the operators to study the anisotropy of the ground.

The square array fell out of use in the UK with the development of the twin probe array but continued to be used in Continental Europe (especially France, Switzerland and Austria). Much of the work in the last 20 years has seen the trend towards towed mobile platforms. The development of mobile sensor arrays has largely been in response to the time consuming nature of collecting earth resistance data and is seen by many as a limiting factor in its use on large-scale high-resolution surveys (Neubauer *et al.* 2002 ; Drahor 2011).

The major development of mobile arrays was the RATEAU system (developed by the French research institute Centre de Récherches Geophysics de Garchy (CNRS)). The RATEAU system could cope with a high contact resistance so that the wheels of a trailer were used as the electrodes (Hesse *et al.* 1986 ; Panissod *et al.* 1998b).

The RATEAU (Autotracté à Enregistrement Automatique: Automatic recording and self-towed resistivity meter) roughly translates to a harrow in English as the array acts in a similar way as a plough or discing system. Collection rates were restricted to approximately 1 m/s (Dabas 2009 105-129). The square array was preferred to collinear arrays as it suffered less from anisotropy and the square array's geometry suited the design for use on a towed trailer system. The early system was capable of sampling at 0.25m intervals (Panissod *et al.* 1998b), but later developments meant a 0.10 m sampling strategy could be achieved (Scollar *et al.* 1990 345). With a 1m sampling strategy it was possible to survey 15 ha or 37 acres per day, far exceeding what was possible by traditional hand-held devices (approximately 1ha. per day at 1m sampling). However, only one orientation configuration Alpha could be sampled as the system was a single quadrupole without multiplexing capabilities. This meant the area would have to be resurveyed entirely for a Beta measurement (Soing and Geocarta 2008 ; Dabas 2009 105-129; Dabas and Gruel 2009).

The RATEAU system underwent further developments with the use of high pressure liquid jets to maintain a continuous contact with the soil surface (Hesse *et al.* 1986 ; Panissod *et al.* 1998b). The main drawback of this system was the need to refill the tanks and maintaining sufficient pressure levels to ensure a consistent contact for earth resistance measurements. A lightweight system was also developed that could be pulled by a single operator; it was trialled at the Roman town of Wroxeter and found to work well on favourable site conditions (flat areas with damp topsoil).

The array had separated mobile (C1P1) and remote probes (C2P2) similar to a twin probe survey (see figure 3.1).
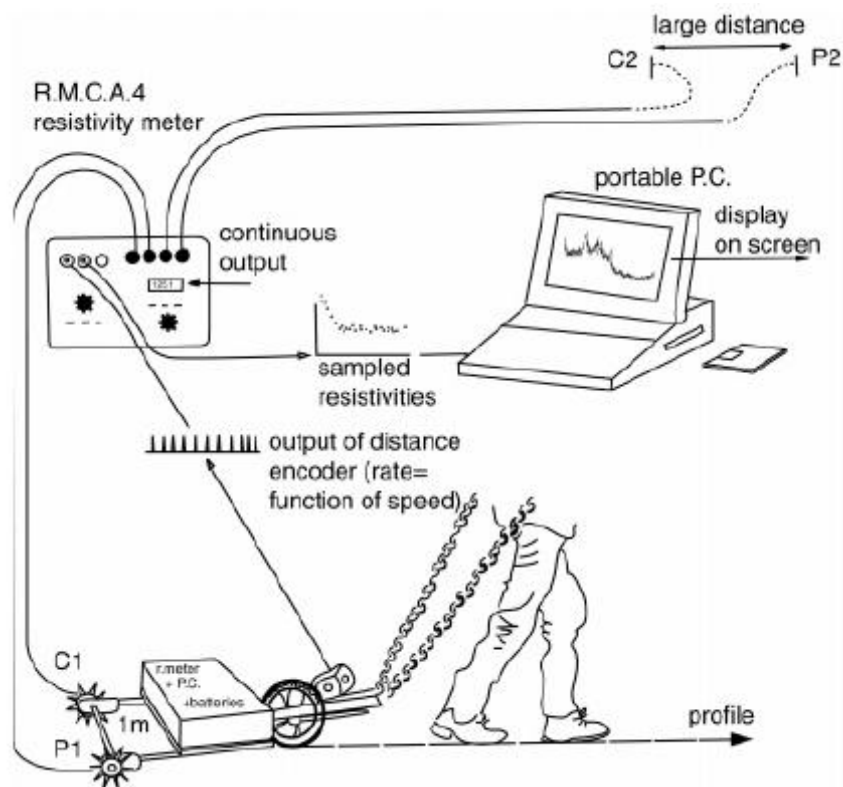
Figure 3.1.　The lightweight RATEAU system tested at the Roman town of Wroxeter noting the C2 and P2 separated from the mobile array (Dabas *et al.* 2000).

Sampling could be achieved at 10 cm intervals and the rate of acquisition could be as fast as 15 ms^{-1} (when towed by a vehicle).

The array used an encoder wheel to sample at the correct position and allowed for variable collection speeds depending on ground conditions and operator fatigue (Dabas *et al.* 2000).

The next big development by the practitioners of the French research group (CNRS) was the MUCEP.MUCEP stands for Multi-pole Continuous Electrical Profiling. The MUCEP system is made up of 8 electrodes that can be configured as a rectangular (panel) or trapezoidal (Vol-de-canard) array. The system's different electrode spacings allowed for various depths of investigations (see figure 3.2). Electrostatic multi-pole measurements can also be taken with the MUCEP which allows for electrical methods of investigation even over resistive surfaces like asphalt (Panissod *et al.* 1997a ; Panissod *et al.* 1997b ; Panissod *et al.* 1998a ; Panissod *et al.* 1998b).

Figure 3.2   The MUCEP array towed behind a Land Rover (Samouëlian *et al.* 2005).

The Automatic Resistivity Profiling (ARP©) and Automatic Magnetic (AMP) system are the most recent mobile sensor systems developed by GEOCARTA (a spinoff company from the CNRS group in France).

The ARP© system can be used to perform rapid resistivity surveys of soil variation at a high spatial resolution as it is pulled on the back of a quad bike.

The ARP© system injects the electrical current through a series of 8 rolling electrode wheels with large cutting spikes. The ARP© has two fixed current electrodes at the front of the array with six potential electrodes staggered behind (with three different probe separations). A new resistance meter was designed to overcome contact resistance issues where dry conditions impede or stop the current flow into the soil. The system was initially developed for agricultural mapping of soils (Gebbers *et al.* 2009). Later developments improved the positional accuracy of the measurement locations making the system suitable for archaeological geophysics surveys.

The ARP© system has three depths of investigation which can be taken simultaneously due to the layout of the array (see figure 3.3-3.5). The approximate depths of investigation are 0 to 50 cm, 0 to 1m and 0 to 2 m depending on the soil moisture and depth of soil (Soing and Geocarta 2008 ; Papadopoulos *et al.* 2009a). Theoretical modelling of the ARP© system suggested a similar depth of detection as a Wenner array with an identical probe separation (Dabas 2009 105-129). The ARP© system can also record digital elevation model (DEM) data alongside the resistivity data by using a dGPS or RTK system. The GPS survey information is also used to guide the quad bike operator across the site. A video of the system in operation can be viewed online, noting the soil displacement caused by the array (Dabas 2008).
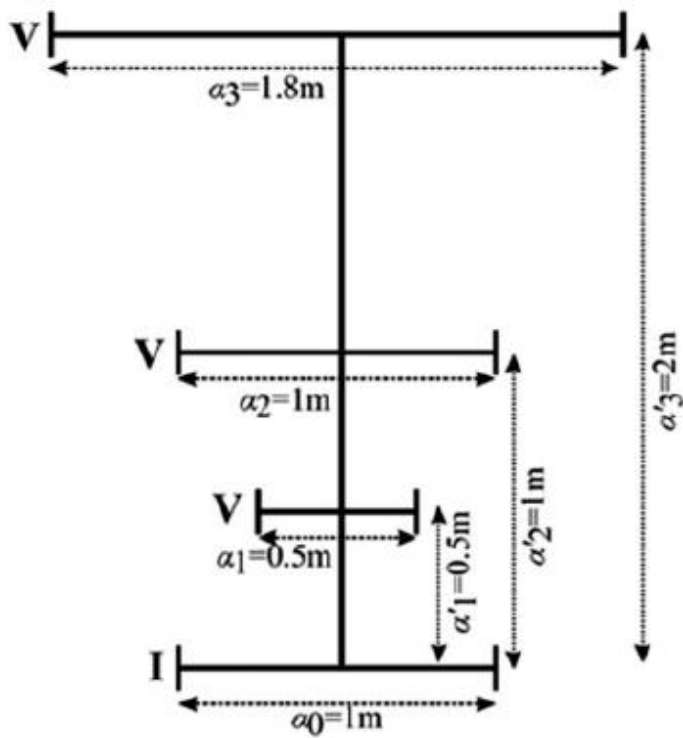
Figure 3.3   The ARP© system configuration with fixed current probes and variable potential probes (Papadopoulos *et al.* 2009a)

The current and potential electrodes are fixed in the direction of the traverse which means the orientation of the array changes on subsequent traverses. This is likely to result in banding between traverses that must be removed during data processing.
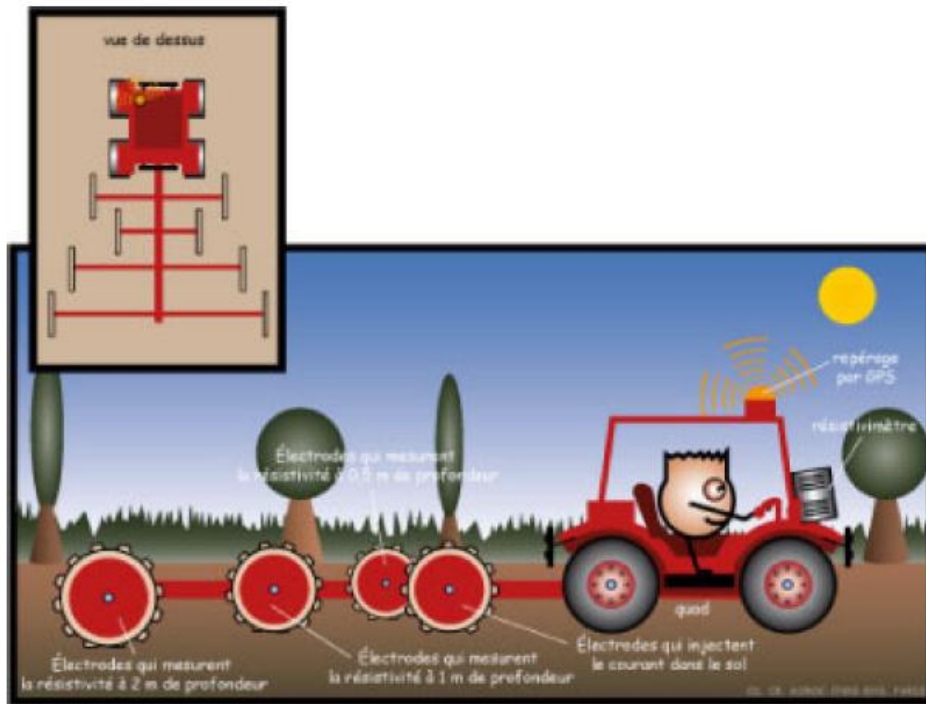
Figure 3.4   The ARP© system configuration with fixed current probes and variable potential probes (Dabas and Gruel 2009).

Figure 3.5   The ARP© system towed behind a quad bike (Dabas and Gruel 2009).

Papadopoulos *et al.*(2009a) discuss how one of the major benefits of the ARP©
system configuration is the reduced effect of the superficial geophysical noise
on the large receiver electrodes. This is achieved by the three investigation
depths being recorded simultaneously without the need for switching between
configurations. It is also possible to perform 3D inversion of the three stacked
data sets to provide additional information about the underlying archaeology
(Papadopoulos *et al.* 2009b).

A typical traverse interval ranges from 0.5m – 1m depending on the skill of the
quad bike driver and sampling intervals are usually fixed to 20cm along traverse
lines. When all three measurement depths are recorded simultaneously a
maximum speed of 6 m/s is possible. This rate means up to 1 ha an hour can
be surveyed. The addition of hydraulics to the array also made significant time
savings (when changing direction) as there was no need to uncouple the array
from the quad bike. However, data collection rates are often reduced to
approximately 4 ha per day for archaeological sites (Campana and Dabas
2011). The resistance meter synchronises the three channels and can update
every 44 mS (Gebbers *et al.* 2009). The development of a real-time software
processing package has also meant data is processed and displayed as it is
collected (both GPS and the three channel resistivity measurements.

However, the system has had difficulties in data collection during the summer
months when the contact resistance can still not be overcome or in colder
winters when the ground is frozen (for more details about seasonal variation
see chapter 4.2).

A range of mobile sensor platforms have also been developed for magnetic prospection, which offers multiple fluxgate gradiometer sensors to increase survey density and significantly reduce survey time. The platforms are often towed behind quad bikes improving the efficiency of the systems. The impact of magnetometer carts is generally restricted to that of the quad bike towing the array, making them suitable for non-invasive investigation. The carts often use GPS to guide and record topography but are not capable of earth resistance surveys. As only a single sensor gradiometer can be mounted on to the MSP40 at the present time only a brief discussion of one system is included for illustrative purposes.

The AMP is a mobile sensor platform also designed by GEOCARTA but is built specifically for magnetic mapping using a series of up to five specifically developed Bartington Fluxgate sensors. The sensors can run at an acquisition frequency of 80 Hz and are designed to produce low noise levels when towed behind a quad bike (see figure 3.6). Dechezleprêtre *et al.* (2009) describe how with a collection rate of 4 m/s the 80 Hz acquisition frequency equates to a sample interval of 5 cm with a 50cm sensor separation (a 2.5 m traverse interval, when all five sensors are used). A dGPS is used for positioning information for the driver of the quad bike. The speed of survey means it is possible to collect >8 ha a day.

The improved rate of data acquisition means larger units of land / whole landscapes can be investigated in significantly less time than has been possible with hand-held collection surveys, Gruel *et al.*(2009) for example collected 15 ha in two days at the city of Allonnes, (Sarthes, France).
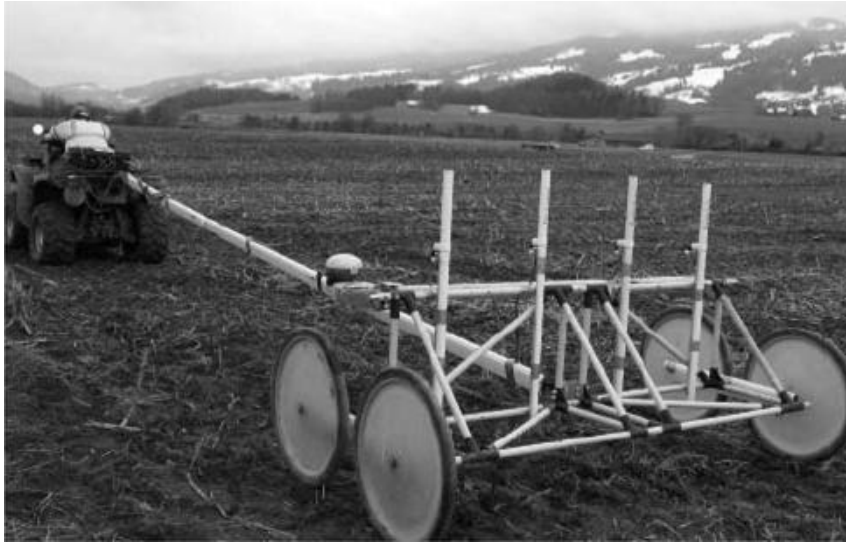
Figure 3.6   The AMP system configuration with four mounted gradiometer sensors (Dabas and Gruel 2009)

The AMP and ARP© systems have been extensively trialled and are now frequently used for large-scale area surveys, an example of which includes a total of 217 ha of AMP data and 215 ha of ARP© data collected for the BREBEMI project in Italy (Campana and Dabas 2011).

A novel approach to continuous electrical profiling was created by the Hydrogeophysics Group from Aarhus University; Denmark. The PA-CEP (Pulled Array Continuous Electrical Profiling) system involves a series of electrodes attached to a cable pulled behind a vehicle like a tail. The PA-CEP has not been used for archaeological purposes; instead research has focused on hydrogeological applications. The electrodes are made of heavy cylindrical mild steel tubes (each current and potential probe weighing between 10-20kg and 10 kg respectively).

The potential probes house processing electronics with a high input resistance (5-10 Mohm) which are used to suppress ground contact resistance and noise within the tail. Additional band pass filters applied to the data also reduces internal noise and interference from power lines etc. (50 and 60 Hz).

Data acquisition and storage is controlled by equipment mounted on the towing vehicle (see figure 3.7). The system works at a frequency of 15-25 Hz with an inbuilt averaging of responses to reject outliers in the data caused by external 'noise' sources, power lines etc. A constant alternating current of 10-30 mA is used with a voltage set at <250 volts. Systems were also implemented to monitor poor galvanic contact at the current electrodes and the contact resistance at the potential probes to improve repeatability of measurements. A cross country caterpillar is used to pull the array. However, even with the systems described above Sørensen (1996) still encountered issues including the distorting effect of noise voltages at the potential electrodes, cross communication between signals in the tail and capacitive coupled noise from the cabling due to the high voltage required.

Earth resistance measurements are updated at a rate of 80Hz and the towed array is pulled at 0.6m s^{-1} (approximately 2 km per hour). Sørensen (1996) suggests profile lengths of 10-15 km are achievable in a day. However, the spatial resolution is significantly coarser than used for archaeological geophysics; the sampling interval is related to the potential electrode spacing (0.1 -0.25 times the potential spacing) of 10m & 30m, equalling a 1m sample interval at its highest resolution (Ernstson and Kirsch 2006 98-104).
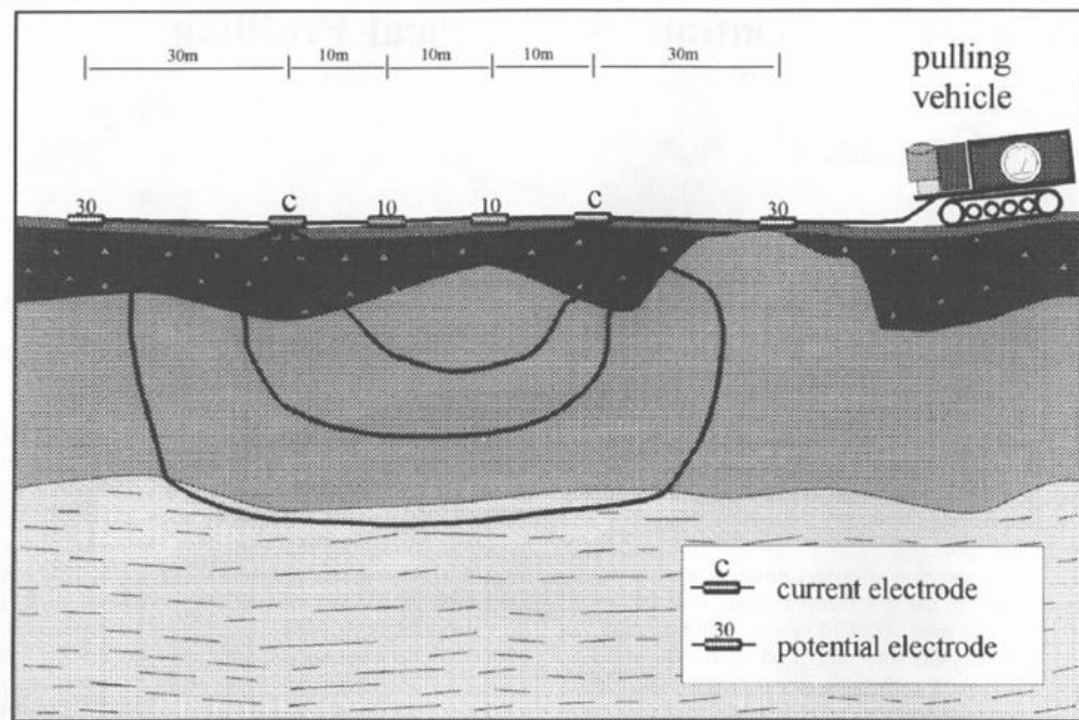
Figure 3.7   A schematic diagram of the PA-CEP system (Sørensen 1996)

Sørensen (1996) compared data from a traditional static collection and the PA-CEP system which indicated a strong repeatability in the PA-CEP data and a good correlation with the static collection method. The weight of the cable, electrodes and towing vehicle are likely to have a significant impact on the soil surface due to the dragging and displacement of soil by the cable and vehicle. The PA-CEP would also compact the soil as the weight of the vehicle and array move across the site.

An additional mobile square array was developed by Juerg Leckebusch; the research was undertaken mainly in Switzerland where the mobile square array was used at the Roman town of Augusta Raurica. The array Leckebusch used consisted of a small tractor with spiked wheels that acted as the electrodes (Leckebusch 2001). Leckebusch's array initially only collected an alpha configuration and had a manual switch required to maintain the correct array orientation when survey data was collected in zigzag as the array would be rotated in the opposite direction.

Potsdam University also developed a mobile array called the 'Geophilus electricus' (nick named after a type of centipede). The array is an equatorial Dipole-Dipole array using one dipole axle for current injection. The array has 5 sets of potential dipoles offering 5 depths of investigation up to an estimated depth of 1.5m (Lüeck and Ruehlmann 2011a). Each dipole axle is separated by 0.5m to a maximum separation of 2.5m x 1m. The array is pulled behind a vehicle and can use either dGPS or a total station mounted on top of the vehicle for positioning (see figure 3.8 & 3.9). The array also collects simultaneous measurements at 4 different frequencies which the manufacture's quote as totalling 40 different possible data sets.

The Geophilus electricus is primarily intended as a soil mapping mobile array that is capable of measuring the conductivity of the soil and spectral induced polarization (to record the amplitude and phase angle) at a frequency range of 1 MHz to 1 kHz. The sampling rate is approximately 1 measurement per second but measures five frequencies simultaneously. The equipment measures signals at a 2 V maximum for the first channel with an incremental reduction of the voltage, the fifth and final channel reduced to 50 mV.

Figure 3.8   The Geophilus Electricus being towed behind a small lorry and its position recorded by a total station (prism mounted on top of the cab) (Simpson *et al.* 2010 2200).
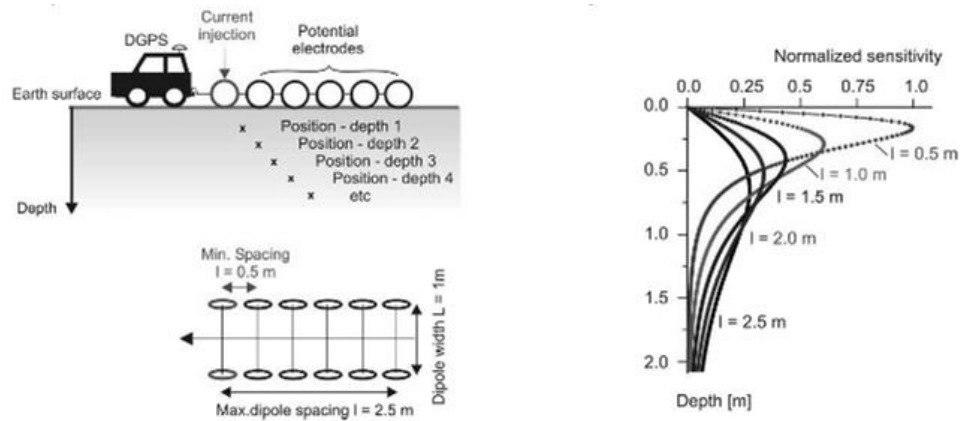
Figure 3.9   A schematic diagram of the Geophilus Electricus and the depth
sensitivities of each potential electrode separation (Lüeck and Ruehlmann
2011a).

The Geophilus Electricus has been used to record soil variation over large
fields. This has often been completed with a coarse sampling and traverse
interval (along the line and between transects). The data is collected at a rate of
one measurement per second, at a velocity of 15 km/h (recording a data point
approximately every 4-5m (Lüeck and Ruehlmann 2011a; 2011b). Traverse
intervals were typically recorded every 18m approximately equalling 100 ha per
day.

However, at least one survey using the Geophilus Electricus was undertaken in
an archaeological geophysics context (Simpson *et al.* 2010). The array was
used on a test site in Germany and was also to be used on a Bronze Age site.
However, the Geophilus Electricus could not be towed on the site so a static
collection was attempted using identical probe separations. The static
measurements were completed to see if theoretically the Bronze Age ditches
could be identified by the array(Simpson 2009). The results of the test site over
a near surface basalt wall suggested similar results between the Geophilus and
static arrays. However, Simpson *et al.* (2010) acknowledge an increase in
conductivity values from the mobile array (see figure 3.10). The results from the
static array identified the Bronze Age ditches (in a similar recording method as a

pseudosections collection) suggesting the Geophilus Electricus could be used in an archaeological context.
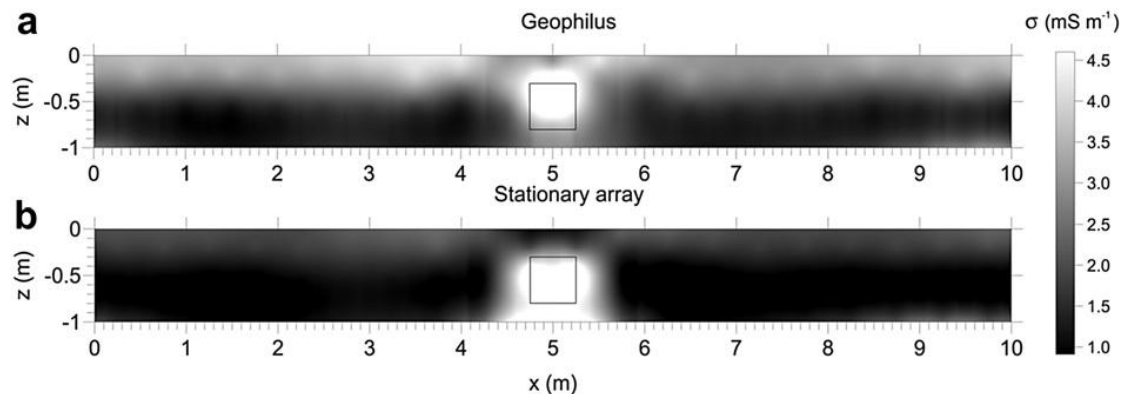
Figure 3.10   Geophilus and stationary array trials, over a basalt wall. The two data sets were collected with the same probe separation, noting the increased conductivity values from the mobile array (a) (Simpson *et al.* 2010: 2202).

The development of the Geoscan RM15 and compatible MPX15 multiplexer meant that the manual square array could be used to its full potential by measuring Alpha, Beta and Gamma, rather than Clark's (1996 39-48) square array that was dependent on the manual switching of the array configurations. Using the PA5 set up also allows for simultaneous 0.5m twin probe survey, Saunders (2002) found it was possible to survey 8 to 12 20m x 20m grids (approximately 0.32 - 0.48 ha) per day with a 1m sampling interval and 1m traverse interval when using the manual frame.

The square array has occasionally been used in the UK and Ireland since Clark's initial work. Recent surveys using the square array were carried out in Ireland where a number of raths were investigated. A manual frame square array was used for the geophysical surveys with several of the sites having limited twin probe surveys carried out for comparison purposes.

Barton and Fenwick (2005) and Waddell et al. (2009) concluded that the square array appeared to have a greater sensitivity as it identified a greater number of anomalies and showed a good correlation with magnetic gradiometer survey results. However, the twin probe and square array surveys were performed at different times of the year so it is not possible to draw very firm conclusions.

The results may have also favoured the square array if the archaeology was near the surface.

A multiplexer similar to the one devised for the RM15 has been developed for the MSP40 (MPX40) to record Alpha and Beta measurements but due to the electronics design restrictions of the RM15 the Gamma configuration is currently not possible. This is because the cart would have moved significantly beyond the sampling position before the Gamma reading had been taken. The Beta readings already have to be shifted during data processing to allow for the time displacement between the Alpha and Beta measurements. Proposed future developments for the RM85 (to replace the RM15, DL256 data logger and multiplexer) will improve the electronic switching time which is needed to collect Alpha, Beta and Gamma measurements whilst maintaining positional accuracy. The MSP40 and PA5 frame with additional square array side wings have a probe separation of 0.75m, which has a similar separation as the original array developed by Clark in the 1960s of 2.5 feet (Clark 1968). The 0.75m probe separation was also believed to produce responses roughly equivalent to a 0.5m twin probe response and so both were incorporated into the seasonality tests to see if this was the case (see chapter 4.2).

A pilot test of the prototype MSP40 was carried out at Drumlanrig in Scotland. The pilot study showed that with a single Alpha measurement it was possible to collect a 20m x 20m grid of data at a 0.25m sampling and 1m traverse in approximately 7.5 minutes (Walker *et al.* 2005). The survey results also indicated that the square array could produce clearer near-surface results than the twin probe whilst also giving satisfactory detection of deeper features.

Additional work and development (see chapter 3.5) has been undertaken by the Geoscan Research North American sales representative Dr Lewis Somers (Somers 2006), whose work has included surveys at Poverty Point, Louisiana, USA amongst others.

Previous research at the University of Bradford has also focused on the square array and the MSP40.

Three main MSc student practitioners must be discussed: Mary Saunders (Saunders 2002 ; Aspinall and Saunders 2005), Tom Sparrow (Sparrow 2004) and Chrys Harris (Harris 2011). For more detailed discussion of Mary Saunders's and Tom Sparrow's research see chapter 2.

Harris (2011) examined the potential use of the MSP40 as a trapezoidal array for archaeological prospection. The array can be modified by adding extension supports to the rear axle of the cart. The extensions increase the wheel / electrode separation to 1.25m. This allows for different depths of investigation (but symmetrical Alpha and Beta measurements are no longer possible). The additional depths of investigation help to differentiate anomalies at variable depths aiding interpretation (Walker 2000 ; Gaffney and Gater 2003 32).

Trapezoidal arrays have been used for different applications including viticulture (wine growing) and exploring soil moisture variation (Soing and Geocarta 2008) and many of the publications have focused on the three-dimensional resistivity modelling of these results (Tabbagh *et al.* 2000). However, Harris's work focused on the MSP40 and potential archaeological applications (see figures 3.11 and 3.12).
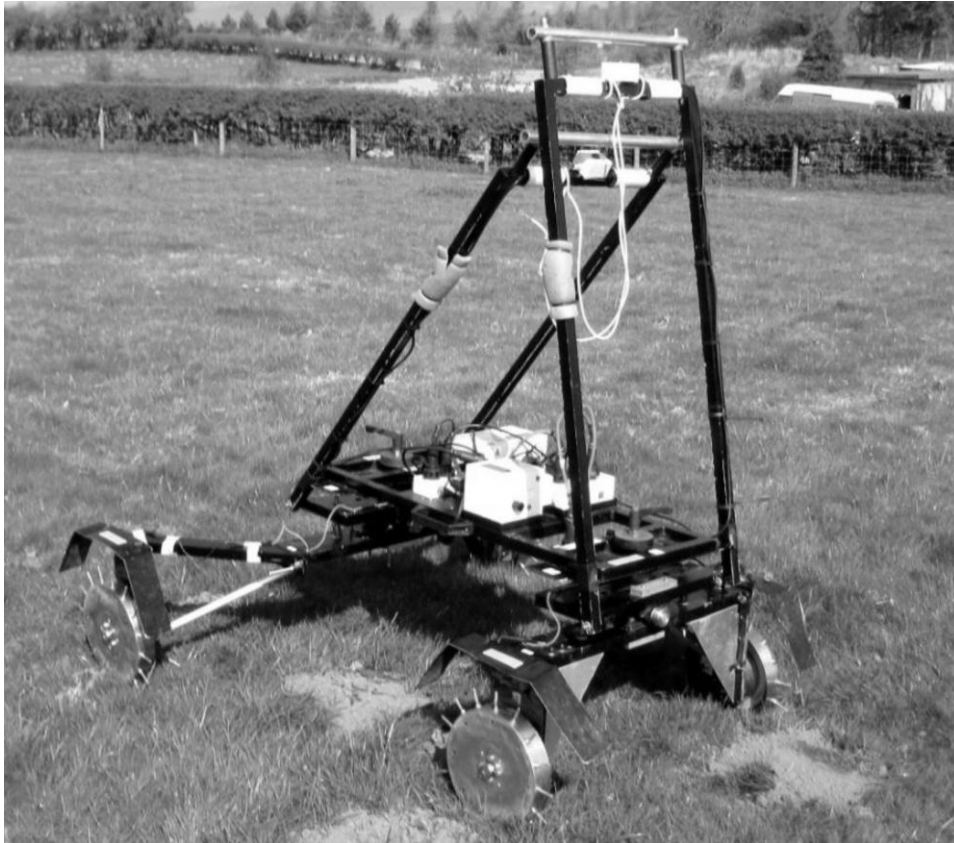
Figure 3.11 The MSP40 with the trapezoidal extensions on the rear of the platform (Harris 2011 42).
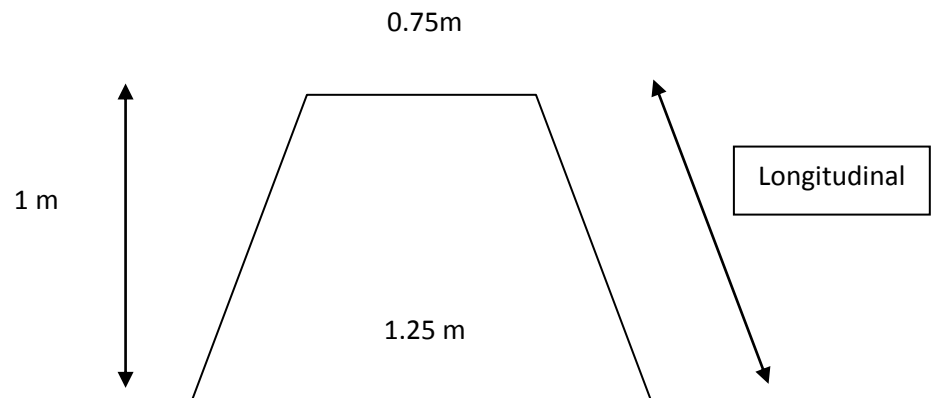
Figure 3.12 The MSP40 axle dimensions when configured as a trapezoidal array. Based on Harris (2011:30).

The research focused on practical field trials, deep tank experiments and data modelling and investigated six main topics:

- The resolution capabilities of the trapezoidal array (being able to distinguish archaeological anomalies from the 'background' soil).
- The depth of investigation, referring to the optimal depth of investigation (greatest current density).
- Apparent anisotropy, changes in the measured resistance of an array dependent on the angle of strike to the anomaly. Ideally arrays would have an isotropic response (no directional influence).
- Practicalities of use in the field, survey logistics and ease of use
- Comparisons with the square array.
- Comparison with modelled response of the trapezoidal array using ResData a software programme based on John Lynam's equations (Lynam 1970).

The research concluded that the trapezoidal and square arrays identified the same anomalies (in practical field trials) and the arrays possessed similar response properties as both had shallow depths of detection with greater sensitivity to near-surface features. However, the response form and magnitude varied between the arrays (Harris 2011). The longitudinal and broadside trapezoidal configurations also showed variation in form, orientation and magnitude of responses related to angle of strike of the anomaly for each configuration.

The trapezoidal array was found to be more cumbersome to position between traverses than the square configuration of the MSP40 due to the wider axle base at the rear of the MSP40.

The trapezoidal gamma measurements showed a significant difference to the square array as the trapezoidal array produced a single peak at depth (in the deep tank experiments) whereas the square array continued to show a double peaking through all investigated depths. Harris (2011) describes this as a consequence of the trapezoidal gamma not sharing two perpendicular potential probe positions.

Therefore the calculated trapezoidal gamma represents the different volumes of soil measured between the longitudinal and broadside configurations (Harris 2011).

The square array and mobile arrays in general have seen significant developments in the last 20 years. Many of the developments with systems such as the RATEAU, MUCEP or Geophilus Electricus systems have focused on increasing the collection speeds but have failed to consider the potential impact of such systems on the soil. The RATEAU system in particular produced significant damage to the soil as the electrodes acted like ploughs. The systems are frequently pulled by cars, tractors or quad bikes (ATV's) which also have a physical impact on the soil. The damage may be caused through compaction or shearing of soil because of the traction required by the vehicles. The MSP40 lightweight multi-sensor platform is intended to be pulled by hand which reduces the impact on the soil helping to protect the buried archaeology. Many of the mobile arrays discussed would also require significant turning circles and are not suitable for smaller or enclosed areas.

Neither the RATEAU or MUCEP systems could collect gradiometer data, although towed fluxgate gradiometer systems are increasing in use for example the Foerster Ferex system (Foerster 2009) and the GEOCARTA AMP system (Dechezleprêtre *et al.* 2009). However, the MSP40 is easily repositioned by using the opposing handles and can collect earth resistance and gradiometer data simultaneously, reducing the survey time and maximising the information gained in a single traverse.

3.2.0 MSP40 hardware description and discussion of functions

3.2.1 Description of the MSP40

The MSP40 is a lightweight hand-pulled mobile sensor platform that can collect gradiometer, RTK GPS collected DEM data and simultaneous earth resistance data (in two orientations Alpha and Beta).

The earth resistance data is collected through 4 stainless steel wheels (with a 0.75m separation). The earth resistance data is measured using an RM15 which sets voltage and current ranges and a DL256 that sets the survey parameters, logging speed and stores the data. The MPX40 is the integrated multiplexer to switch between the directional orientations. The MSP40 is pulled by two handles mounted on the front and back of the array, allowing for easy repositioning of the array. The two handles also help to maintain array orientation as it is not necessary to rotate the array during zigzag data collection.

The MSP40 can log data using two different techniques, a time based collection and a distance based collection (using an optical encoder wheel). Both techniques allow for multiplexing of data (Alpha and Beta only), averaging of data (to reduce interference effects) and the simultaneous collection of a Geoscan Research fluxgate gradiometer survey (FMs). These functions have been designed and tested by Geoscan Research and have not been modified during the research project. The time and encoder based collection allow for specified sampling intervals from 0.125m to 1m. A detailed description of these functions is available in the MSP40 instruction manual (Walker 2006). However, a brief overview of key features is discussed below based on the instruction manual and experience gained during the research project. These points specifically relate to data quality, survey logistics and data collection rates.

3.2.2 Time based collection

The MSP40 can collect data in a time based sample trigger mode; the time function works the same ways as the Geoscan Research FM gradiometers where the operator specifies a pace per metre. The rate of collection ranges from 0.40s to 3.00s with 0.02s increments. Each traverse must be collected within the specified time otherwise the data collected will be unevenly sampled and data will be missing from the end of the traverse. The same pace must be kept throughout the traverse (regardless of topographic changes and site conditions) so that all sampling intervals are equidistant from each other.

The time based collection rate is limited to a maximum rate listed below (dependent on the sampling interval specified).

The use of the MPX40 to collect Alpha and Beta measurements slows the maximum collection speed for both the time and distance based data acquisition (see tables 3.1 and 3.2).

Table 3.1   Maximum collection rates for a single Alpha or Beta measurements.

Sample interval	Samples per metre	Maximum collection speed
0.5m	2	0.4 s/m
0.25m	4	0.7 s/m
0.125m	8	1.2 s/m

Table 3.2   Maximum collection rates for Multiplexed Alpha and Beta measurements.

Sample interval	Samples per metre	Maximum collection speed
1m	1	0.4 s/m
0.5m	2	0.7 s/m
0.25m	4	1.2 s/m
0.125m	8	2.4 s/m

All measurements are with a delay time of 110ms without digital averaging, from Walker (2006).

If the suggested maximum rate is exceeded in multiplexed time based collection then this will produce increased 'noise' levels in the data.

3.2.3 Encoder / distance based collection

The MSP40 can also collect data using a distance based sample trigger; the main advantage of using the optical encoder wheel is that it is not necessary to maintain a constant pace along the traverse. The variable speed of collection is especially useful on sites with sudden changes in topography or poor ground conditions which make it difficult to safely maintain a constant pace.

The distance measurements may improve the reliability of sampling positions on long traverses (>20m) where continuity of pace can be problematic. The distance measurement is calculated from an optical encoder mounted on to the internal drum of wheel 1 and with a perforated ring mounted on the inside faces of wheel 1 (see figure 3.13). As the wheel rotates, the light path between transmitter and receiver is completed each time a perforation passes by, generating a pulse.
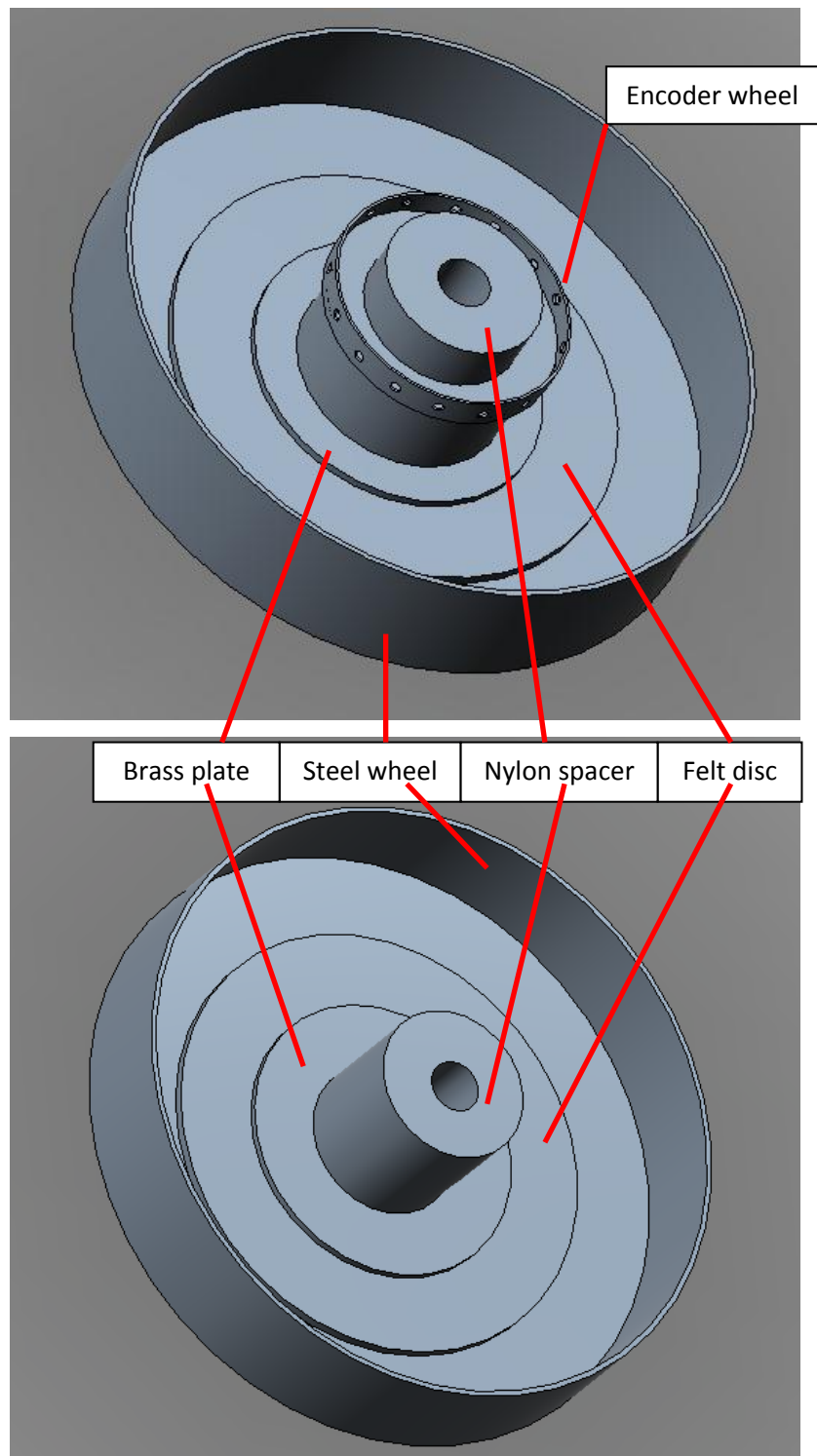
Figure 3.13　The encoder ring mounted on wheel one (top image) with the regular wheel hubs below, drawn in Autodesk 2012.

The optical encoder is calibrated by recording the average number of pulses recorded over three traverses prior to survey. Minor adjustments can be made during a grid by increasing or decreasing the number of pulses per traverse. When significant changes in the topography or errors occur with the traverse distances it may be necessary to repeat the calibration process. A detailed account of the calibration process and setup routine of the MSP40 can be found in the MSP40 instruction manual (Walker 2006).

The maximum sampling / collection rate for the distance measurement collection is slowed by using the optical encoder, with the manufacturer reporting an increase in collection time of approximately 0.3s/m (see table 3.3).

Table 3.3   Maximum collection rates for multiplexed measurement comparisons.

Sample interval	Samples per metre	Maximum collection speed (Timed)	Encoder/ distance collection
1m	1	0.4 s/m	0.7s/m
0.5m	2	0.7 s/m	1.0 s/m
0.25m	4	1.2 s/m	1.5 s/m
0.125m	8	2.4 s/m	2.7 s/m

All measurements are with a delay time of 110ms without digital averaging, from Walker (2006).

If the maximum collection rate for the distance collection is exceeded the MSP40 will overshoot the survey grid. If the maximum collection rate is continually exceeded during a single traverse the MSP40 will stop recording. The recorded data must be deleted and the traverse restarted at a slower pace.

3.2.4 Noise/spike monitoring

The MSP40 has a noise spike monitoring function that emits a warning beep at the end of a traverse if a specified number of spikes are exceeded. Any reading below a specified threshold is recorded as a spike with typically a threshold value of 2 ohms being set. A warning is only given when the number of spikes exceeds a pre-set value. The operator can then choose to accept the spikes or delete the data and resurvey the traverse. This function is especially useful on sites with poor ground conditions (stony soil etc.) or when the soil is very dry and the contact resistance of the electrodes cannot be overcome. These factors often lead to a drop out in data where a negative resistance value or value around zero is recorded as a negative spike.

This function is extremely useful as the operator is positioned at the front of the MSP40 facing away from the instruments making it impossible to view the readings as they are recorded. The data can also be reviewed on the DL256 but this can take up a significant amount of time during a survey. However, using the spike monitor function further slows the maximum collection rate per metre and the spike monitor does not identify large positive spikes between sequential readings.

3.3.0 Delay time tests

3.3.1 Introduction

The delay time function is an operator specified time period that the DL256 should wait for the multiplexed readings to settle before recording the data value.

The delay time can be set at pre-programmed intervals of 0, 50, 80, 90, 100, 110, 200 and 500 mS. The default setting for the DL256 data logger is 110 mS. The chosen delay time affects the collection rate, as the longer the delay / settling time the slower the collection rate. It was not known if the delay time would affect the data quality, as the shorter the delay may lead to an increased risk of noise in the multiplexed data. Therefore an experiment was carried out to study the effects of delay time on data quality.

3.3.2 Method

The amphitheatre test site on the University of Bradford's grounds (see chapter 4.2) was surveyed repeatedly on the same day with delay times of 0mS, 50mS, 110mS and 500mS. Four settings were chosen as the grass would have been damaged by extra trials in the wet conditions. An area 20m x 20m was surveyed with a sampling and traverse interval of 0.5m and 1m respectively. The 500mS delay time was trialled, but the pace required for the 0.5 seconds delay between each Alpha and Beta measurement was difficult to maintain whilst accurately recording the measurements without the DL256 stopping recording or overshooting the grid. Therefore only two traverses were completed.

3.3.3 Data processing

The data was processed using the following parameters for all data sets

- 3 x Despike X=1 Y=1Thr=3 Repl=Mean

- Search and replace any negative values with the dummy value 2047.5

3.3.4 Results

Alpha 0mS delay raw
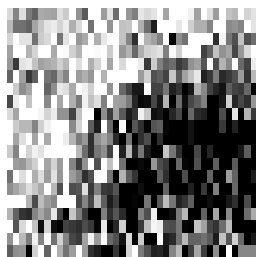
Alpha 0mS delay processed
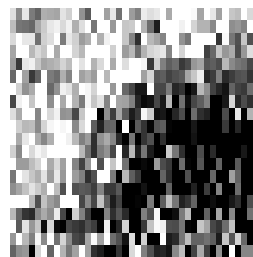
Beta 0mS delay raw
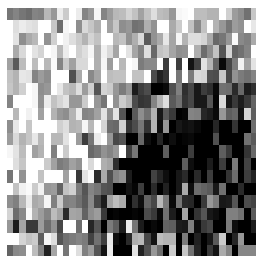
Beta 0mS delay processed
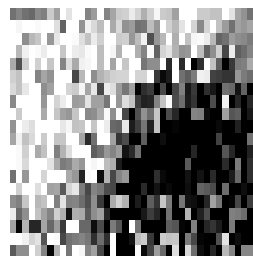
Alpha 50mS delay raw
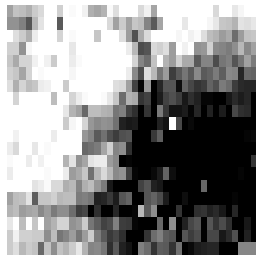
Alpha 50mS delay processed
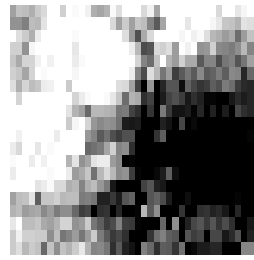
Beta 50mS delay raw
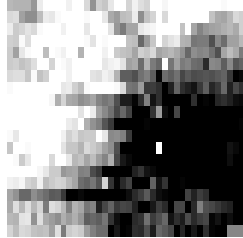
Beta 50mS delay processed
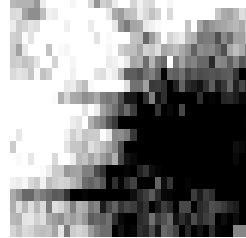
Alpha 110mS delay raw

Alpha 110mS delay processed

Beta 110mS delay raw

Beta 110mS delay processed
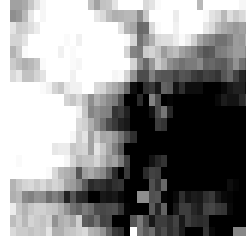
Alpha 500mS delay raw

Beta 500mS delay raw

The processed data sets were exported from Geoplot into Microsoft's Excel 2007.

The data was run through a logic argument programmed in Excel to automatically count the number of spikes between the raw and processed data sets (see chapter 4.5.2 for the formula and greater explanation(see table 3.4 and 4.18)).

Table 3.4   Delay time spike counts

Delay time	Spike count
Alpha 0mS	13
Beta 0mS	25
Alpha 50mS	14
Beta 50mS	11
Alpha 110mS	8
Beta 110mS	5

3.3.5 Discussion

The spike counts indicate that changing the delay time can affect the number of spikes in the data as the spike counts approximately double when the delay time is decreased by half. This indicates an increased variability in neighbouring data points as delay time reduces. However, when the greyscale plots are considered a significant visual difference is apparent between the 0mS delay and the 110mS plots. The 0mS greyscale plots show the broad trends of high resistance in the 110mS data but the subtle linear anomalies are unidentifiable. The diagonal linear anomalies are fragmentary in the 50mS delay plots but other anomalies are identifiable.

The 110mS delay time is the manufacturer recommended setting for the MSP40 so this was used as a 'standard' for data quality checks and comparisons. The individual earth resistance values for the 0mS and 50mS were calculated into a percentage of the 110mS value for each coordinate. This was done to examine the percentage change between the earth resistance readings.

Groups of percentage deviation from the 'standard' were then calculated at ±1%, 5%, 10%, 20%, 50% and 100%. The lower the percentage change in earth resistance values, the greater similarity between the delay time measurements (see table 3.5).

The following example of a logic argument was used in Microsoft's Excel 2007 to interrogate the data and express a true or false response.
=IF(A1>99,A1<101)

- If the value in column A row 1 is greater than 99 and less than 101 the function returns a true answer. If the data value is less than 99 and greater than 101 a false value is recorded.

A numerical count of the 'true values' could then be calculated using the following function.
=COUNTIF(A1:A800,TRUE)

Table 3.5   Delay time effects on the variation in earth resistance measurements.

	Count of data points within ± X % of Earth resistance values compared to the 110mS delay time					
	1%	5%	10%	20%	50%	100%
Delay time 0mS (Alpha)	21	60	122	226	551	764
Delay time 50mS (Alpha)	62	250	449	668	792	800
Delay time 0mS (Beta)	17	66	124	265	607	781
Delay time 50mS (Beta)	36	182	379	612	783	799
110mS Alpha Beta comp.	56	256	506	746	797	800

The percentile variation between the 'standard' 110mS results and the 50mS and 0mS roughly equate to the following ohm variation.

Based on a 12 ohm reading

± 1%= 0.12 ohms   ±5% = 0.6 ohms   ±10% = 1.2ohms

±20% = 2.4 ohms   ±50% = 6 ohms   ±100 % 12 ohms

Slight positional variation between each delay time survey may account for some of the recorded variation. However, the data indicates that delay time does have an impact on data quality. The longer the delay before recording the multiplexed resistance values reduces the risk of noise in the data.

However, this must be considered against the collection rate of the MSP40, as delay time above 110mS (e.g. 500mS) heavily impacts on the data collection by significantly increasing the survey time. The percentage variation between the 110mS Alpha and Beta measurements were also evaluated. The results show a slight improvement in correlation between Alpha and Beta 110mS and the 0mS and 50mS approximately between 2-25%. However, the Alpha and Beta measurements may also be affected by the slight variation in directionality that may explain why the percentile difference closely parallels the 50mS delay time. The results show a clear effect on the data quality of reducing the delay time for the multiplexed MSP40 data. The 110ms is the 'factory default' setting by the manufacturer. From the experiment it shows this setting produces a good balance of data quality and maintainable logging / collection speed.

3.4.0 MSP40 modifications / technology development

3.4.1 Introduction

The following section discusses the modifications made to the prototype MSP40 during the research. Modifications were made as possible solutions to specific problems encountered during the research. Several of the issues are discussed in more detail later on in the chapter. To aid understanding of the issues a series of three dimensional models were drawn in Autodesk Inventor Fusion 2012 to highlight the areas being discussed (see figures 3.14 and 3.15). This was a more appropriate method than photography alone as it allowed for an easier selection of views or angles (see figure 3.16).
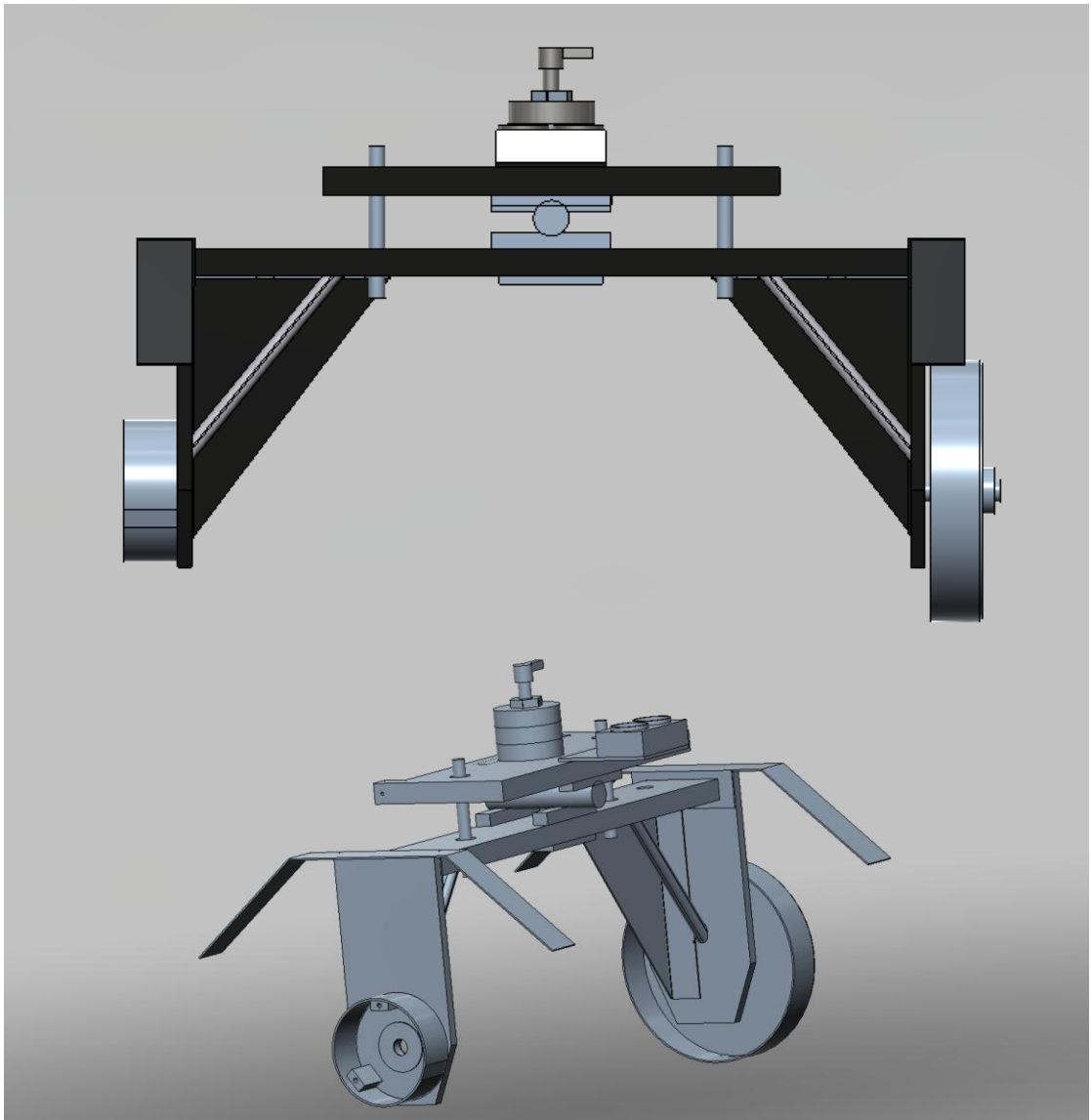
Figure 3.14   The axle of the MSP40 from two angles drawn in Autodesk 2012.
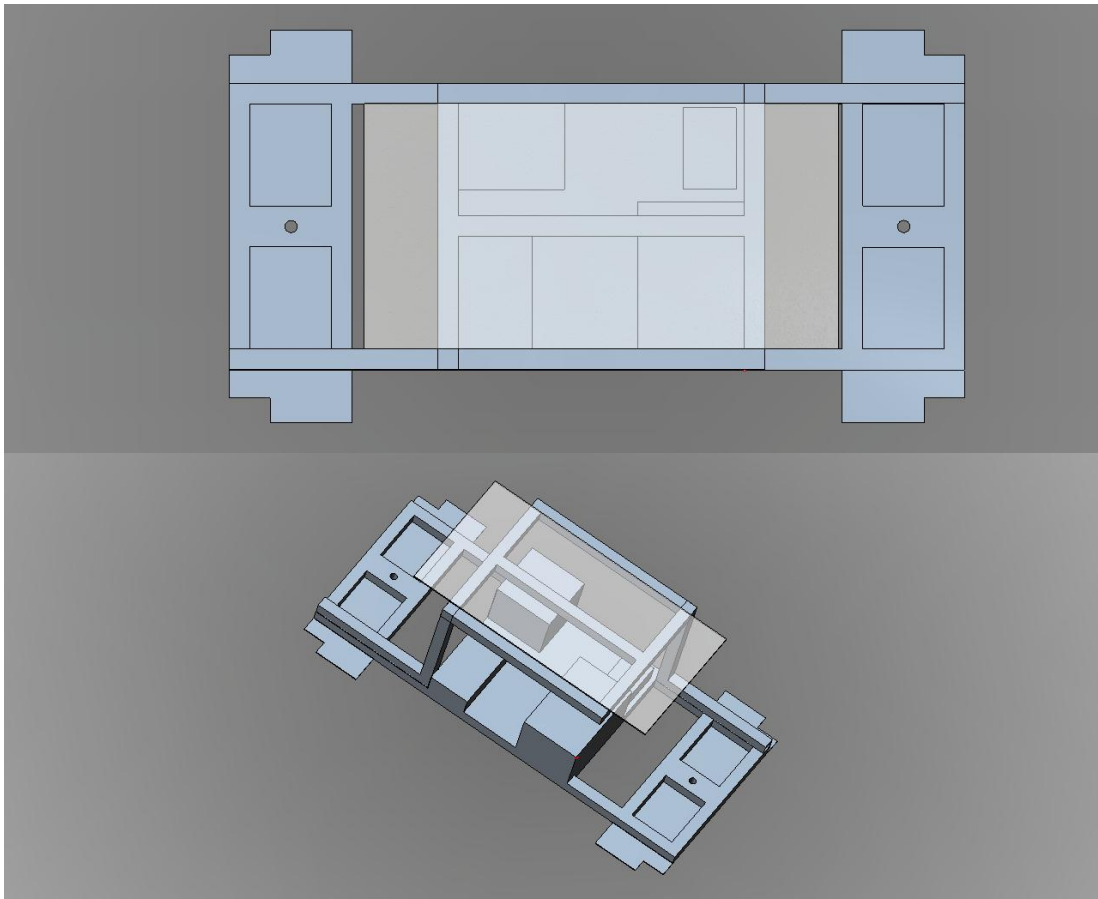
Figure 3.15   The MSP40 platform from two angles drawn in Autodesk 2012.
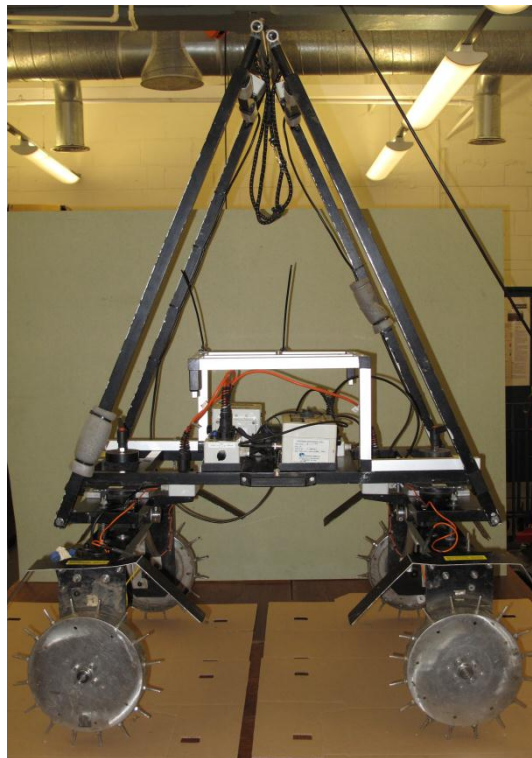
Figure 3.16   The prototype MSP40 used during the research project (Sparrow 2013).

3.4.2 Reinforced axle supports (aluminium)

The aluminium tubing used to provide a diagonal support for the vertical axle support was replaced as the bent aluminium began to sheer at the fold. All four axle supports showed signs of sheering or had sheered so needed to be replaced. This was noticed after c. 20 ha of survey. Thicker walled (3mm) aluminium tubing was used to replace the sheered tubing. The pressure that caused the sheering of the support tubing on the vertical axle plate also showed up as a slight bending of the wheels. This issue became more pronounced on sloping ground and was an indication of the plastic being forced outwards at the base of the wheel (see figure 3.17).

⬤ Replaced aluminium tubing   Position and direction of the vertical plastic axle plate bending outward.
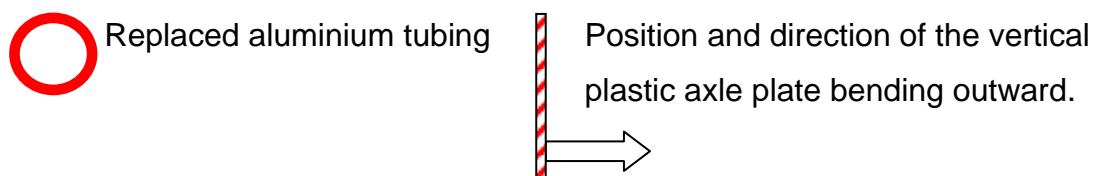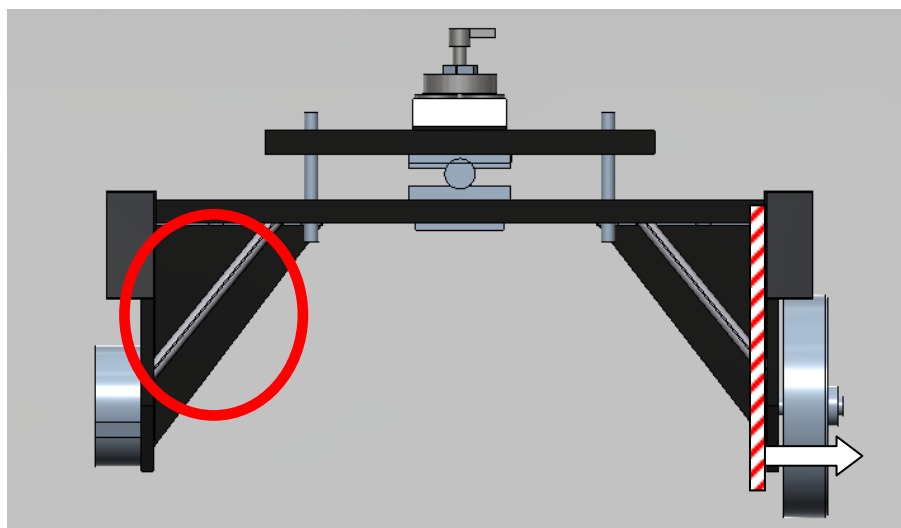
Figure 3.17   The replaced aluminium tubing axle support and the vertical axle plate bending outwards from the forces exerted on the axle drawn in Autodesk 2012.

3.4.3 Right angle aluminium supports

After the reinforced aluminium supports were replaced it was still apparent that additional bracing was required to stop the vertical axle plate from bending. Aluminium sheeting was bent to form a right angle brace (see figure 3.18). The bracing was drilled and bolted on to the axle and vertical axle plate. Additional cut-out sections were made to allow room for suspension springs, pre-existing bolt locations and the wheel encoder (wheel 1 only (see section 3.8.3)).
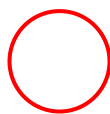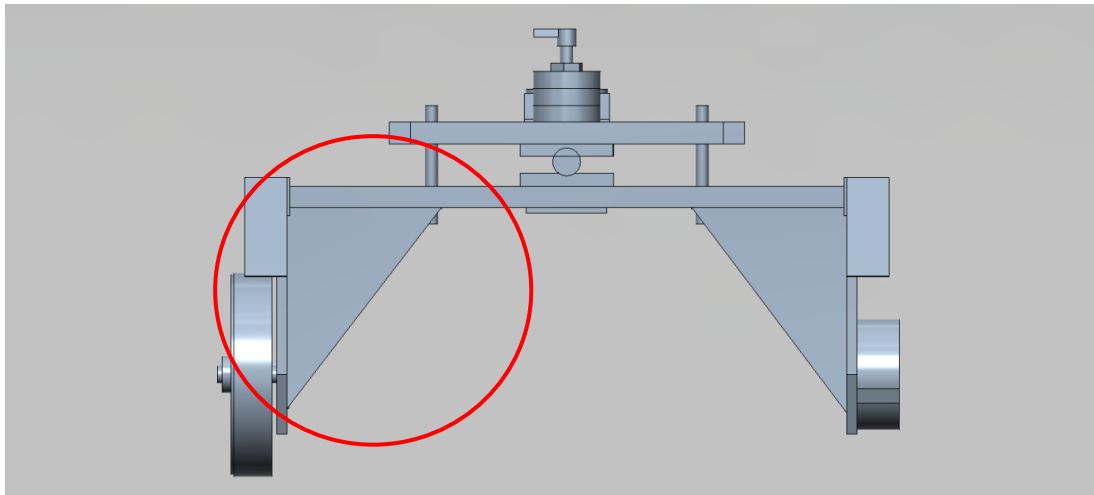
Right Angle Aluminium wheel bracing

Figure 3.18   Highlighting the additional wheel bracing added to the MSP40 drawn in Autodesk 2012.

3.4.4 GPS rear mounting

Initial integration of a global positioning system (GPS) onto the MSP40 had to consider the best position for the GPS receiving unit or Rover. The first mounting position tested consisted of a rear mounted aluminium frame to which plumbers pipe fixing brackets were mounted so that an aluminium detail pole could be inserted.

The height of the pole could be adjusted and was held in place by textured plastic matting inserted between the detail pole and the fixing brackets (see figure 3.19). A more detailed discussion of GPS integration is presented later in the chapter (see chapter 3.6).

Figure 3.19   The 1st generation rear mounted GPS unit attached to the detail pole on the MSP40 (Sparrow 2013).

3.4.5 GPS central mounting

After the initial trials with the GPS rear mounting frame, it was decided that an alternative solution may be more appropriate. Therefore a new aluminium frame was built which situated the GPS directly over the centre of the array (see figure 3.20 and 3.21). The GPS was mounted much lower than the initial rear mounting; this meant that the measurements directly correlated with the earth resistance measurement positions instead of being offset by 0.75m. The lower height of the receiver also meant the GPS would be less affected by tilt.
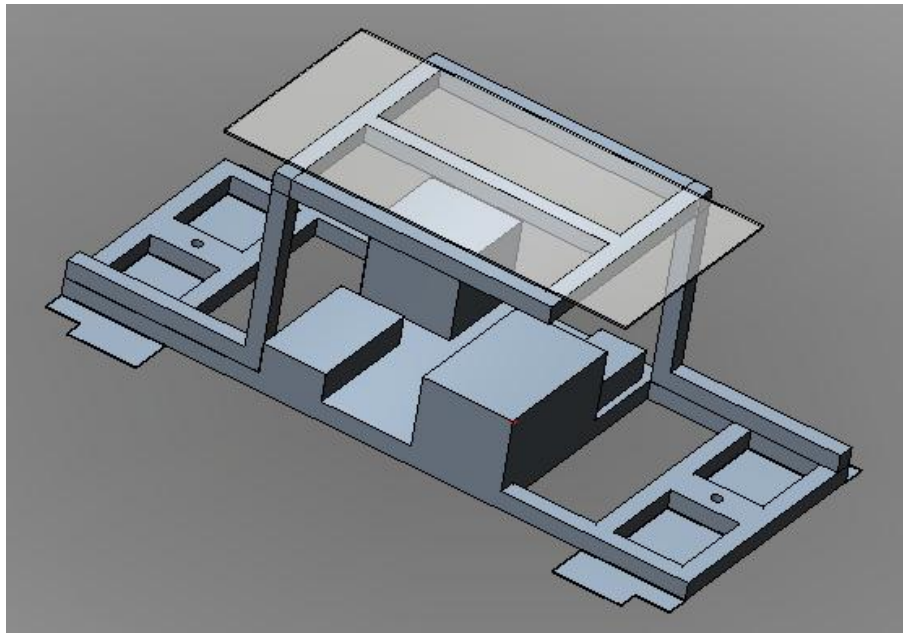
Figure 3.20   The centrally mounted GPS frame mounted on the MSP40 platform drawn in Autodesk 2012.

Threaded for mounting the GPS unit
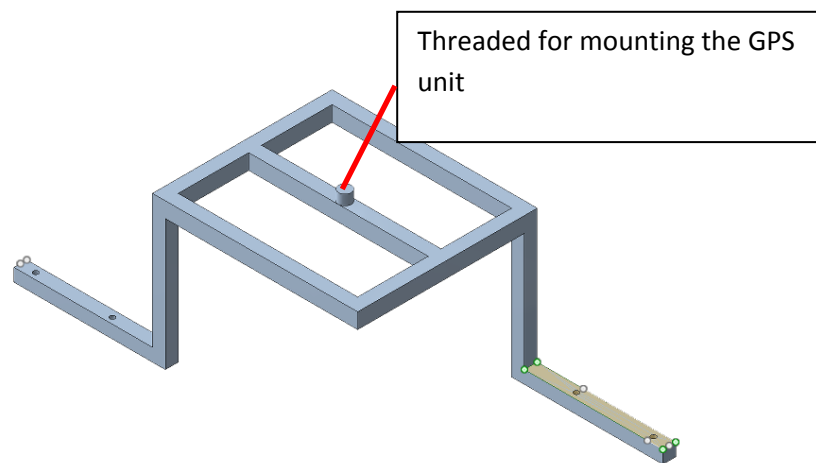
Figure 3.21   The centrally mounted GPS frame drawn in Autodesk 2012.

3.4.6 Bulgin connectors with cable supports

Whilst surveying at the site of Entremont (Provence, France) a heavy rain storm occurred during the survey. At the end of the day the equipment was taken apart and it was noted that water had accumulated in one of the Bulgin plugs that had been sealed (plugged in throughout the storm). Further inspection of the Bulgin plug showed that water was entering the plug from the sealed end of the connector as this was vertical to the cart platform and therefore exposed to the elements. Spiral cable supports were added to the ends of the Bulgin connectors to support the cables and restrict their movement. This would also stop the movement of the rubber grommet / seal in the end of the connector and stop water from entering the Bulgin housing.

3.4.7 Silicon resin filled Bulgin cables connectors

After additional surveys in the rain it was found that water was still entering the Bulgin connectors, which was probably due to the cable flexing and slightly displacing the rubber grommets / seals allowing the water to enter. The water entering the connectors was causing errors in data as the water shorted the wires. The cables were taken apart and allowed to air dry before being reassembled and a silicon resin injected into the connector end to provide a water-tight but flexible seal around the cables.

3.4.8 Rain cover

The centrally mounted GPS frame also had the additional benefit of allowing a rain cover to be built over the platform. Perspex sheeting was drilled and bolted to the Aluminium mounting to act as a rain shield (see figure 3.22). The addition of the rain cover further reduced the risk of water entering the Bulgin connectors (see sections 3.4.6 and 3.4.7) and stopped water collecting on the RM15 and DL256 displays. This protected the instruments and helped improve visibility of the display bar on the instruments.
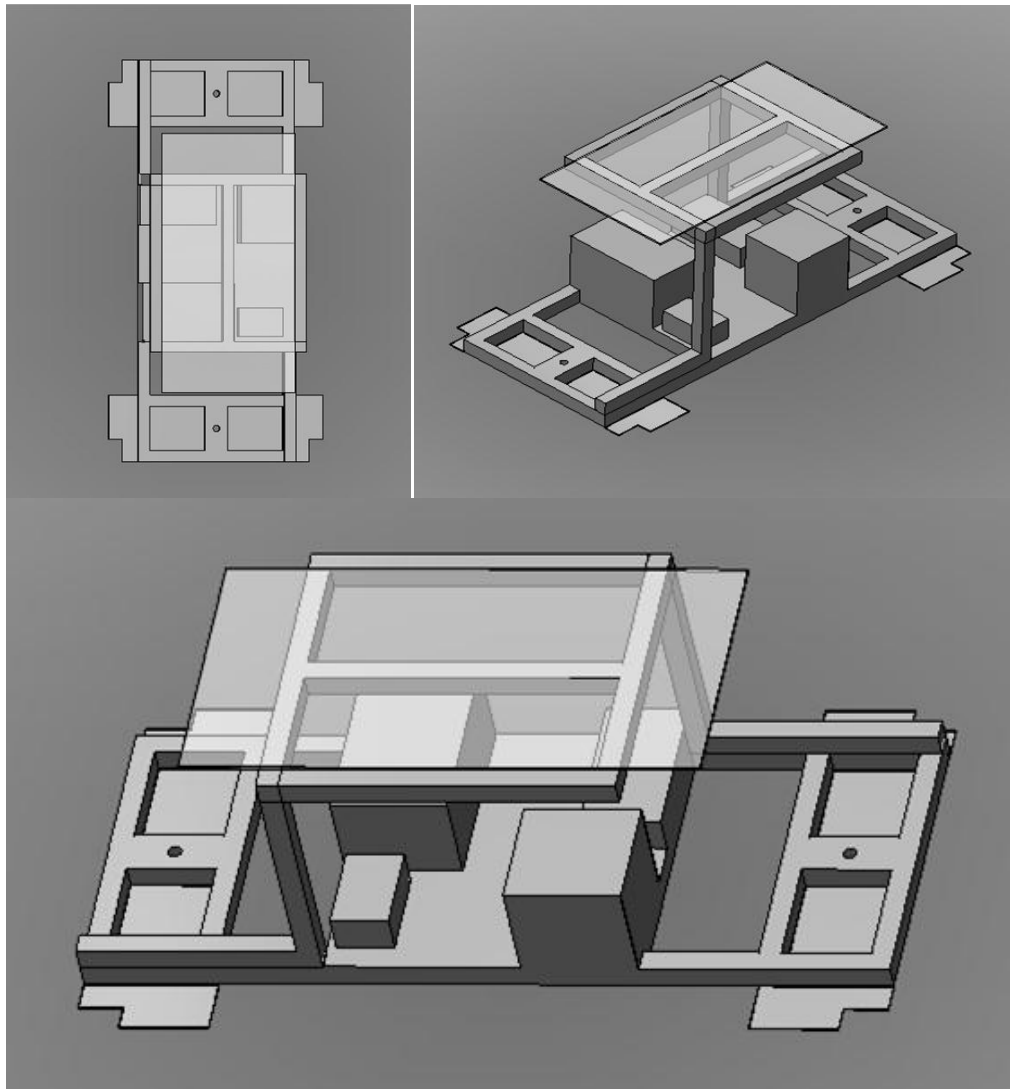
Figure 3.22   The rain cover mounted on to the GPS frame on the MSP40 platform drawn in Autodesk 2012.

3.4.9 Rain holes

After several days of surveying in torrential rain it was decided to drill water drainage holes into the MSP40 platform as rain accumulated in the instrument mounting areas. This was done to help protect the instruments and to speed up the drying time.

3.4.10 Gradiometer mounting

A FM36 / 256 gradiometer can be added to the MSP40 to allow for simultaneous collection of earth resistance and gradiometer surveys.

A bracket supplied by Geoscan research was added to the MSP40 for additional testing during the research.

When a simultaneous earth resistance and gradiometer survey are undertaken the gradiometer is mounted on to the front of the MSP40. The gradiometer aligns with the central axis of the earth resistance array but is mounted approximately 0.875m from the central point. This means it is necessary to shift the measurements after processing of the data (discussed later chapter 3.7). The gradiometer is mounted on an aluminium frame that bolts on to the 1 and 2 wheel end of the MSP40. The gradiometer handle sits within a wooden cradle on the aluminium frame and is strapped into place with the instrument's data logger facing towards the cart (see figure 3.16, 3.23 and 3.24).

As the FM handle is cylindrical to fit more comfortably in the operator's hand when used for hand-held collection, the handle can rotate in the flat bottomed u-shaped bracket. This can result in a pendulum motion on undulating ground creating additional noise in the data.
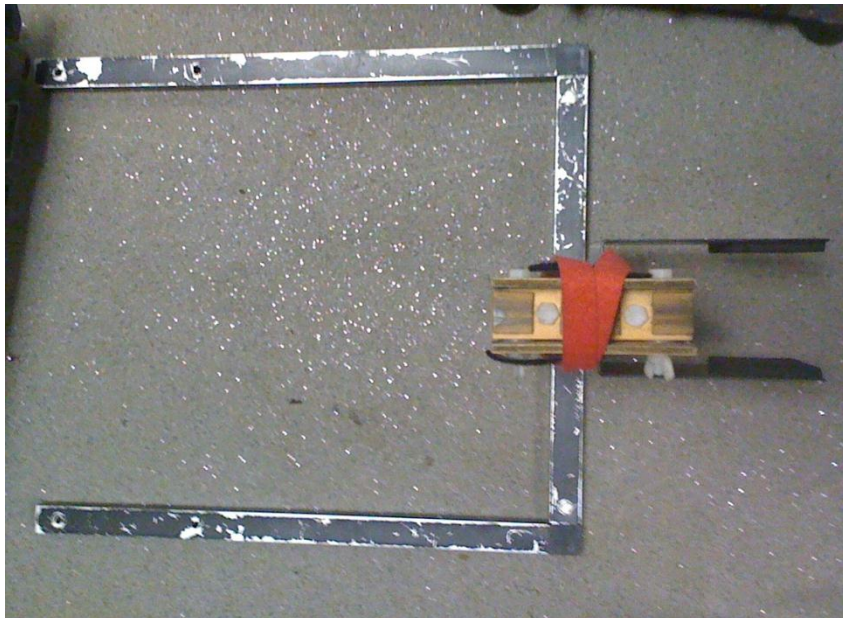
Figure 3.23   A top down perspective of the gradiometer mounting, the FM gradiometer handle sits within the wooden cradle to the right of the picture.

3.4.11 Gradiometer mounting bracket

Geoscan Research supplies a mounting bracket that can be attached on the vertical support of the FM mounting to stop the pendulum motion of the gradiometer (see figure 3.24). However, this also stops any self-correction to a vertical field alignment on sloping ground (discussed later in chapter 3.7.4).
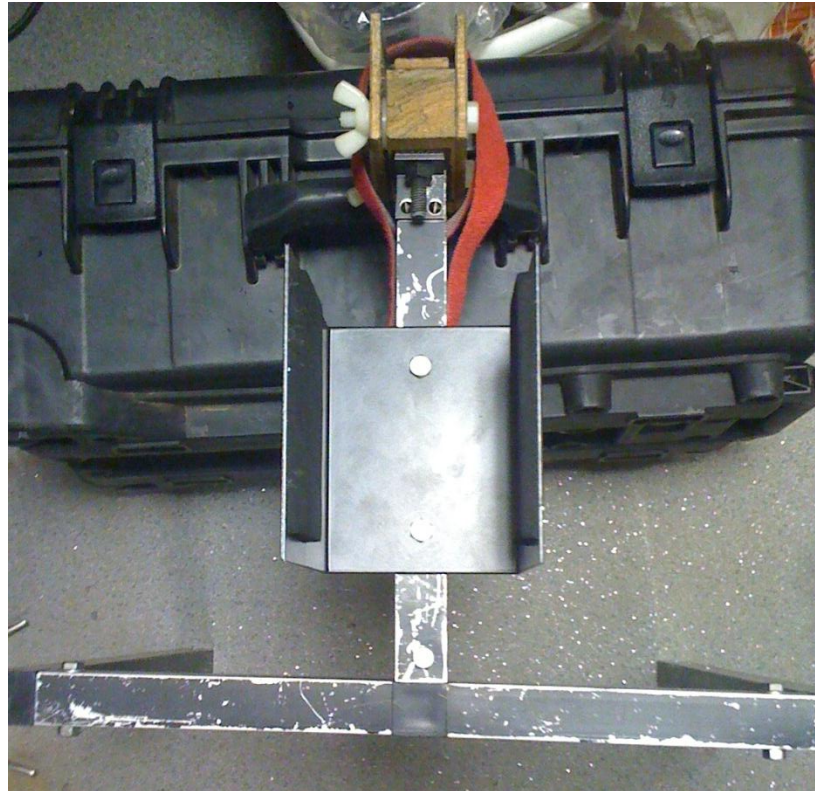
Figure 3.24   An end-on perspective of the gradiometer mounting and the mounting bracket located in the centre of the picture.

3.4.12 Replaced wooden spacers

The MSP40 used throughout the research was a prototype version of the MSP40, which was very similar in design to the commercially available system but small variations did exist. The bearing that allowed the axle to articulate was originally attached to wooden blocks that acted as cushions for the bolts. However, the bolts began to compress the wood causing the bolts to eventually loosen as the bolts could no longer 'bite' into the compressed wooden blocks. These were replaced with blocks of aluminium to help disperse the load along the axle.

The blocks were approximately 7mm thick and were cut to the shape of the existing wooden blocks before they were drilled to match the bolt holes of the axle bearing. The commercial models spacers are made of a filled nylon block (Nylatron GSM MoS2) (Dotmar 2012) and have been equally as effective a solution.

3.4.13 Brass counter weight

The brass rod counter weight provided with the MSP40 is used to counter balance the additional weight of the Geoscan Research FM gradiometer (when in use). As the gradiometer is mounted on to the front of the MSP40 the counter weight is mounted on to the back axle. The original method of mounting the weight was to use strips of Velcro wrapped around the axle, but these would loosen, swing and fall off during the survey. To solve this, the brass rod had two holes drilled through its diameter that could be mounted on to two bolts that were already on the axle. The Velcro could then be used to further secure the brass rod in place.

3.4.14 Sand filled tubes

Sand filled tubes were made by Tom Sparrow and consisted of drain pipes cut to the width of the axle c 0.62m x 0.05m. The tubes were attached to the underside of each axle to weigh down the cart and help reduce contact resistance issues. This proved especially useful on grassed areas that had significant percentage of moss making up the turf layer. Each tube was filled with approximately 2 kg of sand and two tubes could be attached to each axle with bungee cords to secure the tubes in place.

3.4.15 Extended contacts

The current and potential electrodes are wired from the multiplexer to the wheel hubs; the ends of the wires terminate with a banana socket. A short section of wire with a banana plug is then inserted into the socket at one end. The other end of the wire is soldered to the side of a brass rod that acts as an electrode on the inner (brass) surface of the wheel. The brass rod is housed in a drilled Tufnol block that also houses a spring to push the brass rod against the surface of the wheel. The brass push rod completes the circuit and allows the wheel to rotate freely (see figure 3.25).
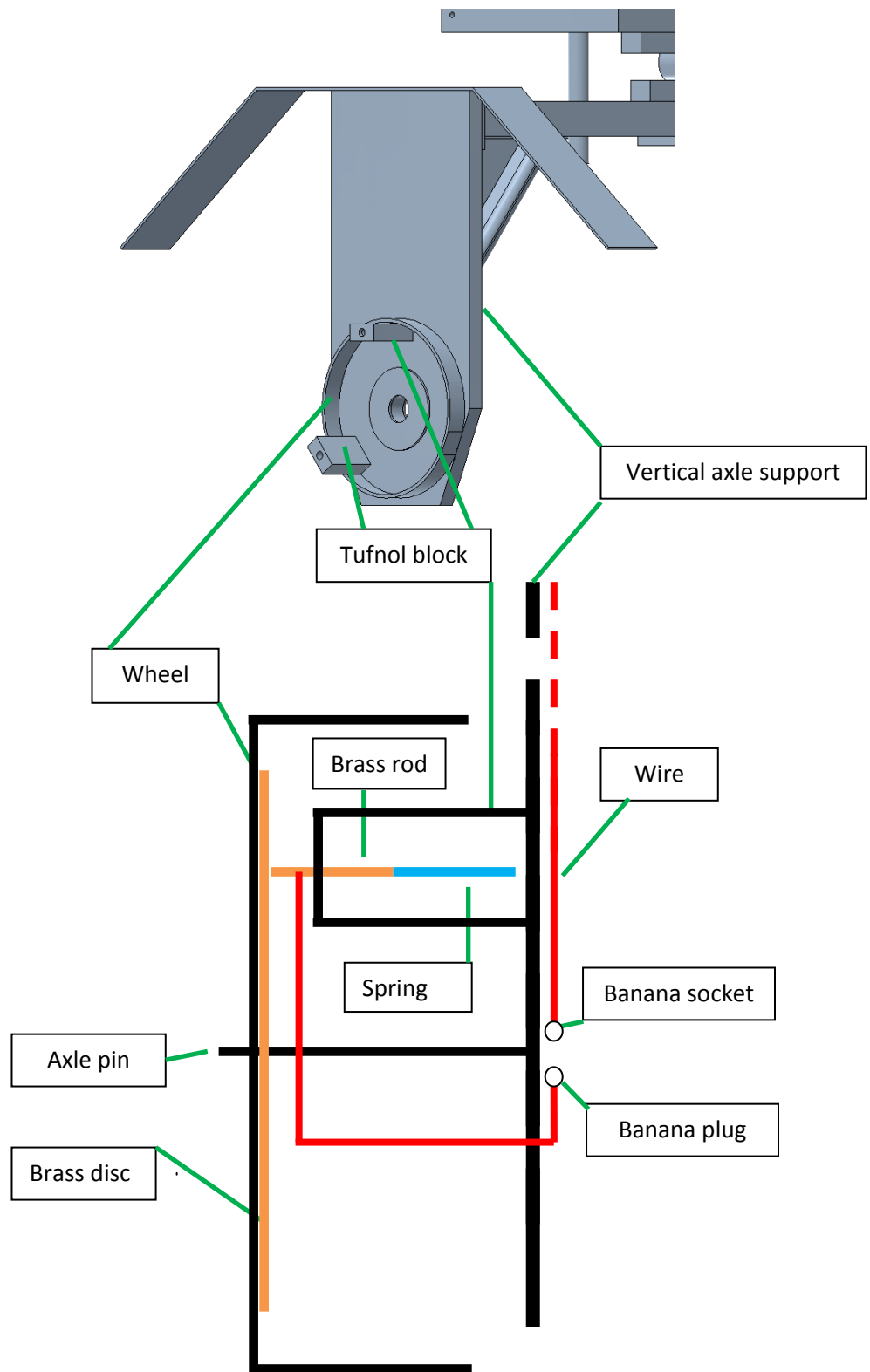
Figure 3.25   A cut away section of the vertical axle support and tuffnol block positions (top image) drawn in Autodesk 2012 with a cross-section diagram of the wheel hub and axle (bottom image not drawn to scale).

As the brass rods / contacts wore down they needed replacing and it was therefore decided that the brass contacts should be extended. The extra length would allow for greater wear before needing to be replaced and would also put the spring under greater pressure helping to ensure contact with the brass plate. The brass rods were increased from 35mm to 40mm in length. However, the wear rate of the brass rods increased initially due to the extra compression on the springs forcing the electrode contacts together. It is also important to note that after replacing the brass rods a 'bedding-in period' was required. During this time the wear and contact between the brass rod and plate may be uneven reducing the surface contact area that may in turn lead to poorer results (more spikes / noise). Burrs formed during the 'bedding-in period' and were filed down so that the rod did not foul / catch on the Tufnol block housing.

3.4.16 Extended spring length

The springs were replaced as they had become slack through wear. The four springs' lengths were also increased to force the brass rod to remain in contact with the brass plate on the wheel. The spring length was increased from 23 mm to 26 mm lengths to increase the compression force on the brass contacts. The increased spring and rod length helped to force contact with the brass plate as seen through the wear pattern on the brass plate after each survey.

3.4.17 Double electrode

In an attempt to produce more consistent result (reduce error / missing readings) a second electrode was added to each wheel. It was hoped that it would ensure at least one electrode would always be in contact with the brass plate on the internal face of the wheel (see figure 3.26). A Tufnol block was used for housing the second electrode as it is a laminated plastic made from modified phenolic resin with a woven glass fibre reinforcement making it an excellent insulator with a high mechanical strength and is not significantly affected by variable weather conditions when used outdoors(TufnolcompositesLtd 2008). The addition of a second electrode reduced the number of open circuit messages and dropouts in data even when the MSP40 was pulled along the contours of a steep slope.

Original electrode position

Additional electrode position
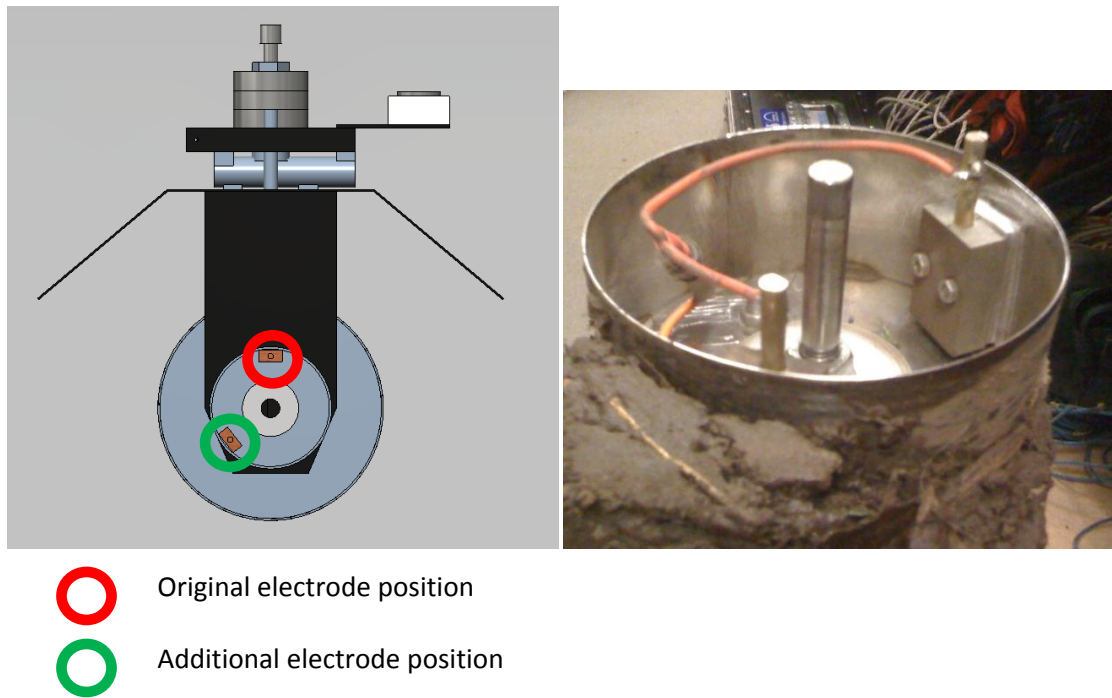
Figure 3.26   The Tufnol block mounting positions on the axle hubs for the two electrodes on each wheel (left hand image) drawn in Autodesk 2012. The right hand photograph shows the two electrodes within the wheel hub.

3.4.18 Rounded handles

After multiple days of survey with the MSP40, it was noticed that the risk of aggravating the carpel tunnel nerves in the surveyor's wrist increased. Therefore, it was decided to modify the handles of the MSP40. The problem was caused by the square box section aluminium tubing and the way in which the hands grip around the bar. The hand bends at the wrist and has continual pressure exerted on it as the cart is pulled. Circular tubing was drilled and bolted on to the existing handles with clearance for hands and not to foul the start stop switch. Saddle collars were used to seat the circular tubing and were bolted into place with high grade stainless steel (non-magnetic). The modification was successful and allows for two grip positions (the original square and the new rounded bar) for personal preference (see figure 3.27).
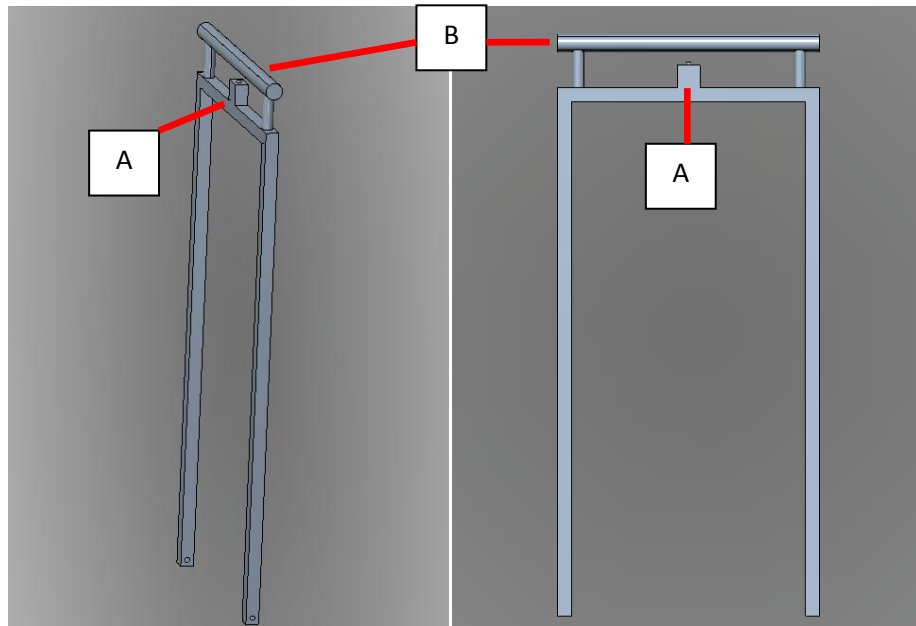
A= Start / stop button   B= Extended circular tubing / handle

Figure 3.27   The MSP40 handles (from two angles) with extended circular tubing / handle drawn in Autodesk 2012.

The remainder of the chapter focuses on further discussion of the key modifications outlined above. With discussion of sensor integration, issues faced during the research project and explanation why the modifications were made. Practical examples of survey data are included to highlight the issues encountered.

3.5.0 Wheel variations

3.5.1 Introduction

The MSP40 uses four wheels as the electrodes for the earth resistance measurements (configured as a square array for the purposes of this research). The wheels therefore became an important topic to research to see if an 'optimal' configuration existed. The easiest parameter to change was the spike lengths as the wheel spikes are simple nuts and bolts that can be removed and replaced (see table 3.6).

Table 3.6   Wheel diameter variations

Wheel configuration	Wheel diameter
Long spike	356 mm
Normal / standard spike	316mm
Short spike	285 mm
Bare wheel	240 mm
Bolt on discs #1	316mm
Bolt on discs #2	285mm

After repeated trials with the spike length variation it was apparent that the standard spike length produced the most consistent results. However, certain vegetation covers proved problematic for survey including lawned areas where the turf contained a high percentage of moss.

The springy nature of the moss reduced the contact area with the soil increasing the number of recorded errors. Therefore a disc system was developed that allows a stainless steel disc to be bolted on to the side of the existing wheel hubs. The 4mm thick stainless steel provided additional weight to the cart whilst providing a continuous edge to bear the full weight of the cart. The disc rim helped to smooth out the 'ride' of the cart, as the spikes can make the platform undulate slightly as each wheel spike enters the ground surface. Two sets of discs were manufactured to the same dimensions as the normal and short spike lengths so that the discs and spikes could be used simultaneously (for further discussion on wheel configurations see chapter 6.3.2).

Using discs on the wheels had been trialled previously by Dr Lew Somers. His discs have sharp teeth mounted on the outside face of the wheel to cut into the ground as the cart is towed along.

His research focused on achieving good ground penetration to overcome the contact resistance issues and was not intended to consider the impact on an archaeological site (see figures 3.28 – 3.30). The MSP40 was also towed behind a small quad or vehicle which once again could cause additional damage to the site. The long-term effects of towing the cart is also a cause for concern due to additional forces acting on the framework that it was not designed for.
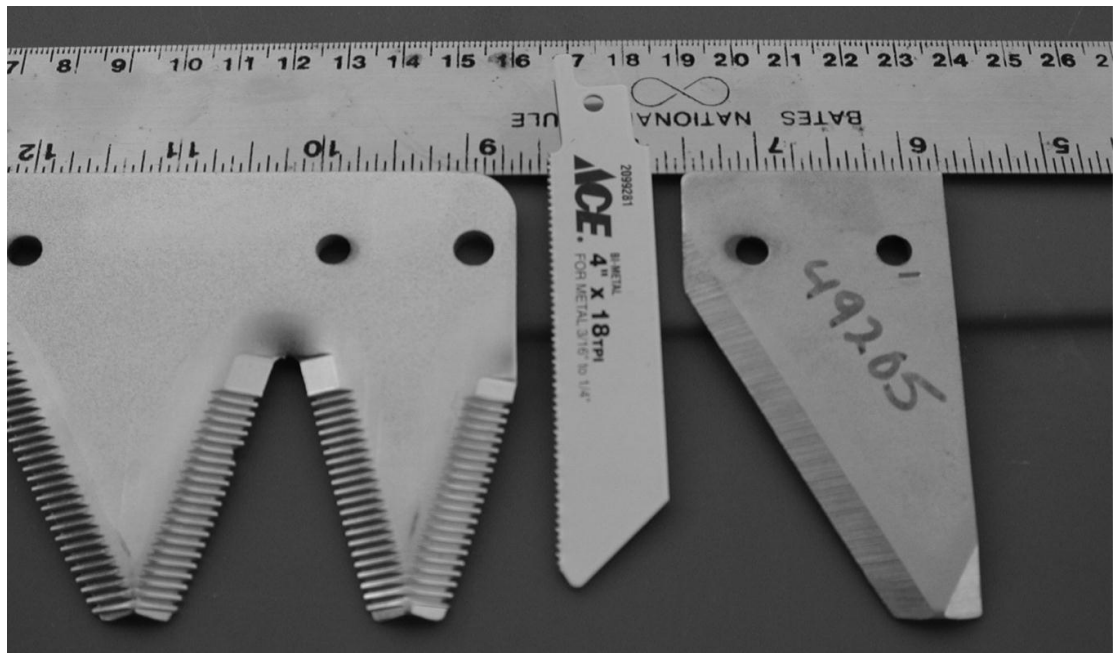
Figure 3.28   A range of teeth options considered for the MSP40(Somers 2010).
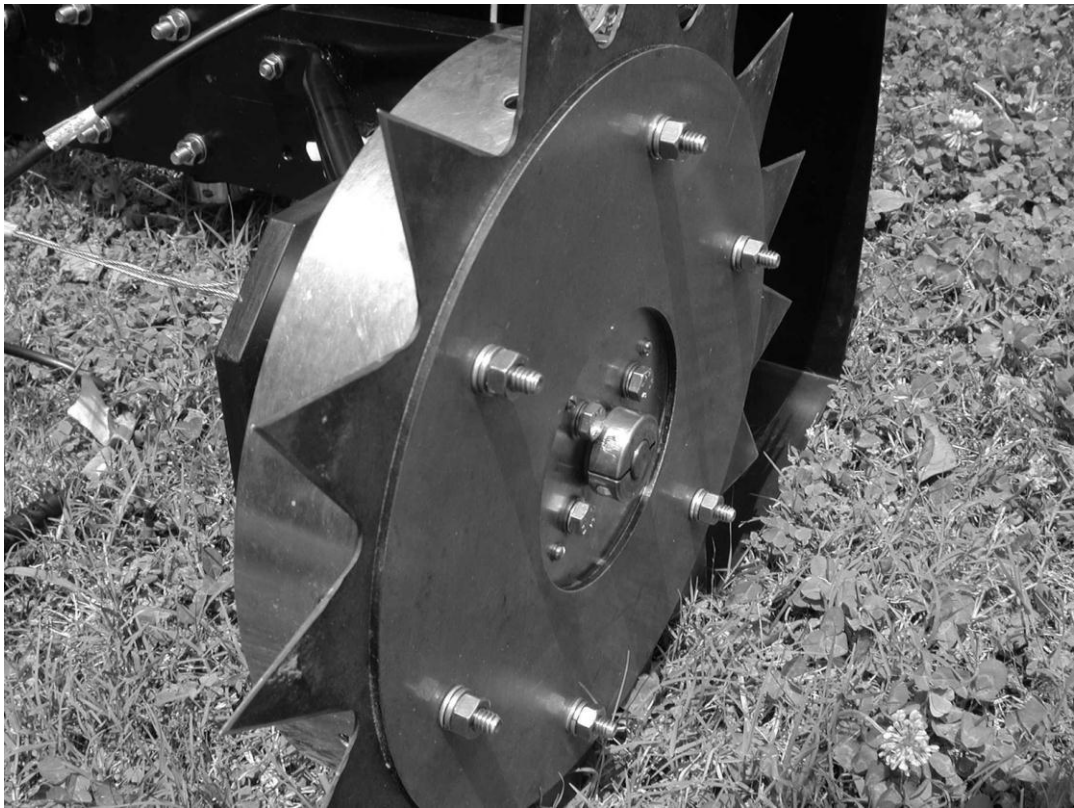
Figure 3.29   A wheel disc with teeth attached to the MSP40 (Somers 2010)**.**

Figure 3.30   The MSP40 with a toothed wheel configuration being towed behind a vehicle (Somers 2010).

3.6.0 GPS integration

3.6.1 Introduction

The MSP40 is a mobile sensor platform that can integrate multiple types of simultaneous survey techniques including earth resistance, GPS and fluxgate gradiometer survey (magnetic survey, see chapter 3.7).The combination of three different methods of survey must be tested to ensure acceptable data quality is achievable for each technique. The following section discusses GPS mounting, integration and issues.

This element of the research was done in collaboration with Tom Sparrow linking the University of Bradford with Geoscan Research specifically looking at GPS integration. The Geoscan Research collaboration focused on how GPS data may in the future be recorded on to the RM85 (still under development and discussed in future research see chapter 7.2). The project also looked at the possibility of Real Time Kinematic (RTK) GPS surveys with centimetre accuracy and the many data formats created by different manufacturers' GPS devices.

3.6.2 GPS rear mounting

The University of Bradford amphitheatre was used for the initial testing. The area made an ideal testing ground for the MSP40 and was the location for the seasonality testing area (see chapter 4.2 for more information).

Primary field trials on the amphitheatre raised a series of issues. As the MSP40 was pulled along the detail pole began to slide down through the fixing brackets before eventually touching the ground surface. This was due to the weight of the antenna and the intended adaptation size of the rings to fit different sized detail poles. The change in height of the antenna would obviously record erroneous elevation data values. The height of the pole raised further issues as slight undulations on the ground surface caused the Rover unit to tilt away from the vertical (see discussion chapter 6.4.5). The GPS data was collected at a rate of 10 Hz.

The result of the GPS trial showed the signal deteriorated over the second half of the grid due to the built up environment surrounding the site. The initial trials only collected with a GPS fix and not an RTK floating signal as the base and rover units were not configured for RTK GPS. The data was logged directly on to the TOPCON HiPer Pro (Topcon 2010a) GPS+ PC-CDU unit / programme which is used to control the GPS and can send scripts to and from the Rover (Topcon 2010b). The data was plotted using a freeware software programme called Visual-GPS (see figure 3.31) which can play-back National Marine Electronics Association (NMEA) (Kingsley-Hughes 2005 195-223) data in a real time window (VISUALGPS 2010).

The data plots showed significant displacement of the X, Y and Z coordinates as the survey data was collected at a 1m traverse interval on a 20m x 20m grid. Traverses were collected in straight lines with measured marker pegs at the beginning and end of each traverse. The GPS data recorded an erroneous change in elevation of approximately 38 feet or 11.5m over the 20m x 20m survey area. The survey area is relatively flat and a value significantly less than 30cm in elevation change would be expected.
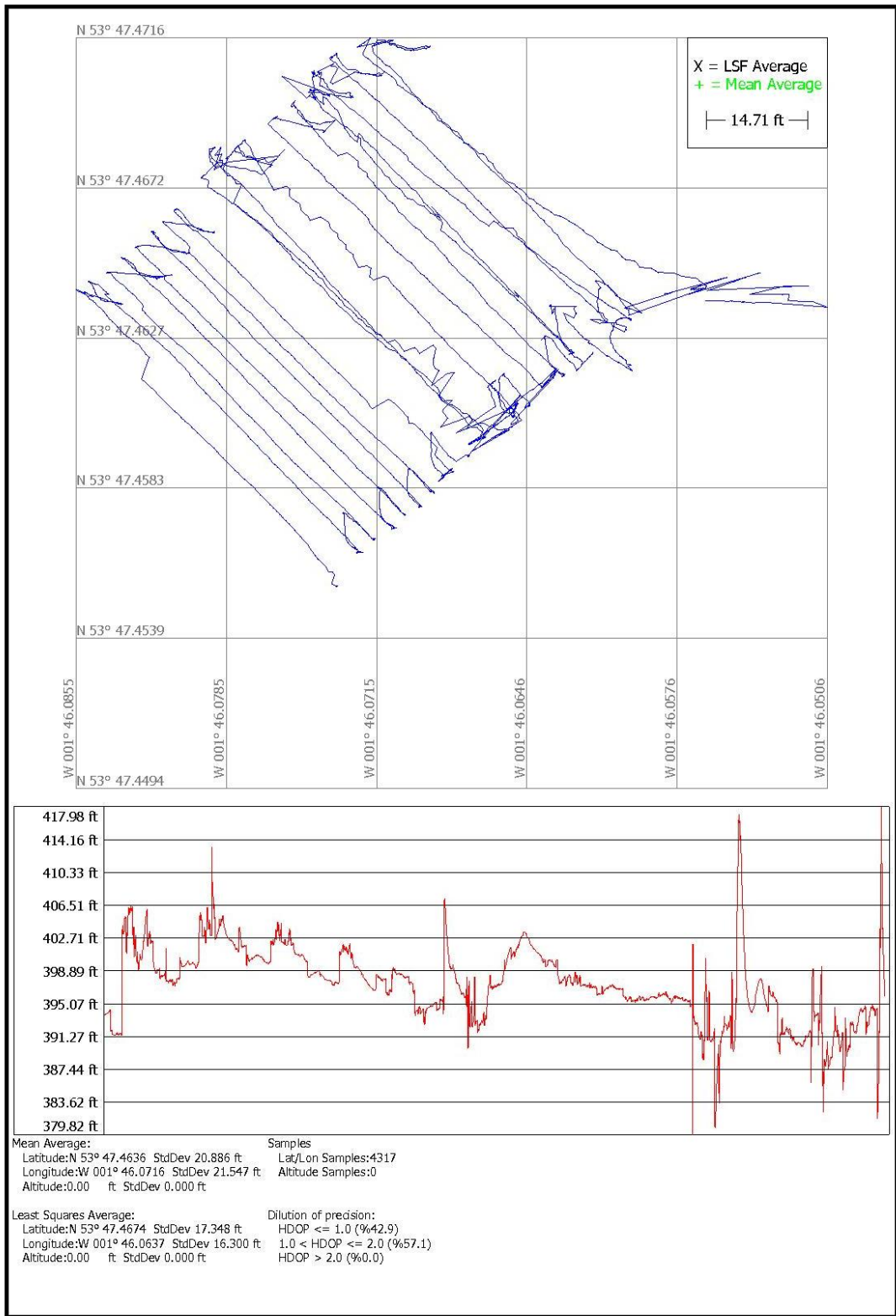
Figure 3.31   The initial plot of the NMEA output of the rear mounted GPS survey (VISUALGPS 2010).

3.6.3 GPS central mounting

The mounting has several advantages over the rear mounting frame as the GPS is low enough that the tilt is minimised. The central location means there is no need to correct for the offset position of the rear mounted GPS and the measurement position corresponds with the centre of the earth resistance array. The frame is made of box section aluminium and plastic corner connectors with an aluminium core (Termotex 2006) which means it can easily support the newer 'all in one' GPS systems that are significantly heavier than regular antennas. For example, the Topcon HiPer Pro RTK Rover unit weighs 1.65 kg or 3.64 lbs. (Topcon 2004). The frame projects 0.25 m above the height of the platform.

Mounting the GPS on a taller central mount would increase the tilt positioning errors and may have impinged on the handle positions when not in use. The lower positioning of the GPS results in a slight disruption of the signal from the rear handle (in relation to the traverse direction). This is because the handle will block part of the GPS skyline. However, tests carried out by Tom Sparrow suggested that with a good satellite constellation (satellite position in the sky) and open sky-line the handles would have minimal effect on the accuracy of the position. The handles produce a greater positional error when there is a poor satellite constellation or when the site is more enclosed and the GPS has a reduced visible skyline. The error terms discussed by Sparrow (2011:24) suggest a shift of 0.05m (in the X or Y direction) is the maximum error term for the handles blocking the signal which is acceptable for most geophysical survey sampling intervals. The Z orientation (elevation) will show the greatest error terms as this calculation will always be more prone to errors.

3.6.4 Potential GPS positioning errors

Errors in GPS positioning may be produced by two main tilt effects,

- The topography of the survey area

If the ground has very small undulations then the cart will have small positional inaccuracies as the cart platform will no longer be horizontal. Larger slopes will have greater errors as the plan (X and Y) and pitch (Z) position will be changed even further from the horizontal and vertical positions relating to the centre of the array.

- Suspension of the MSP40

The suspension of the MSP40 may also create errors as the suspension has a limited travel so may not always be able to keep the platform horizontal. The operator may also hold the handles at a slightly different angle forcing the platform to one side instead of parallel with the ground surface.

3.6.5 Reflection / refraction of signal from the MSP40 platform, handles and operator.

Sparrow (2011) discusses how the operator is likely to be a sufficient distance away from the receiver (approximately 1.5m – 2m distance) that the risk of signal distortion is unlikely. Many of the current GPS units also allow for a cut-off angle (normally between 15 and 30 degrees from the horizontal) where satellites low in the sky are excluded due to the greater ionspheric refraction (Leick 2004 211; Bruyninx *et al.* 2011 420-431). As the highest point of the operator (the head) is likely to be within the cut-off angle any reflection of signal should be ignored.

Sparrow (2011) discusses how the risk of signal reflection caused by the operator are less problematic than those of reflected signals from buildings. The risk of signal reflection from the MSP40 platform is unlikely to have a significant effect on the GPS signal as the reflection would be below the cut off angle.

RTK survey data does not require post processing; however, it is necessary to process the base station data if the base station is not setup on a known point. The base station data can only be processed when the updated satellite data is released approximately 14 days after a survey. The processed base station data will then correct the data shift for all survey points. Post processing of the satellite data from the Topcon HiPer Pro GPS was done in Topcon tools.

3.6.6 Practical examples of GPS survey mounted on the MSP40

The integration of a GPS on the MSP40 was a new development for the cart system that required testing. Practical trials provided the most suitable method to test this new development. Several fieldwork projects were suitable for testing the MSP40 and the GPS integration at Entremont (France), Eining and Pförring (Germany) and Towthorpe (UK). Detailed descriptions of the work can be found in sections 3.6.6, 5.3 and A.1 respectively.

Towthorpe 18 (see Appendix A.1)

The site was a ploughed-out Neolithic ring barrow that had been excavated in the 1800's. There was a high level of uncertainty about the condition and location of the site (see Appendix A). However, a Google Earth image showed a faint soil mark and a visit to the site showed a slight rise in a similar location to the soil marks.

The GPS system was used to locate the geophysics data sets as the site had little tie-in information in the immediate landscape. The MSP40 mounted GPS antenna was positioned over a number of grid pegs and an average calculated over ca. 5 minutes for each peg. The GPS data was collected as a RTK survey with the GPS mounted over the centre of the array. Data was collected at a rate of 20 Hz. The data was post processed and then exported in to ArcGIS 9.2. The elevation data was used to create a surface raster using the following process.

3D Analyst > Interpolate to raster > Natural neighbours > Then selecting the Z data file and the output file name. The generated surface clearly shows the ploughing direction of the ridge and furrow (see figure 3.32).The GPS data covered approximately 60% of the total survey area as the power management settings on the GPS meant the data was not recorded on the initial part of the survey.
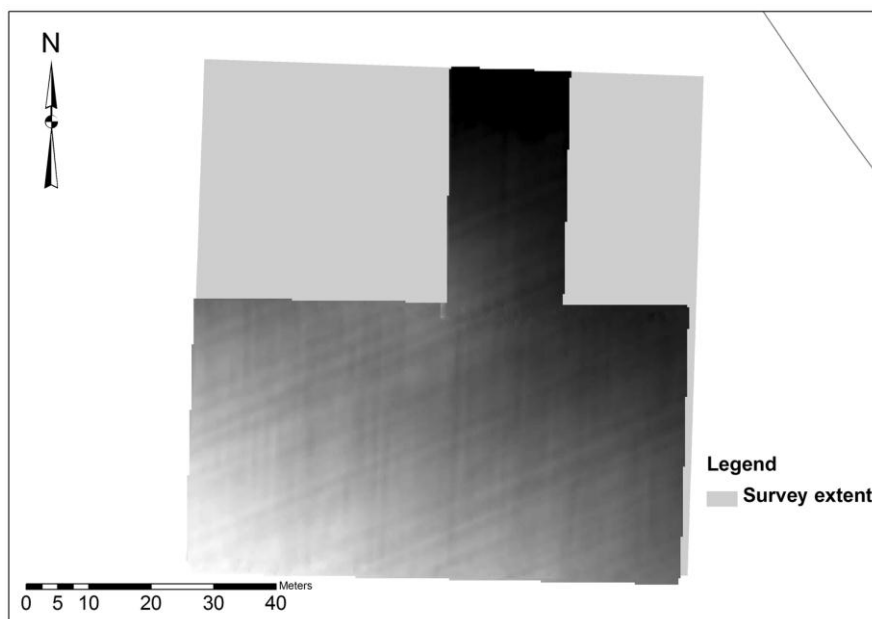
Figure 3.32   A generated raster surface image of the Towthorpe 18 data collected by a GPS mounted centrally on the MSP40.

The raster surface could then be opened in ArcScene and used to create a 3D surface model (see figure 3.33). A vertical exaggeration was applied to the data to highlight the ridge and furrow. The surface model also showed a slight rise in the data where the barrow is located (even though approximately ¼ of the barrow was not surveyed by the GPS).
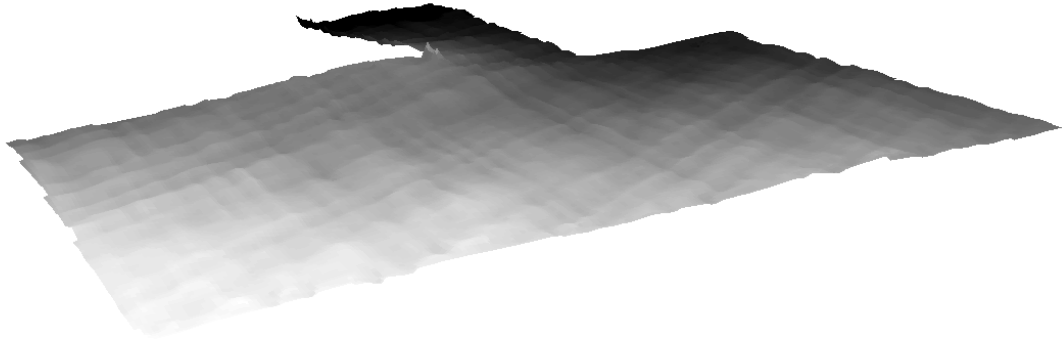
Figure 3.33. A 3D surface model of the Towthorpe 18 GPS survey a vertical exageration has been applied to the data to highlight the ridge and furrow.

Using the information from the GPS survey it is possible to draw the ridge peaks on to the geophyscial data which improves understanding of the data. It is then possible to improve interpretations of geophysical anomalies as some of the ridge lines correspond with high resistance linear anomalies (see figure 3.34).
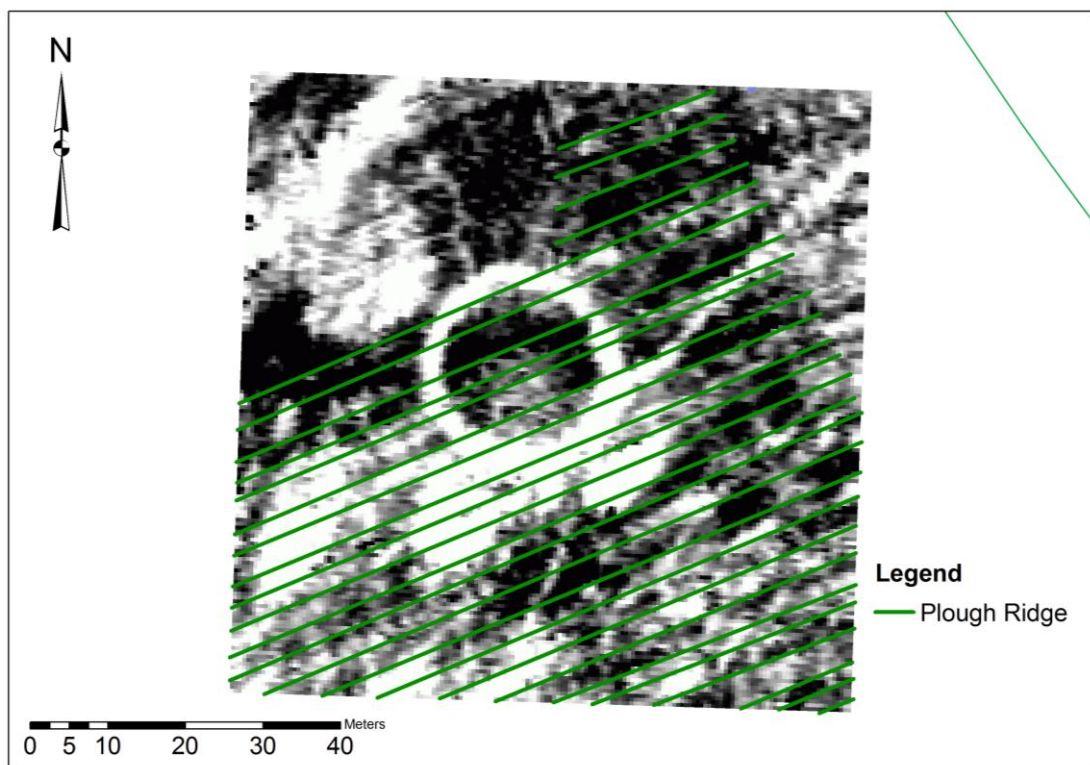
Figure 3.34   The square array earth resistance data collected at Towthorpe by the MSP40 with a plough ridge overlay based on the GPS survey.

RTK GPS DEM / Microtopography survey

The GPS survey underwent additional field trials at the three sites in Germany. A TOPCON HiPer Pro RTK GPS unit was used to collect positional information at a rate of 20 Hz storing the directly on to the handheld data logger / controller (Topcon 2010a). The RTK system boasts sub centimetre accuracy with good satellite coverage, however all three sites had some degree of obstacles partially blocking the skyline including buildings, trees and at the case of Pförring a steep sided hill side. Poor satellite coverage also reduced the survey accuracy.

This meant the elevation data had missing data gaps in the surface models when the fixed solution was lost and floating solutions were discounted as elevation or Z values are prone to the greatest errors.

Area A (Eining) (see figure 3.35)

For survey details, geophysical results and interpretations please see chapter 5.3 and 5.3.5.

Topography, collected using a RTK GPS on the MSP40 (local)
Value
High : 357.366
Low : 354.334
Hillshade of topography, illuminated from NW
Value
High : 253
Low : 0

N

0   20
Meters

UNIVERSITY OF
BRADFORD
MAKING KNOWLEDGE WORK
ARCHAEOLOGICAL SCIENCES © 2010

Eining, Area A Topography (Top), Hillshade (Bottom), Scale 1:750
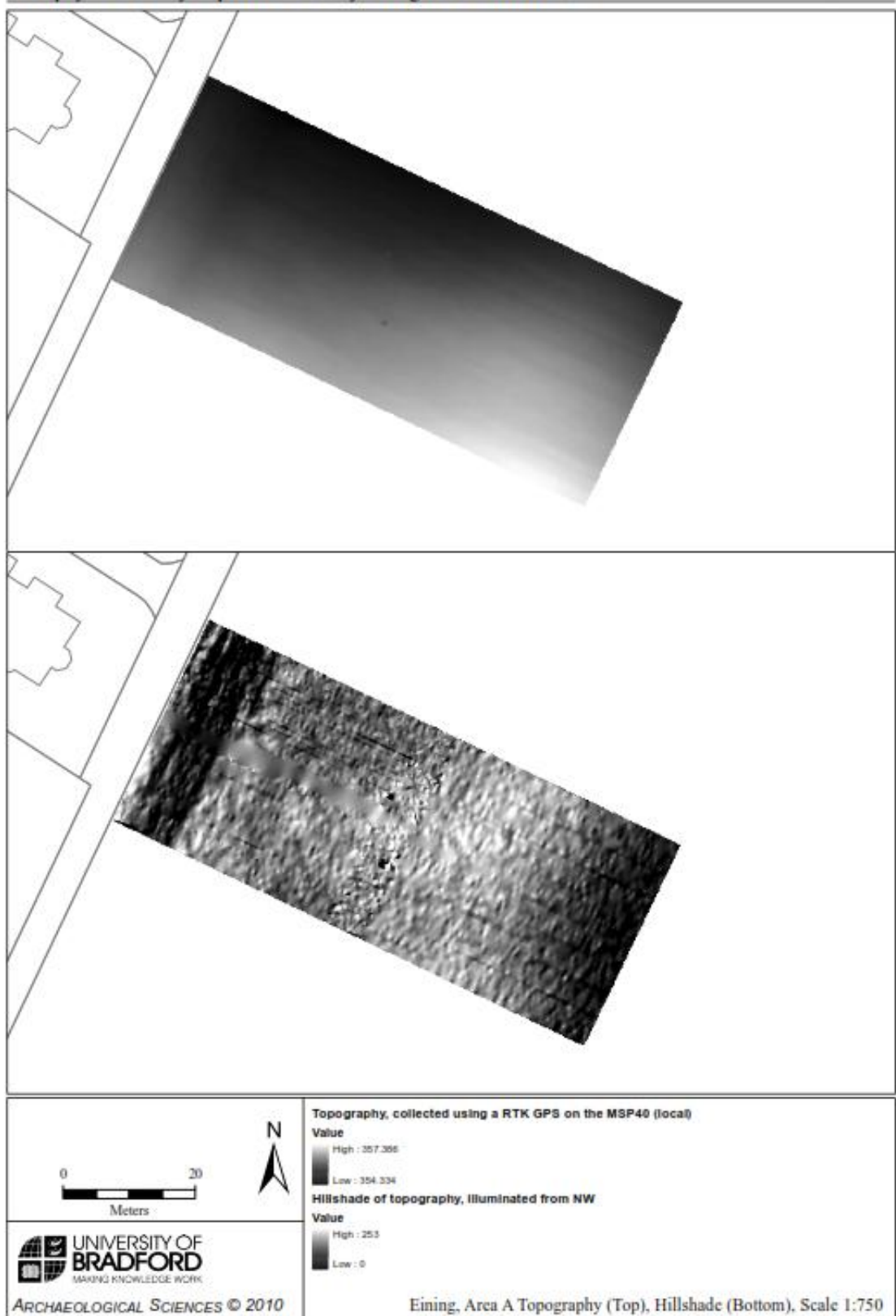
Base mapping provided by The Bavarian State Dept. of Monuments and Sites

Figure 3.35   DEM / microtopographic survey data collected on the MSP40 at Eining Area A (Parkyn *et al.* 2010).

82

The DEM for Eining Area A shows the general topographic variation of the site; however the surface model contains areas of missing data due to errors in the recorded elevation values that were deleted. The errors are due to poor satellite constellations / positions at the time of survey and the close proximity of buildings to the western edge of the survey area. It is not possible to identify any visible archaeology but does indicate the uneven surface of the site (due to rutting and plough ridges).

Area B (Eining) (see figure 3.36 and 3.37)

For survey information and geophysical results and interpretations please see chapter 5.3 and 5.3.9.

Topography, collected using a RTK GPS on the MSP40 (local)

Value

High : 357.386

Low : 354.334

0   40

Meters

N

UNIVERSITY OF BRADFORD
MAKING KNOWLEDGE WORK

ARCHAEOLOGICAL SCIENCES © 2010

Eining, Area B, topgraphy, 1:1000

Base mapping provided by The Bavarian State Dept. of Monuments and Sites
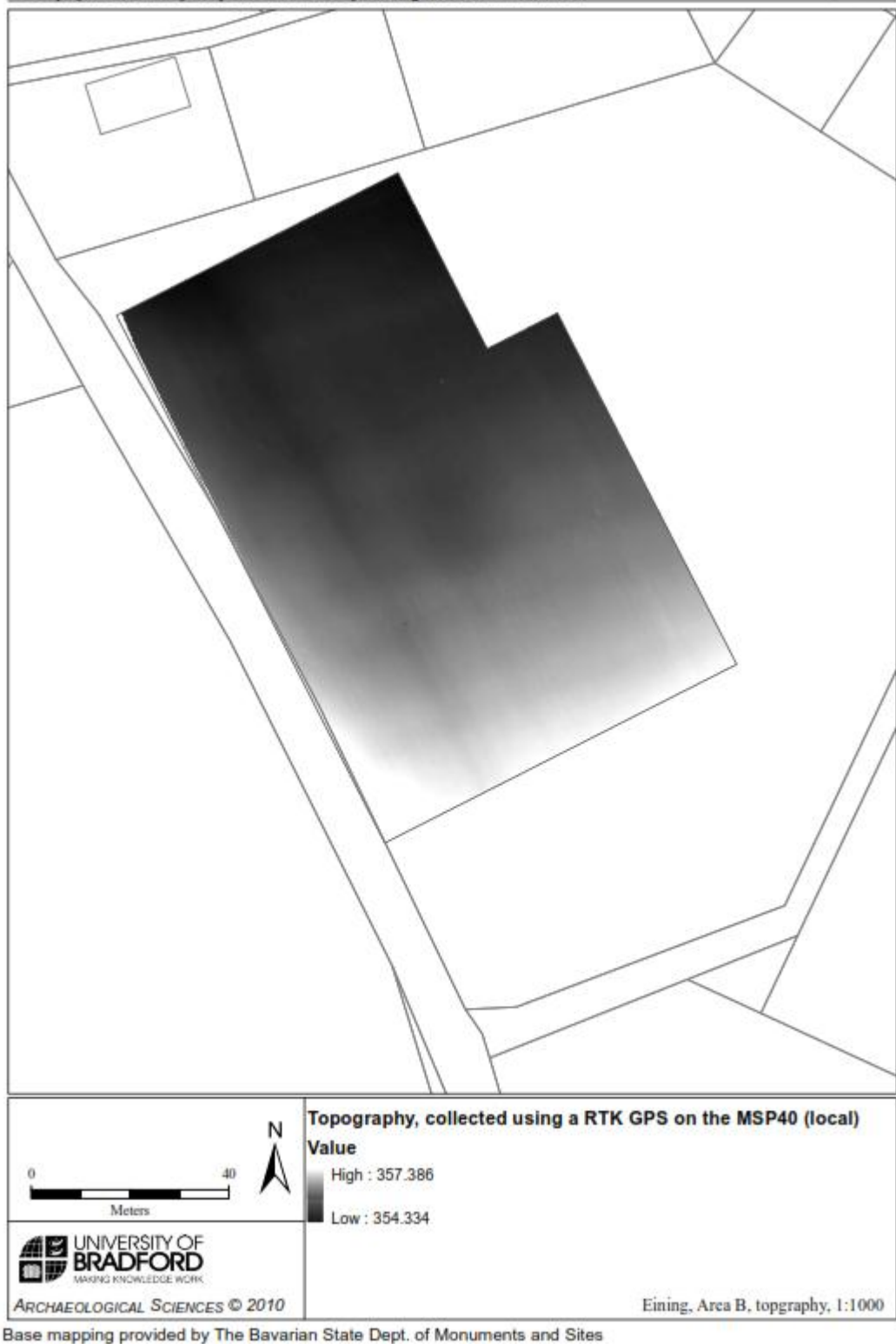
Figure 3.36   DEM / microtopographic survey data collected on the MSP40 at Eining Area B (Parkyn *et al.* 2010).

Hillshade of topography, illuminated from NW

Value

High : 253

Low : 0

0   40
Meters

N

UNIVERSITY OF
BRADFORD
MAKING KNOWLEDGE WORK

ARCHAEOLOGICAL SCIENCES © 2010

Eining, Area B, hillshade, 1:1000

Base mapping provided by The Bavarian State Dept. of Monuments and Sites
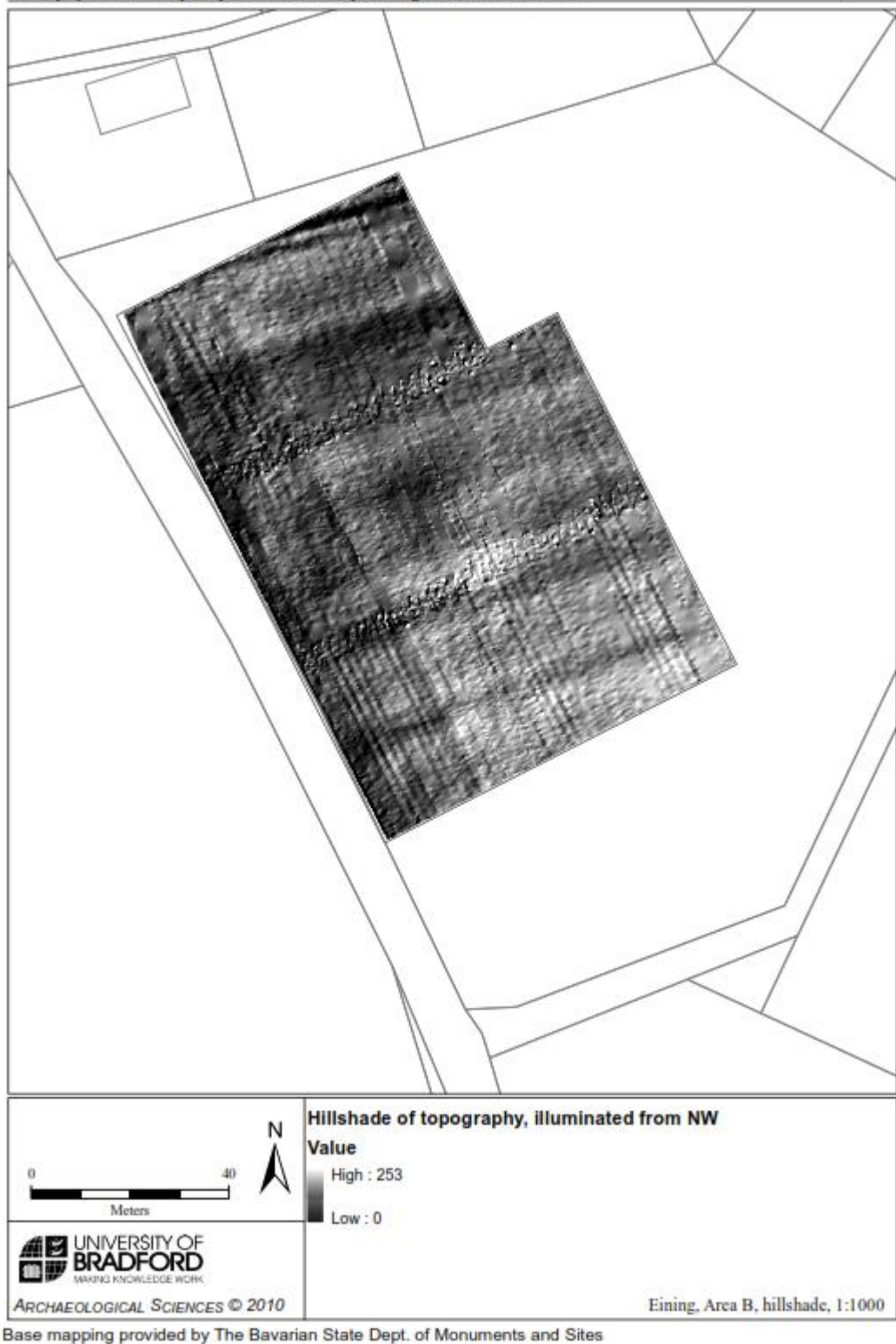
Figure 3.37   A hill shade enhanced topographic surface at Eining Area B (Parkyn *et al.* 2010).

The DEM's for Eining Area B show only subtle variation across the site as the area had been heavily ploughed. The site had been left fallow for a number of years so little evidence of ridge and furrow remained. The variations in topography running approximately north-northeast to south-southwest does correlate with zones of archaeology but are too subtle to pick out individual anomalies. The data also shows variation between the traverse lines, which may be an operator induced error as it was noted that the MSP40 platform tilted when the handles are held at an angle. As a consequence the GPS position will also subtly change in height; if the tilt is not consistent between traverses then such variation could occur in the data. Therefore it is important to try to keep the platform as level as possible throughout the survey even when fatigued at the end of the day.

Area C (Pförring) (see figure 3.38)

For survey details, geophysical results and interpretations please see chapter 5.3 and 5.3.9.

The DEM from Pförring indicates how useful the MSP40 mounted GPS can be for site investigation. The survey provides contextual information for example the sites location in the landscape (in this example on a hillside) as well as the previous or current land use (ridge and furrow from ploughing). On sites with raised features (possible deserted medieval villages or DMV's) the GPS survey would provide a detailed map of the surface that could be directly linked to the geophysical responses. The simultaneous collection with the geophysical survey also saves time and provides additional detail than would normally be collected for topographical surveys. This is due to the density of measurements required for geophysical investigations where traverses are spaced no more than 1m apart and GPS data collected at a rate of 20 Hz (approximately equalling a measurement along the traverse line of every 5 cm).
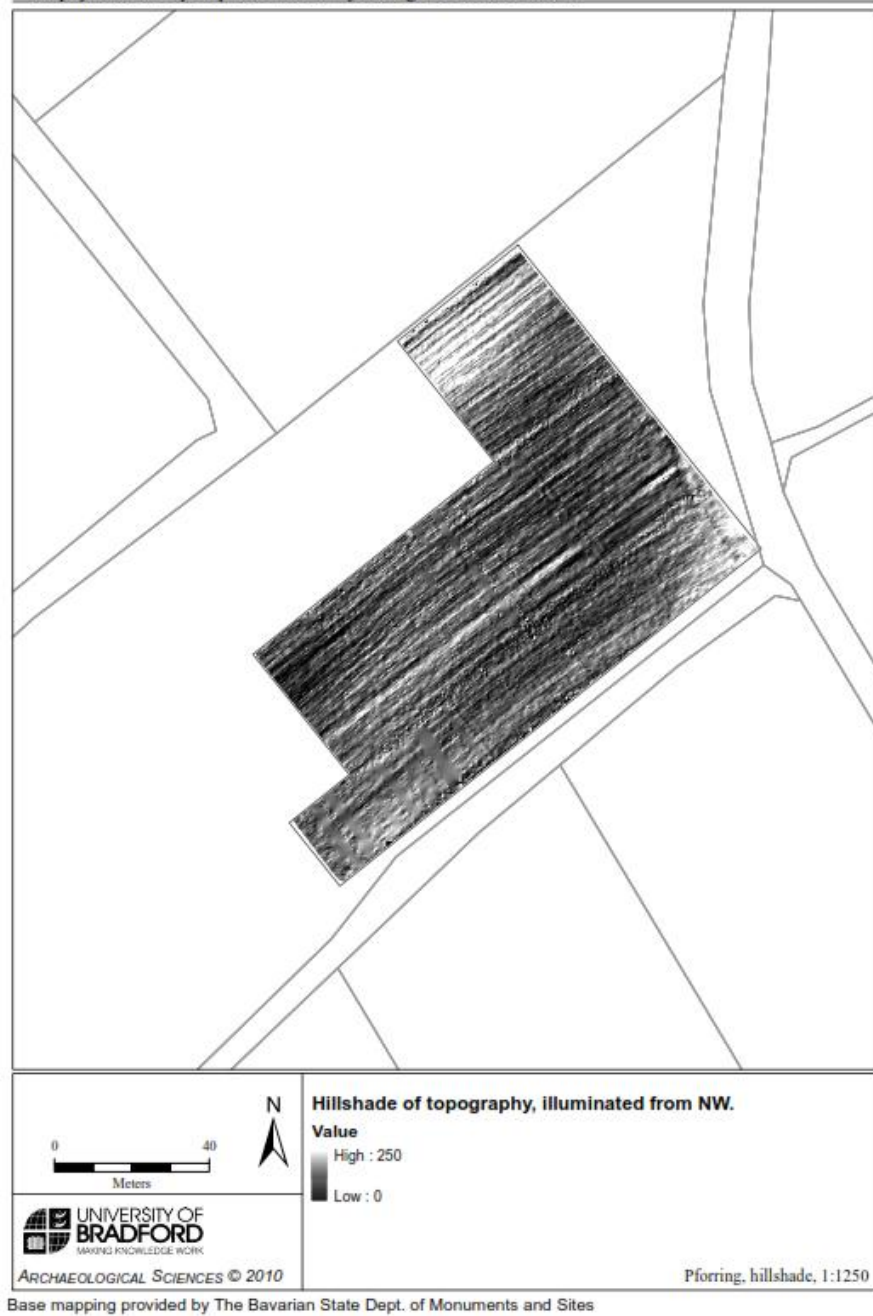
Figure 3.38   A hill shade enhanced topographic survey collected on the MSP40 at Pförring Area C (Parkyn *et al.* 2010).

Entremont, Provence, France

The MSP40 was used to undertake simultaneous earth resistance and gradiometer survey areas both inside and outside the Iron Age Oppidum of Entremont, Provence, France with a research group from the University of Bradford (Armit *et al.* 2012). A high-resolution earth resistance survey was trialled over a 40m x 20m area with an integrated RTK GPS survey. A TOPCON HiPer Pro RTK GPS rover unit (Topcon 2004) was mounted on the custom made framework positioning the GPS above the centre of the MSP40. The high-resolution GPS survey was collected at a rate of 20 Hz and a transect line of 0.25m with a simultaneous earth resistance survey of 0.25m x 0.25m sampling and traverse interval. Data was collected in regularly spaced transects due to the simultaneous earth resistance survey.

The GPS data was downloaded and imported in to ArcMap (ArcGIS 9.2). Only fixed data points were plotted but the data still required editing to remove errors in the elevation data values. Raster plots and a 3D model were generated to display the changes in elevation. A vertical exaggeration of a factor of five was added to the 3D model to show the changes in elevation (see figures 3.39-3.42).
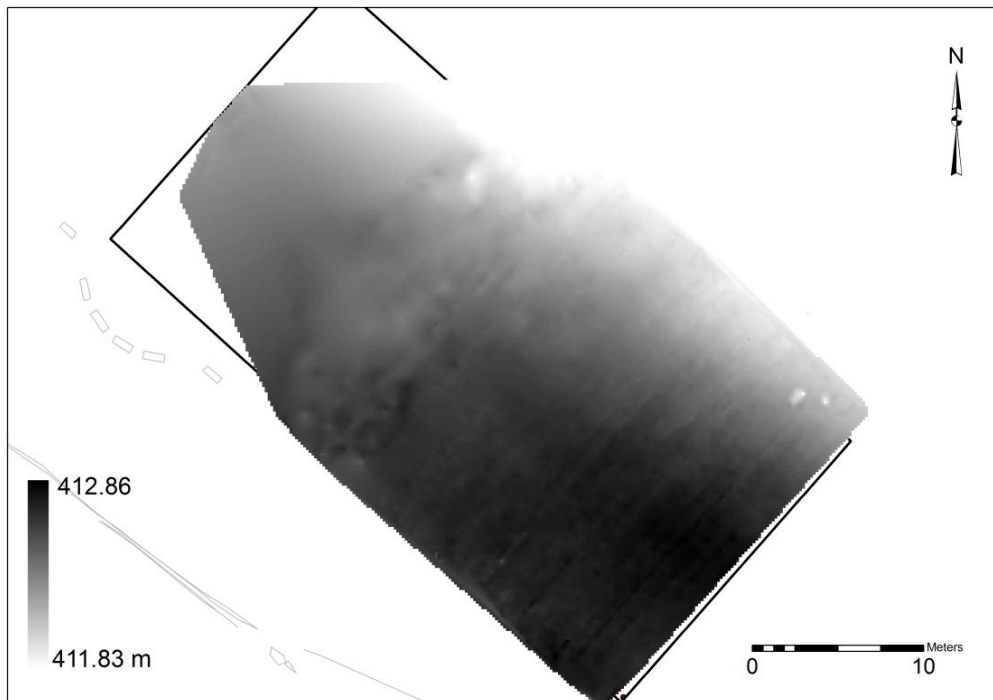
Figure 3.39   A high-resolution GPS survey at Entremont.
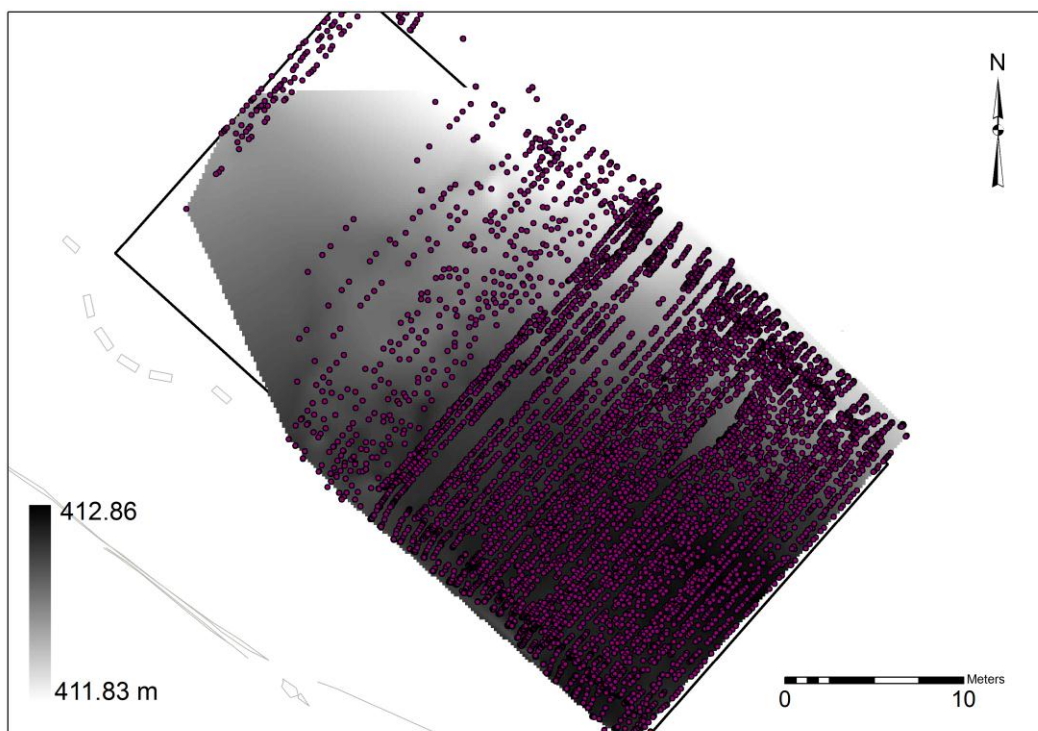
Figure 3.40   A high-resolution raster plot with fixed point overlay from the GPS survey at Entremont.
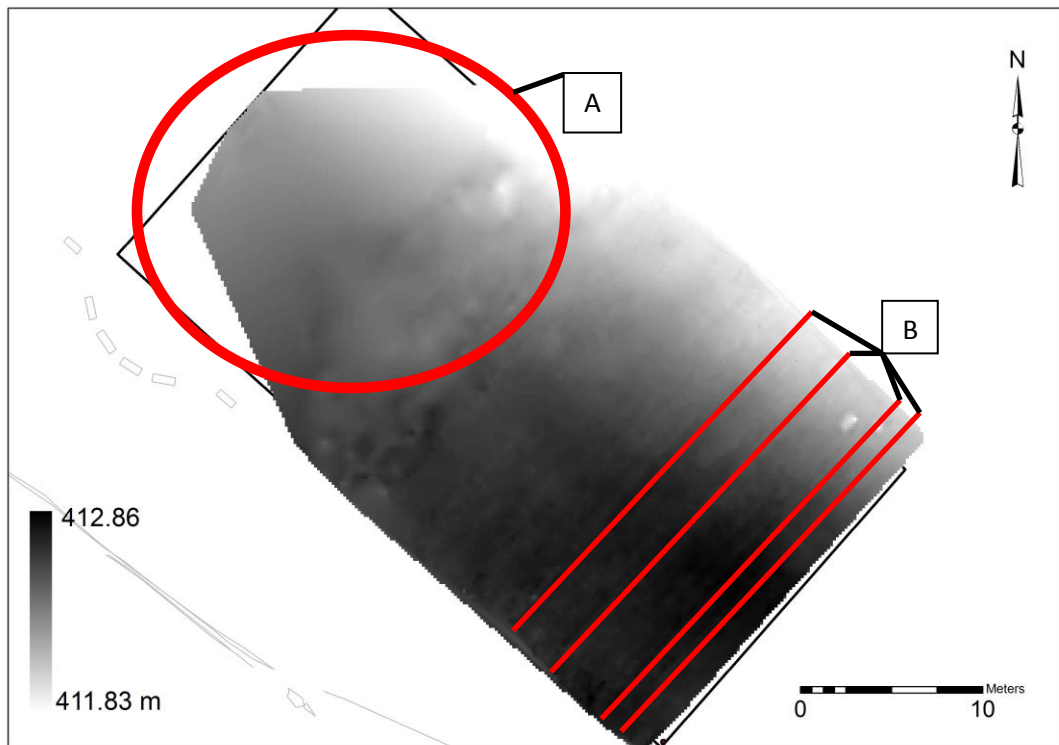
A= Low fixed point density   B= Linear anomalies along transect lines
                                       caused by operator collection errors

Figure 3.41   A high-resolution GPS survey at Entremont with highlighted errors
in the data.

The data plots show the fixed point solutions only (highest precision); floating
data points were edited out due to the high resolution of the survey. The DEMs
show the variability in data quality as there was a poor satellite constellation
when the survey was performed. The survey area was enclosed by trees and
subtle changes in topography also blocked the sky line. The large flat area in
the data (north-west corner (Area A figure 3.41)) is due to a lack of fixed data
points recorded in this area. This is due to the poor satellite constellation
(number and position in the sky) and the reduced skyline, both of which affect
the positional accuracy of the GPS survey.

The reduction in data quality is shown through the reduced number of fixed points and increased number of floating points (where positional accuracy in the X, Y and Z direction is reduced) floating points were removed from the survey data. Therefore the natural neighbour surface created in ArcMap (ArcGIS 9.2) levels out the surface using the positional information available. Further to the south and east the fixed data point density increases producing a more accurate surface model that does not rely on interpolation between data points over large distances. Area B shows the subtle 'noise' that can be recorded in the data along the transect lines. The cause of the noise may result from an operator error as the MSP40 must be held horizontally to reduce subtle changes in elevation between traverses. However, it was noticed that at some points the operator held the handles in a way that tilted the platform to one side, therefore tilting the GPS causing errors in the recorded elevation values.
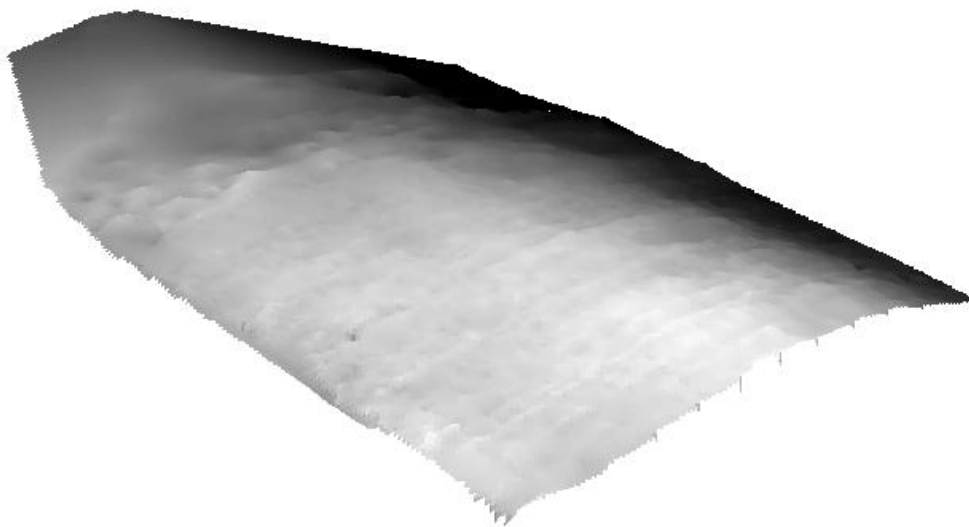
Figure 3.42   A 3D DEM of the high-resolution GPS survey with vertical exaggeration to enhance the subtle changes in elevation.

A larger scale GPS survey was also trialled at Entremont where the operator walked around the site in a semi-random sinusoidal pattern down slope and across slope. Data was collected at a rate of 20Hz with irregularly spaced traverses. No geophysical survey data was collected during the trial as the data could not be gridded. A survey area of approximately 1 ha was covered in approximately 1 ½ hours by a single operator (see figure 3.43-3.48).
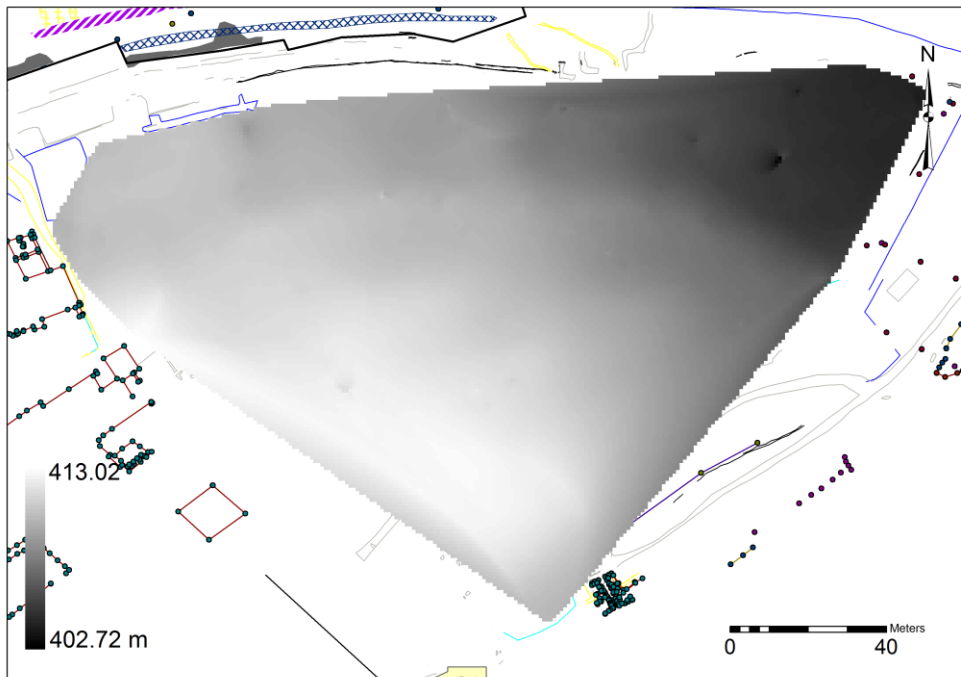
Figure 3.43   An elevation raster of the large scale GPS area survey
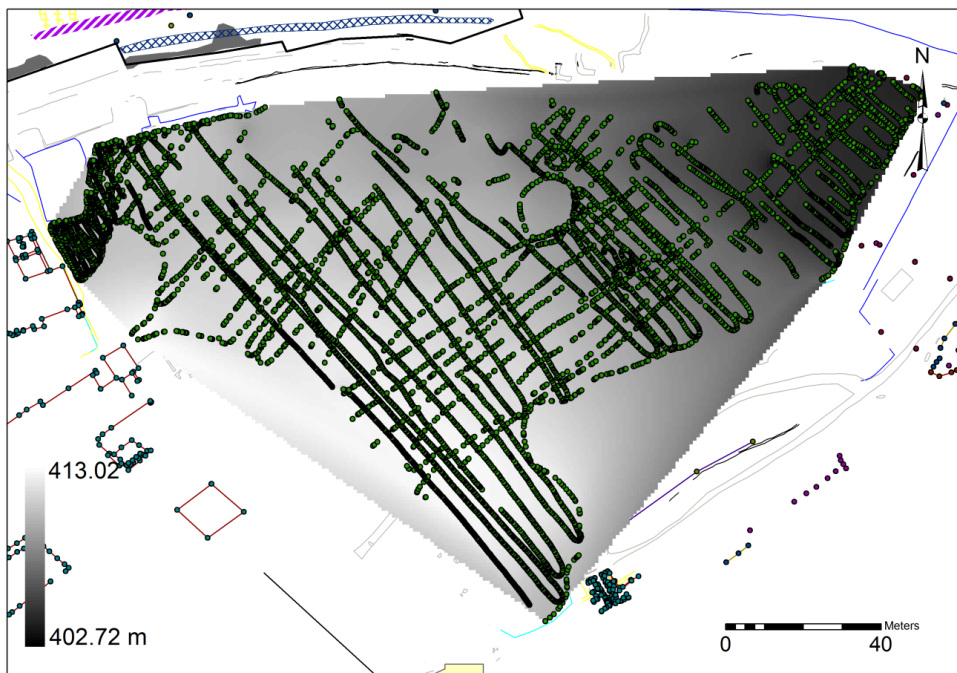
Figure 3.44   The 'fixed' (greatest XYZ positional accuracy) point locations draped over the elevation raster of the large scale GPS survey.
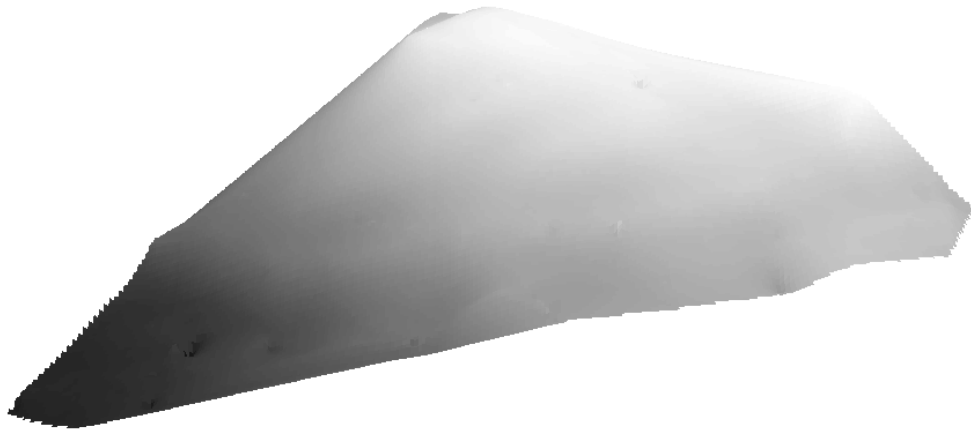
Figure 3.45   A 3D DEM of the large GPS survey with vertical exaggeration to enhance the subtle changes in elevation.
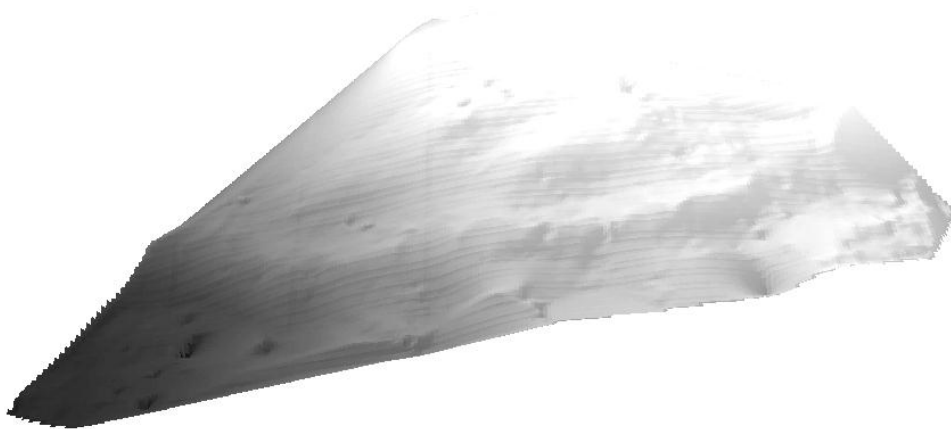
Figure 3.46   A 3D DEM of the large GPS survey with vertical exaggeration to enhance the subtle changes in elevation. A hill shade effect has also been added to highlight the 'noise' banding in the data (both left-right and top-bottom).
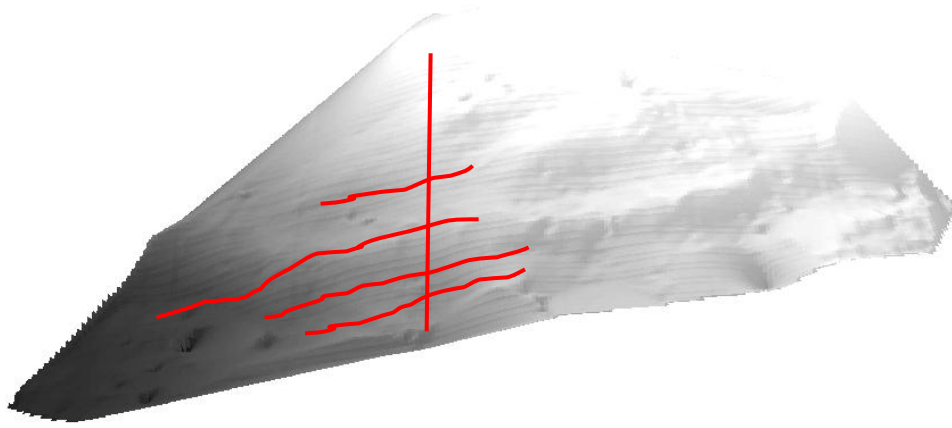
Figure 3.47   A 3D DEM of the large GPS survey with highlighted 'noise' banding.
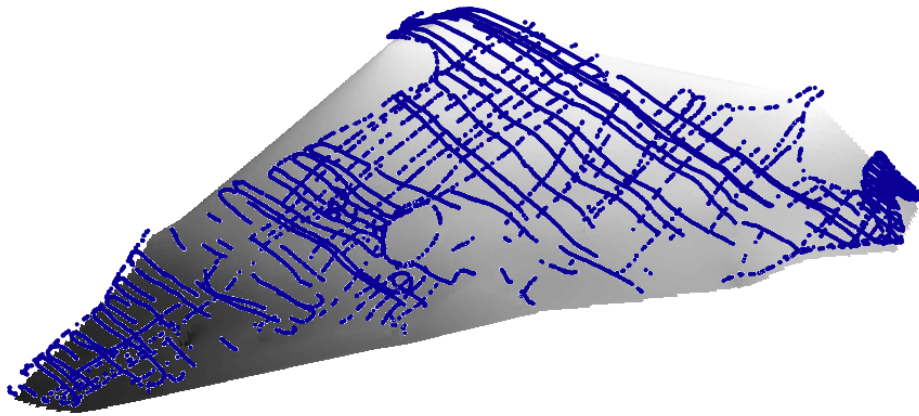
Figure 3.48   A 3D DEM of the large GPS survey with vertical exaggeration to enhance the subtle changes in elevation. The individual data points have been draped over the DEM to show the fixed point densities.

The banding visible in figures 3.46 and 3.47 does not correlate with the traverse directions visible in figure 3.48. This may suggest the additional 'noise' in the data may also be a consequence of the way the DEM is constructed in ArcMap (ArcGIS 9.2) using the natural neighbour function as the 3D surface tries to connect the neighbouring elevation values.

The survey areas missing point information are a consequence of the trees on and surrounding the site blocking the skyline. A raised antenna position may have improved the fixed point coverage of the site but low tree branches would have hit the rover unit.

A final GPS survey, covering an area of approximately 20m x 30m, was performed outside of the oppidum. The recorded elevation values were significantly affected by the enclosed nature of the site. The initial values suggested a change of elevation of approximately 16m. Therefore a band of approximately 1.5 metres in elevation variation was selected, as it had the greatest point density with the outliers clipped from the data set. The GPS survey still contained errors within the elevation values but subtle changes in topography related to the archaeological geophysics results could be identified. Two parallel hollows/channels are visible in the GPS survey that correspond to two high resistance curvilinear anomalies in the earth resistance data (see figure 3.49) and a positive anomaly in the fluxgate gradiometer surveys. It is possible the anomalies may have formed the boundary of a route / road way to a postern gate in to the oppidum (Armit *et al.* 2012).
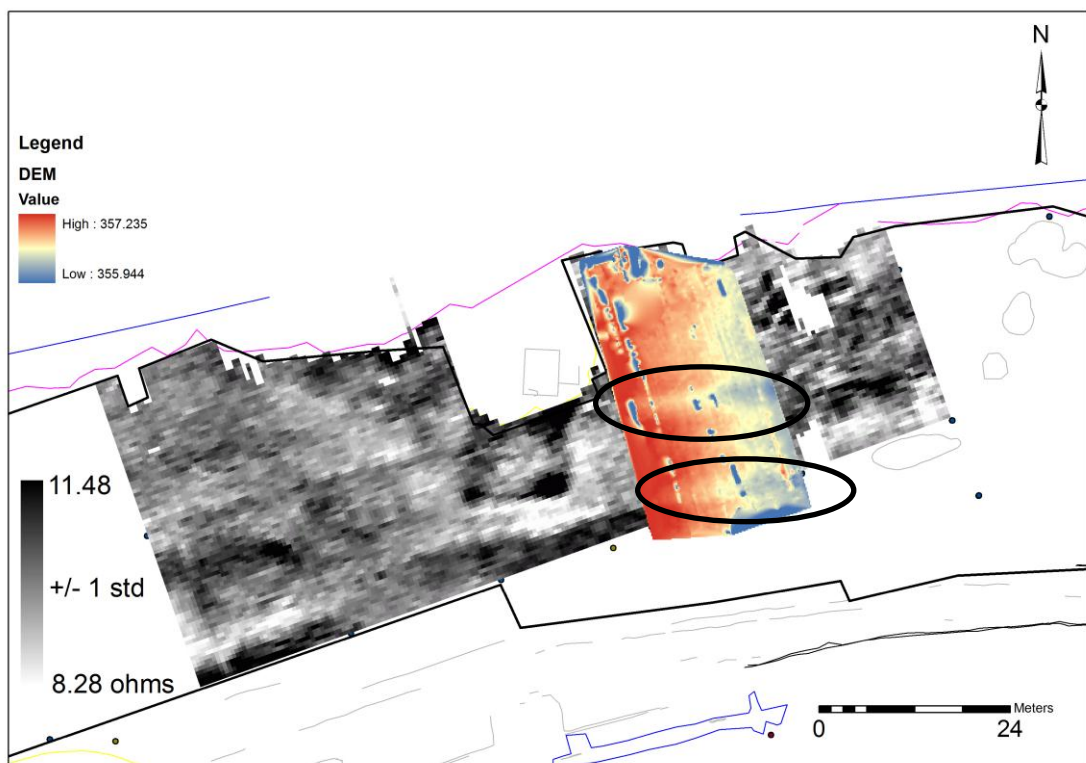
Figure 3.49   Highlighted hollows / dips in the GPS survey that corresponds to high resistance linear anomalies in the earth resistance survey.

The results from Towthorpe, Pförring, Eining and Entremont show that the MSP40 with mounted GPS can be used to survey a large area at a high resolution in a short amount of time. As the rover antenna is a fixed height above the ground it means it is possible to stream data at a rate of 20 Hz and survey quickly over a landscape with a constant offset height (that can be specified as the staff height) (see chapter 6.4 for further discussion on GPS integration).

3.7.0 Gradiometer integration and mounting, processing and issues.

3.7.1 Introduction

The MSP40 is a mobile sensor platform that allows for simultaneous earth resistance and fluxgate gradiometer (FM36 / 256) surveys. The gradiometer is mounted on to the front of the cart on an aluminium and wooden housing. Gradiometers are extremely sensitive to slight variations in the localised magnetic field with some models able to detect changes in the order of 0.01 nT (the earth's magnetic field is in the order of 50,000 nT) (Linford *et al.* 2007). However, Aspinall et al. (2009 84-89) discuss how the sensitivity of a gradiometer varies between manufacturers and individual models. The Geoscan Research FM256 gradiometer has a sensitivity of approximately 0.05nT which makes it extremely sensitive to sources of random or coherent noise.

Coherent operational noise may come from ferrous material on the operator or from the materials used in the construction of the MSP40. The cart frame is made of aluminium tubing and plastic connectors to reduce the potential sources of magnetic noise in the data. However, the prototype cart also had a steel axle pin that locked the axles to the platform surface. The steel rod remains in a fixed location in relation to the gradiometer so any noise was kept to a minimum. However, the decision was made to replace the rod with a stainless steel pin on the front axle closest to the gradiometer to eliminate a source of noise. The rear axle pin is approximately 1.5m away from the gradiometer sensors so is unlikely to have significant effects.

The electronics of the DL256 and RM15 are also a source of 'noise' but as the fluxgate gradiometer is balanced then mounted on the cart before zeroing the instrument then any 'noise' is incorporated as part of the background measurement (including the induced magnetisation of electronic components). As the electronic components if the DL256 and RM 15 are in static position the influence on the background value remains constant.

The MSP40 can collect data in parallel or zigzag traverses. However, when carrying out a hand-held gradiometer survey, using a zigzag method of data collection (heading errors) can affect the quality of the results if the gradiometer is turned between traverses. This is due to slight variations in the directional alignment of the sensors away from the north-south, east-west axis. However, as the MSP40 has two handles for directional pulling means the gradiometer can be maintained in the same orientation. The MSP40 array is not rotated which reduces heading errors between traverses.

3.7.2 Gradiometer field trial

The test area at the University of Bradford was used to test a Geoscan Research FM256 gradiometer mounted on the cart against a hand-held FM256 hand-held survey (see table 3.7).

Data collection methods

Table 3.7   Gradiometer field trials survey parameters.

Equipment	Measurement Configuration	Sampling Interval	Traverse Interval	Method of collection
MSP40 mounted FM 256 Gradiometer	Single gradiometer measurement and earth resistance	0.25m (0.5m)	1m (1m)	Zig Zag (encoder wheel)
Hand-held FM256 Gradiometer	Single measurement	0.25m	1m	Parallel

The gradiometer should be setup in exactly the same way as for a hand-held survey apart from three important differences.

- The sampling interval must be set to double the density of the earth resistance measurements when recording the Alpha and Beta data sets. For example-

  Earth resistance sampling and traverse interval

  0.25m x 0.5 m

  Gradiometer sampling and traverse interval

  0.125m x 0.5m

- The gradiometer should be set to an external trigger source as it receives the pulse from the MSP40 (in timed and encoder based collection).

The gradiometer should be balanced as usual, setting both the mechanical and electronic balance. However, the gradiometer should be mounted and attached to the trigger cable before the instrument is zeroed so that any components with a localised magnetic field can be included as part of the background field.

When surveying using the gradiometer mounted on to the MSP40 it is important to make sure readings match with the recorded earth resistance measurements sampling and traverse positions. If the dummy log function is required to navigate around an object then the start / stop switch is pressed at the last measurable point. The MSP40 can then be repositioned at the next measurable location before dummy logging the necessary positions. The last recorded position on the DL256 must be read to see if the Alpha or Beta measurement was the last recorded point. When only the Alpha measurement was recorded an additional dummy log point should be recorded for the gradiometer to replace the Beta measurement. Double the number of dummy values should be recorded on the gradiometer than on the DL256 (earth resistance data logger) when Alpha and Beta measurements are recorded to maintain the pattern of the measurements.

If dummy values are entered incorrectly when using the encoder wheel to record the earth resistance and fluxgate gradiometer measurements then it is best practice to restart the line as the positioning information (encoder pulses) is lost and will no longer log the data points for the remainder of the traverse.

It is best practice to rebalance the fluxgate gradiometer sensors more frequently during a survey than would normally be done with hand-held collection because of the additional vibrations acting upon the sensors when mounted on to the mobile platform. This should be done to ensure the highest quality results possible through the correct alignment of the sensors.

Grid Size

20m x 20m

After each grid the FM256 sensors were realigned and re-zeroed to take into account any noise from the MSP40 and the variations in sensor heights.

Data processing

As the data was only recorded over a single grid there was little processing required as the instrument was unlikely to drift significantly in the time necessary to survey.

Interpolate Y, Expand – SinX/X, x2

An overview of data processing techniques is discussed in chapter 5.2.4 Detailed processing description are found in the Geoscan Research FM256 manual (Walker 2004)

However, it is important to note that after the gradiometer data has been processed the data set must be shifted forward along the traverse line by + 0.875m as this is the offset distance from the centre of the earth resistance array. The amount of shift will be dependent on the sampling interval e.g. 0.25m sampling equals approximately 3 shifts.

Gradiometer comparisons results.

Figure 3.50 shows comparative plots for hand-held and MSP40 collected gradiometer data. The data sets complement each other and have both identified the same anomalies.
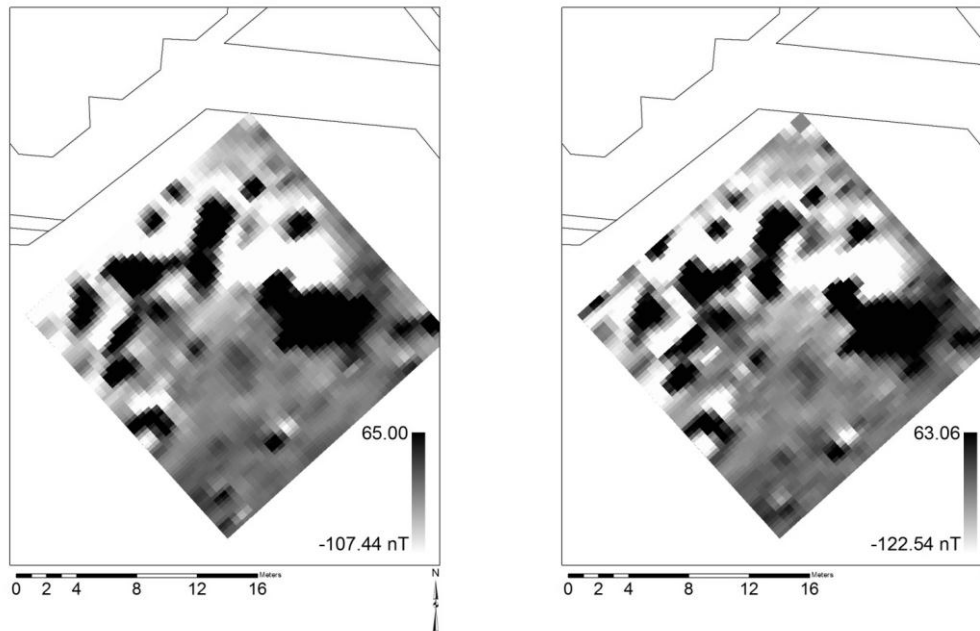
Figure 3.50　The left image is collected using a hand-held FM256 the right image is the FM256 mounted on the MSP40.

The testing area is made up of rubble possibly from the demolition of the old housing stock, or buildings associated with the old mill (now Phoenix SW) which includes brick and metal rebar (see figure 3.51 and 3.52). The brick and rebar will produce strong magnetic anomalies that are likely to dominate the data sets. This explains why none of the anomalies identified in the seasonality tests are detectable.

The earth resistance anomalies are likely to be a series of compacted rubble layers and possible brick lined drainage channels or wall foundations (see chapter 4.2).

Figure 3.51   The mixed nature of the levelled ground after the back to back housing was demolished.

Figure 3.52   Brick and steel rebar that have strong localised magnetic fields.

When the trace plots of each collection method are compared, the differences between the surveys become more apparent. The magnitude of the individual anomalies is greater with the MSP40 mounted gradiometer (see figure 3.53 and 3.54).
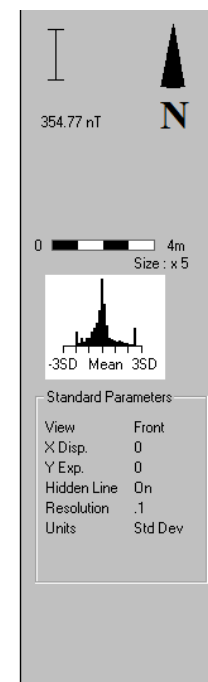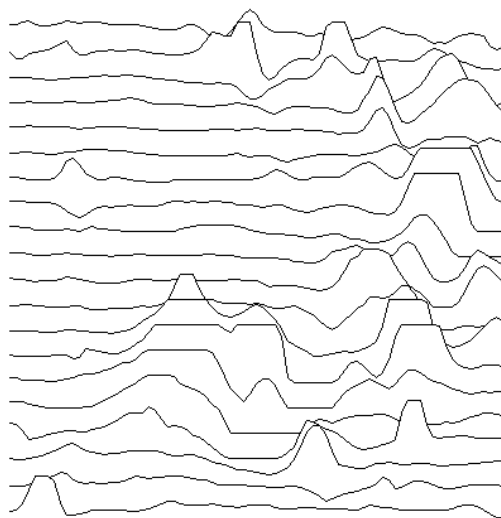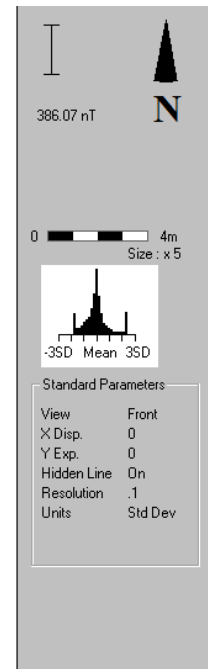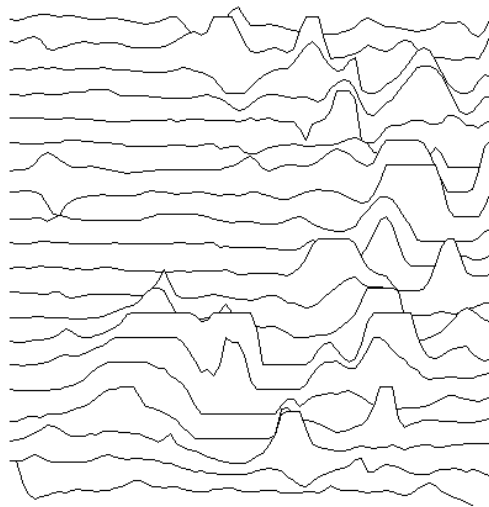
Figure 3.53   X Y traces of the MSP40 mounted (top) and hand-held (bottom)
FM256 gradiometer survey at the University of Bradford.
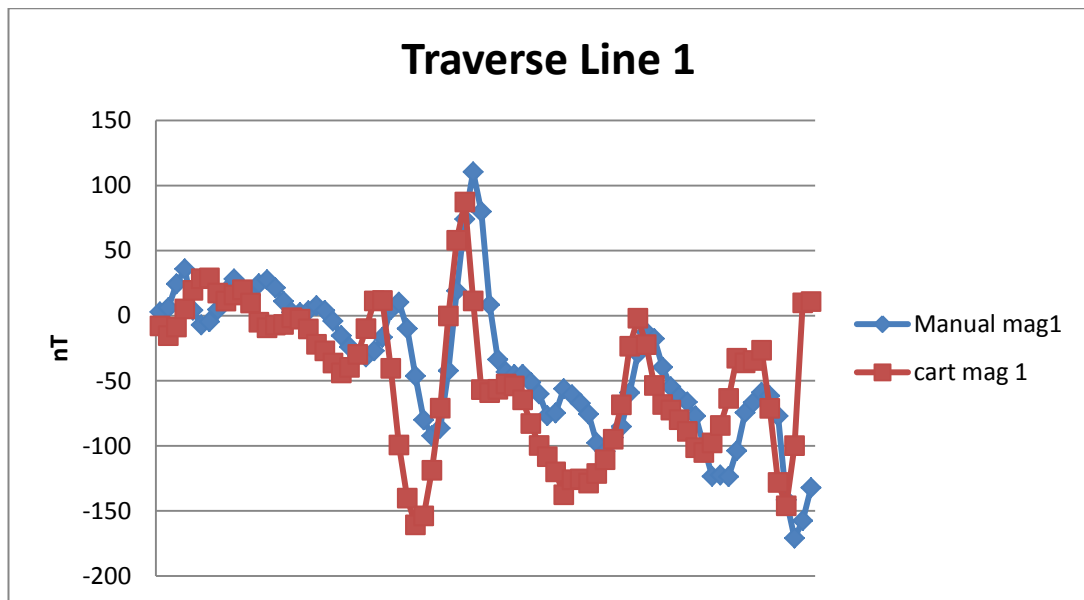
Figure 3.54   A single traverse X Y trace plot of the hand-held and MSP40 mounted FM256 gradiometer survey at the University of Bradford.

3.7.3 Gradiometer collection noise (Barden Tower, N. Yorkshire)

An additional test was performed on data collected at Barden Tower; the data set was chosen as it contained a significant area of low variation / 'quiet' magnetic response. It is therefore possible to examine the 'noise' levels recorded by the instruments mounted on the MSP40 compared to a hand-held collection.

The composites of the data were reduced to a 20m x 100m strip as this area had little archaeology or soil noise. The middle grid of the strip of five was then chosen as there were no strong anomalies in the grid and had a uniformity of response across the grid. An area of approximately 12.5m x 10m was selected at local Geoplot co-ordinates 97, 49 -148, 58 as it showed the least amount of soil noise.

A standard deviation / variance map was then plotted on the area for both the hand-held (see figure 3.55) and MSP40 mounted gradiometer surveys (see figure 3.56). No data processing was performed so that the data could be statistically analysed in its raw state.

Hand-held FM256

A   B   C

A = Raw data

B = selected area (raw data)

C = Standard deviation / variance map

Hand-held FM 256 statistics (all in nT)

0.17 – 0.39 1STD

0.277664 – mean

0.1111742- STD

0.03143865– min

0.7843314 – max

± 1 STD
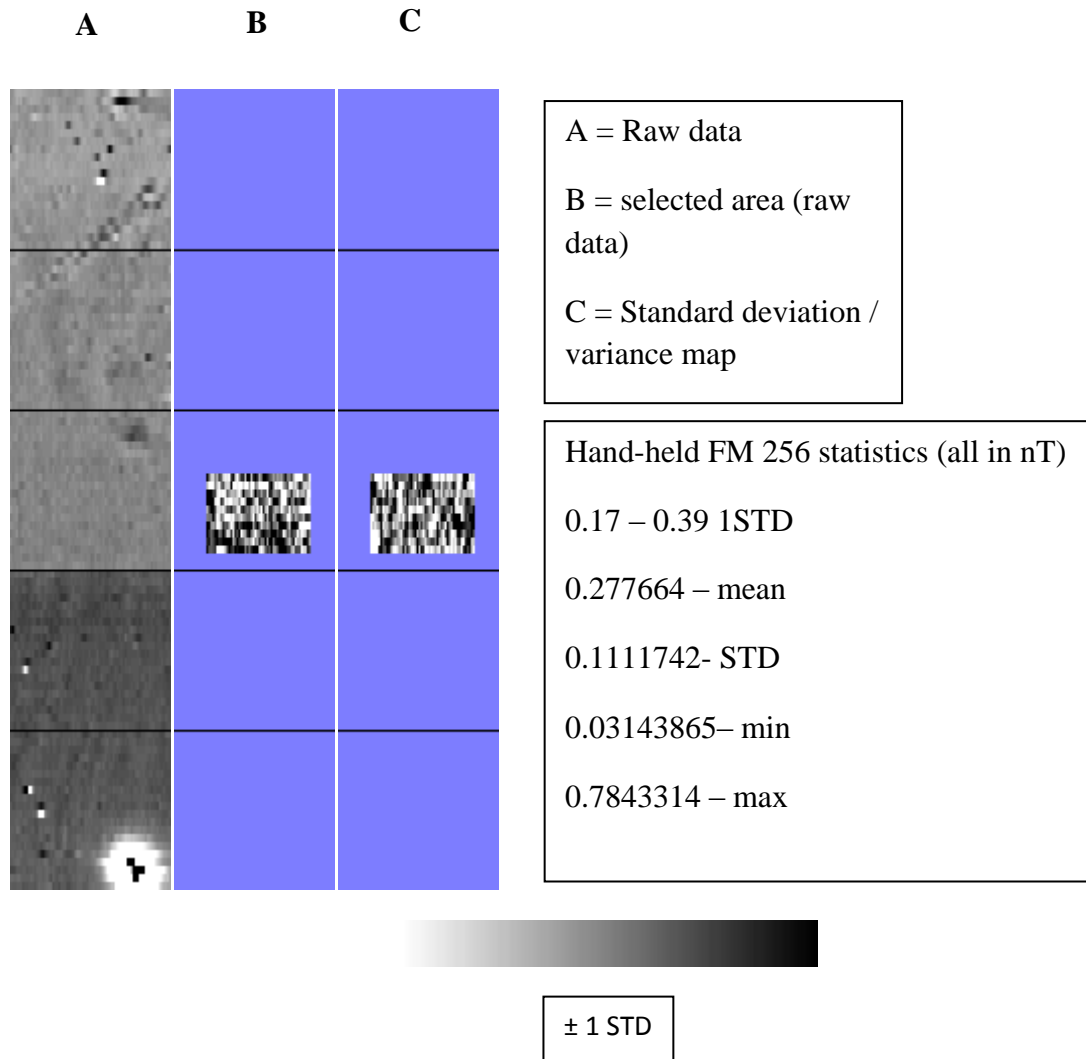
Figure 3.55   An unprocessed greyscale plot with a selected area standard deviation plot of the hand-held FM256 gradiometer survey.

MSP40 mounted gradiometer

A = Raw data

B = selected area (raw data)

C = Standard deviation / variance map

MSP40 FM 256 statistics (all in nT)

0.4 - 1.01 1STD

0.705242 – mean

0.3054532- STD

0.1477877 – min

1.975516 – max

± 1 STD
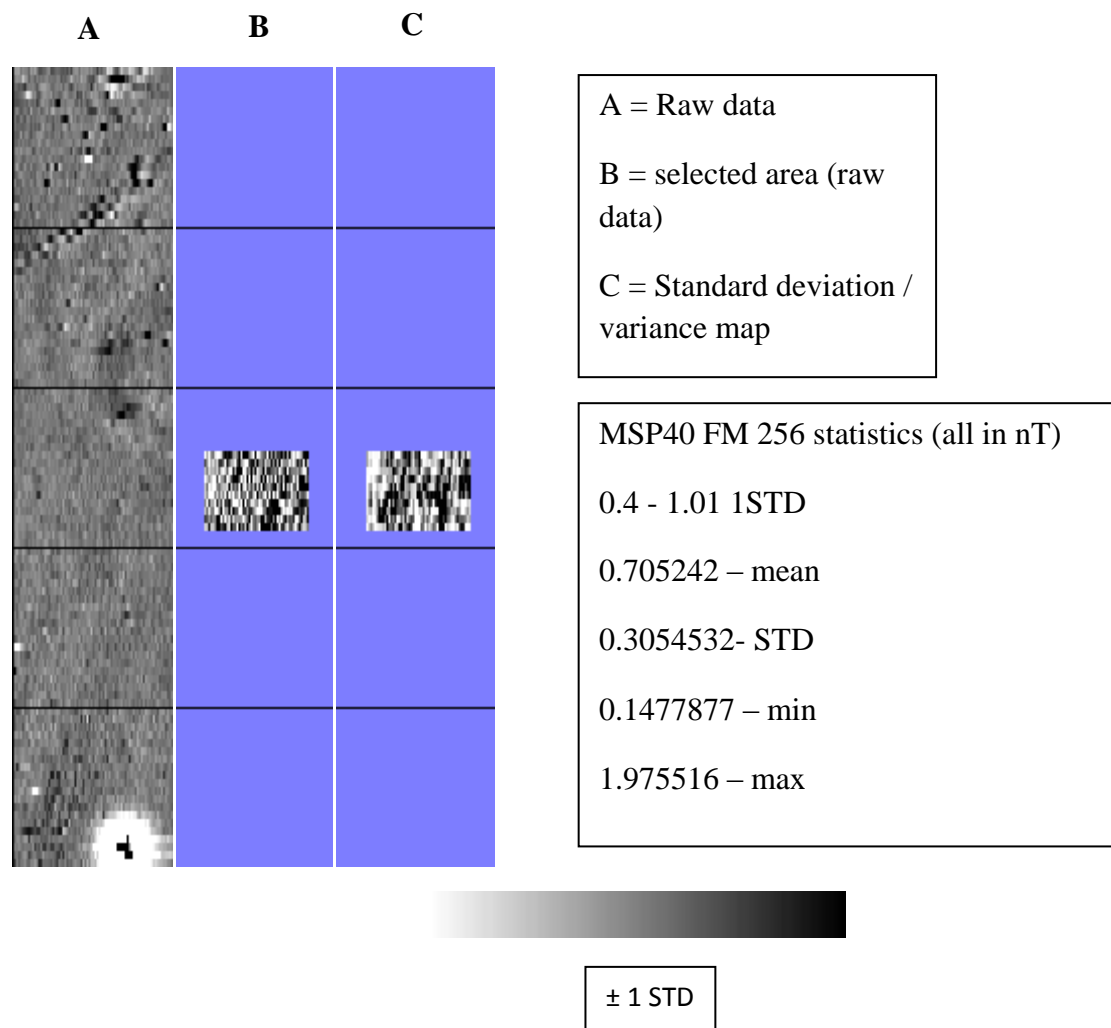
Figure 3.56   An unprocessed greyscale plot with a selected area standard deviation plot of the MSP40 mounted FM256 gradiometer survey.

When the standard deviation results are compared (hand-held 0.11nT and MSP40 0.31nT) there is a threefold increase in noise over the same area on data collected by the MSP40. However, if the data values are considered 0.1 nT and 0.3 nT against archaeological anomalies (often above ± 1 nT) then the additional noise in the MSP40 data is less significant. Data processing may reduce the noise level further using a low pass (X=1 Y=1 Wt=G) filter which reduces the noise in the data to a standard deviation of 0.2795345 nT. The additional noise in the MSP40 data is likely to come from vibration as it is pulled over the ground surface and the oscillation / movement of the gradiometer in the mounting.

3.7.4 Discussion

The increased magnitude of the trace plots is likely to be due to the variations in the height of the bottom sensor. The MSP40 has the bottom of the gradiometer housing 0.24 m above the ground whilst the hand-held survey is positioned c.0.3m above the ground. The closer the sensor is to the ground surface the greater the signal influence of the topsoil. Clark (1996 79) suggests the standard height for carrying an instrument is 20-30cm above the ground as this reduces the effect of localised magnetism in the topsoil. Therefore the MSP40 is towards the lower end of this range and shows why there is a greater response to the local magnetic fields. As a consequence the MSP40 gradiometer sensors are more likely to go over range in both positive and negative measurements as the sensors become saturated by strong localised fields. Rough or rutted ground may cause issues as the bottom of the gradiometer can be knocked affecting the sensor alignment.

The results indicate that the MSP40 mounted gradiometer will produce comparable data sets to hand-held collection. The additional noise of the MSP40 gradiometer data has not hindered interpretation of any of the collected data sets. However, testing on archaeological sites at Entremont (S. France), Barden tower (North Yorkshire, UK) and the St Ives estate (West Yorkshire, UK) indicated the gradiometer was prone to swinging as it rotated in its housing on undulating ground. This potentially led to errors in readings as the top and bottom sensors were not vertically aligned. However, the free moving gradiometer can correct itself back to a vertical position due to the weight of the instrument. The locking mechanism developed by Geoscan Research to stop the pendulum motion works well, but may increase errors if the cart is pulled along a slope where the fixed gradiometer's sensor may remain misaligned (on a diagonal plane, without correction).

The instruction manual for the FM256 suggests ±2.5° tilt from the vertical should produce much less ≤1 nT of noise to the measurements(Walker 2004). However, the greater the deviation from the vertical the more noise is likely to be measured as both sensors will no longer be measuring the vertical component of the localised magnetic field.

The error terms would increase with a poor setup of the two fluxgate gradiometer sensors.

3.8.0 Wheel bracing and double electrode contacts

3.8.1 Introduction

It was observed during fieldwork sessions that the vertical axle supports could bend when the MSP40 encountered certain ground conditions (see figure 3.57).
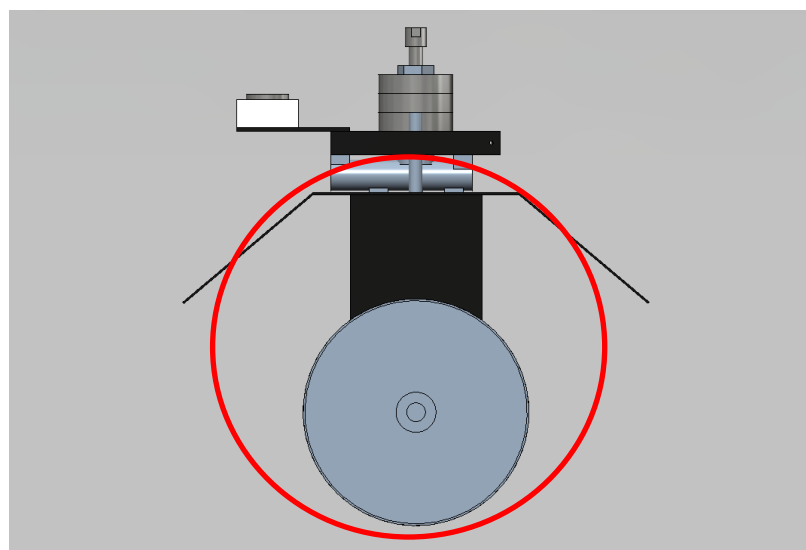
Figure 3.57   Highlighting the vertical axle support made of plastic that splayed outwards during geophysical surveys, drawn in Autodesk 2012.

The effects on the data are very noticeable; one particular example to highlight the effect was provided by Earthsound Archaeological Geophysics which is a commercial company based in Ireland that owns an MSP40. The data was from a survey in County Tipperary, Ireland and shows the results of the splaying wheels. The data highlights the intermittent nature of the issue as the higher resistance values are randomly distributed along the traverse lines. The fault was also unidirectional, with the return traverse being unaffected by the fault. The right edge of the survey was completed on a second day and further highlights the issue as the MSP40 had not been modified between surveys but shows a reduced frequency in spikes (see figures 3.58 and 3.59).

-3.01   48.73 ohms
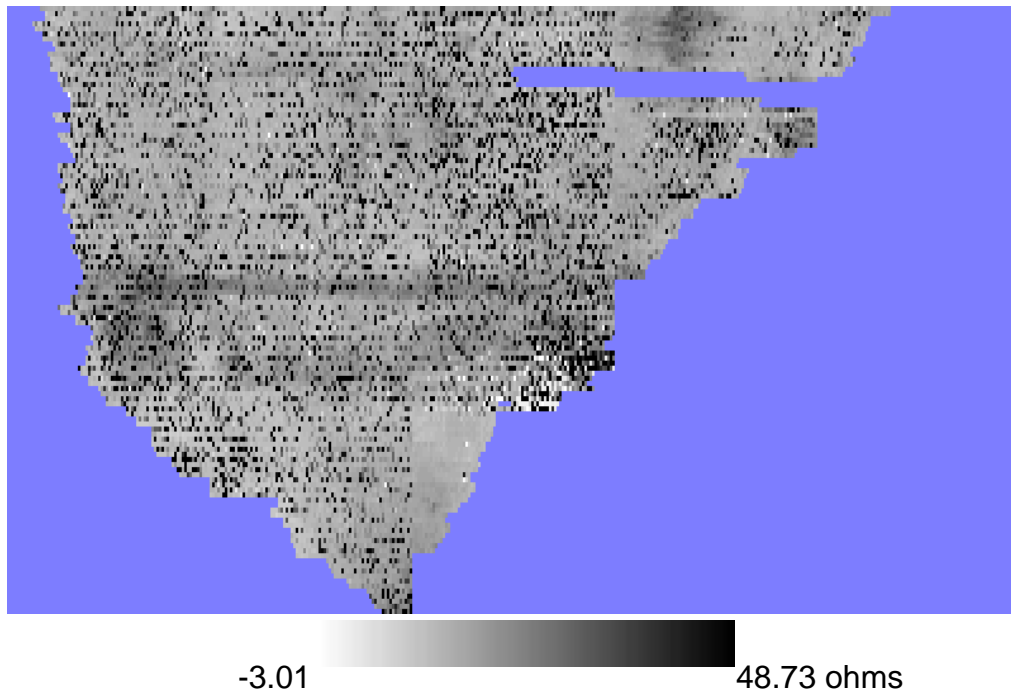
Figure 3.58   The unprocessed earth resistance (raw) MSP40 Alpha data set.

When the data is processed a large number of errors may still remain due to the clustering of erroneous measurements, which are not easily replaced by spike removal. An example of the processing steps may be as follows.

- 4 x Despike X=1 Y=1Thr=3 Repl=Mean

- Despike X=2 Y=2Thr=3 Repl=Mean

- Despike X=1 Y=1Thr=2 Repl=Mean

- Search and replace any negative values with the dummy value 2047.5

Search and replace 50-300 ohm values with the dummy value 2047.5

9.8   21.53 ohms
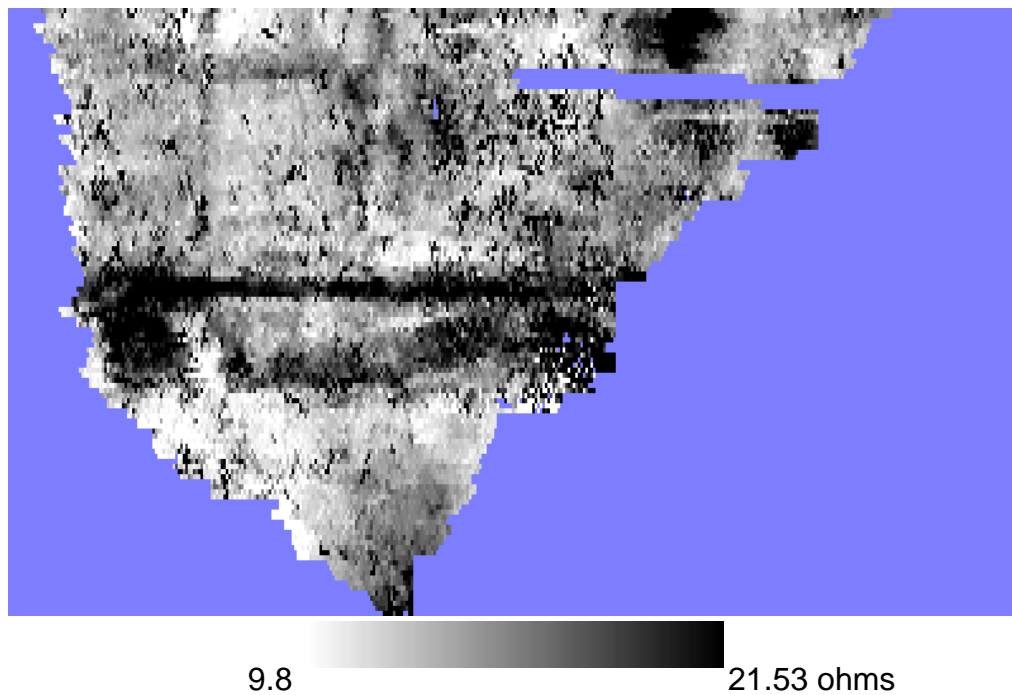
Figure 3.59   The processed earth resistance MSP40 Alpha data set, noting the large number of positive spike clusters still remaining.

The processing has removed many of the individual spikes but many of the grouped / neighbouring errors (along and between traverses) still remain. The visibility of the anomalies has improved by initial processing of the data but the areas of high resistance spikes still remain. Further investigation of data processing steps are discussed in chapter 5. However, the need to heavily process data can be reduced by improving the quality of the data collection. Additional bracing has been one solution to resolve this issue.

The distortion of the vertical axle support is not consistent during a survey. This leads to an increased number of 'spikes' in the data and possibly the creation of anomalies along traverse lines.

The distortion appears to be related to subtle ground variations (slope) or when the cart is pulled over harder surfaces when greater forces are acting on the wheel (less pressure dissipated in to the soil). It was therefore important to brace the bottom of the vertical axle plate (see figure 3.60).
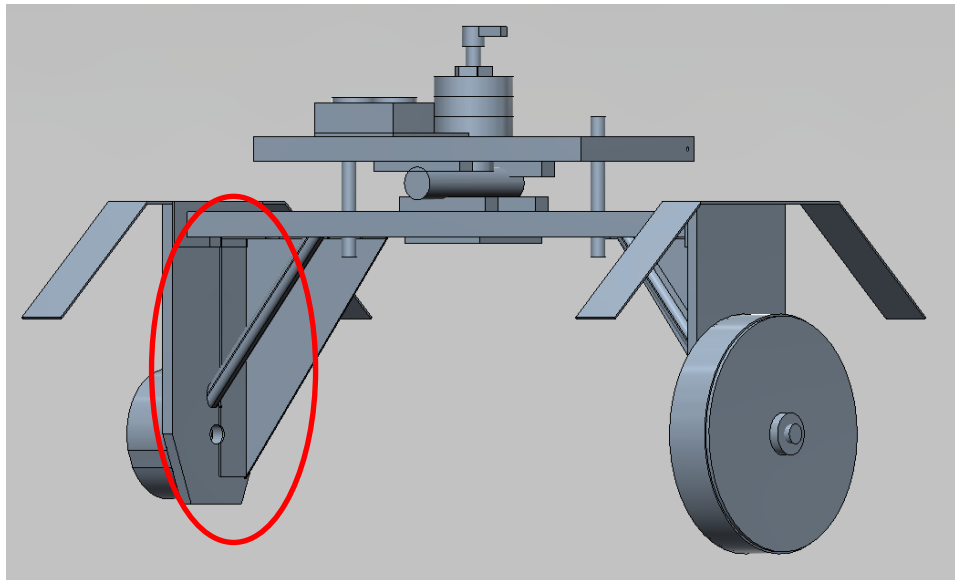
Figure 3.60 The highlighted area shows the low bracing extent on the inside face of the vertical axle support, drawn in Autodesk 2012.

3.8.2 The effect of square array distortion on earth resistance values

The effect of distortion of the axles on earth resistance values can be seen by a simple calculation. The hypotenuse of a 0.75 m square = 1.06066 m (see table 3.8)

Table 3.8   Square array distortion calculations

Probe configuration	C1 – P1	C2 – P1	C1 – P2	C2 – P2
a = probe separation	0.75 m	1.06066 m	1.06066 m	0.75 m

This means the geometry factor

g = geometry factor for a given array

$$g = \frac{1}{[C1P1]} - \frac{1}{[C2P1]} - \frac{1}{[C1P2]} + \frac{1}{[C2P2]}$$

$$g = \frac{1}{[0.75]} - \frac{1}{[1.06066]} - \frac{1}{[1.06066]} + \frac{1}{[0.75]}$$

g= 0.78105 m^{-1}

Therefore K = $\frac{2\pi}{g}$

Or

K = $\frac{2\pi}{0.78105}$ m

K= 8.044537 m

For a 1cm displacement of a single electrode the displaced electrode hypotenuse will equal 1.067755 m and the array is now no longer square, making a shape 0.75m x 0.75m x 0.75m x 0.76m (see table 3.9).

Table 3.9 Square array distortion calculations

Probe configuration	C1 – P1	C2 – P1	C1 – P2	C2 – P2
a = probe separation	0.75 m	1.06066 m	1.06776 m	0.75 m

This means the geometry factor

g = $\frac{1}{[0.75]}$ - $\frac{1}{[1.06066]}$ - $\frac{1}{[1.06776]}$ + $\frac{1}{[0.75]}$

g= 0. 78732 m^{-1}

K = $\frac{2\pi}{0.78732}$ m

K= 7.980472 m

If a hypothetical resistance measurement for both arrays was taken as 20 ohms and converted to apparent resistivity as discussed in chapter 2 the 0.75m square has an apparent resistivity value of 160.8907 ohms m whilst the distorted square array would produce a value of 159.6094 ohms m. This produces approximately a 0.8% decrease in apparent resistivity measurements by a 1cm distortion of a single electrode.

The distortion effect has two main issues. The first is, as outlined above, the subtle change in the array geometry which will affect the recorded earth resistance values (and calculated apparent resistivity values). The second issue would be the relationship between Alpha and Beta measurements, which would no longer hold true due to the distorted geometry, consequently distorting the calculated gamma results.

Subtle changes to the geometry may occur through poor field procedure; the MSP40 can be pulled in two directions as the cart has front and rear handles. The rear handles are locked in place as the cart is pulled along. At the end of each traverse the MSP40 is repositioned at the grid edge of the next traverse over using both the front and rear handles. If the rear handle is not locked in place the axle may be distorted effecting the array geometry. However, greater errors are likely to come from poor alignment of the front axle, which should be parallel to the rear axle. The axles will align when the next traverse is started but distortion of the array geometry may occur for the initial readings. The problem can be solved by careful positioning and aligning the wheel axles at right angles to the grid edge before starting the next traverse (see figure 3.61). In practise these errors remain unnoticeable as it is a subtle change in resistance only effecting the first Alpha and Beta readings but should be reduced where possible.
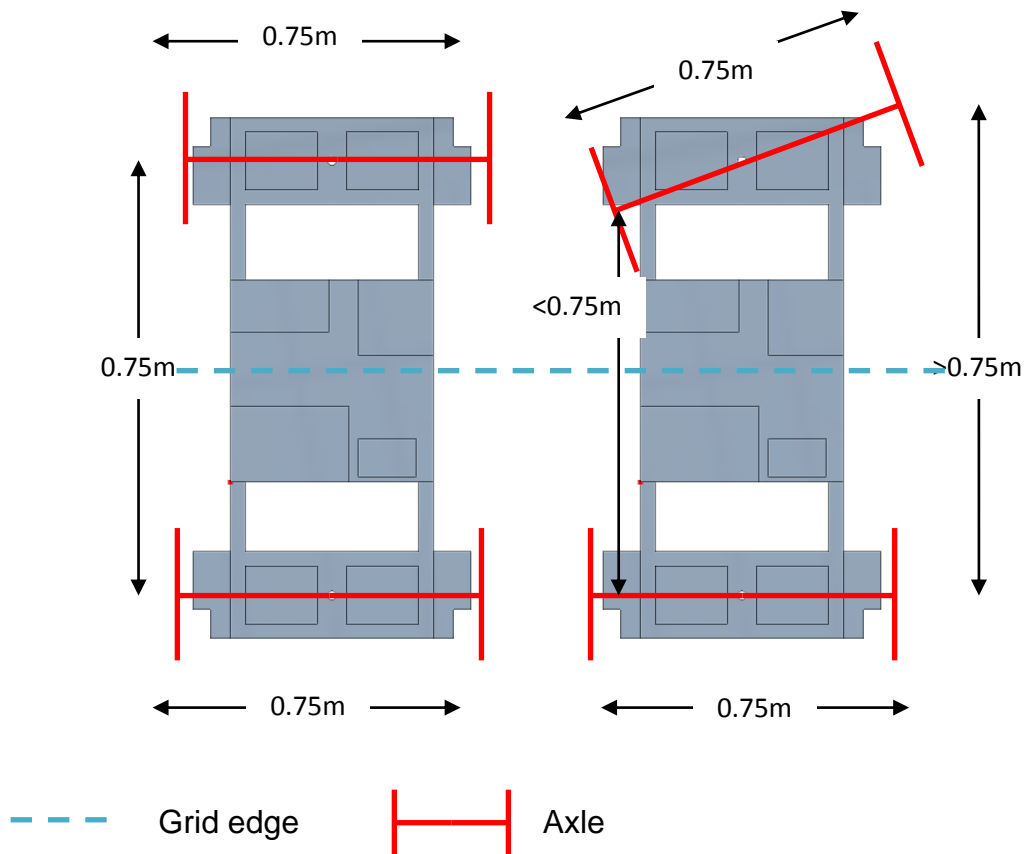
Figure 3.61   The correct alignment of the axles to the grid edge (left hand image) and how the array geometry can be effected by poor field procedure (right hand image).

3.8.3 Slope effect on axle supports.

It was noted that as the axle support bent under the forces exerted on it, the alignment of the wheels shifted away from a vertical alignment. After a day of survey it had been noticed that a polished ring mark is formed on the brass plate this is due to the movement of the plate over the contacts clearing away dirt and having an abrasive effect under pressure. The polished mark should have a continuous thickness however, a number of surveys showed a variable thickness was being left on the plate (see figure 3.62). This indicates the brass rod electrode and brass plate on the wheel are not making flat contact increasing the potential for erroneous readings.
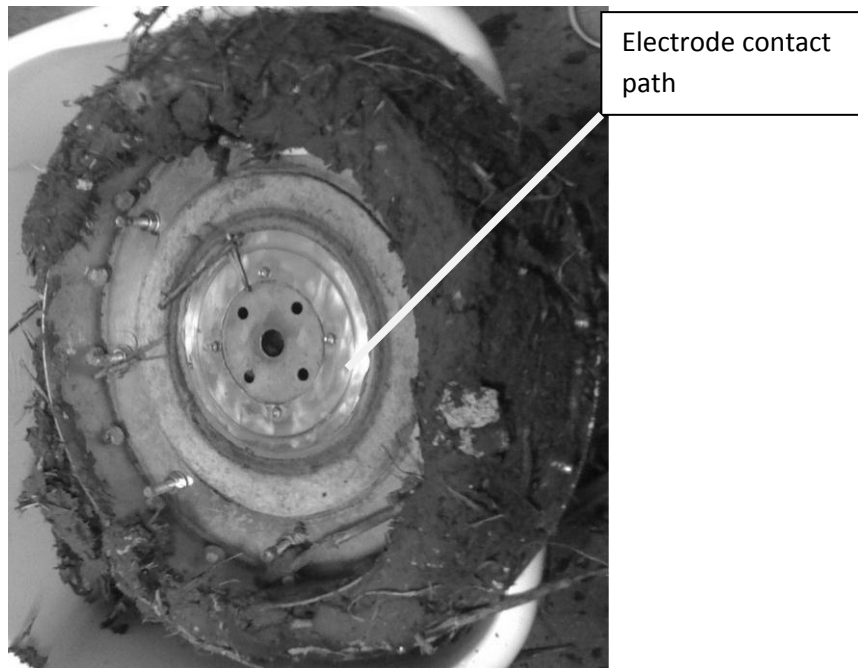
Figure 3.62   The internal view of the wheel hub noting the area where the brass rod and plate make contact.

A second contact electrode was added to each wheel. It was positioned off the centre line at the base of the wheel hub in case the wheel splayed outwards. Adding an additional electrode also meant that if a brass rod temporarily became stuck in the Tufnell housing (or material became trapped between the rod and plate) it would still be possible to take measurements with the second contact (see figure 3.63).

The second electrode was constructed by soldering two wires of equal rating to a single banana plug at one end then having the two wires divide out to the two individual brass rods and Tufnol housing located on different parts of the wheel drum. The brass rod is located a few millimetres closer to the centre of the wheel so that if material builds up on the brass plate the likelihood of both electrodes being affected is reduced.
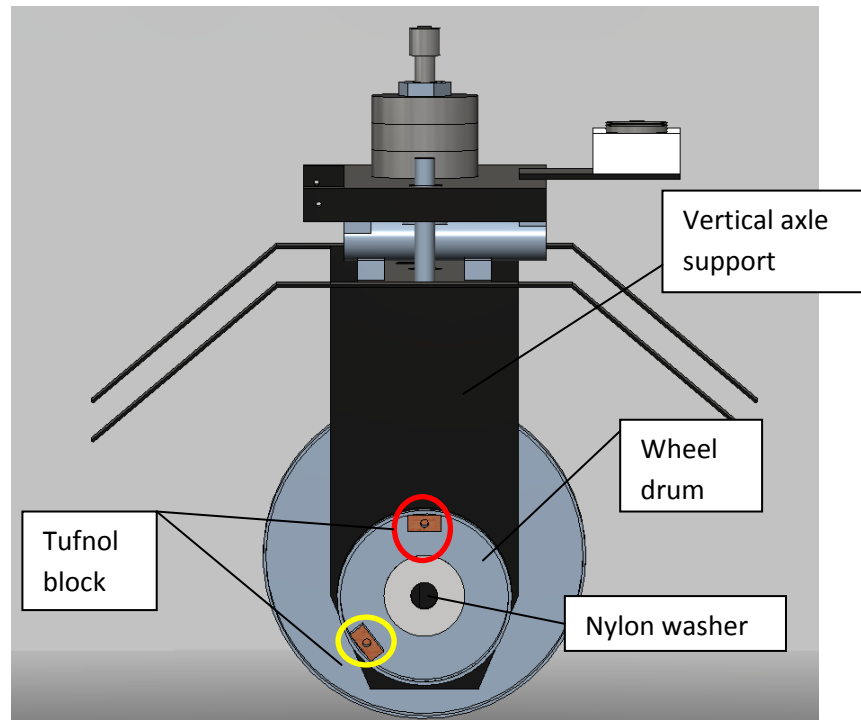
 Original electrode position / Tufnol block

 Additional electrode position / Tufnol block

Figure 3.63   The internal view of a wheel drum with the highlighted electrode positions (red and yellow) drawn in Autodesk 2012.

3.9.0 Regular checks for wear and replacement of parts (frequency where appropriate)

3.9.1 Before Every survey

Cleaning Brass contact plate

The brass contact plate on the internal face of the wheel must be cleaned before every survey to ensure a clean contact surface. Other practitioners of the MSP40 had previously encountered issues with noisy data which was diagnosed by the manufacturer (Geoscan Research) and solved by cleaning the brass regularly. The brass surface begins to oxidise producing a film of copper and zinc oxide particles which effect the earth resistance readings.

Checking on brass rod length (electrode)

Checking the brass rod electrodes length is important as the wearing down of the brass rod shortens the length of the rod. As the rod wears away the pressure placed upon the spring to push against the brass rod is reduced. This will lead to increased risk of detritus trapping between the brass rod and plate which may lead to broken contact between the two components (missing readings). It is also useful to check for burrs forming on the side of the rods which may be an indication of uneven wear. The burrs will also catch on the Tufnol housing and may break the contact with the brass plate.

3.9.2 Once a month

Cleaning optical encoder lenses

During the research project an issue arose from using the optical encoder where the MSP40 would over-shoot the edge of a traverse (sometimes over 2 metres). The error was not repeatable (to the same extent) which suggested it was not an effect of surface undulations during the calibration process. Lab tests involving jacking up the front axle and rotating the wheel a prescribed distance did not indicate any issues with the encoder.

Diameter of encoder wheel = 9 cm

Circumference of encoder circle = c. 28.27 cm

Number of holes in encoder = 16

Over a 20 m traverse the encoder wheel revolves = 70.75 times

Over a 20 m traverse the encoder should record = 320 pulses

There was no visible material on the encoder lenses but the decision was taken to clean the lenses. A cotton bud was gently wiped over the surface and traces of a fine dust were removed by the cotton wool. Later trials on the amphitheatre indicated that the encoder was more accurate in its positioning over a 20m traverse. Therefore the build up of material on the lenses must have been sufficient to diffract the signal from the optical transmitter to the receiver.

The material on the lenses may move because of the vibrations from the wheel explaining the random errors in distance.

The calibration process can therefore be used to check the encoder is working correctly before a survey as it measures the pulses seen over three traverses before averaging the results for the traverse. If a traverse records less than the minimum 320 pulses there may be an issue with the encoder that may be solved by cleaning the encoder. If pulse numbers exceed 320 then this is probably due to slight topographic change increasing the distance travelled and the number of pulses recorded. Minor adjustments can then be made to the number of pulses recorded per traverse to improve the positional accuracy.

Lubricating the vertical axle pins and nylon spacers

Lubricating the vertical axle pin and the internal faces of the nylon spacers with silicon grease helps to reduce wear and ease the rotation. The grease should be cleaned off each month before being replaced to remove any dirt and abrasives from the grease.

3.9.3 Every 3 - 4 months

The following should be checked every 3 – 4 months or more frequently depending on the amount of use. The information is based on personal experiences of the author and the experiences of other practitioners (Bonsall 2011).

Checking for water entering the multiplexer and Bulgin plug boxes

As discussed previously in the chapter water was found to be entering the Bulgin connectors and plug housing. Even though modifications had been made to the prototype MSP40 it is still necessary to check the MSP40 for water entering these areas of the cart.

Cleaning the internal face of the nylon wheel drums

Dirt and metal filings can collect in the space between the wheel axle pin and the nylon drum. The material may collect in the wheel drum and explain the dirt build up on the optical encoder lenses. The nylon drum can be cleaned by using a bottle brush to clean the inner face of the drum and reduces the need to clean the optical encoder lenses as frequently (see figure 3.64).

Internal face of nylon drum
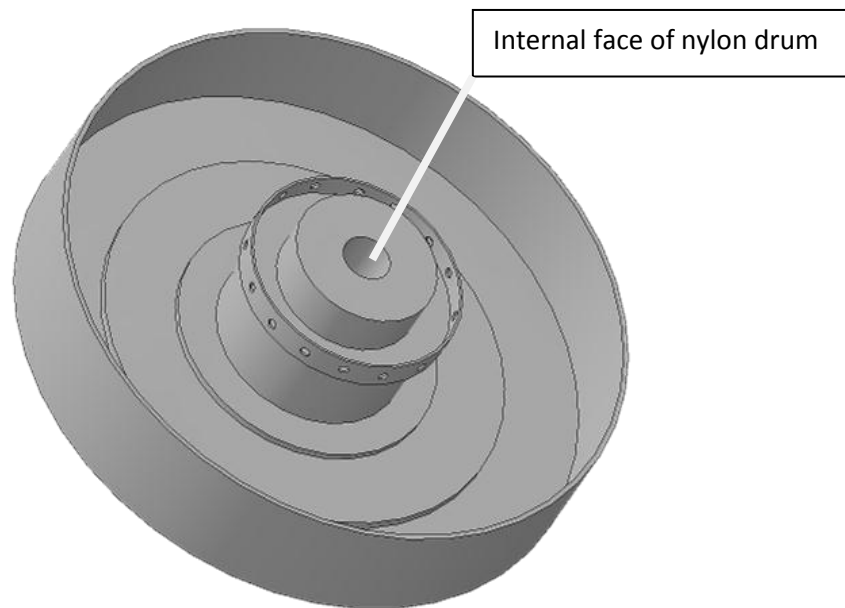
Figure 3.64   An internal view of the front left axle (wheel 1) highlighting the internal surface of the nylon drum, drawn in Autodesk 2012.

Wear on axle pins and wheel mounts

The wheel mounts and vertical axle pins should be monitored as both can show signs of wear (see figure 3.65). The wheel mounts show signs of wear around the collar that holds the wheel in place. This is due to abrasive material trapping between the wheel and collar and grinding down the wheel mount. An examination of a commercial model MSP40 indicated how the wheel could become misaligned by a significant groove forming on the wheel mount at an uneven rate. The vertical axle pins are also prone to wear, which is caused when the axle twists or jack-knifes beyond its normal range of motion (on undulating ground or when the axle nuts loosen excessively).

As the vertical axle pin is a threaded stainless steel rod it 'cuts' into the 'softer' aluminium box section used to construct the axle. This would eventually lead to a widening of the vertical hole increasing the risk of the axle twisting and distorting the array dimensions.
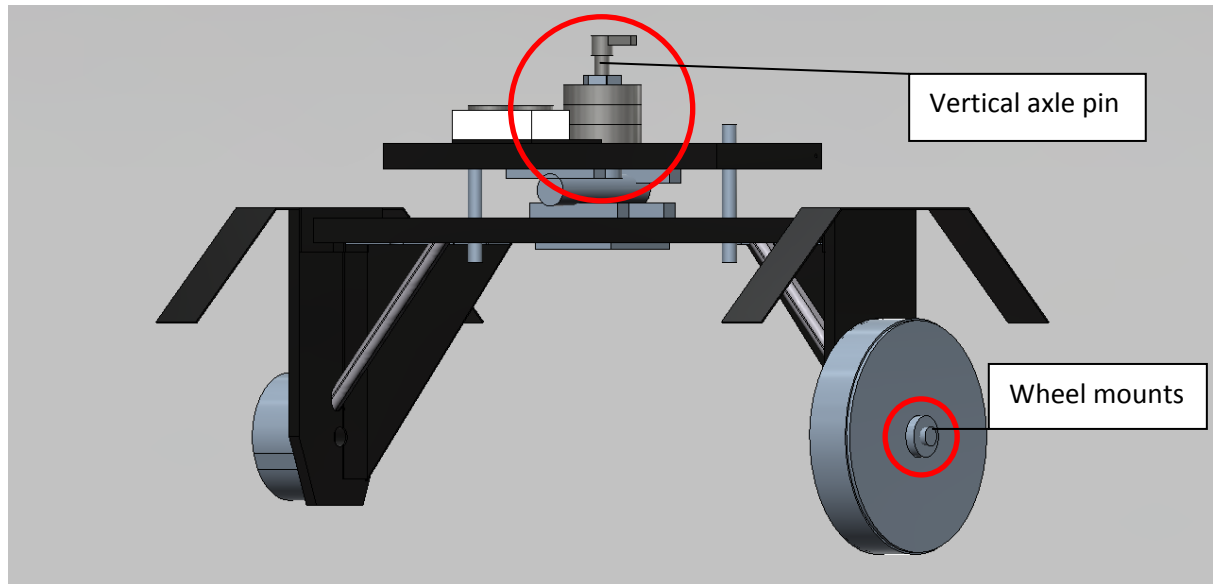
Figure 3.65   The highlighted vertical axle pin and wheel mount areas prone to wear, drawn in Autodesk 2012.

Wear on platform edge from handles

The metal plate that acts as a rest for the handle when not in use can become damaged if the handle is not locked properly into position. The commercial version of the MSP40 has had large gouges taken out of the handle and metal when the axle twists if not correctly located. The gouges then make the handle sit incorrectly against the platform exacerbating the problem (see figure 3.66). The operator only needs to monitor the affected areas every three to four month as it is likely to take some time for this to become a significant issue. The problem can be solved by reinforcing the platform edges with sheet metal bolted through the original platform. A bungee cord tied between the two handles can help to keep the rear handle locked in place.
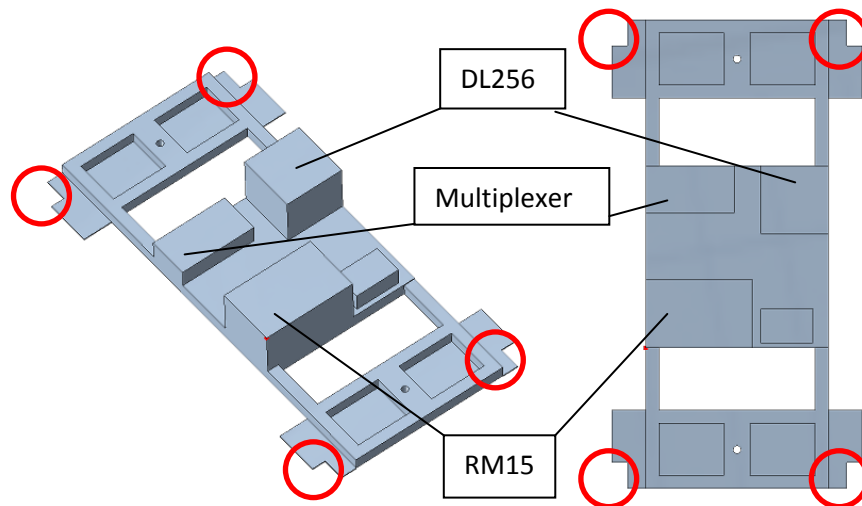
Figure 3.66　The MSP40 platform areas that can be damaged by an improperly secured handle when the axle twists (red), drawn in Autodesk 2012.

Check for metal fatigue on handle pins

The pins that connect the handles to the platform have been prone to bending when the axles are put under significant pressure or twisting so should be monitored for damage or distortion.

3.10. Discussion

The MSP40 has a range of attachments (or add-ons) that can be used for surveying on different types of site conditions. Careful selection of wheel configuration may improve survey success (discussed further in chapter 6.3.2). Weather conditions prior to survey should also be considered (discussed further in chapter 4.2) when trying to record the best quality data. The 'factory default' setup for equipment settings does provide the most appropriate configuration for the majority of sites and surveys. However, additional factors may influence decisions made before the survey to optimize the results. These factors include ground cover (bare soil or planting types), the weather regime prior to the survey, soil types (clay or sandy soils may influence setup choice) and any restriction placed on the survey area (reduced impact). Many of the factors are linked together; for example the weather regime prior to survey will affect the soil moisture content of clay or sandy soils.

This can influence the viscosity of the soil and therefore the soil build up on the wheels especially on clay site (increasing impact on the site). If there have been extended dry periods prior to survey then an increase in the contact resistance on free draining sandy soil is likely. When more problematic survey conditions arise it is useful to adapt the MSP40 configuration to improve the success rate of the survey.

The addition of the gradiometer on the MSP40 increases the information gained from a single traverse. Having multiple data sets for an archaeological site aids understanding and interpretation of the anomalies. Many archaeological sites will have complimentary earth resistance and gradiometer data sets but the research has shown that relying solely on one technique can mean much of the information could be missed (see chapter 4.1).

The MSP40 mounted gradiometer tests show a positive comparison with the hand-held collection although a slight increase in noise is noticeable. Magnetically quieter archaeological sites may show a higher level of noise created by vibration and instrumental movement. However, when the two collection methods have been compared on archaeological sites the same anomalies have been identified.

The integration of a GPS adds an extra data set from the same traverse reducing the impact on the site. The GPS can be used to locate the survey when a lack of location information is available to geo-reference the data to a map projection in a GIS package. The GPS survey also aids the interpretation of the geophysical data as it is possible to confirm anomalies that are a result of land use or a natural change in topography.

The experiences of the research and communication with other geophysicists using the MSP40 highlight a need for careful maintenance from the very beginning of ownership of the equipment. This will ensure an increased lifespan of the components and lead to improved performance during a survey, leading to better quality results. An overhaul of components may also be necessary after 20 – 30 ha of survey based on this research and commercial companies' experiences. Ideally the MSP40 needs to have a nominated individual to monitor the condition of the MSP40 and make appropriate modifications and repairs when necessary.

Chapter 4 examines the data from several practical trials intended to test the potential MSP40 applications. In light of discussion from chapter two the testing included an investigation of the multiple square array measurements, a seasonality test, wheel type and general configurations. This chapter culminates in an assessment of the physical impact of the MSP40.

4.0.0 Practical field work trials

4.1.0 Introduction

A major part of the research project was to examine the multiple applications and configurations of the MSP40 by using fieldwork to test the various parameters. This chapter focuses on the practical testing of the mobile sensor platform considering the potential benefits of collecting multiple earth resistance data sets. Additional testing included the feasibility of using the MSP40 throughout the year, in the form of a seasonality test. Where possible the similarities / differences between the earth resistance arrays were compared (when data sets overlapped). An investigation of the wheel configurations available to the cart was also examined to explore wheel type choice on different site conditions. Finally an assessment of the physical impact of the MSP40 was completed to understand the damage caused to the soil surface during a survey.

4.1.1 Alpha, Beta & Gamma tests

Square array configurations are orientation dependent, as Clark (1996 46-47) and Aspinall and Saunders (2005) both showed how Alpha and Beta responses can vary over a feature. One orientation may show double peaking over an anomaly depending on the angle of strike to the anomaly and the resistivity contrast of the anomaly (see figure 4.1).
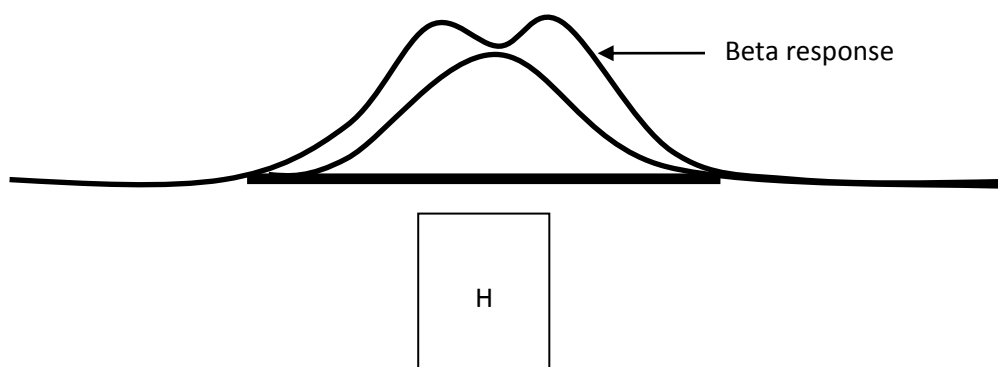
Figure 4.1   Alpha and Beta response curves over a high-resistivity feature. Based on Clark (1996 39).

As the square array has a two dimensional configuration it was important to understand the directional dependence of the array and how to maximise the information gained. A project at the St Ives estate in Bingley, West Yorkshire provided a suitable early case study. The site formed part of the Ferrand family estate and early Ordnance Survey maps indicate the area under geophysical investigation formed part of the estate plantation (see figure 4.2). The estate was sold to the rural town of Bingley by the Ferrand family in the 1920s and is currently run by the City of Bradford Metropolitan District Council with support from the Friends of St Ives. The Friends of St Ives (2010) website provides a more detailed history and discuss previous archaeological geophysics work carried out on another area of the site.

The project was an exploratory survey as nothing was known of the archaeological potential for the site. The area was chosen as it was suitable for use as a geophysical training area (run by the university) for a local historical society Bingley and District Local Historical Society. The 1893 Ordnance Survey map of the area appears to show a linear track way and field boundary in the survey area whilst the general area is labelled as plantation property.

Figure 4.2   The 1893 Ordnance Survey map of the St Ives estates (left image) with the survey area highlighted (right image).

4.1.2 Survey details

St Ives Estate, Bingley, West Yorkshire (Grid Ref: SE096391).

4.1.3 Method

Survey equipment

MSP40 configured with normal spiked wheels (RM15 and DL256 data logger).

Mounted FM256 gradiometer.

Survey parameters

Data was collected in a zigzag pattern without rotating the array. The encoder wheel was used to trigger measurements at the specified intervals. Data was collected in 40m x 40m grids with sighting poles at the grid edges.

Sampling strategy (see table 4.1)

Table 4.1   Survey parameters (St Ives Estate)

Equipment	Measurement Configuration	Sampling Interval	Traverse Interval	Method of collection
MSP40	Alpha & Beta	0.5m	1m	Zig Zag
FM 256 Gradiometer	Single measurement (MSP40)	0.25m	1m	Zig Zag

4.1.4 Data processing

Processing of the earth resistance data was restricted to despiking and the removal of errors in readings. The despike parameters are as shown below. Any negative values in the data set was replaced with a dummy value of 2047.5 (the standard value recognised by Geoplot) using the search and replace function.

MSP40 Alpha and Beta

2 x X=1, Y=1, Threshold=3 and Replace=Mean

1 x X=2, Y=2, Threshold=3 and Replace=Mean

Additional Beta

Destagger All Grids, X dir, Shift =-1, Line Pattern -2-4-6-8

Shift +1

The additional destagger for the Beta measurement was to compensate for the slight displacement of anomalies between traverses due to positional errors from the encoder over a changing topography.

The shift function is recommended by Geoscan Research in the MSP40 manual to account for the time displacement between the Alpha and Beta measurements. However, when sampling intervals of $\geq$0.25m are used the displacement may over compensate for the slight time delay although this is dependent on the collection rate. It was therefore decided not to shift data on subsequent site investigations.

Geoscan Research FM256 gradiometer processing

The data was initially analysed for periodic noise by performing a spectrum analysis of the entire data set. Periodic frequencies were then filtered out using the following parameters.

Zero Mean Grid, Threshold = .25

Zero Mean Traverse, Grid=All LMS=On (Threshold not applied).

Per. F, Index 131-141 & 237-246, Grid=All, Spike=On (Threshold not applied).

2 x Low pass filter X=1, Y=0, Weighting = Gaussian

4.1.5 Results of Alpha, Beta and Gamma tests

The results show a series of high resistance linear anomalies that show the subtle anomaly extent variation associated (see figure 4.3) with Alpha and Beta measurements (longitudinal and broadside surveys). See figure 4.4 for the archaeological interpretations.

12.02 ohms 23.28	12.83 ohms 24.93
±1STD	±1STD
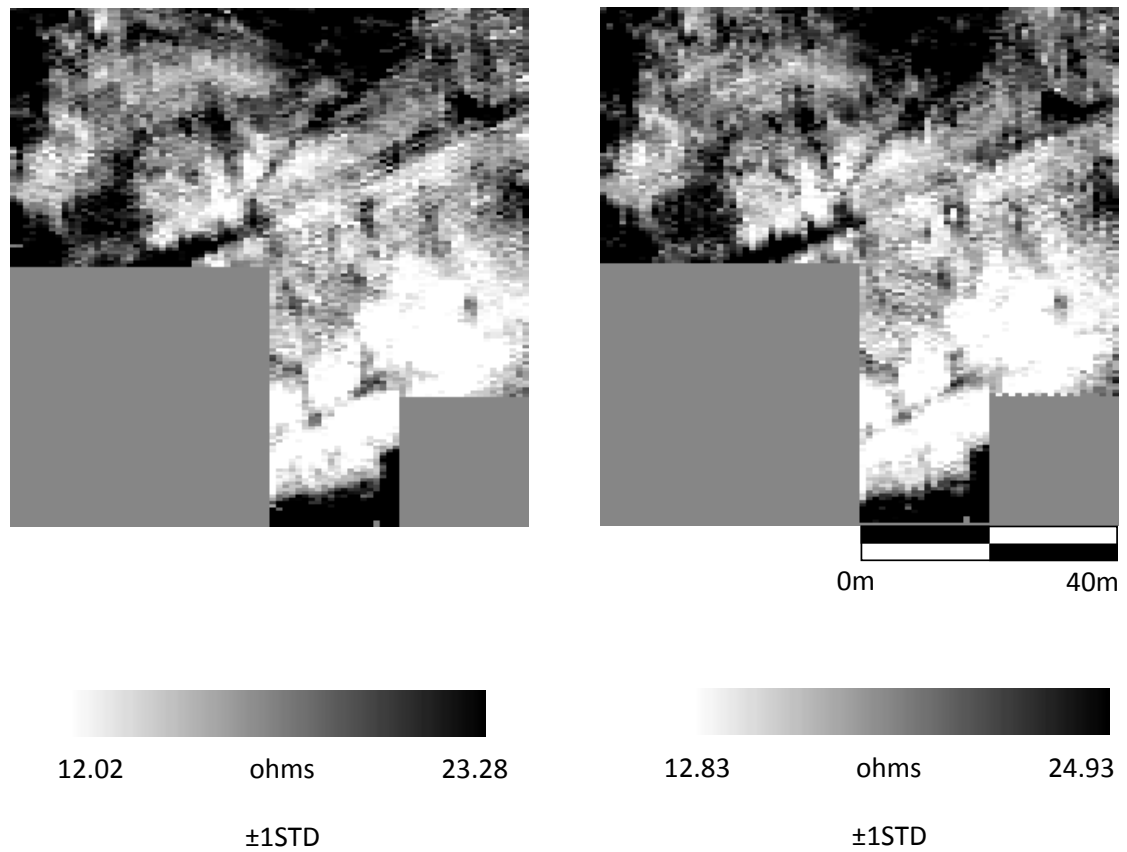
Figure 4.3   Alpha and Beta data sets from the MSP40 at the St Ives estate, Bingley, West Yorkshire, with subtle anomaly variations between datasets.

Figure 4.4   Archaeological interpretations of the earth resistance data.

The Alpha and Beta data sets show subtle changes in anomaly extent depending on the array orientation, the Alpha measurement showing increased anomaly sizes along the north-south axis whilst the Beta measurement has broader anomalies in an east west orientation.

The differences between the two data sets can be seen in the calculated Gamma measurement (see figure 4.5). The Gamma measurement was calculated following the examples given in Aspinall and Saunders (2005).

-3.45   ohms   0.89

±1STD
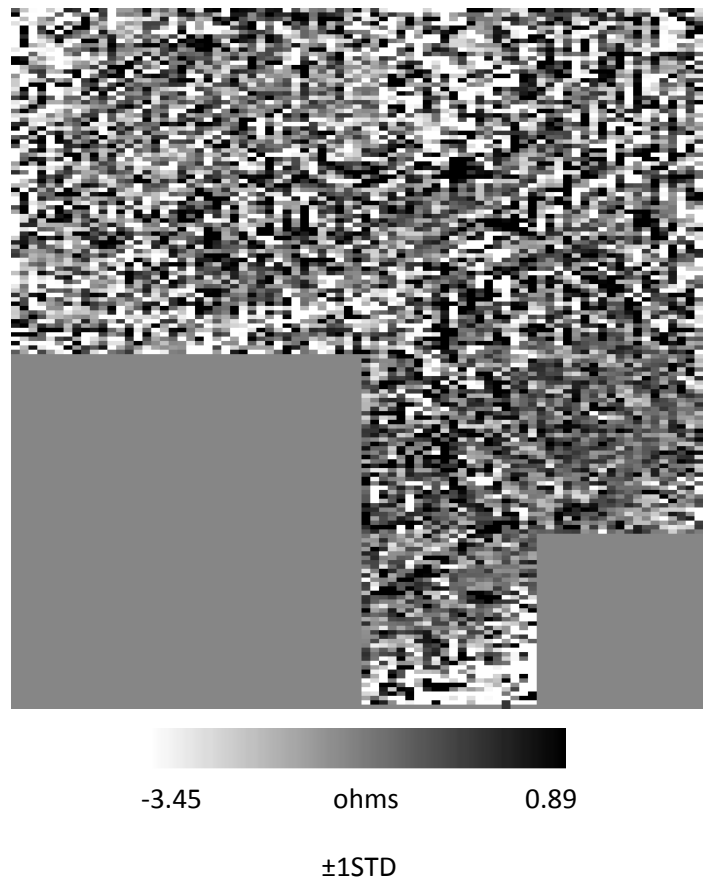
Figure 4.5   The MSP40 calculated Gamma measurement showing areas of disturbance and edges of features.

In an isotropic medium the Gamma measurement will have a value of 0 as there is no directional dependence in either the Alpha or Beta measurements. From the Gamma measurement the Azimuthal Inhomogeneity Ratio (A.I.R.) was calculated. A.I.R. calculations were generated following the method discussed in chapter 2.8 (see figure 4.6).
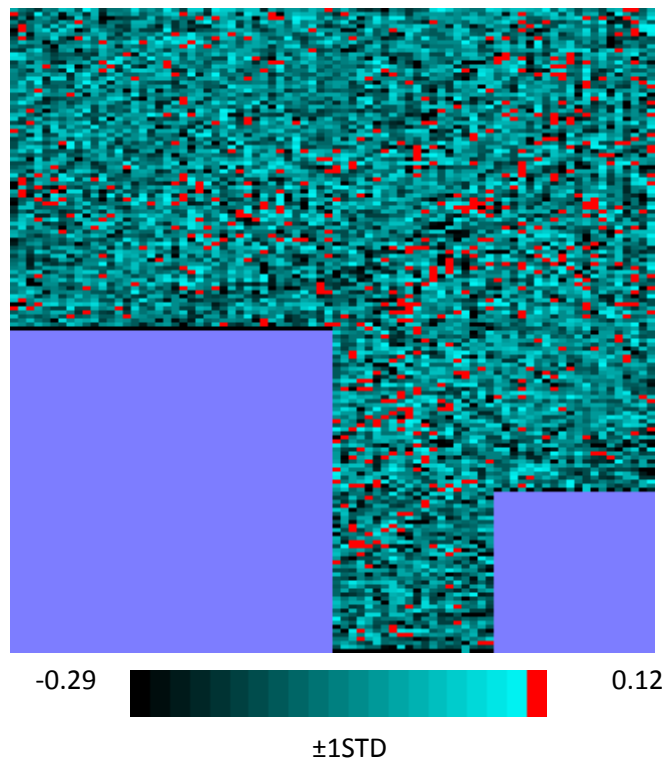
Figure 4.6   The calculated MSP40 A.I.R. display, colours closer to red and black show areas of greater anisotropy.

The A.I.R. display may improve the visualisation of the anisotropy of the anomalies but as with the Gamma display the data set cannot be clearly interpreted in isolation from the Alpha and Beta data sets.

Small scale changes in the form and extent of anomalies (between Alpha and Beta measurements) were identified in many of the surveys undertaken during the research project. However, only one clear example of the anisotropic effect of archaeological anomalies was identified during the research project where a complete anomaly could only be identified in a single data set. This was from the extramural investigation of the Iron Age Oppidum at Entremont, Provence, France (Armit *et al.* 2012). The Alpha and Beta measurements showed a clear variation in the survey data with a large curvilinear anomaly only visible in the Beta data set (see red highlighted anomalies in figure 4.7). The anomaly is likely to be a near surface feature possibly caused by a boundary marker (bank).
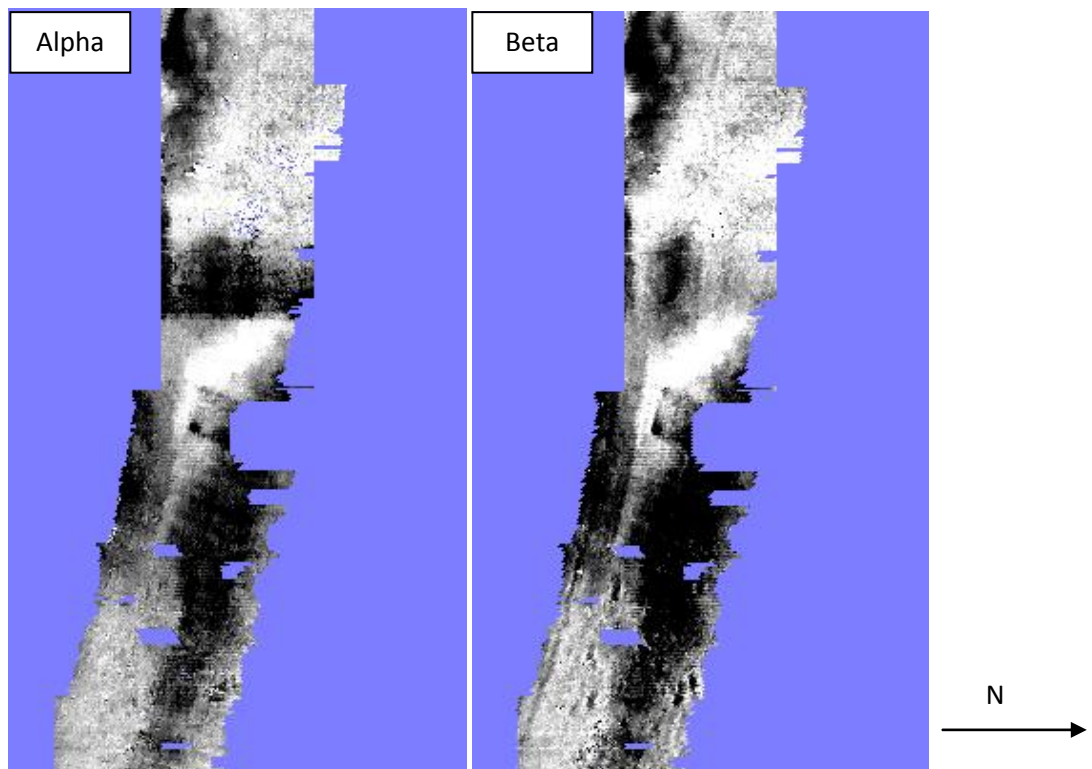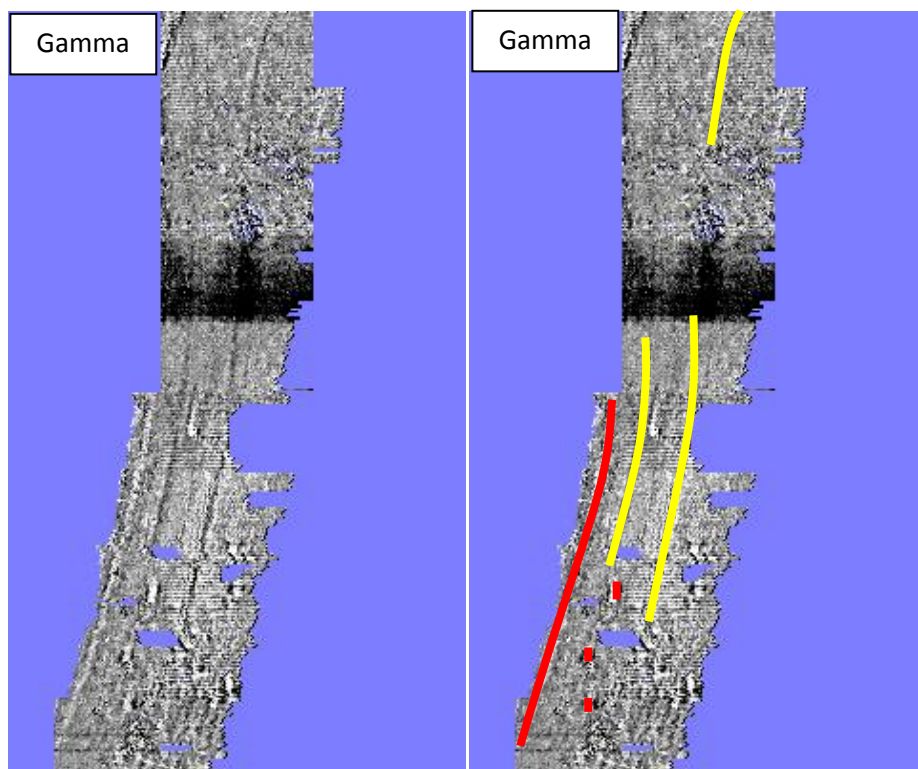
Figure 4.7   Alpha, Beta and calculated Gamma data sets with geophysical anomalies showing anisotropic responses to the electrical current.

4.1.6 Discussion of Alpha, Beta and Gamma configurations

Alpha and Beta measurements can identify anisotropic properties of current flow through the soil. Gamma and A.I.R calculation highlight the differences between the two measurements and for edge detection but cannot be used independently to interpret archaeological anomalies. The combination of the Alpha, Beta and Gamma data in the A.I.R. calculations shows that the data set is dominated by the Gamma measurement. Saunders (2002) believes that both Gamma and A.I.R. measurements will show the same broad trends and the extra calculations for the A.I.R. may not warrant the extra processing.

4.1.7 Combined earth resistance and gradiometer surveys

The results from the St Ives estate survey highlight the benefits of collecting multiple data sets when investigating previously unidentified sites. The gradiometer surveys do not show many of the anomalies identifiable in the earth resistance measurements and when they are visible only have a weak magnetic signal. The reduced level of information in the gradiometer data may be due to the nature of the archaeology. If the recorded earth resistance anomalies are constructed from the local parent geology it is likely to show little variation above the magnetic background. Alternatively the soils in the area may have had limited magnetic enhancement (through burning or addition of magnetic minerals in the soil) resulting in the gradiometer survey only identifying weak geophysical responses from the potential archaeology.

As the MSP40 allows simultaneous gradiometer and earth resistance data collection it is more likely to identify a larger number of geophysical anomalies than choosing a single method of investigation (see figure 4.8). The improved collection time for earth resistance measurements also make the MSP40 ideal for pilot studies, to get a more detailed investigation of a site by maximising information gained within project time constraints.
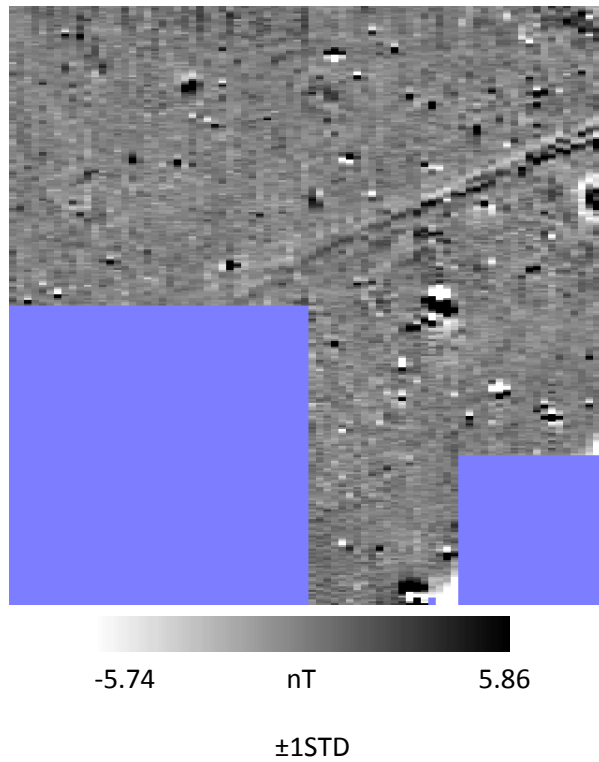
Figure 4.8   Processed gradiometer data which fails to identify many of the anomalies in the earth resistance data at the St Ives estate.
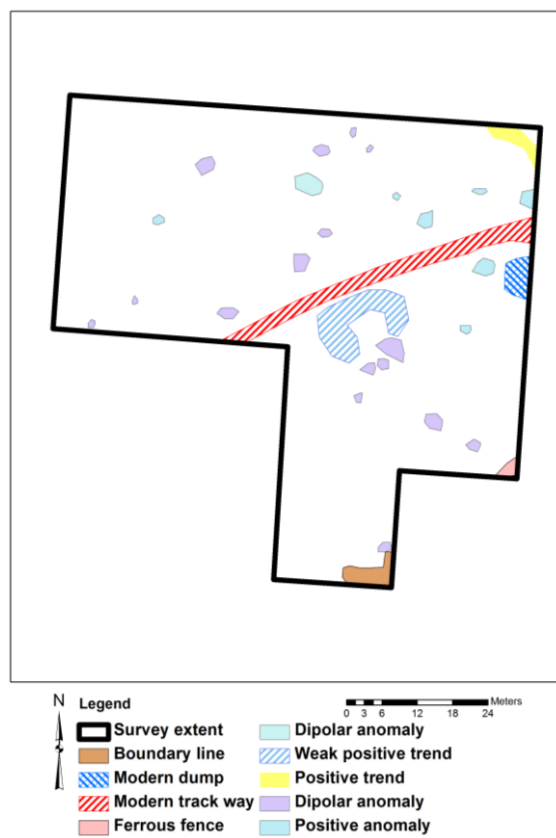
Figure 4.9   Archaeological interpretations of the fluxgate gradiometer survey of the St Ives estate.

Gradiometer surveys have found favour with commercial geophysics as larger areas of survey data can be collected at a higher resolution than traditional earth resistance arrays. However, as the St Ives data has shown earth resistance measurements can provide extra information not always recorded by magnetometer surveys. As commercial geophysical investigations of archaeological sites are performed throughout the year, gradiometer surveys are also preferred as they are not affected by seasonal variations or suffer from loss or detection of anomalies with change in soil moisture.

Therefore the research incorporated a seasonality test to examine the changing soil moisture level effects on the earth resistance values and the monthly responses from the MSP40 to further understand these issues.

4.2.0 Seasonality measurements

4.2.1 Introduction

Earth resistance measurements are affected by variations in soil moisture content as the water within the soil contains electrolytes that are capable of holding a charge that allow an electrical current to flow. Variations in the moisture and electrolyte content will directly affect the resistance values recorded during a survey, as Scollar (1990 350) discusses that earth resistance measurements are directly dependent upon the displacement of ions in the interstitial water in the soil.

Changes in earth resistance values can be detected on an hourly (Benderitter and Schott 1999), diurnal, weekly or monthly basis and are influenced by the localised weather parameters including rainfall, evapotranspiration and temperature. It was important to establish whether the MSP40 could be used throughout the year or whether the continuous data logging would be significantly affected by changes in soil moisture and fail to record 'accurate' earth resistance values when the contact resistance of the electrodes cannot be overcome.

4.2.2 Previous seasonality investigations

Al Chalabi and Rees (1962) were one of the first to investigate the effects of environmental moisture change on earth resistance measurements. Their work focused on the site of Wall in Staffordshire, a Roman military encampment that consisted of seven defensive ditches.

The net water contribution was considered (the cumulative difference between the amount of precipitate and evapotranspiration) alongside the resistance values. The data was split in to various size blocks of time preceding the monthly testing and the results found a correlation coefficient of ≥75% when the net water contribution (cumulative total) was considered for the 2 - 4 months prior to survey. The authors believed this time lag was due to the considerable time required for the water to percolate through the upper horizons of the soil. Further conclusions were drawn that suggested that short or long periods of rain had little to no immediate effect upon measurements. This may be a result of the ditch fill being a mix of turf and clay that are likely to retain water for significant periods of time before showing signs of water loss or gain.

Hesse (1966) carried out research on the effects of weather on earth resistance measurements in France. One of the major findings of the research was that a number of ditches initially produced a low resistance anomaly that disappeared under drought conditions or produced a high resistance anomaly as the ditch fill dried out. This is because the fill of the ditch dries to such a degree that no contrast can be recorded between anomalies and background resistance values. In certain conditions very large ditches cut into clay can show up as a high resistance anomaly as part of the lower ditch acts as a sump for the surrounding material and the upper ditch fill remains free draining.

Hesse's range of probe separations showed the immediate effects of precipitation on earth resistance readings. After a period of drought, a prolonged period of precipitation showed a ten-fold decrease in earth resistance values for the 0.06m probe separation whilst the 1m probe separation showed only a 10% drop in resistance readings.

Hesse's work at Camp des Matignons at Charente in France highlights the complexity of resistance measurements for soil moisture monitoring. The site was enclosed by a large Neolithic ditch cut into the chalk bedrock. The ditch fill consisted of a black earth which would normally produce a low resistance response compared to the surrounding soil. However, a high resistance response was recorded over the ditch. The ditch fill, with its larger pore spacing, is likely to have shown change in moisture quicker as the water moves more freely through the soil. This may explain the positive response as the ditch fill dried out.

This is an important result as many of the site investigations undertaken during the research project were carried on chalk or limestone bedrock. Many of the sites had thin soils over chalk bedrock so it was possible that such anomaly responses may be recorded.

The main conclusions by Hesse were that during prolonged dry periods, changes to earth resistance values were gradual but any rain falling during the dry periods caused a rapid decrease in resistance that continued to drop as the water percolated through the soil.

Clark (1980) performed a series of experiments looking at cross sectional traverses over ditches using Wenner, Double Dipole, Twin probe and Square arrays. Clark's (1996 48-56) work at Durrington Walls also incorporated measurements over undisturbed soil which was found to have a thickness ≤0.15m. The measurement of the thin soil using the 1m and 1.50m Wenner array continued to produce high resistance readings throughout the 16 month experiment regardless of precipitation volumes. This may be a result of the free draining chalk bedrock. The thin soils therefore remaining largely drained throughout the year. However, the increased density of the chalk compared to the thin top soil and wide probe separations with deeper current pathways is likely to have the greatest effect. The 1m probe separation current pathways will be at a decreased density at the near surface.

Therefore greater influence to the resistance values will come from the underlying geology due to the wide probe separation and greater depth of detection.

Clark correlated the measured resistance of the ditches with the moisture content of the soil. The net water level for each month was calculated by subtracting the potential evapotranspiration values from the amount of precipitate for the same month from information obtained from local weather stations. Clark identified that when the soil moisture content changed from a net gain to a net loss (or vice versa), then the earth resistance values varied accordingly with little lag time in response. This was identified by a phase reversal of the trace plots.

Aaltonen's (2000) research in Sweden considered the importance of seasonal variations when studying groundwater contamination due to leakage from landfill with case studies showing a variation of 15% in resistivity values throughout a year on a site of silty clay / sandy till on a crystalline bedrock. Sites located over sand and gravels with boulders on a crystalline bedrock showed fluctuations of approximately 20 % but Aaltonen (2000) suggests this reflects fluctuations in groundwater level. Karstic limestone also showed significant groundwater fluctuations over a short time due to the free draining bedrock.

Aaltonen (2001) also researched seasonal variations in resistivity measurements in five distinct geological regions in Sweden. The results showed that coarse grained soils and Gyttja clays showed a 68% and 90 % variation in mean values. Correlations were tested between resistivity with groundwater levels, precipitation and a simulated water content of the soil. Aaltonen believed such variation in resistivity values was related to groundwater levels and soil water content but not precipitation.

Aaltonen also discusses the considerable effect soil temperature has on resistivity measurements as resistivity increase significantly closer to 0°C (this is also influenced by soil type). Aaltonen used a continuous vertical electrical sounding (permanent installation) with a 5m probe separation for the research.

The coarser grained soils showed the greatest absolute resistivity changes (440 Ω m) but relative variation was greatest in the Gyttja clays (120Ωm) based around a mean of (130Ωm). Interestingly the maximum resistivity values were recorded during the autumn months (September – November) before decreasing during the winter months. This followed a similar trend in groundwater levels (as groundwater levels increase resistivity values decrease). Aaltonen used a linear correlation regression to analyse the data. The linear correlations suggested a significant correlation between groundwater and resistivity fluctuations in approximately half of the comparisons.

Only a very weak correlation (<0.1) was found between precipitation and resistivity changes. Aaltonen explains the lack of correlation as a result of precipitation often accumulating as snow so the water does not immediately enter the soil profile. Aaltonen (2001) also discusses that July- August produce the highest volumes of precipitation (in Sweden) but this is also the time of greatest potential evaporation so less precipitation enters the soil profile. However, the large probe separation (5 m) hinders the potential correlation as the depth of detection is measured over a large volume of soil and the current is interacting with the groundwater levels on several of the sites so the relative reduced influence of precipitation would be lost.

A smaller probe separation and shallower depth of detection may have produced a significant correlation between resistivity and precipitation.

Buselli *et al.* (1992) also investigated the effect of seasonal variation during ground water pollution investigations. It was noted that the narrower probe separations used in the investigation AB/2 of 10m & 20m showed significantly more variation in apparent resistivity sounding (configured as a Schlumberger array). The greater depths were likely to show less variation as the DC current is likely to be interacting with the groundwater levels which are likely to remain more stable at depth. The study also identified a 14% variation in Transient Electromagnetic Method measurements (TEM).

The change in conductivity was also believed to reflect seasonal variation in soil moisture content. Little analysis of the variation was completed but it was noted decreases and increases in apparent resistivity occurred shortly after wet or dry periods.

Cott's (1997) MPhill thesis further investigated seasonality measurements by recording results from a site at Caistor St Edmunds, Norfolk. The research focused on a 10 m x 10m grid over an archaeological ditch. Cott found that at no point did the ditch fill dry out sufficiently that the resistance values became positive above background levels with the resistivity always below the background response as has been reported elsewhere. However, Cott suggested that feature definition changed during the year and noticed differences in definition between the 0.5m and 1 m separations which Cott ascribed to the near surface ditch fill drying out at an increased rate to the lower ditch fill detected in the 1m probe separation.

Cott (1997) also critiqued previous seasonality tests that tried to correlate moisture content directly to earth resistance values. Cott suggested two main errors with such comparisons: the moisture balance does not take into account any surface run off as it assumes all precipitate is held within the soil's field capacity and that the rate of evapotranspiration is always fixed at the highest rate also referred to as the potential rate (PE).

Smith (1967; 1976) discusses a more detailed model for rates of evapotranspiration where the soil is split in to several distinct bands.

1, Soil to a depth of ≤50mm the rate of evapotranspiration is equal to the potential rate (maximum rate).

2, Soil at a depth of approximately 50mm – 100mm the rate of evapotranspiration is equal to half the potential rate.

3, Soil at a depth of approximately 100 mm – 125 mm the rate of evapotranspiration is equal to a quarter of the potential rate.

4, A total soil depth of 125mm is assumed to be the maximum depth influenced by evapotranspiration.

5, When the net gain of soil moisture content is positive the input influences the upper layers first.

If the weekly rainfall and PE are incorporated into the model then the soil moisture deficit can be calculated.

Tables of potential evapotranspiration have been established for 15 and 20 year blocks which the Metrological Office uses for its suite of information called MORECS (Metrological Office Rainfall and Evaporation Calculation Service). The MORECS information lists soil moisture balance considering potential and actual evapotranspiration for various crops by splitting the UK in to 40 km x 40 km blocks. The data set is the calculated average of weather parameters collected by weather stations within the 40 km^2 as well as the average soil type for each individual square. A grass crop is the standard ground cover used in the calculations.

Cott (1997) compared the MORECS results with those based on the specific soil type of a site with local weather station information and found a similar broad trend in results, but the values produced varied significantly due in part to the MOREC results being based on an average of a 40 km^2.

English Heritage completed an area investigation over a 18 month period (David *et al.* 2008) at the site of Stanwick Roman Villa, Northamptonshire. MORECS information was also collated to consider the soil moisture deficit for each month (Linford 2009). The English Heritage research indicated high resistance anomalies were clearest during the winter period when the soil has high moisture content, whilst low resistance anomalies were clearest in the summer months, when there was a high soil moisture deficit.

4.2.3 Current / on-going investigations

In addition to the seasonality investigation that formed part of this research, two seasonality tests are currently underway as part of on-going research at the University of Bradford. The first forms part of a PhD. research topic (by James Bonsall) considering the impact on Archaeological Geophysics by the Irish National Roads Authority NRA developing road network over the last 10 year (Bonsall 2010b ; Bonsall *et al.* 2010). The test site is at Kilcloghans Ringfort, County Galway in the Irish Republic. The project is the first test carried out on Irish soils and will provide a valuable future resource. Three array configurations are under investigation: Twin-probe, Square (MSP40) and a Wenner array (Bonsall 2010a). The seasonality testing is being carried out on a monthly basis and is intended to consider the moisture variations typical for Ireland which has a different weather regime to many areas of Northern Europe(Bonsall *et al.* 2011).

The second seasonality investigation forms part of another PhD. research project (by Robert Fry). The work forms part of a collaboration between the University of Leeds, Birmingham University and the University of Bradford. The seasonality tests form part of the DART project (Detection of Archaeological Residues using remote sensing Techniques). The work focuses on earth resistance, Electrical Resistivity Tomography (ERT), dual frequency Ground Penetrating Radar (GPR) and Electromagnetic survey (EM) to monitor changes in response over archaeological features and 'natural' soils. The aim is to increase our understanding of moisture change on geophysical results over a range of anomalies and soils (Fry *et al.* 2011).

4.2.4 Method

Test site location and information
A test site location was chosen on the grounds of the University of Bradford due to its ease of access throughout the year. The seasonal data was collected across a 20m x 20m grid (see figure 4.10). The site forms the base of the re-landscaped amphitheatre.
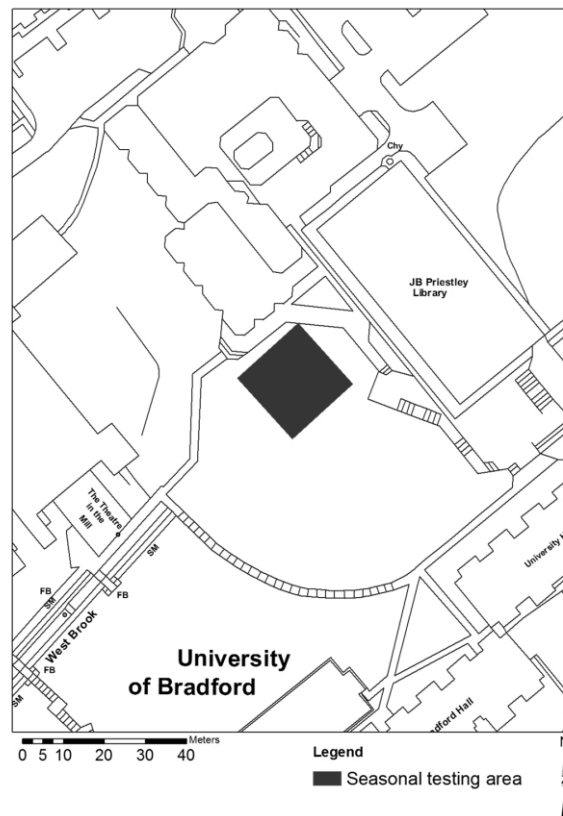
Figure 4.10   The location of the seasonality testing area at the University of Bradford (© Crown copyright / data base right 2009. An Ordnance Survey/Edina supplied service).

Geology

The underlying geology for the site and across much of West Yorkshire is part of the Coal measures (Upper Carboniferous) 280 - 240 m.y.a (Chisholm *et al.* 1996 ; Bell 2007 ; Tymon 2011).

Soil type

 Large areas of soils around Bradford city centre are unmapped (Carroll *et al.* 1979). However, Carroll *et al.* (1979) discuss the surrounding soil type as a mix of brown earths made up of coarse to fine loam. Other areas of the city are identified as Stagnogley soils and Pelo-stagnogley soils. The site has a loamy soil with the inclusion of mixed deposit top soil used to landscape the area after the demolition of the surrounding terraced housing.

Site history

The University grounds used to be a mix of back to back terraced housing that was subsequently demolished and reconsolidated with demolition rubble and auxiliary buildings associated with the Phoenix mill (see figure 4.11).

Figure 4.11   A historical map regression of the test site at the University of Bradford.

A service trench was dug across the width of the grid after 10 months of measurements that provided an opportunity to 'ground truth' the soil make up whilst introducing an additional anomaly to the data set (see figures 4.12 & 4.13). The soil profile showed 'lenses' of hardcore material and rock mixed with steel rebar. The trench was back filled with coarse sand and topped with mixed backfill.

Figure 4.12   The compacted rubble layer in the trench section.

Figure 4.13   The piping for the cabling being laid before sand was added then finally levelled with the previously excavated material.

4.2.5 Survey parameters

Multiple arrays were used to provide as many comparative data sets as possible. They were a 0.5m and 0.75m separation twin probe a 0.75m manual square and MSP40 array. The 0.75m separation twin probe was chosen as it had identical dimensions to the square arrays whilst the responses from the 0.5m twin probe were believed to more closely parallel to the depth of detection of the square array (Roy and Apparao 1971).

It was decided that monthly testing would provide sufficient information of the seasonal variation on the site. Surveys were carried out where possible in the middle of each month but this was occasionally moved to a more suitable date. A total of 16 months of survey data was collected with the MSP40 and a minimum of 13 months were collected for the twin probe surveys.

Sampling strategy (see table 4.2)

Table 4.2   Seasonality test survey parameters

Equipment & probe separation	Measurement Configuration	Sampling Interval	Traverse Interval	Method of collection
MSP40 (0.75m)	Alpha & Beta	0.5m	1m	Zig Zag (encoder wheel)
Manual square (0.75m)	Alpha, Beta, Gamma & 0.5m Twin probe	0.5m	1m	Zig Zag
Twin probe (0.75m)	Single measurement	0.5m	1m	Zig Zag

4.2.6 Data processing

Manual Square and twin probe arrays

Despike parameters

1 x X=1, Y=1, Threshold=3 and Replace=Mean

MSP40

```
2 x X=1, Y=1, Threshold=3 and Replace=Mean

1 x X=2, Y=2, Threshold=3 and Replace=Mean
```

The MSP40 data showed a greater number of spikes in the data sets (discussed later) so had additional processing to remove the additional errors in the responses.

4.2.7 Weather station information

From the research undertaken by Cott (1997) it became apparent that MORECS information would only produce an approximate moisture change for the area. However, a localised weather station would be more accurate. An evapotranspiration calculator was downloaded from Cranfield University website (Hess 2010). When weather station parameters are missing the calculator uses in-built default values for the missing data as not all weather stations have the 'complete' set of data necessary to complete the calculations. Two weather stations were found within a 4 mile radius of the site; the two sets of weather station information were collated to improve the accuracy of the evapotranspiration calculations.

Cartwright Hall (Bradford) c. 2.5 miles from test site was used for the precipitation and sun shine hours (Lat. 53.8134 Long.-1.77234).

Bingley 2 c. 3.7 miles from test site was used for the wind speed, maximum and minimum air temperatures and soil temperatures (Lat. 53.811 Long. -1.86526).

The data from two local weather stations was accessed through the BADC NERC website (2011). Data sets were combined to produce a daily and monthly output for precipitation, and net moisture (precipitation - evapotranspiration) soil and air temperatures were also collated (see figures 4.14 and 4.15). The monthly output was calculated in 30 day blocks prior to each survey day.

Occasional gaps and overlaps exist in the data due to changing time periods between survey days. The day of the survey was included in the 30 day precipitation and evapotranspiration calculations as it is likely that the weather station would have the precipitate from the previous day stored until the survey day (before being measured and emptied). The data was run through the evapotranspiration calculator using a Penman Monteith equation (Hess 2010), and the rate of evapotranspiration was then subtracted from the amount of precipitation to produce a net moisture value.
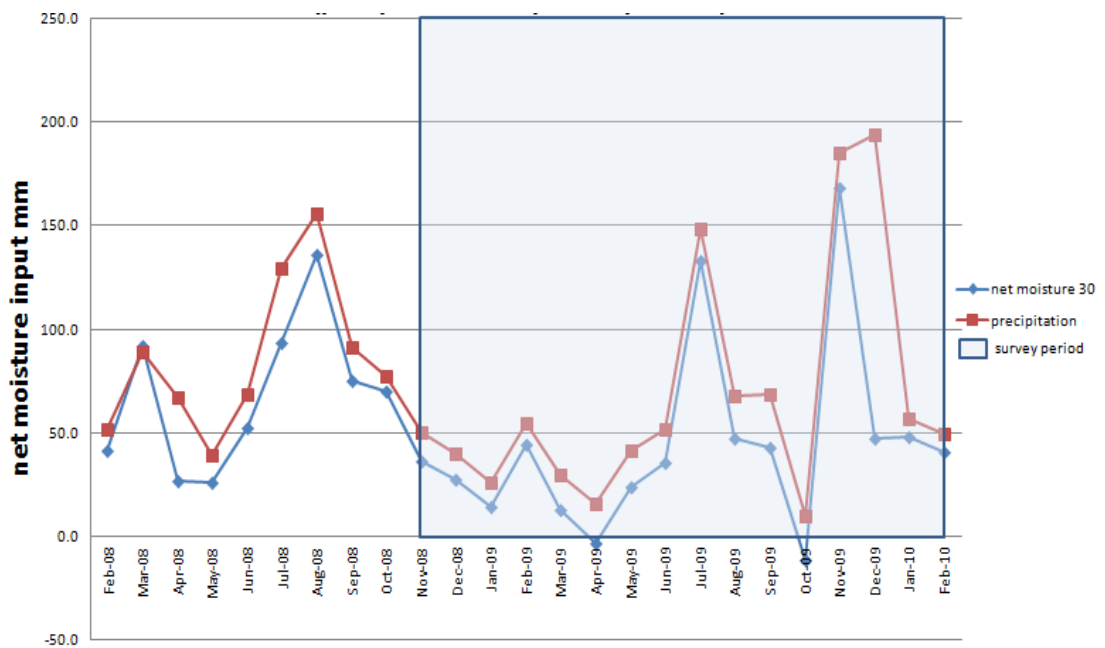
Figure 4.14   Monthly precipitation and net moisture values 30 days prior to survey (precipitation-evapotranspiration).
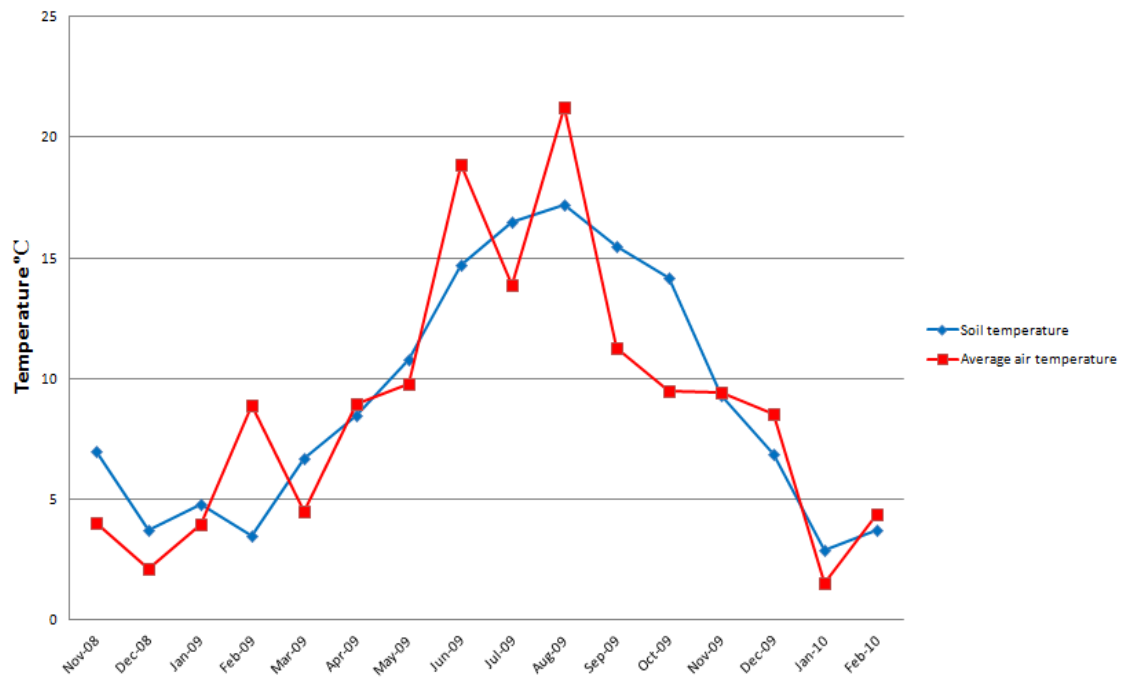
Figure 4.15   Soil and air temperatures collected on the day of survey (BADC 2011).

As the test site was flat it was not necessary to account for surface run off in the net soil moisture values, as all precipitation would infiltrate down through the soil profile or be evaporated off from the surface and be accounted for in the evapotranspiration calculations. Due to the budgetary constraints of the research detailed soil analysis was not possible as suggested by Cott (1997) so the maximum evapotranspiration rate was used throughout the experiment.

Earth resistance measurements were converted to apparent resistivity (see figure 4.16). Apparent resistivity values were then corrected for soil temperature variation based on the equation below (Keller and Frischknecht 1966 ; Scollar *et al.* 1990 19)

$$\varrho_t = \frac{\varrho 10}{1+\alpha_t (t - 10°)}$$

Key

$\varrho 10$= rho (ϱ) reference temperature

t = ambient temperature (in °C)

α = temperature coefficient of resistivity (approximately 0.022 per °C)

A reference temperature of 10 °C was chosen as this was the approximate mean value of the soil temperature through-out the testing period.
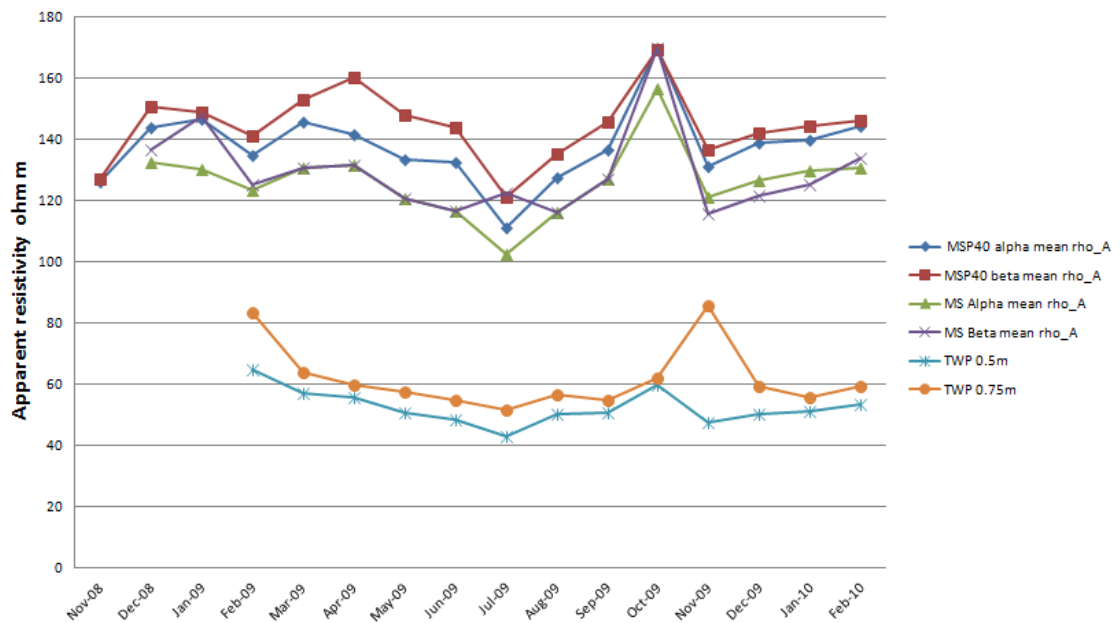
Figure 4.16   Mean apparent resistivity values of a 20m x 20m grid corrected for soil temperature variation.

Resistivity values increase significantly when soil temperature becomes closer to 0°C and so must be corrected for; see the table below for percentage change in apparent resistivity values after correction for soil temperature. Samouëlian *et al.* (2005) discuss how ionic agitation increases with temperature as water viscosity decreases. This results in a drop in resistivity values as temperature increases.

They also note that in the northern hemisphere the greatest resistivity values are recorded between September and November whilst the lowest are recorded between June and July (Samouëlian *et al.* 2005). This trend is generally seen in the Bradford seasonality data with the highest mean resistivity values in October-November and the lower resistivity values around June and July (see figure 4.16 and table 4.3).

Table 4.3   **Percentage change in resistivity for soil temperature correction.**

Survey day	% percentage change for soil temp correction
25.11.08	93
11.12.08	86
19.01.09	89
18.02.09	86
30.03.09	93
09.04.09	97
05.05.09	102
23.06.09	110
30.07.09	114
20.08.09	116
17.09.09	112
06.10.09	109
25.11.09	98
09.12.09	93
26.01.10	84
26.02.10	86

The twin probe measurements also show a significant difference in apparent resistivity values compared to the square array measurements (approximately half of the recorded apparent resistivity). This is not expected as converting to apparent resistivity should remove geometric factors associated with different arrays. The variation is likely to be caused by using the idealised twin probe conversion which specifies the remote probe at an infinite distance (Scollar *et al.* 1990 340).

However, the 0.5m twin probe does show the same broad trend but shifted downward from the square array measurements whilst the 0.75m shows a different trend.

4.2.8 Contrast factors

In order to study the effect of seasonal variations of moisture change for the different arrays it was decided to calculate a contrast factor for each array. This information could then be used to consider an optimal time of year for survey. Two methodologies for calculating contrast factors were trialled. The input data was based on earth resistance measurements which were converted to apparent resistivity to remove the array geometry effects.

The first contrast factor values (CF1 in table) were based on a fixed low resistance point and a high resistance data point chosen at random in the survey area. The low resistance value was subtracted from the high resistance value before an additional operation was performed to normalise the data. The first normalization experiment used the calculated mean of each month's data for each array.

Worked example

High rho data point November 2008

273.5

Low rho data point November 2008

55.7

Mean rho data point November 2008

135

$$\frac{(273.5 - 55.7)}{135} = 1.61$$

The second experiment used the median to normalise the data to reduce the influence of outliers in the data (CF2 in table 4.4).

High rho data point November 2008

273.5

Low rho data point November 2008

55.7

Median rho data point November 2008

127.3

$$\frac{(273.5 - 55.7)}{127.3} = 1.71$$

Table 4.4   Contrast factor results

	CF1	CF2	CF1	CF2	CF1	CF2	CF1	CF2	CF1	CF2	CF1	CF2
Nov	1.61	1.71	1.41	1.52								
Dec	1.40	1.44	1.47	1.54	1.48	1.56	1.21	1.25				
Jan	1.32	1.39	1.17	1.23	1.39	1.44	1.37	1.40				
Feb	1.20	1.28	1.23	1.30	1.20	1.25	1.24	1.32	0.94	1.31	0.88	1.54
Mar	1.42	1.53	1.21	1.27	1.21	1.17	1.21	1.10	1.11	1.63	1.26	1.23
Apr	1.41	1.55	1.40	1.83	1.34	1.40	1.34	1.45	1.35	1.92	1.38	1.30
May	1.32	1.42	1.09	1.17	1.26	1.31	1.26	1.33	1.15	1.63	1.28	1.27
Jun	1.67	1.79	1.13	1.21	1.33	1.38	1.33	1.44	1.26	1.80	1.31	1.56
Jul	1.30	1.39	1.03	1.10	1.35	1.43	1.35	1.10	1.14	1.60	1.13	1.17
Aug	1.95	2.25	1.36	1.51	1.49	1.63	1.49	1.52	1.39	1.97	1.38	1.21
Sept	1.29	1.41	1.35	1.45	1.31	1.42	1.31	1.53	1.28	1.82	1.35	1.10
Oct	1.19	1.25	1.10	1.18	1.41	1.51	1.43	1.48	1.33	1.86	1.32	1.51
Nov	1.19	1.31	1.01	1.08	1.18	1.27	1.25	1.36	1.14	1.63	0.59	1.45
Dec	1.12	1.22	1.23	1.32	1.20	1.28	1.14	1.22	1.02	1.45	1.06	1.18
Jan	1.28	1.36	1.16	1.23	1.18	1.25	1.18	1.24	1.07	1.50	0.73	1.08
Feb	1.18	1.24	1.18	1.25	1.14	1.20	1.08	1.12	1.00	1.39	1.04	1.32

Key

MSP40 Alpha

MSP40 Beta

MS Alpha

MS Beta

0.5 TWP

0.75 TWP

Highest contrast factors for each array

4.2.9 Contrast factor discussion

The results indicate August would be the optimal survey time with 8 out of 12 values having the greatest contrast. Generally late summer to early autumn would produce the best contrast for earth resistance surveys.

The 0.75 m twin probe and MSP40 Beta measurements show the greatest deviation from this trend. The 0.75 m twin probe measurement variations may be due to the enlarged volume of soil being measured with a greater depth of detection due to the wider twin probe separation. This suggests the 0.75 m twin is less prone to seasonal variation as it is less affected by the upper soil horizon and the zone of evapotranspiration.

Experiments with the use of the mean or median as a normalising factor suggests using the median value produces the best results as larger contrast factors are produced (as it is less influenced by outlier values).

4.2.10 Seasonality measurements, spatial extents of anomalies

It was decided to study the effect of seasonality measurements with relation to sizes / extent of anomalies. As the net moisture levels change, the size of anomalies as perceived in the greyscale plot are also likely to change as the soil around the periphery react to changes in moisture. The peripheries of the anomalies are likely to be shallower and more affected by the surrounding soils moisture change. Six anomalies were identified from the seasonality tests. The anomalies were chosen as they provided a range of 'types' including several linear anomalies in different orientations, a large area of high resistance and a small area of medium to low resistance.

4.2.11 Method

The data sets were exported from Geoplot 3.0 in to ArcGIS 9.3 and polygon shape files were manually created for each anomaly for each month and array. Each image exported from Geoplot was always plotted at ± 1 standard deviation so that anomalies could be compared between months and between arrays (normalised). The extent of each anomaly was calculated in ArcGIS (see figure 4.17).

4.2.12 Results

The results were tabulated and analysed for each anomaly by considering the average area in m^2, the standard deviation value for each array (for all months of available survey), the standard deviation for each anomaly (based on the averages of each array) and the total average spatial extent of the anomaly in m^2 (based on all calculated areas) (see tables 4.5 - 4.10).
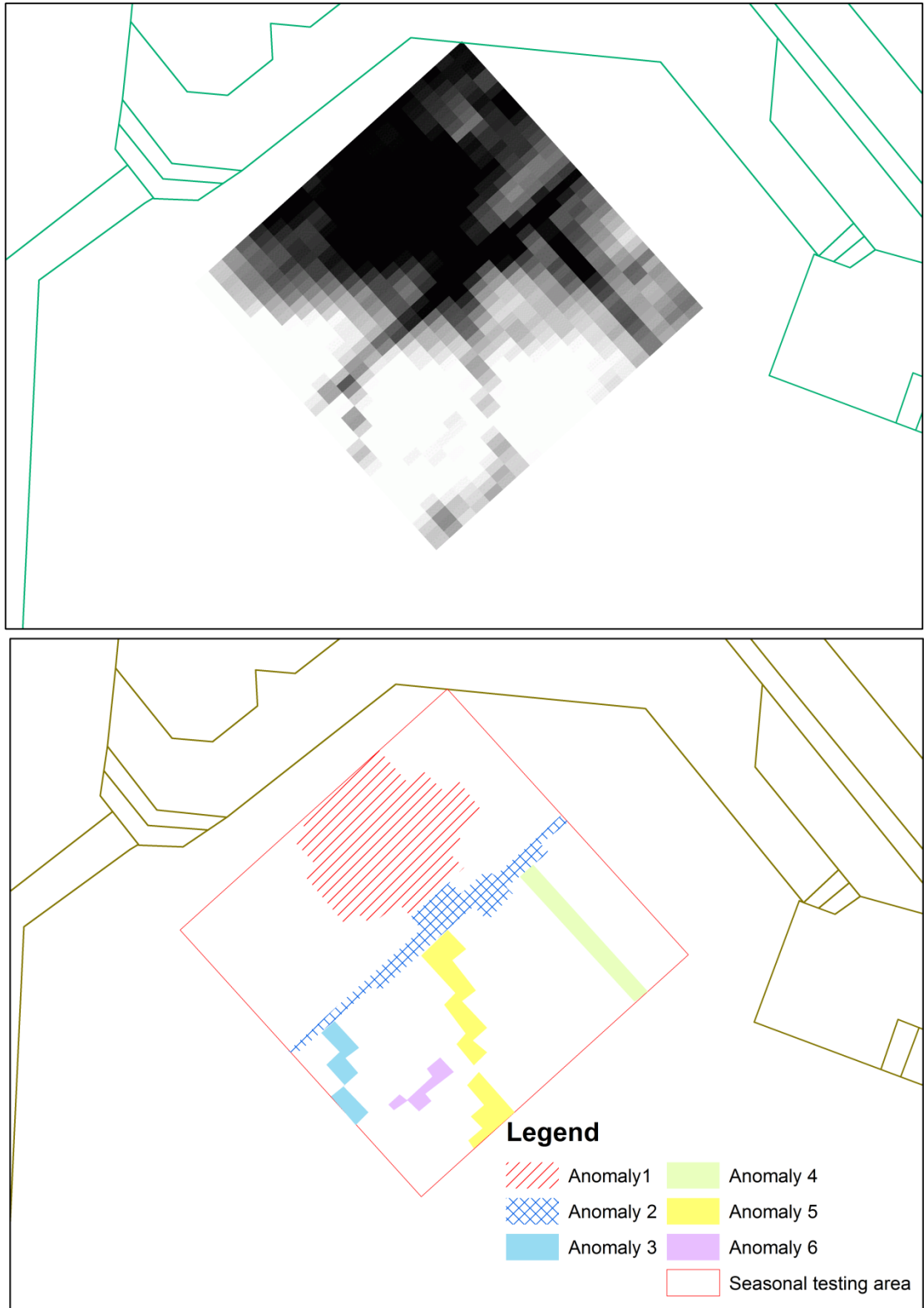
Figure 4.17   The spatial extent of the anomalies used for the area comparisons

Anomaly 1

Table 4.5   Anomaly 1 extent variation for each array.

Array	Average for array m²	STD for array	Total STD	Total average m²
MSP40 Alpha	60.7	4.4	3.1	59.6
MSP40 Beta	61.5	6.9		
Manual Alpha	61.6	2.8		
Manual Beta	61.0	4.0		
Twin 0.5m	57.1	8.3		
Twin 0.75m	54.1	6.5		
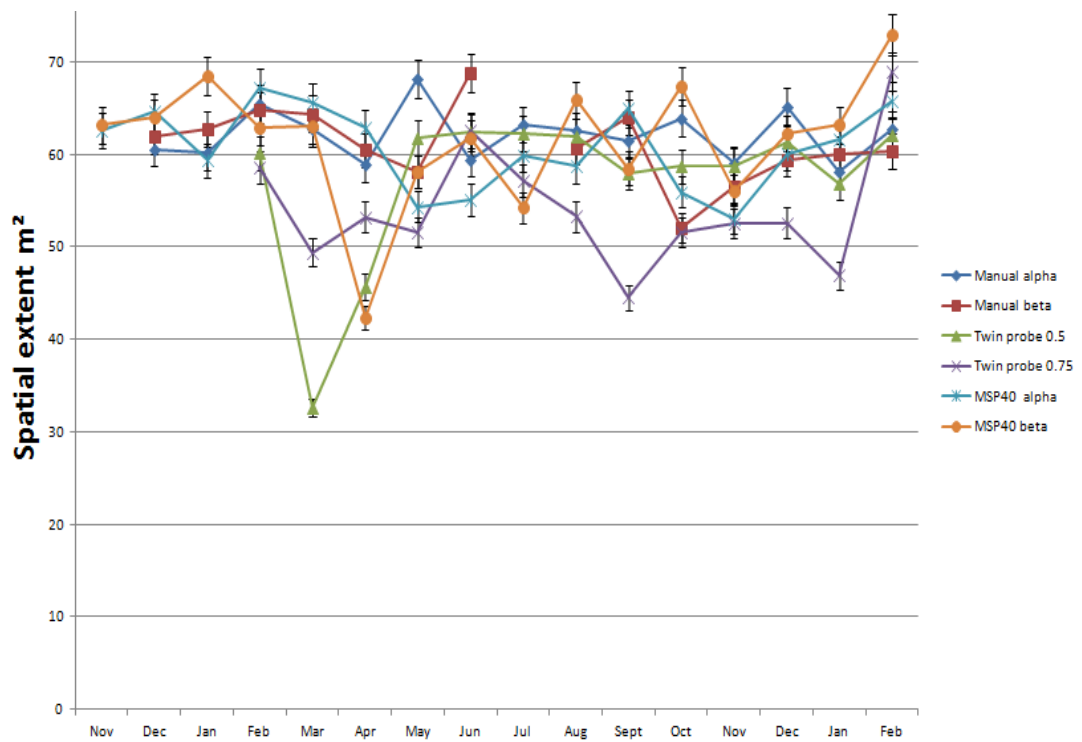
Figure 4.18   The changing spatial extent of anomaly one for different array types over a minimum thirteen month period.

Anomaly 2

Table 4.6   Anomaly 2 extent variation for each array.

Array	Average for array m^2	STD for array	Total STD	Total average m^2
MSP40 Alpha	21.4	6.2	2.4	23.1
MSP40 Beta	20.2	6.3		
Manual Alpha	27.3	5.3		
Manual Beta	24.3	7.3		
Twin 0.5m	22.9	3.6		
Twin 0.75m	23.0	3.0		
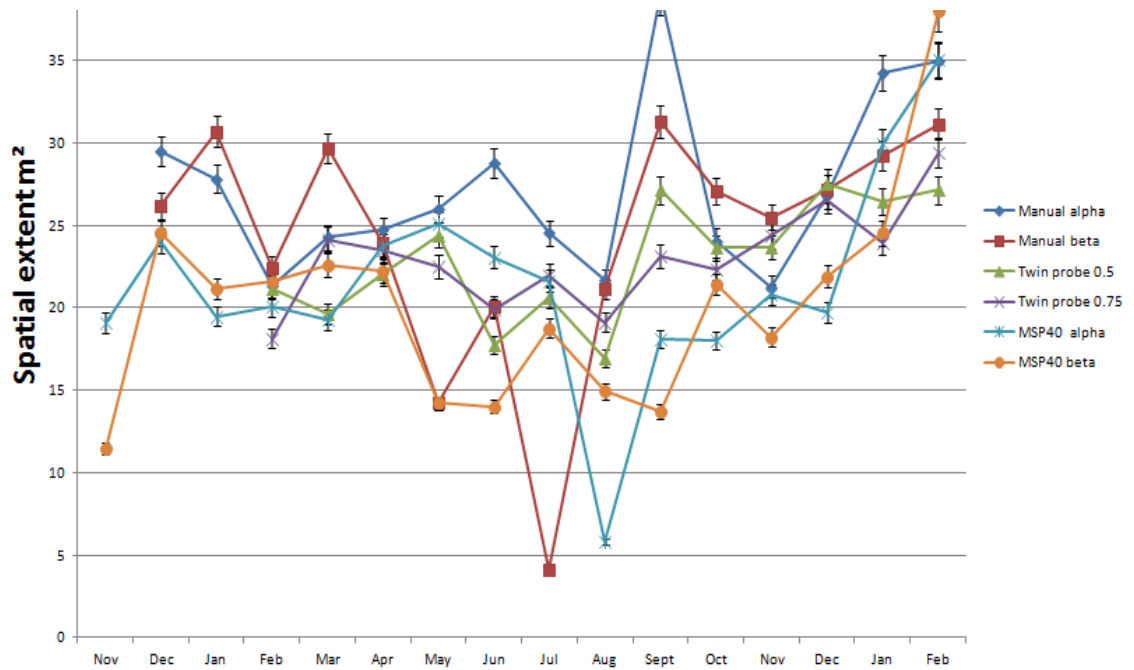
Figure 4.19   The changing spatial extent of anomaly two for different array types over a minimum thirteen month period.

Anomaly 3

Table 4.7   Anomaly 3 extent variation for each array.

Array	Average for array m^2	STD for array	Total STD	Total average m^2
MSP40 Alpha	6.6	1.4	0.8	6.3
MSP40 Beta	6.7	1.4		
Manual Alpha	6.4	0.7		
Manual Beta	7.1	1.0		
Twin 0.5m	5.6	0.7		
Twin 0.75m	5.0	1.3		
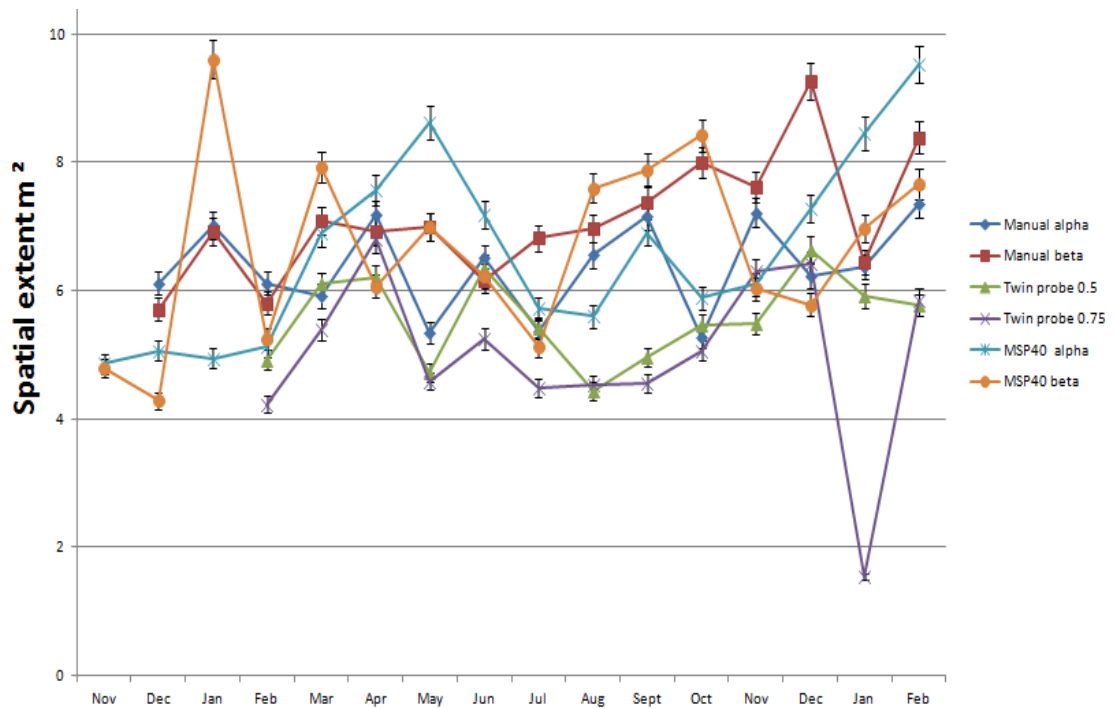
Figure 4.20   The changing spatial extent of anomaly three for different array types over a minimum thirteen month period.

Anomaly 4

Table 4.8   Anomaly 4 extent variation for each array.

Array	Average for array m^2	STD for array	Total STD	Total average m^2
MSP40 Alpha	9.2	1.1	0.3	9.5
MSP40 Beta	9.1	2.2		
Manual Alpha	9.7	1.0		
Manual Beta	9.7	1.4		
Twin 0.5m	9.8	0.4		
Twin 0.75m	9.6	0.3		
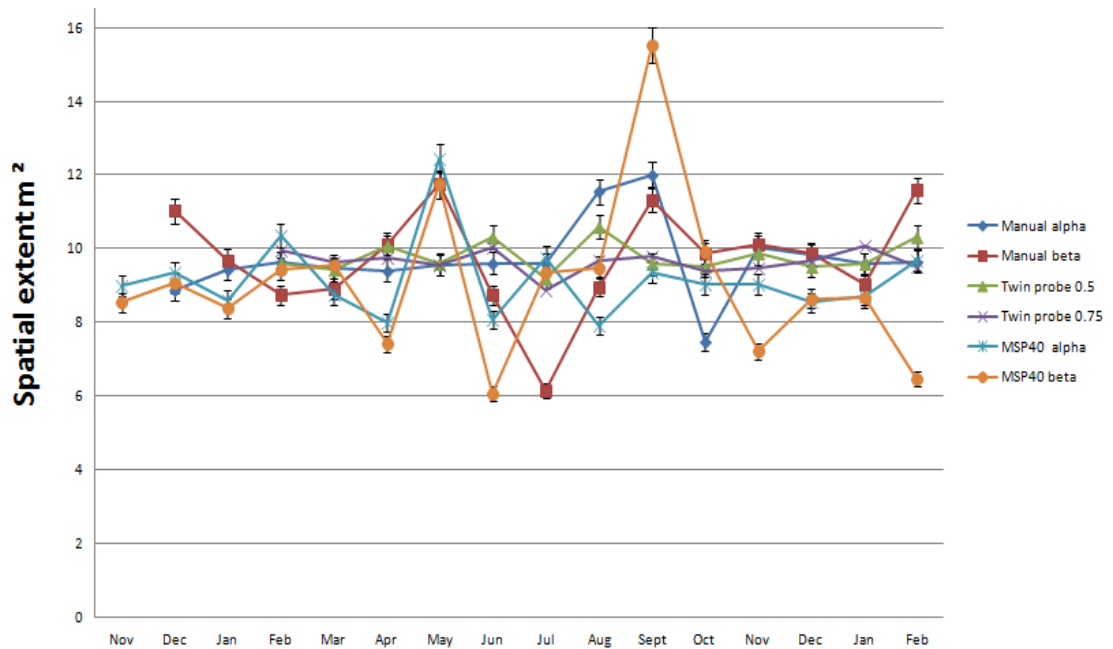
Figure 4.21   The changing spatial extent of anomaly four for different array types over a minimum thirteen month period.

Anomaly 5

Table 4.9   Anomaly 5 extent variation for each array.

Array	Average for array m²	STD for array	Total STD	Total average m²
MSP40 Alpha	13.6	2.0	0.6	13.6
MSP40 Beta	12.4	2.8		
Manual Alpha	14.2	1.6		
Manual Beta	13.9	3.0		
Twin 0.5m	13.5	1.3		
Twin 0.75m	13.7	1.6		
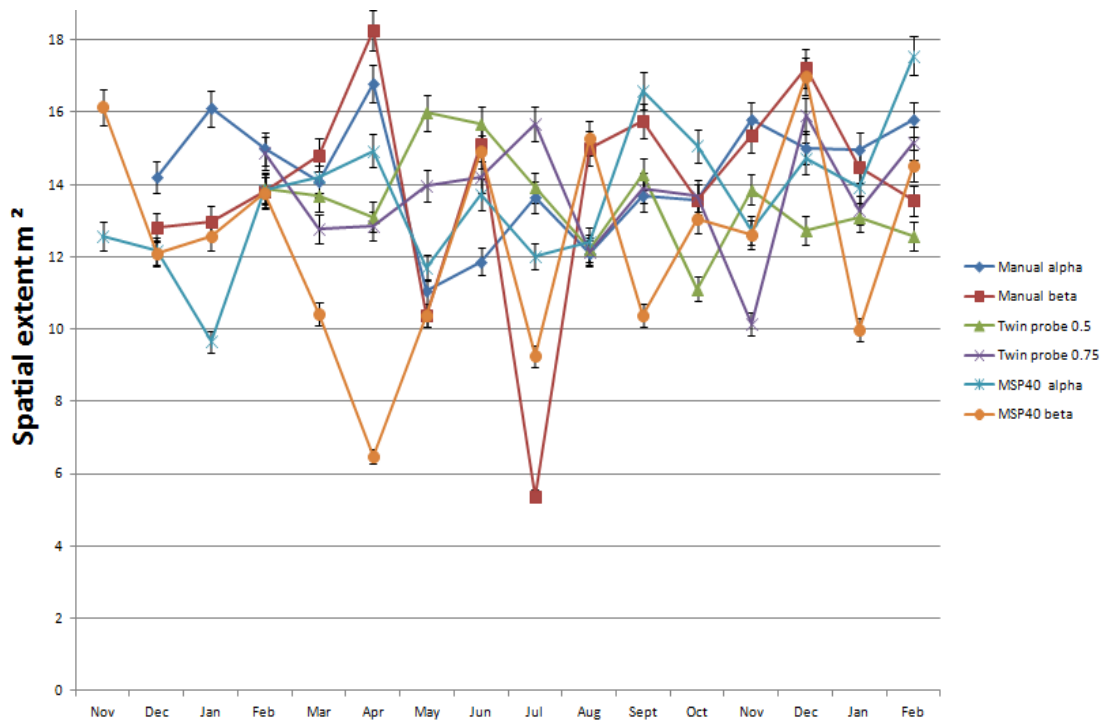
Figure 4.22   The changing spatial extent of anomaly five for different array types over a minimum thirteen month period.

Anomaly 6

Table 4.10   Anomaly 6 extent variation for each array.

Array	Average for array m^2	STD for array	Total STD	Total average m^2
MSP40 Alpha	3.8	1.8	0.2	3.7
MSP40 Beta	3.8	1.2		
Manual Alpha	3.5	2.9		
Manual Beta	3.5	2.9		
Twin 0.5m	3.9	2.7		
Twin 0.75m	4.0	4.3		
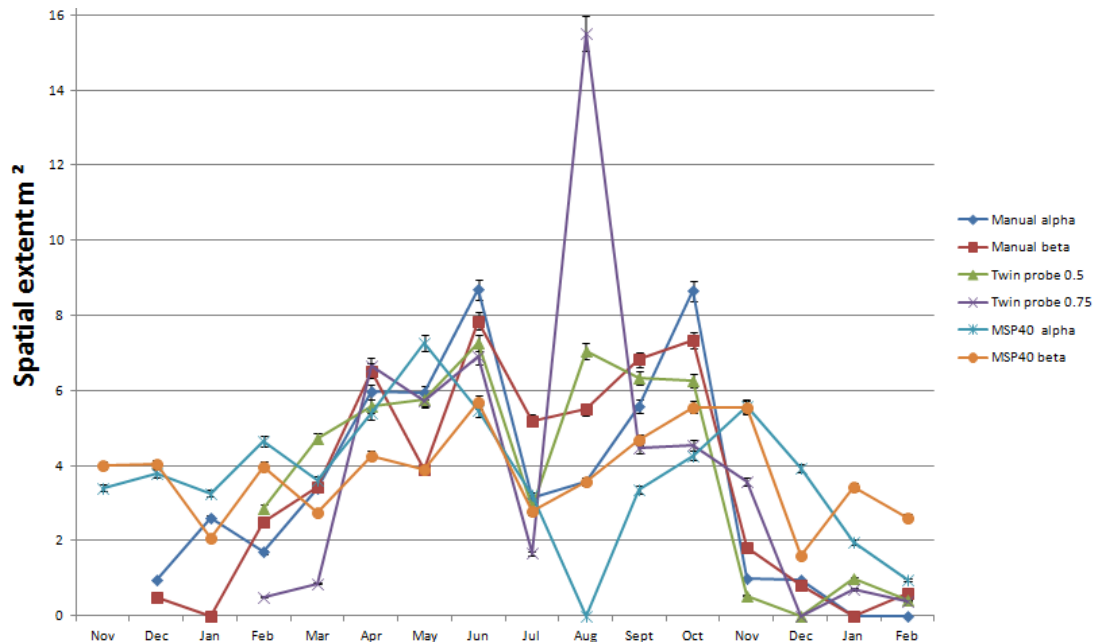
Figure 4.23   The changing spatial extent of anomaly six for different array types over a minimum thirteen month period.

Spatial extent calculations contain an average ±3% relative error based on repeatability of interpretation diagrams. Smaller anomaly areas produce large error terms in repeatability (larger anomalies produce smaller relative errors in repeatability).

4.2.13 Discussion of variations of spatial extents of anomalies

The results are qualitative in nature as it is a subjective measurement of the anomaly extent biased, by an individual interpretation. However, the results have validity as it is the same method that would be employed in any archaeological geophysics report where a decision must be made as to the extent of the anomalies.

The square array shows a greater range of standard deviation value for many of the spatial extent calculations even with a larger population size, 15 months compared to 13 months for the twin probe measurements. This may indicate the square array is more susceptible to seasonal variation as it is more likely to measure the peripheral areas of the anomaly. The results show that the MSP40 has the greatest change in anomaly size (standard deviation), which is due to the variations and errors of a near continuous collection of the MSP40 as opposed to the static collection of the manual arrays (square and twin probe). However, the spatial extent of the anomalies only shows small changes in anomaly areas throughout the year, indicating that interpretation of anomalies should be possible even at times of low contrast.

4.2.14 Seasonal variations earth resistance grey scale plots

A selection of minimally processed earth resistance data plots all plotted at ±1 STD showing the variation in data quality for the MSP40, manual square and twin probe arrays recorded during the seasonality tests.

November 2008

MSP40 Alpha   MSP40 Beta
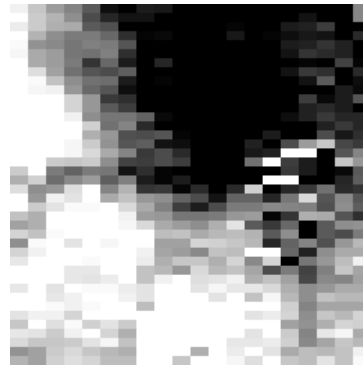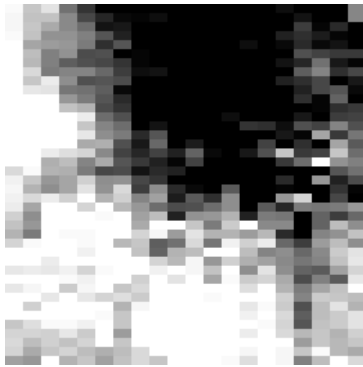
December 2008

MSP40 Alpha   MSP40 Beta
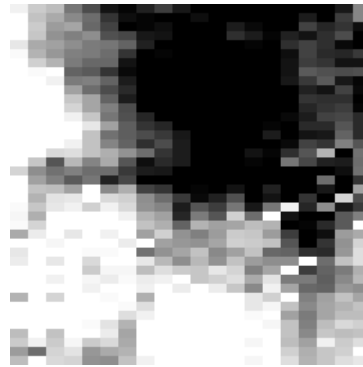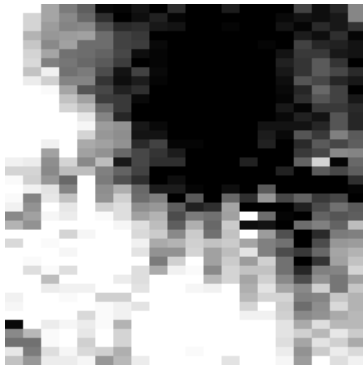
Manual square Alpha   Manual square Beta
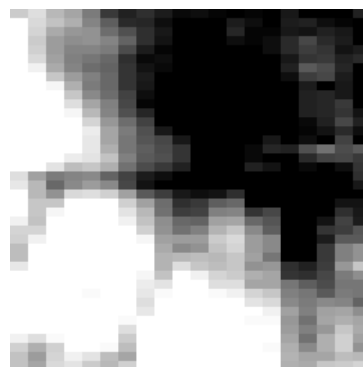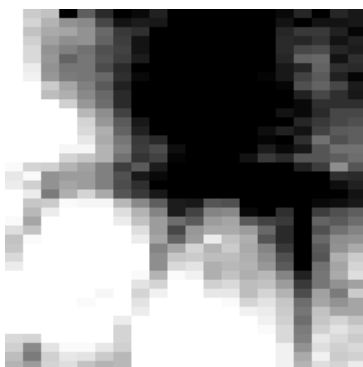
August 2009

MSP40 Alpha

MSP40 Beta
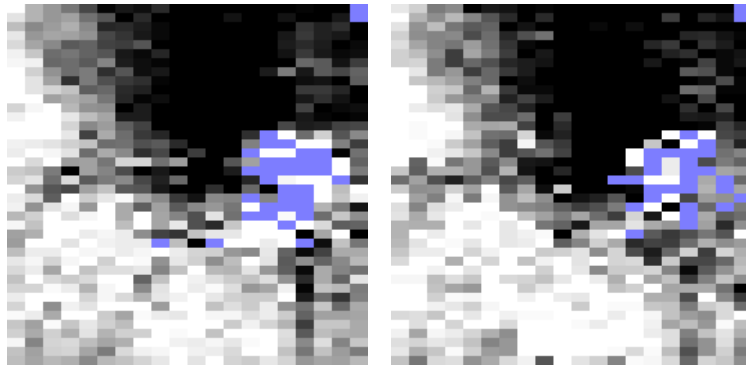
The August 2009 MSP40 data shows the issues encountered when the ground surface dries out and compacted. The large blue areas show dummy values that were used to replace erroneous negative resistance values due to poor contact and impeded current flow. For comparison see the twin probe plots below.

August 2009

Twin probe 0.5 m

Twin probe 0.75 m
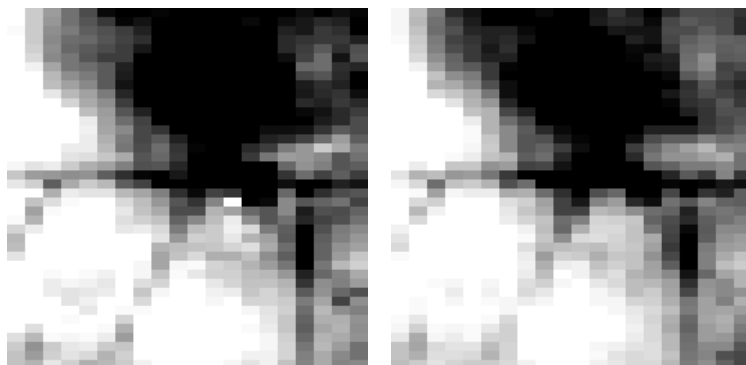
4.2.15 Precipitation, Evapotranspiration, net soil moisture and earth resistance measurements.

Seasonality tests examine the changing earth resistance measurements throughout the year. It is therefore important to consider the relationship between earth resistance values and the localised hydrological cycle. As the hydrological cycle is an open ended system both with inputs and outputs it was necessary to examine the different factors that may affect the relationship between the two variables.

4.2.16 Method

Correlation coefficients were calculated to explore the relationship between changes in apparent resistivity values compared to precipitation and net moisture change (precipitation-evapotranspiration). Correlation coefficient values were calculated for the mean apparent resistivity of each month, a single data point of 'high' and 'low' apparent resistivity values and the difference between these 'high' and 'low' values.

It was hypothesised that a negative linear relationship existed between the variables as increases in net soil moisture should reduce the apparent resistivity as the electrical current flows through the soil medium more easily (see figure 4.24 and 4.25). As a 'low' resistance data point was also measured the correlation coefficient values were expected to show a weak positive relationship (closer to 0) as the value remains low throughout the year.
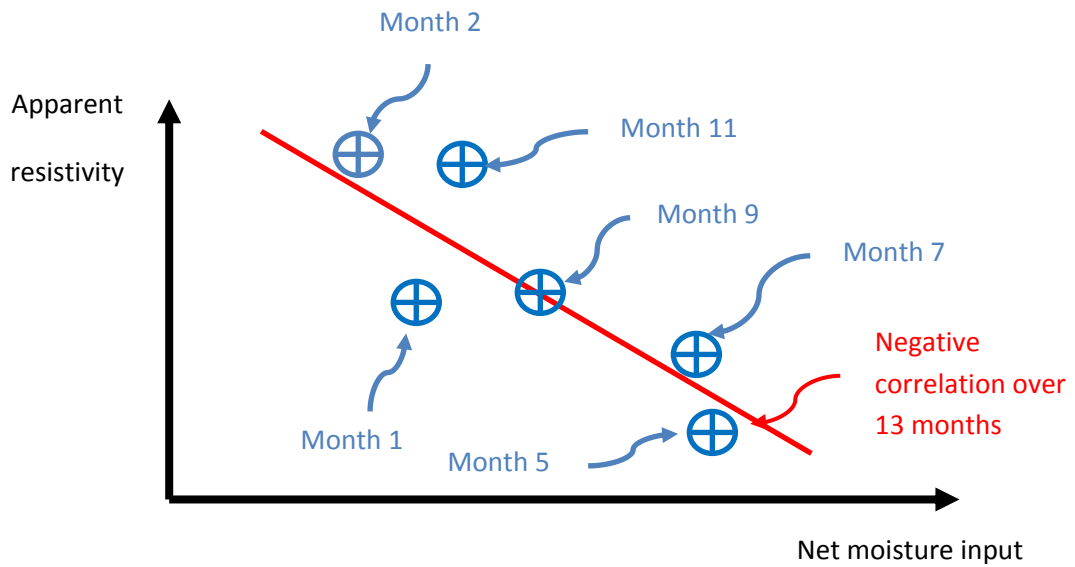
Figure 4.24   The negative linear correlation coefficient relationship between resistivity and net moisture input based upon Parkyn *et al.* (2011).
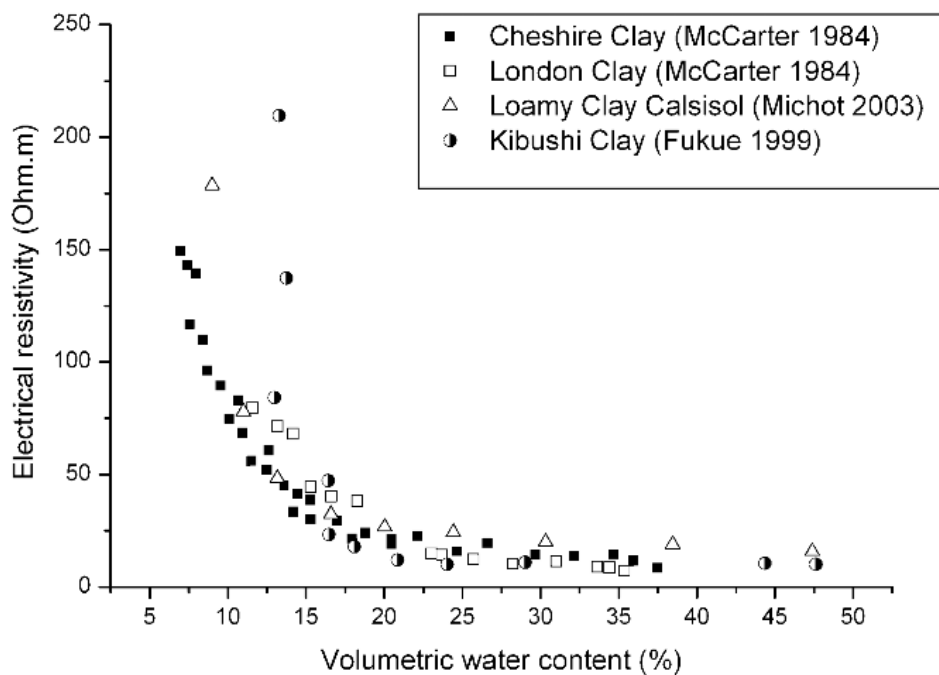
Figure 4.25   The recorded variation in volumetric water content and electrical resistivity for four different clay soils. From Samouëlian *et al.* (2005):178.

Part of the investigation included looking at lag effects on earth resistance measurements after precipitation events. Some previous investigations suggested precipitation shortly before a survey had a greater effect on earth resistance values than long term weather patterns. Therefore lag times of multiple 30 day periods were considered (up to 11 months prior to survey) alongside a daily cumulative net moisture running total, to examine the time required for the water front to reach the archaeological feature (see figure 4.26).
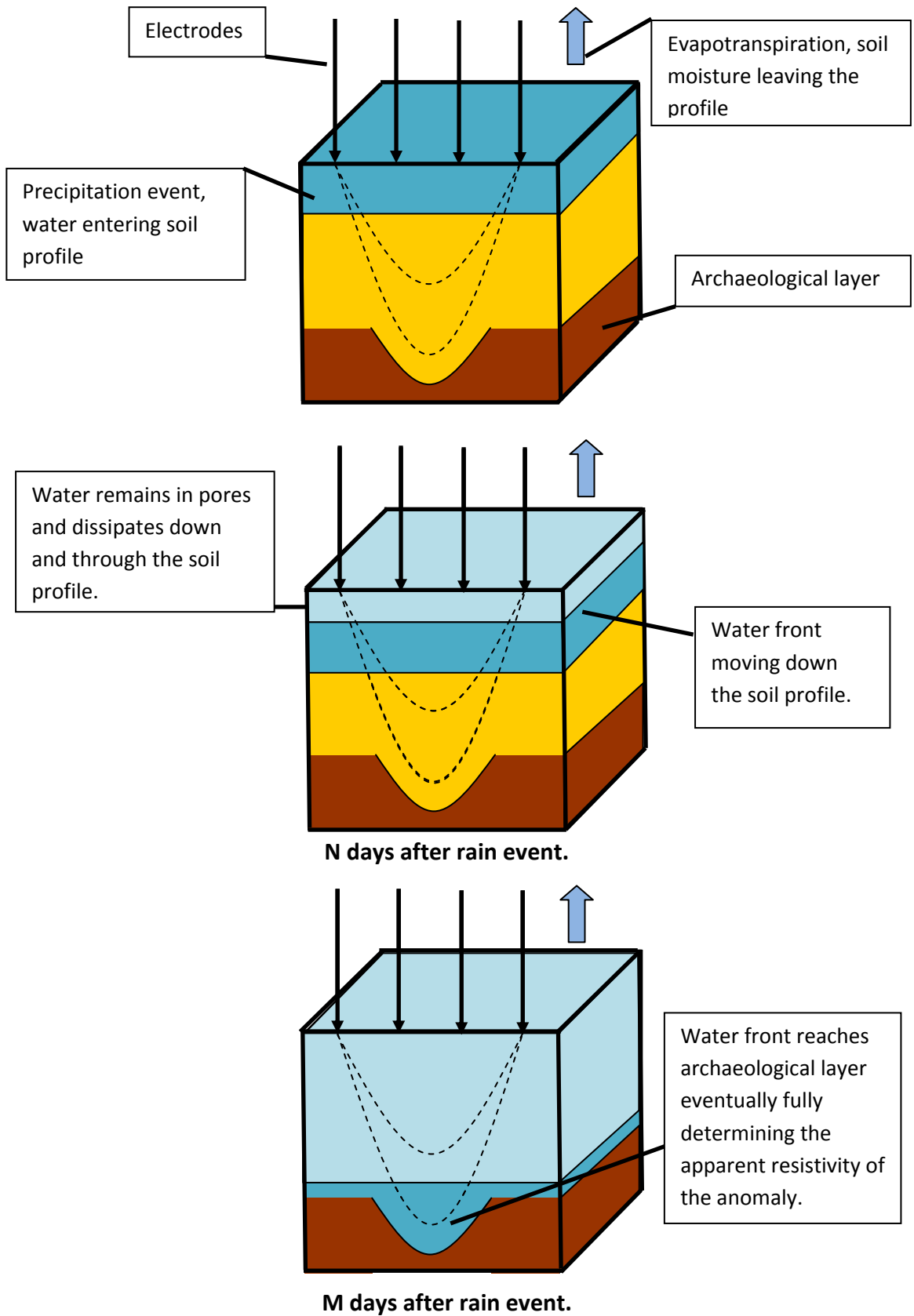
Figure 4.26   A simplified water front moving down a soil profile to an

archaeological feature (based upon (Parkyn *et al.* 2011)).

4.2.17 Results

As evapotranspiration calculations require additional time to compute it was decided to consider if precipitation alone would provide a suitable comparison for correlation coefficient test. The results indicated in over 75% of the results that the correlation coefficient values increase in significance when using the net moisture calculations (precipitation – evapotranspiration) (see figure 4.27). Therefore the extra information should be considered and provides a more accurate understanding of the soil moisture content (see figures 4.28-4.35).

Figure 4.27 A line graph plot of the calculated correlation coefficient values for the mean resistivity of the manual square (Alpha), MSP40 (Alpha) and 0.5m twin probe array compared to the net soil moisture input and precipitation alone in 30 day blocks prior to each survey.
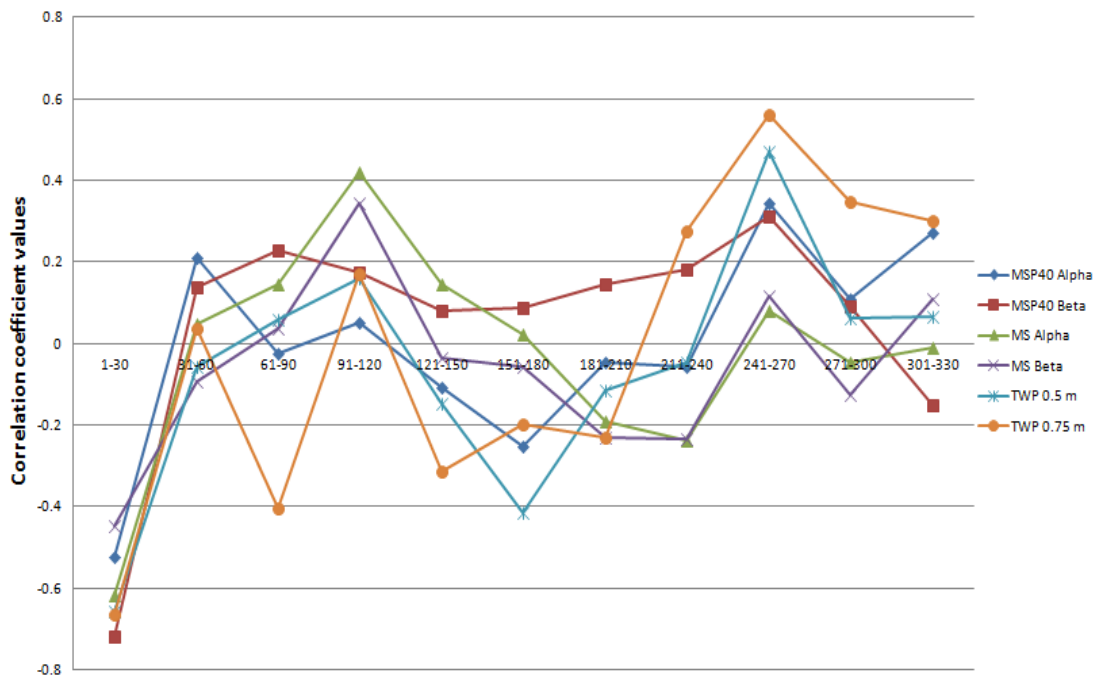
Figure 4.28   A line graph plot of the calculated correlation coefficient values for the calculated difference in resistivity values of a 'high' and 'low' data point for each earth resistance array compared to the net soil moisture input in 30 day blocks prior to each survey.
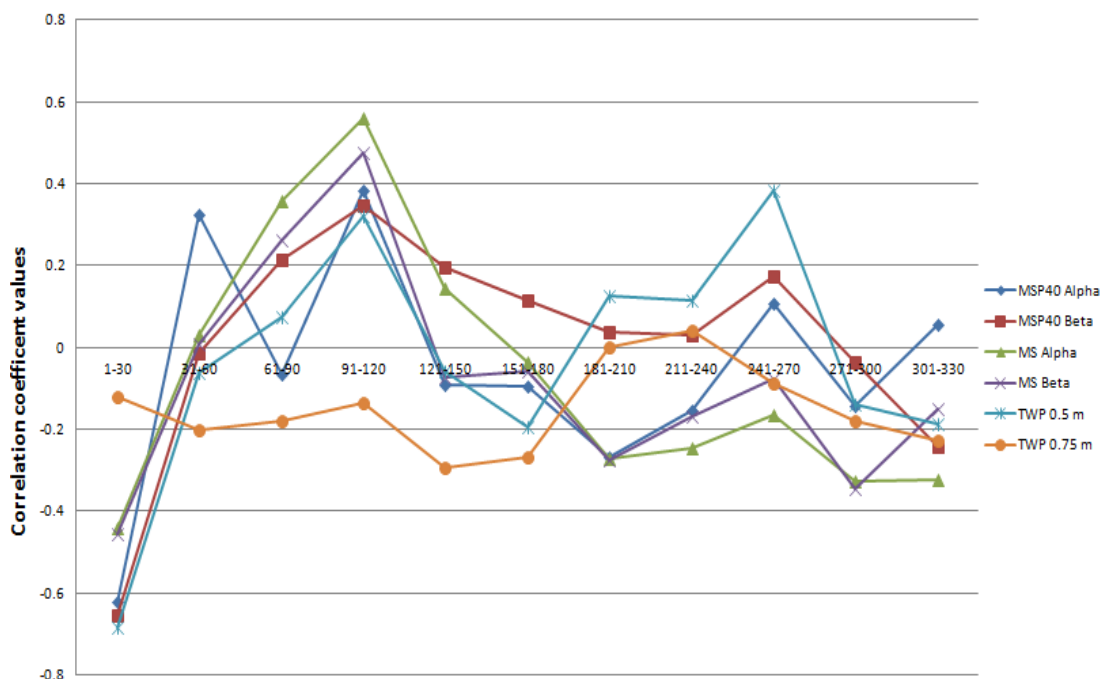
Figure 4.29   A line graph plot of the calculated correlation coefficient values for a 'high' resistivity data point for each earth resistance array compared to the net soil moisture input in 30 day blocks prior to each survey.
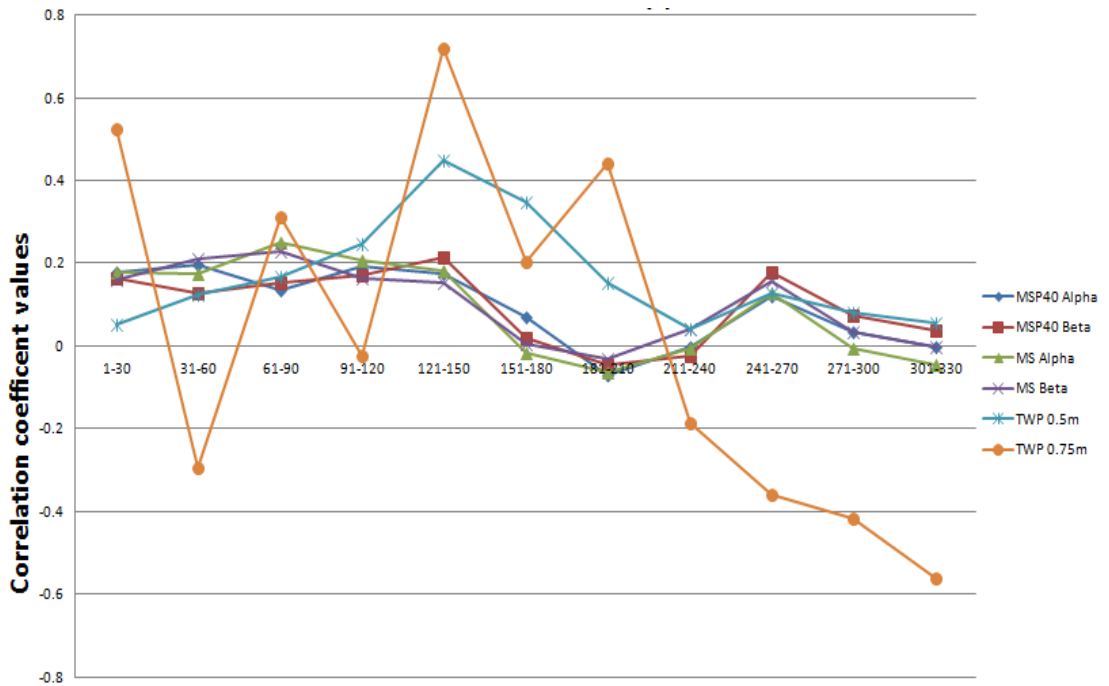
Figure 4.30   A line graph plot of the calculated correlation coefficient values for a 'low' resistivity data point for each earth resistance array compared to the net soil moisture input in 30 day blocks prior to each survey.
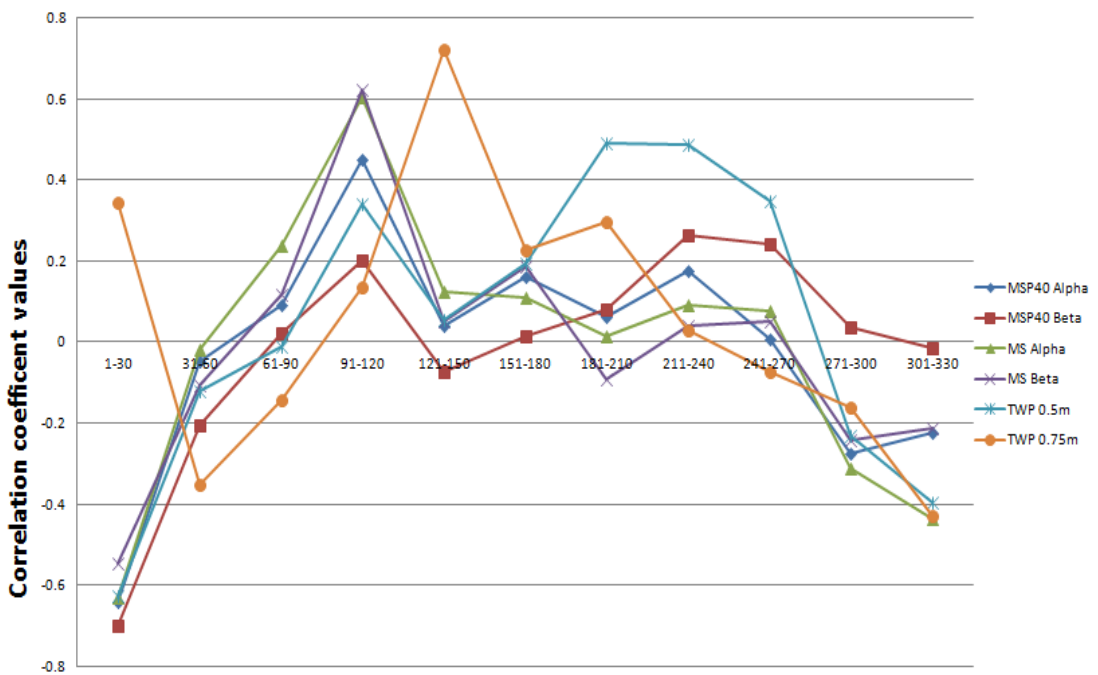
Figure 4.31   A line graph plot of the calculated correlation coefficient values for the calculated mean resistivity values for each earth resistance array compared to the net soil moisture input in 30 day blocks prior to each survey.
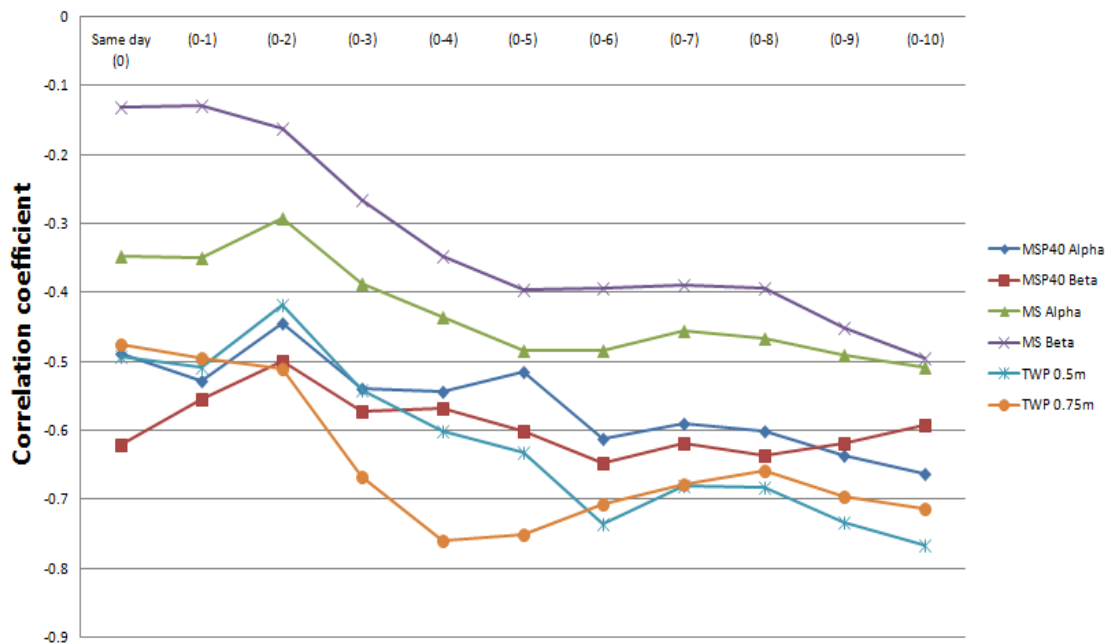
Figure 4.32   A line graph plot of the calculated correlation coefficient values for the calculated difference in resistivity values of a 'high' and 'low' data point for each earth resistance array compared to the net soil moisture input in days prior to each survey.
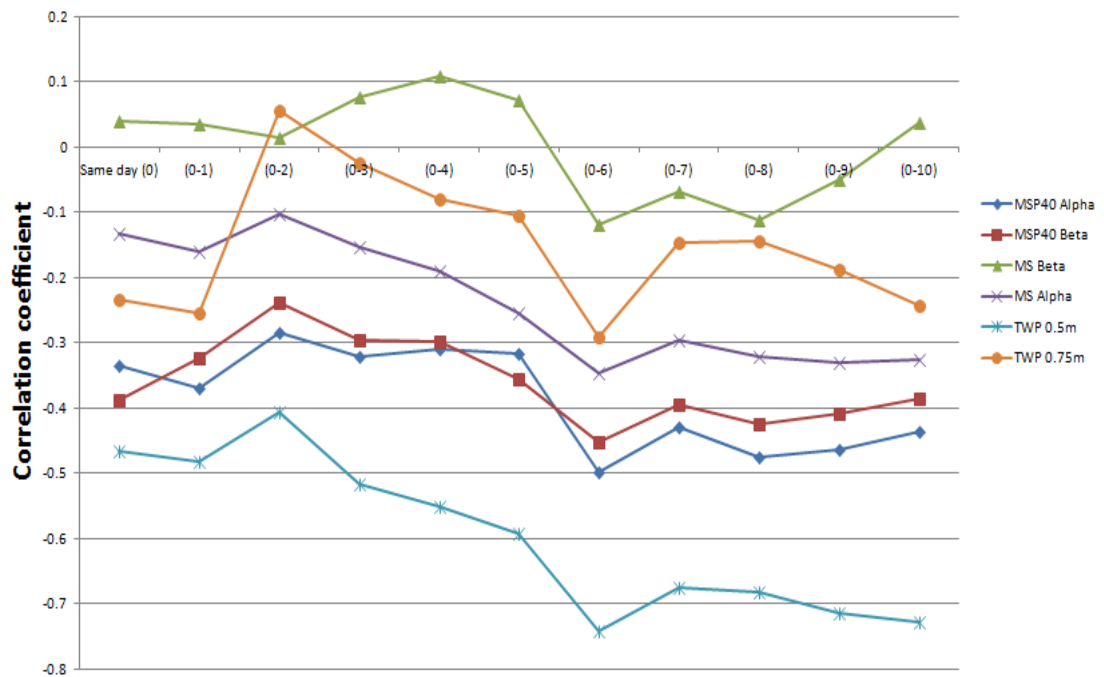
Figure 4.33   A line graph plot of the calculated correlation coefficient values for a 'high' resistivity data point for each earth resistance array compared to the net soil moisture input in days prior to each survey.
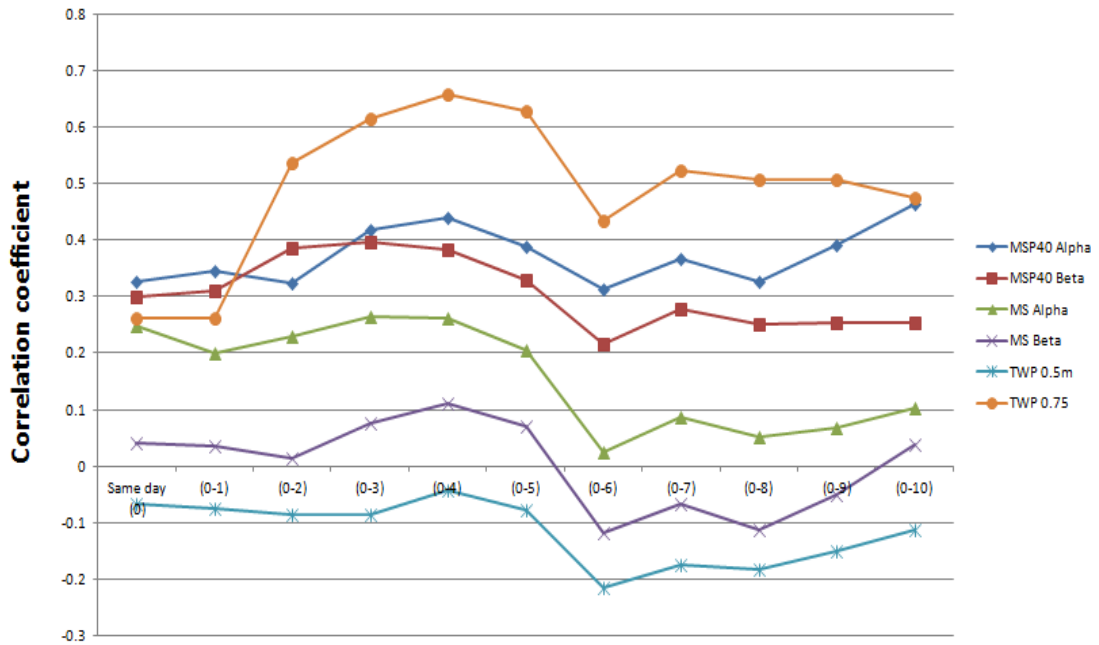
Figure 4.34   A line graph plot of the calculated correlation coefficient values for a 'low' resistivity data point for each earth resistance array compared to the net soil moisture input in days prior to each survey.
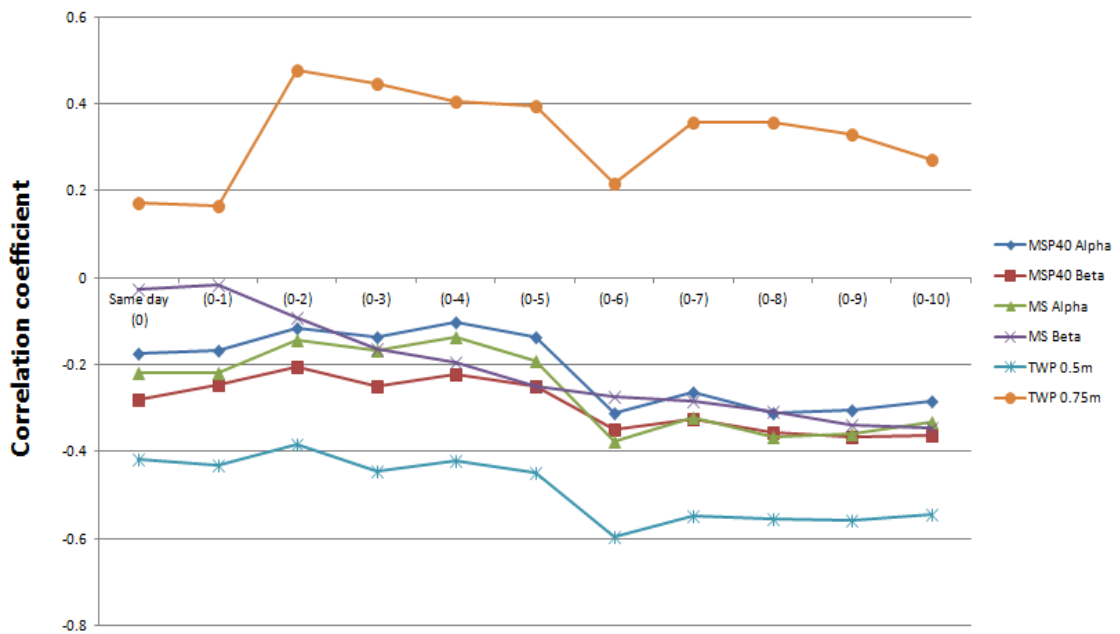
Figure 4.35   A line graph plot of the calculated correlation coefficient values for the calculated mean resistivity values for each earth resistance array compared to the net soil moisture input in days prior to each survey.

4.2.18 Discussion

The results show that as net soil moisture input increases apparent resistivity decreases producing a negative linear correlation (see figure 4.32). However, the low resistance anomaly shows a weak positive correlation (see figure 4.34).

When considering lag times the strongest negative correlation occurs between the net moisture input and the apparent resistivity in the 1-30 day period prior to survey. With the cumulative net moisture values of approximately 5-6 days before the survey showing the strongest negative correlation coefficient.

The results show that in all investigated conditions the 0.5m twin probe array behaves similarly to a 0.75m square array. However, the 0.75m twin probe array measures a different soil volume with increased depth of detection so is influenced less (under these conditions) by water entering the soil (compared to the 0.5m twin).

The seasonality data shows the MSP40, manual square and twin probe arrays can be used throughout the year but the MSP40 is prone to recording more errors when the soil has dried out and become compacted. This may occur as large spikes or areas of negative values where the MSP40 has failed to record an accurate measurement. However, the results are biased against the MSP40 as it uses continuous collection whilst the other arrays are manually inserted so additional pressure or repositioning of the array can be performed to get an accurate reading.

Achieving greater electrode (wheel) penetration of the ground surface would be a possible solution to more compact and dried out top soils but this would have greater impact on the archaeological layers. Wheel choice and impact assessment forms an important part of the MSP40 research and is discussed in more detail below.

4.3.0 Wheel tests, impact assessment and ground cover variation

4.3.1 Introduction

Chapter 3's discussion of additional gradiometer and GPS instruments showed how the MSP40 can be used to reduce impact on archaeological sites by integrating additional sensors to the cart-based earth resistance array. The reduction of physical impact coming from an ability to maximise the amount of information gained from a single traverse therefore reducing trampling across the site.

However, it is important to assess the physical impact of the MSP40 and identify ways to reduce impact without sacrificing data quality. One important aspect to consider when trying to reduce the damage caused to archaeological sites is the wheel option as the spikes penetrate the ground surface. The wheel choice (see chapter 3.5) can influence the success of a survey; an optimal configuration should reduce contact resistance issues, remain unaffected by vegetation cover and soil types whilst still being practical to pull by hand.

4.3.2 Spike impact assessment

As the project's aim is to develop and test the system for rapid low impact assessment on archaeologically sensitive sites it is vital to assess the MSP40's potential impact on the soil. The cart uses small bolts as probes on the wheels, which add grip and act as additional contact points with the soil medium. Therefore it is necessary to consider the potential damage to the top soil that the insertion and rotation of spikes may have.

The MSP40 spikes leave visible impressions in the ground and it was important to measure and model the depth of penetration. As the spike damage was fairly ephemeral it was decided to research how forensic investigators produce casts of tyre and foot imprints.

Tyre and shoe evidence in forensics can leave both three-dimensional impressions and two dimensional patterns on hard surfaces. Gardner (2005) argues the primary method for recovering impression evidence is the use of rubberized casting compounds such as silicon and rubber for tool marks and stone cast for three-dimensional impressions. Two pilot study tests were trialled to assess the most suitable casting medium, the first using silicon based resin, the second using stone cast (a fine grade Plaster of Paris). Fisher (2004 253) suggests more accurate casts are produced by pouring the stone cast away from the impression and letting the casting material flow into the cast area. This helps maintain the original shape as pouring can destroy the impression.

4.3.3 Method

Two wooden sand boxes were built with the dimensions of 180cm x 8cm x 6cm; each box was lined with low density Polyethylene sheeting to retain the moisture. The boxes were filled with fine grade sand so that any disturbance from the cart wheels would be preserved. Sand was chosen as a suitable medium as it is frequently used as a mould in casting processes due to its cohesive nature but is still friable enough to model the cutting action of the spikes. A fine grade children's play sand was purchased as it had been cleaned and sorted and would not raise an issue of disposing of 'soil' after the experiments.

The MSP40 was assembled then lifted directly on to the surface before the cart was pulled along the box and lifted off at the other end. The RM15 and DL256 were also fixed to the cart so that the cart was at the usual survey weight.

After the imprints had been made several tests were performed to identify the most suitable casting medium. A silicon based resin compound was trialled after necessary health and safety forms were completed. The catalyst was added at a 1:50 ratio to the resin and mixed together following the instructions supplied with the chemicals. The resin was poured on to the sand surface away from the holes and allowed to gradually fill the spike impression.

The silicon resin was then allowed to cure for a 48 hour period before being removed from the sand boxes (see figure 4.36).

Figure 4.36   The impressions left in the sand from the normal spiked wheel, the spikes cut and ripped the sand surface whilst the wheels compacted the sand.

For the stone cast trials crushed coloured chalk was lightly sprinkled into the impressions as the chalk was chemically similar to the stone cast so it would not affect the casting process and acted as a visual confirmation that the plaster had moulded the full impression.

The experiment was repeated with several wheel options. The initial testing was performed using a normal spike which projects 40 mm above the wheel rim. The short spikes were also tested and these have a 25mm length. The third setup was a bare wheel with the bolt holes covered on the inner rim with electrical insulation tape to stop material being forced up through the bolt holes.

4.3.4 Spike impact assessment results

The casts from the silicon resin showed that the viscous nature of the resin forced the sand apart as it was flowing in to the spike impressions creating an unrepresentative cast. However, the resin did achieve good surface impressions of the tearing of the sand surface but no further tests were performed (see figure 4.37).

Figure 4.37   A close up of the surface 'tearing' and the results of the unsuccessful silicon resin experiment.

The imprints left by the cart clearly show the damage caused by the cart spikes (see figure 4.38). The normal spikes unsurprisingly do the most damage causing v shaped gouges. However, all three wheel variables showed significant signs of compression on the wet sand with approximately 10mm of compression on average below the surface.

Figure 4.38   A photograph of the stone casts of the normal spiked wheel experiments with the crushed blue chalk adhering to the cast.

Normal Spike 40 mm

6mm

7mm

36m

12mm

27mm

600 mm
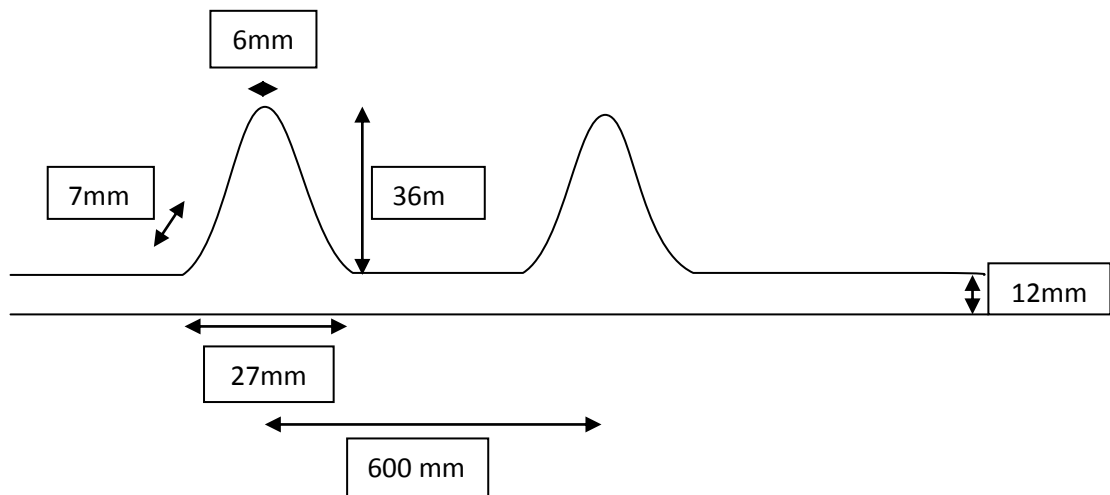
Figure 4.39   The dimensions of the normal spiked wheel experiments measured from the cast.

Short spike 25mm
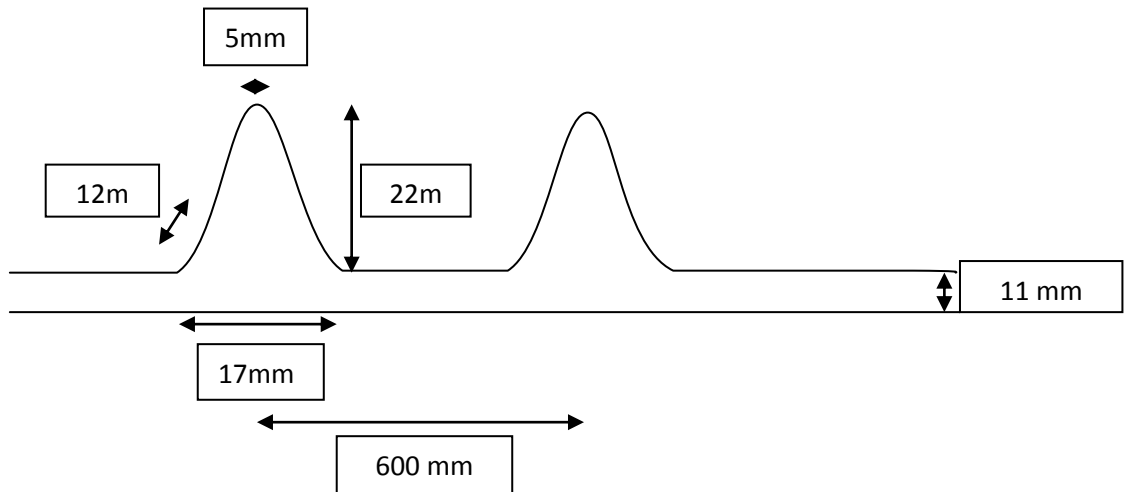
Figure 4.40   The dimensions of the short spiked wheel experiments measured from the cast.

Non-spiked wheel
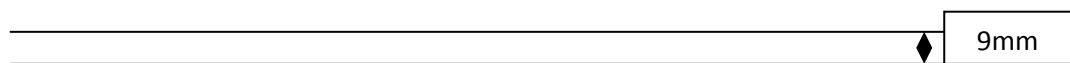
Figure 4.41   The compression depth of the sand under the bare wheel tests.

For comparison purposes a twin probe spike was also cast.

Twin probe spike
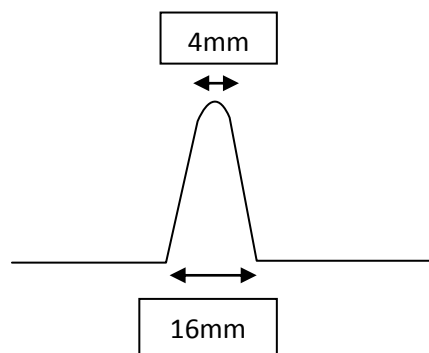
Figure 4.42   The dimensions of a Geoscan Research PA5 frame spike measured from the cast spike model.

The maximum spike penetration of a twin probe electrode is 125mm but this is rarely achieved unless the site is frequently ploughed with friable soil or has high moisture content. A 20-50mm average penetration is more likely depth extent.

4.3.5 Spike impact assessment discussion

The results show that a bare wheel system would be the optimal configuration to reduce the damage to archaeological sites; however it is important to understand the limitations of such a configuration. The amount of compaction of the sand may also indicate a significant impact on the soil as research looking at the effects of agricultural machinery on soils suggests compaction of the soil profile can drastically alter the soil processes and increase erosion (Horn and Fleige 2003).

The seasonality test site provided further observational information on the potential damage caused by the cart. When the soil was dry virtually no damage was visible other than the small incisions from the wheel spikes (see figure 4.43 and 4.44).

Figure 4.43   Small cut marks of the normal spiked wheels from the MSP40 visible in the dry turf layer.

Figure 4.44   Faint track lines left by the MSP40 during a survey, which is due to the light reflecting off the compressed grass which quickly recovers. Some are highlighted in red.

Several of the monthly tests had significant quantities of rainfall on the days immediately preceding the test days and during the survey. This increased the ground disturbance as the spikes cut into the soil and picked up wet grass and soil much more easily (see figure 4.45).

The build up of material may have consequences for survey results. When using the optical encoder wheel the sampling accuracy may also be affected as the material accumulates. The accumulation of material changes the diameter of the wheel which in turn increases the distance travelled per revolution. This affects the calibrated sampling intervals established at the beginning of the survey. These issues can be solved by regular cleaning of the wheel rims or by the use of the time based collection mode but need to be incorporated into good survey practises.

Figure 4.45   The normal spiked wheel rims 'caked' with material after partially surveying a 20m grid.

Further discussion of the build up of material can be found in section 4.4.2. As the spike impact results showed a bare wheel had the least physical impact on the soil it was decided to investigate further with a bare wheel configuration.

4.3.6 Bare wheel tests

As the spike's length is directly related to the depth of soil penetration and potentially the amount of soil displacement then it was important to test the non-spiked wheel as a means of site investigation. As a considerable amount of data had been collected on the Bradford University test area it was decided that this would be a suitable location for a pilot study.

4.3.7 Method

Survey details (see table 4.11)

Table 4.11   Bare wheel test survey parameters

Equipment & probe separation	Measurement Configuration	Sampling Interval	Traverse Interval	Method of collection
MSP40 (0.75m) normal spike and bare wheel.	Alpha & Beta	0.5m	1m	Zig Zag (encoder wheel)

4.3.8 Data processing

(All data sets were despiked using the parameters)

X=1, Y=1, Threshold 3 & replace with mean.

X=2, Y=2, Threshold 3 & replace with mean.

The Beta data with normal spiked wheels had a destagger applied of -1 across the grid with a line pattern of -2-4-6-8 to account for the visible displacement of data on the alternating traverses of the linear anomalies.

4.3.9 Bare wheel vs. normal spiked wheel tests results

Bare wheel Alpha measurements	Normal spiked wheel Alpha
09.04.09	measurements
	20.03.09

-1 STD   +1 STD

Bare wheel Beta measurements	Normal spiked wheel Beta measurements
09.04.09	20.03.09
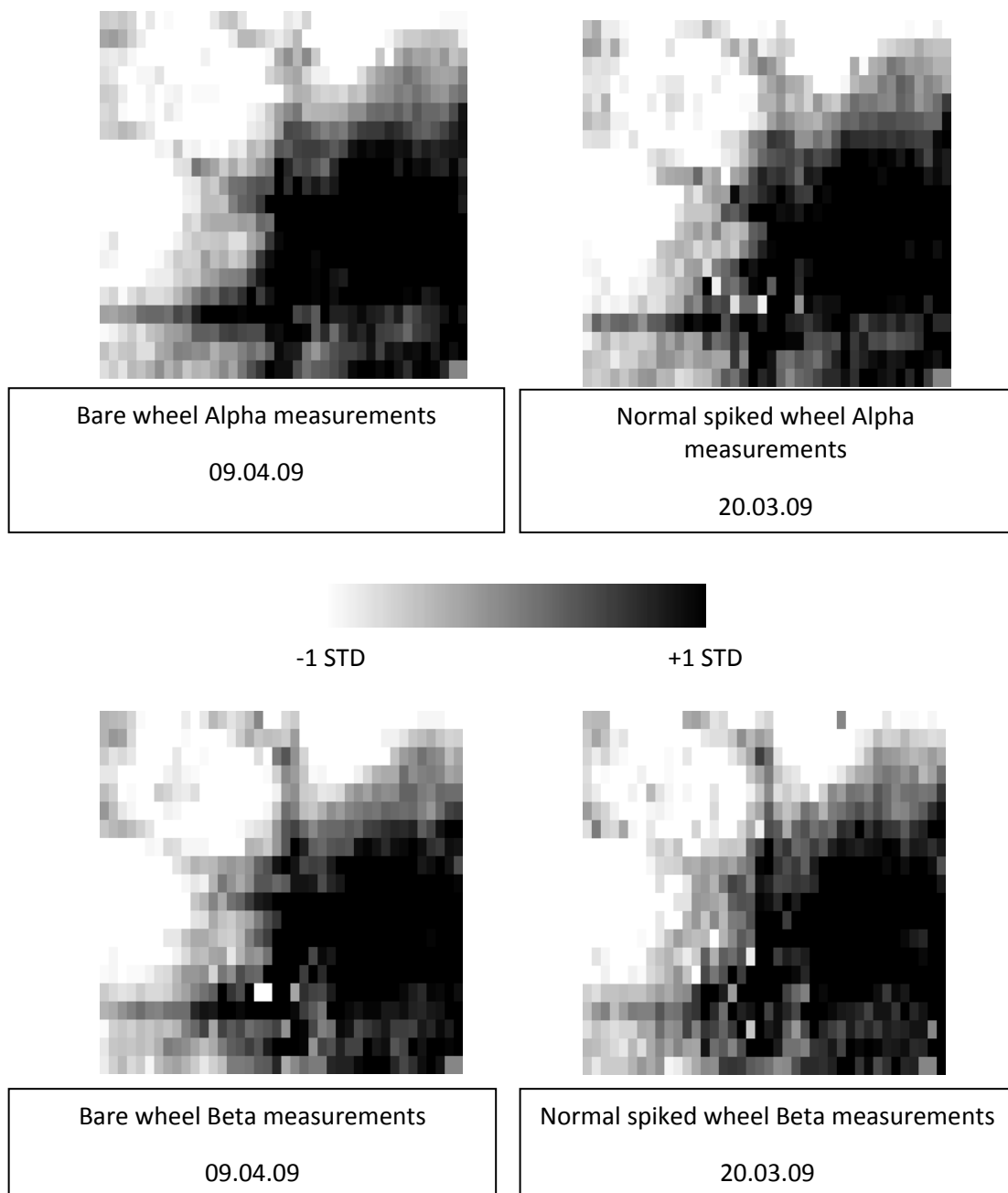
Figure 4.46   Data set comparisons of the differences in resistance measurements between the bare wheels and long spiked Alpha and Beta configurations of the MSP40.

The three week delay in measurements between the bare wheel test and the normal spike test was due to the time required to replace the 64 bolts on the wheels as only one set of wheels was available at the time. The replacement of bolts is labour intensive as the threaded bolts fill up with material picked up during the survey which must be cleaned to manually loosen the bolts. Later bolt replacement involved using a right angle drill bit and a long socket attached to an electric hand drill to speed up the process.

- Care should be taken when using this method as significant heating of the bolts through friction can occur. The risk of stripping the thread off the bolts also increases as does the risk of slipping the spanner off the bolts and injuring yourself. However, this method proved necessary when the threads have been clogged with material.

The data sets show a good visual correlation between the bare wheel and normal spiked data and all of the major anomalies were identified (see figure 4.46). Slight variations in shapes of anomalies are likely to be due to the three week gap between the surveys as the soil moisture levels changed.

The bare wheel survey was carried out after a day of rain which may have improved the contact resistance issues that are evident in the spiked wheel test. The contact resistance issues are shown by the increased variability of anomaly extent and greater variation of values within anomalies in the spiked wheel test due to poor spike penetration and insufficient current flow through the resistive top soil.

The variations between the two data sets displayed below were calculated by subtracting one array measurement from the other. Greater variation in the earth resistance values between the bare wheel and normal spiked wheels are plotted as red or dark blue whilst stronger correlations between data sets are plotted in green (see figure 4.47 and 4.48).
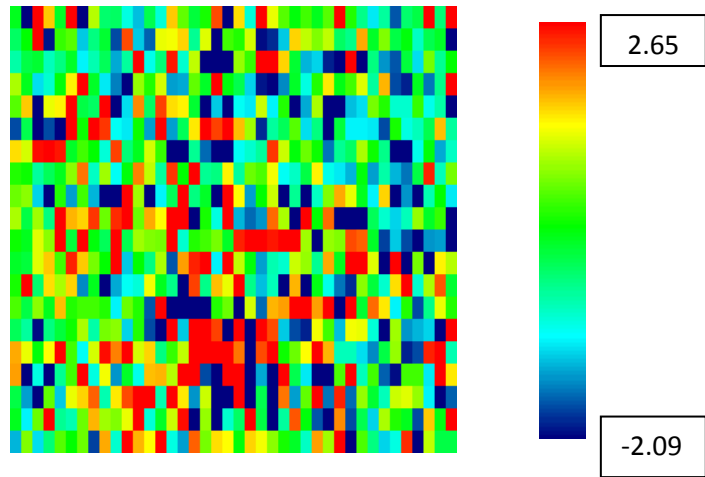
Figure 4.47   A visualisation of the differences in resistance values between the bare wheels and normal spiked Alpha configurations.
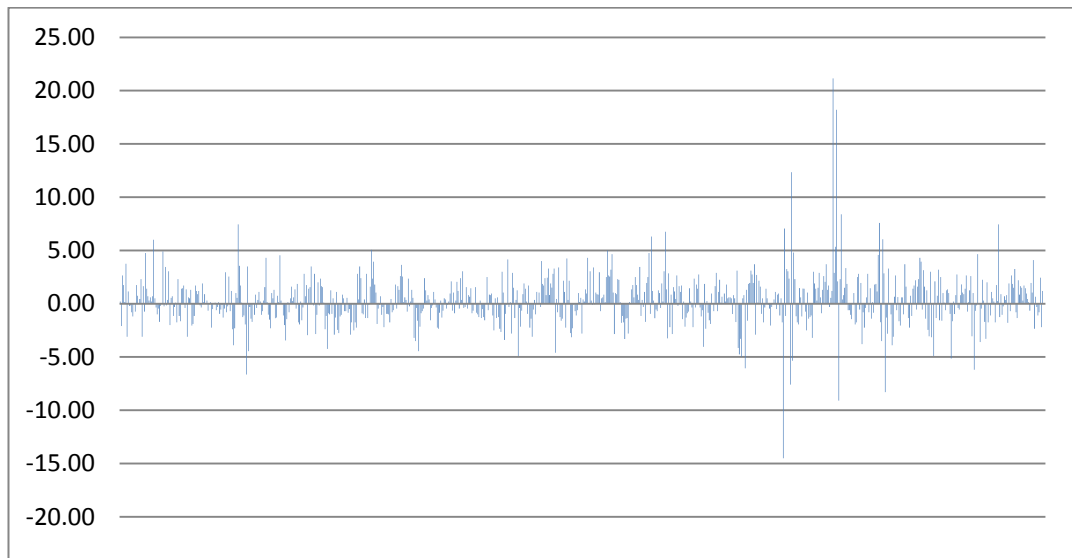
Error terms ± STD 0.06

Figure 4.48   A chart of the differences in individual data points of resistance values between the bare wheel and normal spiked configurations of the MSP40.

The variations in resistance results are likely to be a consequence of three factor variation in soil moisture, slight positional differences or variations in electrode contact with the soil.

4.3.10 Bare wheel tests discussion

The bare wheel experiment produced encouraging results but further testing was necessary to assess the application of the bare wheels. There are two key factors that need to be considered: the first and probably most important is the ability to use the bare wheel on a variety of ground covers consistently through the year. The key period would be during the summer months when the soils moisture is likely to be at its lowest. The dry topsoil may mean that the contact resistance is too great to take accurate earth resistance measurements. A further issue with using a bare wheel is the potential inaccuracies of measurement locations. A spiked wheel configuration will have at least one spike penetrating the ground directly beneath the wheel; however, on undulating ground the contact area for the bare wheel may cover a greater area (see figure 4.49).
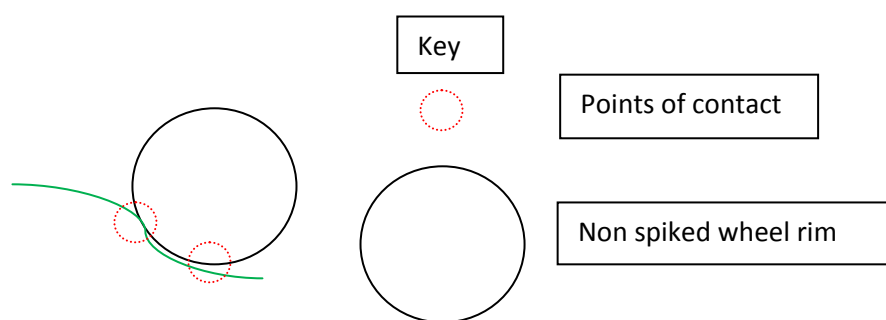
Figure 4.49   The bare wheel configuration may have multiple contact points with the soil surface which may distort the array geometry.

4.3.11 Geophysical investigation of a 'sensitive' landscape using bare wheels

The MSP40 has the potential to provide a means of performing a rapid site assessment collecting multiple data sets whilst minimising the physical impact on the most sensitive of archaeological sites (compared to other mobile arrays). Having gained a greater understanding of the array and instrumentation a sensitive landscape was chosen for investigation where previous knowledge could be tested on an archaeological site.

The site was on Bingley Moor and formed part of an on going collaborative project between the University of Bradford and the Bingley and District Local Historical Society (BDLHS). The moorland has a significant number of sites of prehistoric cup and ring rock art and the BDLHS wanted to examine the associated landscape change through prehistory and the historical period. Moors are a fragile ecosystems; the Yorkshire Dales National Park Authority (Yorkshire Dales 2009) describe how much of the Moor deposits are dependent on the drainage characteristics of the underlying geology. Limestone parent materials tend to produce shallow free-draining loamy soils whilst sandstones and grit stones tend to develop peatier, poorly drained acidic soils. Both parent materials produce poor soils that are not suitable for agriculture and only suitable for light sheep grazing. Although Bingley Moor is not part of the Yorkshire Dales National Park it is still a sensitive landscape in terms of its soil. The site was used by the Home Guard during World War II as an artillery range; preliminary gradiometer, metal detecting and field walking surveys have identified a number of potential unexploded shells.

Surface finds included mortar fins and shrapnel and an unexploded Bakelite hand grenade (see figures 4.50 and 4.51). The British Army's Bomb disposal unit were deployed and many of the identified mortars were disposed of accordingly. The decision was taken to use the bare wheels for the survey as it was necessary to undertake remote sensing with minimal impact so as not to disturb any buried ordnance.
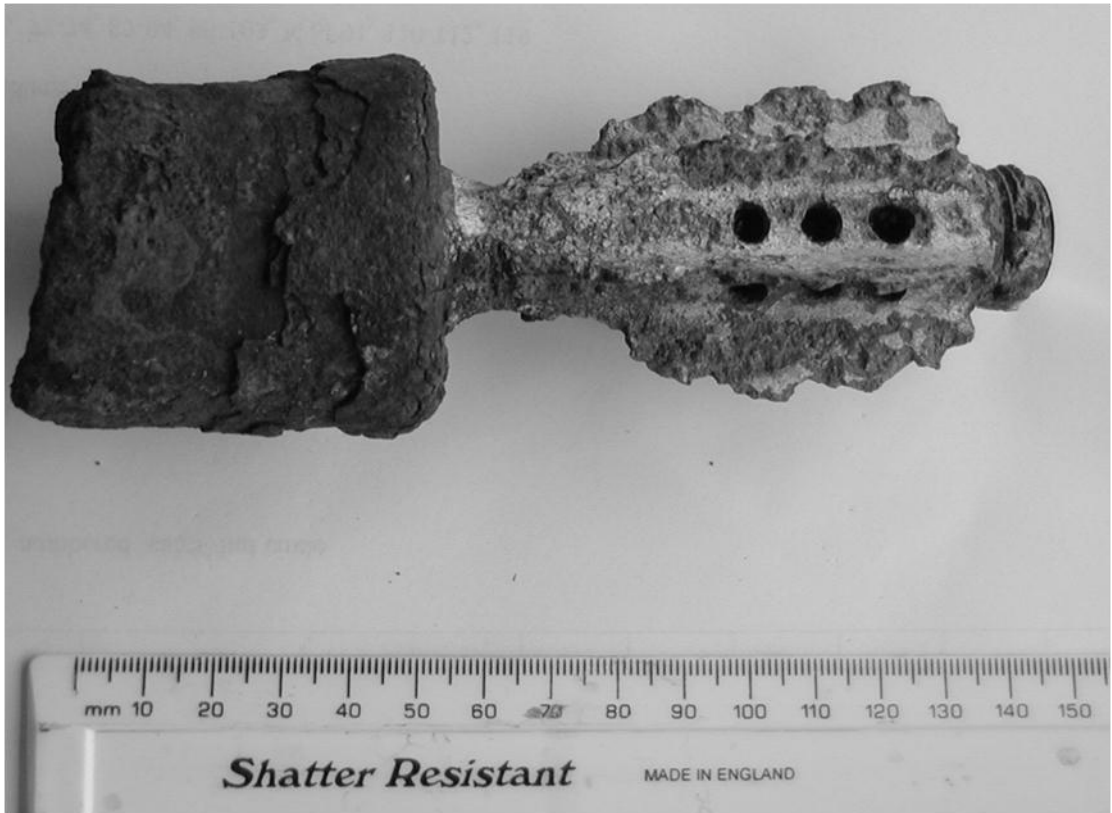
Figure 4.50   The remains of a ML2 mortar found on the Bingley Moor site, picture courtesy of the Bingley and District Local Historical Society (BDLHS 2009).

Figure 4.51   A Bakelite hand grenade found on the surface of Bingley Moor, picture courtesy of the Bingley and District Local Historical Society (BDLHS 2009).

4.3.12 Method

Survey equipment (see table 4.12)

Table 4.12   Bingley Moor survey parameters

Equipment & probe separation	Measurement Configuration	Sampling Interval	Traverse Interval	Method of collection
MSP40 (0.75m) Bare and normal spiked wheels	Alpha & Beta	0.25m	1m	Zig Zag (encoder wheel)
FM 256 Gradiometer	Single measurement (MSP40)	0.125m	1m	Zig Zag (external trigger)

Grid Size

20m x 20m

4.3.13 Data processing

Earth resistance

All four days of data were processed independently as the surveys were in small discrete areas. However, the same processing parameters were used for each survey area.

3 x X=1, Y=1, Threshold 3 & replace with mean.

X=2, Y=2, Threshold 3 & replace with mean.

The Beta data sets were also shifted by +1 to allow for the time displacement between Alpha and Beta measurements. The Alpha and Beta measurements were then merged in Geoplot using the merge MSP40 composite option applying a high pass filter with X=8, Y = 2 and a Gaussian weighting.

Low pass filter with parameters of X=0, Y=2

Interpolated data Y= SinX/X, x2

Geoscan FM256 gradiometer processing

The data was initially analysed for periodic noise by performing a spectrum analysis of the entire data set. Periodic frequencies were then filtered out.

Zero Mean Grid, Threshold = .25

Zero Mean Traverse, Grid=All LMS=On (Threshold not applied).

Destagger all grids, X dir, Shift=2, line pattern -2 -4 -6 -8

Low pass filter, LPF X=2, Y=0, Wt=Gaussian

2 x Interpolate Y, Expand – SinX/X, x2.

4.3.14 Results

56.30

30.72 ohm

3.52

-3.21 nT

0m   20m

N
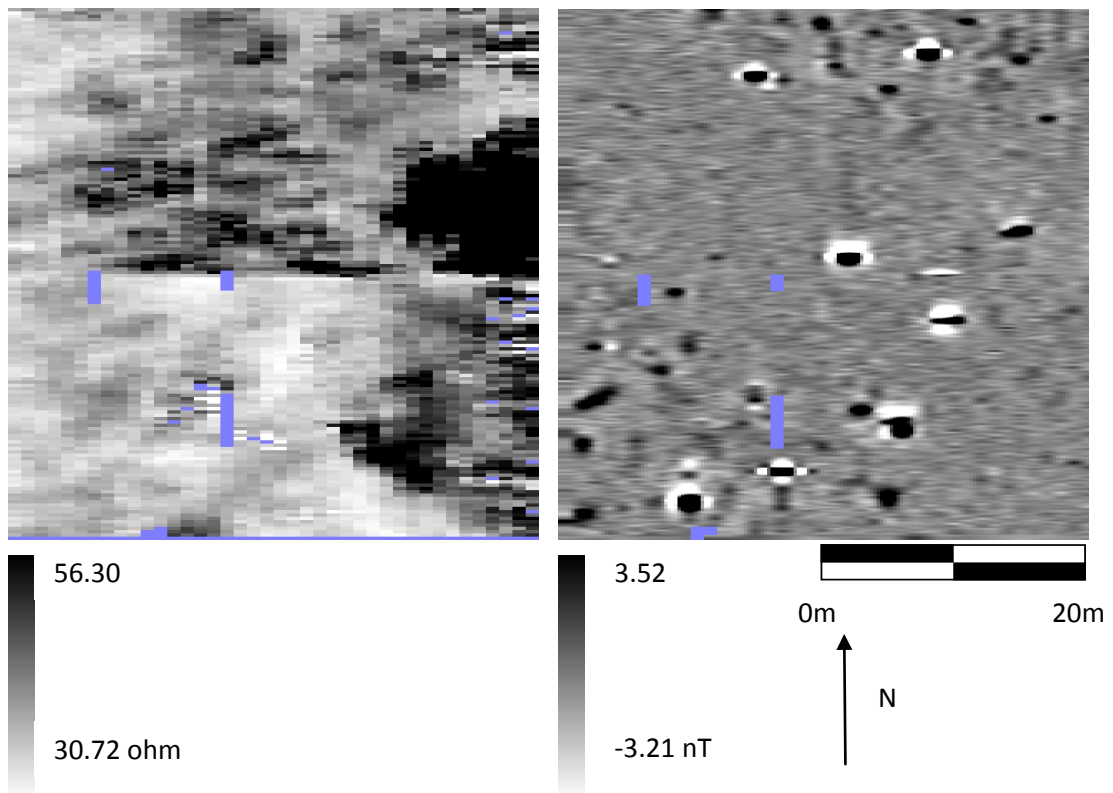
Figure 4.52   The MSP40 earth resistance and gradiometer survey data using a bare wheel configuration on Bingley Moor.

The first day on site culminated in a successful survey using the bare wheel setup. However, subsequent surveys were beset with contact issues as the soil dried out. The moor is partially covered in woody heather over 30cm thick in parts. The initial survey area had shorter heather and it had rained in the days immediately preceding the survey allowing sufficient ground contact to inject the electrical current into the ground (see figure 4.52).

Subsequent days of survey saw the weather improve and areas of the Moor soon dried as did the heather. As the heather is woody in texture along with the depth of the vegetation meant that ground surface acted as an insulating layer and no circuit could be completed. It was therefore necessary to re-evaluate the MSP40 configuration and to continue surveying with the normal spikes.

As the potential damage from the wheels had been modelled previously in the sand box it was possible to say with some confidence that spikes would penetrate no deeper than 35mm into the ground. Information from the army bomb disposal squad and from the metal detectorists suggested that the ordnance was buried approximately 10cm down. The acidic nature of the soil had also corroded the housing of the ordnance which had led to the leaching of the reactive chemical reducing the risk further. It was therefore decided that the survey could proceed with the normal spikes and the issues of contact were immediately overcome as the electrical circuit with the soil could be completed and resistance values measured (see figure 4.53).
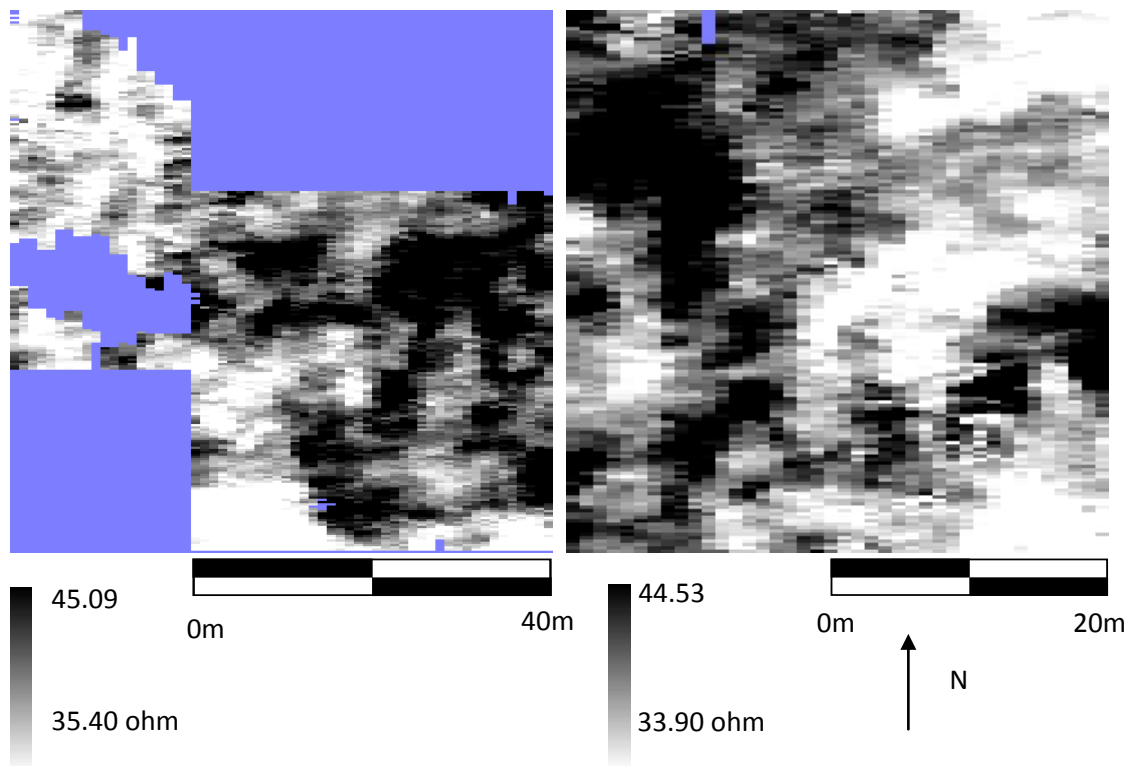
Figure 4.53   Two separate area surveys of MSP40 combined Alpha and Beta data sets collected on Bingley Moor with a normal spike wheel configuration.

The results produced a clear image of the subsurface features and identified a number of anomalies, many of which are likely to be geological or pedological features. However, the survey also shows the extent of the rock groupings visible on the surface that appear to be the remains of small cairns. The MSP40 gradiometer results produced a comparable data set with the Bartington gradiometer survey that had been completed as part of the primary investigation (see figure 4.54).

-4.5   ±1STD   5.0 nT
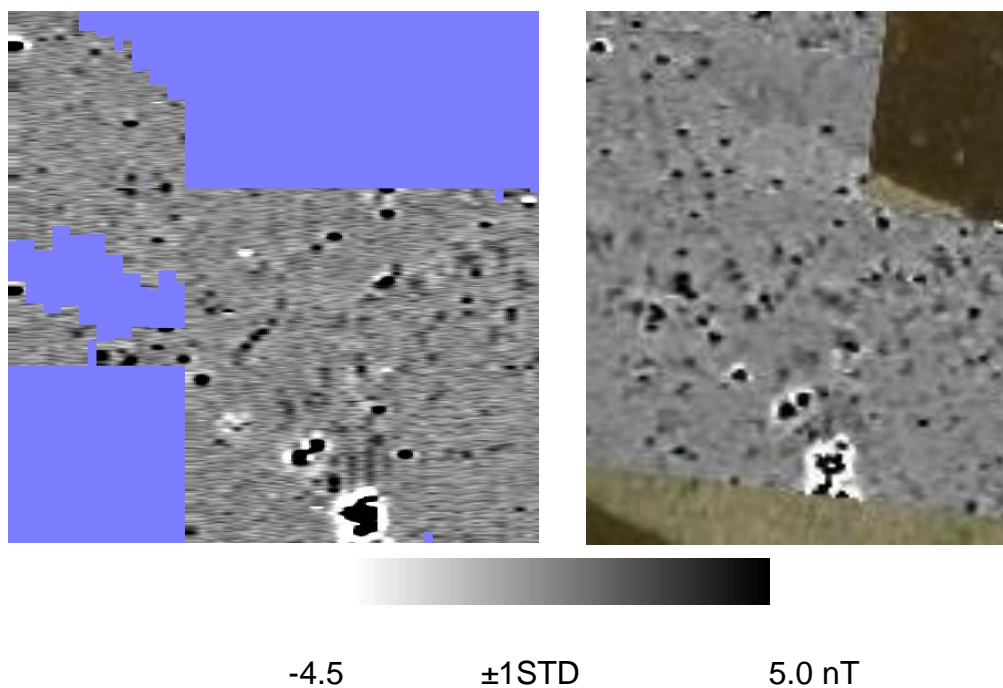
Figure 4.54   Comparison data sets of a Geoscan Research FM256 (mounted on the MSP40) and Bartington Grad 601 Gradiometer on Bingley Moor, courtesy of Bingley and District Local Historical Society (BDLHS 2009).

4.3.15 Discussion

The investigations on Bingley Moor show the adaptability of the MSP40 and how increasing knowledge and confidence in the various configurations will lead to informed decisions as to the most appropriate setup on a site-by-site basis. However, it has also highlighted the need for additional testing of the earth resistance variables to achieve the best possible results. The initial bare wheel survey indicated that surveys are possible without spikes but the choice of wheel must be appropriate for the ground cover and weather conditions before survey commences.

The MSP40 mounted gradiometer identified the same anomalies as the hand-held Bartington survey; additional noise is visible in the mounted FM256. This may come from the lower mounted position of the FM256 compared to the carried Bartington Grad 601 but is more likely a consequence of vibration and movement associated with pulling the MSP40 across undulating ground (see chapter 3.7).

As the MSP40 can record measurements using a time based or encoder wheel trigger, there was no need for marker ropes to be laid before survey commenced. This reduced the trampling across the site. The thick heather and grass would also distort measurement ropes which may have lead to positional errors.

4.3.16 Compaction assessment

At an IFA meeting in 2007 (Reading, UK) English Heritage had a discussion with geophysical practitioners about the use of vehicles on archaeological sites. It was discussed how a quad bike / ATV load can be as much as 60 kg per tyre and a Land Rover can have a load of 500 kg per tyre (Gaffney 2011). Quad bikes and Land Rovers are often used to pull mobile arrays so have a significant impact on the soil in terms of compaction but also the sheering of the soil surface when driven at speed.

The spike impact assessment trial looked at different wheel configurations effects on a ground surface (tearing and ripping) but also indicated soil compaction was an additional source of damage that should be considered. As the MSP40 is used for field work it was important to consider possible methods or measures that might be applied to future practical field trials.

4.3.17 Introduction

Soils can undergo significant physical alterations to structure both through natural processes and human interference. Damaging processes may include ploughing, compaction, extraction and erosion (either from wind or water, this can be a natural or human induced process). From an agricultural perspective compaction (through vehicular traffic) and erosion have the greatest consequences (Horn *et al.* 2003). Compaction reduces productivity and increase ground water pollution and gas emissions. Damage to the soil can take several years to repair and will lead to significant loss of productivity without human intervention.

Håkansson and Medvedev (1995) report topsoil takes approximately 4-6 years to recover naturally from soil compaction but state that subsoil compaction at depths of $\geq$ 40 cm may never recover and are beyond the range of most modern tillage equipment. According to Dain-Owens *et al.(2009)*, whilst the upper 200 mm of soil is directly affected by cultivation or machinery, from 200mm down to 1m may be indirectly affected by soil deformation through pressure transfer or compaction.

Oldeman (1992) quantified the extent of the problem with up to 32 Mha of arable land in Europe having been significantly damaged by wheel compaction. Van den Akker *et al.* (2003) provide a good overview of the situation in the European Union relating to soil compaction in an agricultural context. This issue will have direct consequences for archaeological sites as they are at risk from damage (through compaction and erosion). In England alone nearly 3000 scheduled monuments are impacted by intensive cultivation or livestock farming and one third of all scheduled monuments in the East Midlands area was classified as vulnerable to damage from agricultural practises (EnglishHeritage 2003)

Having a quantifiable measure of the physical impact on soils may encourage increased use of the MSP40 as several landowners encountered during the field work portion of the research were initially reluctant to allow access. This was overcome by highlighting the lightweight features of the cart and the benefit of being pulled by hand.

Previous research on the impact assessment of soil has predominantly focused on agricultural machinery, the wheels used on tractors and other heavy machinery before analysing the subsequent effects on the soil physical properties and soil structure. Rasool Mari & Changying (2008) describe the soil compaction by wheeled vehicles as a decrease in soil porosity, localized to the zone beneath the wheel often with visible surface rutting.

Changes to soil pore shape and size can significantly influence the natural physical, chemical and biological processes within the soil, including water and gas movement, the reduction in pore space and shape can also reduce the productivity of the soil (Håkansson and Medvedev 1995 ; Pagliai *et al.* 2003). It is important to not damage the buried archaeology and to reduce the impact on the soil structure so that damage is limited and the extent of compaction and erosion is not exacerbated.

A detailed evaluation of the methods frequently used in the study of agricultural soil compaction was reported by Fritton (2008). Arvidsson (1999) and Rasool Mari & Changying (2008) discuss further how vehicular compaction of soil is dependent on the soils mechanical strength (linked to texture and organic content), soil structure, water content of soil and loads applied (affected by axle load, tyre dimensions, velocity and soil/tyre interaction (grip patterns)). Bulk density tests have frequently been used to identify compaction of soil but this only shows evidence of compaction or loosening of the soil.

Horn *et al.* (2003) suggested that soil sheering is equally important as it homogenizes and deforms the pore space in the soil whilst showing little to no change in bulk density. Their research showed both horizontal and vertical displacement down the soil profile with changes in hydraulic conductivity due to altered pore spacing. However, this analysis involves the insertion of displacement transducer systems (DTS) and stress and strain tensors (SST) into a soil profile (in this case inserted into the side of a soil bin).The DTS and SST research was too complicated a system to implement for the purposes of this research project. Therefore an infield measurement was attempted using earth resistance survey with penetrometer measurements.

Seger *et al.* (2009a ; 2009b) considered the application of 2D & 3D electrical resistivity measurements to identify compacted zones, loose material or clods formed in a soil profile.

Their experimental soil profile had been compacted by a vehicle running over the soil surface before ploughing the test area to simulate the different soil components. The research indicated it was possible to record the position of such structures but geometrical characteristics could not be recorded.

From an archaeological perspective studying the impact assessment of vehicular traffic has focused on artefact damage. In one study a dynamic load was applied to a soil box representative of a range of pressures from field-going vehicles both through tyre inflation and load (Dain-Owens *et al.* 2008 ; Dain-Owens *et al.* 2009), the results of which indicated that the choice of tyre and pressure significantly affected the impact on the soil and artefacts.

McBride and Mercer (2011) also investigated the damage to archaeological artefacts but used Micro-CT scanning to identify damage whilst still inside soil blocks. By leaving the artefact insitu additional damage of artefact recovery would be negated and would allow for the re-examination of the artefact after each traverse.

Multiple pressures of static compaction were trialled up to 600 kPa. The results indicated slight distortion/damage occurred to fragile artefacts (freshwater clam shells) at 50- 100 kPa and severe damage between 300- 600 kPa. Moderate strength artefacts (burnt maize kernels) showed dimensional distortion but high strength lithic artefacts remained unaffected at 600 kPa. 50-300 kPa is a typical pressure for tractors or similar vehicles, whilst 300-600 kPa can be encountered from construction class vehicles.

Additional studies related to archaeological sites and site formation processes have considered the damage and displacement of artefacts through trampling (Gifford-Gonzalez *et al.* 1985a ; Nielsen 1991). The research measured the damage to lithic objects and the three dimensional migration of the objects in different types of soil.

Gifford-Gonzalez *et al.* (1985a) indicated artefacts showed significant horizontal displacement with little vertical displacement in the loamy soils. However, the loose surface layer doubled in depth suggesting the compacted soil was disturbed through trampling across the site. Sandy soils showed a significant vertical displacement with artefacts being displaced by almost 11 cm down the soil profile. Lithic damage occurred through breakage and edge damage. The effect of trampling on sites is important as the repeated walking across a site may displace objects (Villa 1982) and cause damage to artefacts (McBrearty *et al.* 1998) and sites. However, the main impact relating to the MSP40 comes from the displacement / loosening of soil material which increases the risk of soil erosion of the soil surface with compaction taking place deeper down the soil profile. By integrating multiple survey techniques on the cart the amount of trampling and damage can be reduced. The level of damage to a site through trampling is not as significant as ploughing or the towing of heavy mobile arrays but still should be considered as part of the physical impact on a site.

4.3.18 MSP40 soil compaction tests

It is important to know the weight and pressure of the instrument so each component was weighed and is listed below.

MSP40 weights	Total
Each axle including 2 wheels* = 9.5 kg	19 kg
MSP40 platform = 4 kg	4kg
Each handle = 2 kg	4kg
Multiplexer = 0.9 kg	0.9 kg
DL256 = 1.2 kg	1.2 kg
RM15 = 1.65 kg	1.65 kg
Total weight	30.75 kg

*Each wheel hub weighs 2.75 kg.

30.75 kg = 301.35 Newtons (1 kilogram weighing = 9.8 Newtons under standard condition on the earth surface).

Each wheel on the MSP40 has a diameter of 0.24 m x 0.045 wide (surface width). If the wheels are considered to be perfect circles and standing on a perfectly flat hard surface then only a small area will be in contact with the surface (for this example 1mm contact is used) the surface area can be calculated as follows based on an online calculator (Nave 2011)

0.001m x 0.045m = 0.000045 m^2 per wheel, as the weight is theoretically dispersed equally amongst the 4 wheels the surface area can be multiplied by four.

0.000045m^2 x 4 = 0.00018m^2 total surface area for all four wheels.

To calculate the pressure it is necessary to divide the force by the area

301.35 Newtons / 0.00018m^2 = 1674166.6666....... Pa (Pascals) which is roughly equivalent to 243 lbs. per $inch^2$

However, a more realistic surface area reduces the pressure on the ground significantly based on natural undulations on a soil surface and slight compaction of the surface due to the natural compression of soil.

0.03 m x 0.045m = 0.00135 m^2

0.00135m^2 x 4 = 0.0054 m^2

301.35 Newtons / 0.0054m^2 = 55805.5555....... Pa roughly equivalent to 8 lbs. per $inch^2$

Increasing the wheel size would provide an easy solution to reducing the physical impact on an archaeological site. This would lead to a slight weight increase but would be offset by the increased weight distribution.

However, increasing the wheel surface area has the negative effect of increasing the variability of the measurement position. If only part of the wheel is in contact with the ground surface then the dimensions of the array may be altered and this can have a significant effect on the recorded resistance measurements (see chapter 3.8.2).

4.3.19 Method

As the MSP40 inevitably causes soil compaction, which contributes to the potential damage of archaeological site it was decided to try and identify a way of measuring the compaction rates. A soil box was built measuring approximately 2.4m x 0.9 m x 0.18m. Additional vertical partitions were inserted to reduce the amount of soil required for the experiment. Each soil box was approximately 0.2m wide and separated by 0.5m so that the MSP40 wheels could span the two boxes. The box was constructed with dimensions that allowed the MSP40 to be lifted and rolled into place at either end before the electrode bank so that the measurements would only record the rolling compaction of the MSP40 (not static compaction). The electrodes were also positioned so that both axles would roll over the same area of soil to simulate the full pressure of the MSP40 on the ground surface as the beginning and final 0.75m of the soil boxes would only be run over by one set of wheels (see figure 4.55 and 4.56).

Figure 4.55   A photograph of the MSP40 as it was pulled past the banks of electrodes (highlighted in red).

A series of stainless steel screws were screwed into one side panel. Four rows of 21 screws were fixed 3 cm apart and the upper three rows were separated by 3cm whilst the fourth row was positioned 5cm below the third to offer a greater depth of measurement. The first row was positioned 1cm below the top of the box (see figure 4.56). The four rows of electrodes were to allow for horizontal pseudosections (or horizons) to be measured through the soil boxes to measure soil compaction at different soil depths after each traverse.
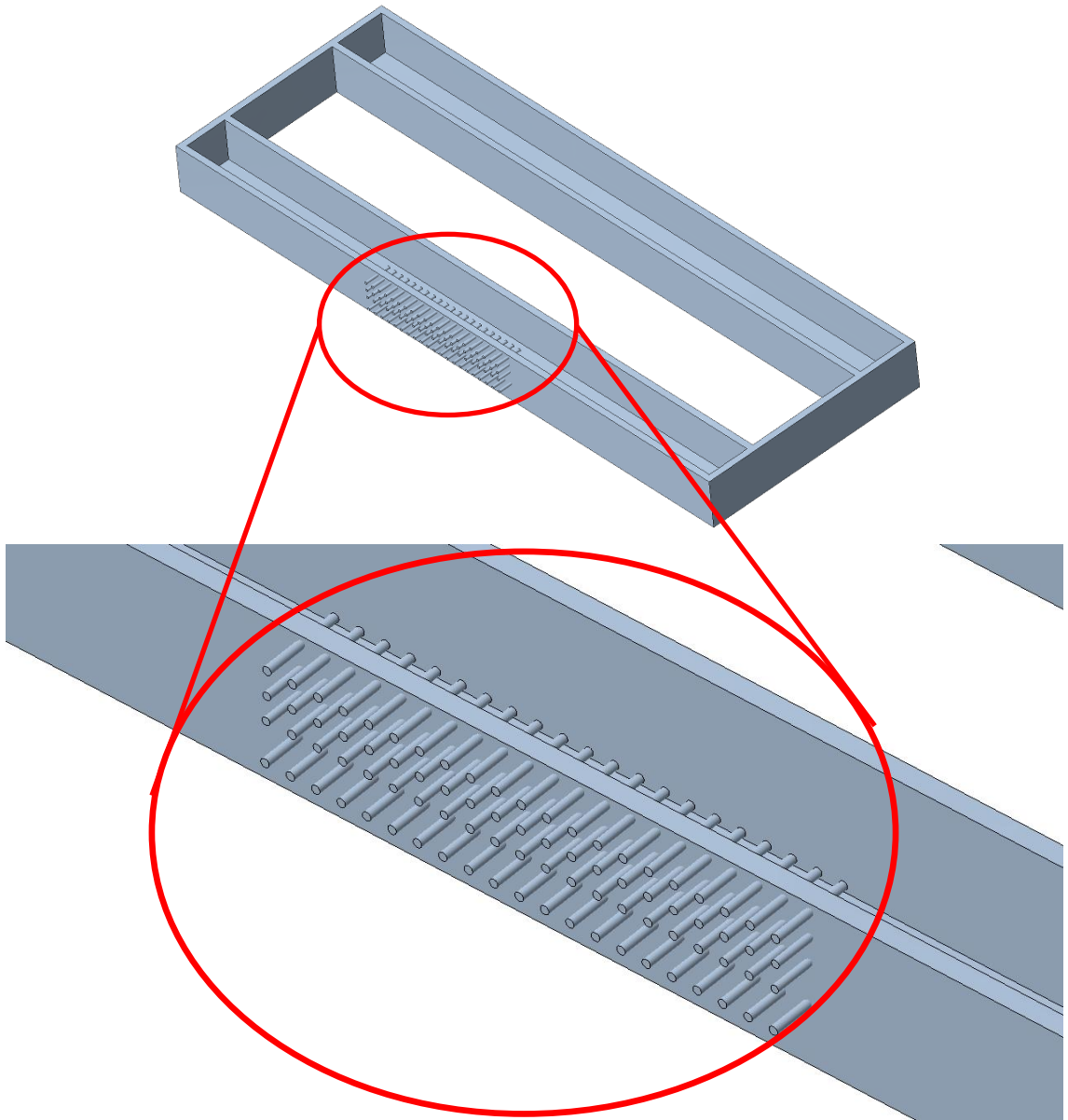
Figure 4.56   The highlighted electrode position in the side panel of the soil box (top image) and a close up of the electrode positions (bottom image).

Additional measurements were recorded across the soil surface using a probe separation of 3 cm. The measurements were to test if it was possible to measure compaction from the surface and relate it to changes in resistance down a soil profile.

A Geoscan Research RM15 resistance meter was used to record the horizontal and vertical pseudosections. Crocodile clips were attached to the remote and mobile probe pins on the back of the RM15 with the other end of the clip attached to the stainless steel electrodes in the soil box. The pseudosection was configured as a Wenner array for this experiment. The smallest probe separation for each pseudosection was recorded first before expanding out the probe separations (leaving the current probe on the left hand side in the same position). When every probe separation had been recorded the left-most current probe was moved across one electrode position then the process was restarted until all possible measurements were recorded. The next pseudosection down the soil profile was then recorded in the same way.

First measurement position

```
A     M     N     B
○     ○     ○     ○     ○     ○     ○     ○
```
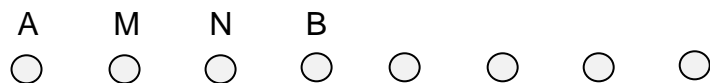
Second measurement position

```
A           M           N           B
○     ○     ○     ○     ○     ○     ○     ○
```

Nth measurement position

```
      A     M     N     B
○     ○     ○     ○     ○     ○     ○     ○
```

The boxes were filled with approximately 10cm of sand and 10 cm of topsoil to offer two different materials with different resistances. A 3 kg weight was applied across the subsoil (sand layer) for a period of 24 hrs. to gently compress the layer to simulate a more accurate soil horizon. The top soil layer was compressed for 6 hrs. to replicate a ploughed soil surface where the soil has been turned over and made more friable. The soil boxes were dampened down with approximately 5 litres of water to reduce variations in resistance due to dry sand or soil from the bags. The soil boxes were then left exposed to the elements for 4 weeks for the water to equalise and soil to settle.

The four rows of electrodes were positioned so the upper three rows (Horizons A-C) were in the upper topsoil layer whilst the bottom row of electrodes (Horizon D) was positioned within the sand layer. Horizon A was located 1cm below the original soil surface, Horizon B 4cm and Horizon C 7cm below original surface layer and Horizon D 11cm below original surface level (located in sand layer).This was done to examine the possible compaction effects in two different soil mediums.

A hand-held penetrometer pen was used to measure the penetration resistance / compaction of both the sand (before the topsoil was added) and topsoil before the experiments ran. A SOILTEST CL700A pocket penetrometer was used to measure the unconfined compression strength in kilograms per centimetre square (kg/cm^2). The penetrometer was also used to measure the topsoil compaction after each traverse. Measurements were taken within the MSP40 wheel ruts. An average of 5 measurements was calculated for each series of compaction tests to reduce errors.

An additional surface measurement was taken to consider the amount of soil displacement / compaction in the track way left by the MSP40 (see figure 4.57). This was done by measuring from the base of the rut vertically up to the soil surface. Once again five measurements were taken after each traverse and a range is quoted below to account for variation along the rut (see table 4.13).

Figure 4.57   A photograph of the rut left by the MSP40 running alongside the electrode bank.

4.3.20 Results

Table 4.13   Compaction results

	Sand kg/cm^2	Topsoil kg/cm^2	Compaction in mm
Pre compaction	0.1	0	N/A
Run 1	N/A	0	20 - 25
Run 2	N/A	0.1	25 - 45
Run 3	N/A	0.2	45 - 47
Run 4	N/A	0.4	47 - 50
Run 5	N/A	0.5	47 – 52.5

The results from the surface measurements show that the MSP40 compacted the soil surface. The measured compaction indicates the first and second traverses have the greatest affect on the soil structure as the soil compacted by 20-25 mm each traverse.

The later traverses also increase the compaction depth from the soil surface but at a significantly reduced level (2-3mm) suggesting the soil structure has condensed and pore spaces/voids within the soil reduced. This would reduce the transfer of moisture and air through the soil affecting the recorded earth resistance values. However, as long as the equipment functions correctly there is no reason to repeatedly resurvey the same traverse line and it is unlikely to run along the exact same rut for every traverse. The results also suggest that single traverse surveys with a multi-sensor platform reduce physical impact compared to multiple individual instrument surveys.

Earth resistance data values from the horizontal and vertical pseudosections were exported from Geoplot and inserted into a text document that could be read by Res2Dinv. The least squares inversion processing was applied to all data sets (Loke and Barker 1996).

The following Res2Dinv plots consider each horizontal pseudosection in turn starting with a pre-compaction display and then a new figure for each subsequent traverse, moving down the soil profile to the next pseudosection line / horizon.

Pre-traverse Horizon A
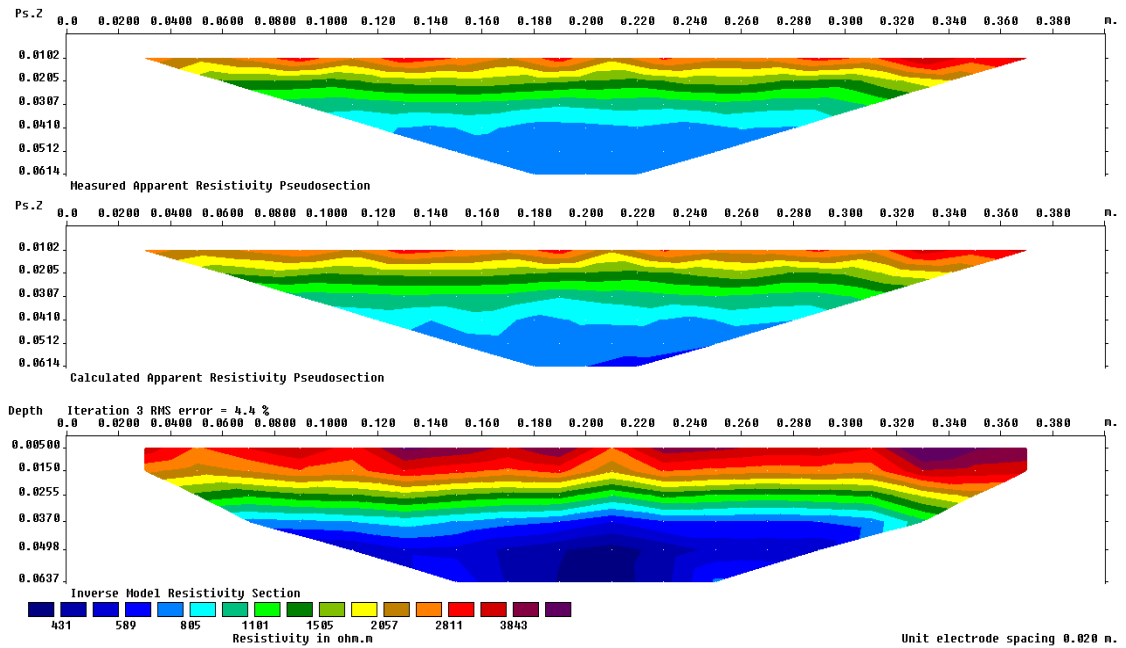
Figure 4.58   The undisturbed horizontal pseudosection of Horizon A.

Traverse 1 Horizon A
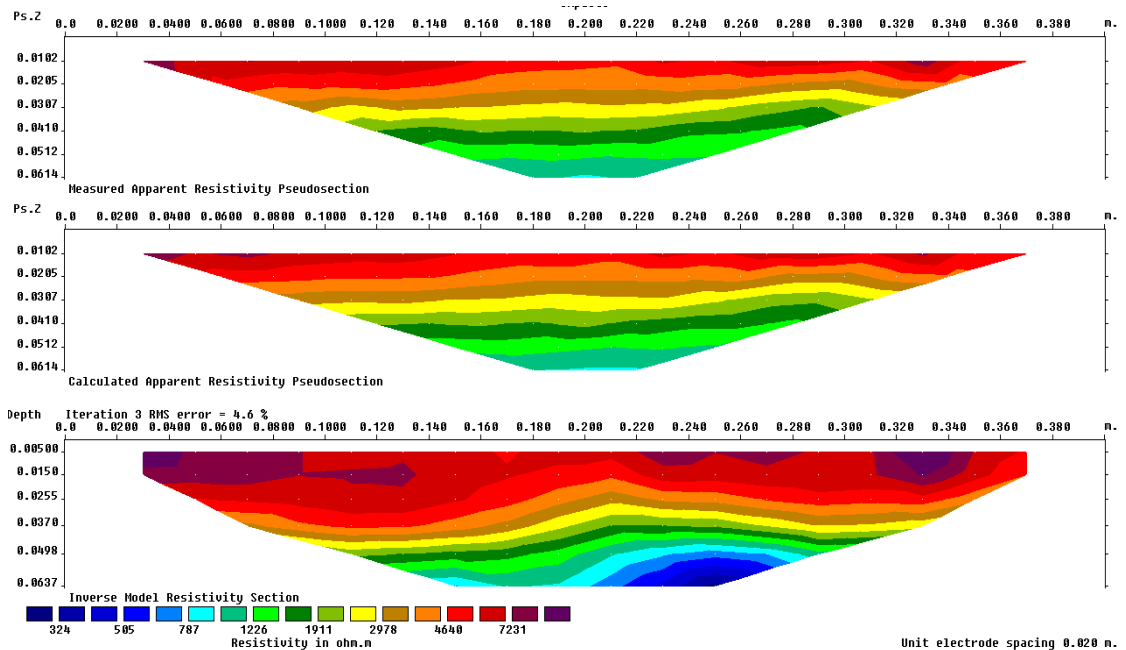
Figure 4.59   The pseudosection of Horizon A after one traverse with the

MSP40.

Traverse 2 Horizon A
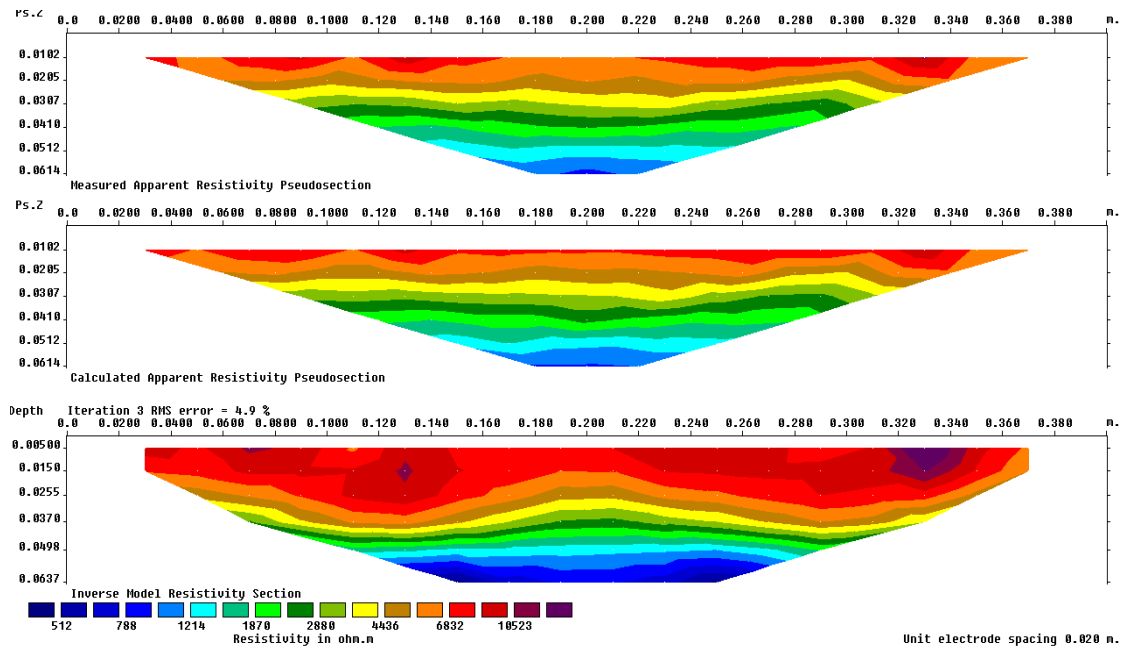
Figure 4.60   The pseudosection of Horizon A after two traverses with the MSP40.

Traverse 3 Horizon A
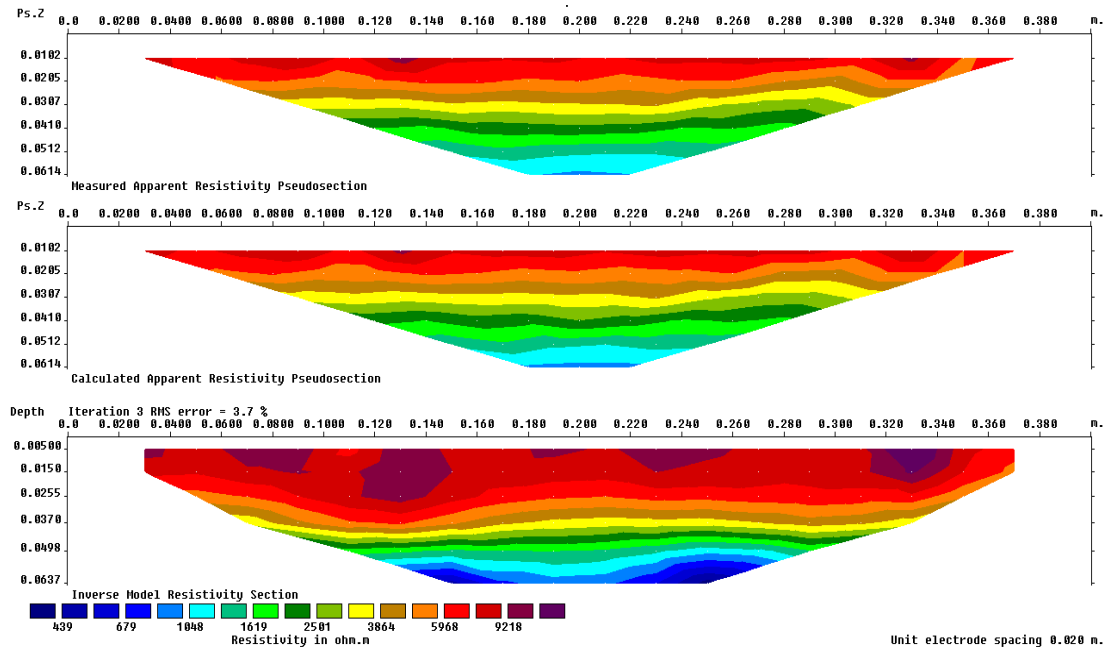
Figure 4.61   The pseudosection of Horizon A after three traverses with the MSP40.

Traverse 4 Horizon A
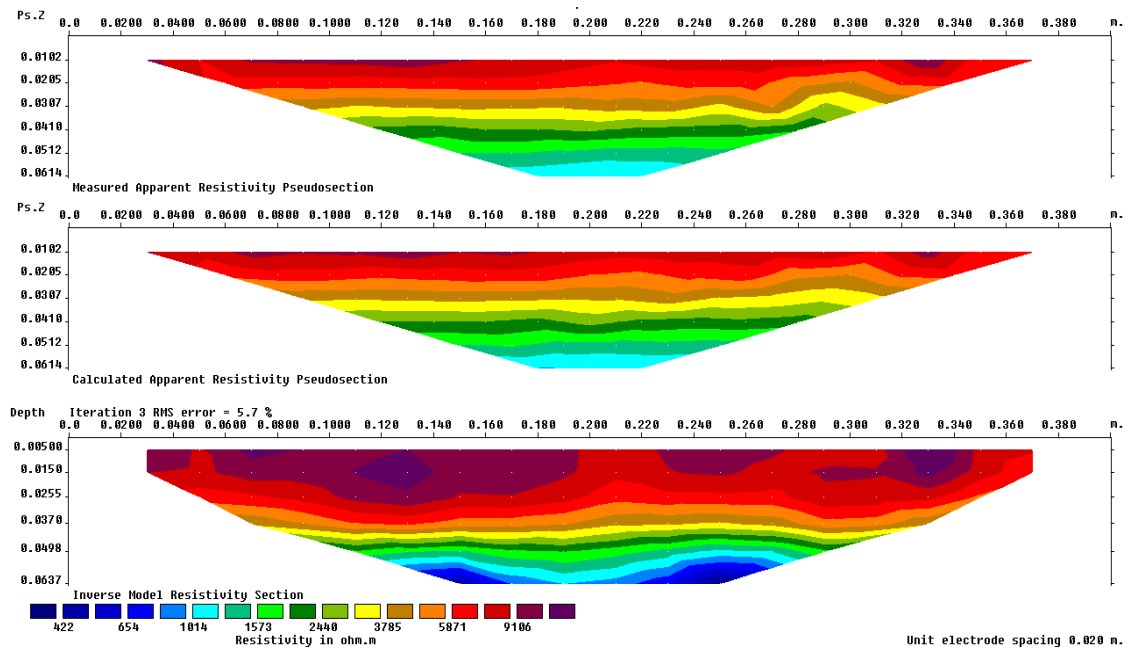
Figure 4.62   The pseudosection of Horizon A after four traverses with the

MSP40.

Traverse 5 Horizon A
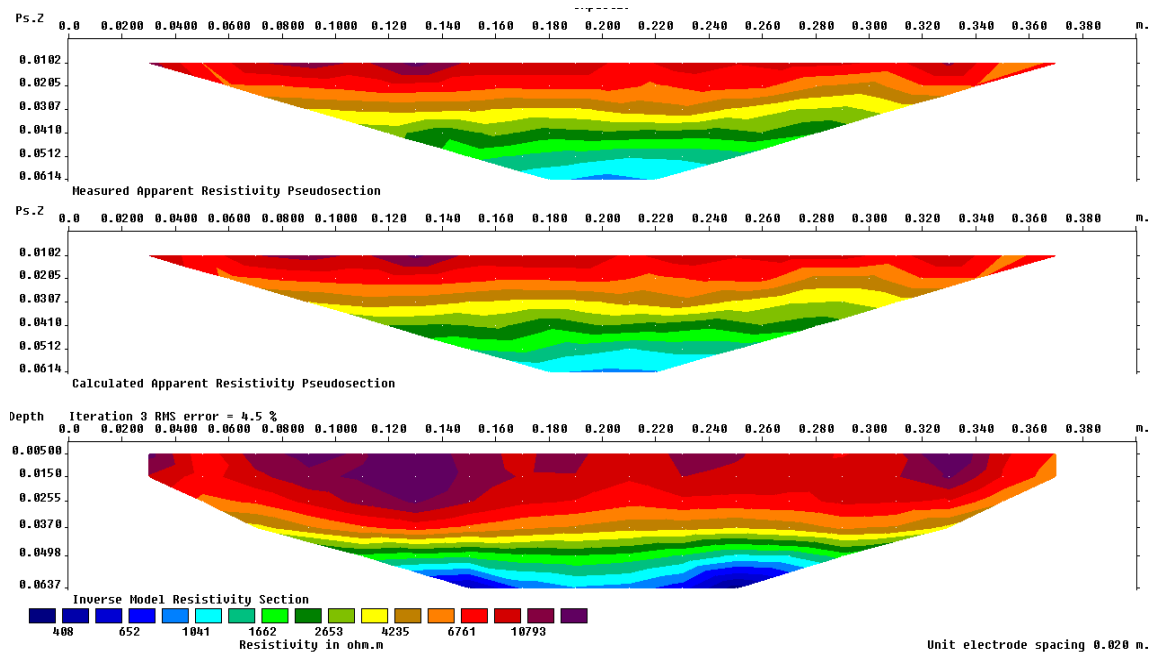
Figure 4.63   The pseudosection of Horizon A after five traverses with the

MSP40.

The high apparent resistivity band along the top edge ('surface') of the pseudosection is a result of the insulating wooden box edging combining with the narrow probe separation. The smaller area of very high apparent resistivity probably resulting from air pockets or stones around the electrodes as the soil was difficult to pack between the electrodes.

The horizontal pseudosection from Horizon A shows a significant increase in apparent resistivity values between the pre-compaction (431-3843 ohm.m ± 4.4% error) and traverse 5 results (408-10793 ohm.m ± 4.5% error). This is likely to be due to the surface compaction of the soil after the initial traverse as the soil was compacted by 20-25 mm reducing the soil surface to a level approximately 10 -15 mm below the initial bank of electrodes (Horizon A). This reduced the amount of soil medium surrounding the electrodes restricting the current pathways and increasing the recorded apparent resistivity values. The increasing resistivity value between subsequent traverses is likely to be the further displacement of soil medium around the electrodes (see figure 4.64).
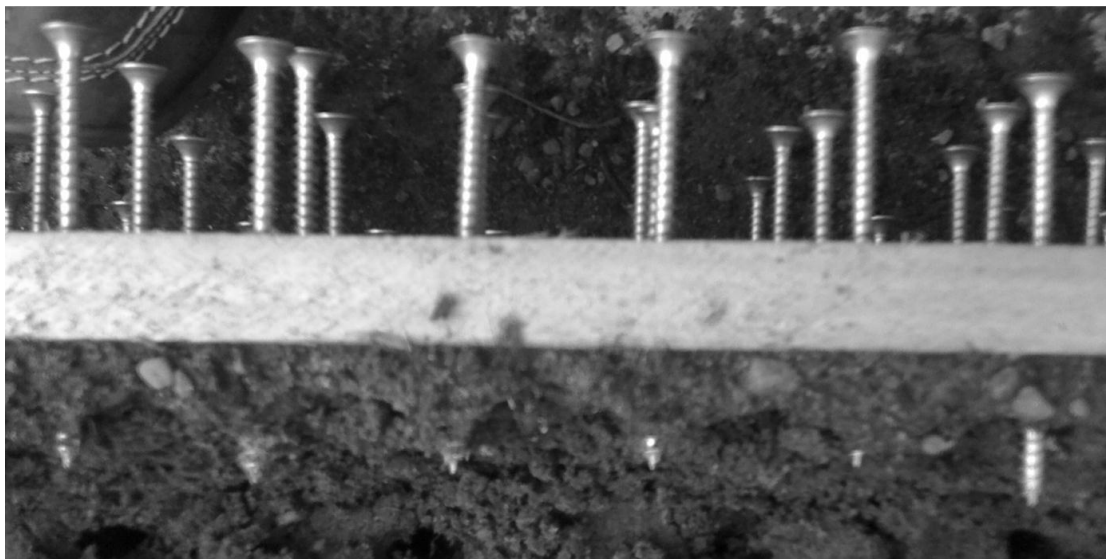
Figure 4.64   A photograph of the exposed electrodes of Horizon A after repeated traverses with the MSP40.

Pre-traverse Horizon B
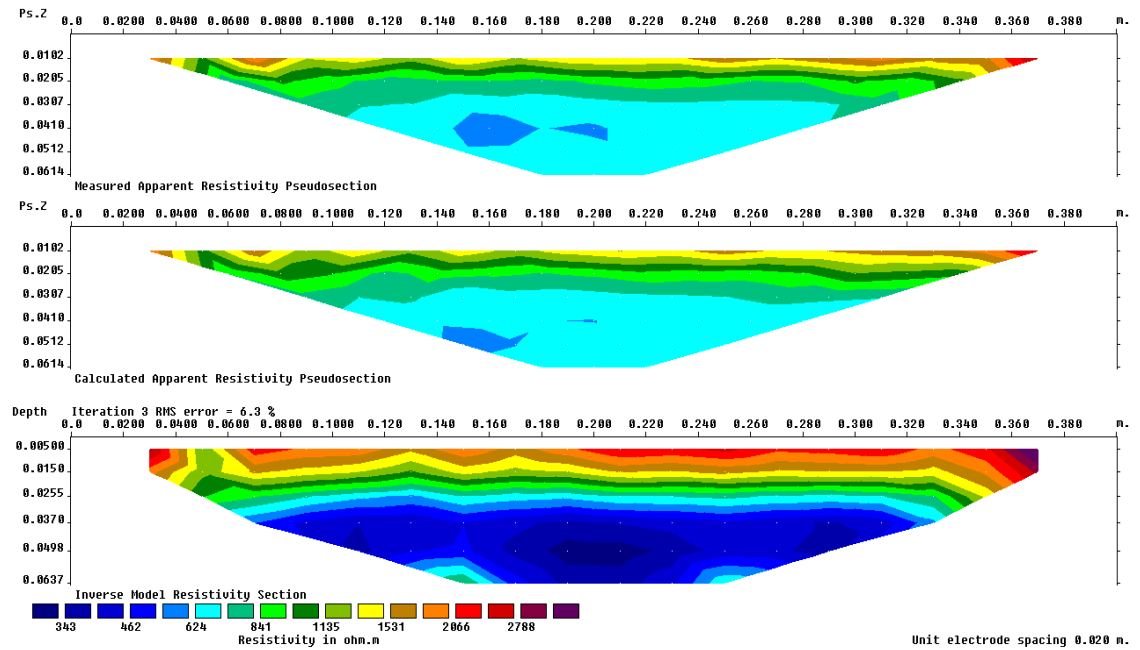
Figure 4.65   The undisturbed horizontal pseudosection of Horizon B.

Traverse 1 Horizon B
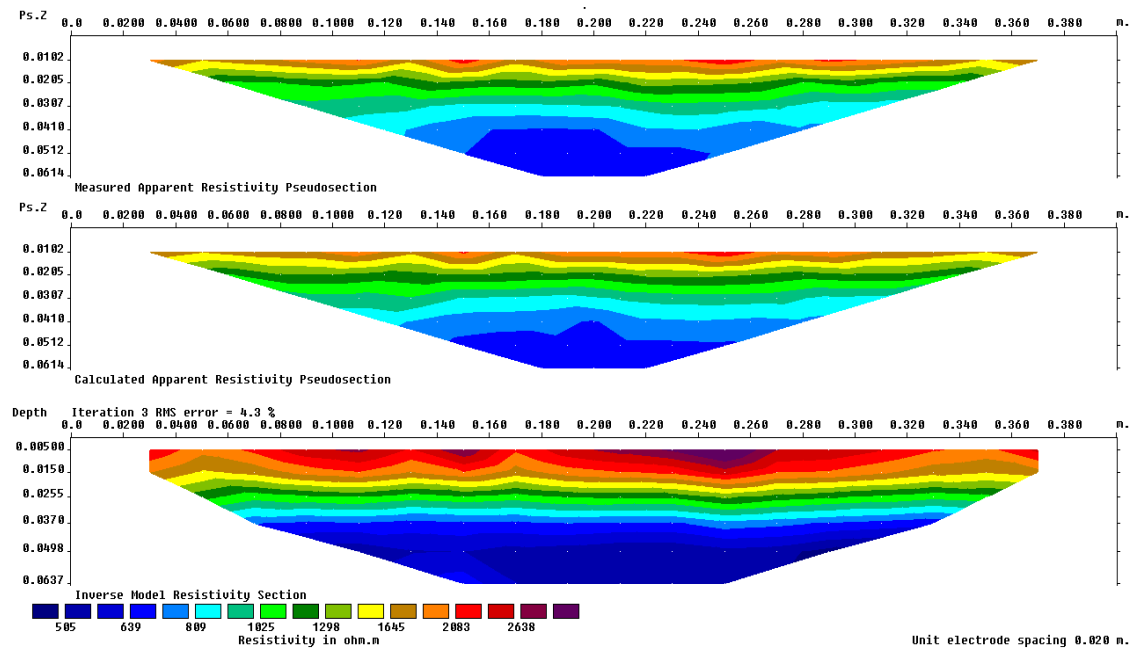
Figure 4.66   The pseudosection of Horizon B after one traverse with the

MSP40.

Traverse 2 Horizon B
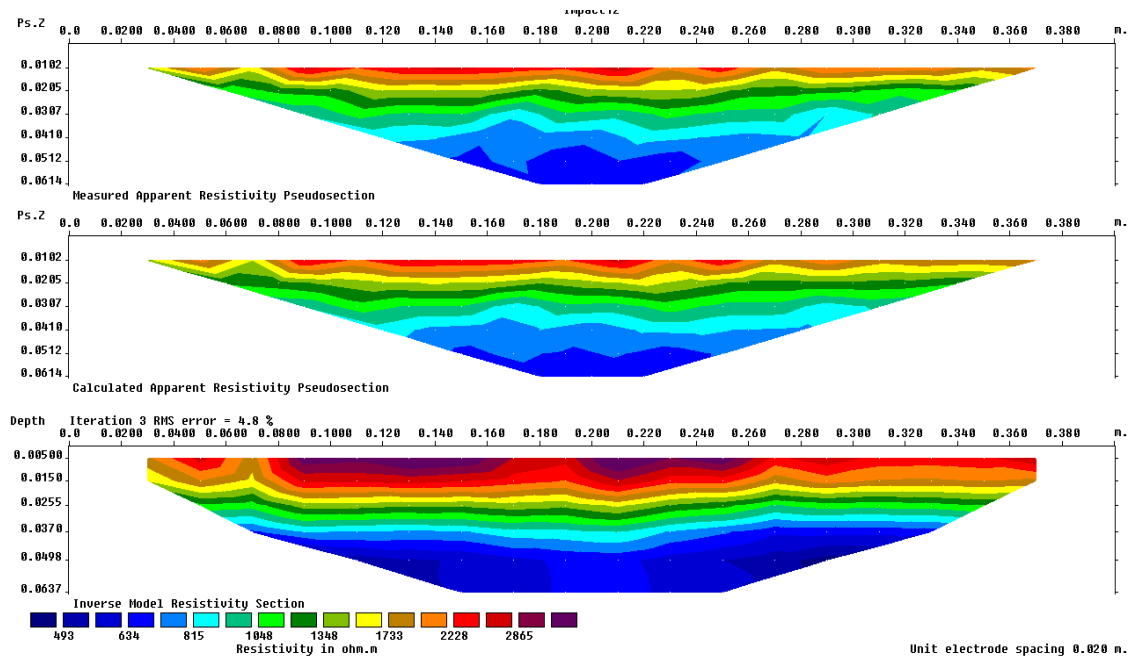
Figure 4.67   The pseudosection of Horizon B after two traverses with the

MSP40.

Traverse 3 Horizon B
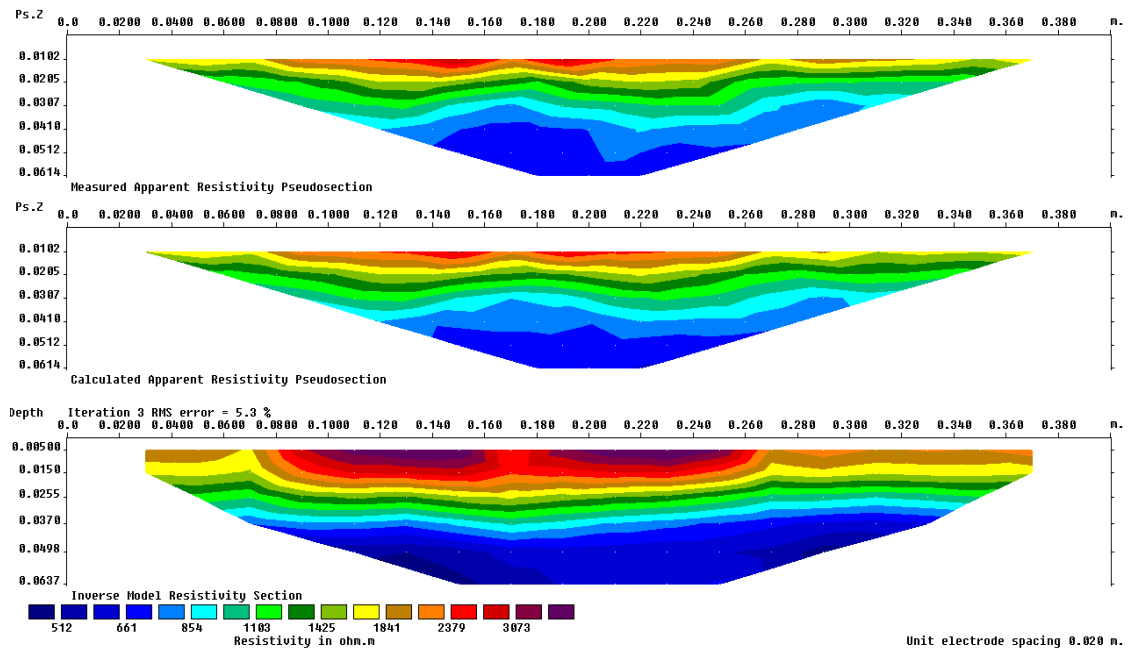
Figure 4.68   The pseudosection of Horizon B after three traverses with the

MSP40.

Traverse 4 Horizon B
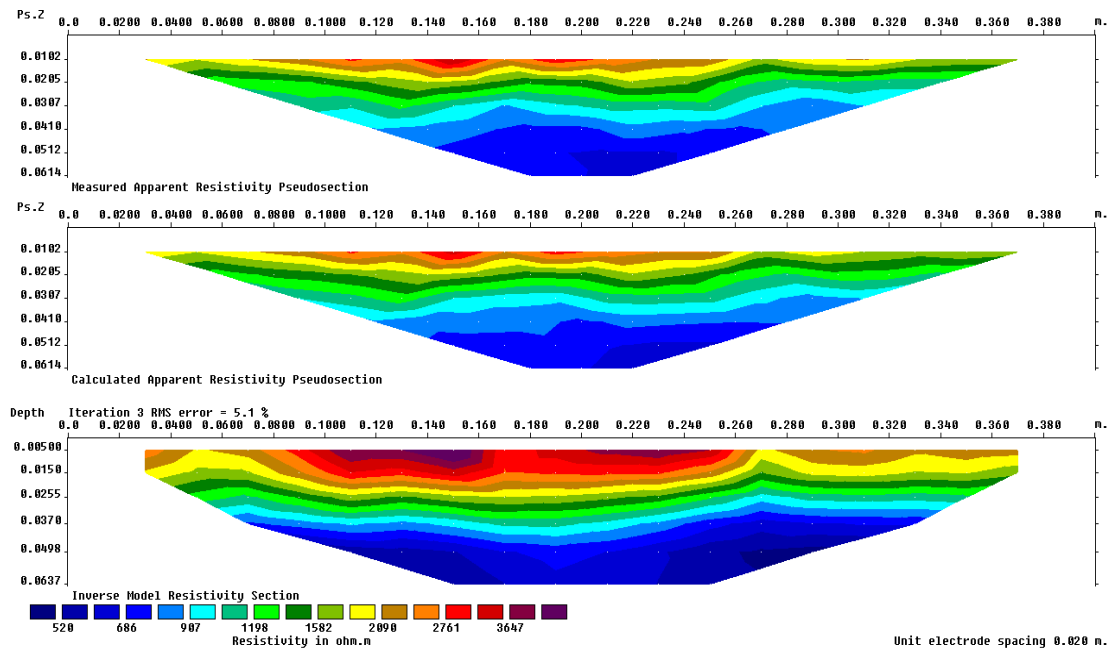
Figure 4.69   The pseudosection of Horizon B after four traverses with the

MSP40.

Traverse 5 Horizon B
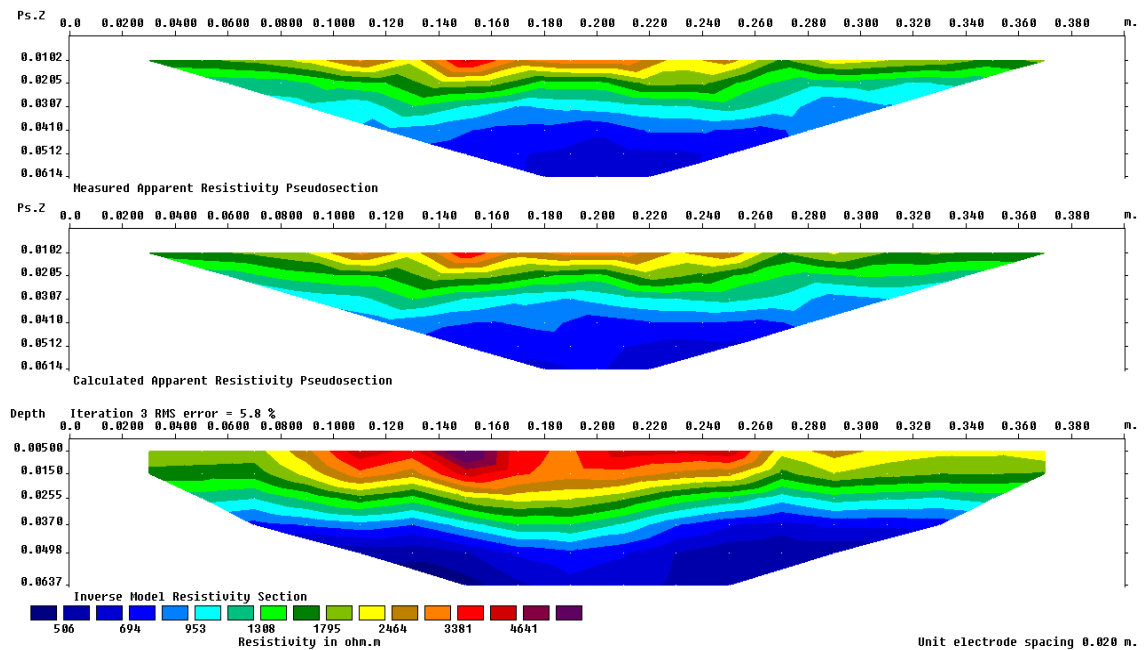
Figure 4.70   The pseudosection of Horizon B after five traverses with the

MSP40.

The Horizon B apparent resistivity values all show an increase in the plotted ranges from the initial pre-compaction soil conditions apart from the first traverse which shows a slight reduction in apparent resistivity. The reduction in apparent resistivity may be a result of errors in recording but is more likely to be a result of the consolidation of the soil reducing hollows or air pockets and the forced movement of soil moisture down the soil profile reducing the apparent resistivity for the horizon. The lowering of resistivity values due to the compaction effects of vehicular traffic have been reported elsewhere (Besson *et al.* 2004 ; Samouëlian *et al.* 2005) (see figure 4.71). The highlighted low resistivity values corresponding to the areas under vehicular compaction with values of 1.53 Mg m^{-3} compared to 1.39 Mg m^{-3} in the surrounding soil matrix. The low resistivity band at the bottom of the data relates to a different soil horizon.
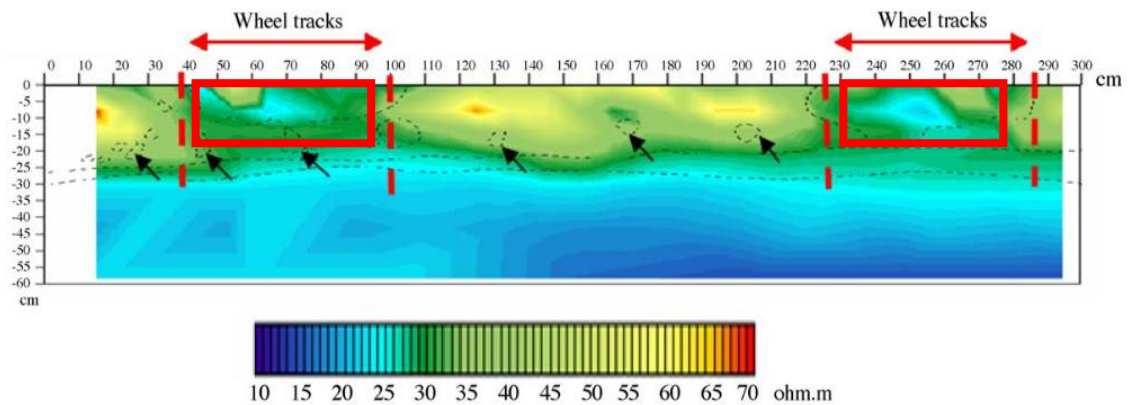
Areas of low resistivity values through compaction of soil.

The black arrows represent individual clods of soil identified and drawn by the original author Samouëlian *et al.* (2005).

Figure 4.71 A vertical pseudosection showing the low resistivity values caused by soil compaction from vehicular traffic (after Samouëlian *et al.* (2005)).

The increasing apparent resistivity values for subsequent traverses is due to an increase in compaction of the soil as shown by the penetrometer measurement and the reduced theoretical half space for the current. The surface layer was compacted down to a level approximately equal to the position of the Horizon B electrodes by the third traverse. The Horizon B electrodes retained more soil around the electrodes as any material from Horizon A would have slumped down to cover the lower electrodes explaining why the plotted ranges for the apparent resistivity is approximately half the maximum of Horizon A after the fifth traverse (506-4641 ohm.m ± 5.8 % error compared to 408-10793 ohm.m ± 4.5% error).

Pre-traverse Horizon C
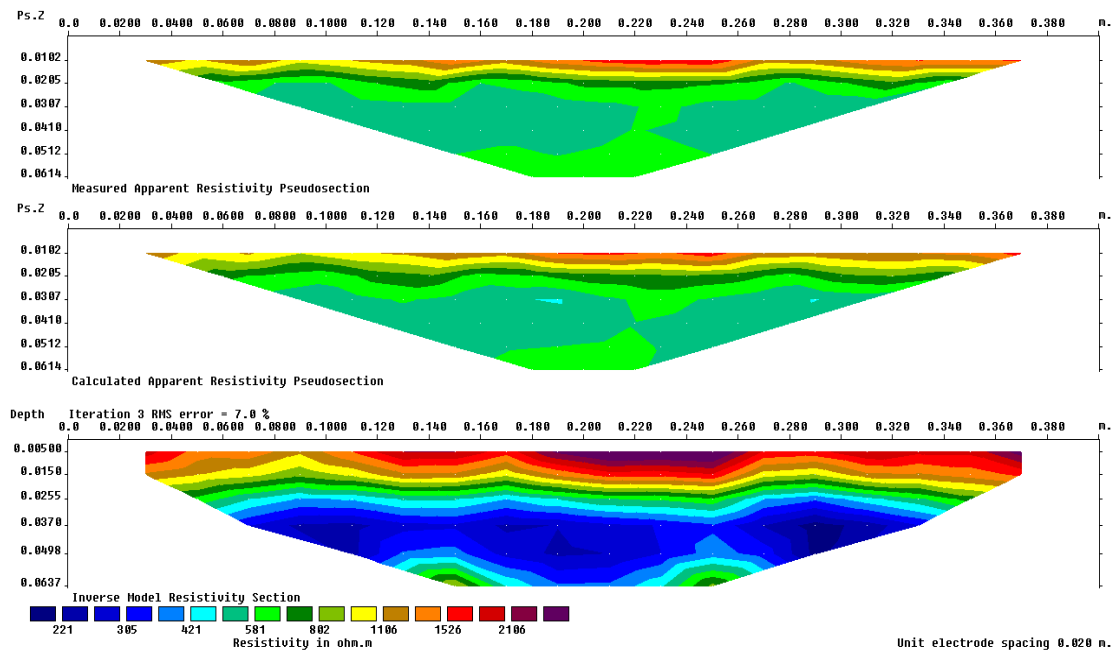
Figure 4.72   The undisturbed horizontal pseudosection of Horizon C.

Traverse 1 Horizon C
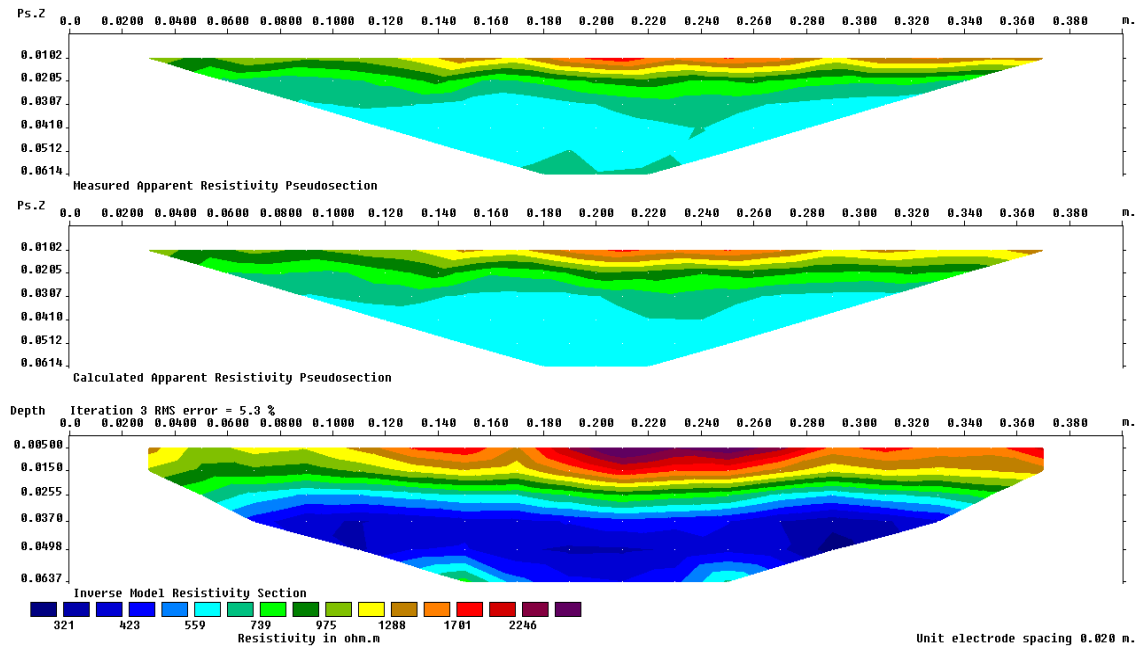
Figure 4.73   The pseudosection of Horizon C after one traverse with the

MSP40.

Traverse 2 Horizon C
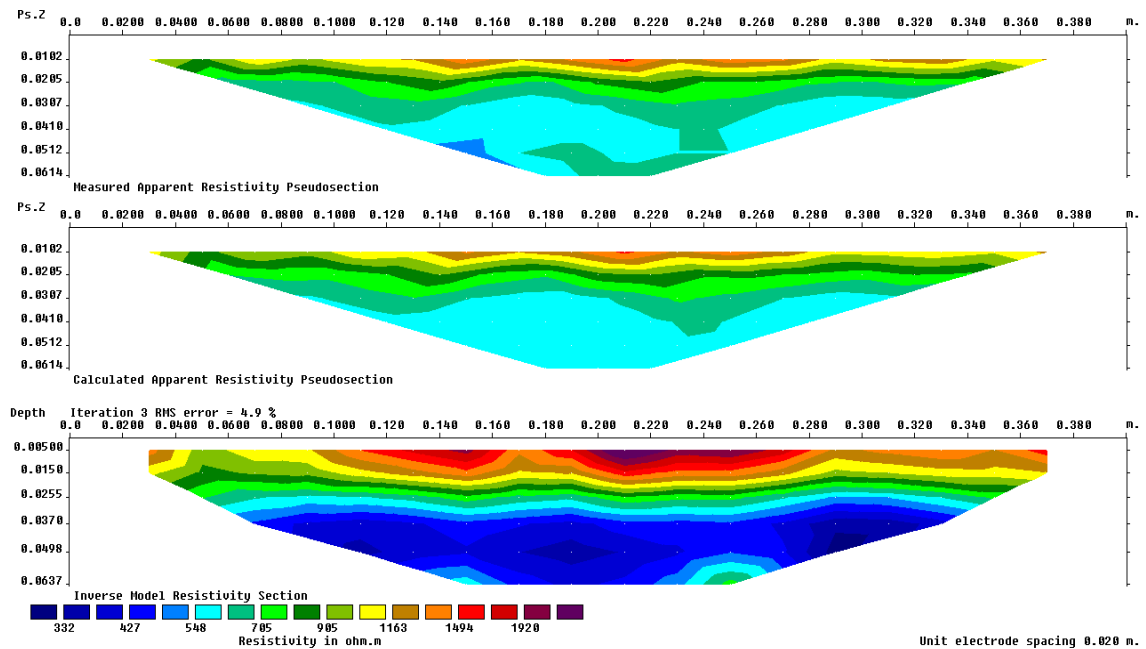
Figure 4.74   The pseudosection of Horizon C after two traverses with the

MSP40.

Traverse 3 Horizon C
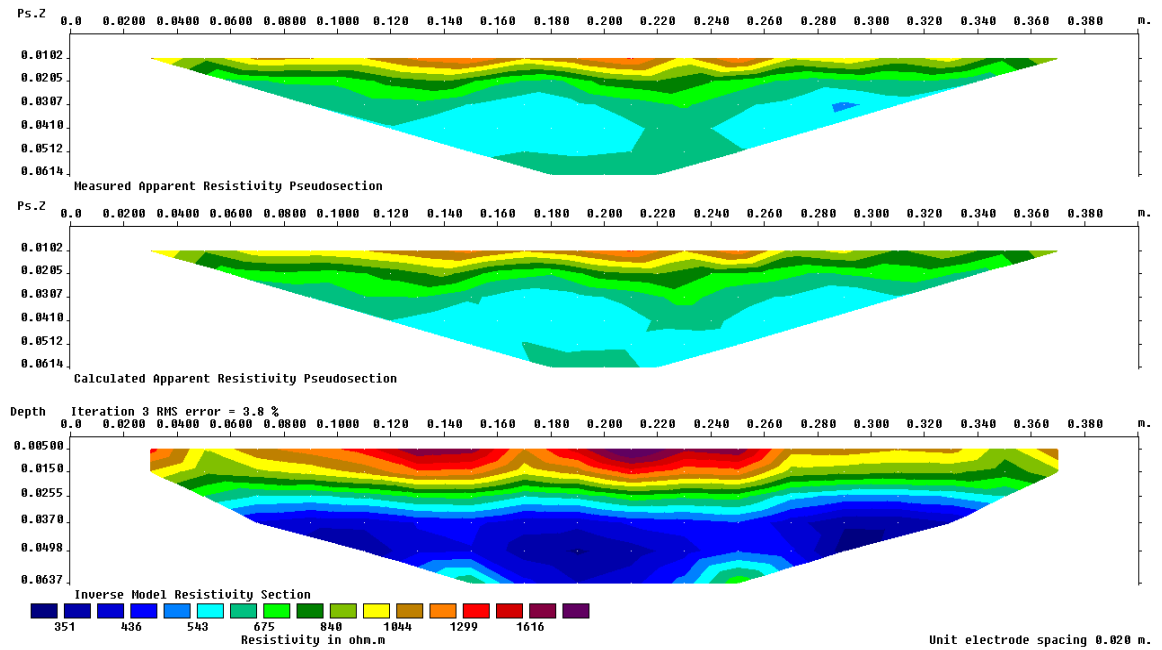
Figure 4.75   The pseudosection of Horizon C after three traverses with the

MSP40.

Traverse 4 Horizon C
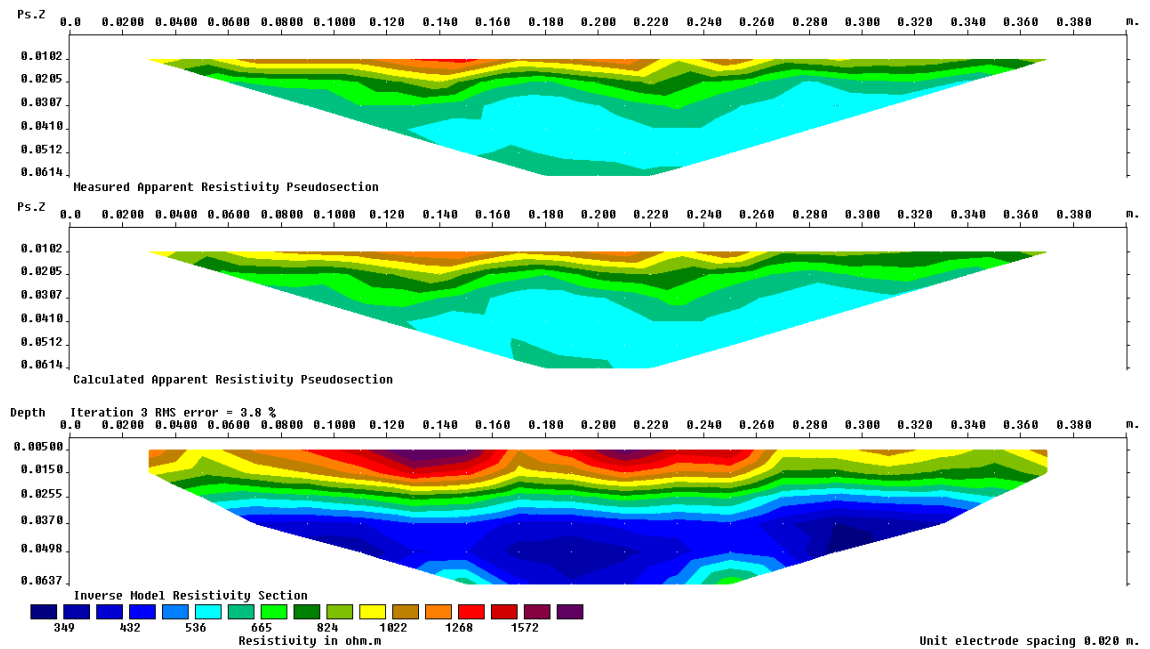
Figure 4.76   The pseudosection of Horizon C after four traverses with the

MSP40.

Traverse 5 Horizon C
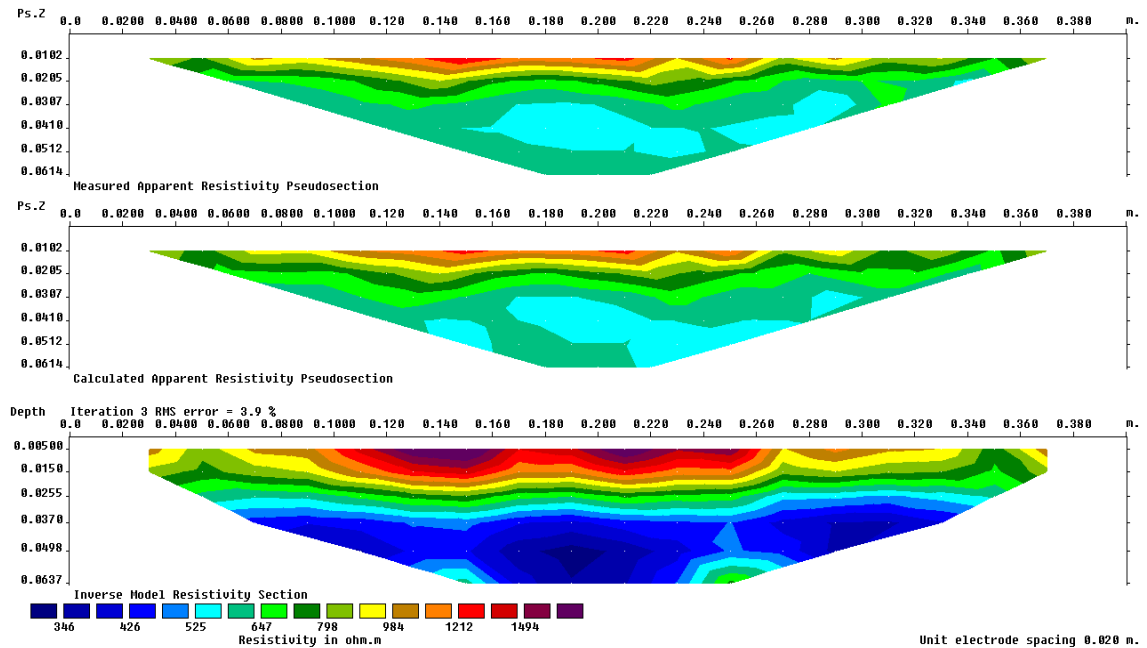
Figure 4.77   The pseudosection of Horizon C after five traverses with the
MSP40.

Horizon C profiles show a decreasing apparent resistivity range after repeated traverses which is due to consolidation / compaction of soil reducing airspace and the possible movement of water down the soil profile filling the pores causing reduced apparent resistivity measurements. The results show a reduction in resistivity values that also confirm compaction from the MSP40 is affecting the soil properties at a depth of over 7cm. The loosely compacted soil (pre-traverse) may be the main influence of the depth of compaction results as the soil remained friable even after the four week 'settling period'. Field measurements may produce less significant changes to apparent resistivity results as the soil is likely to be more compacted before any measurements are recorded.

The Horizon C profiles show the lowest apparent resistivity ranges of the three 'topsoil' (Horizons A, B and C). This is likely to be due to the natural movement of water down the soil profile through infiltration. Such findings have also been reported elsewhere Cousin *et al.* (2009).

Pre-traverse Horizon D
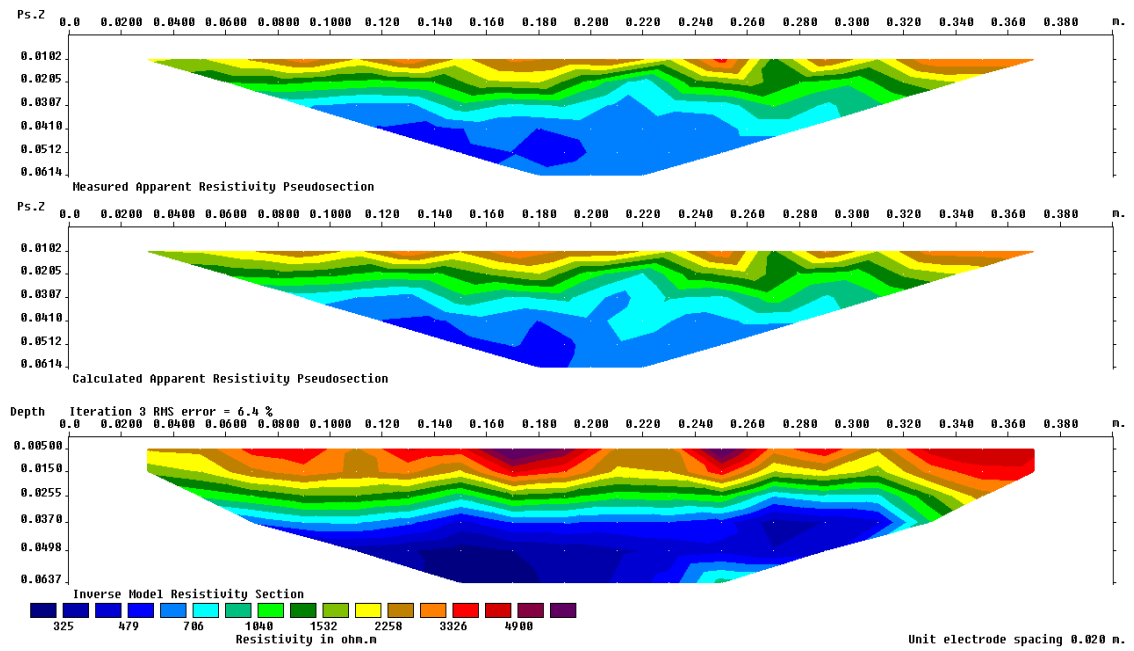
Figure 4.78   The undisturbed horizontal pseudosection of Horizon D.

Traverse 1 Horizon D
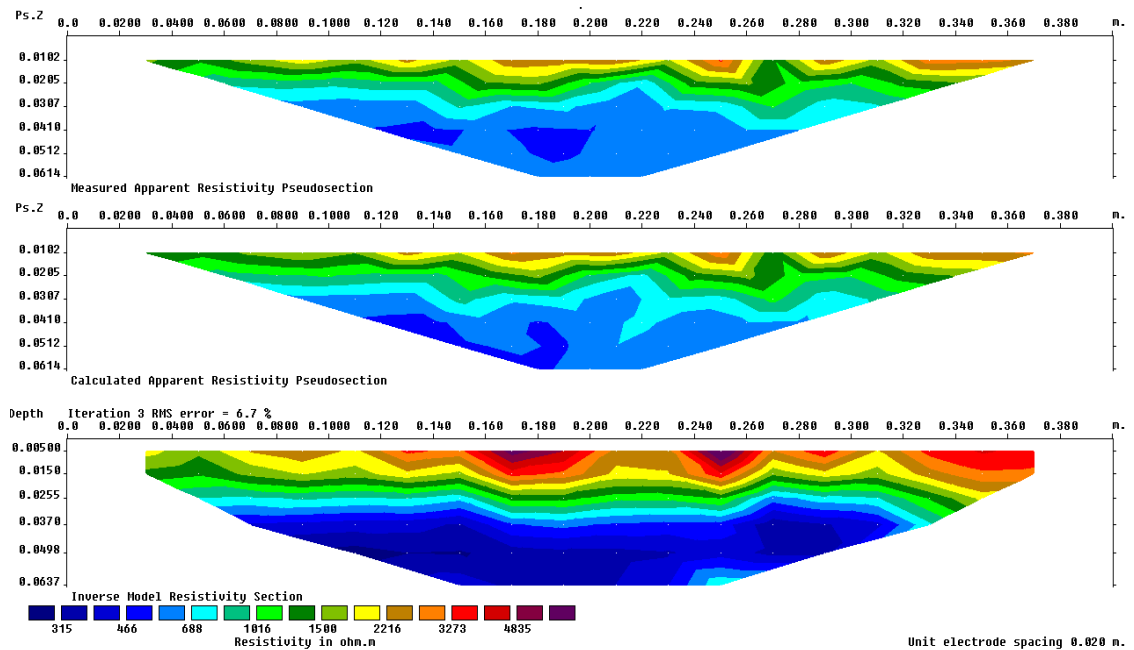
Figure 4.79   The pseudosection of Horizon D after one traverse with the

MSP40.

Traverse 2 Horizon D
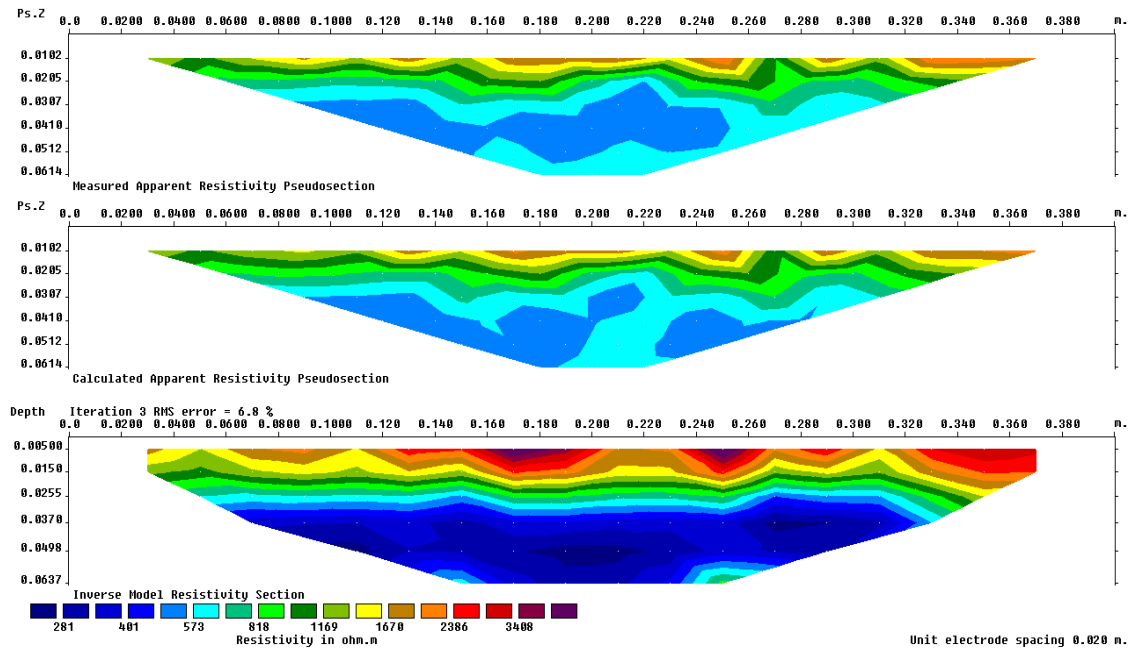
Figure 4.80   The pseudosection of Horizon D after two traverses with the

MSP40.

Traverse 3 Horizon D
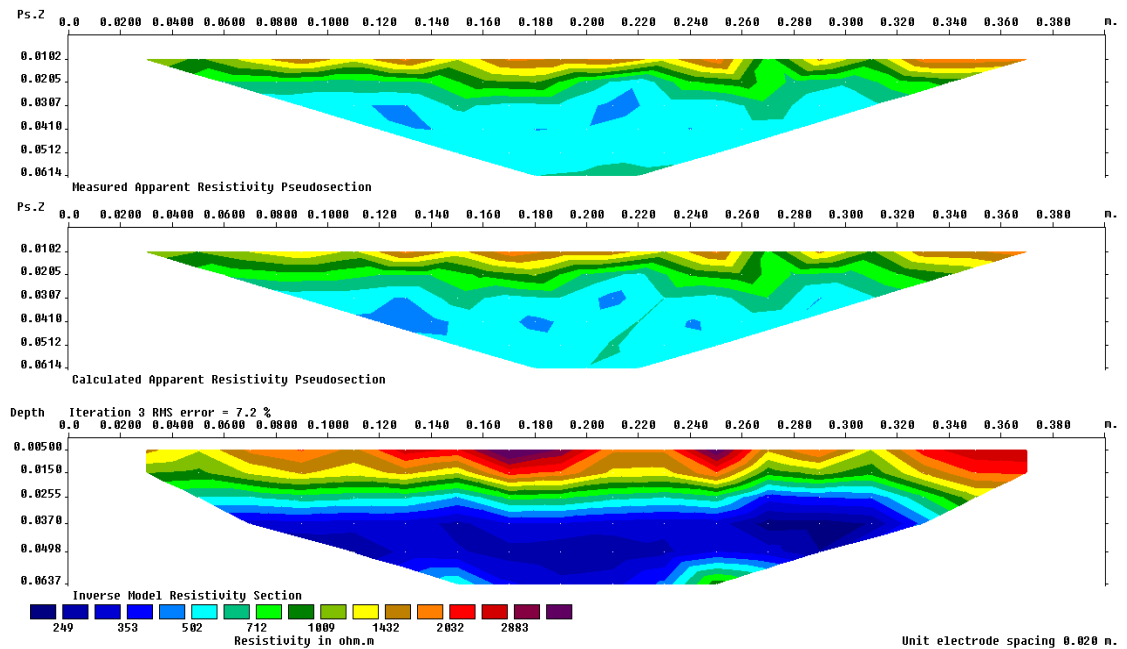
Figure 4.81   The pseudosection of Horizon D after three traverses with the

MSP40.

Traverse 4 Horizon D
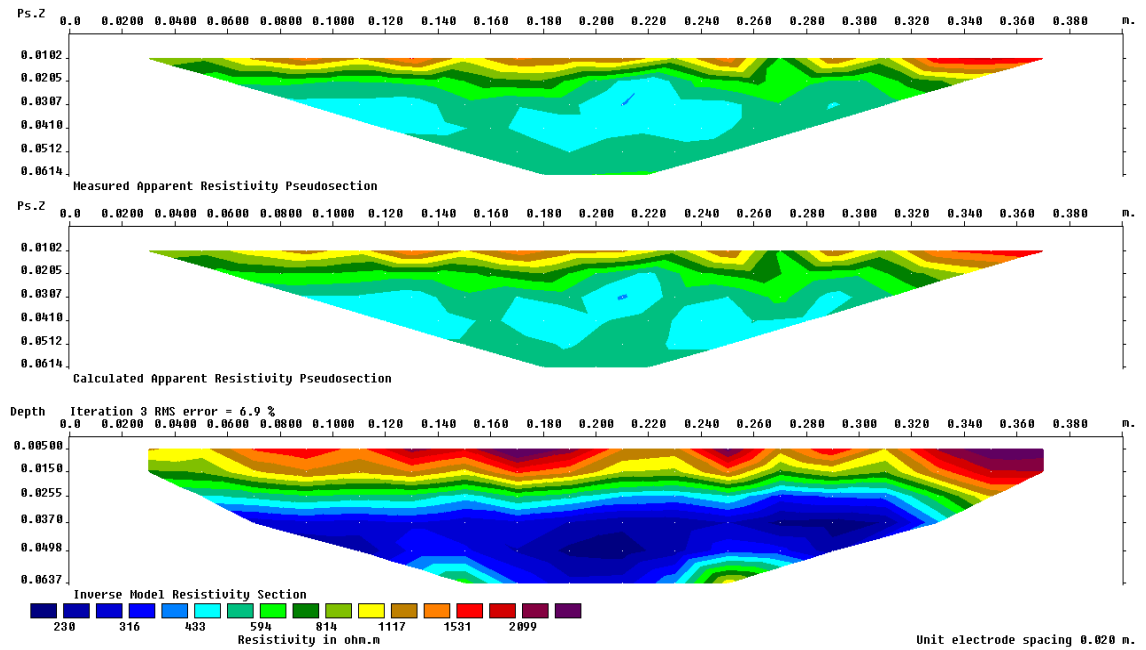
Figure 4.82   The pseudosection of Horizon D after four traverses with the

MSP40.

Traverse 5 Horizon D
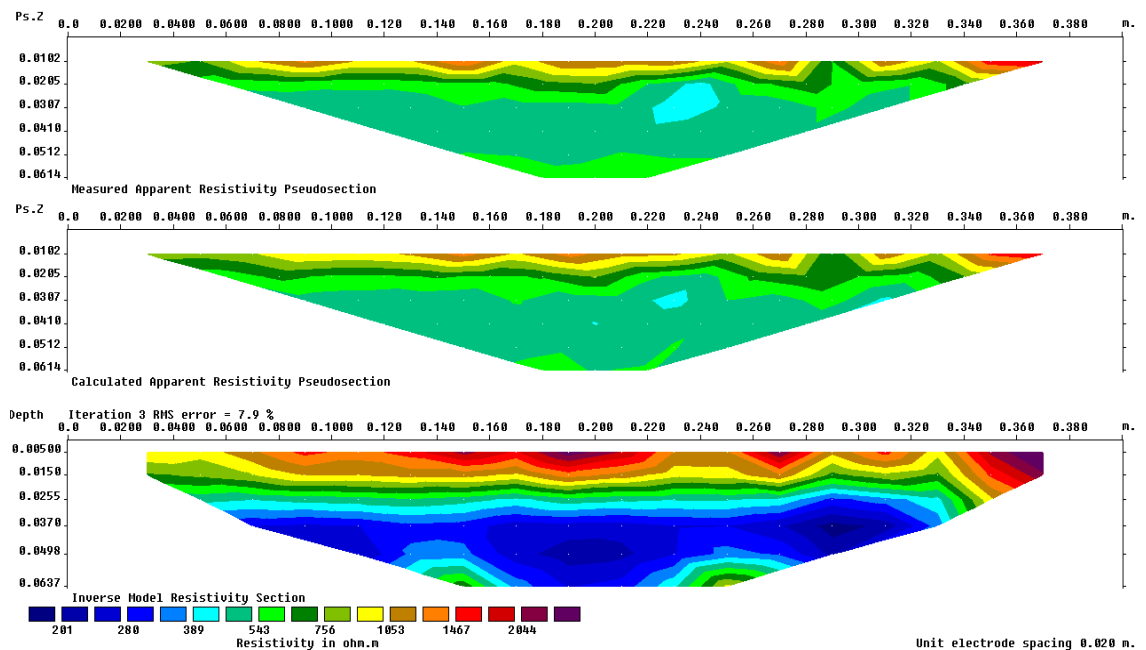
Figure 4.83   The pseudosection of Horizon D after five traverses with the

MSP40.

Horizon D horizontal profiles are the only electrodes buried in the sand layer; the apparent resistivity values for the sand layer are the highest apparent resistivity values for any horizon in the pre-compaction measurements (325-4900 ohm.m). Each subsequent traverse shows a reduction in the recorded ranges of apparent resistivity values. This may be a result of the compaction of the 'top soil' forcing soil moisture down the soil profile to the 'subsoil' layer. However, if significant compaction had taken place the electrodes may have been in contact with the 'topsoil' layer explaining the halving effect of apparent resistivity values as the electrodes would no longer be measuring the sand layer. It was decided to excavate a section of the sand box near the electrodes to examine if the probes were still buried in the sand layer.

Careful excavation revealed that the sand layer had compacted by approximately 5mm-10mm but was still covering the electrodes; however, the current is likely to flow through the topsoil due to the decreased resistance of the topsoil compared to the sand layer (see figure 4.84).
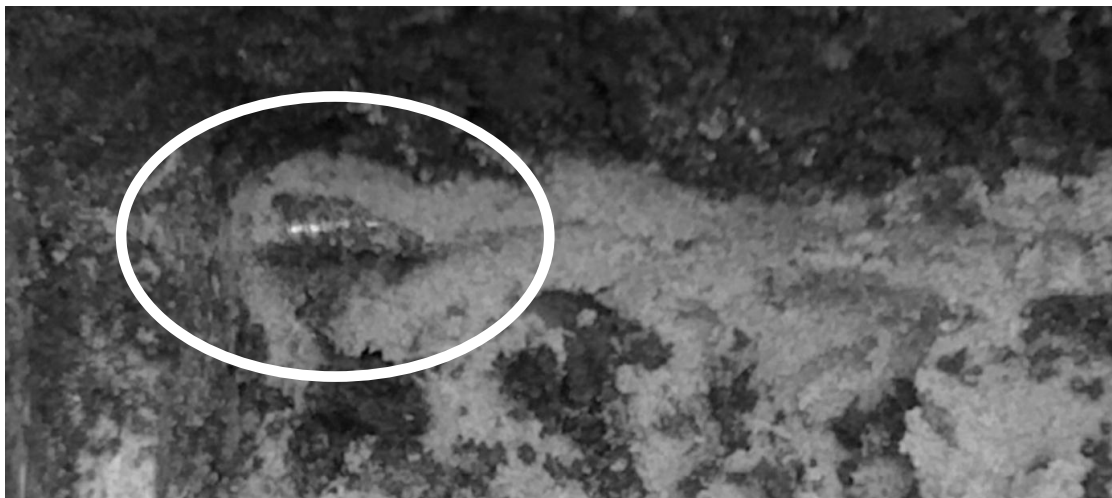
Figure 4.84   The excavated Horizon D electrode still buried in the sand.

4.3.21 Surface measurements

A miniature Wenner array was built for surface measurements. The electrodes had a probe separation of 3cm and were measured at the same time as the pseudosections (after each traverse). The array was constructed as a single depth pseudosection so that only the near-surface measurements were recorded. This was due to the limited space in the box that would not allow for increasing probe separations (see table 4.14).

Table 4.14   Surface earth resistance measurements

Measurement number	Pre-compaction	Traverse 1	Traverse 2	Traverse 3	Traverse 4	Traverse 5
1	1270	1330	1460	1175	1445	1415
2	1050	1490	10180	3930	10345	10900
3	990	2375	10255	8550	13620	13910
4	1405	1500	13730	13920	13055	13115

All earth resistance values are quoted in ohms

The surface measurements recorded perpendicular to the traverse direction show a significant increase in the earth resistance measurements after each traverse. As the electrodes were mounted on to a wooden frame it was difficult to adjust the height of the electrodes to account for the changes in the ground surface. It is therefore possible that a poor contact on one of the potential probes may explain some of the variation between traverses.

The first measurement for each traverse was positioned so that it always lay outside the zone of compaction; this is why there is a reduced variation between the recorded earth resistance measurements. What variation there is was likely to come from a change in the position of the electrodes between measurements as the frame had to be removed and repositioned after every traverse. However, the results do indicate that the compaction of the soil surface is measurable by a simple linear array measurement with a small probe separation. The problem with this method in the field comes from measuring the surface before compaction then measuring the same position post traverse and to ensure the MSP40 runs over these measured areas.

4.4.0 Wheel configuration / choice

4.4.1 Introduction

Whilst carrying out the research into the MSP40 it became apparent that the level of success of earth resistance surveys could be affected by the wheel configuration. The number of erroneous readings in data and the effort to pull the MSP40 are also related to the wheel choice.

A number of different wheel options were trialled during the research. The following section highlights factors that can influence wheel choice and summarises the benefits and limitations of each configuration.

4.4.2 Factors affecting wheel choice

4.4.3 Soil moisture

The seasonality tests have shown how the quality of results can vary with variations in soil moisture change. Only the standard spike lengths were used for the entire testing period but showed the issues that arise in both dry and wet conditions. Both wet and dry soil conditions need to be considered as both extremes can influence the decision making process.

Dry soil

Dry soil causes two main issues for the MSP40. The first is poor spike penetration as the wheels cannot cut into the ground surface has dried out and compacted. This reduces the surface area of the electrodes in contact with the soil medium which also leads to the second issue of overcoming contact resistance. As the soil dries out the contact resistance of the electrodes increases which can lead to a blocking of the current flow from the electrode to the soil medium. The reduced surface area of the electrode makes the issues worse by restricting the contact points from which current can flow. In the case of the MSP40 this leads to drop out in data i.e. negative / erroneous values recorded as the continuous collection of the MSP40 means a value must be recorded regardless of errors.

Long spikes may help to reduce the contact resistance problem by penetrating deeper into the soil. However, this is dependent on the spikes being able to cut deep enough into the ground to interact with areas of increased soil moisture lower down the soil profile. However, longer spikes cause more damage to archaeological sites and require more effort to pull the cart. Additional weight may also be added to the cart in the form of sand filled tubes (see chapter 3.4.14) to increase the spike penetration but once again increases the physical impact on the soil surface.

A more appropriate solution is likely to come from the future development of a new resistance meter with variable current options to hopefully reduce the contact resistance issues (see chapter 7.2).

Wet soil / material build up

Wet soil conditions are generally not affected by contact resistance issues as the current can flow freely between the electrodes and soil. However, material build up on the wheels of the MSP40 can effect the positional accuracy of measurements. This is only an issue when using the optical encoder to trigger the sampling positions As material collects on the wheel it increases the diameter of the wheel resulting in less revolutions to cover the same distance (see chapter 4.4.9). The soil build up on the wheels can be reduced by choosing a shorter spiked wheel as the spikes help to bind the soil and plant material to the wheel.

The survey at Towthorpe (see Appendix A) highlighted the issues with the MSP40 in extremely wet conditions. The site is located on the Yorkshire Wolds in North Yorkshire. The parent geology of the area is chalk that was formed during the Cretaceous period. The upland areas remained unaffected by the glaciations of the Devensian period. However, windblown sand was deposited during this period which covered much of the Yorkshire Wolds.

The soils that cover the upland areas of the Wolds are a mix of Rendzinas and Brown Earths. The soils on the upper slopes are often less than 20cm thick and tend to be the Rendzinas made from the chalk parent material (from the East Riding of Yorkshire Council website unknown author (2005)).

The disc wheels (discussed in chapter 3.5) were trialled on the site but before any survey work could commence the MSP40 had to be pulled approximately 100m to reach the survey area. The build up of soil material encased the wheel in over 3 cm of material. The trial was aborted due to the additional weight and effort required to pull the MSP40.

The survey was completed with the short spikes to reduce the potential soil build up. Each wheel was weighed shortly after the survey and found to weigh approximately 4.75 kg per wheel including the wet soil (each clean wheel weighs 2.75 kg). A similar test was performed on the seasonality testing site using the normal spiked wheels; the dry weight of material totalled 3.5kg from the four wheels over a single 20m grid.

4.4.4 Soil composition and stone content of the soil surface

The quality of results can be affected by the soil composition in terms of the type of soil and the quantity of the inclusions within the soil. Sandy soil can cause problems as the soil is free draining and results in issues with contact resistance especially during the summer months.

A MSP40 earth resistance survey at West Heslerton, North Yorkshire was carried out in May 2011 over a site covered in approximately one metre of windblown sand. The site had not had significant rainfall for over a month. The disced wheels were fitted to the normal spike length wheels (see figure 4.85).
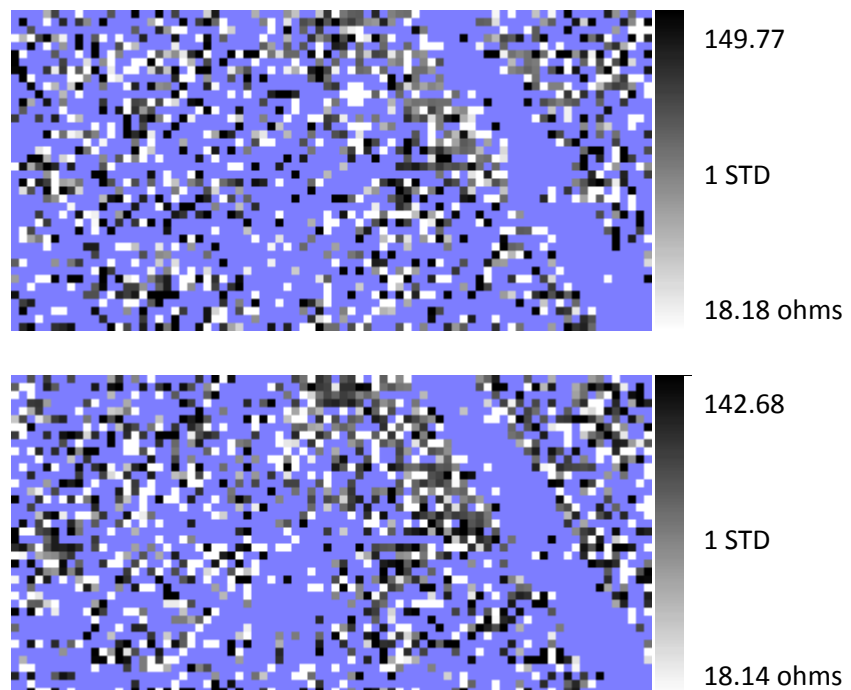
Figure 4.85   MSP40 Alpha (top) and Beta (bottom) earth resistance data display from West Heslerton, North Yorkshire with the negative values replaced with dummy values.

The greyscale plots show the significant drop out in data due to the dry sand conditions. The only data processing carried out on the data sets was the removal of all negative values. No archaeological interpretations could be made due to the lack of recorded information.

Long spikes may improve the success of surveys in these conditions but extended periods of dry weather will make survey success unlikely without additional options to alter the current settings to overcome the contact resistance.

The cohesive nature of clay soils will often lead to soil and material build up on the wheel especially in wet conditions. Fine-grained soil particle may stick to the wheels when the soil is wet especially if mixed with loose vegetation (cut crops or leaf litter). Clay soils are best surveyed with a shorter spike wheel to reduce the build up of material on the wheels.

The stone inclusions of the soil can significantly effect the number of spikes recorded in the data. The data quality of the survey at Pförring, Germany was affected by the near-surface limestone geology being brought to the surface through deep ploughing (see chapter 5.3.11 and 5.3.12). Large numbers of limestone fragments lay on or near the surface of the soil. The dense distribution of fragments restricted the spike contact with the soil causing a large number of high resistance spikes or negative readings where no resistance value could be recorded.

The normal spike length was used for the survey but the short spikes were trialled to see if it improved the data as short spikes were more likely to miss the limestone fragments. However, the trial was aborted as the site had been harvested but was covered in dry straw that acted as an insulating layer that the short spikes could not cut through. The short spikes were replaced with the normal spikes and the survey continued with the acceptance of spikes in the data due to the limestone fragments.

4.4.5 Vegetation cover

As described above the vegetation cover on the site should also influence wheel choice. The survey at Pförring was not the only survey where vegetation proved problematic. The geophysical investigation on Bingley Moor (see chapter 4.3.11) was initially surveyed with a bare wheel configuration due to the sensitive nature of the previous land use. The first day on site produced encouraging results but subsequent days over thick dry heather meant the bare wheel could no longer record resistance measurements due to the springy insulating plant layer.

A commercial geophysical survey carried out by the University of Bradford at Wykeham Abbey used the MSP40 for earth resistance measurements. The grounds of the abbey were covered in well-kept short grass; however, the grass also contained a high percentage of moss. The moss and grass were thick enough to spring against the weight of the MSP40 and stop contact with the soil.

The long spikes could have been used for the survey but would have caused too much damage to the lawn. Instead the sand-filled tubes were used to add additional weight to the cart and this was sufficient to make a good electrical contact with meaningful resistance measurements.

An additional earth resistance site survey at Kilnsey in the North Yorkshire Moors (see chapter 6.3.2) had a similar moss component as Wykeham Abbey but mixed with long grass. A disced wheel was trialled on the site and was shown to be very successful with low spike numbers and little to no drop out in data values.

4.4.6 Ground conditions

Surface rutting caused by wheel and animal hoofs has also influenced the data quality of earth resistance surveys. The direction of the rutting in relation to the traverse direction can effect the results. Rutting that lies perpendicular to the traverse direction can cause the optical encoder to stop working if the MSP40 wheels lurch down into a rut. Generally wheels with normal spikes dealt the best over rutted ground as the bolts helped to grip the soil and reduce the lurching of the wheels.

4.4.7 Inertia tests

The amount of energy required to pull the cart is directly affected by the wheel choice; the longer the spike the harder it is to pull the cart especially on soft ground which the spikes can easily penetrate. As part of the research a spring balance was used to approximate the amount of effort required to pull the mobile platform; the initial inertia was recorded i.e. how much effort is required to start moving. This was recorded through a visual check of the spring balance dial at the beginning of each traverse. The maximum inertia across the entire traverse was also recorded which was achieved by a second needle on the spring balance that recorded the maximum effort and stayed in place till manually reset (see table 4.15).

Table 4.15   Inertia measurements

Date of survey	Wheel type	Initial inertia	Maximum inertia
06.05.2009	Bare	13 lbs.	13 lbs.
06.05.2009	Short	20 lbs.	24 lbs.
06.05.2009	Normal	31 lbs.	37 lbs.
06.10.2009	Normal	43 lbs.	54 lbs.
25.11.2009	Normal	29 lbs.	36 lbs.
09.12.2009	Normal	28 lbs.	37.5lbs
26.01.2010	Normal	32 lbs.	35 lbs.
26.02.2010	Normal	28 lbs.	41 lbs.

The inertia tests clearly show the advantage of using a bare wheel configuration in reducing the physical effort of pulling the MSP40. When the normal spike, short spike and bare wheel configurations are considered the normal wheels shows a doubling in effort required compared to the bare wheels. The results also show the effort required to pull the MSP40 varies from month to month and is linked to the changing soil moisture.

4.4.8 Wheel choice summary (see table 4.16)

Table 4.16   Wheel choice summary

Wheel type	Long spike	Normal spike	Short spike	Bare wheel	Disc
Penetration depth	< 60mm	< 40mm	< 35mm	n/a	<40mm & <25mm
Compaction risk	Moderate	Moderate	Moderate	Reduced	Increased
Material build up	High	Medium	Low	Lowest	High
Inertia/effort	High	Medium	Low	Lowest	High / medium

Additional considerations

Long spike

Positives=   Offers greater penetration for drier soils.

Negatives=   Reduced penetration on stonier soils (reliant on small surface area for contact (bolt dimensions)) a significant amount of inertia/ force is required to pull the MSP40, increased spike penetration depth (more damage to sites).

Normal spike

Positives=   Best all-around performance for most site types and ground covers.

Negatives=   Material build up in wet conditions.

Short spike

Positives=   Reduced impact and inertia / force to pull the MSP40.

Negatives=   Can have reduced success on thick vegetation. Slight increase in spike numbers.

Bare wheel

Positives=   Reduced impact and inertia / force to pull the MSP40.

Negatives=   Will not work on thick vegetation or dry soil surfaces.

Disc wheel

Positives=   Smoother traverse (less vertical movement), continuous electrode contact at depth (for drier soils), weighted edge (greater pressure on small surface edge 4mm thick).

Negatives=   Increased physical impact on the soil, high levels of material build up in wet conditions and additional effort required to pull the MSP40.

4.4.9 Optical encoder testing

The amount of soil picked up on the wheels is an indication of the impact the MSP40 has on a site as small amounts of soil are displaced. The soil build up also affects the effort required to pull the MSP40 as it adds to the weight of the MSP40. In addition the material build up may affect the positional accuracy of the optical encoder-based measurements. The number of encoder pulses recorded during the calibration process was noted down before a number of seasonality surveys when the wheels were clean. The calibration was repeated at the end of the survey of the 20m x 20m grid without cleaning the wheels to see if soil build up affected the encoder measurements (see table 4.17).

Table 4.17   Optical encoder pulses

Date	Traverse 1	Traverse 2	Traverse 3	Average
Nov 2009 clean	338	338	339	338
Nov 2009 after	337	338	337	337
Dec 2009 clean	331	331	333	331
Dec 2009 after	337	328	324	328
Jan 2010 clean	333	334	333	333
Jan 2010 after	332	333	332	332
May 2010	331	327	329	329
May 2010	362	361	355	359
May 2010	383	363	374	373

☐ Short spike wheels   ☐ Bare wheels

The results show a slight decrease in the number of recorded pulses seen by the encoder after the survey suggesting the diameter of the wheel has increased due to the build up of material. This would affect the positional accuracy of subsequent grids especially over longer traverses ($\geq$40m). The problem can be reduced by monitoring the build up of material and cleaning the wheel when necessary. The short spiked and bare wheels have a larger number of recorded pulses as the maximum diameter of the wheel is reduced.

The variability in pulse counts on the same set of traverses is a result of dirt building up on the optical encoder lenses leading to a number of missed pulses.

4.5.0 Spikes in earth resistance data

4.5.1 Introduction

The amount of 'noise' or spikes in earth resistance data is an important area of investigation as it relates directly to data quality. As the research project incorporated a multi-array seasonality test it provided a comprehensive data set to investigate the number of spikes in the data.

4.5.2 Method

Each data set was processed with the following parameters, without the influence of different levels of processing of the data.

- 3 x Despike X=1 Y=1Thr=3 Repl=Mean

- Search and replace any negative values with the dummy value 2047.5

- Search and replace any values over 100 ohms with dummy value of 2047.5

The decision to replace any values over 100 ohms (an arbitrary value) with the dummy value was because these data points were deemed to be outliers in the data from examining the statistics. Negative values or drop out in data are a result of errors in recording which may be due to poor spike penetration and / or an inability to overcome the contact resistance at the electrode / soil interface.

The raw and processed data was exported from Geoplot and imported into Microsoft's Excel 2007. A logic argument was used to analyse the data.

=IF(ISERROR(VLOOKUP(C1,$D$1:$E$800,2,FALSE)),D1,VLOOKUP(C1,$D$1 :$E$800,2,FALSE))

The logic argument analyses the data in columns C and D (raw and processed data), if the values are identical then the information in column E (NO_CHANGE) is inserted in column F. However, when the processed column D is different to C then column D value is inserted in column F (see example table).

To calculate the number of spikes another logic argument was used for column G

=IF(ISNUMBER(F1),1,0)

This argument refers to column F if any number is present a 1 is returned in column G, if NO_CHANGE is in column F then a 0 is returned in column G. The total spikes were then calculated from column G using the SUM function (see table 4.18).

Table 4.18   Example table

A	B	C	D	E	F	G
0	0	19.9	19.9	NO_CHANGE	NO_CHANGE	0
0.5	0	22.2	22.2	NO_CHANGE	NO_CHANGE	0
1	0	2	21.6	NO_CHANGE	21.6	1
1.5	0	-23	2047.5	NO_CHANGE	2047.5	1
2	0	156	2047.5	NO_CHANGE	2047.5	1

A = X coordinate

B = Y coordinate

C = Raw data (Z)

D = Processed data (Z)

E = Information for logic argument

F= Result of logic argument NO_CHANGE = no spike, numerical values = spike replaced value

G= Spike count 0 = no spike 1= spike

An issue with the data import or a glitch in Excel meant that not all spikes were recorded properly; therefore a visual check was performed over all data sets to identify spikes not reported in the worksheet. When spikes were identified an e (for error) was inserted next to the column C input and this recorded a spike (see table 4.19).

4.5.3 Results

Table 4.19   Spikes per month

Date	# of spikes per 800 measurements for each array						Monthly average
	MSP40 Alpha	MSP40 Beta	MS Alpha	MS Beta	TW 0.5	TW 0.75	
Nov-08	5	21					13.00
Dec-08	15	14	2	0			7.75
Jan-09	14	12	1	3			7.50
Feb-09	13	7	4	0	1	0	4.17
Mar-09	14	20	4	0	29	0	11.17
Apr-09	36	88	18	7	12	4	27.50
May-09	33	61	3	2	2	2	17.17
Jun-09	27	46	6	2	4	2	14.50
Jul-09	23	32	4	18	1	2	13.33
Aug-09	61	41	20	16	2	0	23.33
Sep-09	25	22	18	3	3	3	12.33
Oct-09	16	17	16	21	0	2	12.00
Nov-09	25	8	8	4	1	2	8.00
Dec-09	12	11	5	2	3	1	5.67
Jan-10	13	15	8	4	1	1	7.00
Feb-10	17	12	4	2	3	1	6.50
Total	349	427	121	84	62	20	
Average	21.81	26.69	8.07	5.60	4.77	1.54	

4.5.4 Discussion

The manual square array shows 1.17-5.24 fold increase in the average number of spikes compared to the twin probe measurements throughout the year. This is likely to be because the twin probe has a current and potential probe inserted deep in to the ground (remote probes). Therefore errors should only occur at the two mobile current and potential probes.

The survey logistics of only inserting two probes into the ground also explains the lower spike counts for the twin probe array as the square array must have sufficient penetration to overcome the contact resistance of all four electrodes at every sampling interval making it more prone to error. Poor contact at the current probes impedes the current flow into the ground however; a false earth resistance measurement can still be recorded with a single potential probe if the electrical circuit is complete.

The results show a significant 2.7-17.3 fold increase in the number of spikes recorded by the MSP40 compared to the manual square and twin probe arrays. The increased number of spikes in the MSP40 data must be a consequence of the different methods of data acquisition, as the MSP40 has a near continuous collection whilst the manual square and twin probe are static measurements. The MSP40 must collect data in an allotted time or distance interval regardless of errors in the data. If the contact resistance cannot be overcome a value is still recorded. The MSP40 also requires a faster logging speed on the RM15 compared to the manual arrays which results in a reduced settling time for individual measurements making it more prone to spikes. The static collection also allows for the retaking of measurements if errors are spotted. The MSP40 does have a spike monitor, (see chapter 3.2.4) but is more difficult to perform a visual check on the data whilst it is being recorded. The static frames can also be repositioned or more pressure applied to record an accurate measurement. The MSP40 array also shares the same issue as the manual square (discussed above) with trying to achieve good ground contact with all four electrodes at once compared to the twin probe's two.

The 0.5m twin probe also showed approximately two to three times the average number of spikes compared to the 0.75m twin probe surveys. The increased spike noise may result from incorporating the 0.5m twin probe survey on the manual square array frame (see figure 4.86). The manoeuvrability of the frame is reduced as the square array probes are mounted on the corners of the array. Therefore subtle changes in topography can lead to reduced electrode surface area in contact with the soil as six electrodes must be inserted into the ground.
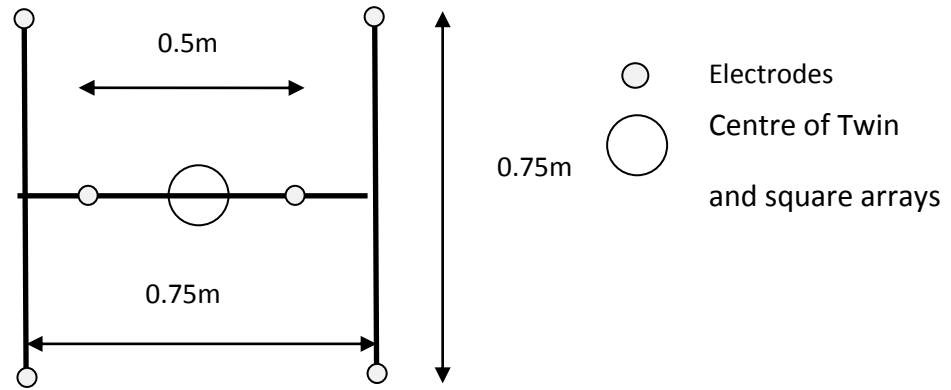
Figure 4.86   The manual square array dimensions with a 0.5m twin probe mounted on the same frame.

An additional factor in the increased number of spikes may be the electronic switching between Alpha and Beta and between the programmed arrays (manual square and 0.5m twin probe) as the analogue switching of configurations may introduce additional noise (Walker 2011a). This may further explain the additional noise in the 0.5m twin as the 0.75m twin probe was the only singly recorded data set e.g. no multiplexing.

Chapter 5 focuses on data processing and considers the effects of reduced data quality. The chapter discusses the different methods of combining the Alpha and Beta data sets before examining a theoretical data set with different percentages of errors and what can be done to remove many of the errors.

5.0.0 Processing earth resistance data

After the geophysical surveys have been collected it is necessary to process the data for interpretation and reporting purposes. As previously mentioned in chapter 2.9 the Alpha and Beta data sets can be combined in different ways ranging from mathematical combinations to RGB composites. This chapter discusses these methods in more detail and considers additional processing techniques, and what can be done when instrumental issues lead to reduced data quality.

5.1.0 Combining Alpha and Beta data sets.

5.1.1 Introduction

The Alpha and Beta (for definitions see chapter 2.3) readings may show subtle directional differences in current flow through the soil medium. It was therefore useful to combine the results into a single data set to display the maximum level of information about the geophysical anomalies. There are three commonly used methods of combining the data which will be discussed and the benefits and limitations of each will be highlighted.

5.1.2 Averaging

The simplest way to combine the Alpha and Beta data sets is to perform an averaging function by using the cut and combine function (using the add option) in Geoplot on the data and then divide the created data set by two (multiplying by 0.5) to return the resistance values to the recorded ranges.

However, the averaging of the two data sets can over-smooth the data loosing definition of anomaly edges. Weak anomalies in either the Alpha or Beta data set may also be lost by the averaging process (see figure 5.1). The highlighted areas in this combined data set show the subtle loss of information caused by averaging the data sets. The linear anomalies that are more pronounced in the Alpha data but are more fragmentary in the image of the combined data.
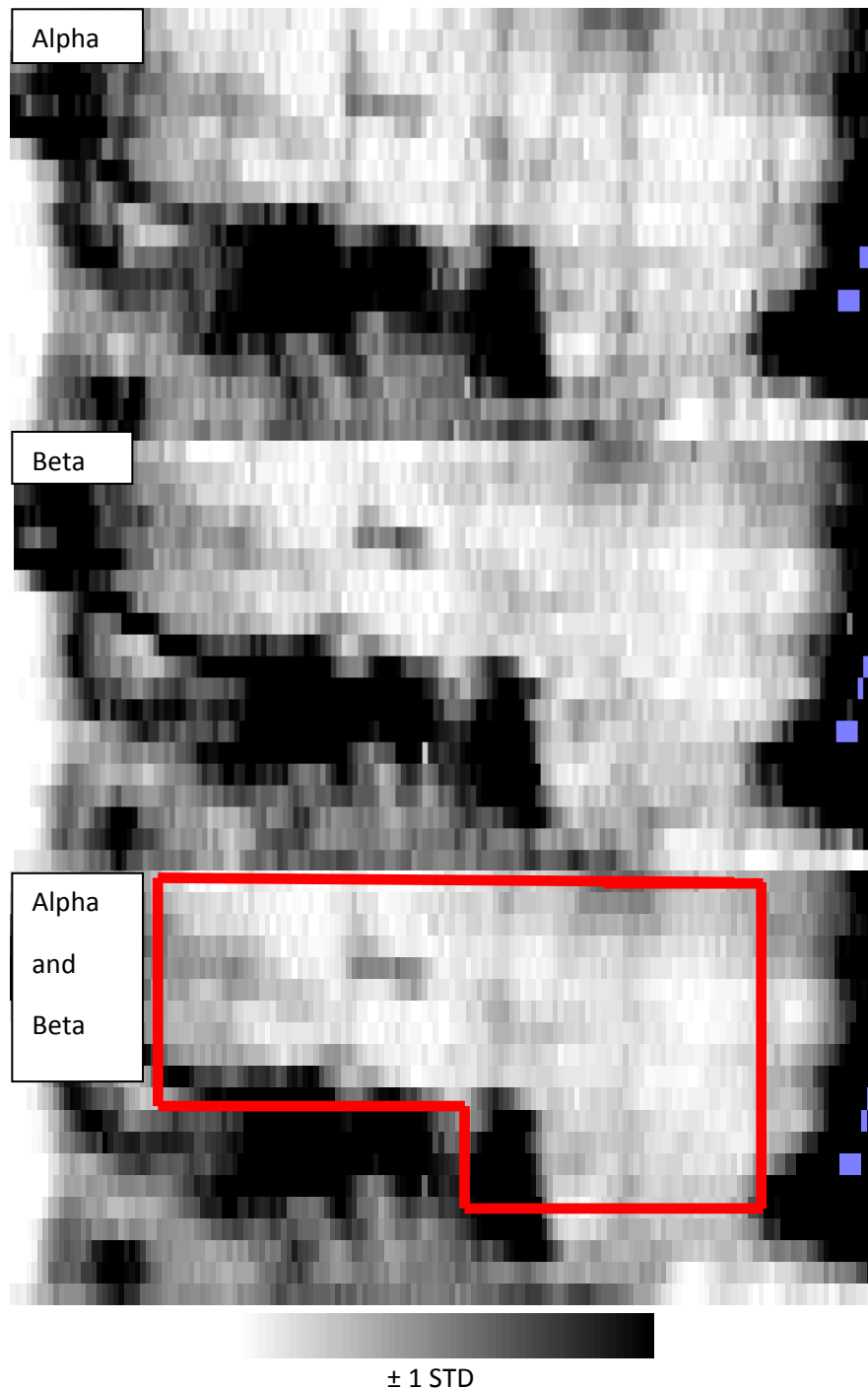
Figure 5.1   Littlemoor castle survey highlighting the smoothing and loss of
subtle information, using the averaging method of data combination. The red
box shows the area of reduced definition of linear anomalies. The survey extent
is 80m x 40m. Data provided by Geoscan Research (Walker 2005).

5.1.3 Mathematical combinations

An alternative method of combining the two data sets is to use a combine function written into the Geoplot software. The 'merge MSP40 composites' function allows the combination of Alpha and Beta sets by an algorithm that applies high pass filters to each data set before combining the data. The high pass filtering effect is then removed from the resulting data set (see figure 5.2).

The merge function allows the selection of a high pass filter window size and the type of weighting required (Gaussian or uniform). The window size is usually equal to a symmetrical window size in metres i.e. taking into account the sampling and traverse interval ratio. However, experimentation with window sizes may be required to improve the results for individual sites.

7.00   ohms   16.59

±1STD
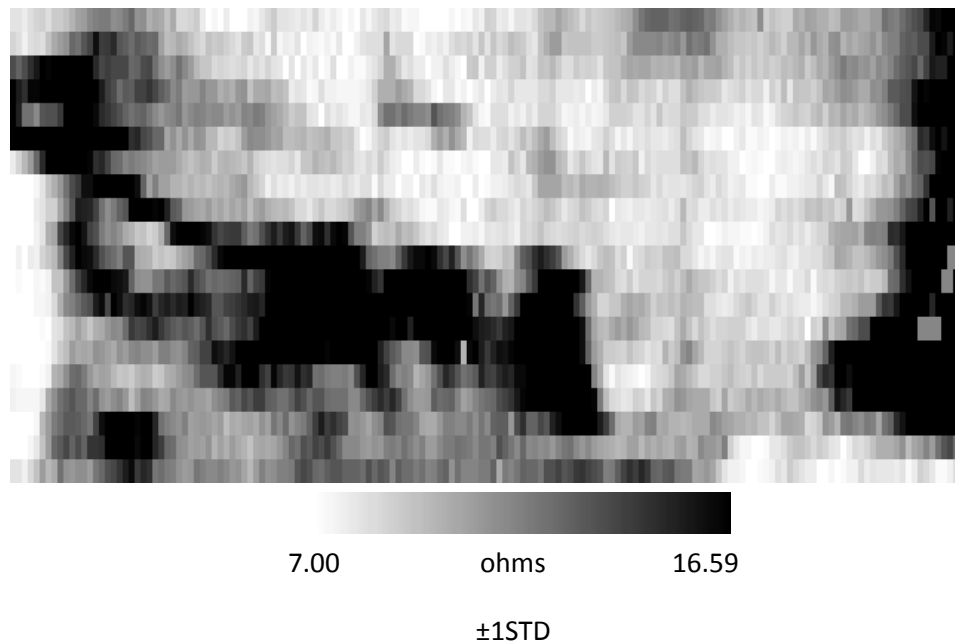
Figure 5.2   The results of Geoplot's MSP40 Alpha and Beta merge function. Survey data from Littlemoor Castle. Raw data provided by Geoscan Research (Walker 2005).

The merge function still shows a slight reduction in the visibility of the linear anomalies from the Alpha display but is more prominent than the average function.

By using the high pass filter combination it should be noted that although the data ranges are shifted back to the original values, the process can still create small 'halos' around spikes in the data (see figure 5.3-5.5). The halos are small but should be reported as a processing artefact in a report. This effect can be reduced by despiking both data sets multiple times (e.g. 3x Despike X=1 Y=1Thr=3 Repl=Mean) to remove the spikes before combining the data.

4.44   ohms   7.45

±1STD
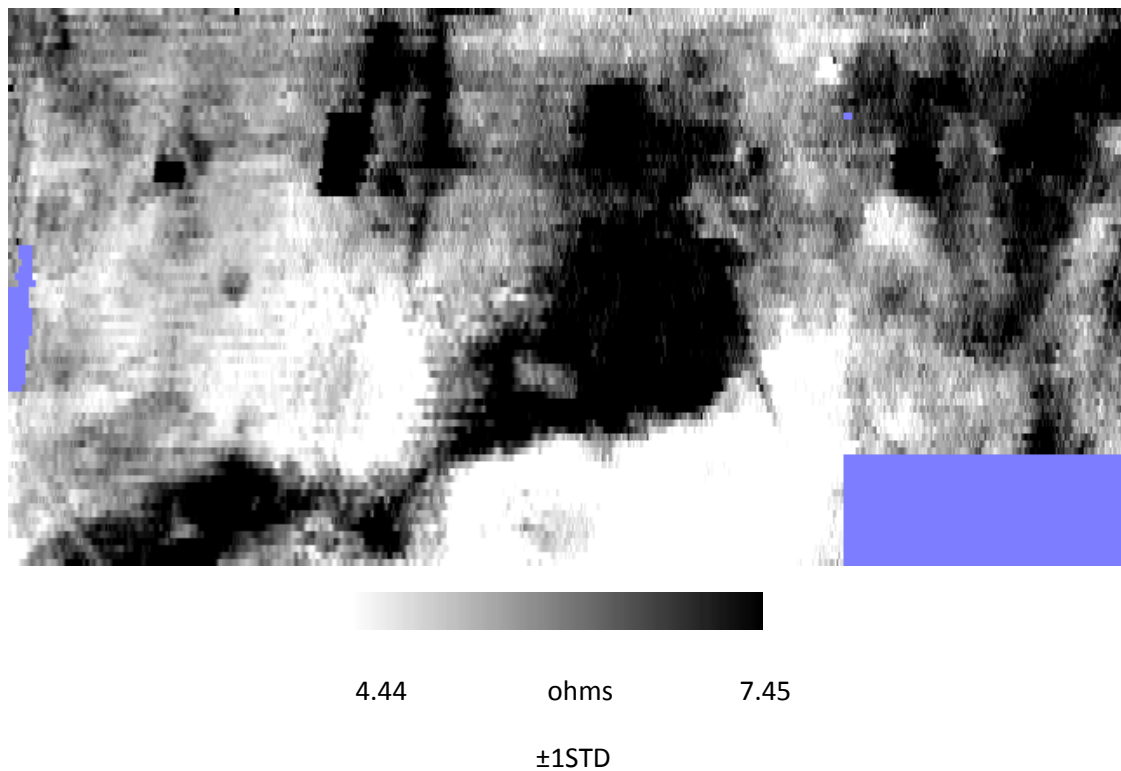
Figure 5.3   A processed MSP40 Alpha data set from Eining, Germany (survey extent 160m x 80m).
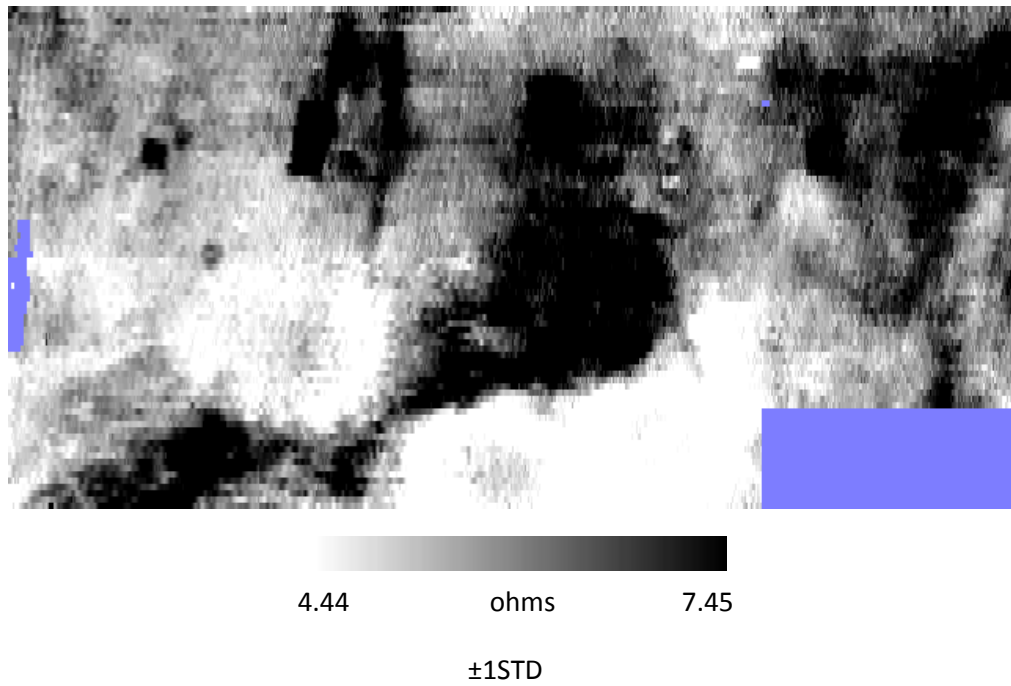
Figure 5.4   A processed Beta data set from Eining, Germany.
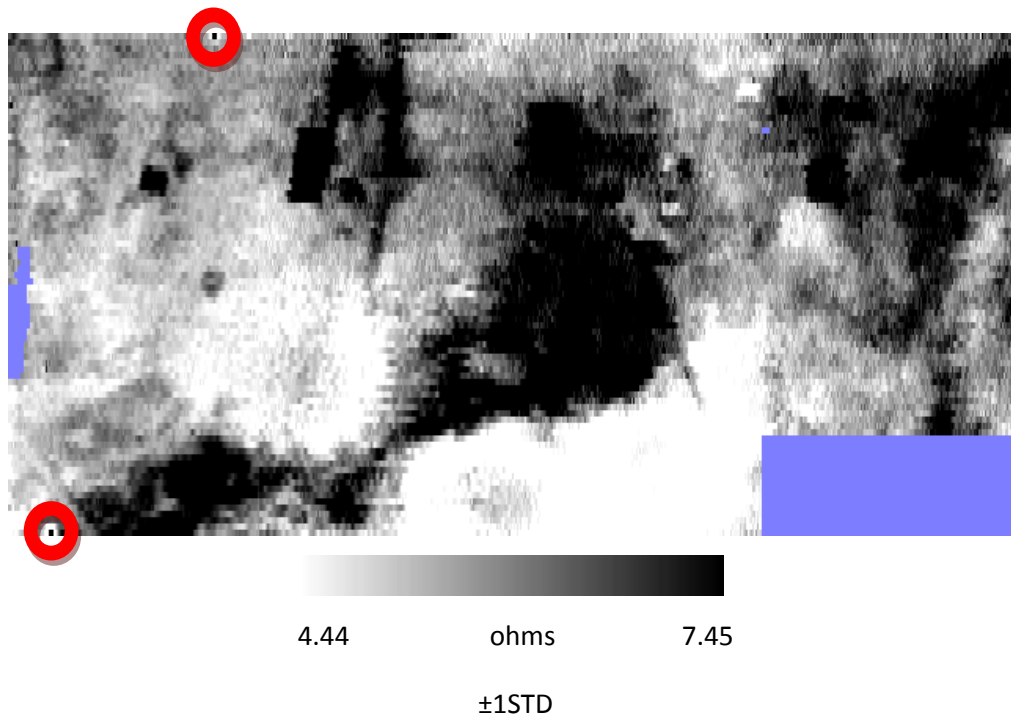
Highlighted Halo from processing

Figure 5.5   The combined data displays showing the artificial creation of
geophysical anomalies halos by processing choices. Data from Eining,
Germany (Area B) (see chapter 5.3.8 for archaeological interpretations and
detailed discussion of results).

To further examine the effect of data combination the Littlemoor data sets were exported from Geoplot and imported in to Excel in an XYZ comma separated variable format. The individual traverses were separated out and plotted as line graphs. The data sets were clipped to reduce the traverse lengths and focus in more detail on the anomalies visible in the Alpha data set. Only the first nine traverses were chosen as these had the strongest anomaly definition. Three linear anomalies were chosen and the highest resistance value of each anomaly from each traverse was compared.

The comparisons focused on the Alpha, Beta, averaging combination and MSP40 merge function. The test is important as there is little point combining data if the combination process removes the subtle differences between the data sets (see figure 5.6 and 5.7).

Care was taken when combining the Alpha and Beta data sets as any filtering will alter the data so that the relationship between data sets may no longer exist.
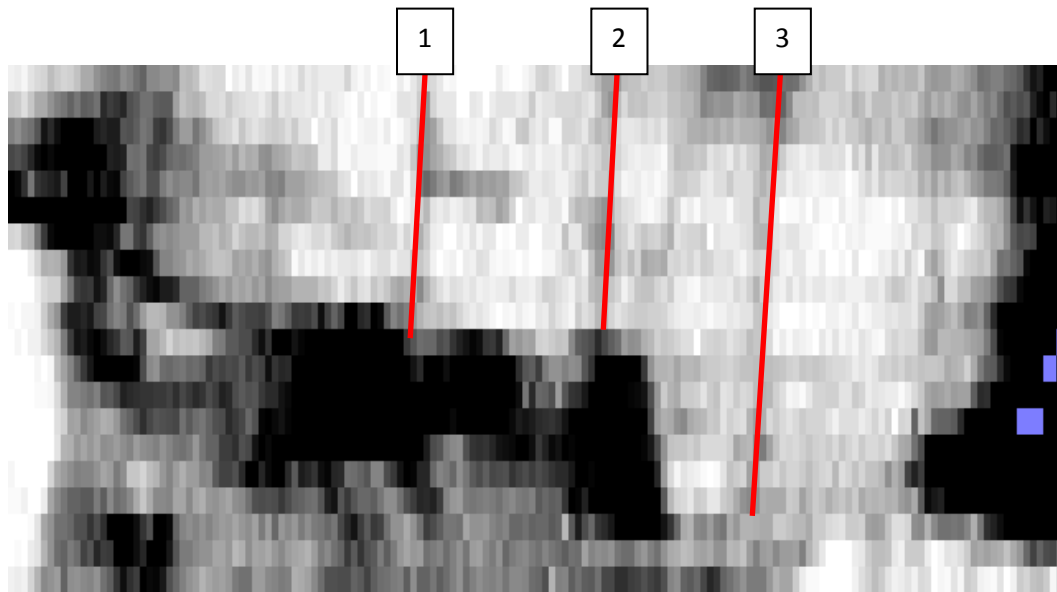
Figure 5.6   Three highlighted (Alpha) anomalies selected to investigate combination effects on the earth resistance data. Survey data from Littlemoor Castle.
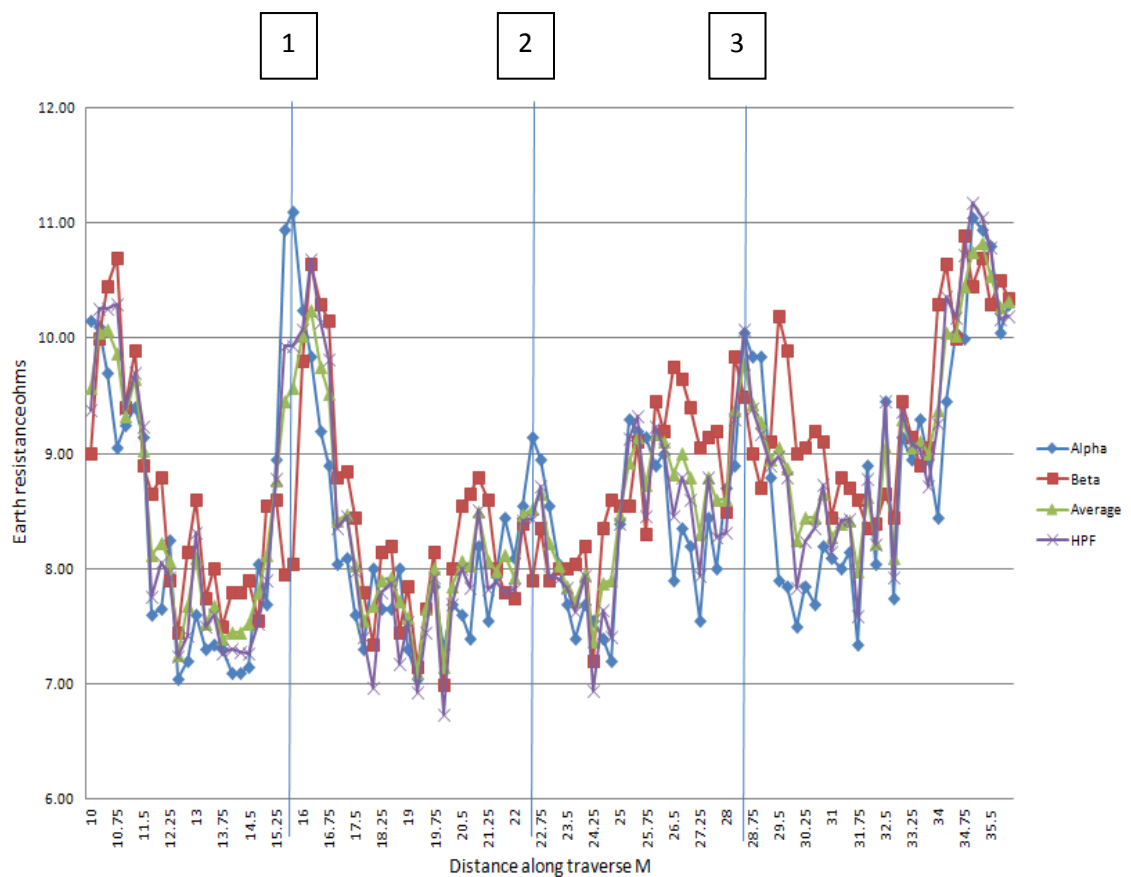
Figure 5.7   The effects of data combination on an X Y plot of earth resistance data with highlighted anomaly position.

The percentile difference between the Alpha & Beta earth resistance measurements, average combination & MSP40 merge (HPF) were calculated. A higher percentage means the greater the parallel to the Alpha anomalies (see table 5.1). This in turn leads to an increased visibility of the anomaly in the data sets.

Table 5.1   Alpha and Beta data combination effects.

Anomaly 1	Alpha	Beta	Average	HPF	Beta_diff_%	Avrg_diff_%	HPF_diff_%
Traverse 1	8.55	8.10	8.33	8.43	94.74	97.37	98.64
Traverse 2	10.65	8.10	9.38	10.39	76.06	88.03	97.54
Traverse 3	10.80	8.10	9.45	10.10	75.00	87.50	93.53
Traverse 4	11.10	8.05	9.58	9.93	72.52	86.26	89.46
Traverse 5	12.40	10.55	11.48	12.27	85.08	92.54	98.94
Traverse 6	9.45	8.35	8.90	8.95	88.36	94.18	94.66
Traverse 7	9.85	7.60	8.73	8.88	77.16	88.58	90.18
Traverse 8	9.20	7.10	8.15	7.23	77.17	88.59	78.54
Traverse 9	11.25	10.30	10.78	11.39	91.56	95.78	101.27

Anomaly 2	Alpha	Beta	Average	HPF	Beta_diff_%	Avrg_diff_%	HPF_diff_%
Traverse 1	10.45	9.75	10.10	10.32	93.30	96.65	98.75
Traverse 2	10.85	9.90	10.38	10.81	91.24	95.62	99.59
Traverse 3	9.60	8.95	9.28	9.59	93.23	96.61	99.93
Traverse 4	9.15	7.90	8.53	8.44	86.34	93.17	92.21
Traverse 5	9.45	7.70	8.58	8.55	81.48	90.74	90.43
Traverse 6	10.90	8.95	9.93	10.64	82.11	91.06	97.60
Traverse 7	11.30	9.70	10.50	11.16	85.84	92.92	98.74
Traverse 8	10.70	9.00	9.85	10.32	84.11	92.06	96.48
Traverse 9	9.75	9.40	9.58	9.48	96.41	98.21	97.24

Anomaly 3	Alpha	Beta	Average	HPF	Beta_diff_%	Avrg_diff_%	HPF_diff_%
Traverse 1	13.15	11.65	12.40	12.94	88.59	94.30	98.38
Traverse 2	12.50	10.90	11.70	12.30	87.20	93.60	98.44
Traverse 3	11.40	9.00	10.20	10.31	78.95	89.47	90.42
Traverse 4	10.05	9.50	9.78	10.07	94.53	97.26	100.23
Traverse 5	9.65	8.25	8.95	9.02	85.49	92.75	93.48
Traverse 6	9.65	8.35	9.00	9.44	86.53	93.26	97.79
Traverse 7	9.75	8.35	9.05	9.74	85.64	92.82	99.86
Traverse 8	8.60	8.25	8.43	8.57	95.93	97.97	99.60
Traverse 9	9.75	8.30	9.03	9.71	85.13	92.56	99.62

High pass filter increasing resistance values (MSP40 merge function).

Averaging combination resistance value exceeds MSP40 merge function.

The MSP40 merge function retains a greater percentage of the linear Alpha anomalies. However, the MSP40 merge function only increases the original resistance values on two occasions out of twenty seven tests.

The averaging function 'dilutes' or smooths out the differences between the Alpha and Beta measurements. Only four out of twenty seven Alpha resistance measurements exceeded the MSP40 merge function.

The analysis of the combination methods (visual and percentile change) indicates that the MSP40 merge function is the most appropriate technique for combining Alpha and Beta data sets. Subtle but important anomaly differences can be masked during the averaging process. The MSP40 merge function also suppresses the data but produces an anomaly response on average 3% greater than the averaging combination (based on the original Alpha response).

Any MSP40 report should display the Alpha and Beta data displays alongside any attempts at data combination. This ensures the reader can see which data set contributed which responses. It should be noted that when combining the Alpha and Beta data sets using the averaging or the merge MSP40 composites functions in Geoplot a dummy value in either data set will override a value from the other data set (see figure 5.8).

Alpha

Beta

Negative averaged

Negative MSP40 merge
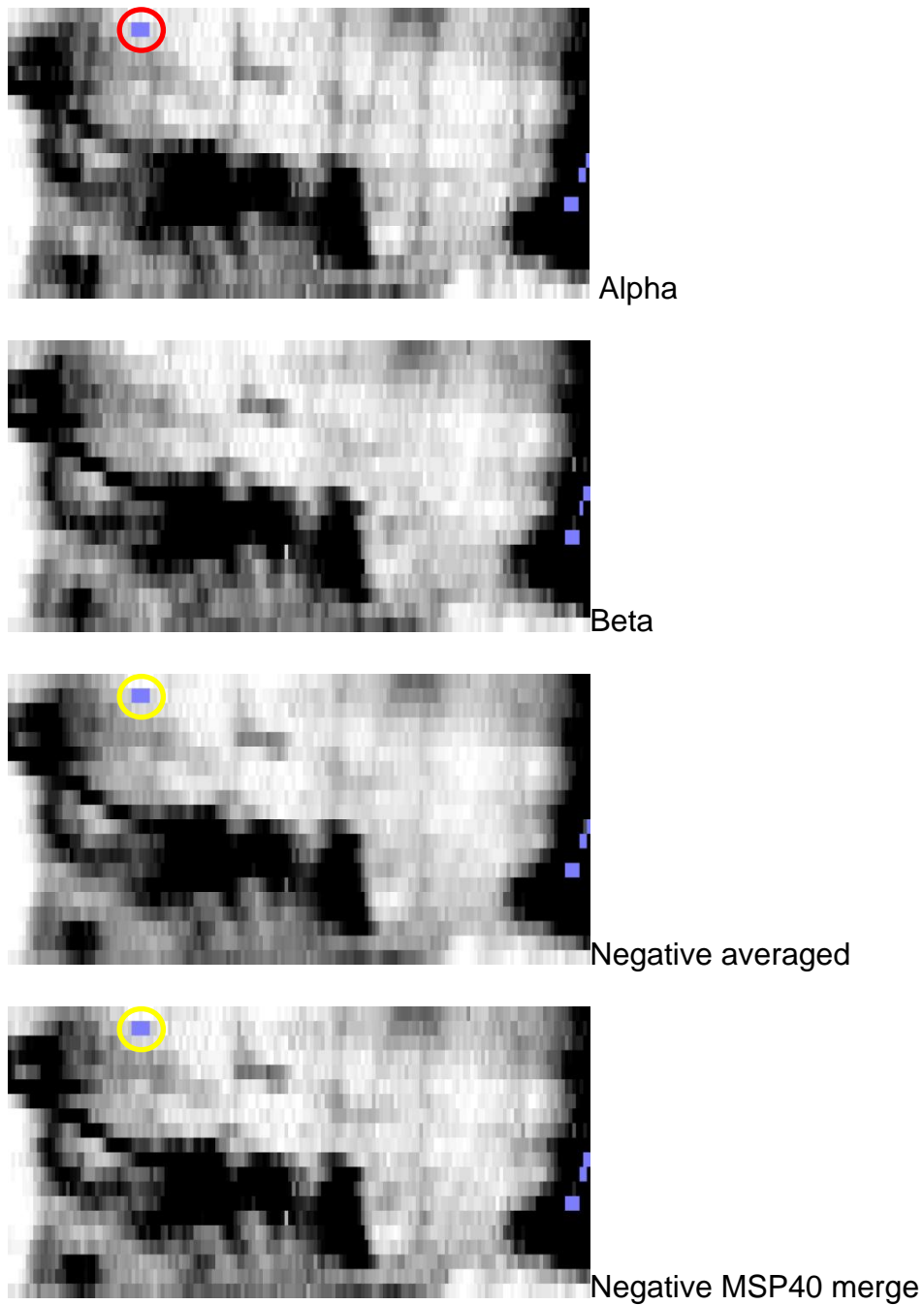
⭕ (red) Inserted dummy readings   ⭕ (yellow) Dummy readings after data combination

Figure 5.8   Four greyscale plots showing how Geoplot overwrites data with dummy values when data sets are combined.

5.1.4 ArcGIS RGB data combination

After Alpha and Beta data sets have been separately processed in Geoplot they can be combined in a variety of different software packages including ArcGIS as Red, Green and Blue (RGB) composites. This method can be used show variations between Alpha and Beta measurements.

The combined data set will show the areas of significant differences between Alpha & Beta data sets - where one colour will dominate an area (Red, Green or Blue). When only two data sets are combined one data set will contain two bands. The obsolete band can be turned off (see figure 5.9 and 5.10).
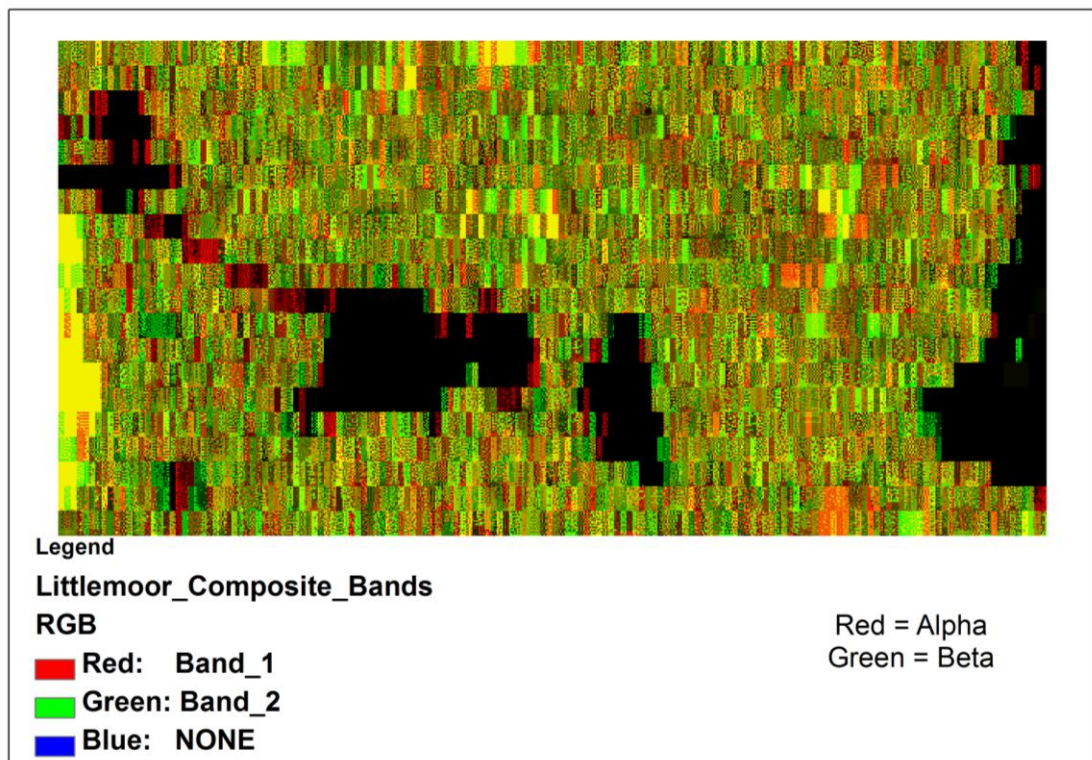
Figure 5.9   An RGB composite of Alpha and Beta data from Littlemoor Castle. Raw data provided by Geoscan Research (Walker 2005).

Legend
Eining_Area_B_Composite_Bands
RGB
Red: Band_1
Green: Band_2
Blue: NONE

Red = Alpha
Green = Beta
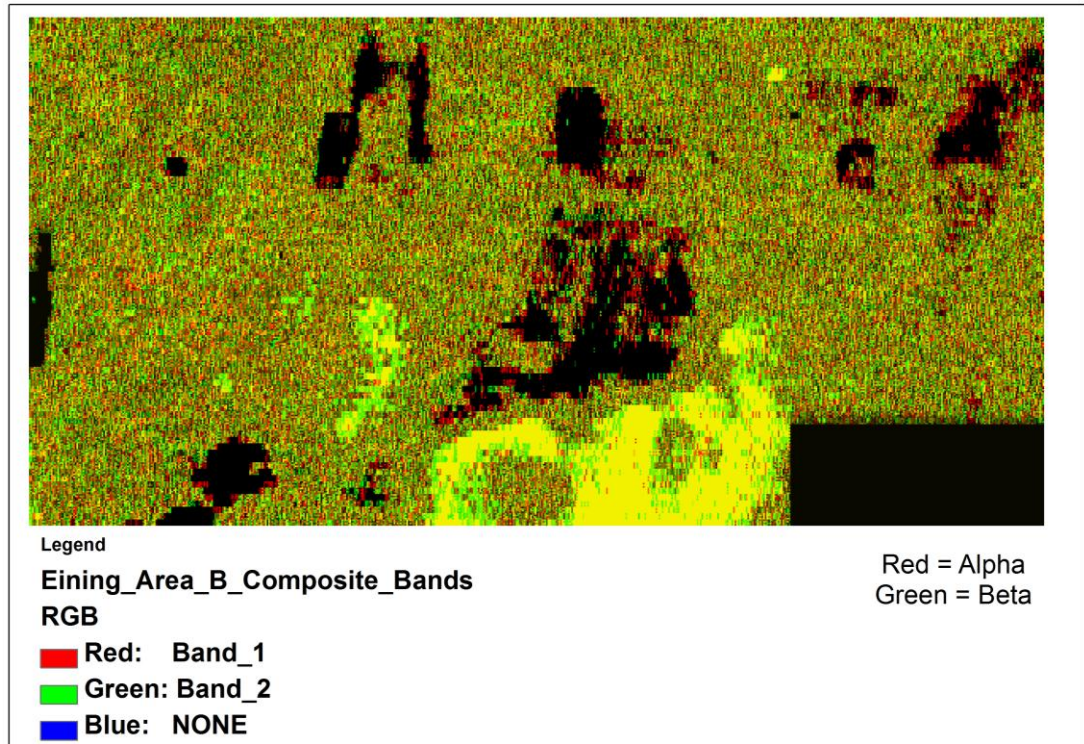
Figure 5.10   An RGB composite of Alpha and Beta data from Eining, Germany (Area B).

The RGB composites do indicate variation between the Alpha and Beta data sets but do not show the difference in areas of high resistance (black). The darker shades of grey in the greyscale range also mask the subtle differences between the two images. One solution would be to import the numerical data values into a GIS package and assign a suitable colour ramp to each individual data set. However, this limits the processing capabilities of the data.

5.1.5 Transparency layers

An additional way of combining the data is through the use of transparencies and layers. Many software packages that specialise in photographic editing and Geographic Information Systems (GIS) can create image transparencies.

Therefore images can be overlaid and data can be analysed in a combined image (see figure 5.11). The main problem with transparencies is the inability to distinguish between the two data sets without separate images of the individual Alpha and Beta data sets.
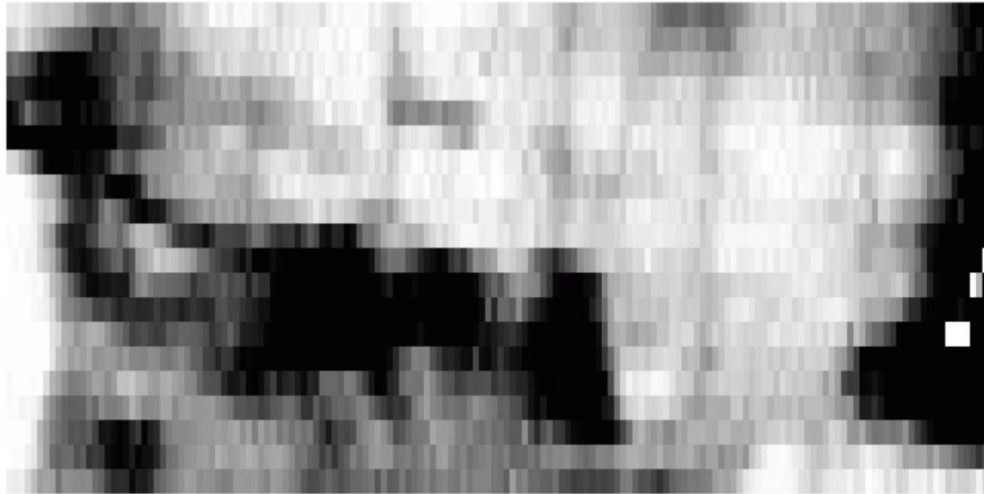
Alpha and Beta data set overlay

Beta data set at 60% transparency

Figure 5.11   A transparency overlay of the Alpha and Beta data sets from Littlemoor Castle. Raw data provided by Geoscan Research (Walker 2005).

5.1.6 Further processing considerations

As the MSP40 allows for a faster collection rate than 'traditional' earth resistance surveys the possibilities of higher resolution survey becomes more realistic in the commercial sector. However, as the MSP40 is a single earth resistance sensor array there is likely to be a significant difference between the sampling and traverse intervals. It is therefore necessary to be cautious when processing earth resistance data so not to distort the data between the traverse lines (see figure 5.12). This can be overcome by using unidirectional processing parameters (processing in the X or Y direction only) or by interpolating between traverse lines earlier in the processing steps to reduce the distortion effect.
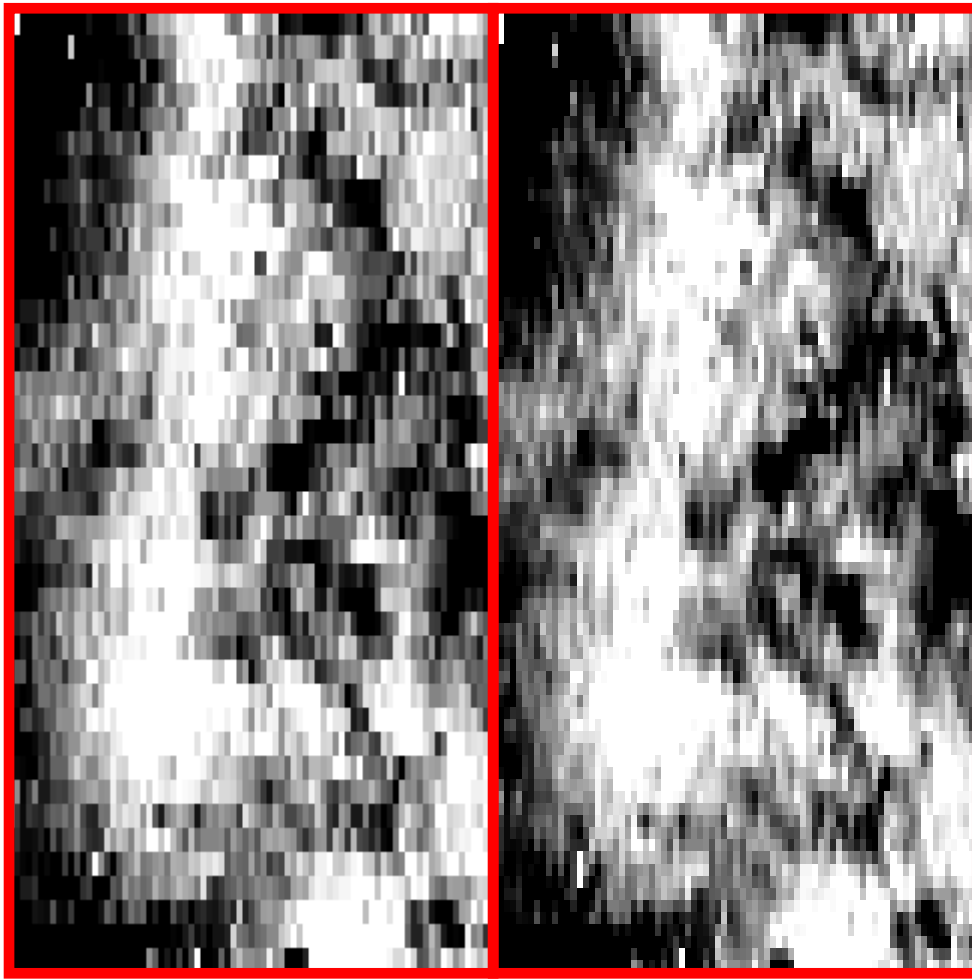
6.35   ohms   8.12

±1STD

Sampling Interval 0.25m   Sampling Interval 0.25m

Traverse Interval 1m   Traverse Interval 0.5m

Figure 5.12   The right hand image shows the stretching affect of a single interpolation in the Y direction. Data from Entremont, an Iron Age Oppidum, Provence, France.

5.2.0 When data goes bad – Instrumental noise & mechanical faults-Processing techniques, what to keep and what can be done.

5.2.1 Introduction

During this research project a number of issues arose when collecting data, ranging from loosening wheels to twisting of the axles. Many of these issues had to be overcome through mechanical developments (as discussed in chapter 3.4). However, it raised the important research question of what could be done to improve the data after problems arose. It was important to consider how data processing may be used to salvage the survey data as and when mechanical faults developed. A discussion of the processing options available and their effects on the data with case studies is therefore important.

5.2.2 Useful processing tools (pre-combination of Alpha and Beta data) Earth resistance survey

Despiking

The MSP40 continuously samples the earth resistance measurements at a rate of 13 Hz, based on the fastest logging speed possible on the RM15 (Walker 2006). As the RM15 must be set to the fastest logging speed possible the readings are continually fluctuating as the MSP40 is pulled along. The near continuous logging increases the variation in neighbouring earth resistance values compared to 'traditional' earth resistance survey. During 'traditional' earth resistance survey the probes are inserted into the ground and a slight delay time allows for the readings to 'settle' (data logging speeds are usually recorded at the 'medium' setting). The increased fluctuation in MSP40 readings can be reduced by using the despiking option in Geoplot. Increasing the X & Y radius and reducing the threshold can be useful to remove larger spikes in the data.

5.2.3 Useful processing tools (post-combination of Alpha and Beta data) earth resistance survey

Destagger

The destagger function can correct the displacement of anomalies during zigzag data collection or when a surveyor's walking speed is not consistent for the entire traverse (time based collection). The function is more commonly used for gradiometer surveys but can also be used to correct positional errors in earth resistance data. The function corrects variable collection rates for time-based earth resistance correction as would be done for gradiometer surveys. However, it may also be necessary to correct the optical encoder collected data as errors in sampling intervals can occur. Usually this results from dirty encoder lenses (missing pulses) or varying topography. Operator error can also cause a displacement of anomalies if the centre of the array does not align with the grid edge at the beginning of each traverse. The function can be run on alternative or paired traverses and can be applied to entire composites, individual grids or lines. The amount of displacement can be specified in a positive or negative direction by the operator (only in the X direction). When data points are shifted beyond the grid edge the values are discarded. Blank spaces created at the opposite end of the traverse are replaced by the calculated mean of the two adjacent traverses (Y direction).

Low pass filtering

The filter removes high frequency small-scale details and is commonly used to smooth data displays or to enhance large subtle response features. The low pass filtering can also be used to smooth out the resistance data when variations exist between traverse lines. Using a weighting of X=0 & Y=1 multiple times will reduce traverse discontinuities without over-smoothing the data.

High pass filtering

The filter removes low frequency large-scale spatial details. The filter can be useful to remove geological responses in earth resistance data.

The high pass filter may also improve definition of high resistance anomalies. However, the filter shifts the data to a zero midpoint and can create processing artefacts such as halos and bipolar anomalies.

Interpolation

The interpolation function creates additional data points between sampling intervals or traverse intervals by statistical analysis of neighbouring data points. This can be useful when combining surveys that have different sampling strategies. The interpolation function also softens the edges of anomalies by doubling the number of pixels in one direction which can improve the aesthetics of the data displays. However, interpolating the data excessively will 'blow out' the data by over-smoothing the image. It can also stretch / distort anomalies if over-used in the X or Y direction (depending on sampling and traverse intervals).

Periodic defect filtering

The spectrum analysis and periodic filtering tools can be useful to suppress geophysical anomalies created by ridge and furrow. These linear and periodic anomalies may mask older archaeological features and so can be removed to aid earlier landscape / site identification. The periodic filters may also be used to remove collection errors in gradiometer data if the data shows a regular periodicity (caused by the gradiometer swinging from side to side on undulating ground).

5.2.4 Useful processing tools – Fluxgate Gradiometer survey

In addition to many of the processing tools listed above the following are useful when improving gradiometer data.

Zero mean grid

The function sets the background mean of a grid to zero, this helps remove grid edge variations caused by drift of the instruments between grids.

Edge match

The edge match function can be used to remove grid edge discontinuities caused by the instrument drifting between grids. However, unlike the zero mean grid function, the edge matching works on individual grids rather than the entire data set by comparing the mean edge difference between two neighbouring grids and subtracting the mean from one grid to balance the grids.

Zero mean traverse

The function sets the background mean of each traverse to zero, which helps remove variations between traverses. The function is especially useful when surveying in a zigzag formation to reduce heading errors.

5.2.5 Data collection issues- a theoretical case study

A data set collected at Eining, Germany, was initially despiked to remove many of the defects from the survey collection (see figure 5.13). The data was then exported into MS Excel in a Z data format. A spread sheet was created with columns as follows to introduce deliberate random errors into the data set.

Raw Alpha data (after despiking)

4.1   ohms   6.82

±1STD
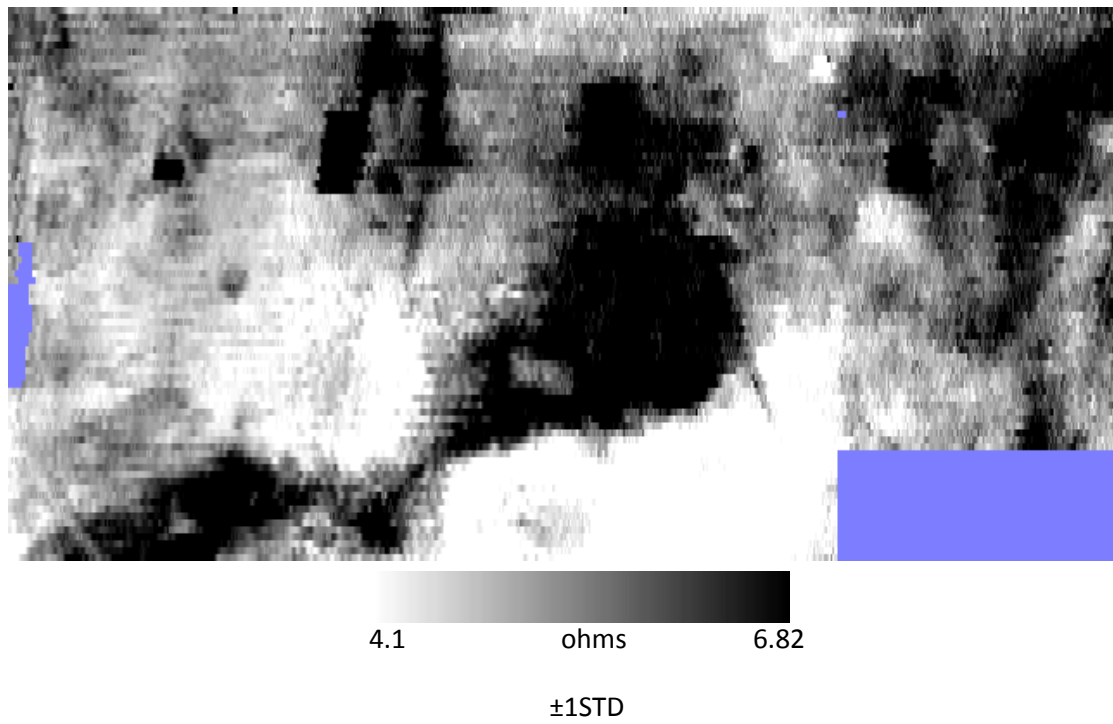
Raw Beta data (after despiking)

4.43   ohms   7.47

±1STD
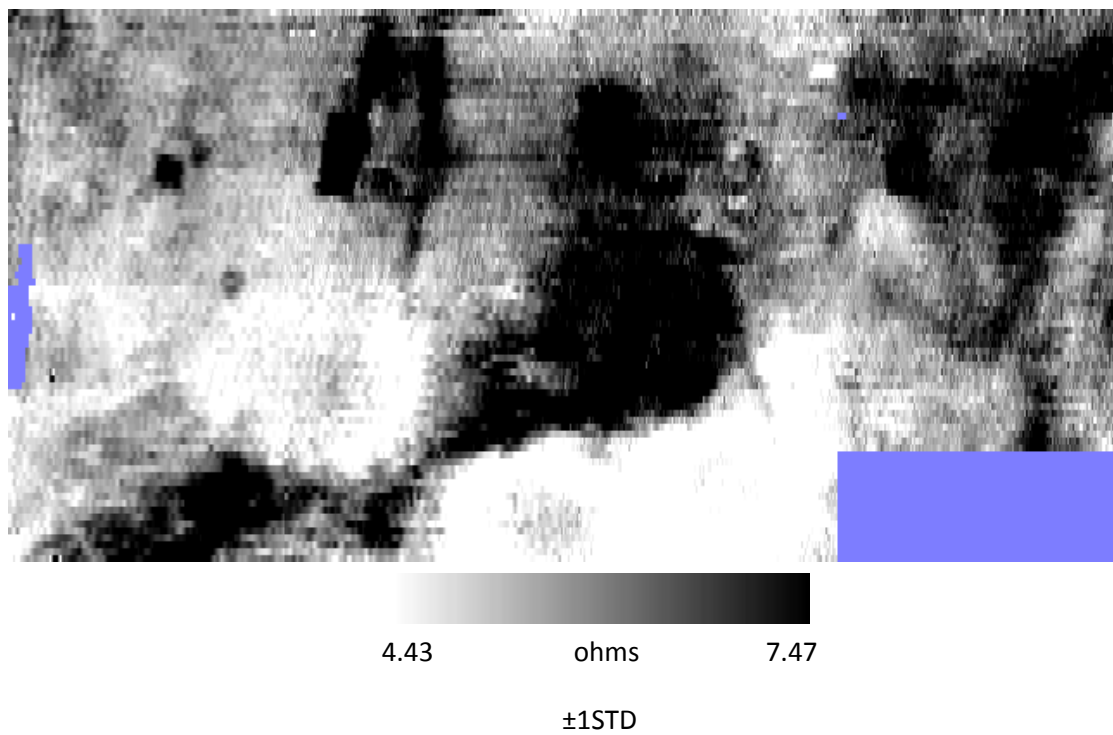
Figure 5.13 Despiked Alpha and Beta MSP40 earth resistance survey data from Eining (Area B), Germany.

The data set is intended to simulate a number of scenarios that may occur during a survey including dry soil surfaces, poor spike penetration, problematic survey conditions (stones / vegetation) and issues with overcoming contact resistance.

Column A = The measurement number, listed from 1- 51,200

Column B = The original Z data, earth resistance data exported from Geoplot.

Column C = Random number generator, based on the number position of measurement (column A) using the function below to generate a unique value between 1 and 51,200.

=INDEX($A:$A,RANDBETWEEN(1,COUNTA($A:$A)),1)

Column D = Random earth resistance number generator using the function below to assign values between -247 & 247 ohm (duplicate values were allowed).

=RANDBETWEEN(-247,247)

Negative values were included as drop outs in data are often recorded as a negative reading (when the MSP40 cannot resolve a stable measurement for the sampling position) or when the contact resistance is too great to overcome (also related to poor electrode penetration).

Column E = Modified Z data, using the logic argument listed below. This function examines column C, and if the number corresponds with a number from column A then the random earth resistance error measurement (column D) is inserted into the corresponding row in column E.

If however, the number in column A is not listed in column C then the Z data value from column B is automatically listed in column E (see table 5.2).

=IF(ISERROR(VLOOKUP(A1,$C$1:$D$200,2,FALSE)),B1,VLOOKUP(A1,$C$1
:$D$200,2,FALSE))

Table 5.2   Worked example of how the random errors were generated.

A	B	C	D	E
# position of measurement	Original Z data (earth resistance ohms)	Random position of measurement	Random earth resistance error value	Modified Z data
1	5.77	5005	204.7	5.77
2	5.66	2	120.5	120.5
3	5.55	21976	9	5.55
4	5.44	4	-62.5	-62.5

The data set (Eining area B) was made up of 51200 data points, the raw data was run through the MS Excel spread sheet with a range of percentages of errors (see table 5.3) before processing was attempted to improve the data. In the actual MS Excel spread sheet column C (described above) consisted of 4 columns, each one containing the desired percentage of random position of measurements to be used for each display. The process has been simplified for descriptive purposes.

Table 5.3   Number of erroneous data points inserted at each percentage level.

Percentage errors	# of erroneous data points from 51,200
1%	512
5%	2560
10%	5120
25%	12,800

The following images represent the Alpha and Beta data sets after the intentional errors have been inserted into the survey data and then imported back into Geoplot for processing. Alpha and Beta data sets both contained intentional errors and were merged together using the two methods (averaging and high pass filtered merging) discussed previously.

-9.13   ohms   19.86
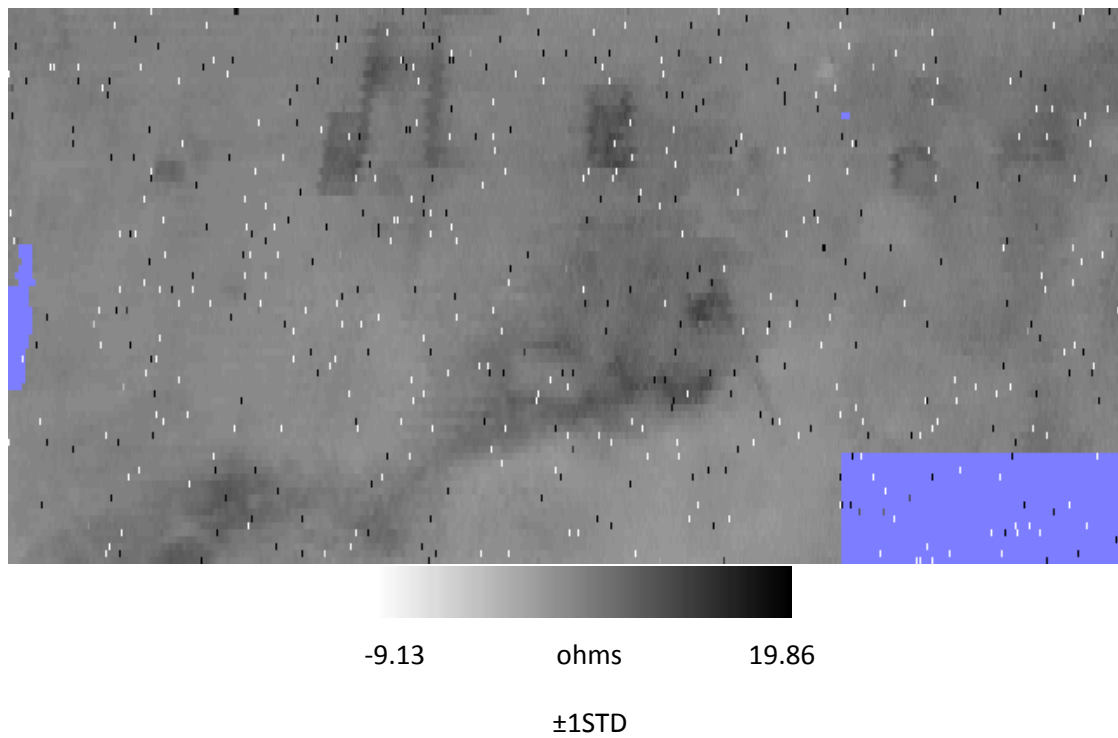
±1STD

Figure 5.14 MSP40 earth resistance Alpha data with random 1% errors included.

-27.93   ohms   37.77
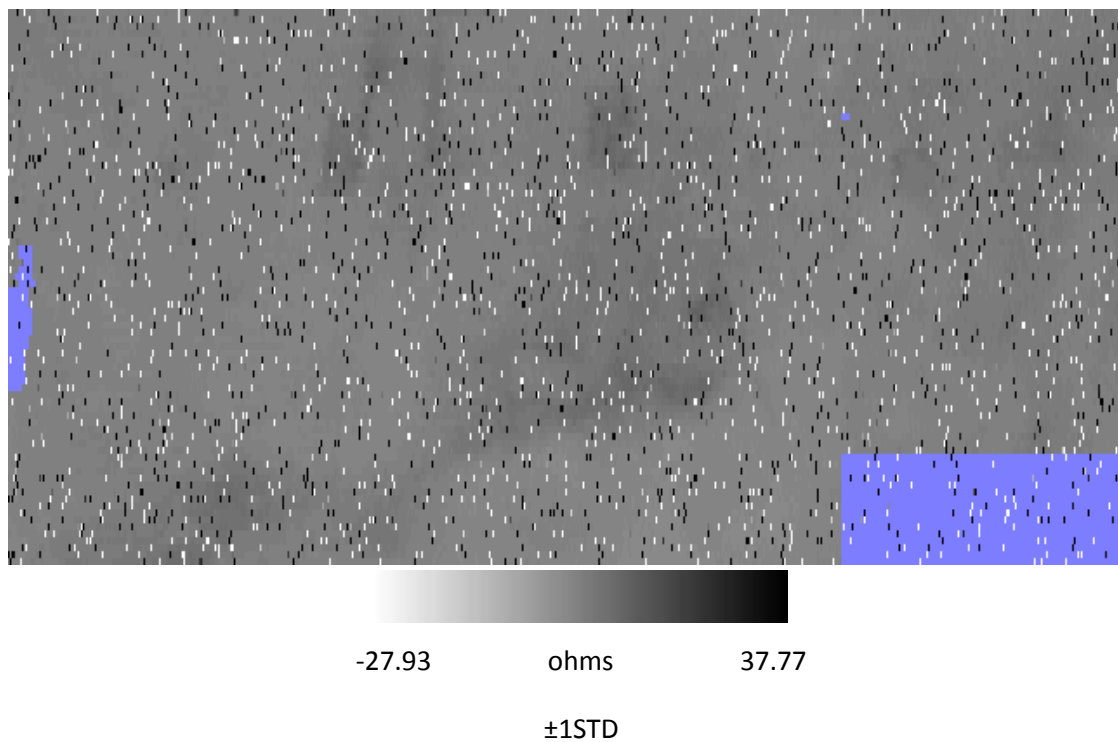
±1STD

Figure 5.15 MSP40 earth resistance Alpha data with 5% random errors included.

-41.72   ohms   51.95
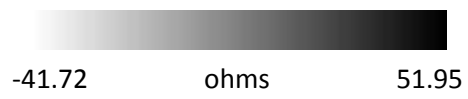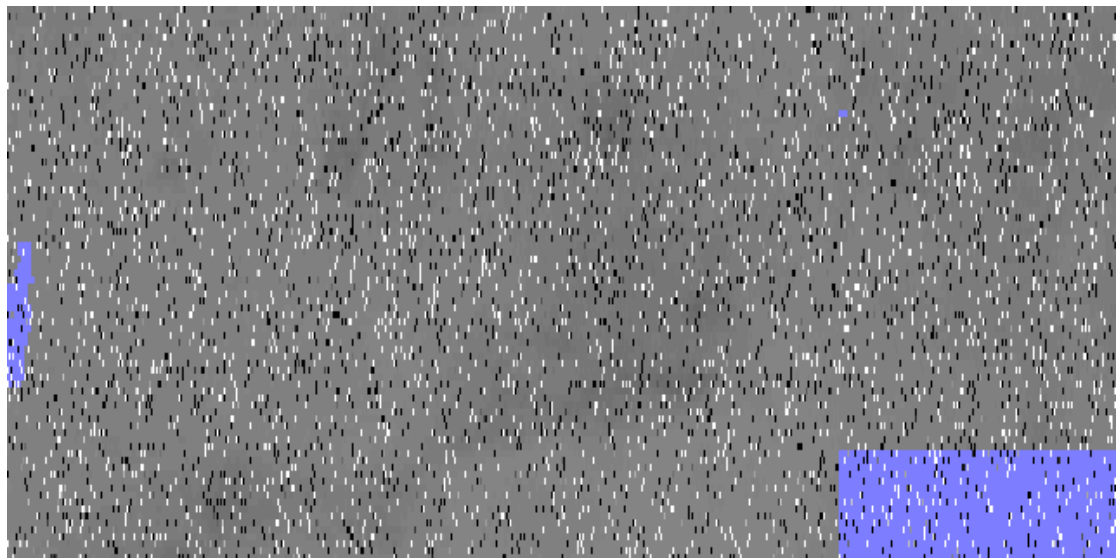
±1STD

Figure 5.16   MSP40 earth resistance Alpha data with random 10% errors included.

-69.42   ohms   77.19
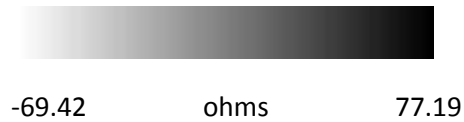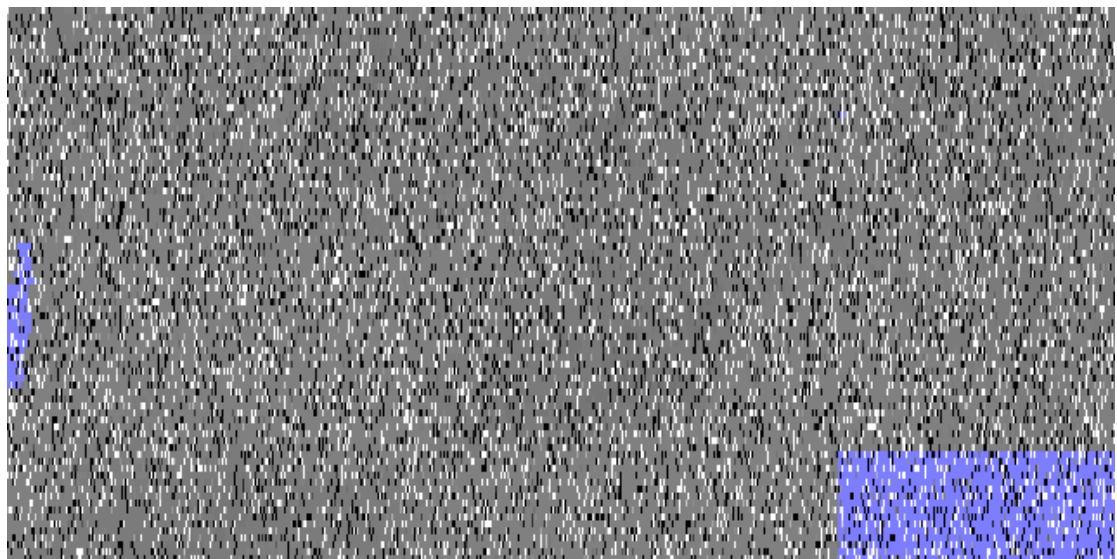
±1STD

Figure 5.17   MSP40 earth resistance Alpha data with 25% random errors included.

Results

The following data displays are post processed images with a description of the processing parameters involved and a discussion of the salient points. Bullet point processing steps represent the stages done to each individual data set before the Alpha and Beta data sets were combined.

1% Error, combined & averaged data

Processing

- 2x Despike X=1 Y=1Thr=3 Repl=Mean

- 1x Despike X=2 Y=2Thr=3 Repl=Mean

- Search -500 to 500- Replace= 2047.5 Block on inclusive 481,65 641,80

Cut c:\geoplot\comp\error\erora1%p.cmp, 1, 1 640, 80, Combine (Add) to 1, 1 Multiply .5

Despike X=2 Y=2Thr=3 Repl=Mean

Destagger All Grids, X dir, Shift= 1- Line Pattern -2-4-6-8

Search -500 to 0 - Replace=2047.5

Search 50 to 500 - Replace=2047.5

LPF X=1 Y=1 Wt=G
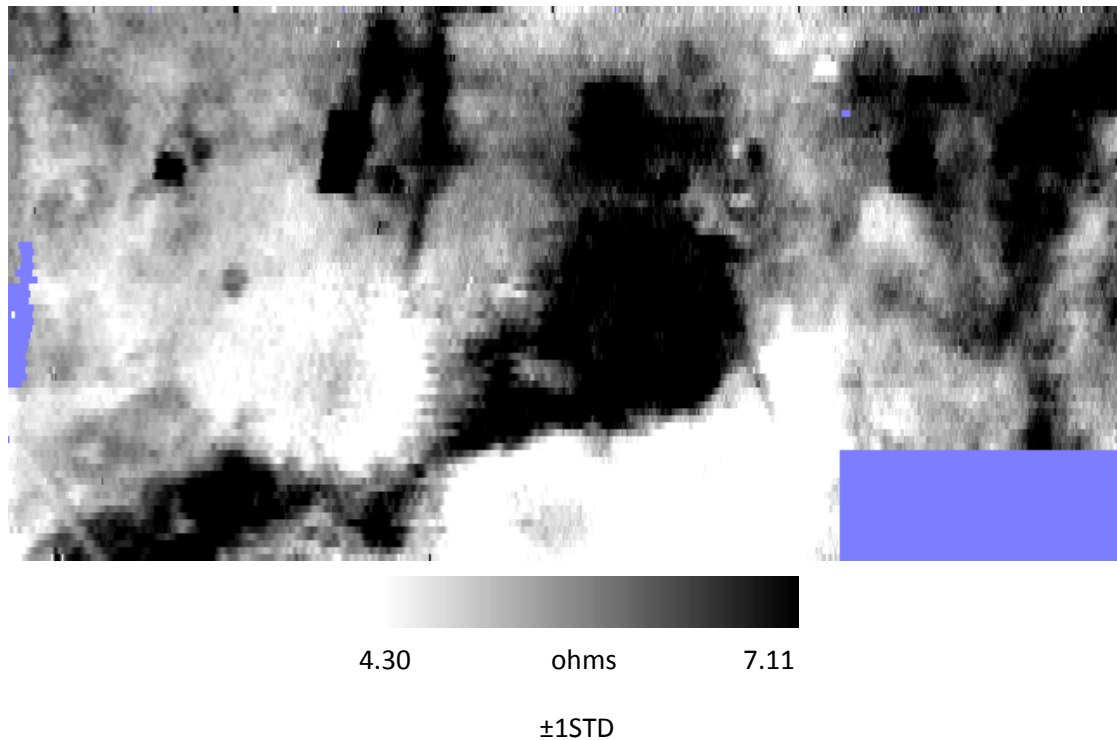
Figure 5.18   Processed 1% error MSP40 earth resistance Alpha data combined using the averaging method.

The 1% averaged data set processing shows no evidence of the introduced errors, largely removed through the despiking. The combined data set has a smoothed out appearance when compared to the original Alpha and Beta images. This is due to the averaging process and the low pass filtering (LPF). The banding between traverses visible in the original images has also been removed by the averaging process and filtering.

The destaggering was applied to correct for the slight displacement between traverses caused by slight discrepancies in reading positions when using the distance encoder and collecting data in zigzag traverses. The block on inclusive tool was used to remove the random errors inserted into the areas filled with dummy values (e.g. areas not surveyed).

1% Error, combined data using Geoplot's MSP40 merge function

Processing

- 2x Despike X=1 Y=1Thr=3 Repl=Mean

- 1x Despike X=2 Y=2Thr=3 Repl=Mean

- Search -500 to 500- Replace= 2047.5 Block on inclusive 481,65 641,80

Merge Composites (HPF X=6 Y=3 Wt=G) 1%p & 1%bp

Despike X=2 Y=2Thr=3 Repl=Mean

Destagger All Grids, X dir, Shift= 1- Line Pattern -2-4-6-8

LPF X=1 Y=1 Wt=G

4.26   ohms   7.16

±1STD
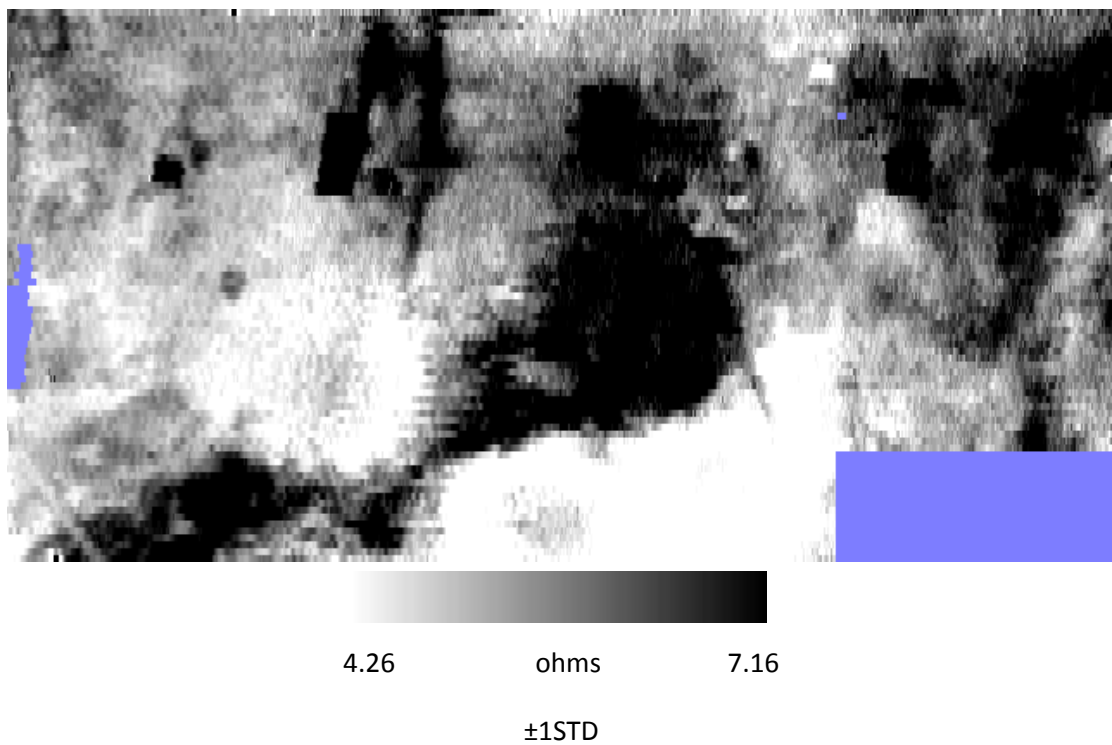
Figure 5.19 Processed 1% error MSP40 earth resistance Alpha data combined using the MSP40 merge function.

The use of the Geoplot MSP40 merge function as discussed previously (see 5.1.3) once again produced low resistance halos artefacts due to the high pass filtering. Increasing the window size of the filter to match the sampling and traverse intervals ratio increased the halo sizes so a smaller window ratio was chosen to reduce the processing artefacts.

5% Error, combined & averaged data

Processing

- 3x Despike X=1 Y=1Thr=3 Repl=Mean

- Despike X=2 Y=2Thr=3 Repl=Mean

- Search -500 to 500, Replace=2047.5, Bl(Inc) 481,65 641,80
- Search -500 to 0, Replace=2047.5, Search 50 to 500 Replace=2047.5

Cut c:\geoplot\comp\error\5%p.cmp, 1, 1 640, 80, Combine (Add) to 1, 1

Multiply .5

Despike X=2 Y=2Thr=3 Repl=Mean

Destagger All Grids, X dir, Shift= 1- Line Pattern -2-4-6-8

LPF X=1 Y=1 Wt=G

4.30   ohms   7.11

±1STD
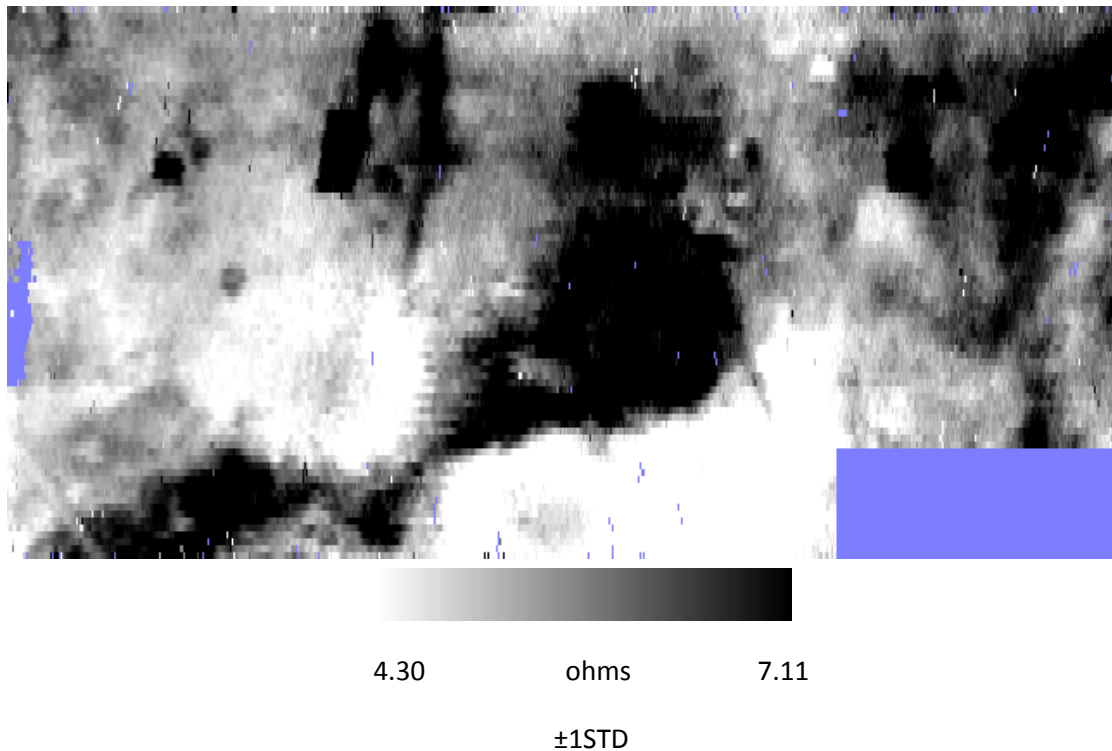
Figure 5.20   Processed 5% error MSP40 earth resistance Alpha data combined using the averaging method.

5% Error, combined data using Geoplot's MSP40 merge function

Processing

- 3x Despike X=1 Y=1Thr=3 Repl=Mean

- Despike X=2 Y=2Thr=3 Repl=Mean

- Search -500 to 500, Replace=2047.5, Bl(Inc) 481,65 641,80

- Search -500 to 0, Replace=2047.5, Search 50 to 500 Replace=2047.5

Merge Composites (HPF X=6 Y=3 Wt=G): 5%p & 5%pb

Despike X=2 Y=2Thr=3 Repl=Mean

Destagger All Grids, X dir, Shift= 1- Line Pattern -2-4-6-8

LPF X=1 Y=1 Wt=G

4.24   ohms   7.17

±1STD
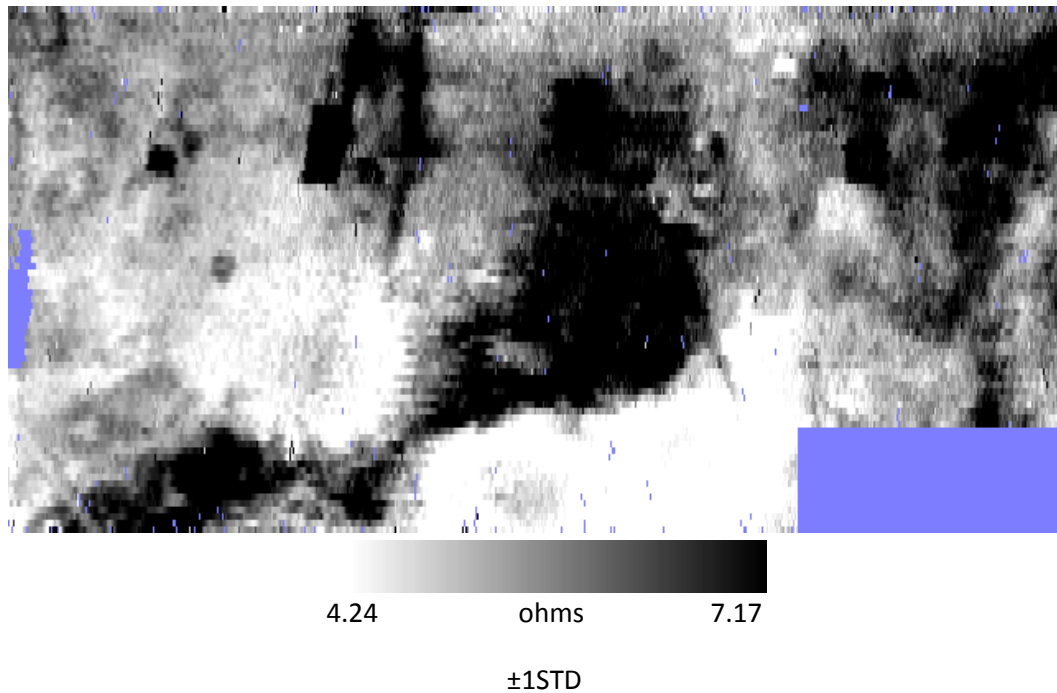
Figure 5.21   Processed 5% error MSP40 earth resistance Alpha data combined using the MSP40 merge function.

The 5% error data sets have had the additional processing step where the entire data sets have had a search and replace function applied to them to remove values below zero and above 50 ohm as these values would likely be measurement errors.

10% Error, combined & averaged data

Processing

- 3 x Despike X=1 Y=1Thr=3 Repl=Mean

- 2 x Despike X=2 Y=2Thr=3 Repl=Mean

- Search -500 to 500- Replace=2047.5, Bl(Inc) 482,65 641,80

- Search -500 to 0- Replace=2047.5
- Search 50 to 500- Replace=2047.5

Cut c:\geoplot\comp\error\10%p.cmp - 1, 1 640, 80, Combine (Add) to 1, 1

Multiply .5

Despike X=2 Y=2Thr=3 Repl=Mean

Destagger All Grids, X dir, Shift= 1- Line Pattern -2-4-6-8

LPF X=1 Y=1 Wt=G
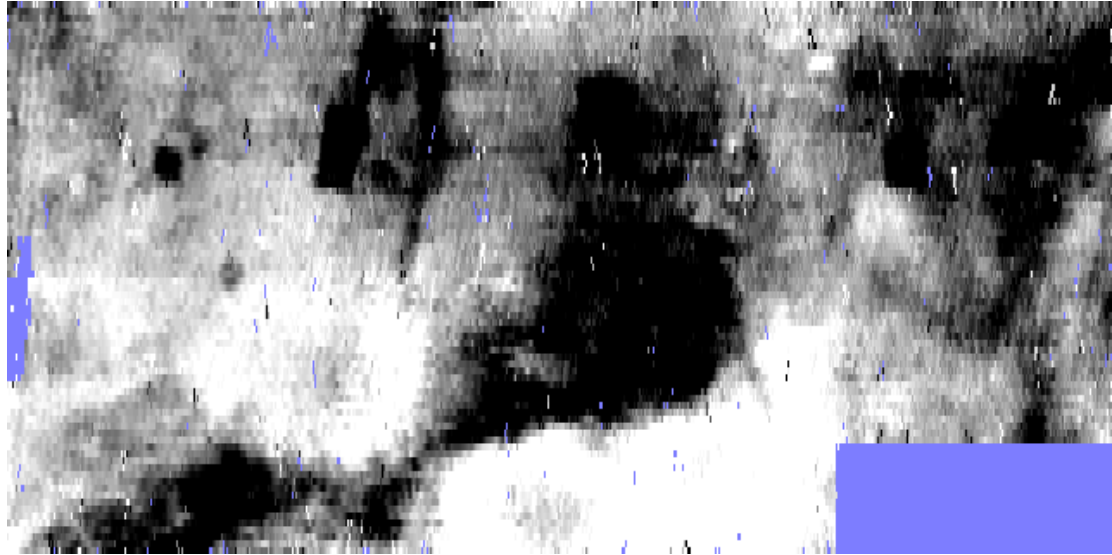
4.44   ohms   7.46

±1STD

Figure 5.22   Processed 10% error MSP40 earth resistance Alpha data combined using the averaging method.

10% Error, combined data using Geoplot's MSP40 merge function

Processing

- 3 x Despike X=1 Y=1Thr=3 Repl=Mean

- 2 x Despike X=2 Y=2Thr=3 Repl=Mean

- Search -500 to 500- Replace=2047.5, Bl(Inc) 482,65 641,80

- Search -500 to 0- Replace=2047.5

- Search 50 to 500- Replace=2047.5

Merge Composites (HPF X=6 Y=3 Wt=G): 10%p & 10%bp

Despike X=1 Y=1Thr=2 Repl=Mean

Destagger All Grids, X dir, Shift= 1- Line Pattern -2-4-6-8

LPF X=1 Y=1 Wt=G

4.41   ohms   7.48

±1STD
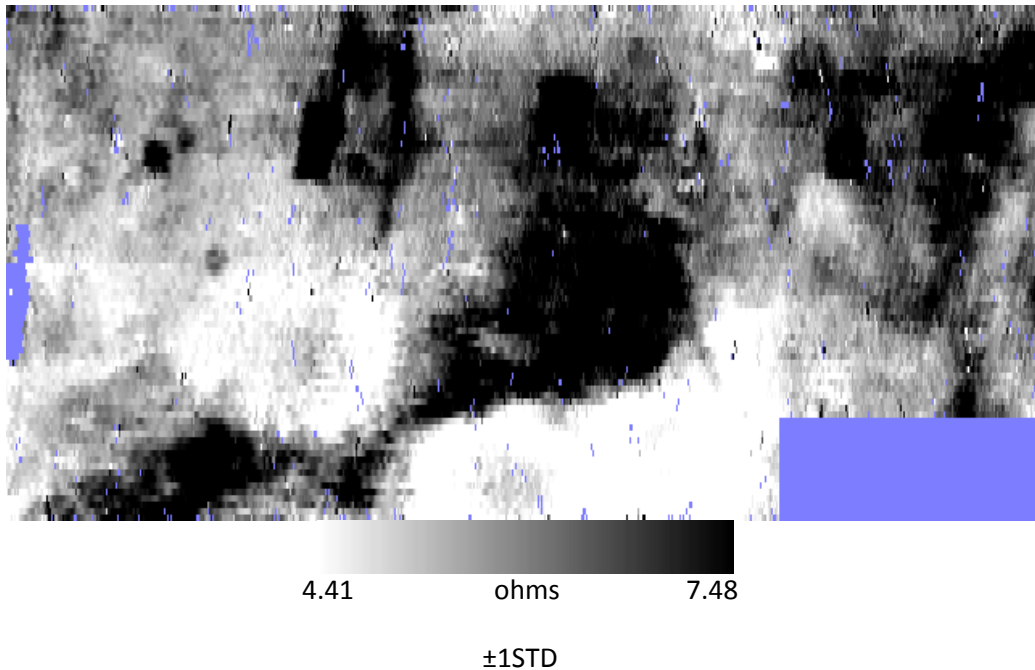
Figure 5.23   Processed 10% error MSP40 earth resistance Alpha data combined using the MSP40 merge function.

25% Error, combined & averaged data

Processing

- 3 x Despike X=1 Y=1Thr=3 Repl=Mean

- Despike X=2 Y=2Thr=2 Repl=Mean

- Search -500 to 500 - Replace=2047.5, Bl(Inc) 480,65 641,80

- Search -500 to 0 - Replace=2047.5

- Search 40 to 500 - Replace=2047.5

Cut c:\geoplot\comp\error\25%p.cmp - 1, 1 640, 80 Combine (Add) to 1,1

Multiply .5

2 x Despike X=2 Y=2Thr=2 Repl=Mean

Despike X=2 Y=2Thr=3 Repl=Mean

Destagger All Grids, X dir, Shift= 1- Line Pattern -2-4-6-8

LPF X=1 Y=0 Wt=G

LPF X=1 Y=1 Wt=G

4.16   ohms   7.10

±1STD
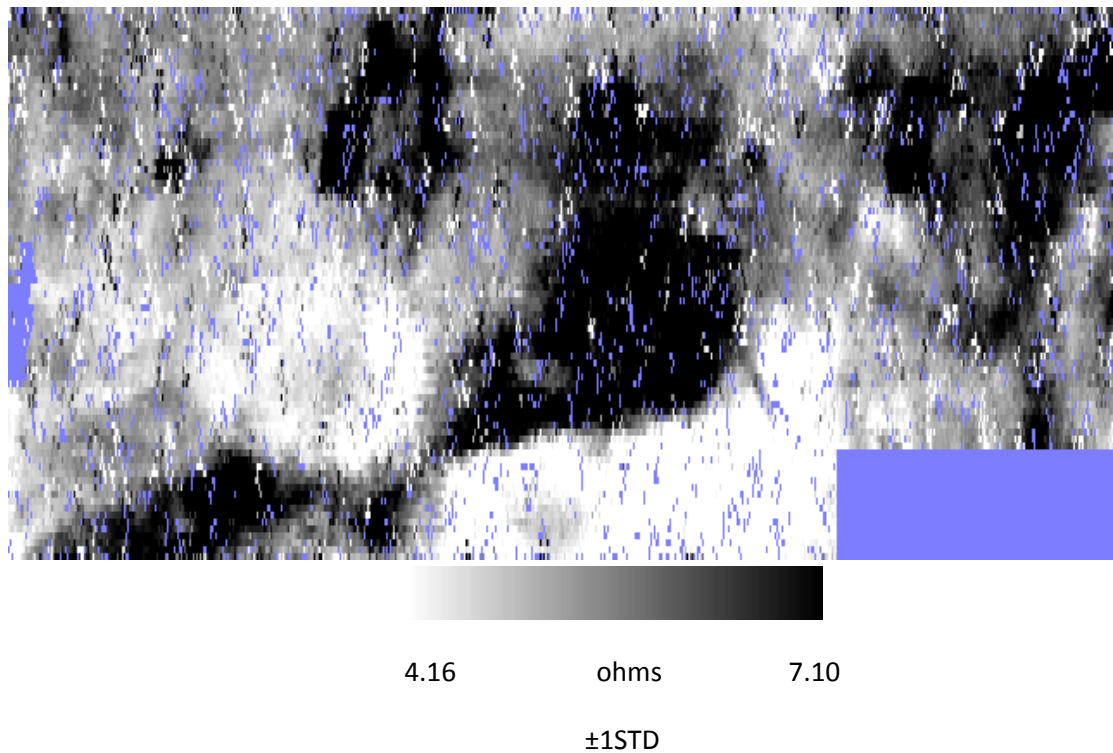
Figure 5.24   Processed 25% error MSP40 earth resistance Alpha data combined using the averaging method.

25% Error, combined data using Geoplot's MSP40 merge function

Processing

- 3 x Despike X=1 Y=1Thr=3 Repl=Mean

- Despike X=2 Y=2Thr=2 Repl=Mean

- Search -500 to 500 - Replace=2047.5, Bl(Inc) 480,65 641,80

- Search -500 to 0 - Replace=2047.5

- Search 40 to 500 - Replace=2047.5

Merge Composites (HPF X=6 Y=3 Wt=G): 25%p & 25%bp

Despike X=2 Y=2Thr=2 Repl=Mean

Destagger All Grids, X dir, Shift= 1- Line Pattern -2-4-6-8

3 x LPF X=1 Y=0 Wt=G

LPF X=1 Y=1 Wt=G

3.88   ohms   7.15

±1STD
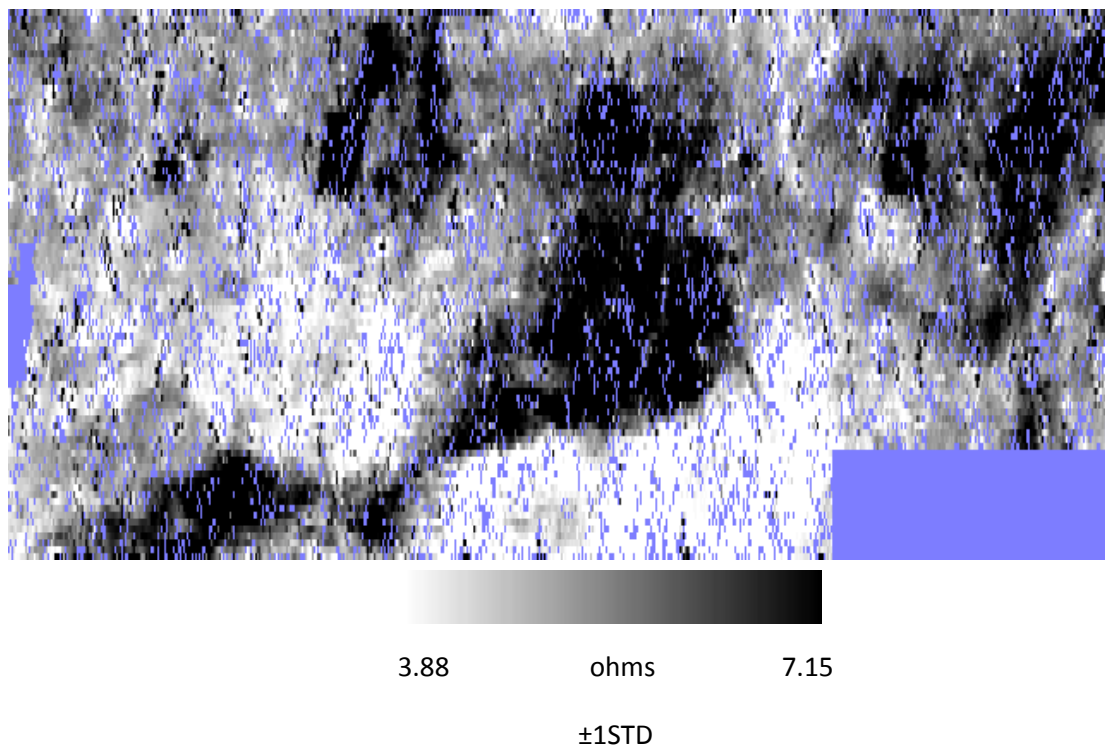
Figure 5.25   Processed 25% error MSP40 earth resistance Alpha data combined using the MSP40 merge function.

The 25% error data sets showed a significant increase in missing data values (dummy values). Additional error levels of 50% and 75% were also created but too much of the data was lost during the error removal process (replaced by dummy values). There for the data was not included.

5.2.6 Discussion of error tests

The theoretical testing suggests that the interpretation of anomalies is significantly hindered by a lack of information when 25%-50% of values are erroneous readings. The random generation of errors may have increased the processing success as localised concentrations of errors are more likely to be recorded with field measurements (based on experience). This is because single data points are easier to correct than blocks of errors.

A drawback of both combination methods within Geoplot is when a dummy values is found in one data set and not the other as the dummy value overrides the other value and replaces it with a dummy value. Therefore search and replace functions should be carefully chosen so not to remove 'correct' readings before data combination. The following section highlight the issues faced when errors occur in data collection and provides practical examples of processing (see section 5.3 and appendix A).

5.3.0 Practical data processing based on fieldwork reports.

5.3.1 Introduction (Limes frontier, Germany)

The German-Raetian Limes was used to separate the Roman Empire from independent Germany. The Upper German-Raetian Limes road or frontier runs approximately 550 kilometres (340 miles), making it the longest archaeological monument in Europe (Fassbinder 2010). The road / frontier was straddled by forts, watchtowers alongside stretches of walls and palisades and often followed natural boundaries such as the (Rhine and Danube) (Unknown 2013). In 2005 UNESCO declared the German-Raetian Limes a world heritage site.

Visitors to the Limes can see excavations and building reconstructions (Breeze and Jilek 2009) based on the archaeological investigations. The fortifications along the Limes ranged from small fortlets (under one hectare) to auxiliary forts (larger than three hectares) and were originally built of earth and timber.

The exact location of the frontier remains an area of research still under investigation. Geophysics has been used extensively in Bavaria to locate and identify many of the fortified areas on the Limes (Fassbinder 2010). The University of Bradford was invited to survey the sites of Eining and Pförring in Bavaria as part of the on-going research project (see figure 5.26). The Bavarian State Department of Monuments and Sites wished to undertake large scale earth resistance survey to complement their Caesium Vapour magnetometer surveys of the Vicus surrounding the forts / fortlets and the MSP40 was of interest to them. The sites were suitable for the PhD research project as they were on prime agricultural land that was prone to damage from heavy machinery and had shallow top and subsoil (≤25cm total depth) on limestone geology.

The site of Eining may have originally been a Flavian strong hold (Czysz *et al.* 2008) which developed as one of the larger frontier garrisons in the area during the second half of the third century to mid fifth century (Czysz *et al.* 2008). Major reconstruction also took place during this time to the road and associated buildings due to the demand of increasing troop numbers and usage.

Czysz *et al.* 2008 describe how Eining (or Abusina) was built as an earth and timber fort for Emperor Titus (circa 79-81 AD) by the cohors IV Gallorum near a pre-existing crossing point in the Danube. The vicus and civilian settlement spread along three sides of the fort (the fourth side backed against the side of the Danube). The fort was rebuilt in stone after a fire in 125 AD destroyed much of the earlier timber structures. Smaller rebuilding projects continued in to the early third century before another fire completely destroyed the fort and vicus (possibly related to Germanic attacks).

A smaller fortified strong hold was built in the southwest corner of the site to house a reduced military presence until 430 AD when a final fire destroyed the stronghold. The civilian population continued to occupy the site until the mid-fifth century when the site was finally abandoned.

Two areas of investigation were undertaken at Eining (Area A & B). Area A focused on a freshly harvested field and was an exploratory survey. Area B focused on a field directly opposite the fort and was attempted to identify evidence for the Vicus continuing on the other side of the modern road. Pförring (or Celeusum) was a smaller fortlet on the Limes that was located on top of a small hill; the vicus was believed to surround the site on the slopes of the hill.

A digital elevation model (DEM) was to be produced; this was collected using a RTK GPS mounted on the MSP40. This method of topographic data collection was undergoing evaluation and refinement during the survey. The GPS and earth resistance survey area covered approximately 1.5ha at Pförring and 1.6ha at Eining.

It was anticipated that the geophysical survey would help to confirm the accuracy of aerial photographs of the sites, whilst also adding additional information to the understanding of the sites. However much of the aerial photography for the areas that have been surveyed lacked enough control points to enable them to be fully rectified. However the buildings identified during this survey may help confirm the locations of these building and others identified on the aerial photography.
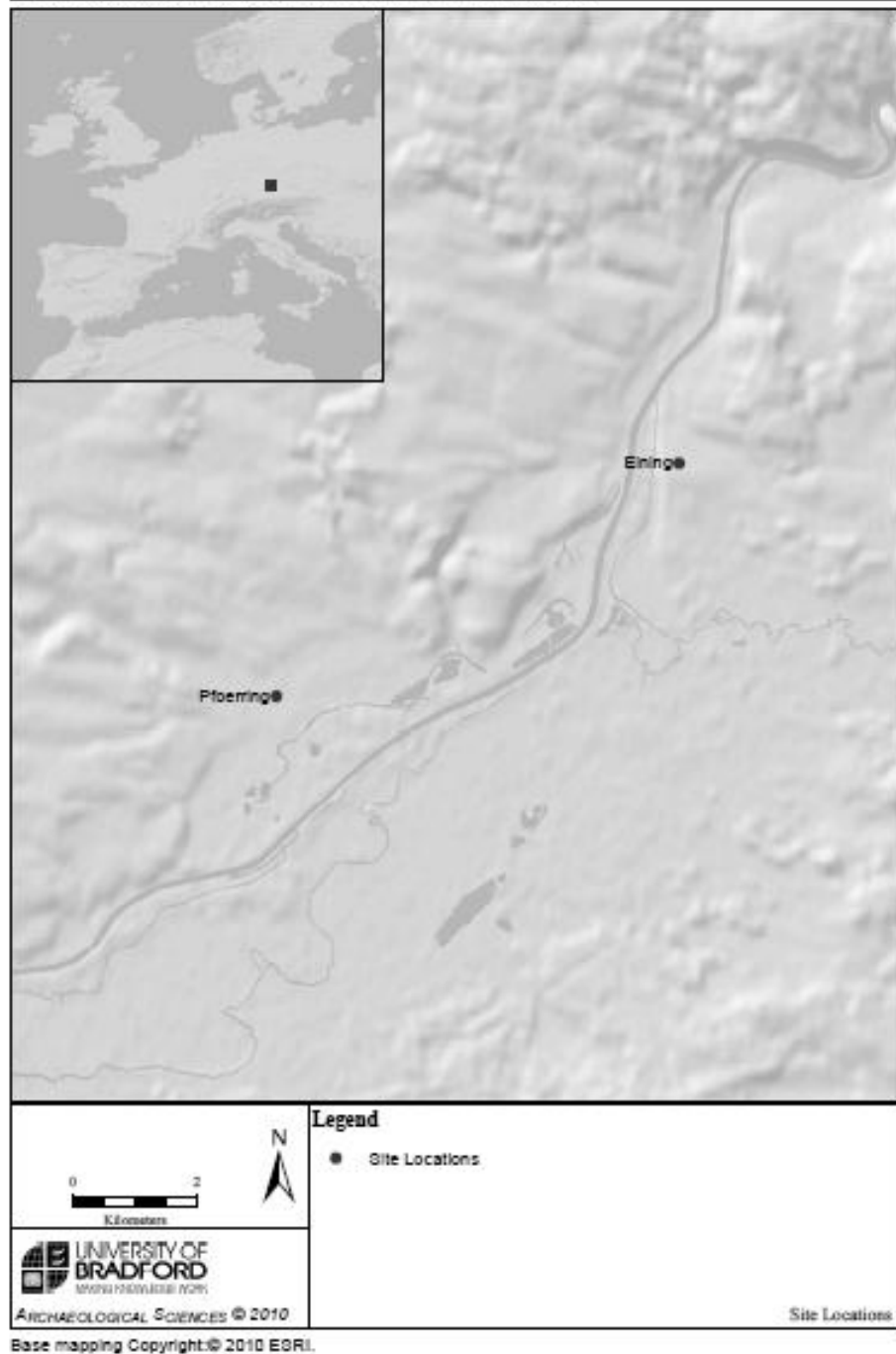
Figure 5.26   The location of the sites Pförring and Eining part of the Limes frontier, Germany.

The two site (3 areas) investigations all took place over a chalk / limestone parent material with shallow top and subsoil < 25cm deep.

All three areas had been used for agricultural purposes. Eining Area A and Pförring Area C were recently harvested (bare soil and plant stubble) whilst Eining Area B had previously been ploughed but had been left fallow for approximately 5 years and was covered in short grass. The three sites had been heavily ploughed which brought large concentrations of chalk to the surface (due to the shallow soil depth) which meant the archaeology was also at risk in these areas. The project provided an opportunity to investigate the MSP40 on different soil types with a variety of current land uses.

5.3.2 Aim of survey

The aim of the geophysical survey was to gather sufficient information to establish the location and extent of archaeological features if present within the survey area and, where possible, to characterise the archaeology identified. Data from the caesium vapour magnetometer survey, DEM and air photographs were also used, where available, to aid interpretation and improve confidence in the archaeological interpretations of the earth resistance survey.

5.3.3 Method

Eining, Germany (Area A)

- MSP40 configured with normal spiked wheels.

- RM15 & DL256 data logger
- Data was collected in a zigzag pattern without rotating the MSP40. The encoder wheel was used to trigger measurements at the specified intervals (see table 5.4). Data was collected in 40m x 40m grids with sighting poles at the grid edges.

Table 5.4   Eining (Area A) survey parameters.

Equipment	Measurement Configuration	Sampling Interval	Traverse Interval	Method of collection
MSP40	Alpha & Beta	0.5m	1m	Zig Zag

Eining, Germany (Area B)

- MSP40 configured with normal spiked wheels.

- RM15 & DL256 data logger

- Data was collected in a zigzag pattern without rotating the MSP40. The encoder wheel was used to trigger measurements at the specified intervals. Data was collected in 40m x 40m grids with sighting poles at the grid edges.

Manual square

- Manual square measurements were used to increase survey area using the RM15 mounted on a PA5 frame with square array side wings (see table 5.5)

- Data was collected in 20m x 20m grids.

-

Table 5.5   Eining (Area B) survey parameters.

Equipment	Measurement Configuration	Sampling Interval	Traverse Interval	Method of collection
MSP40	Alpha & Beta	0.25m	1m	Zig Zag
Manual Square	Alpha & Beta	0.5m	1m	Zig Zag

After initial trials of the MSP40 in Area B it was decided to increase the sampling interval to 0.25m sampling for the earth resistance survey. There were two main reasons for the change in sampling. The excavated fortified site of Eining had upstanding walls and these were approximately 0.5m-0.75m in width. Therefore a 0.5m sampling interval may have been insufficient to identify any walls in the data.

The MSP40 encoder wheel was also overshooting the grid edge with the 0.5m sampling which was affecting the accuracy of the sampling positions. The calibration process was repeated several times and the collection rate was reduced but positional accuracy still remained an issue. The sampling interval was reduced to 0.25m as the collection rate at this sampling interval significantly restricts the speed at which the data is collected. If too many pulses are missed by the encoder then the instrument stops logging data. This helped to significantly reduce the sampling interval errors.

Pförring, Germany (Area C)

- MSP40 configured with normal spiked wheels.

- RM15 & DL256 data logger

- Data was collected in a zigzag pattern without rotating the MSP40. The encoder wheel was used to trigger measurements at the specified intervals. Data was collected in 40m x 40m grids with sighting poles at the ends of each traverse.

Manual square

- A manual square measurement was used to increase survey area using the RM15 mounted on a PA5 frame with square array side wings.

- Data was collected in 20m x 20m grids (see table 5.6).

Table 5.6   Pförring (Area C) survey parameters

Equipment	Measurement Configuration	Sampling Interval	Traverse Interval	Method of collection
MSP40	Alpha & Beta	0.25m	1m	Zig Zag
Manual Square	Alpha & Beta	0.5m	1m	Zig Zag

5.3.4 Data processing

Eining, Area A

Alpha and Beta processing

> 2x Despike X= 1 Y=1 Thr=3 Repl=Mean
>
> 1x Despike X= 1 Y=1 Thr=2 Repl=Mean
>
> 1x Despike X= 2 Y=2 Thr=3 Repl=Mean
>
> Low Pass Filter (LPF) X= 0 Y= 1 Wt = Gaussian
>
> Combine Gera1app & Gera1bpp using the combine msp40 composites in Geoplot.
>
> Merge composites (High pass filtered (HPF) x = 5 Y= 5 Wt=G)
>
> LPF X= 0 Y= 1 Wt = Gaussian
>
> LPF X= 0 Y= 1 Wt = Gaussian

5.3.5 Results

Area A (Eining) see figures 5.27 – 5.29

A1- Trend, high resistance anomalies possibly associated with moisture uptake from the maize crops in the neighbouring field. Alternatively the high resistance may be a result of the underlying geology being closer to the surface at the southern edge of the survey area (also further up slope).

A2- Trend, low resistance trend lines. The fragmented lines running across the survey area may be due to the ploughing of the field as the ridges run across the line of slope

A3- ? Archaeology, high resistance amorphous anomaly (5-10 ohms). The data does not show any clear shape or structure but may result from a dump of modern material or compaction associated with access into the field.

A4- ? Archaeology, Medium – low resistance anomaly, sub rectangular in plan. The anomaly is indistinct and may or may not be archaeological in origin.

A5- ? Natural, low resistance, large amorphous anomaly. Likely to be localised variation in soil depth or a result of increased soil water retention properties.

A6- ? Natural, high resistance sub circular anomalies. May be a result of accumulations of stone brought up into the plough soil by ploughing or near surface geology increasing the earth resistance values on a localized scale.
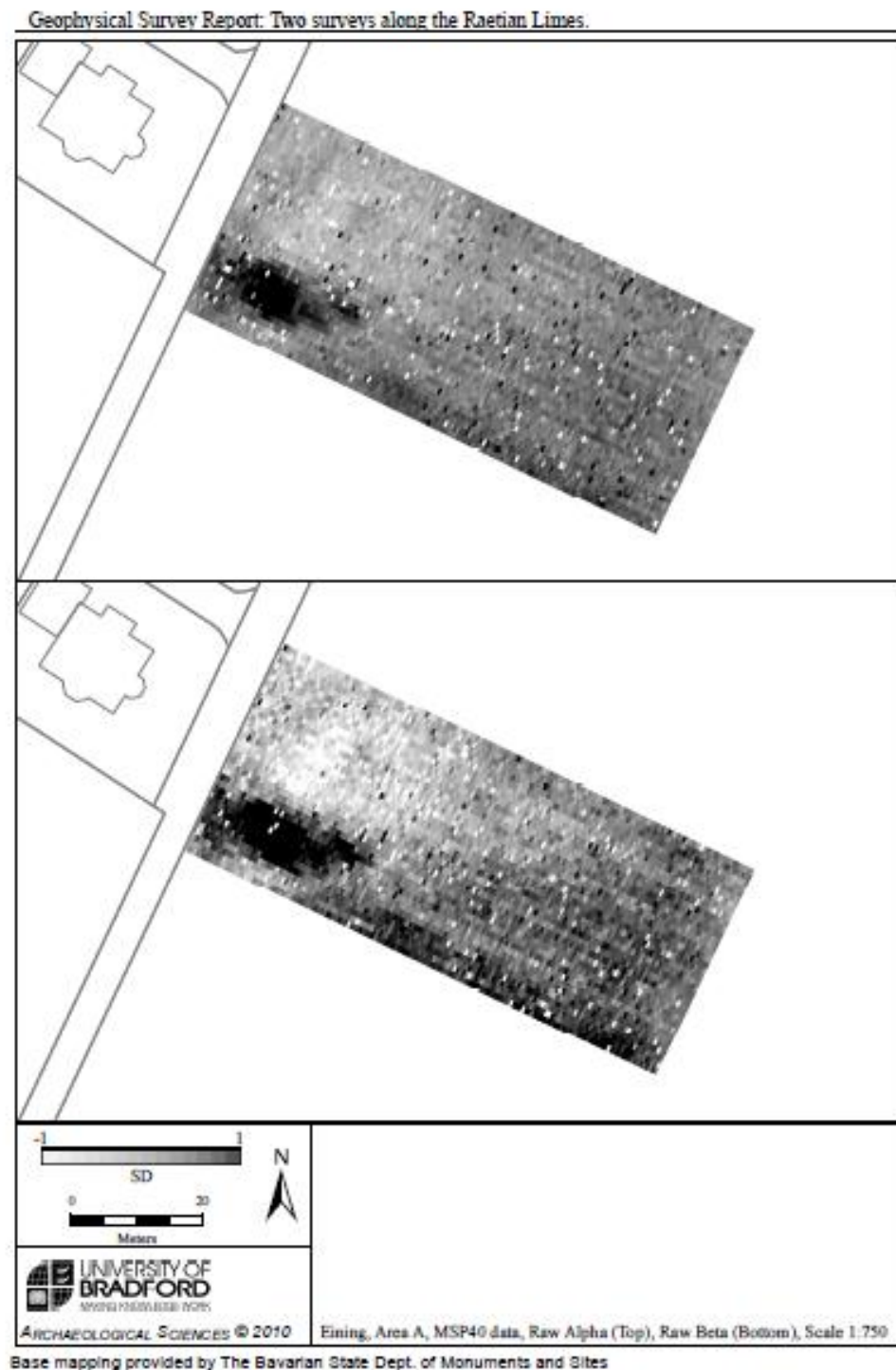
Figure 5.27   Raw earth resistance data (Alpha and Beta) from Eining area A.

SD

N

0   20
Meters

UNIVERSITY OF
BRADFORD
MAKING KNOWLEDGE WORK
ARCHAEOLOGICAL SCIENCES © 2010

Eining, Area A, MSP40 data, combined Alpha and Beta (Top),
combined Alpha and Beta, processed (Bottom), Scale 1:750

Base mapping provided by The Bavarian State Dept. of Monuments and Sites
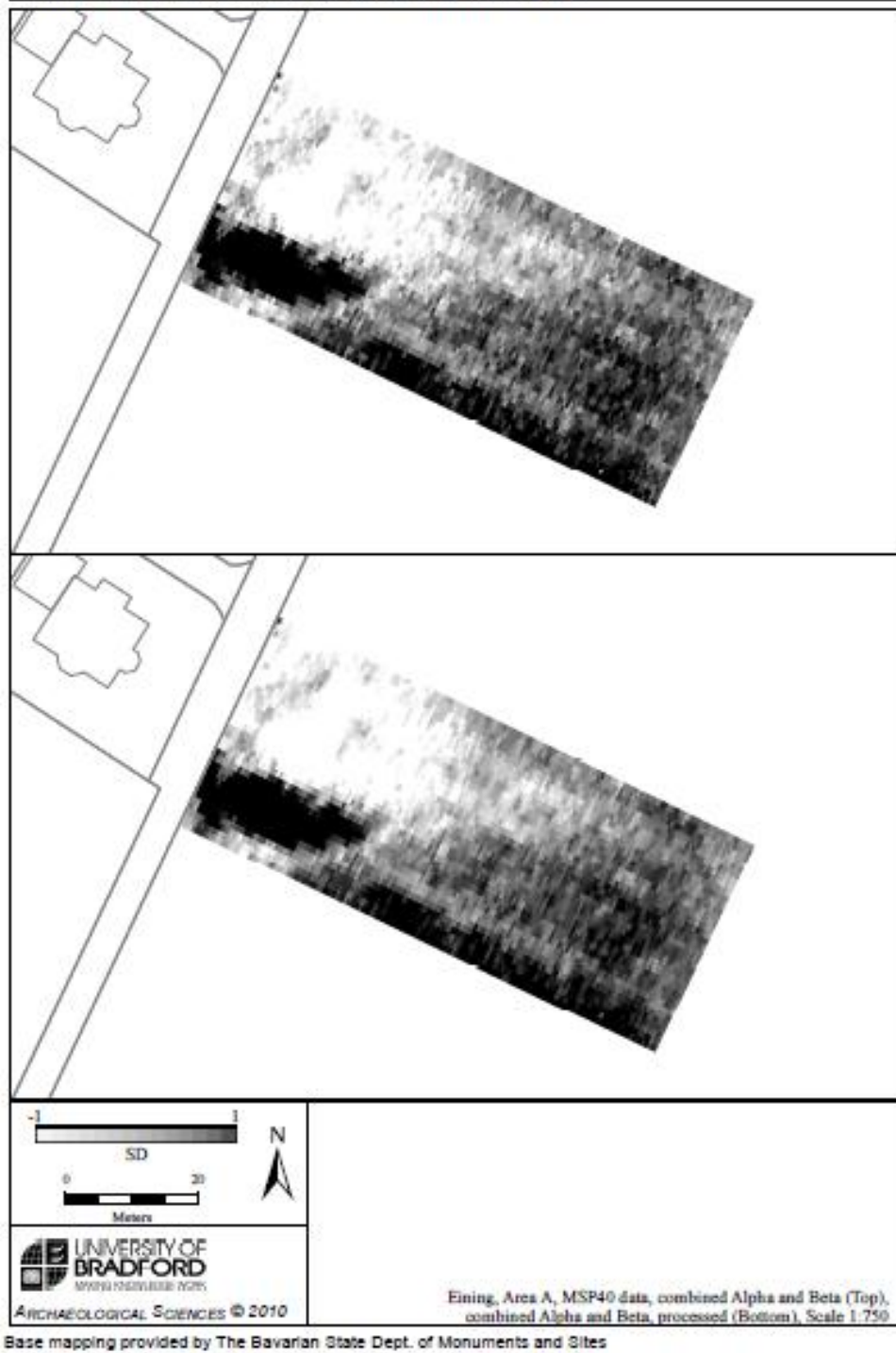
Figure 5.28   Processed earth resistance data (combined Alpha and Beta data sets) from Eining area A.
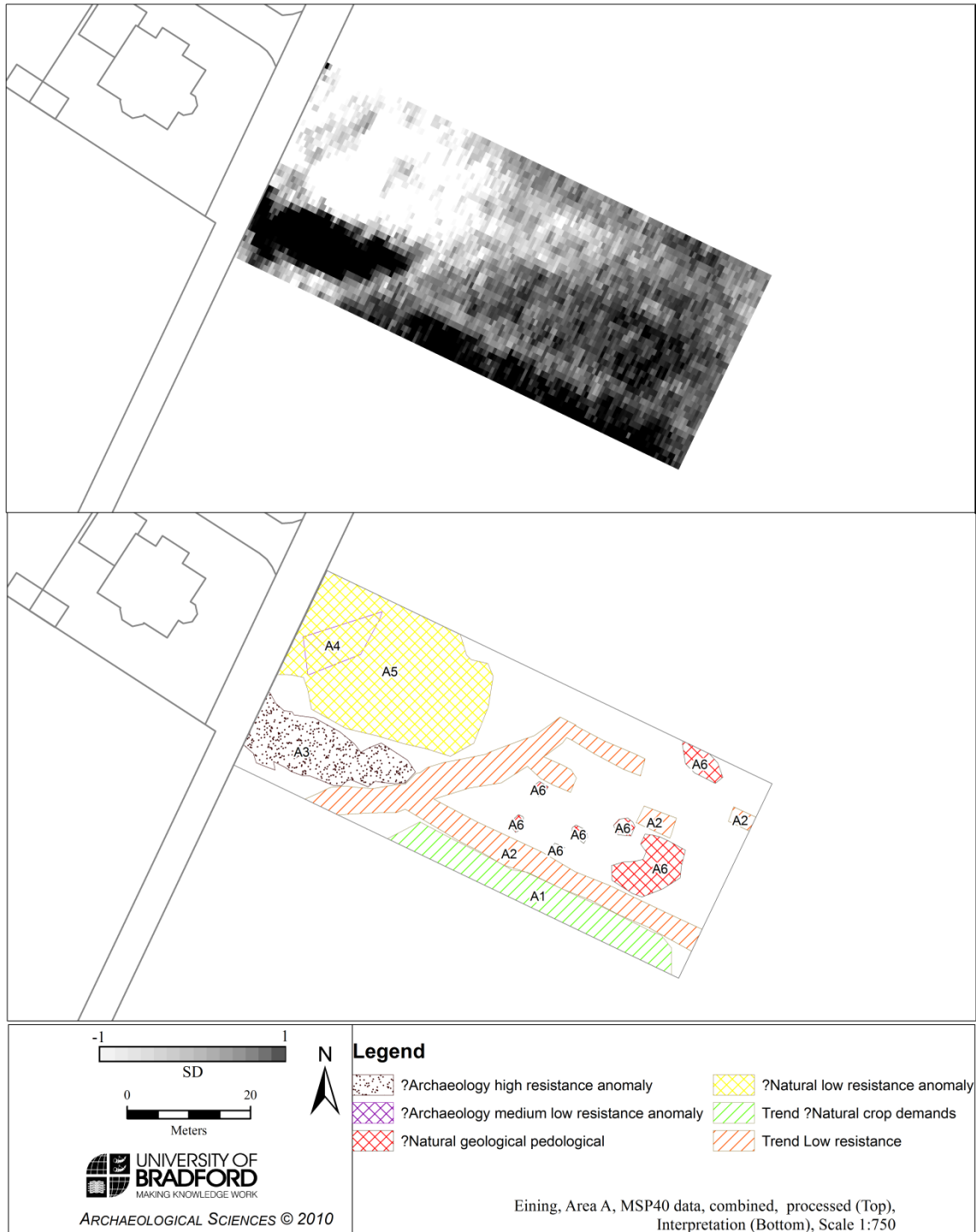
Figure 5.29   Processed earth resistance data (combined Alpha and Beta data sets) and archaeological interpretations of the major anomalies.

5.3.6 Eining Area A discussion

The Eining survey (Area A) showed no clear evidence for any settlement or archaeological features / anomalies.

The anomalies that have been identified are likely to be the result of the agricultural practice (ploughing) or natural variations possibly a result of the shallow topsoil and subsoil on Limestone geology.

5.3.7 Eining, Area B & Pförring

A manual square array survey and MSP40 earth resistance survey was undertaken at both sites to increase the survey area investigated.

5.3.8 Eining data processing

Manual square array processing

The survey was carried out with a 0.5m sampling interval and traverse interval of 1 m therefore it was necessary to interpolate the data set (Interpolate X, Expand –SinX/X, x2) before combining with the MSP40 data sampled at 0.25m and traverse interval of 1m (see figures 5.30, and for results 5.31--5.37).

MSP40 and manual square array (combined) processing

Alpha

- Combine composites (i.e. join them): (Alpha MSP40 and manual square)

- C:\geoplot\comp\gerb1\a at 1, 1

- C:\geoplot\comp\gerb1\gerbca at 161, 1

- Edge match EM2L, EM6L

- 2x Despike X= 1 Y=1 Thr=3 Repl=Mean

- 1x Despike X= 1 Y=1 Thr=2 Repl=Mean

- 1x Despike X= 2 Y=2 Thr=3 Repl=Mean

Beta

Combine composites (i.e. join them): (Beta MSP40 and manual square)

- C:\geoplot\comp\gerb1\b at 1, 1

- C:\geoplot\comp\gerb1\gerbcb at 161, 1

- Edge match EM2L, EM6L

- 2x Despike X= 1 Y=1 Thr=3 Repl=Mean

- 1x Despike X= 1 Y=1 Thr=2 Repl=Mean

- 1x Despike X= 2 Y=2 Thr=3 Repl=Mean

Combined Alpha and Beta

- Merge composite (HPF X=5 Y= 5 Wt=G) Gerbccap & Gerbccbp

- Search 0 to 50 Replace= 5.5, B (Inc) 130, 1 137, 2

- Destagger All Grids, Xdir, Shift= 1 Line pattern -2-4-6-8

- LPF X=0 Y=1 Wt=G

- LPF X=1 Y=1 Wt=G

- Interpolate Y, Expand –SinX/X, x2
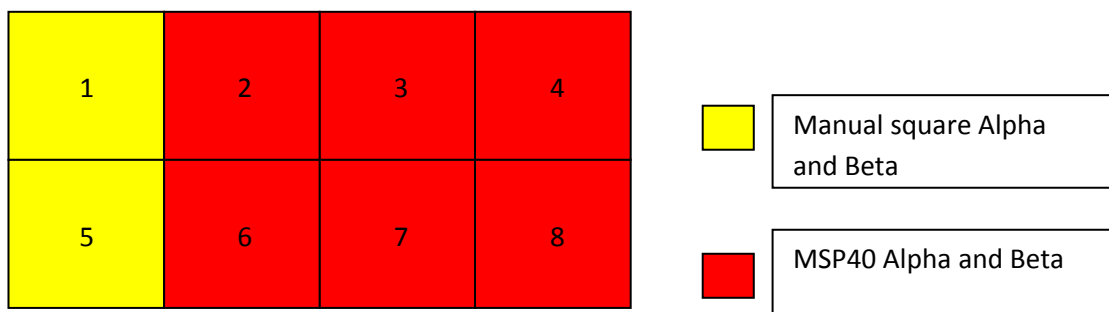
Figure 5.30   The combined composite survey areas of Eining (Area B).

5.3.9 Results Eining Area B

Geophysical Survey Report: Two surveys along the Raetian Limes.

Legend

SD

Meters

UNIVERSITY OF
BRADFORD
MAKING KNOWLEDGE WORK
ARCHAEOLOGICAL SCIENCES © 2010

Eining, Area B, combined raw Alpha data, 1:1000

Base mapping provided by The Bavarian State Dept. of Monuments and Sites
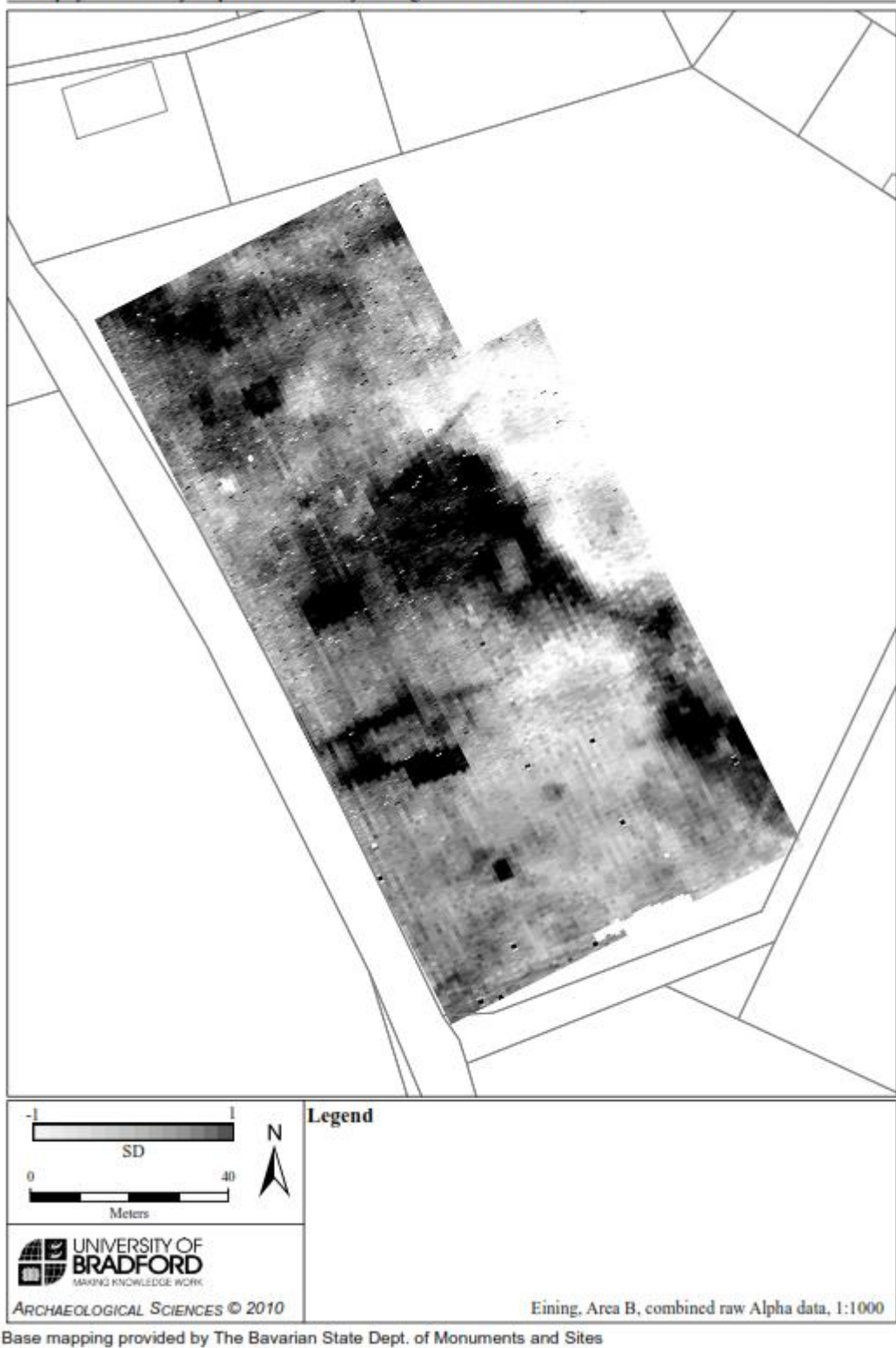
Figure 5.31   Unprocessed earth resistance data (Alpha) from Eining Area B.

Legend

SD

0   40
Meters

N

UNIVERSITY OF
BRADFORD
MAKING KNOWLEDGE WORK

ARCHAEOLOGICAL SCIENCES © 2010

Eining, Area B, combined raw Beta data, 1:1000

Base mapping provided by The Bavarian State Dept. of Monuments and Sites
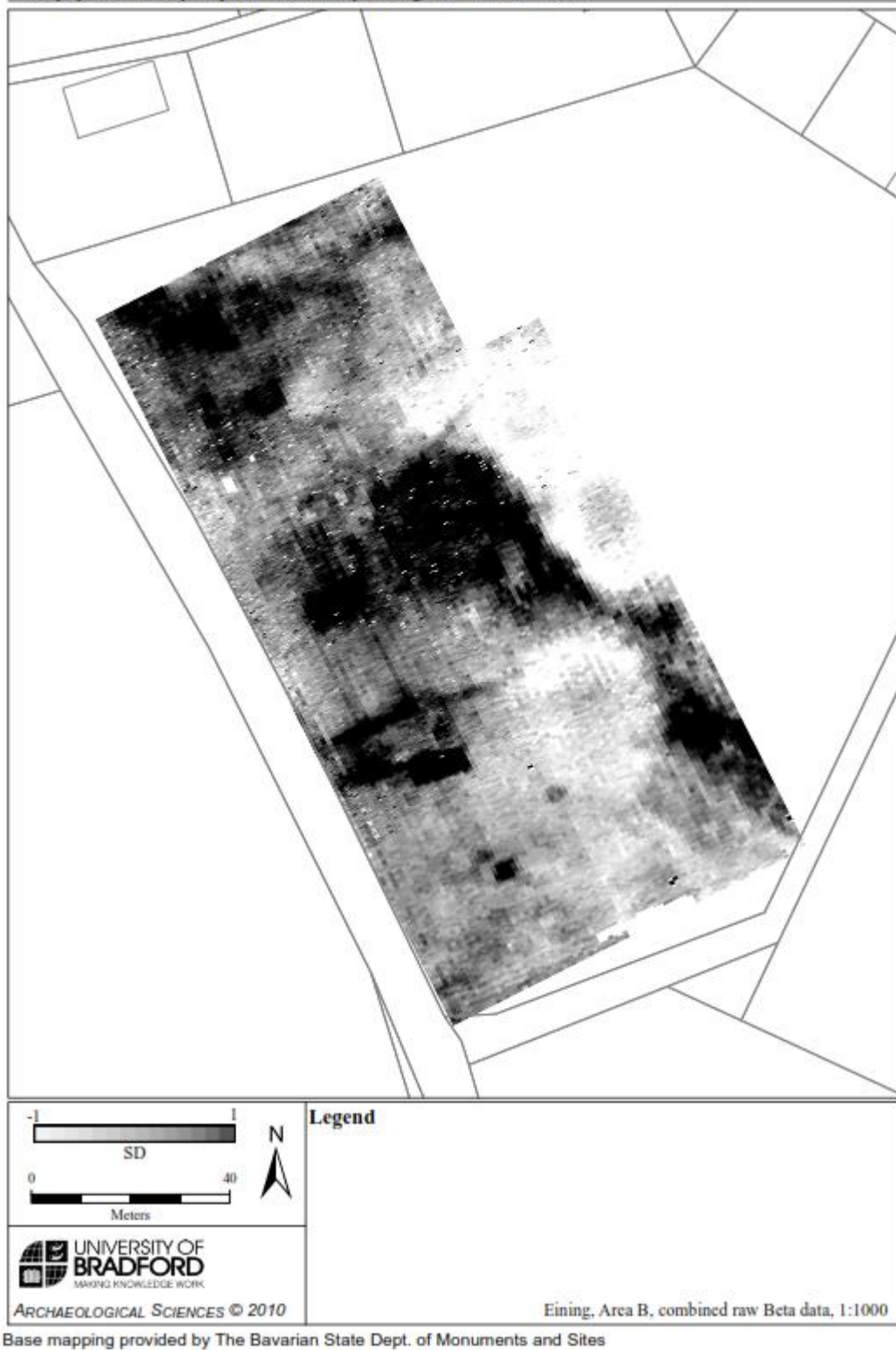
Figure 5.32   Unprocessed earth resistance data (Beta) from Eining Area B.
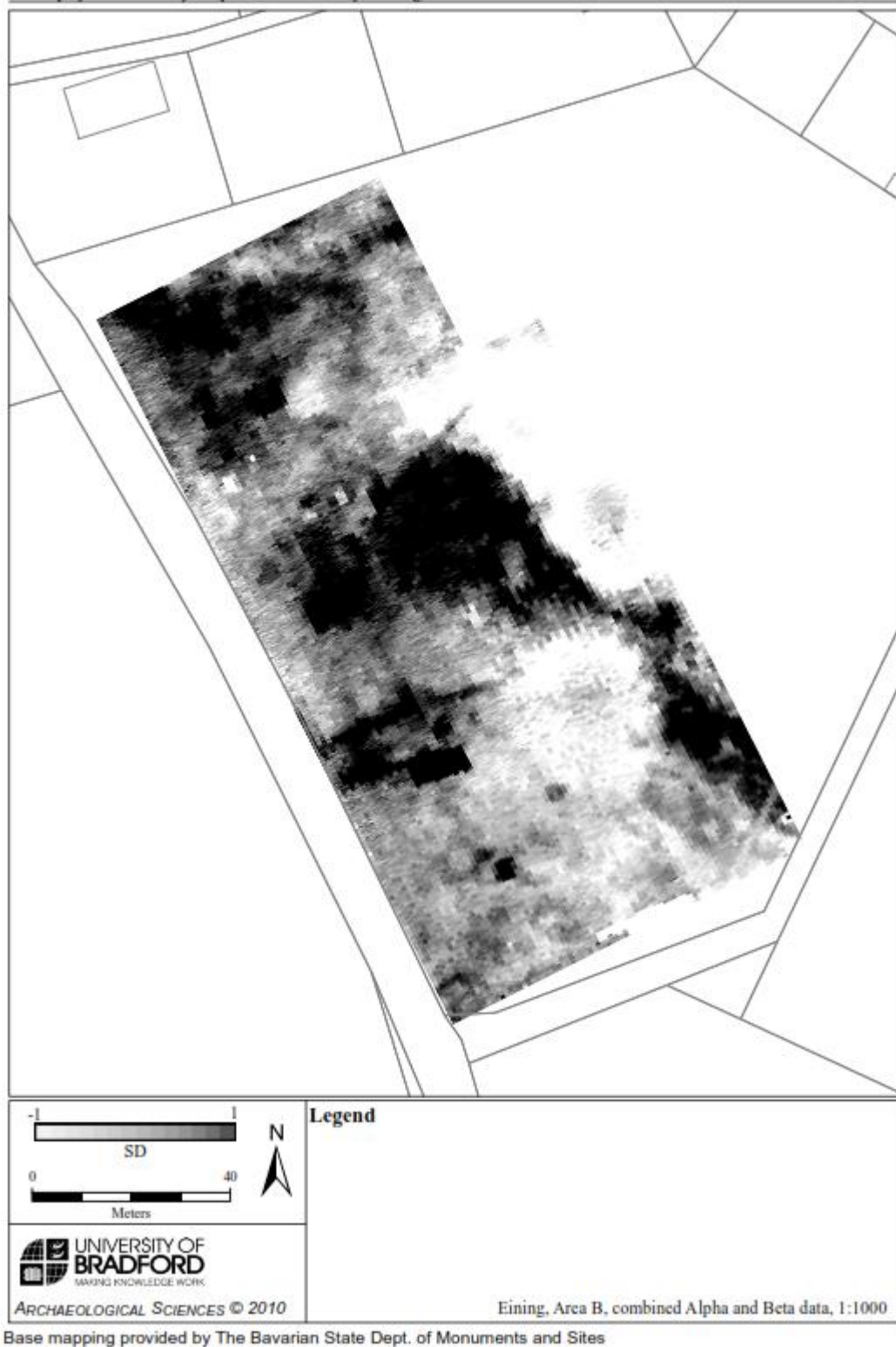
Figure 5.33   Minimally processed earth resistance data (combined Alpha and Beta datasets) from Eining Area B.
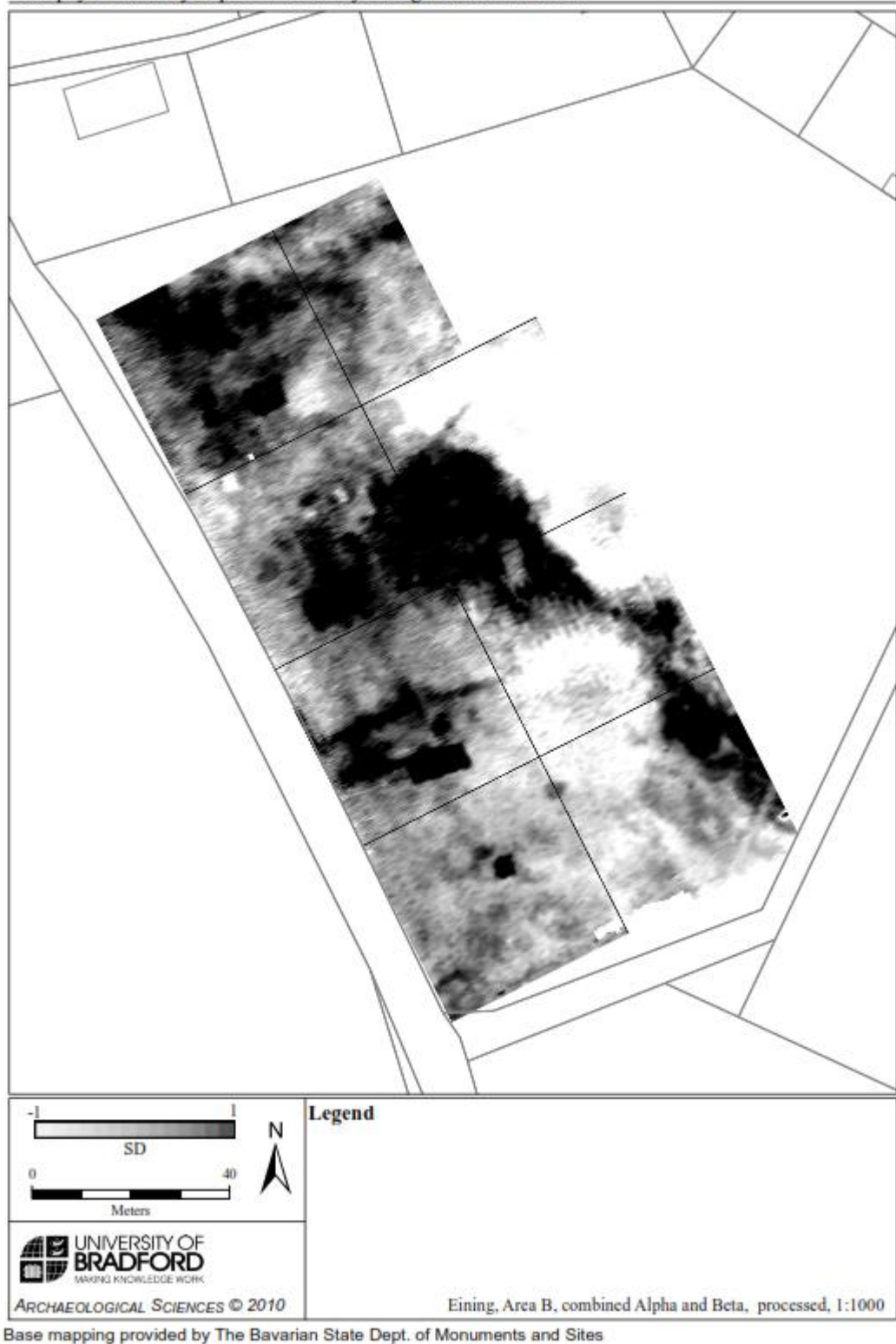
Figure 5.34   Processed earth resistance data (combined Alpha and Beta datasets) from Eining Area B.
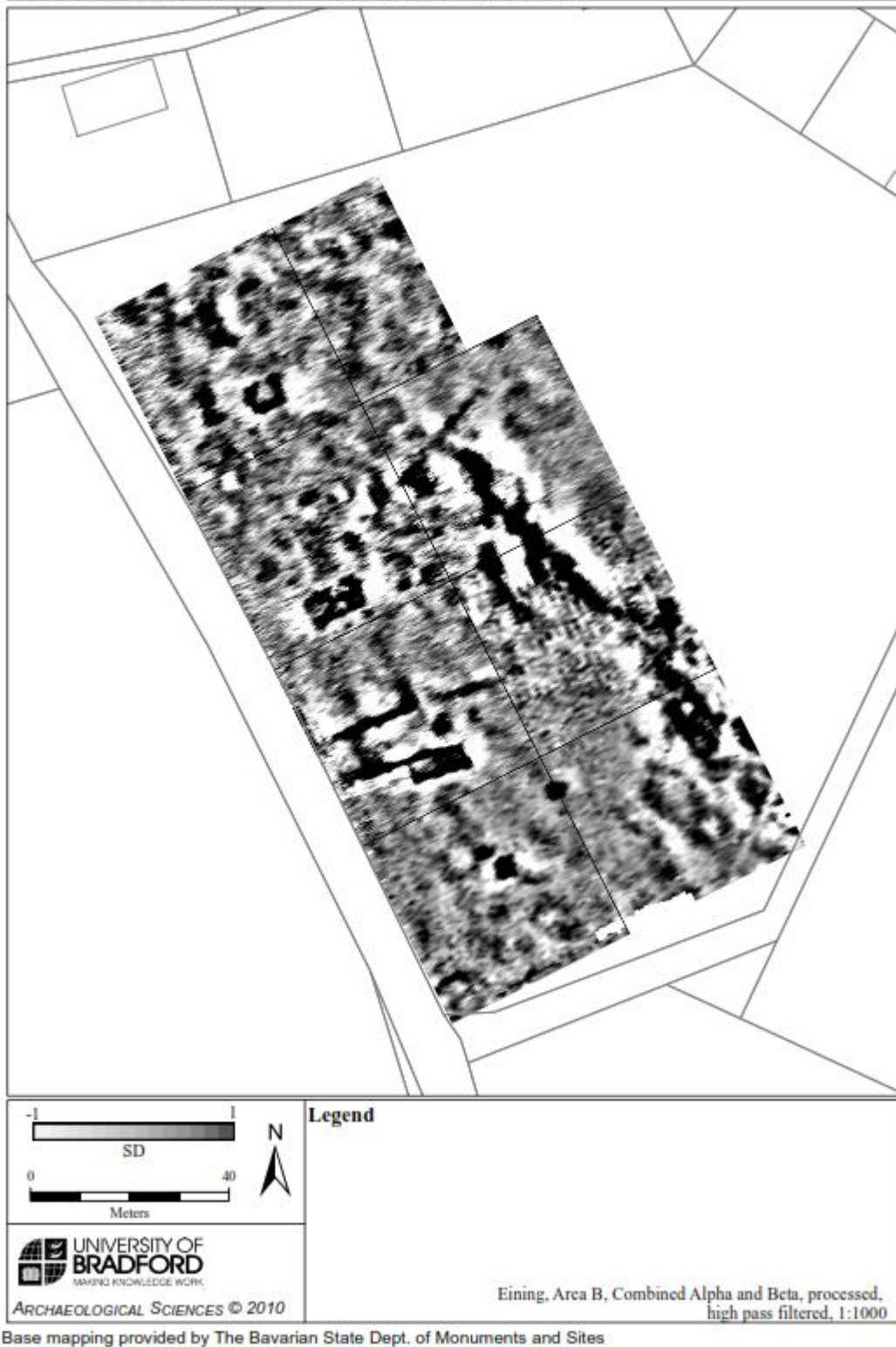
Figure 5.35   Processed and high pass filtered earth resistance data (combined Alpha and Beta datasets) from Eining Area B.

Legend

Caesium vapour magnetometer survey

1:1000

Base mapping provided by The Bavarian State Dept. of Monuments and Sites
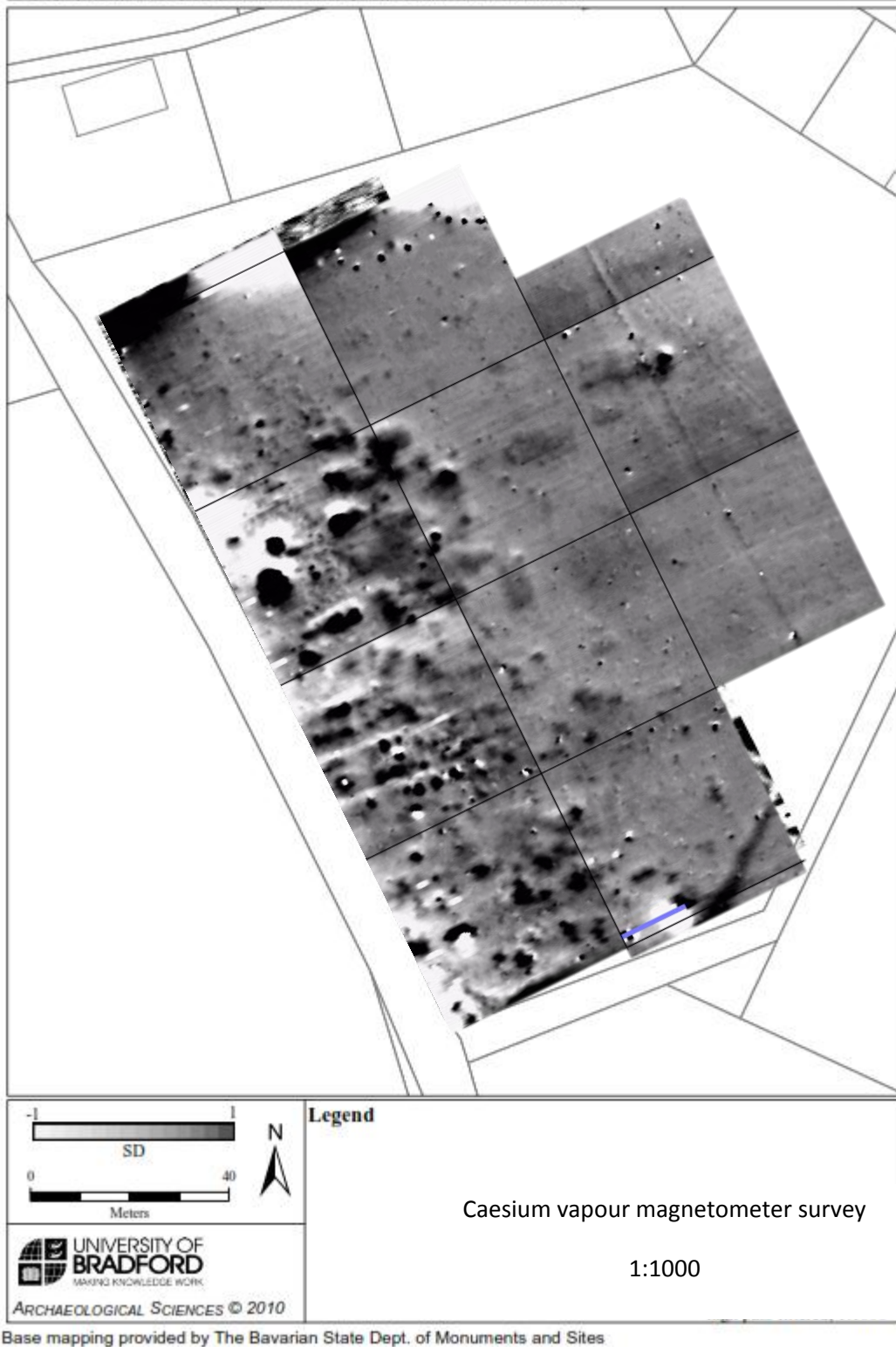
Figure 5.36   Processed Caesium vapour magnetometer survey results from Eining Area B. Data provided by The Bavarian State Department of Monuments and Sites

■ **Archaeology Building**		▨ **?Archaeology ?Building**	
▨ **High resistance anomaly**		▨ **?Archaeology ?Pits**	
▨ **Low resistance anomaly**		▨ **Natural geological pedological**	
▨ **Area of disturbance**		▨ **?Natural high resistance anomaly**	
▨ **Modern road edge**		▨ **Trend**	
▨ **Archaeology ?Ditch**		▨ **Trend High resistance**	
▨ **?Archaeology high resistance anomaly**			

UNIVERSITY OF
BRADFORD
MAKING KNOWLEDGE WORK

ARCHAEOLOGICAL SCIENCES © *2010*

Eining, Area B,Interpretation, 1:1000
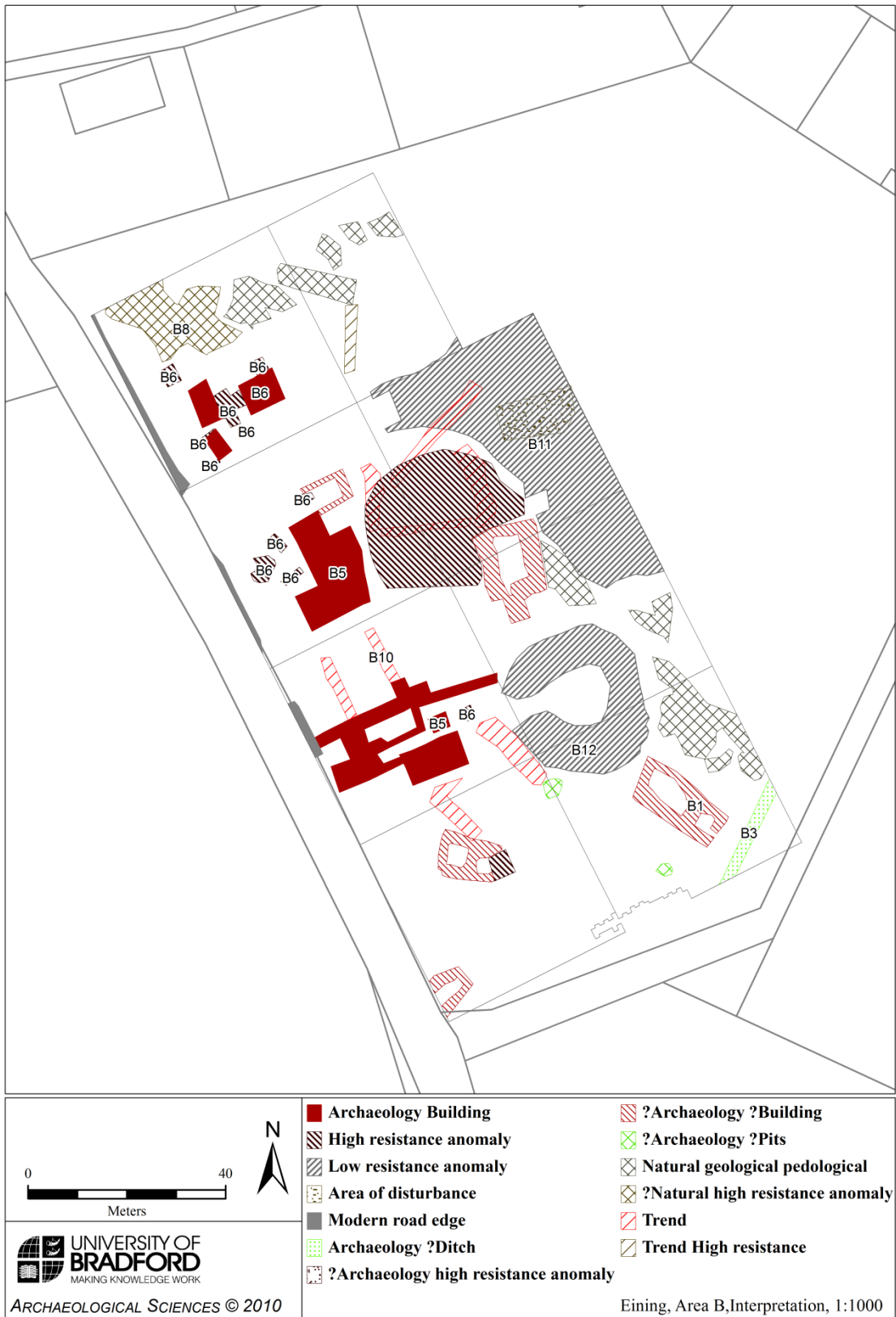
Base mapping provided by The Bavarian State Dept. of Monuments and Sites

Figure 5.37   Archaeological interpretations from Eining Area B.

B1- Archaeology, low – medium resistance anomaly likely to be part of a building. The anomaly is not easily visible in the caesium vapour magnetometer survey but by comparison can be seen along with the other building identified during the survey. The orientation of the anomaly approximately north-west to south-east with is different to the likely Roman buildings, suggesting it is not contemporary with the other buildings identified in the resistance survey.

B2 – Archaeology, high resistance anomalies likely to form a complex of buildings. The buildings are in close proximity to the excavated Roman archaeological site at Eining and possibly indicate a continuation of the site across the road. The fortified site of Abusina is likely to have had a vicus associated with it and the area to the north east and east of the site is the most suitable area due to the steep embankment to the west and close proximity to the tributary of the Danube. As the anomalies suggest the buildings are made of stone then it is likely they date to shortly after 125 AD - prior to this wooden buildings were erected before being burnt down at this time - and before the middle third of the third century AD when a fire again burnt down much of the fort and vicus.

B3 – Archaeology, very low resistance linear anomaly also identifiable in the magnetometer survey as a strong positive anomaly. The anomaly may indicate evidence for a ditch.

B4 – Archaeology, high resistance rectangular anomaly, the archaeological feature appears as a high resistance anomaly and may indicate the remains of a building with a surviving floor surface or a layer of demolition. The caesium vapour magnetometer survey also identified the building. The walls are recorded as a strong negative anomaly whilst the internal area has a strong positive signal indicating a magnetically enhanced signal which may suggest an in situ floor surface.

B5 – Archaeology, high resistance sub rectangular anomalies possibly forming a range of buildings or structures associated with the building B4.

B6- ? Archaeology, high resistance anomalies rectangular in plan possibly part of a small structure / building.

B7 –? Archaeology, medium resistance sub rectangular shaped anomaly with two separate low resistance centres. The anomaly is indistinct which may indicate the archaeology is at the limits of the 0.75m square array's depth of detection. The anomaly appears similar to B1 (a possible building).

B8 –? Natural, amorphous high resistance anomaly. The magnetometer survey shows no anomalies that correlate with the high resistance readings and this may suggest that the high resistance is a result of localised near surface geological variation.

B9 –? Archaeology, high resistance linear anomaly/trend, possibly archaeological but little certainty of interpretation is possible.

B10 – Trend. Low - medium resistance linear trend lines which are clearly visible in the magnetometer data but also more visible in the high pass filtered resistance data - the anomalies may be associated with the probable building B2. However, more precise interpretations of the anomalies cannot be made due to the poorly defined anomalies.

B11 – Natural, low resistance anomaly covering a large area to the eastern extent of the survey. Likely to be an area of poorly draining soil and / or have a greater overburden of topsoil.

B12 –? Archaeology, low resistance sub circular (possibly c shaped) anomaly which correlates with an area of a weakly negative anomaly in the caesium vapour magnetometer data. The inner area of the anomaly has raised resistance and shows up as an increased magnetic enhancement - this suggests the feature is some form of ditched enclosure.

5.3.10 Discussion

The surveys at Eining showed how data sets with different methods of collection could be combined with limited indication of reduced data quality resulting from the faster collection rate of the MSP40. The results show the field immediately to the north east of the fort at Eining (Area B) showed a range of buildings present that are likely to form part of the vicus associated with the fort of Abusina. The earth resistance surveys showed that the settlement continued beyond the modern road and may continue into the field to the east of the fort. The survey also indicates a different phase of occupation with two possible structures (B1 & B7) on a different orientation to the other buildings identified. The increased distance of B1 from the other buildings may also indicate a different phase of occupation.

5.3.11 Pförring, Germany (Area C)

5.3.12 Introduction

The first day at Pförring provided an opportunity to trial the MSP40 over a freshly harvested field covered in hay / straw off cuts and stubble. The ground surface was also covered in aggregates of stone brought to the surface through ploughing and soil creep. The conditions produced a noisy data set with negative readings and spikes in earth resistance measurements.

5.3.13 Processing

To reduce the effects of the erroneous readings the first day's results were exported from Geoplot and an algorithm was used that compares the Alpha and Beta data sets for each survey point. If either of the readings had a negative value then it was replaced by the other, positive measurement; if the two corresponding survey points have negative values then both were replaced by the Geoplot dummy value of 2047.5 (see table 5.7). The Alpha and Beta data sets are then combined this can be done by averaging the data or by re-importing the data back in to Geoplot and using the MSP40 merge function.

Table 5.7   Example of processing

Alpha	Beta	Combined Alpha & Beta (averaged)
5.6	4.8	5.2
-5.9 (replaced with Beta value of 2.5)	2.5	2.5
3.4	-6.7 (replaced with Alpha value of 3.4)	3.4
-5.9	-6.8	Both values replaced with dummy value of 2047.5

Day two allowed for more testing with a new wheel set, using short spikes to reduce the potential of errors created by the spikes hitting the surface stones. Initial trials indicated the cart rolled more smoothly over the surface as the spikes could penetrate the ground without hitting as many stones. However, after viewing the readings on the DL256 data logger erroneous readings were still an issue. This was due to the thin layer of freshly harvested straw having dried out and acting as an insulating layer and impeding the spike penetration into the ground. The MSP40 was changed back to the normal spikes and additional weight was added to the cart to increase the chance of sufficient spike penetration for accurate earth resistance readings.

On the final day of survey the MSP40 developed a fault which saw the Alpha readings suffer from increased noise in the data (see figure 5.38). The fault may have resulted from an electrode not being sufficiently in contact with the brass plate on the wheel hub possibly as a result of movement of the wheel hub created by surveying across the line of the slope. Alternatively the fault may have been due to an ingression of water into the axle junction box creating a short between the wires.

-3.75   ohms   14.21

±1STD

-6.75   ohms   20.28

±1STD
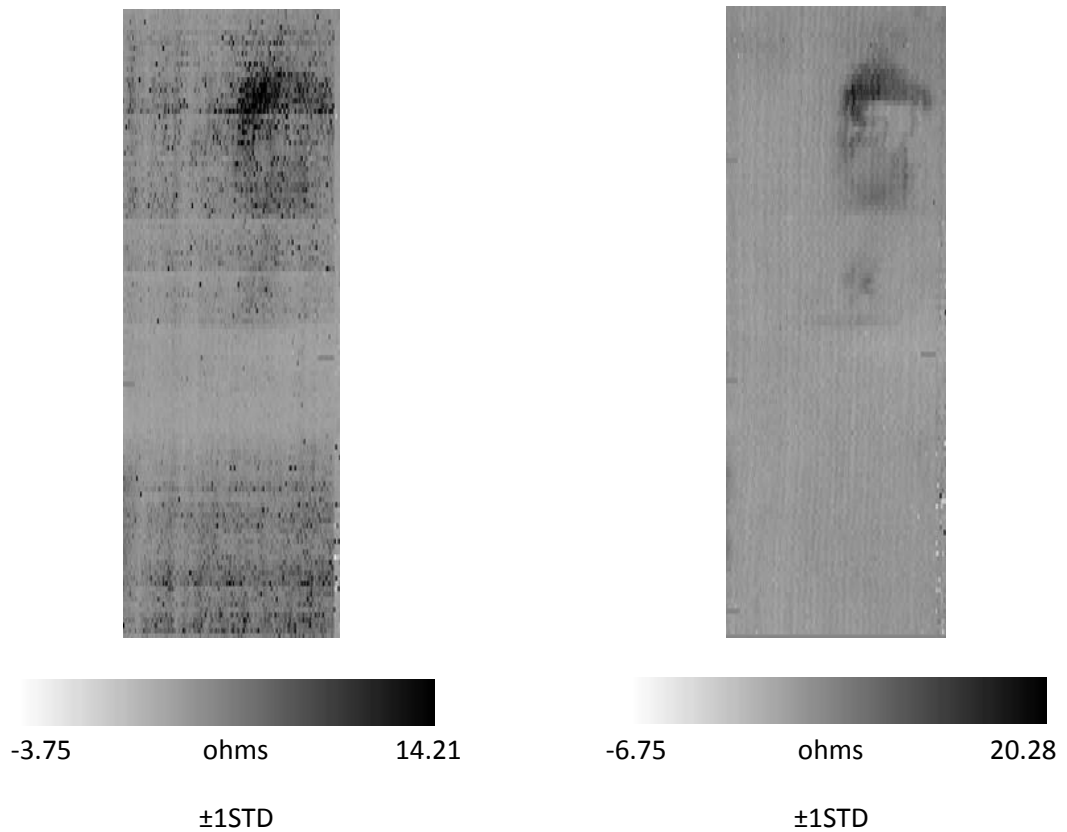
Figure 5.38   Raw Alpha (left) and Beta (right) data sets - the Alpha plot has increased noise spikes and bands of increasing or decreasing resistance across grids.

A decision was made to not process the Alpha measurements from the three affected grids (see figure 5.39 grids 2, 5, 8); instead it was decided to just use the Beta measurements as the grids appeared to be less affected by the fault (the anomalies in the Beta data set also correlated with those in the Caesium vapour magnetometer survey (see figure 5.45).
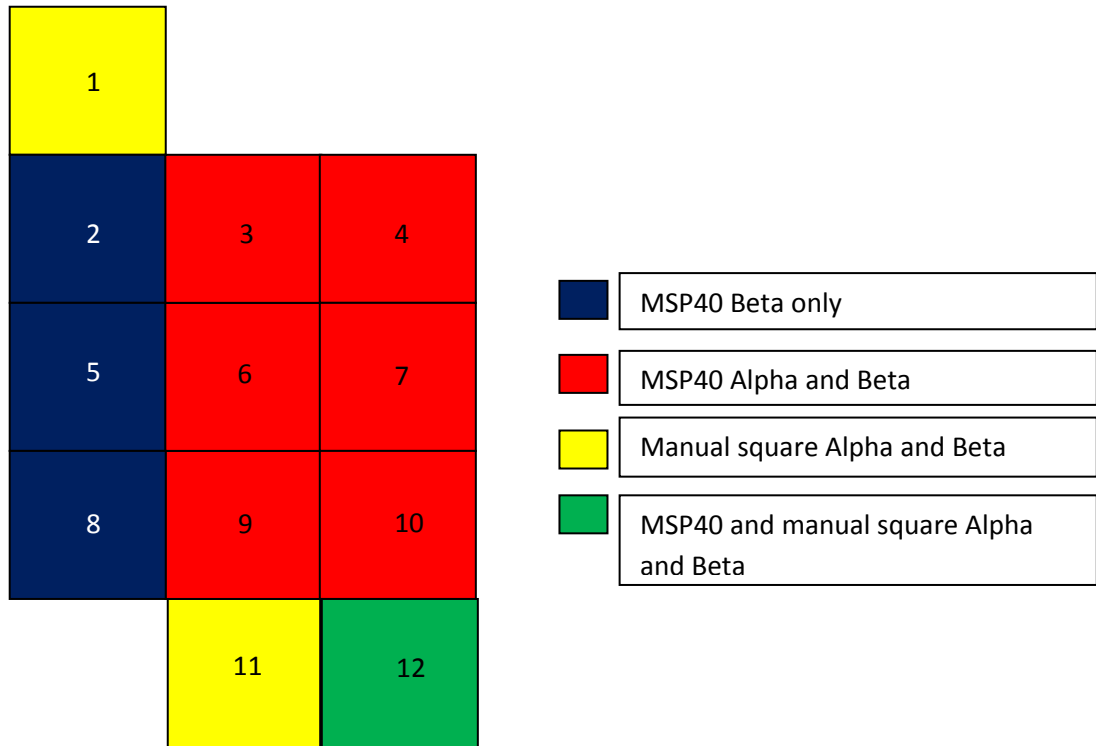
Figure 5.39   The combined composite survey areas of Pförring (Area C).

Grid 12 was processed by interpolating the manual square array data, before exporting the data from Geoplot (as Z data) and combining with the MSP40 grid data in Surfer 8 and re-importing back into Geoplot. The data was cut and pasted into the relevant column position to join the two surveys together. The process was completed in Surfer as it is possible to open the list of Z data points and save in the original file location without affecting file formats in Geoplot.

Processing

Combine composites:

C:\geoplot\comp\gerc\gerc3c at 1, 1 to C:\geoplot\comp\gerc\b at 161,161

C:\geoplot\comp\gerc\gerc3c at 1, 1 to C:\geoplot\comp\gerc\b2p at 1, 1

1x Despike X= 1 Y=1 Thr=3 Repl=Mean

Edge match EM4T, EM11B, EM12B

2x Despike X= 1 Y=1 Thr=3 Repl=Mean

1x Despike X= 2 Y=2 Thr=3 Repl=Mean

1x Despike X= 1 Y=1 Thr=2.5 Repl=Mean

Per. F., Index =61-65, Grid=All, Spike= On, thresholds not applied.

Per. F., Index =105-108, Grid=All, Spike= On, thresholds not applied.

Per. F., Index =122-125, Grid=All, Spike= On, thresholds not applied.

Per. F., Index =132-136, Grid=All, Spike= On, thresholds not applied.

Per. F., Index =244-246, Grid=All, Spike= On, thresholds not applied.

LPF X= 0 Y= 1 Wt = Gaussian

LPF X= 1 Y= 1 Wt = Gaussian

Interpolate X, Expand – SinX/X, x2

Interpolate Y, Expand – SinX/X, x2

Per. F = Periodic filtering (see p289 for more detail)

5.3.14 Results Pförring

The entire data set is covered by agricultural plough lines running down slope. The data has been processed (periodic filtering) in such a way to suppress the effects of the ploughing but not completely remove the landscape artefacts. The linear anomalies generally alternating between high-low resistances correlated with the dimensions of the plough lines.

C1- Archaeology, low resistance curvilinear anomalies. The ditches, easily visible in the caesium vapour magnetometer survey (see figure 5.45), are very hard to distinguish in the earth resistance data (see figure 5.43 and 5.46). The poor anomaly definition is due to the weather conditions as there had been torrential rain in the weeks and days preceding the survey. There was also significant rain fall during the survey. This could drastically reduce the contrast between the background values and geophysical anomalies.

C2- Archaeology / modern, high resistance linear anomaly running approximately across the site. The anomaly may be a field boundary.

C3- Archaeology, very high resistance anomalies forming a range of buildings. The anomaly is displayed as a high resistance anomaly with little definition of the internal structures. This is because the range of the resistance values in this area compared of the whole survey area means the internal divisions of the buildings are masked. A clipped plot was produced focusing on this building area. The data was reprocessed and a high pass filter was applied to the data set to remove the low frequency, large-scale spatial detail. The high pass filter shifts the data around a zero point creating a bipolar display (Black-White). The black anomalies represent the higher resistance values and show a good correlation with the caesium vapour magnetometer results which are displayed as a strong negative anomaly. The high resistance linear anomalies are likely to be walls of a building. The geology in the surrounding area is limestone, and is likely to have low magnetic susceptibility values.

Limestone is a likely source of building material, therefore the foundations are likely to show up as a negative anomaly when cut into the magnetically enhanced topsoil and subsoil.

C4- Archaeology, high resistance linear anomalies. Probably an isolated building again visible in both the earth resistance and magnetometer surveys. An amorphous high resistance anomaly is located on the south-west edge of the building which may be a surviving floor surface or more likely be the result of plough damage dragging material down slope increasing resistance in the area & explaining the lack of definition to the wall. A very high resistance anomaly is located on the north-east end of the building and may also be a result of plough damage.

C5- Archaeology, high resistance rectangular anomaly. The anomaly is poorly defined and shows little of the detail of walls visible in the magnetometer survey. This may be an indication of the depth of the feature as it may be on the limits of the depth of detection of the MSP40.

C6- Archaeology, high resistance anomaly forming a sub-rectangular anomaly probably associated with the anomaly C3 although no internal divisions can be identified.

C7- ? Archaeology, high resistance sub-circular anomalies. Several of the anomalies correlate with the strong positive magnetic anomalies (+10, -15 nT) and may be indications of hearth locations or waste from industrial activity. Where there is no correlation, then the anomalies may indicate small accumulations of higher resistance material.

C8- ? Archaeology, high resistance area / trend correlating with a broad trend of magnetically enhanced material. The anomaly may be a result of plough movement and topsoil wash down the slope.

C9- ? Archaeology, A high resistance 'L' shaped anomaly running approximately north-west to south-east across the site. Possibly a boundary of an enclosure.

C10- ? Archaeology, high resistance linear anomaly possibly forming part of a wall of a building and related to C11.

C11- ? Archaeology, high resistance linear anomalies possibly forming part of a wall of a building and related to C9/10.

C12- Curvilinear anomaly possibly from the hedgerow field boundary to the far north-east of the site.

C13- Two high resistance linear trend lines running approximately across the site possibly forming an enclosed area adjacent to the building complex C3

C14- Isolated linear trend line approximately 22.5 m in length and 3 m wide there are no visible anomalies in the magnetometer survey.

C15- ? Archaeology, faint curvilinear, located in the western corner of the survey area. This may form the end of the Pre-Roman enclosures identified in the magnetometer survey.

C16 - ?Archaeology, high resistance anomalies possibly a building although this is not visible without high pass filtering the data. There is less correlation with the magnetometer data in this area than on the building complex further down slope so only a more tentative interpretation is possible.

C17 –? Natural /? Geological, a high resistance anomaly that may be masking archaeological anomalies. The magnetometer data indicates an area of weak-strong negative values which may indicate the near surface geology. Alternatively the localised area of high resistance may also result from a layer of demolition or localised drainage variation. No clear interpretation can be made.

Geophysical Survey Report: Two surveys along the Raetian Limes.

SD

0   40
Meters

N

UNIVERSITY OF
BRADFORD
MAKING KNOWLEDGE WORK

ARCHAEOLOGICAL SCIENCES © 2010

Pforring, raw unprocessed Alpha MSP40 data, 1:1250

Base mapping provided by The Bavarian State Dept. of Monuments and Sites
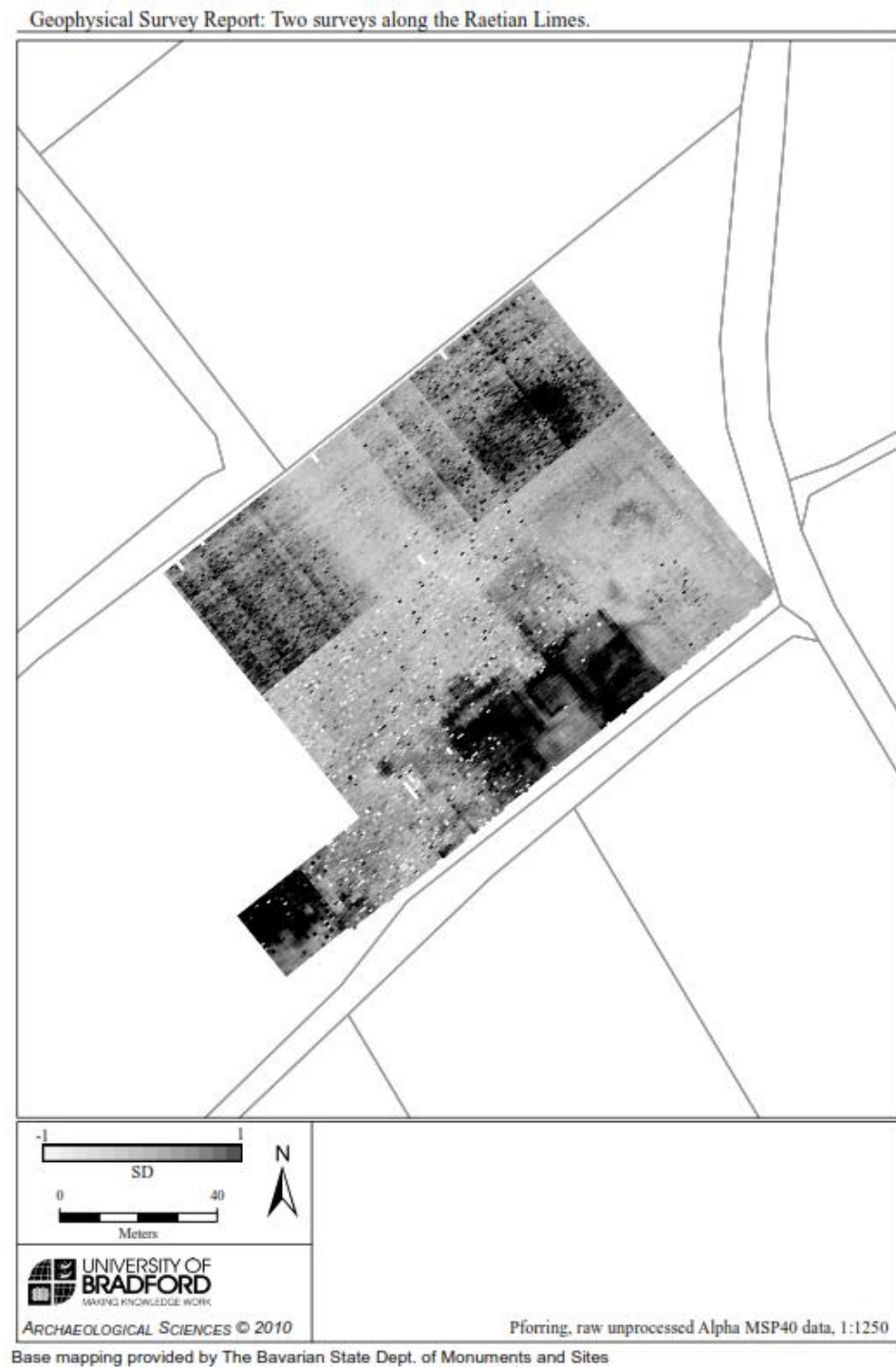
Figure 5.40   showing the unprocessed earth resistance data (Alpha) from Pförring Area C.

Base mapping provided by The Bavarian State Dept. of Monuments and Sites

Figure 5.41   Processed earth resistance data (Beta) from Pförring Area C.

Figure 5.42 Minimally processed earth resistance data (combined Alpha and Beta data sets) from Pförring Area C.

Base mapping provided by The Bavarian State Dept. of Monuments and Sites

Figure 5.43   Processed earth resistance data (combined Alpha and Beta data sets) from Pförring Area C.

-I   I

SD

N

0   40

Meters

UNIVERSITY OF
BRADFORD
MAKING KNOWLEDGE WORK

ARCHAEOLOGICAL SCIENCES © 2010

Pforring, detail of building area, clipped and high pass filtered,
1:1250

Base mapping provided by The Bavarian State Dept. of Monuments and Sites

Figure 5.44   Processed and high pass filtered earth resistance data (combined Alpha and Beta data sets) from Pförring Area C

307

Caesium vapour Magnetometer survey results

N

0   40

Meters

UNIVERSITY OF
BRADFORD
MAKING KNOWLEDGE WORK

ARCHAEOLOGICAL SCIENCES © 2010

-1   1

SD

Base mapping provided by The Bavarian State Dept. of Monuments and Sites   Pfoerring, ,Interpretation, 1:1250

Figure 5.45   Processed caesium vapour magnetometer survey from Eining Area B. Data provided by The Bavarian State Department of Monuments and Site.

Legend

■ (red)	Archaeology Building / walling	▨ (purple)	?Archaeology ?Building
▨ (red hatched)	Archaeology Building extent	▨ (blue hatched)	?Archaeology ?Building platform
▨ (cyan hatched)	High resistance anomaly	▨ (blue lines)	?Archaeology ?Enclosure / ?Walling
▨ (green hatched)	Low resistance anomaly	▨ (light blue cross)	?Archaeology ?Floor surface
▨ (blue hatched)	Curvilinear trend	▨ (red cross)	?Archaeology ?demolition material
■ (brown)	Archaeology Hearths? High resistance anomaly	▨ (purple cross)	?Archaeology ?enclosure
▨ (green dots)	?Archaeolgy Ditch complex	▨ (blue cross)	?Natural high resistance anomaly
▨ (tan dots)	?Archaeology Field boundary	▨ (red hatched)	Trend

Base mapping provided by The Bavarian State Dept. of Monuments and Sites   Pfoerring, ,Interpretation, 1:1250

Figure 5.46   Archaeological interpretations of the earth resistance data from Pförring Area C.

5.3.15 Discussion

The data sets from Pförring showed how the use of high pass filtering can reveal additional information in geophysical data. Initially the building complex to the southern edge of the survey area showed as a high resistance block. However, when the survey extent is clipped and high pass filtered then individual wall features are visible in the data.

The issues encountered in the Alpha data set also highlight the benefit of collecting Alpha & Beta data sets as the final day of survey could not be satisfactorily processed with confidence in the final Alpha output. Therefore the MSP40 has the additional benefit of collecting Alpha and Beta data sets so if problems arise from a single data set the second data set can be used as a single plot or aid in the processing when combining the data. The algorithm used to pre-process the data helped to improve the final image by reducing the number of dummy values, but it is important to compare the data with a 'standard' data set.

The geophysical survey of the vicus at Pförring (Area C) has identified a large complex of buildings covering an area of approximately 80m x 40m along the south-west side of the survey area. The buildings may have formed part of the vicus of the associated fort of Celeusum. However the survey area suggests sparse settlement in this area of the vicus and is situated 80m away from the closest corner of the fort. Further survey north of the fort may provide additional evidence for the extent of the vicus and its associated buildings.

The MSP40 earth resistance survey has shown that the system can be used on freshly harvested sites even when the field is covered in stubble. The adverse weather conditions (torrential rain) meant that the ground conditions reduced the contact resistance issues that are normally an issue with surveys during the summer months. However it also meant that contrast was reduced possibly explaining the poor definition of the fort ditch complex (Pförring) that was clearly visible in the magnetometer data.

The MSP40 has also shown it is possible to produce a large scale earth resistance survey in a shorter period of time than traditional equipment (approximately 3 ha in 4.5 days) even when a high sampling interval (0.25m x 1m) is employed. This does not factor in time lost through trialling different configurations and time taken to make small repairs on site.

After trialling the MSP40 at the locations in Germany an additional site investigation was made available at Towthorpe 18 (a ploughed out Neolithic Round Barrow) North Yorkshire, UK. The site located in the Yorkshire Wolds has been used extensively for agriculture prior to 1864 to the present day. The project allowed for further testing of the GPS unit (see section 3.6.6) and provides further examples of 'vulnerable; archaeological sites and data processing (see Appendix A for full site report).

5.4.0 Comparisons of Geoplot's MSP40 merge function with the Excel pre-processing method

5.4.1 Introduction

The algorithm used in Germany to improve the data was created in MS Excel 2007 (see section 5.3.13). It was decided to compare the pre-processing step with comparisons data from the error tests to see if there was an improvement in the final output. The data sets with 1%, 5%, 10% and 25% errors were used for the experiment. The main purpose of the pre-processing is the replacement of negative values from the data set with an earth resistance value over the same volume of soil (with a different array orientation). This step may help to reduce the number of dummy values inserted into the data.

5.4.2 Processing

The raw data was exported in a Z data format and processed in Excel before being re-imported in to Geoplot and processed with the same processing routine as the MSP40 merge function outlined in the induced error tests.

The processing used the following routines

Column A

Raw data imported (Alpha)

Column B

Raw data imported (Beta)

Column C

$$=IF(A1<0,0,A1)$$

The logic argument interrogates the data values if the value is less than 0 (i.e. a negative number) then a zero is inserted into the cell. If the value is greater than zero the original value is inserted into column C.

Column D

The same logic argument is used to investigate the Beta data set from column B.

Column E

$$=IF(C1=0,D1,C1)$$

The fifth column modifies column C by identifying zero values (the changed negative values). If a zero is identified then the data from column D is inserted into the cell. If the number is a positive value (including large positive spikes) then the original value is kept.

Column F

$$=IF(D1=0,C1,D1)$$

The sixth column works the same as column E but examines the Beta data set and replaces zero values with an Alpha value.

Column G and H

$$=IF(J1=0,2047.5,J1)$$

The final two columns replace any remaining zero values (where Alpha and Beta values are both zero) with the dummy value used in Geoplot, in this case 2047.5.

5.4.3 Results (also see table 5.8)

4.26   ohms   7.16
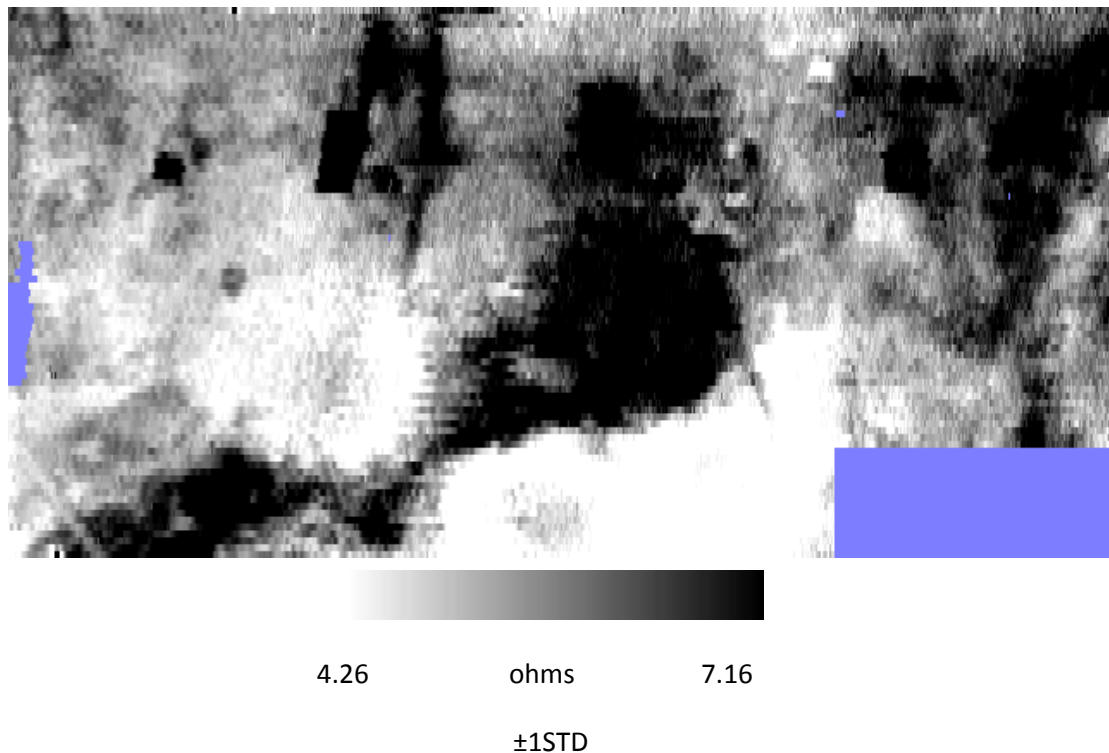
±1STD

Figure 5.47   Processed 1% error pre-processed algorithm results.
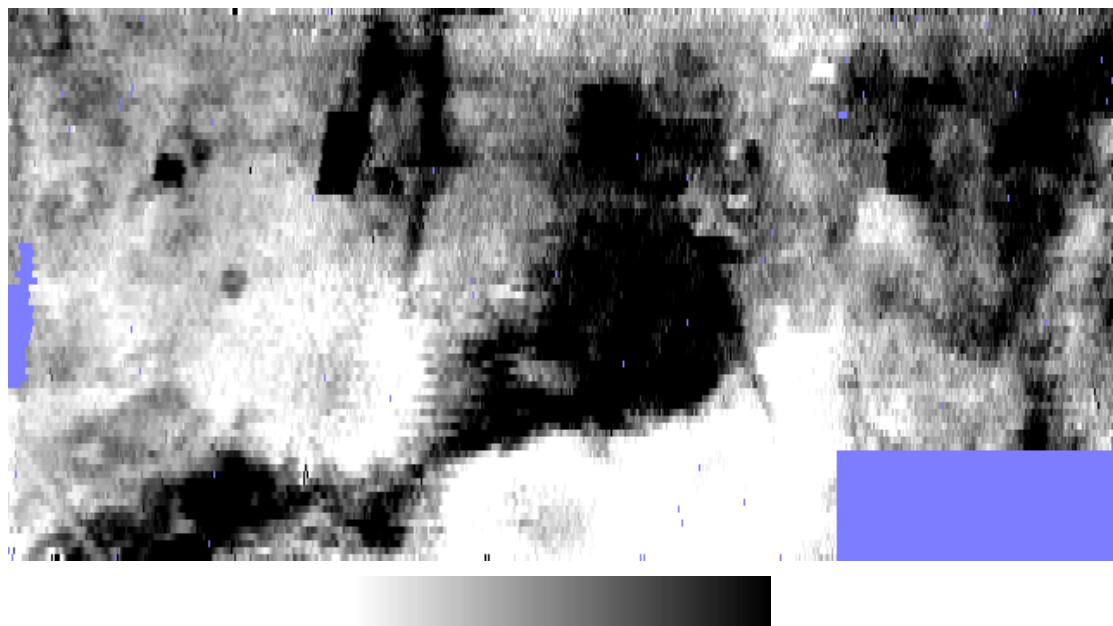
4.24   ohms   7.17

±1STD

Figure 5.48   Processed 5% error pre-processed algorithm results.
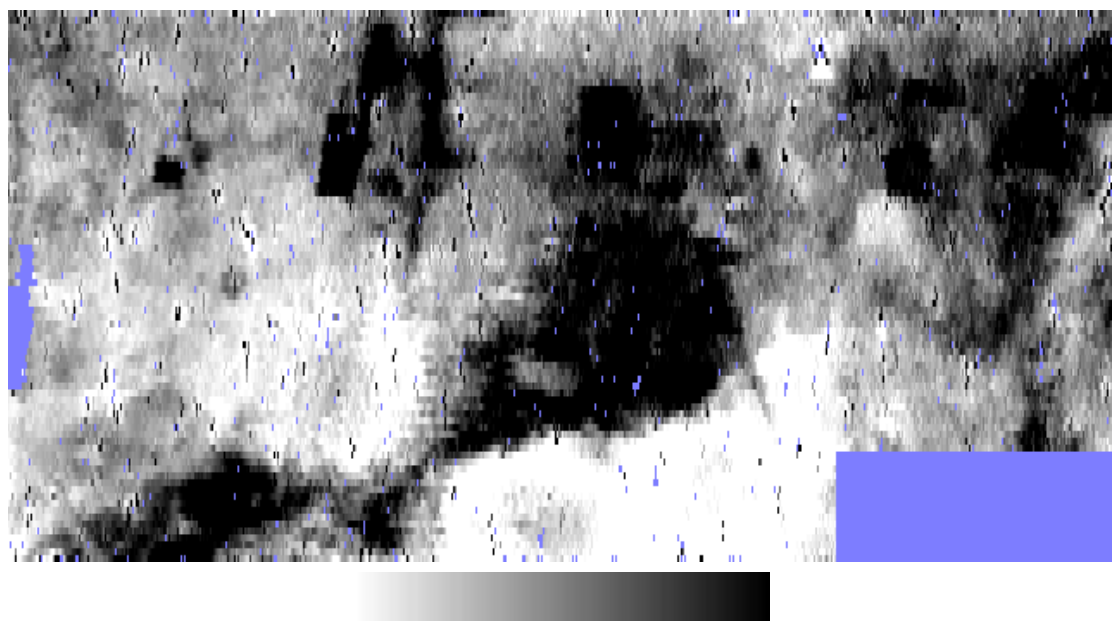
4.07   ohms   7.31

±1STD

Figure 5.49   Processed 10% error pre-processed algorithm results.

4.11   ohms   7.11

±1STD
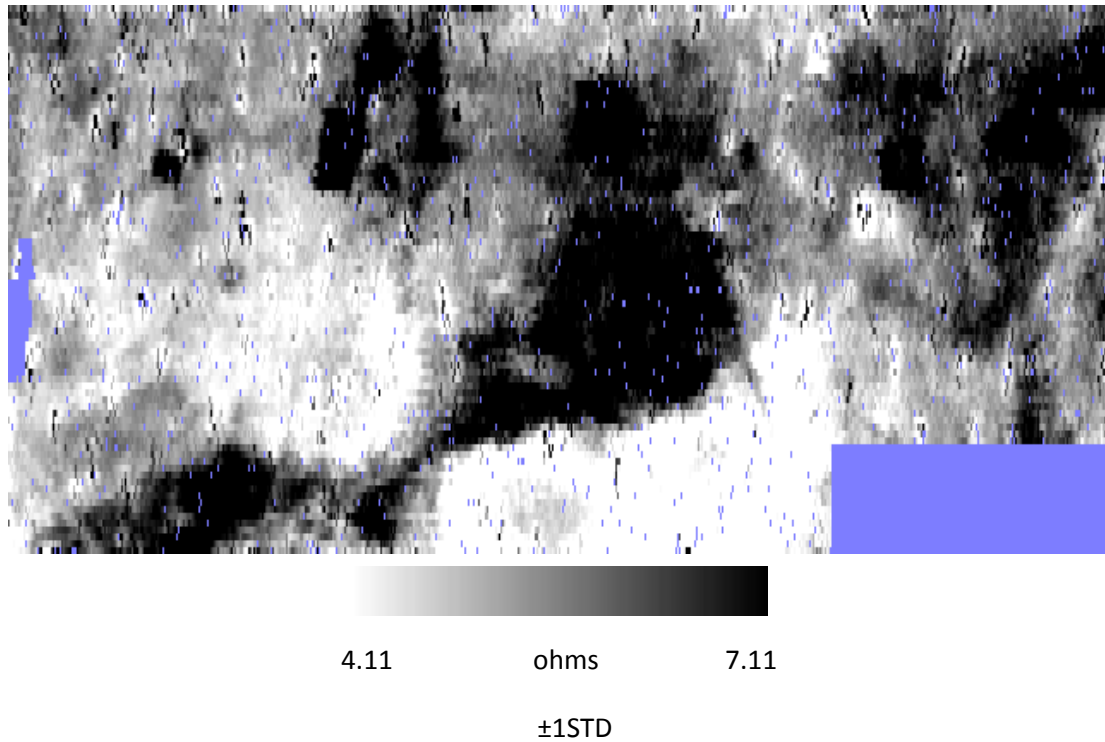
Figure 5.50   Processed 25% error pre-processed algorithm results.

Table 5.8   Number of dummy values for each error percentage level

Error percentage	# of dummy values MSP40 merge function	# of dummy values Excel pre-processing
1%	2806	2798
5%	2972	2846
10%	3315	3307
25%	9404	3663
Original dummy value total	2790	2790

5.4.4 Discussion

The numbers of spikes indicate that the pre-processing in Excel shows improved results at each error level. However, the pre-processing is significantly more efficient when the raw data contains larger numbers of errors. This equals a reduction in dummy values of almost 66% at the 25% error level.

Interestingly the 10% error data set shows a greater clustering of high resistance spikes both along and between traverses than the MSP40 merge function. This is probably due to the replacement of dummy values with an increased resistance value from the other data set. The positive clusters could be removed through additional processing but have not been removed for comparison purposes. The algorithm could also be expanded to include an upper limit cut off at which point any resistance values above a specified threshold would not replace a negative value.

Greater success may have been achieved by despiking the data initially then exporting the data and removing the negative values. The processing is intended to aid the production of the combined image using one of the two recorded data sets to reduce the gaps in the data.

5.5.0 Conclusions

The MSP40 varies significantly from more traditional earth resistance equipment, as the MSP40 offers near continuous collection. The increased collection rates can cause additional 'noise' or spikes in the data (as discussed in chapter 3.3, 3.7and 4.5) for both the earth resistance and gradiometer surveys. A careful selection of settings (delay times, current selection) and good field practice (rebalancing the gradiometer regularly) can reduce the possibility of errors in the data.

Mechanical failures can also influence data quality; this can range from loose wheel connections to axles twisting. Mechanical developments have reduced the frequency of failures, but there are always risks of reduced quality data being collected. It is therefore important to consider the most appropriate ways of processing and combining data to 'improve' the final output when errors arise.

The improved rate of collection and the potential for higher resolution surveys means that processing of MSP40 data must be handled differently. However, careful processing can still produce good-quality images. It is therefore important to understand how the processing techniques work to avoid distortion of the data.

The simultaneous collection of the Alpha and Beta measurements offers additional information about an anomaly. However, care must be taken when combining this information so that the processing steps preserve the subtle directional information in both the data sets. The additional data set can also be used when errors occur in one dataset as the individual data can be merged so that erroneous measurements are discounted and only 'correct' values used.

The use of RGB and transparency composites is a simple solution to combining the data as both data sets are preserved as separate layers. However, the data sets must be processed independently of each other which could mean the relationship between the Alpha and Beta data sets are lost as additional filtering acts separately on each individual data set.

The mathematical combination of the Alpha and Beta data means that the relationship between the two measurements is preserved but subtle variation of anomalies may be lost by a simple averaging of the data. Alternatively the use of more sophisticated mathematical combinations (high pass filter merging) preserves subtle directional variation but may introduce processing artefacts. The solution to this problem therefore must be the inclusion of individually processed Alpha and Beta data sets and carefully selected and processed combined image. By displaying the three data sets it is still possible to examine which responses are from which electrode configuration.

Chapter 6 forms the discussion chapter that draws on practical examples (where appropriate) to highlight the salient points identified during the previous chapters in greater detail.

6.0.0 Discussion / potential benefits of a mobile sensor array

6.1.0 Introduction

The aim of the research / fieldwork was to investigate how the Geoscan Research mobile sensor platform (MSP40) could be optimized for rapid assessment of archaeological sites, maximizing the information gained from a single traverse and minimizing the physical impact on the soil. This has involved experiments and observations both in the field (during survey) and practical measurements on the University of Bradford's grounds. The properties investigated include speed trials, high resolution survey capabilities, sensor integration, impact assessment, developing wheel configurations / option, array variations and seasonality testing.

6.2.0 Towthorpe and Germany geophysical surveys

The two main case studies discussed in detail are based on fieldwork in Germany (Eining and Pförring see chapter 5.3) and Towthorpe (Appendix A) showed how the MSP40 can be used to investigate 'vulnerable' archaeological sites. However, a number of topics can be highlighted from the case studies that require further discussion (using additional case studies where appropriate) these range from assessment of the physical impact on archaeological sites to data processing and seasonal variability.

6.3.0   Assessment of physical impact investigation

6.3.1 Introduction

As the aim of the research project was focused on reducing the impact on archaeological sites whilst undertaking surveys with a mobile array this is the most important area to be discussed. The additional research areas are then related to reducing the physical impact on 'sensitive' archaeological soils by optimising the MSP40 to reduce survey time and through additional sensor integration.

Whilst the MSP40 has a physical impact on the soil it must be considered less destructive than other mobile earth resistance arrays used in geophysical investigations. It does not require plough like blades that rip through the soil (RATEAU and to a certain extent the Geophilus (see chapter 3.1.2)), neither does it require huge tanks of water that compact the soil. As the MSP40 is a hand-pulled cart system it means no quad bikes or large four wheel drive vehicles are required to pull the array, thus reducing the sheering of the top soil / vegetation layer and reducing compaction of the soil profile.

As with all earth resistance arrays the (with the exception of the mobile electrostatic multi-pole array or MPU (Panissod *et al.* 1998a)) penetration of the soil surface helps to overcome contact resistance issues by increasing the surface area of each electrode in contact with the soil. The amount of damage to the archaeological deposits will depend on the mobile array used, the ground cover and the depth of the archaeology. However, as the depth of the archaeology is often unknown it is best practice to limit the intrusion of the soil to reduce the impact on the soil environment. The maximum penetration of the wheels of the MSP40 is restricted to the length of the spike being used (normally 40 mm), however a number of configurations are available to reduce the impact (short spikes / disc and bare wheels) for a variety of site conditions. These are discussed in more detail in section 6.3.2.

6.3.2 Wheel configurations

The choice of wheel configurations for the MSP40 can affect the success of the survey and general data quality. The decision as to the most appropriate wheel choice can be influenced by the ground cover (grass, crop, bare soil etc.), the seasonal variation in soil moisture content and the sensitivity of the archaeological site being investigated. The various configurations are discussed in more detail below.

Bare wheel

The bare wheel tests indicate that the wheels can be used to minimise impact on archaeological sites but will work most effectively on short vegetation / ground cover (see chapters 4.3.10 and 4.4.5). Higher quality results (reduced data spikes and drop out in data) are achievable when the ground conditions are sufficiently damp (ideally after light dew). However, dry ground conditions or sites with thick vegetation will limit the success of bare wheels survey.

Short spike

The short spiked wheel provides an additional option for the MSP40 as the shorter spikes benefit the system by reducing the damage to the soil surface (see chapter 4.3.1 - 4.3.5). The physical effort is also significantly reduced (compared to the normal spikes) by using the short spiked wheels, seeing a decrease of 2-3 times less force required to pull and maintain motion of the cart (see chapter 4.4.7). The short spikes however, produce slightly noisier data than the normal spike length due to the reduced penetration (increasing the risk of drop out in readings).

The geophysical survey at the Roman Vicus at Pförring (part of the Limes Germanicus, Bavaria) trialled short spikes on a recently harvested wheat field (see chapter 5.3.11). The short spikes were trialled because the field was covered in loose hay material and limestone fragments brought to the surface through ploughing. The surface stone and hay restricted the normal spikes from entering the soil causing an undulation between the four wheels.

It was thought that the small spikes may avoid more of the limestone fragments reducing drop out of signal. The trial showed that the smaller spikes did improve the smoothness of the traverses suggesting it was less affected by the limestone fragments. However, the drop out of signal increased as the spikes could not penetrate through the scattered straw material which acted as an insulating layer.

Approximately 75% of all measurements from four repeated traverses were erroneous (drop out in signal or positive spikes). The data was not saved as the trial was unsuccessful and the wheels were exchanged back to the normal spike length as it was trialled in the middle of a survey. However, trials on the amphitheatre at Bradford University were successful suggesting the ground conditions and land use can and will have an effect on the successful deployment of different spike lengths.

Normal spike

The default spike length supplied with the MSP40 provides the best option for many site investigations. The spikes will usually overcome issues of contact resistance as the spikes can penetrate sufficiently into the soil for the electrical current to flow even when the ground surface has dried out. The damage to the soil is restricted to the depth of the spike (<40mm) and does not significantly tire out the operator (see chapters 4.3.4. and 4.4.7). However, it is worth considering the alternative wheel configurations on difficult site conditions or where the archaeology is believed to be extremely near surface. This makes it important to try and minimise the damage caused by the MSP40 so other wheel configurations should be considered.

Long spike

The long spiked wheels (60mm bolts) were not trialled as part of this research project but were experimented by Tom Sparrow at Stonehenge in Wiltshire (Sparrow 2010). The following summation is based on Tom Sparrow's and the researchers own observations with other wheel configurations. The long spikes have the greatest physical impact on the ground surface and should only be used on sites with thick vegetation that is resilient (springing back / spongy) enough to prevent sufficient contact with the soil surface. Alternatively the long spikes could also be used on free draining dry sites where the upper surface layer has dried out significantly but remain friable enough for the spikes to cut into the ground surface (ploughed soils).

However, the long spikes significantly increase the effort required to pull the MSP40, whilst increasing the stresses on the framework and the physical demands on the practitioners.

Disced Wheels

The disced wheels were developed late in the project to try and find a solution for poor contact issues. However, the trials were not completely successful as two sites were not favourable to survey; Towthorpe 18 had significant issues due to the fine grained soil over limestone / chalk bedrock (see Appendix A). The site had been covered in snow for several weeks and had just thawed so the soil was saturated with water. The soil developed a clayish consistency that led to a significant build up of material on the wheels even before carrying out the survey.

An additional trial at West Heslerton, North Yorkshire, also proved unsuccessful but for the opposite reasons. The site had not had a significant amount of rain for several weeks and the site has deposits of windblown sand around a metre deep (confirmed through coring on the day). The free draining nature of the sandy soil made it impossible to record readings that were not affected by drop outs in data or over range spikes (see chapter 4.4.4).

However, a single day investigation in the Kilnsey North York Moors showed the potential applications of the disced wheel. The site was covered in moss and thick grasses which have been problematic on other field trials carried out during the research. The results were extremely successful with a low number of spikes and good quality data even though the area was lacking in archaeological features (see figure 6.1).

20.33   47.51 ohms

21.59   53.09 ohms
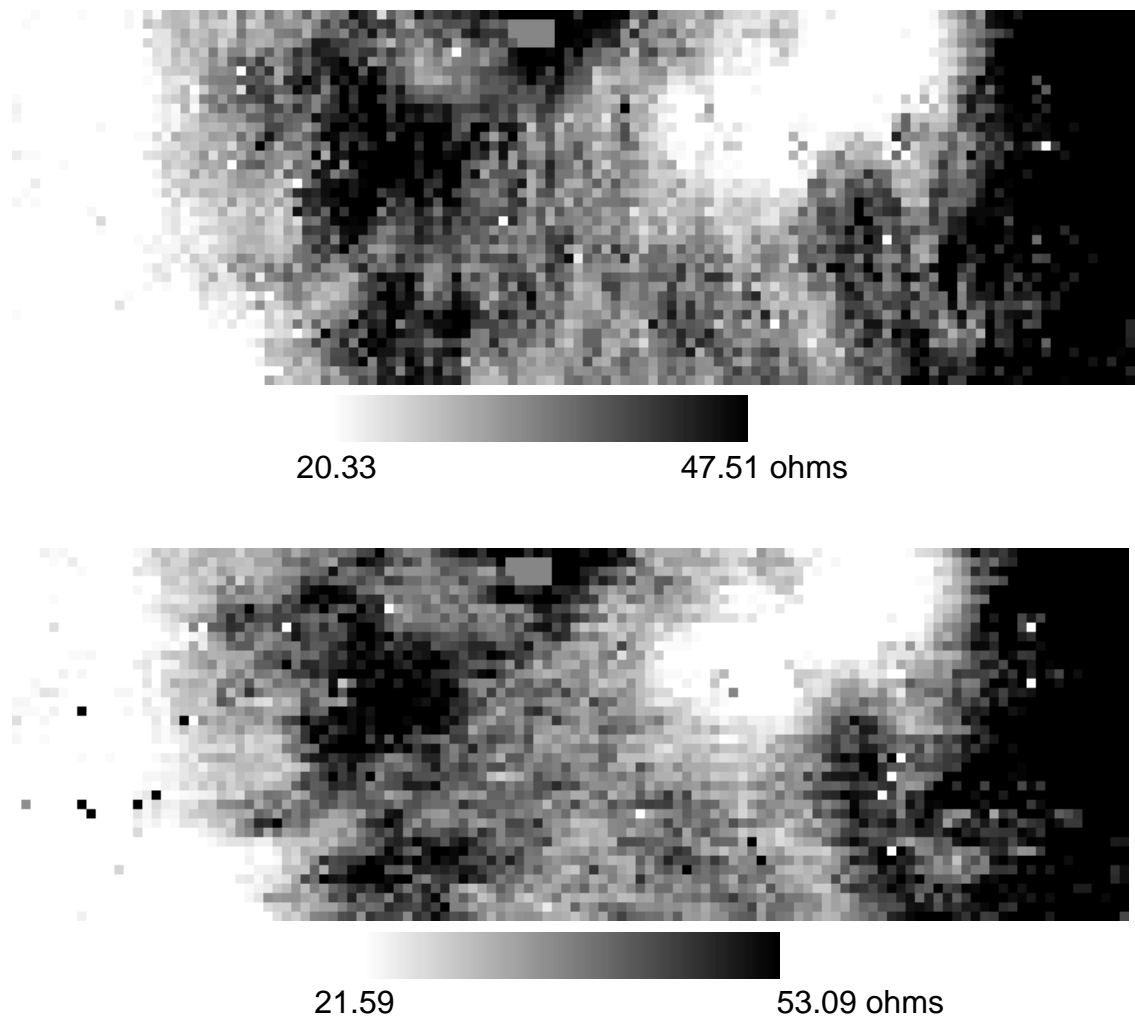
Figure 6.1   Disced wheel data collected at Kilnsey (unprocessed data, Alpha top image, Beta bottom image).

The disced wheels require more testing but are envisioned to be useful on sites with dense vegetation (as they provide a continuous narrow edge to make contact with the ground. The discs may also prove useful for ploughed sites where the upper layer of the soil is drier as the discs will increase the surface area of the electrodes beneath the soil surface achieving a more accurate reading of soil moisture.

6.3.3 Soil compaction

The physical impact on archaeological site does not just include the penetration of electrodes into the soil surface and must include compaction of the soil. This can take two main forms, firstly the weight of the mobile array (and towing vehicle where necessary) and secondly the physical trampling / compaction of the soil under foot.

The compaction of soil has been widely investigated in relation to agricultural vehicles (Rasool Mari and Changying 2008) and research has also considered the effect of trampling on archaeological sites(Gifford-Gonzalez *et al.* 1985b) see chapter 4.3.18-4.3.21 for more detail. A decision was taken to access the physical impact of the MSP40 alone as the geophysical surveyor would vary in size and weight potentially effecting the amount of damage to the site.

The impact assessment tests confirmed a degree of soil compaction does take place when using the MSP40. However, the experiment is likely to show the worst case scenario (if the MSP40 were used on a freshly ploughed friable soil) with surface compaction of approximately 4-5 cm after repeated traverses. However, the horizontal pseudosections showed changes in the recorded resistivity values beyond 7 cm in depth suggesting further compaction through the soil profile. In practice a transect line is only likely to be surveyed once and the soil would already be more compacted than in the soil box tests (due to previous land use and natural settling of soil over time).

The experiment shows that by using a pocket penetrometer and a closely spaced linear array (2-3cm probe separation) it would be possible to monitor soil compaction on a variety of soil types in the future.

As the MSP40 is a hand-pulled lightweight mobile sensor platform (30.75 kg total weight) the impact on a site is reduced when compared to other mobile arrays.

This is because there is no need for a quad bike (350-550kg) (Directgov 2011) or four wheel drive vehicle to tow the array (approximately 2095 kg for a 2002 Land Rover Discovery series II) (FindTheBest.com 2012). These values do not factor in the towed mobile array weights and the operator weights driving the vehicle.

The manoeuvre ability of the MSP40 further reduces impact as it can be easily positioned at the next traverse line without the need to uncouple the vehicle or to have large turning circles potentially adding to the compaction across the site. As the MSP40 is hand-pulled it means there are no pollutants given off which cannot be said for towed mobile arrays.

A key benefit of the MSP40 in physical impact reduction is the multiple sensor options allowing for earth resistance, gradiometer and GPS surveys all to be carried out simultaneously on a single traverse. This significantly reduces the trampling of a site as there is no need to resurvey the same traverses with the three individual instruments. The following sections 6.4 & 6.5 discuss sensor integration and testing.

6.4.0 GPS sensor mounting and integration

6.4.1 Introduction

A key element of the research project was the integration of additional sensors to the MSP40 to enable the maximum information to be collected from a single traverse thus reducing the survey time and impact on an archaeological site. A number of mobile (ARP (Dabas 2008; 2009 105-129), Foerster Ferex (Gaffney *et al.* 2008 ; Foerster 2009) arrays already use GPS for navigation and for the collection of elevation information.

The GPS was to be used on the MSP40 for data collection opposed to navigation as this was beyond the time constraints of the research.

The integration of a GPS unit provides additional information (elevation values) to aid the interpretation of the geophysics results. The benefits of a mounted GPS include collecting a microtopography survey simultaneously with geophysics data collection, locating and confirming grid location and variable mounting positions for different environments. However, the drawbacks of a GPS mounted on the MSP40 include tilt errors and an increased mass of the array; each aspect is discussed below.

6.4.2 Microtopography

A microtopographic survey can be performed at the same time as earth resistance and gradiometer surveys. This makes it possible to produce a high resolution surface model that can identify surface features that are visible in the geophysics results (Towthorpe ridge and furrow / plough damage see Appendix A). It can also provide additional location / contextual information for the site position (Pförring's vicus hill side location see chapter 3.6.6).

The experimentation discussed in chapter 3.4 clearly shows a high level of information can be collected as the TOPCON HiPer Pro and A100 Smart Antenna GPS by Hemisphere GPS collected data at a rate of 20 Hz with a traverse interval dependant on the geophysical survey interval. This is likely to be at a greater density than would be collected for a normal topographic survey (possibly every 0.5m depending on requirements) and has the added benefit of being collected at the same time as the geophysical survey.

The research project highlighted the need for linear or gridded collection of GPS data as a random walking approach was adopted during initial trials and was found to produce a more variable 3D DEM (Entremont, see chapter 3.6.6).

However, data collected during a geophysical survey produced a more regularly spaced point cloud giving a more accurate surface model (Towthorpe, Eining and Pförring, see chapter 3.6.6). This was due to the more even coverage and reduced point clustering of data through random collection.

6.4.3 Grid location in wide field locations/uniform landscapes

When surveying in remote locations it is often difficult to identify sufficient numbers of points to accurately locate the survey grids on a base map. However, by using an RTK system mounted on the MSP40 this becomes less of an issue, as the array can be centred over a grid peg and left to collate positional points over several minutes. An average position can then be calculated using the fixed GPS points (greatest positional accuracy) to locate the grids. This was trialled at the site of Towthorpe 18 and when used alongside a total station survey gave positional accuracy within three centimetres.

6.4.4 Variable mounting positions

The design and construction of the MSP40 allowed for two GPS mounting positions to be trialled in both rear and centrally mounted positions. The centrally mounted GPS rover unit was found to be the best solution for the work carried out during the research. The GPS was positioned in the centre of the array which correlated with the centre of the earth resistance array.

The trials indicated that handles and operator did not create significant shadowing / blocking of the sky line or refract the signal. The low positioning also reduced issues associated with tilt (see section 6.4.5). The custom built mounting could also be adapted with plastic sheeting to act as a rain guard for the instruments on the platform.

The rear mounted position may still prove useful for more enclosed sites as the higher mounted sensor position potentially gives a greater sky line for the detection of satellites improving the positional accuracy. However, further refinement of the mounting is required to fix the pole to the frame and stop the lowering of the rover sensor (see chapter 3.6.2). The major drawback of the rear mounted position is the offset position of the sensor, which means a correction based on the sensor offset and vector information of the MSP40 would be required to shift the data to correlate with the geophysics results.

The higher the rover unit off the ground surface the greater the positional errors on undulating ground due to the angle of tilt.

6.4.5 Tilt sensor correction.

By integrating the GPS mounting on the MSP40 an error in the positioning accuracy of the recorded topography can be introduced. This is because the platform tilts under the varying ground conditions making the GPS tilt at the same angle producing a different position to the centre of the array (see figure 6.2) The tilt errors could be solved by a gimbal bearing system that would mechanically correct the tilting of the sensor caused by ground undulations.

However, a tilt sensor could be developed using a system like the open source electronics development system such as Arduino which has a range of accelerometers and gyroscopes. From the recorded angles of tilt it would be possible to correct the errors in positioning. However, the time constraints of the project did not allow for this to be developed fully.

High mounted GPS

Low mounted GPS

MSP40

GPS position centred over array

High mounted GPS

Low mounted GPS

Increasing displacement from the array centre
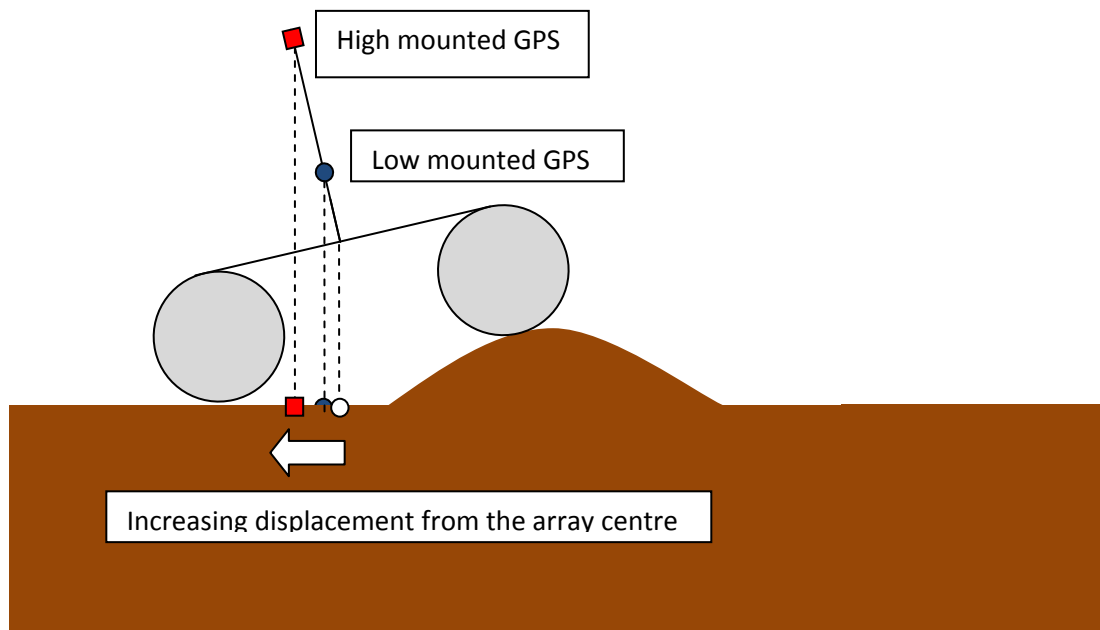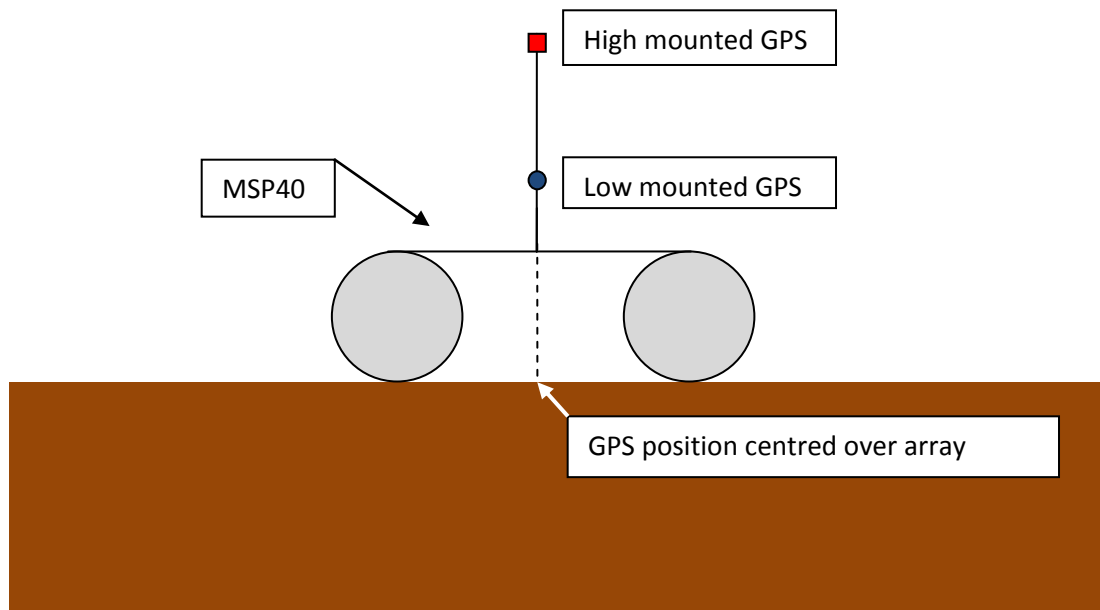
Figure 6.2   A schematic diagram of the positional errors recorded by the GPS

on undulating ground surface with increasing sensor height.

6.4.6 Additional mass

The integration of the GPS adds additional mass to the MSP40. Two GPS units were trialled during the research the TOPCON HiPer Pro rover unit adds on approximately 2kg of additional mass to the MSP40 (30.75 kg) plus an additional 1.65 kg for the hand-held data logger. The A100 Smart Antenna GPS by Hemisphere GPS adds an additional 3.5 kg including the battery packs used to power the Rover unit (not including cabling).

The increased mass adds pressure to the framework and causes additional physical impact to the soil surface. But the additional information and simultaneous collection with the geophysics data offset any damage the slight increase in mass may cause. However, the additional pressure exerted on the frame is a potential area for additional research as it is not known what the load bearing capacity of the MSP40 components are especially after long-term use.

6.4.7 Developments

The next logical step for GPS integration would be data that is synced to data output from the MSP40 sensors. This could eventually lead to a navigated system that would direct the operator and mean non-gridded data would be achievable (a system already achieved by the Foerster Ferex system (Gaffney *et al.* 2008 ; Foerster 2009)). This would improve the productivity rate of MSP40 survey by reducing setup time by not having to layout grids.

In addition to the GPS survey a gradiometer survey can also be taken simultaneously with a single gradiometer mounted on to the front of the MSP40. The gradiometer survey also improves efficiency as a single operator can perform all three methods of survey. The GPS unit has little effect on gradiometer data as the GPS can be mounted at the centre or rear of the mobile array (>0.75m away from gradiometer).

The GPS must be positioned before the gradiometer is zeroed so that any 'noise' is incorporated into the 'background zero value' as the sensor is fixed in one position so does not change in relation to the sensors and is a constant source of coherent 'noise'.

6.5.0 Gradiometer integration

6.5.1 Introduction

The optional mounting of a gradiometer on the MSP40 increases the efficiency when undertaking rapid geophysical assessments of archaeological sites. The use of two complimentary techniques improves interpretation of anomalies by increasing knowledge of the individual anomaly responses.

Using multiple techniques for exploratory surveys should always be encouraged as one technique may not always be suitable for successfully identifying the archaeology (see St Ives chapter 4.1.7). When combining the two techniques, it is important that a sufficient data quality is achievable.

6.5.2 Data collection 'noise'

The amount of 'noise' in data was investigated as part of the research, for quality comparison between the hand-held gradiometer data collection and the data from the MSP40. The MSP40 mounted gradiometer introduces additional noise into the data when compared to hand-held collection (see chapter 3.7.3). The additional noise levels associated with the mounted gradiometer do not detract from the data interpretation as the 'noise' is lower than most archaeological signals. Processing the data will remove much of the additional noise caused by the gradiometer mounting on the MSP40. Periodic filtering may remove some of the additional noise if it is a repeatable pattern. However, a more appropriate form of processing may come from a weighted low pass filter along the line of traverse direction only (x=1, y=0) to smooth out the additional noise.

Much of the noise comes from vibration of the sensor as the MSP40 is pulled along the ground surface and from the rotation / oscillation of the MSP40 in the gradiometer mounting bracket. Noise levels can also be reduced by careful balancing of the gradiometer at the start of the day and performing the rebalancing procedure every few hours.

The use of the additional mounting bracket to stop the sensor rotation needs to be used appropriately. The bracket can reduce the noise introduced by the pendulum motion of the sensors but on steeper slopes stops the weighted rotation of the sensor back to vertical alignment. This leads to subtle misalignment of the sensors meaning the vertical magnetic field component is no longer measured. The additional 'noise' in the data collected by the MSP40 has not hindered the interpretations of any of the sites investigated during the research project, and best practice techniques of rebalancing during the day reduce the noise levels. The time savings that can be made by the simultaneous data collection outweigh the slight drop in data quality for the gradiometer surveys.

6.5.3 Time saving

Having the gradiometer mounted on to the MSP40 has the advantage of increasing productivity by collecting two sets of data simultaneously. The obvious benefits for commercial and research projects are that it is not necessary to have two people survey the same grid with the two techniques meaning time can be spent surveying elsewhere on site. As the gradiometer is mounted on the central axis of the array (offset, forward by 0.75m) it means that both earth resistance and gradiometer surveys have surveyed the same ground foot print, making it possible to draw more accurate comparisons about the varying geophysical responses of the anomalies. The MSP40 has the potential to appeal towards a multiple technique approach for commercial surveys due to the time saving capabilities.

Only a single sensor configuration is available at the current time which limits the productivity of the gradiometer survey. This means that it is necessary for an equal traverse interval between earth resistance and gradiometer surveys. Having additional mounting options for multiple gradiometer sensors would be more attractive for commercial companies as many commercial investigations require higher sampling density (increased number of traverses). English Heritage guidelines (David *et al.* 2008) recommend a sampling strategy of 0.25m sampling and 1m traverse interval (for gradiometer surveys) and 1m by 1m (for earth resistance survey) as the coarsest sampling strategy they accept.

The gradiometer must be set to double the density of the earth resistance survey (when collecting Alpha and Beta data sets) as the gradiometer acts as a slave to the MSP40 pulses from the external trigger (either time based or encoder pulses). Therefore it is necessary to have a minimum sampling interval of 0.25m for gradiometer surveys and a 0.5m sampling interval for the earth resistance survey to ensure surveys are performed at the English Heritage recommendations. If a single earth resistance measurement is recorded (Alpha) then the same number of gradiometer measurements is recorded. However, the RM85 will have an option to specify the number of pulses at 1, 2 or 4 times the earth resistance sampling interval in single or multiplexed mode (Alpha and Beta) (Walker 2012c).

By integrating additional sensors on to the MSP40 (GPS and gradiometer) the efficiency of a single surveyor is increased. However, it was also important to investigate the time taken for earth resistance surveys and evaluate if a hand-pulled mobile array was more efficient than a frame-mounted survey.

6.6.0 Survey speed trials

The multiple field trials completed during the research project indicate that MSP40 can save significant amounts of time for carrying out a geophysical investigation of an archaeological site.

Survey experience gained during the course of the research suggests it is possible up to and over a hectare of earth resistance survey in a day with a sampling of 0.25m or 0.5m and traverse interval of 1m.

Examples of field experience, approximate survey area per day

Towthorpe	Area covered	Sampling and Traverse intervals
	80m x 80m	0.5m x 1m
Eining Area B	Area covered	Sampling and Traverse intervals
	120m x 80m	0.25m x 1m
Pförring (1 1/2 days)	Area covered	Sampling and Traverse intervals
	120 m x 120m	0.25m x 1m

The total area surveyed over each day was limited by equipment issues, for example setting up and re-establishing the GPS when the communications went down. Time was also lost through setting up grids and equipment failures and weather related issues.

Additional efficiency could be achieved through having two operators survey the area taking it in turns to allow time to recuperate on alternative runs. Trials by the manufacturer suggest a rate of 7.5 minutes per 20m grid using a single measurement (0.25m sampling interval and 1m traverse interval) is achievable but maintaining this collection rate is difficult for a single operator (Walker 2012a). The additional level of information gained by collecting the Alpha and Beta data sets halve the time necessary to complete an earth resistance survey as opposed to collecting the same information using a linear array as the area would need to be surveyed from the 90° orientational angle to the original survey. However, this is unlikely to ever be used in a commercial survey due to time constraints of such projects.

The time saving capabilities of the MSP40 increase the opportunity to undertake high resolution surveys in the same time scale as a 'normal' earth resistance survey. A high resolution speed trial at the Iron Age oppidum of Entremont (France) showed a significant time saving to perform high resolution surveys compared to traditional linear arrays (see chapter 6.7). However, a major issue encountered during the research involved the logging speed of the RM15 and DL256. The higher the resolution the slower the collection rate must be (see table 6.1). This in turn reduces the survey coverage achievable in a day.

Table 6.1   Sampling interval (time based collection and digital averaging turned off with delay time of 110ms between Alpha and Beta)

Sampling interval	Maximum collection rate multiplexed Alpha and Beta
1 m	0.4 s/m
0.5 m	0.7s/m
0.25 m	1.2s/m
0.125 m	2.4s/m

A recent firmware update to the DL256 has reportedly improved the electronic design restrictions of the MSP40 (Walker 2011b). This has enabled data collection using the encoder wheel and multiplexer at a rate of 0.6 s/m for a 0.5m sampling interval. If the operator exceeds the maximum collection rate warning messages are displayed. A data recovery system has also been included to allow the surveyor to continue to record data, as previous firmware versions stopped the MSP40 recording additional data points if the maximum collection rate was exceeded. The firmware improvement has not been trialled as part of this research project.

Future developments by the manufacturer will see the replacement of the RM15, DL256 and MPX40 multiplexer with a single unit RM85 (see chapter 7.2.1).

The RM85 will see a fivefold decrease in logging times between Alpha and Beta measurements. Increasing the collection rate and improving the operator experience of high resolution earth resistance surveys.

6.7.0 High resolution survey

6.7.1 Introduction

An advantage of the MSP40 over hand-held arrays is the increased capabilities of high resolution survey. The near continuous collection of the MSP40 significantly decreases the collection time for high resolution survey. Three sites were explored at a significantly higher resolution sampling than recommended by English Heritage guidelines (David *et al.* 2008).

6.7.2 Entremont survey

As discussed in chapter 6.6, a sampling and traverse interval of 0.25m was performed over two 20m x 20m girds collecting both Alpha and Beta measurements. The survey time for the two grids was approximately 1 ½ hours compared to 3 ½ hours for a similar area with a survey resolution of 0.5m x 0.25m (Parkyn 2010). As the MSP40 only has a single probe separation it meant the cart surveyed over similar volumes of soil with only a small increment between traverses. However, the results did provide extra definition to the wall / building structures when compared to a coarser sampled twin probe survey (0.5m x 0.5m sampling and traverse interval) (Hayes 2010).
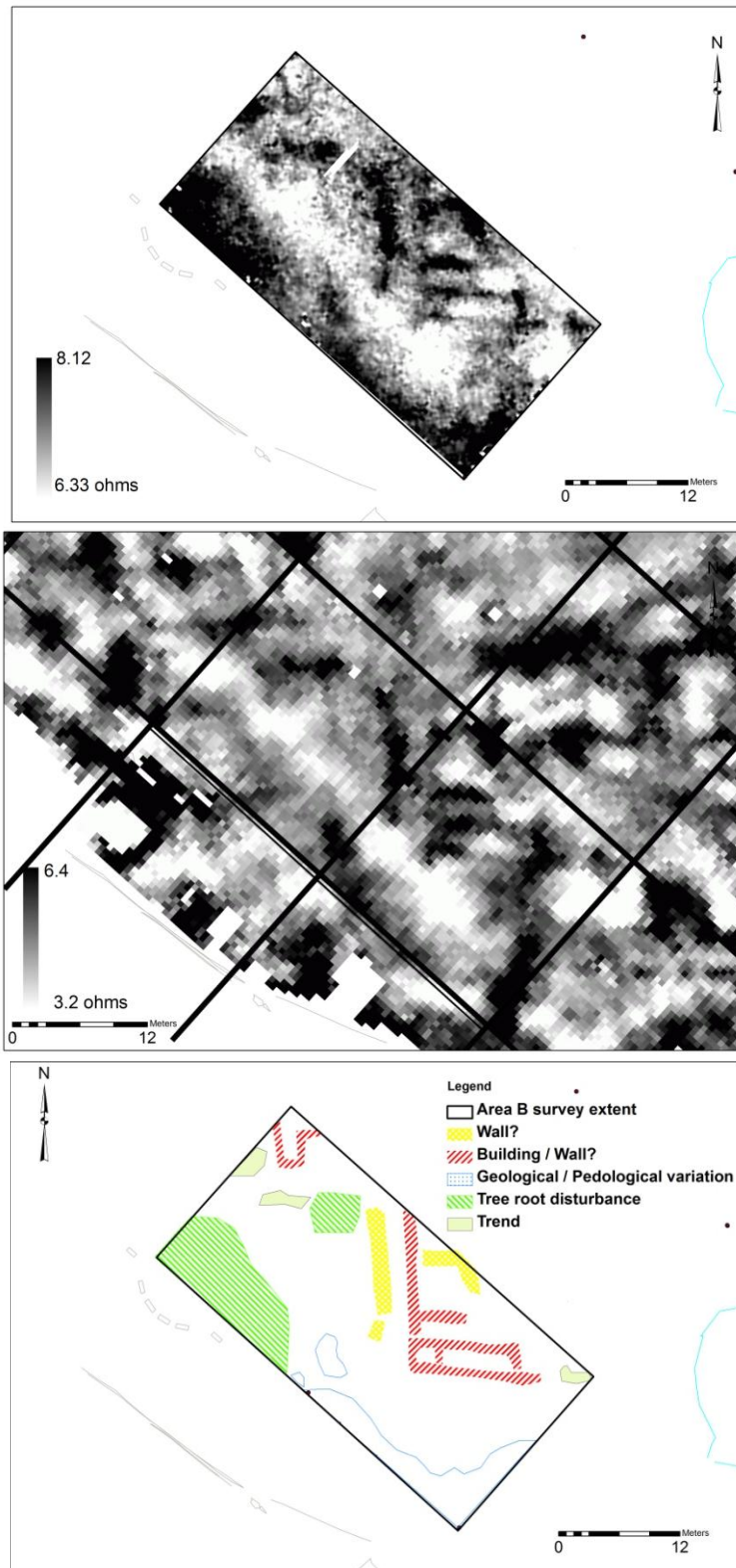
Figure 6.3   A high resolution MSP40 survey (top image) with a coarser 0.5m x 0.5m sampling (middle image (Hayes 2010)) and the archaeological interpretations (bottom image).

6.7.3 Eining and Pförring

Two additional larger scale surveys were performed at Eining and Pförring in Germany with a 0.25m (sampling interval) x 1m (traverse interval). The reasons for the choice of sampling are discussed in chapter 5.3.3. The processed data sets from the two sites were desampled for comparison purposes to see what effect the sampling interval had on anomaly definition.

The three data sets from Eining and Pförring all show the same anomalies however; the higher resolution survey shows greater definitions of the vicus buildings than the desampled surveys (survey data removed in Geoplot through the interpolation, shrink – delete option). The extra definition helps to accurately record an anomaly's extent and may identify more ephemeral archaeological features on different site types.

The increasing commercial and research interest in high resolution and large landscape surveys requires a high level of reliability of instrumentation to enable accurate surveys. During the research project a number of issues were identified with the data collection process, these are discussed in more detail, see section 6.8.
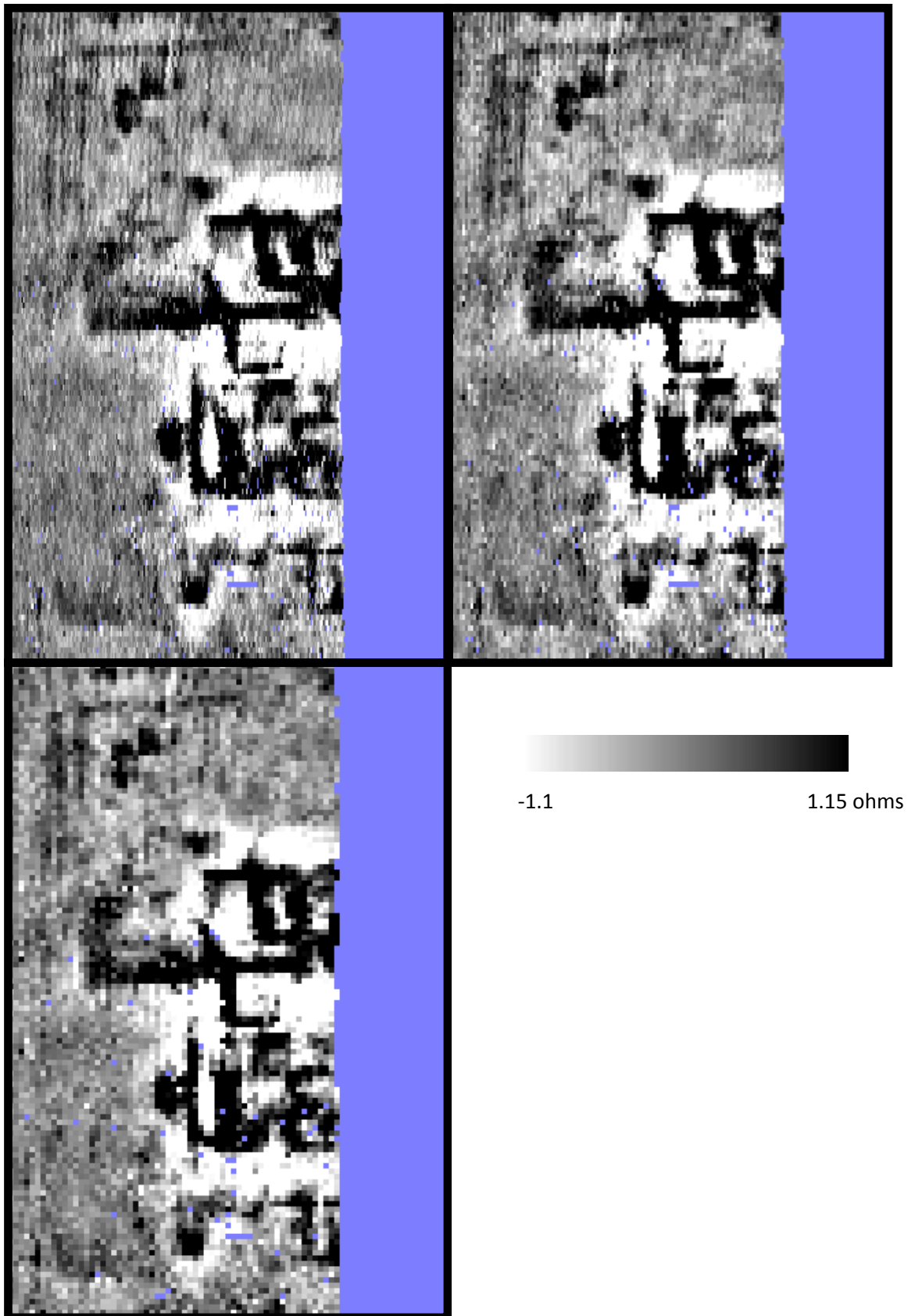
Figure 6.4 A high resolution 0.25m x 1m MSP40 survey (top left image) with the same area at a coarser 0.5m x 1m sampling (top right image) and 1m x 1m sampling (bottom left) from the vicus at Pförring, Germany.
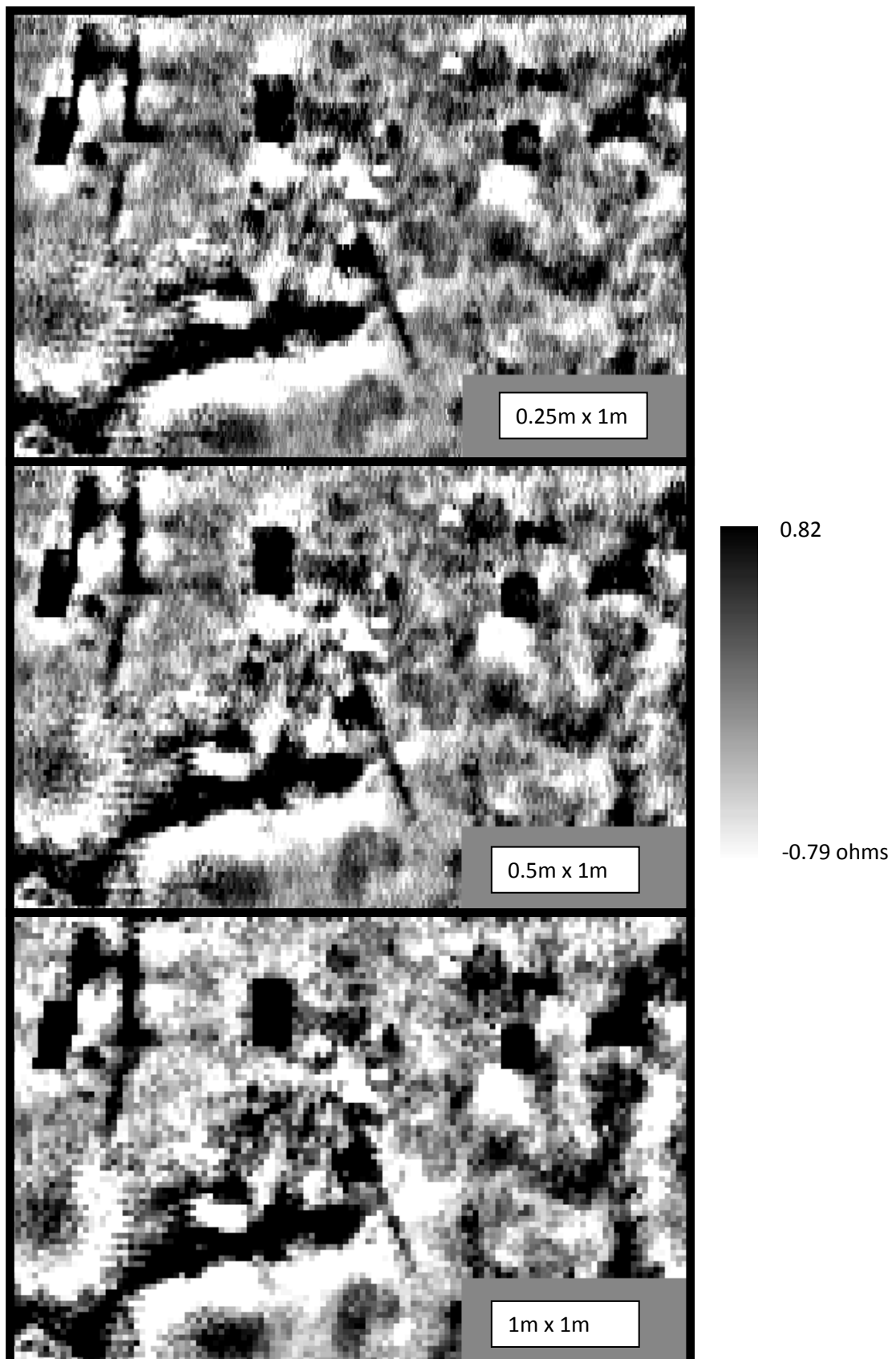
Figure 6.5   A high resolution 0.25m x 1m MSP40 survey (top image) with the same area at a coarser 0.5m x 1m sampling (middle image) and 1m x 1m sampling (bottom image) from the vicus at Eining, Germany.

6.8.0 Logging speed (issues with the RM15, DL256 & MPX40)

The electronic design restrictions of the MSP40 have been a limiting factor when considering the MSP40's potential for high resolution survey. The current configuration of equipment restricts the rate of collection at resolutions below a 0.5m sampling intervals due to the time required to multiplex the array between the Alpha and Beta measurements. The logging speed issue manifests itself as an over shooting of the grid edge when using the encoder as the MSP40 skips pulses so that the MSP40 fails to record enough measurements by the end of the traverse. When using the distance encoder a sudden change of speed or jerking movement (going over thick vegetation or rutting) may also affect the data collection. If the rate of collection is significantly exceeded the MSP40 will stop recording completely as it cannot resolve the missing measurements. In both cases the traverse must be deleted and resurveyed.

As the maximum rate of collection slowed significantly with higher resolution surveys, no surveys were completed at a higher resolution than 0.25m sampling. This was due to the frustration encountered by surveying at higher resolutions as the signal dropout became more frequent due to the electronic design restrictions of the equipment. There are several options to improve the logging speed but raise other issues that must be considered.

- The operator can slow down the rate at which they walk, but this can be difficult to maintain over long periods of time due to the reduced stride length.

- Turning off spike monitoring, will improve the logging rate for the MSP40, but this function offers a form of quality control for the data as it monitors the number of spike per traverse (see chapter 3.2.4).

- Time-based collection will also improve the logging speed compared to the encoder based collection. However, the time-based collection can be difficult to maintain at a constant pace (especially over longer traverse +40 m) throughout the day. The problem is made worse by undulating terrain when it is more difficult to pull the MSP40 at a constant pace.

- Only measuring a single Alpha or Beta measurement, without the additional multiplexing for the additional measurement may also improve the logging rate but this halves the information recorded by the MSP40 (see chapter 6.10).

The logging restrictions and optical encoder on the MSP40 can cause additional problems for the operator even at coarser sampling intervals (+0.5m) as the MSP40 can overshoot the grid edges. The issues of overshooting the grid when using the encoder can be rectified by the following solutions.

- Minor adjustment of the encoder pulses

Small adjustments can be made to the encoder to compensate for undershoots and overshoots of the grid. This is useful for subtle changes in topography that were not encountered when calibrating the MSP40 at the beginning of the survey, especially over longer traverses (>40m).

- Recalibration of the encoder

When larger positional errors develop it is advisable to recalibrate the encoder to reduce larger errors as it calculates an average over three repeated traverses. This process can be done mid grid without losing information and positioning.

- Increase sampling interval to 0.25m reduces the MSP40 overshoot

The surveys at Eining and Pförring (see chapter 5.3) suffered from repeatedly overshooting the grid edge. When recalibration and adjustment were attempted the problem could not be solved. After trials at reducing the speed of collection still failed to rectify the problem it was decided to try and increase the sampling interval to 0.25m from 0.5m. The premise was that the restricted collection speed would reduce the potential for missing pulses as to many would stop the data collection. This was found to be a workable solution and provided accurate positioning for the rest of the survey.

- Cleaning the optical encoder lenses

By gently wiping the encoder lenses it is possible to improve the reliability of the encoder significantly and should be incorporated into part of the regular maintenance routine to ensure successful operation of the MSP40. The lenses can accumulate a small film of dust from the wheels which may block or refract the optical signal explaining why the encoder misses certain pulses. A small cotton bud (ear bud / Q-Tip) is a perfect size for cleaning between the transmitter and receiver on the encoder and not damaging the lenses.

The electronic design restrictions and encoder issues that were encountered during the research may be overcome by future developments of a new resistance meter, regular maintenance or adaption of the sampling strategies.

It was also important to test how well the MSP40 performs throughout the year as soil moisture levels change. Therefore earth resistance surveys were carried out over a 16 month period to test the MSP40 responses with changing soil moisture content.

6.9.0 Seasonality testing

The seasonality tests show that the MSP40 can be used throughout the year but suggests that the summer months can produce an increase in the number of spikes or drop out (negative values recorded) in the data. This was due to two main reasons; the first related to poor spike penetration in a drying surface layer that had also been heavily compacted by the testing area being used as a football field and general leisure area.

The second and most important factor, (also related to the first (due to the reduced surface area in contact with the ground because of the poor penetration)), is the inability of the array to overcome the contact resistance issues of the drying soil. This is an issue for other mobile arrays (Dabas *et al.* 2000) and manual systems but can be reduced by a careful selection of current settings.

The larger number of spikes recorded in the MSP40 data compared to the manual square and twin probe arrays is directly related to the different collection methods. The MSP40 uses a continuous collection method as it attempts to record data at a specified interval no matter what the ground conditions may be. This inevitably means that there will be an increased risk of errors in the data as a measurement must be recorded at each sampling interval. The waiting time for the manual frames also allows time for readings to settle and electrodes can be repositioned or additional pressure applied to the frame over heavily compacted surfaces.

The optimal time for performing geophysical investigations (based on a calculated maximum contrast factor between high and low resistance values) for twin probes and square arrays was August (see chapter 4.2.8). However, when the spatial extent of six chosen anomalies was considered the area of each anomaly only showed small amounts of fluctuation throughout the year, suggesting that even when contrast factors are low interpretations can still be accurately made. However, it should be noted that the weather was unseasonably wet during the summer months with the Met Office at the time recording the wettest July on record and twelfth wettest year since 1910 in the UK (MetOffice 2012).

As a negative correlation exists between net moisture change (precipitation – evapotranspiration) and changes to apparent resistivity (when net soil moisture increases' apparent resistivity values decrease) it is possible to use correlation coefficient tests to examine the two variables relationship. By analysing the correlation coefficient values (a linear relationship test) the research suggested that the 30 day block of weather history immediately before the survey had the greatest effect on the changing apparent resistivity values than subsequent 30 day periods. However, when the lag time for the net moisture change is considered on a daily basis the strongest negative correlation is achieved after a 6 day lag time in the weather history prior to survey.

Throughout every aspect of the seasonality testing, the 0.5m twin probe and 0.75m square array showed very similar responses to changes in weather history. This must support the research by other practitioners regarding the similarity of the twin probe and square arrays (Saunders 2002 ; Aspinall and Saunders 2005) . The similar lag times of the 0.5m twin probe and 0.75m square arrays also indicates the two arrays are likely to have a similar optimal depth of detection previously researched by Roy and Apparao (1971) as the arrays responded with similar lag times and general trends in responses. The 0.75m twin probe responded differently to the lag time in soil moisture change due to the increased depth of detection of the array. The seasonality tests show the significant effect of soil temperature on the recorded earth resistance values with up to a ±15 % change in apparent resistivity values after correction highlighting the importance of correcting for temperature (whenever possible).

The conversion to apparent resistivity also showed the significant effect of using the idealised twin probe apparent resistivity conversion (using an infinity term for the distance between mobile and remote probes) as the square array apparent resistivity values were over 100 ohm m greater than those of the twin probe arrays.

6.10 Alpha Beta Gamma

The discussion of Alpha, Beta and Gamma measurements is important to the potential benefits of the MSP40. As the MSP40 is only capable of Alpha and Beta measurements due to its current hardware restrictions Gamma will only be briefly discussed. The Gamma measurements are aligned so that the potential probes are at right angles to the current probes meaning that the measurements are taken across the lines of equipotential. Therefore all measurements are based around zero and any variation between the Alpha and Beta measurements should be recorded in the Gamma data (or calculated Gamma measurement). The Gamma measurement can be useful for detecting edges of anomalies but cannot be used for interpretation and understanding of anomalies by itself.

As the MSP40 does not have the capabilities to record Gamma with the current hardware the calculated Gamma must be used (see Chapter 2.7, 4.1.5 and 4.1.6).

The tests exploring the use of Azimuthal Inhomogeneity Ratio (A.I.R.) calculations do not show significant levels of information to warrant the extra processing steps beyond the calculated Gamma measurements for most archaeological geophysics investigations (see chapter 2.8 and 4.1.5 and 4.1.6). This is because the calculations failed to show significant extra information not identifiable in the Gamma and A.I.R. data sets as both are dependent on the relationship between the Alpha and Beta measurements.

From a research objective it is recommended to always measure Alpha and Beta measurements. However, for a commercial investigation the potential for extra directional information is likely to be of less importance. This does not mean it should not be recorded as it is not known until the data is reviewed if directional variation of anomalies has been recorded.

During the research investigation only one clear example has been identified where the Beta data set has shown an anomaly not identified in the Alpha data set. The extramural settlement at Entremont (France) showed such an example (see chapter 4.1.5), however other practitioners have had greater variation between the two data sets (Walker 2005) (see chapter 2.2).

This directional variation may result from very near surface (narrow linear) features which are only detectable in one orientation (Walker 2011a). This would fit with the work by previous studies (Roy and Apparao 1971 ; Saunders 2002 ; Sparrow 2004 ; Aspinall and Saunders 2005) suggesting the optimal depth of detection (greatest current densities) for the square array is shallower than the Twin Probe.

No ground truthing has been carried out on the anomalies so it is not possible to say with any certainty. The low numbers of sites showing anomalies with directional orientation may also be down to the choice of sites and the archaeological anomalies they contain.

Collecting the Alpha and Beta data sets also serve an additional purpose as data collection errors may only affect one of the measurements. It is possible to combine data sets to reduce errors in one or both of the data sets caused by drop outs in data (negative readings). An alternative solution to overcome the drop out in the recorded data may be to sample only the Alpha or Beta measurements but double the density / sampling interval. This would provide an additional level of information that could be desampled (halving the data) to be recombined to remove errors in the data (Walker 2011a). Additionally by restricting the MSP40 collection to a single measurement it may provide a more stable signal (when noise levels are problematic). It is believed that the lack of switching of the analogue signal for the two orientations may stabilise the signal (Walker 2011a).

The increasing use and technological developments of mobile arrays will continue to gain importance as larger areas of land (even whole landscapes are investigated) (Gaffney *et al.* 2012). The MSP40 has a number of benefits yet to be fully utilised by archaeological geophysicists as it can perform good quality low impact rapid site assessments of archaeological sites.

6.11 Earth resistance data combination / visualization and data processing.

The processing chapter evaluated the different methods of data combination as a means of maximising the information within the Alpha and Beta data sets. This can be achieved through a visual combination of layers in an RGB format or through mathematical combinations.

The RGB visualisation can be a useful indicator of significant differences between the Alpha and Beta data sets but can make the data look 'too busy' especially when a site has significant background noise.

The mathematical combinations of data sets allow for greyscale images to be used (a more conventional display for geophysical data) but at least three images should be produced. This allows the subtle variations of the Alpha and Beta data sets to be differentiated from a combined image.

- Alpha (raw and processed)
- Beta (raw and processed)
- A combined Alpha and Beta (processed)

However, the type of data combination technique should also be considered, if a simple averaging is used then subtle variation of anomalies may be lost (especially on weak directional responses). When more complicated combinations are attempted (Geoplot combination routine) then it must be remembered that processing artefacts can be created.

These are small artefacts but should be highlighted as part of the report as a consequence of the processing. Data can also be lost if a dummy value is in one data set but not the other (no matter which order they are combined). This would be an issue if the errors in the data were replaced with the dummy value (using the search and replace function). Negative values in the data will also influence the combination process as they are still considered in the mathematical combination. The result is a low resistance area or point in the data. Negative values are often recorded in error when the contact resistance cannot be overcome or when the collection rate exceeds the maximum rate for the MSP40.

The additional processing step of replacing an error in one data set (e.g. Alpha) with a recorded resistance value from the remaining data set (e.g. Beta) can help data combination. The pre-combination processing will also reduce the occurrences of negative and reduced resistance values discussed above. However, the directional information for the data point is skewed towards the data set from which the value was taken.

When poor quality data has been collected a number of processing steps have been documented (see chapter 5.2 and 5.3) to try and improve that data through processing techniques. The data collection error trials indicated that a value of 25% of the original data containing errors could be recovered through processing of the data that would then allow for all anomalies to be identifiable. Between 25- 50% and only the larger scale anomalies are identifiable.

The random error experiment shows that even when there are issues with data quality the data can still be processed and interpretations made. However, data collection issue from practical field work also included areas or blocks where no data is recorded (drop outs of data or Alpha and Beta both recording negative values for multiple measurements). When this occurs it is not possible to interpret the data in these areas due to a lack of information. Therefore the best results will come from highest quality of data collection that is possible.

The discussion chapter has brought together the main findings of the research project by highlighting the multiple research areas investigated whilst assessing the MSP40 as a means of achieving a low impact assessment of 'sensitive' archaeological sites. The inclusion of two case studies is important as they highlight the field observations made during the research project which must form the basis of an investigation of this type. Comparisons have been made with hand-held data collection where available and appropriate. The future research areas of the MSP40 and final conclusions of the research project are discussed in the subsequent chapter (chapter 7).

7.0.0 Conclusions and future research

7.1.0 Conclusion

Archaeological geophysics can be seen as a non-destructive means of investigating the buried archaeological remains of a site. A wide variety of techniques are available for geophysical investigation, each with its own benefits and limitations. A more detailed understanding of the origin of the geophysical anomalies can be achieved by combining multiple geophysics techniques. In the past this could only be achieved through resurveying the area with each technique. The Geoscan Research mobile sensor platform has been successfully adapted to combined earth resistance, fluxgate gradiometer and GPS survey on to a lightweight mobile sensor platform.

The on going development of mobile arrays has focused on increasing survey resolution, data acquisition rates and increasing the survey areas being investigated to whole landscapes. Little attention has been focused on the physical impact of these systems and the damage the arrays (and towing vehicles) cause. The MSP40 is a lightweight mobile array that can be pulled by hand reducing the physical impact on archaeological sites. The multi-sensor integration also reduces the amount of trampling across sites as a maximum amount of information can be gained from a single traverse. It is useful at this time to consider the aims and objectives of the research for the basis of the conclusions.

7.1.1 Aim of the project

- The aim of the project is to investigate how the MSP40 can be used for rapid assessment of archaeological sites, whilst maximizing the information gained from a single traverse and minimizing the physical impact on the soil.

Rapid site assessment evaluation
The MSP40 offers an improved rate of collection compared to traditional manual arrays as a 20m x 20m grid can be surveyed in less than 10 minutes.

Over one hectare of earth resistance survey is also achievable within a single day. The additional functions of the mobile sensor platform allows surveys of larger grids (>40m) than is usually possible with traditional earth resistance arrays. This improves the survey time by halving the number of times the cart must be repositioned between traverses. The optical encoder also proved effective over these distances giving confidence in the positional accuracy of measurements.

The improved efficiency of the mobile sensor platform allows for greater exploration of larger survey areas and / or higher resolution surveys in the same timeframe as hand-held collection techniques. The simultaneous collection of three sets of survey data offers a more detailed assessment of an archaeological site. The simultaneous collection also means any additional geophysical surveyors on site can survey other areas of the site at the same time.

Maximising information

The addition of a GPS sensor and further trials of the gradiometer mounting has been an important development as it allows three surveys to be performed simultaneously by a single operator. The three complimentary data sets increase our understanding of the geophysical anomalies and aid the interpretations process as well as providing contextual information about the site, through the DEM from the GPS survey. The simultaneous collection of Alpha and Beta data sets add additional information about the soil properties in relation to the directionality of current flow. To achieve the same level of information with a linear array would require the resurveying of a grid at an orthogonal angle to achieve longitudinal and broadside surveys.

Reducing physical impact to sites

The development and testing of new wheel configurations alongside an impact assessment evaluation has meant it is possible to monitor the physical impact on a site caused by the MSP40. The physical impact is likely to be restricted to the upper 10 cm of soil or less, which includes the insertion of bolts and any compaction of the top soil as indicated through the various tests.

The lightweight frame also reduces the potential damage to sites when compared to many towed mobile arrays as the framework does not need to withstand the same forces as a heavier towed system. This means plastic and aluminium can be used extensively in the design. The level of soil compaction is also significantly reduced as there is no need for a quad bike or off-road vehicle to pull the array. Physical impact can be reduced further by collecting multiple data sets at once which reduces the level of trampling across the site.

7.1.2 Objectives

- Compare 'traditional' geophysical survey instrument collection rates with the MSP40 and develop ways to further improve survey time.

The MSP40 survey can save archaeological geophysicists significant time on site due to the additional sensor integration because the earth resistance, fluxgate gradiometer and GPS survey can all be completed by a single operator.

The practical field work results recorded during the research project and from other practitioners indicate that a larger area can be surveyed in a day than would usually be possible with traditional earth resistance surveys (+1 hectare). The MSP40 also saves significant amounts of time (approximately 1/3 of the time) when completing high resolution earth resistance survey ($\leq$0.25m sampling) compared to traditional collection due to the near continuous sampling rate.

When a gradiometer is mounted on to the mobile platform the collection rates is slightly decreased as the gradiometer is restricted to the maximum speed of the earth resistance measurements. The collection rate for earth resistance measurements are dependent on the sampling interval, delay time, spike monitoring use, time-based or encoder-based triggering and multiplexing settings (Alpha and/or Beta). Additional time is lost by the need to rebalance the gradiometer more frequently (best practice) because of the additional vibrations acting upon the sensors when mounted on to the mobile platform.

This is necessary to ensure the sensors remain in alignment. However, time is saved by combining the gradiometer measurements with the earth resistance survey as opposed to surveying with each instrument separately. When the GPS survey is factored in, the time savings are increased by almost two thirds as all three techniques are completed in the time taken to complete the earth resistance survey.

Additional time savings can be made by surveying over larger grids (40m x 40m) as it requires less repositioning between traverses than to cover the same area using 20m x 20m grids. It was also found that 40m traverse markers could be easily sighted at this distance to keep the traverse straight.

- Assess the data sets collected by the MSP40 with 'traditional' geophysics instruments considering responses and 'noise' in the data.

When the noise levels from the earth resistance measurements are considered, the instruments show a small level of instrumental noise of ± 1 Std. Dev. of 0.06. The effect of the near-continuous collection of the mobile array compared to a static manual square array survey with the same dimensions, equates to an increase in magnitude of responses between 4-12% for the MSP40.

The number of spikes in the data also showed the variability in responses between the two square arrays with a 3-5 fold increase in the number of spikes recorded by the mobile array during the seasonality tests.

The additional noise reflects the differences in data collection; the MSP40 uses a fast logging speed and offers near-continuous collection regardless of contact resistance issues. The manual square array is generally set at a medium logging speed so that readings have time to settle before being recorded. The manual positioning of the electrodes also reduces errors as greater time is taken to ensure the probes have good contact with the soil surface. The twin probe arrays showed the fewest numbers of spikes in the data, which may be due to the two remote probes being inserted deep into the soil profile for the twin arrays whilst all four probes must make sufficient contact at every sample interval with the square array.

The combination of techniques can increase the noise levels in the survey data but good practice during survey and careful processing reduce these effects. The fluxgate gradiometer shows a two-three fold increase in noise levels (0.2 - 0.3nT) compared to a hand-held survey (0.1nT) but the noise levels are significantly less than most archaeological responses. Additional processing / filtering will reduce the noise from the data sets.

The GPS surveys at the Oppidum of Entremont, Provence, France indicated noise in the data (subtle variation between traverses). This was likely to be operator induced so can be reduced by careful data collection. However, the DEMs showed similar 'noise' in an orientation that did not correlate with a traverse direction which suggests the options chosen to generate the 3D surface may also have an effect.

When all of the noise experiments are considered, the MSP40 does show increased noise in all of the techniques. The additional noise is caused by one or more of the following: the continuous rolling contact with the ground surface, issues with overcoming contact resistance or the vibrations caused by movement and / or tilt effects. All of these possibilities can influence the data quality. If the three techniques are performed individually, the noise levels would be reduced. However, the slight reduction in data quality is offset by the increased efficiency and reduced physical impact the MSP40 offers. Future hardware development (see section 7.2) should reduce some of the earth resistance noise resulting from the current hardware limitations. Only the site investigation at West Heslerton has been uninterpretable due to issues with spikes and contact resistance. If a magnetometer survey had been incorporated as part of the investigation, then the project would have been more successful. The development of a multi-sensor mobile platform means it is not necessary to make choices regarding instrumentation as both techniques can be performed concurrently. This makes multi-technique mobile sensor platforms ideal for pilot studies where little is known of the archaeological potential in an area.

When comparing the twin probe with the MSP40 / square array, the research has shown that the responses of the arrays are very similar. The peak width and response closely matching for the same array orientation / angle of strike to the anomaly. The 0.5m twin probe has a similar depth of detection as the 0.75m square array as reported elsewhere (Roy and Apparao 1971 ; Sparrow 2004), and this has also been indirectly shown during the seasonality research by a similar lag time response in soil moisture variation.

- Increase knowledge of square arrays and cart-based systems and the potential advantages/ disadvantages.

The square array's two dimensional configuration offers an alternative approach for geophysical investigations of archaeological sites; it differs from collinear arrays by allowing two measurements to be recorded over the same volume of soil (Alpha and Beta). A third measurement can be used to identify the directional variation of current between the two configurations (Gamma). The orthogonal arrangement of the array can be used to show directional bias of current flow through one orientation; the occurrences of this may be limited but the additional data set can be collected with minimal effect on collection rates and provides additional information about a site.

Although the MSP40 may not match the collection rates of other mobile sensor platforms (towed arrays), it does offer an alternative for use on smaller, less accessible sites. The array can be carried by hand in smaller component parts and be reconstructed on site. The reduced physical impact on a site may also improve access issues to sites that are under short crops in the early spring as the MSP40 has a minimal impact on the site. The MSP40 does not show the same tearing of the soil as with systems like the MUCEP; the MSP40 can be hand-pulled, further reducing the physical impact on a site because no towing vehicle is required.

Several peer-reviewed conference papers / posters have been delivered at the last two ISAP (International Society of Archaeological Prospection) international conferences in Turkey 2011 and Paris 2009 relating to the research.

This has enabled the dissemination of some of the results reported in the research and provided opportunity for constructive criticism as well as helping to promote the potential applications of the MSP40.

- Aid further development of a lightweight mobile sensor platform through additional sensor testing and integration whilst increasing our understanding of the MSP40's potential applications.

The additional testing of the fluxgate gradiometer has shown that the data can be collected at a high quality that is comparable with hand-held collection. The data quality is only slightly reduced by mounting the fluxgate gradiometers on the mobile platform.

The GPS integration is a significant development in site investigation as it is the first time Geoscan Research equipment has integrated a simultaneous GPS survey alongside geophysical data. The microtopography survey / DEM can show subtle changes in elevation related to the buried archaeology and can be directly linked to the geophysical anomalies. The survey data also provides location information for the survey grids and adds to the sites contextual information. With data collection rate of 20 Hz available on many modern RTK GPS systems, a high resolution survey is easy to complete alongside a geophysical investigation.

The testing and development of several new wheel configurations provided an interesting area of research as the choice of wheel configuration directly effected the quality of the results. The 'normal' spike length wheels provided the best all around performance but the research has shown that physical impact to the soil can be reduced by altering the spike length. However, during extended periods of dry weather the disced wheel may be the optimal configuration to overcome the issues of contact resistance.

Approximately 15 different modifications were made to the prototype MSP40, which ranged from minor changes for example, the replacement of worn components (wooden spacers) with hard wearing materials to improving the structural integrity of the framework (additional wheel bracing).The implementation of additional wheel bracing on the vertical mounting plate alongside such additions as the double wheel electrodes were solutions to fix potential errors within the data caused by subtle distortion of the array and or wheels. The system would still function without such modifications, but the relationship between the Alpha and Beta measurements may no longer be valid.

The inclusion of a rain cover and the rounded handle redesign amongst other minor changes were intended to provide solutions to small issues encountered during the research. Even though these issues would not drastically impede the survey, the solutions were intended to improve the operator's experience with using the MSP40.

- Increase efficiency in data collection rates, to encourage the use of earth resistance data in the wider archaeological geophysics community.

The MSP40 has been trialled on a number of different sites at various times of the year and has shown a good level of success. However, the near-continuous collection rate of the mobile array does mean a slight drop in data quality is inevitable.

When problems with data collection quality were identified, solutions have been sought to improve the reliability and new approaches to data processing have been attempted.

- Perform monthly testing of the MSP40 earth resistance array to investigate the seasonal effects of soil moisture on the recorded earth resistance values and the appropriateness of using the MSP40 during drier periods. This will include other earth resistance arrays for comparison purposes.

The inclusion of a seasonality test showed the MSP40 can be used throughout the year but overcoming the contact resistance of an electrode as soil moisture decreases remain an issue. This is shown by the increasing number of spikes and dropout / errors in the data values. A greater number of spikes occur in the mobile sensor platform data, but this is a reflection of the difference between the collection methods (continuous versus static) rather than being related to the array configuration.

- Assess the level of physical impact the MSP40 has on the soil surface. In order to identify and quantify the potential damage to archaeological sites and where appropriate reduce this impact.

The last fifteen to twenty years has seen an increased interest in mobile arrays, as the desire for faster collection, higher resolution survey and surveying large landscape projects have been met by the developments in sensor technology, multiple sensor arrays and increased storage capacity of field data. This enabled geophysicists to survey larger areas of land in a reduced time. However, the physical impact of towed mobile arrays has not been fully considered. The towing vehicle impacts the soil surface through sheering of the surface layer and compaction through the soil profile due to the mass of the vehicles. Whilst it was not possible to directly compare the impact of the MSP40 with other mobile arrays during the research project, it is possible to infer the physical impact based on photographic and video information.

Earth resistance arrays on a towed system can also have a negative impact on the soil from the tearing of the soil surface with plough-like electrodes to the significant mass of the early RATEAU system that used a constant water jet pressure to complete the electrical circuits.

The use of a square array naturally lends itself to the development of a cart-based system. The symmetry of the array records additional data sets that can indicate directional variation of current flow through the soil / anomaly.

The orthogonal data set also can be used to improve the data quality, as a second value over the same volume of soil (but with a different angle of strike) can replace erroneous resistance measurements.

However, it may be argued that an additional depth of detection may offer more information on the majority of sites than the directional information provides. The research by Harris (2011) showed the potential of a trapezoidal configuration and the additional programmable configurations and functions of future resistance meters can only benefit this development (see section 7.2).

The continuing developments by the manufacturer will reduce the issues encountered during the research project by making the MSP40 more efficient and adaptable which will ensure successful surveys.

7.2.0 Future research

The MSP40 provides a unique multi-sensor approach to archaeological geophysical investigations. The research project has identified the advantages and disadvantages of the system as a means of achieving low impact, rapid site assessment of archaeological sites. However, the wider acceptance of the MSP40 amongst archaeological geophysicists will come from additional 'proven' performance on 'challenging' sites. This is specifically related to free draining sites where the contact resistance of the soil / electrode interface continues to be an issue. It is hoped that the future technological developments of a new resistance meter will reduce the issues of contact resistance effects on data quality.

7.2.1 RM85

The RM85 will condense the existing hardware components of the MSP40 into a single unit (RM15, DL256 and MPX40 (multiplexer)). The RM85 (not available during the research project) should offer additional settings to give the operator greater control over the survey parameters and improve the capabilities of the MSP40.

The advanced RM85 will allow for a GPS measurement to be logged and make data integration easier. Earth resistance, gradiometer and GPS measurements will all share the same time stamp, giving the geophysics measurements a fixed coordinate position. The GPS integration will require additional research and may open up a new series of research questions relating to grid less data and how to process this data.

7.2.2 Variable current options to overcome contact resistance issues

A wider range of current options and increased voltage output may reduce contact resistance issues currently faced by the MSP40 (Walker 2012b). A reduced current option would also allow modification of the signal to noise ratio against the electrode contact resistance. However, this will require additional testing and another seasonality test would prove a useful method of investigation.

7.2.3 Logging speed improvements

One of the major limitations with the current MSP40 configuration has been the logging speed restriction (electronic design restrictions) that severely limits the speed that data can be collected. The issue is especially problematic at sampling $\leq$ 0.25m. The multiplexer timing splits a 1 second time interval equally between the Alpha and Beta sampling interval. For example a 0.5m sampling interval collected at a rate of 1 metre per second, the measurements would be Alpha 1, 0.25s, Beta 1 0.25s, Alpha 2 0.25s & Beta 2 0.25s equalling a positional difference of 0.25m between Alpha and Beta measurements.

Upgrading the electronic components of the earth resistance meter would reduce the necessary switching time and therefore the positional difference between measurements.

Logging speed improvements would help to reduce the frustrations of high-resolution survey, as the current system frequently stops recording when the current maximum collection rate is exceeded.

7.2.4 Trapezoidal array

Harris (2011) provided an excellent insight into the potential development of the MSP40 as a trapezoidal array offers multiple depths of investigation. However, the limitations of the pre-programmed multiplexer restricted how many configurations could be investigated. A multiplexer that enables different programmable configurations would open up another area of future research. An additional wheel could also be incorporated into the design to offer further permutations of the electrode configurations.

7.2.5 Wheel configurations

The development of new wheel configurations during the research project has provided additional ways to reduce physical impact and attempts to overcome the contact resistance issues. The late development of bolt-on discs has had limited success on two of the three test investigations. However, the discs may still prove successful on sites not covered in a metre of windblown sand.

Therefore additional testing is essential. A disced wheel that can be bolted directly on to the wheel hub could also be developed. This would reduce the horizontal surface area of the wheels reducing build up of soil material (as seen during the Towthorpe 18 survey). However, an assessment of the impact would be needed as the disc edge may penetrate deep into the soil profile due to the increased pressure on a reduced surface area.

7.2.6 Noise reduction

Reducing the amount of noise in the geophysics data caused by the combined collection on the MSP40 must be considered. Overcoming the contact resistance of the electrodes as discussed above remains the major source of error in the earth resistance data. However, the larger number of spikes (compared to traditional manual square and twin probe surveys) and increased variability of the responses should also be addressed.

Reducing the variability recorded in the data sets will make a significant improvement to data quality. These issues may be solved by improvements to the earth resistance meter.

The gradiometer data also contains additional noise compared to hand-held collection. Much of the noise comes from the vibration through the cart as it rolls across undulating surfaces. The mobile platform has a suspension system on both axles but additional vibration damping should reduce the noise levels in the data.

7.2.7 Combining multiple data sets

The research project has shown the difficulties in combining multiple earth resistance measurements. Combination of data sets can be achieved through mathematical combinations (averaging or algorithms) or through visual combinations (RGB composites and transparencies). The individual data sets contain unique information that increases understanding of the buried archaeology. The problem that needs to be addressed is how best to preserve as much of the unique information from the different configurations but still combine the data to ease the interpretation and visualisation process. A new algorithm may help to reduce the 'dilution' effects of mathematically combining data sets. This leads on to a similar topic of how best to visualise the multiple survey methods.

7.2.8 Visualising the data

The collection of different data sets (multiple techniques) raises issues with how to combine the individual data sets or layers to aid the interpretation and visualise the entire archaeological geophysics investigation.

The challenge to be considered is how to visualise all of the earth resistance permutations with the magnetometer and the microtopography data so that the maximum level of information can be gained about individual anomalies. The combination of all of this information should improve the accuracy of the geophysical and archaeological interpretations.

Entire landscapes are being surveyed by mobile sensor platforms and it is important to display the results appropriately. Small scale, high resolution detail of anomalies must also be displayed appropriately to allow for interpretation of results at both levels of detail, otherwise the additional information is redundant. The most appropriate way to visualise the data must be considered for future investigations.

7.2.9 Interpretation

The increasing extent of survey areas being investigated by mobile sensor platforms and the visualisation challenges it brings also impacts on the interpretation of anomalies. Wide scale contextual information is becoming more significant but this must not be at the expense of the small scale detail of individual anomalies. The scales must be juxtaposed for a full assessment of the entire survey area. This area of geophysical research must be explored further in future research.

Appendix A

A.1.1 Introduction

The aim of the project was to investigate any potential remains of a round barrow thought to have been fully investigated by J.R. Mortimer c.1864-1868. In addition to the excavation the barrow was reported by Mortimer (1905) to have been completely removed in 1887 by the tenant farmer at the time. The barrow was described by Mortimer as being constructed almost entirely of Kimmeridge clay believed to have been transported from 'Low Mowthorpe' approximately 1 mile away. The barrow also contained local soil mixed in with the clay or inter-dispersed between construction layers.

Even before excavation the barrow had been significantly damaged by ploughing, Mortimer (1905) describes the barrow as having a circumference of 75 yards but only surviving to a height of 3 feet. Since the Mortimer excavations the land has continued to be used for agriculture and has been all but flattened. Only a slight rise is visible approximately at the centre of the mound; however a Google Earth image of the area shows a clear ring ditch soil mark and chalk disk where the mound was located (see figure A1).

54.072503, -0.627256

Figure A1   A faint ring ditch / barrow soil mark of the ploughed out round barrow (Towthorpe 18) visible in the 2006 Google Earth image (Google 2011).

A recent study of round barrows in the Upper Great Wold Valley (Yorkshire) (Gibson and Bayliss 2008 (published 2010)), included C14 dating of the multiple interments from Towthorpe 18. The artefacts suggested a Neolithic date for the barrow, however the Carbon 14 dates suggested a period of use between the mid-4th millennium BC to the end of the 3rd millennium BC indicating a multiphase use of the site (Neolithic and Early Bronze Age).

At the time of the research the poor preservation of the ploughed out barrow dissuaded the authors from any further work as the site was not considered suitable for investigation. However after the artefact analysis had been performed a decision was taken to investigate the barrow when the agricultural regime allowed.

It was decided to use the Geoscan Research MSP40 to undertake a rapid earth resistance survey of the site as the landowners were keen to replant the land. A digital elevation model (DEM) was also to be produced; this was collected using a Real Time Kinematic (RTK) GPS, A100 Smart Antenna by Hemisphere GPS (HemisphereGPS 2010) mounted on the MSP40. A gradiometer survey of the same area was also undertaken using a Bartington Grad 601 dual sensor gradiometer.

The detailed earth resistance and gradiometer surveys were undertaken over the round barrow at Towthorpe, North Yorkshire, England, see figure A2 and A3. The survey area covered approximately 80m x 80m square. It was anticipated that the geophysical survey may help to confirm the position of the barrow based on information from the Google Earth image whilst adding additional information to the understanding of the site.
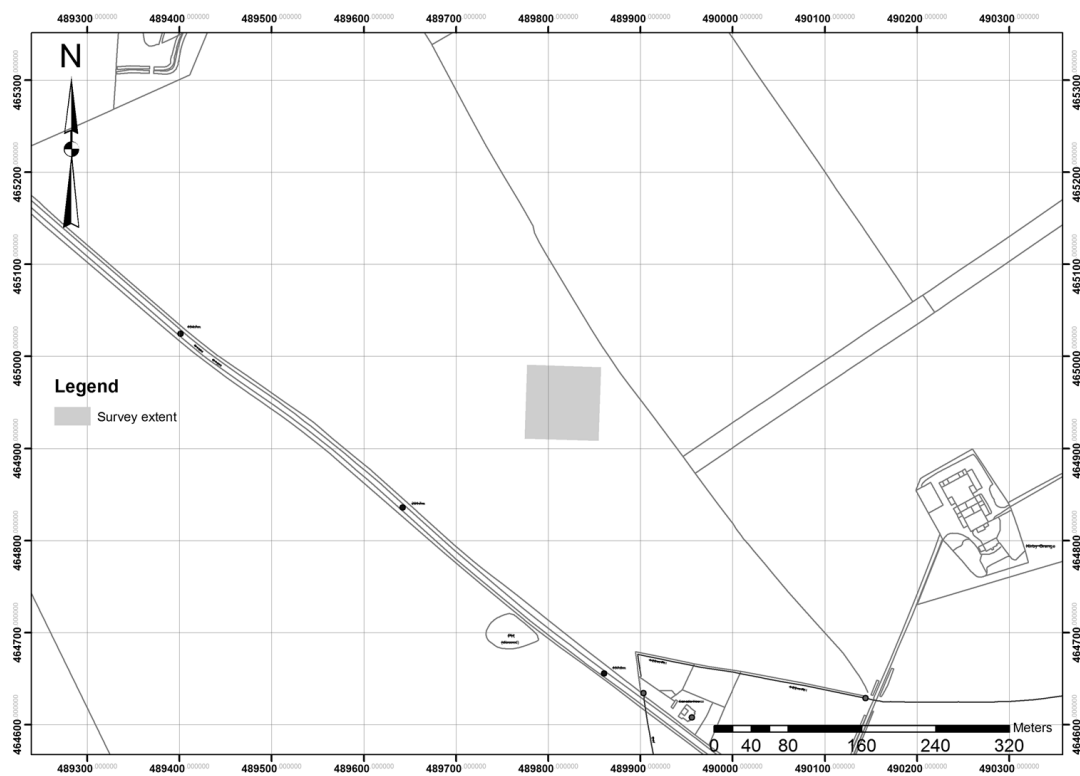
Figure A2   The geophysical survey extent of Towthorpe 18. © Crown copyright / database right 2011. An Ordnance Survey / Edina supplied service.
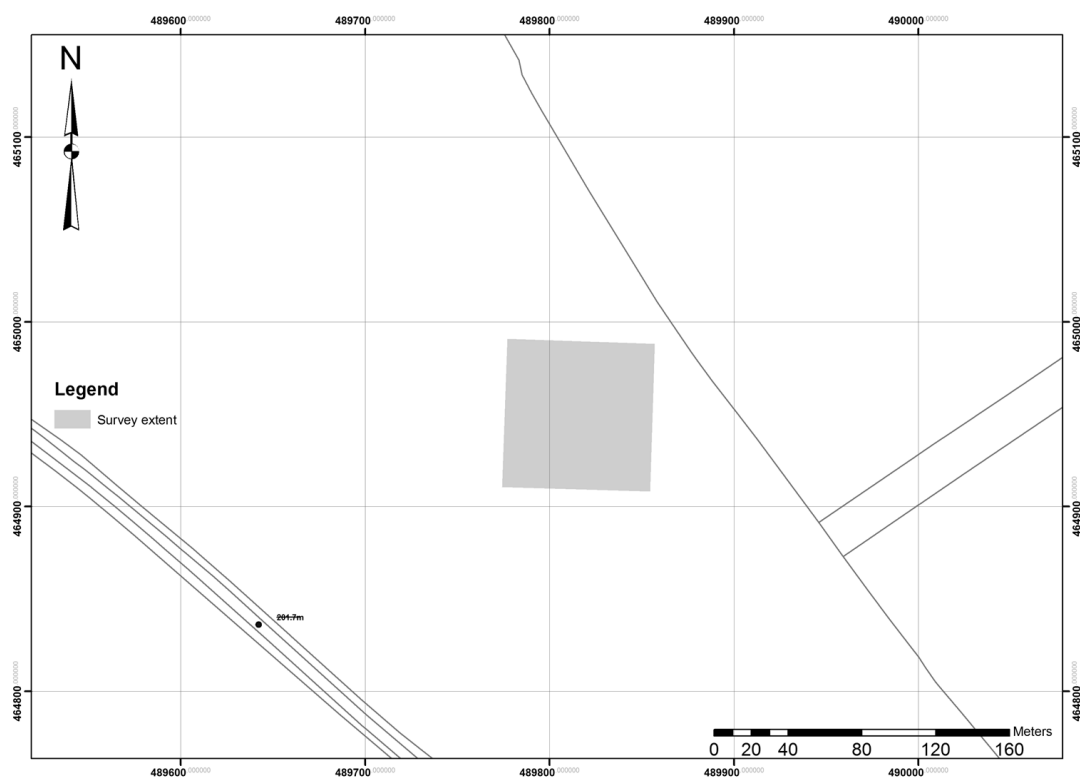

Figure A3   The geophysical survey extent plotted at 1:2000. © Crown copyright / database right 2011. An Ordnance Survey / Edina supplied service. For additional location information see section 3.6.6 page 79.

A.1.2 Site Information

National grid reference - SE89816495

Soil type and Geology

The site is located on the Yorkshire Wolds in North Yorkshire the parent geology of the area is chalk that was formed during the Cretaceous period. The upland areas remained unaffected by the glaciations of the Devensian period. However, windblown sand was deposited during this period and covered much of the Yorkshire Wolds contributing to the soil composition.

The soils that cover the upland areas of the Wolds are a mix of Rendzinas and Brown Earths. The soils on the upper slopes are often less than 20cm thick and tend to be the Rendzinas made from the chalk parent material. The thicker soils (between 30cm and 50cm) further down slope tend to be the brown earths soils (Unknown 2005). Towthorpe 18 barrow is located on the top of a hilly ridge and is likely to form part of the Rendzinas soil range.

Weather / site conditions

The site had been covered in snow for several days prior to survey and the ground had been heavily frozen. A warmer spell three days before the survey meant the snow cover had melted and the ground had begun to defrost. The snow melt water meant the soil was saturated at the time of the survey (possibly reducing contrast in earth resistance measurements). The ground cover was bare plough soil with stubble from the harvested winter crop still on the ground.

A.1.3 Description of the works

Aims and Objectives

The aim of the geophysical survey was to gather sufficient information to establish the location and extent of archaeological features if present within the survey area and, where possible, to characterise the archaeology identified.

Data from the gradiometer survey and DEM were to be used, where available, to aid interpretation and improve confidence in the archaeological interpretations of the earth resistance survey.

The project provided an opportunity to further test the mounted a A100 Smart Antenna by Hemisphere GPS (HemisphereGPS 2010). This helped increase the information gained from a single traverse during a rapid assessment of the site.

A.1.4 Method

Towthorpe earth resistance and gradiometer survey

MSP40 earth resistance survey

- MSP40 configured with short spiked wheels.
- RM15 & DL256 data logger

Data was collected in a zigzag pattern without rotating the MSP40. The encoder wheel was used to trigger measurements at the specified intervals. Data was collected in 40m x 40m grids with sighting poles at the grid edges.

Gradiometer survey (see table A.1)

- Bartington dual sensor grad 601
- Data was collected in a zigzag pattern in 20m x 20m grids.

Table A.1   Towthorpe sampling strategy

Equipment	Measurement Configuration	Sampling Interval	Traverse Interval	Method of collection
MSP40	Alpha & Beta	0.5m	1m	Zig Zag
Grad 601	Gradiometer	0.25m	0.5m	Zig Zag

RTK GPS survey

The GPS unit was mounted on the custom made frame positioning the GPS Antenna over the centre of the earth resistance array. Data was collected at a rate of 20Hz.

Site / Survey conditions

The ground conditions were extremely muddy as the weeks prior to survey had seen a significant snow fall on the ground surface alongside frozen ground. The first day on site was used to establish the survey grid and trial a new set of disced wheels for the MSP40 (see chapter 3.5.1). However the saturated soil and fine grained soil particles meant that the soil developed a clayish consistency that stuck to the wheels and was blocked by the discs on the outer face of the wheel. The soil encased the wheel rim to a depth of over 4 cm significantly adding to the weight of the cart and making measurements impossible (see figure 6.18). As the soil accumulation was so significant even before survey was attempted the field trial was aborted and the wheels were replaced with a short spike configuration.

Figure A.4   A mud encased wheel from the MSP40 after a field trial at Towthorpe 18 round barrow.

A.1.5 Data processing

Earth resistance survey data processing

Alpha and Beta data set processing (before combining)

---

2 x Despike X=1 Y=1Thr=3 Repl=Mean

Despike X=2 Y=2Thr=3 Repl=Mean

Alpha and Beta dataset combining and additional processing

Merge Composites (HPF X=6 Y=3 Wt=G) : towthap & towthbp

Destagger Grid 3, X dir, Shift=-2, Line Pattern -2-4-6-8

Destagger Grid 1, X dir, Shift=-1, Line Pattern -2-4-6-8

Despike X=2 Y=2Thr=3 Repl=Mean

LPF X=1 Y=1 Wt=G

LPF X=1 Y=1 Wt=G

Interpolate Y, Expand - SinX/X, x2

Gradiometer survey data processing

Zero Mean Grid, Threshold = .25

Zero Mean Traverse, Grid=All LMS=On Thresholds not applied

Periodic filtering, Index=60-66, Grid=All, Spike=On Thresholds not applied

Destagger Grid 16, X dir, Shift= 1 Line Pattern -2-4-6-8

Destagger Grid 15, X dir, Shift= 2 Line Pattern -2-4-6-8

Destagger Grid 14, X dir, Shift= 1 Line Pattern -2-4-6-8

Destagger Grid 13, X dir, Shift= 2 Line number 1-16

Destagger Grid 12, X dir, Shift= 1 Line Pattern -2-4-6-8

Destagger Grid 11, X dir, Shift= 1 Line Pattern -2-4-6-8

Destagger Grid 10, X dir, Shift= 1 Line Pattern -2-4-6-8

```
Destagger Grid 9, X dir, Shift= 3 Line Pattern -2-4-6-8

Destagger Grid 8, X dir, Shift= 1 Line Pattern -2-4-6-8

Destagger Grid 6, X dir, Shift= 3 Line Pattern -2-4-6-8

Destagger Grid 5, X dir, Shift= 3 Line Pattern -2-4-6-8

Destagger Grid 4, X dir, Shift= 2 Line number 1-14

Destagger Grid 3, X dir, Shift= 1 Line number 1-7

Destagger Grid 2, X dir, Shift=-4 Line number 28-37

Destagger Grid 1, X dir, Shift= 2 Line Pattern -2-4-6-8

Destagger Grid 2, X dir, Shift= 2 Line Pattern -2-4-6-8

Destagger Grid 13, X dir, Shift= 2 Line Pattern -2-4-6-8

LPF X=1 Y=2 Wt=Gaussian
```

A reconstruction of the archaeological excavation data reported by Mortimer (Mortimer 1905 ; Gibson and Bayliss 2008 (published 2010)) was created in ArcGIS. Distances were converted to metric measurements. The centre of the mound was calculated in ArcGIS using the centroid function of the ring ditch shape file to produce the most accurate centre position. After the centre of the barrow was located it was possible to draw the approximate positions of the archaeological finds to see if any indication of geophysical anomalies correlated with the find positions (excavation trenches etc.).

A.1.6 Results

The earth resistance and gradiometer data sets are strongly influenced by the heavy ploughing (ridge and furrow) running across the site (approximately southwest-northeast). With the inclusion of the RTK GPS DEM it is possible to link the subtle changes in elevation to the geophysics data. The deeper plough soil on the ridge showed a decrease in the earth resistance measurements; this may be due to the increased soil moisture of greater soil volume caused by the act of ploughing (depositing the furrow material on the ridge). The porous nature of the limestone and thinner soil deposits in the furrow therefore can be identified as a high resistance anomaly (reduced soil moisture content).

However, the build up of material on the plough ridge increased the magnetic responses of the ridge. This is due to the build up of top soil on the ridge and the thinner soil deposit in the furrow cut into the parent geology (Chalk / Limestone). Topsoil (generally) has increased magnetic enhancement compared to the subsoil and Limestone (generally) has a low magnetic susceptibility so produces a weaker response (in this case a negative anomaly).

RTK GPS Digital Elevation Model (DEM)

The missing DEM data resulted from the data logger powering down to save battery life. It was not immediately noticed, explaining why certain areas of the survey area are missing data. Unfortunately this also meant that approximately ¼ of the survey area is missing topographic information and time constraints did not allow for this area to be resurveyed.

However the data does show that a small rise in the ground surface at the centre of the survey area does relate to the position of the barrow (based on the identification of the ring ditch associated with the barrow visible in the geophysics results). Hill shade and 3D surface plots were generated in ArcGIS 9.3.1 software packages ArcMap and ArcScene respectively. A vertical exaggeration (Z unit conversion factor of 20) was added to the DEM information to highlight the subtle changes in elevation (see figure A.5 & A.6).
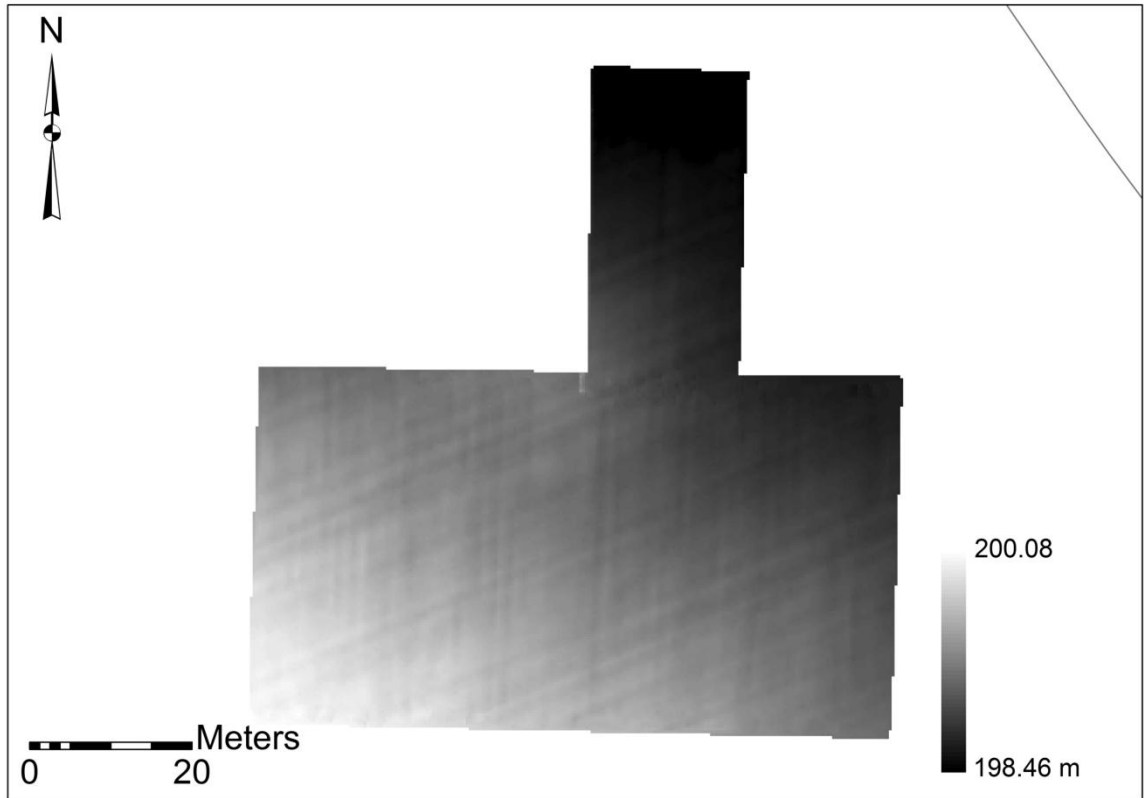
Figure A.5   A GPS survey / DEM of Towthorpe 18 collected on the MSP40 with added hill shade to differentiate the high and low of the surface ridge and furrow caused by ploughing.
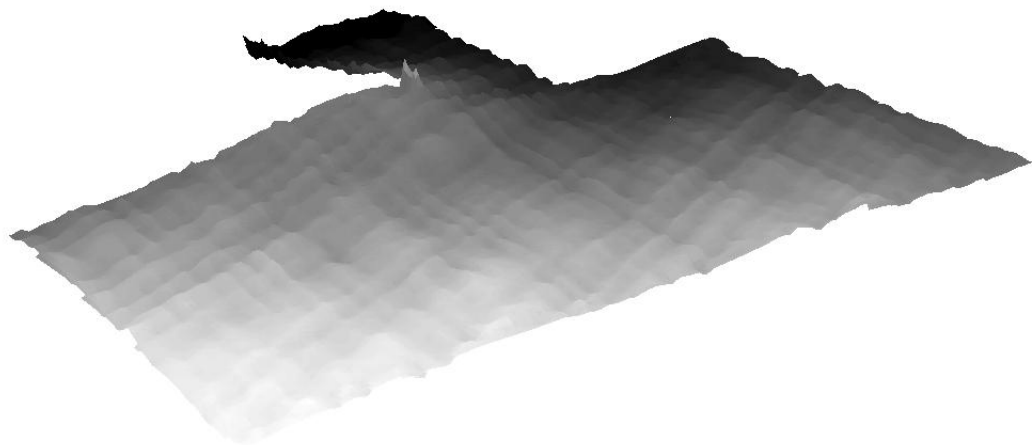

Figure A.6   A 3D DEM surface model of Towthorpe 18 barrow (with vertical exaggeration). The ridge and furrow clearly visible and the rise in the middle of the data set showing the location of the round barrow.

The DEM shows a series of ridges running along the line of transects (approximately north-south) which may result from the surface creation of the DEM. As each transect is approximately 1m apart but has a greater density of data points along the transect line (data collected at 20 Hz). Alternatively it is an operator induced error resulting from the operator twisting the handle as they walk (no longer parallel to the ground surface). The slight twisting of the platform could result in a slight change in the recorded elevation along the traverses explaining the ridges in the data that were not caused by ploughing.

Earth resistance survey results

A1 – Archaeology, Low resistance anomaly, probably forming a circular ring ditch around the mound, a low resistance anomaly forming the boundary of the round barrow. The dimensions approximately equal the dimensions discussed by Wheeler (current circumference = 67.98m or diameter of approximately 21.64m, wheelers circumference description (75 yards) = 68.58m or diameter of approximately 21.83m.

A2 – Archaeology, High resistance anomaly forming part of the barrow material. The barrow is still slightly raised above the surrounding ground level as shown in the (RTK GPS) micro topography survey.

A3 – Archaeology, Low resistance anomaly, curvilinear feature, possible old field boundary ditch, the curve of the anomaly arcs around the barrow from the east to the south suggesting the feature respected the position of the barrow. This may indicate it was dug at a time when the mound was more prominent in the landscape.

A4 – Archaeology? Low resistance linear anomaly. The anomaly is a large low resistance band in the northwest corner of the survey area. The anomaly is approximately 5-6m wide and runs approximately SW-NE.

As only a small area was surveyed it is difficult to assign an archaeological interpretation but may be a ditch feature or could be a naturally deeper deposit of soil. An expansion of the survey area would identify the extent of the anomaly and would aid confidence in the archaeological interpretations.

A5 – Natural? Low resistance amorphous anomalies, the features are probably areas of deeper plough soil / soil filled hollows in the underlying geology as they have no clear shape.

A6 – Natural / Geological? A series of very high-high resistance anomalies or areas. The high resistance values are probably due to areas of near surface geology (shallow top and sub soils).

A7 – Natural? Low resistance amorphous anomaly, probably similar to the A5 group of anomalies but may also include ploughed out barrow material (increasing soil depth) due to the close proximity to the round barrow.

A8 – Archaeology, ridge and furrow (probable mix of old and new). The site has been heavily ploughed for many years as the mound had been heavily ploughed away even before wheeler began excavating the site.
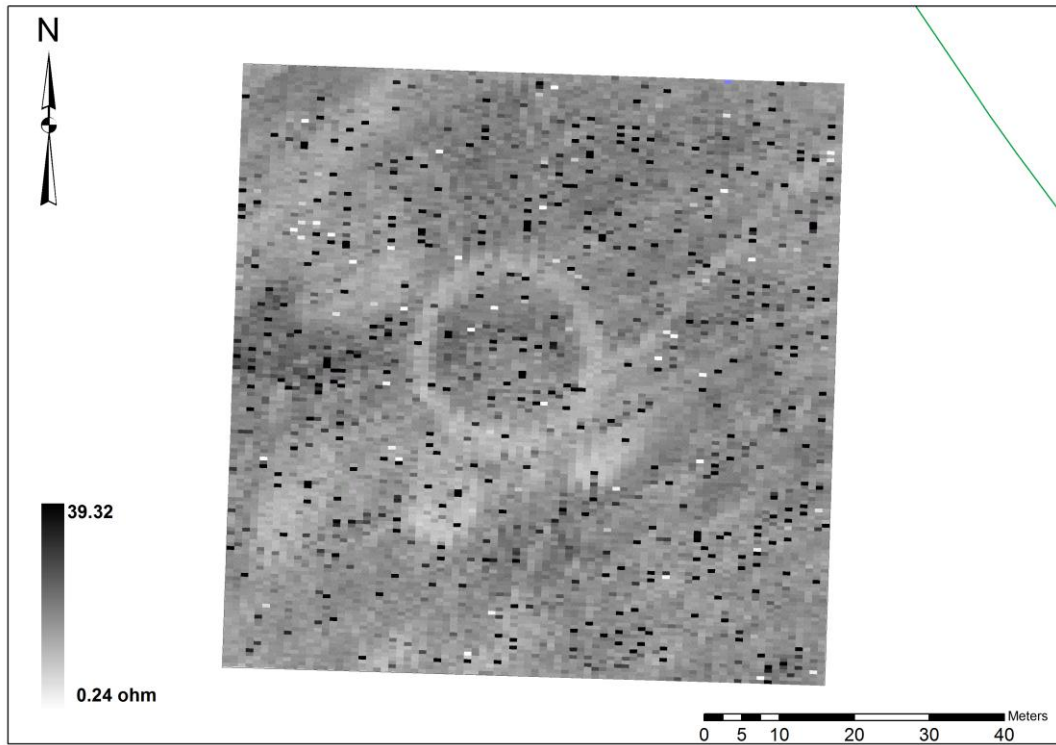
Figure A.7   MSP40 Earth Resistance data (Alpha measurement unprocessed)
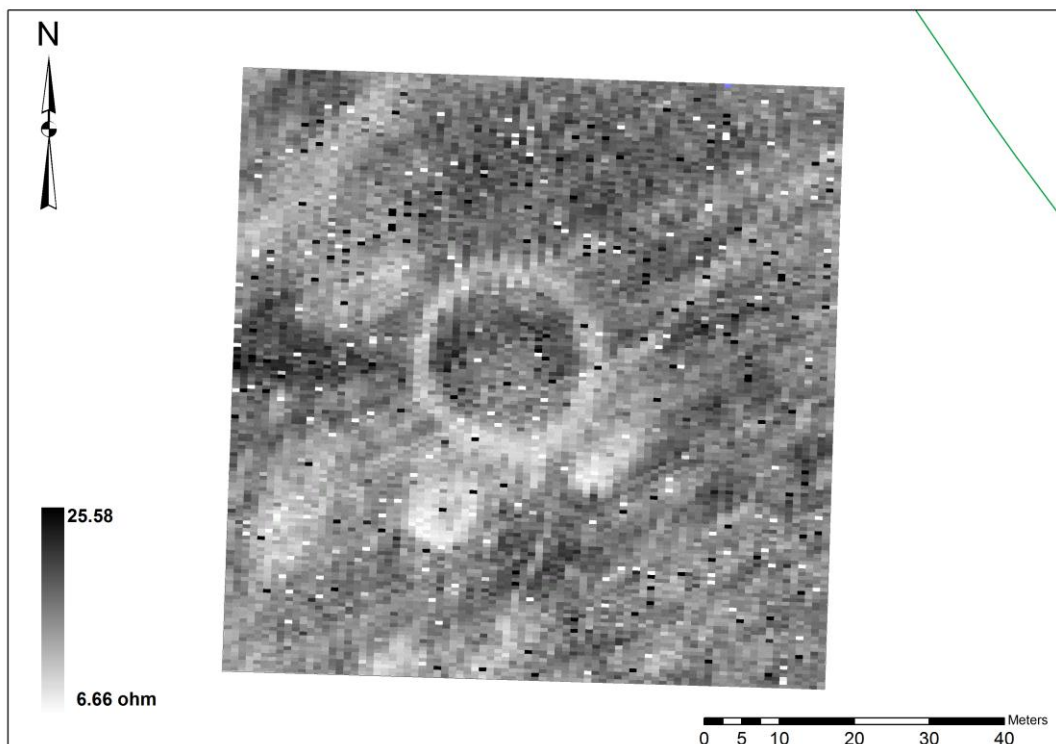

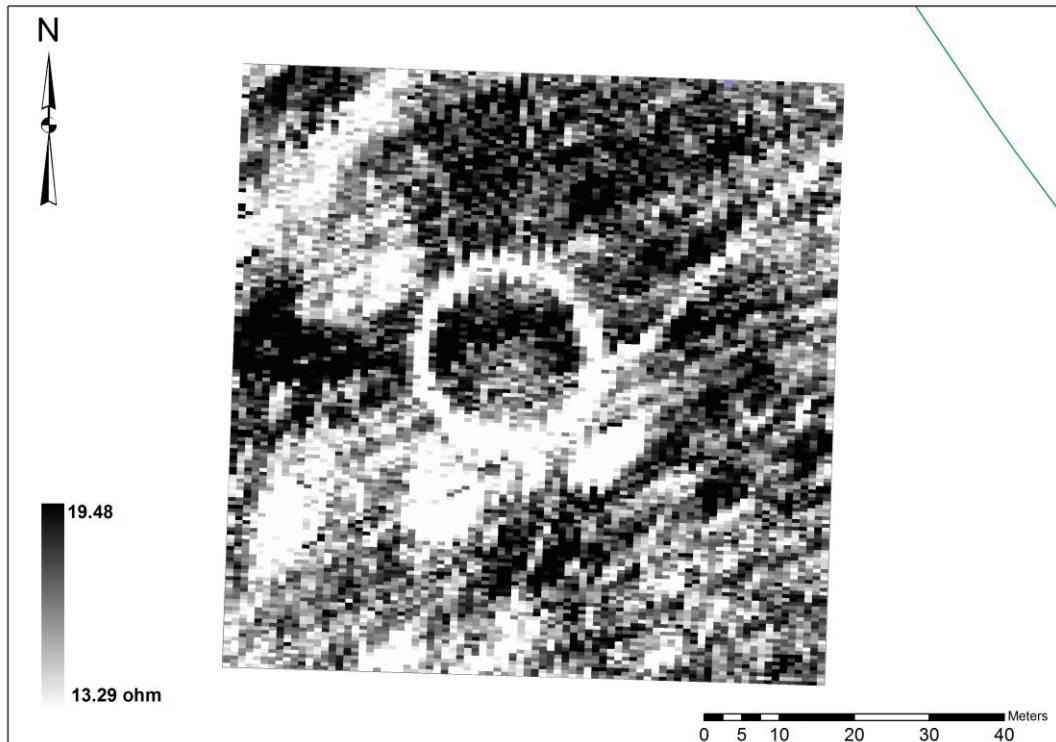Figure A.8   MSP40 Earth Resistance data (Beta measurement unprocessed).

Figure A.9   MSP40 Earth Resistance data (combined Alpha and Beta measurements minimal processing).

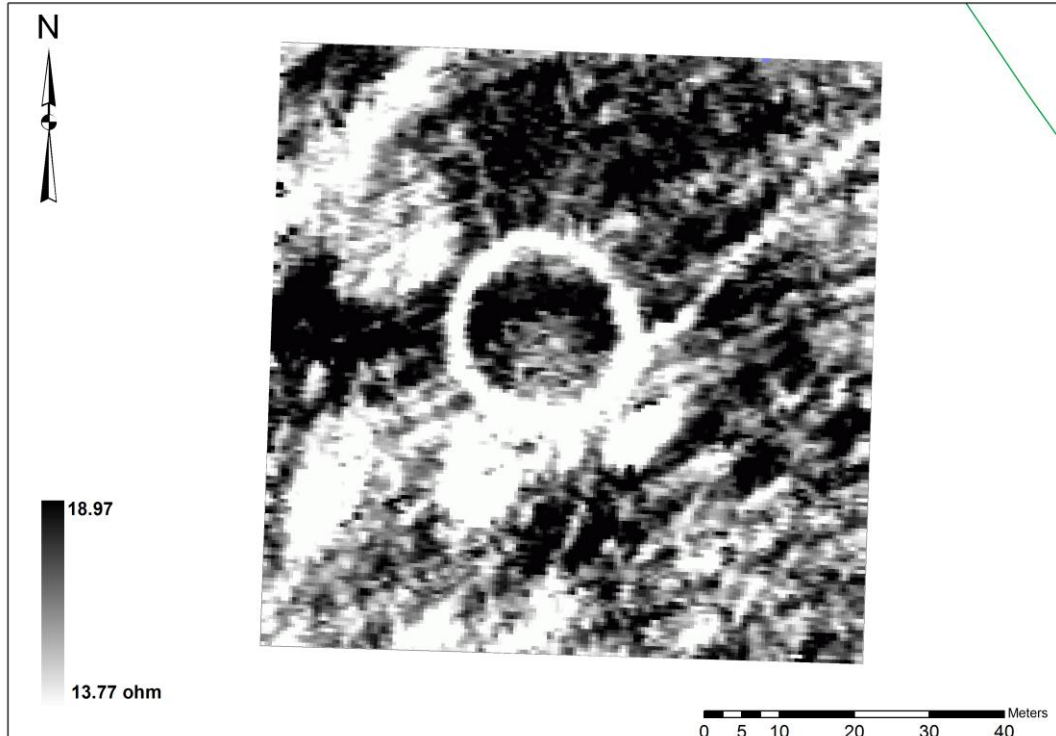Figure A.10   MSP40 Earth Resistance data (combined Alpha and Beta measurements processed).

Figure A.11   MSP40 Earth Resistance data (geophysical interpretations).

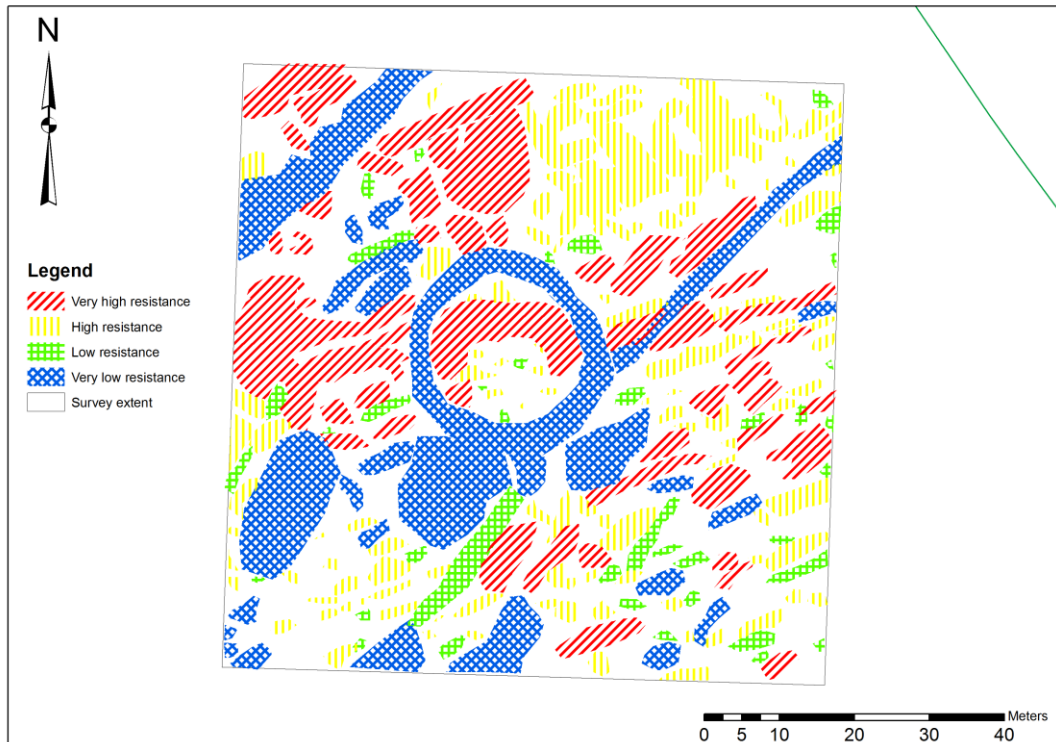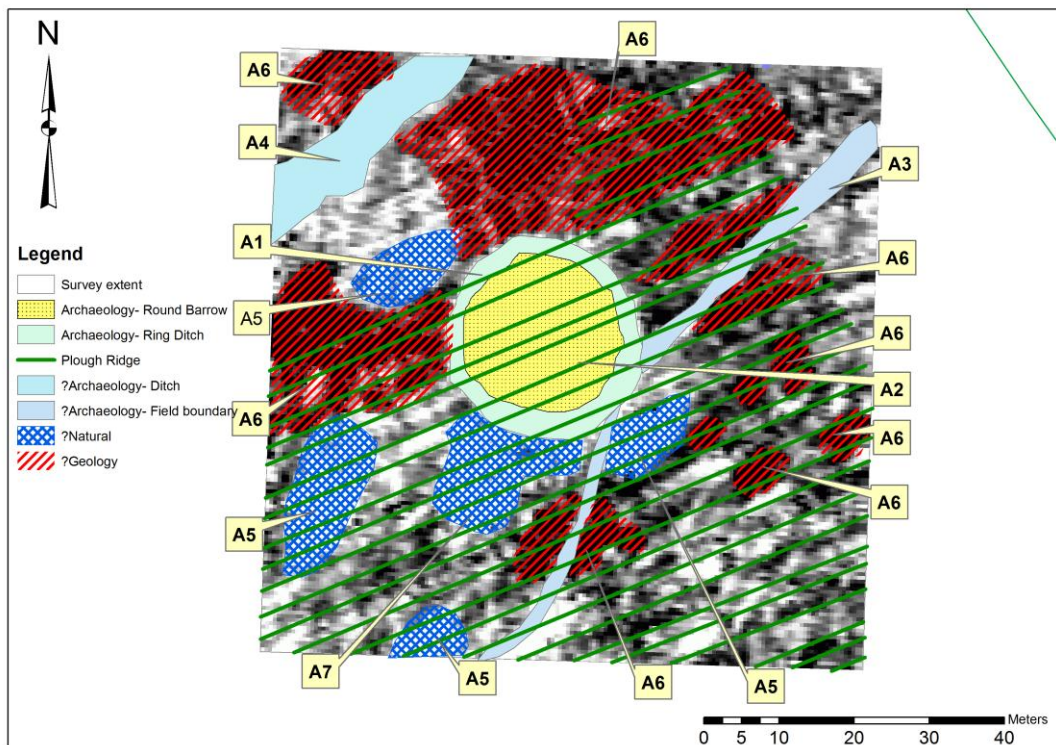Figure A.12   MSP40 Earth Resistance data (archaeological interpretations).
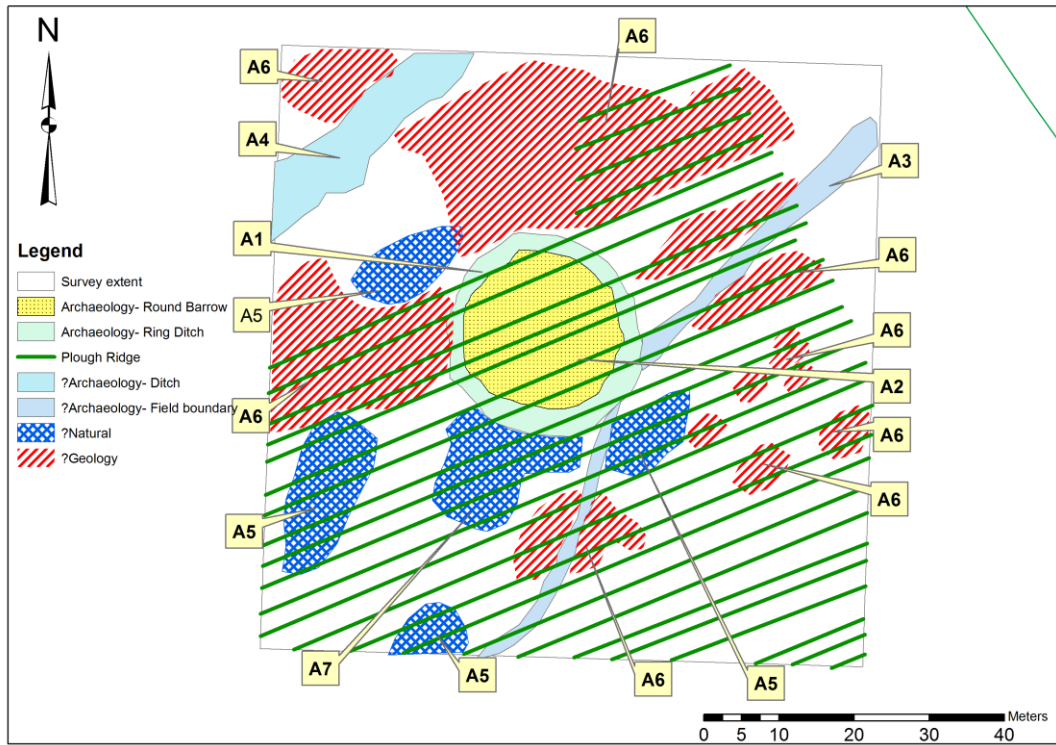
Figure A.15   MSP40 Earth Resistance data (archaeological interpretations).

Figure A.16   Bartington dual sensor Grad 601 gradiometer data (unprocessed).

Figure A.17   Bartington dual sensor Grad 601 gradiometer data (unprocessed XY trace plot).
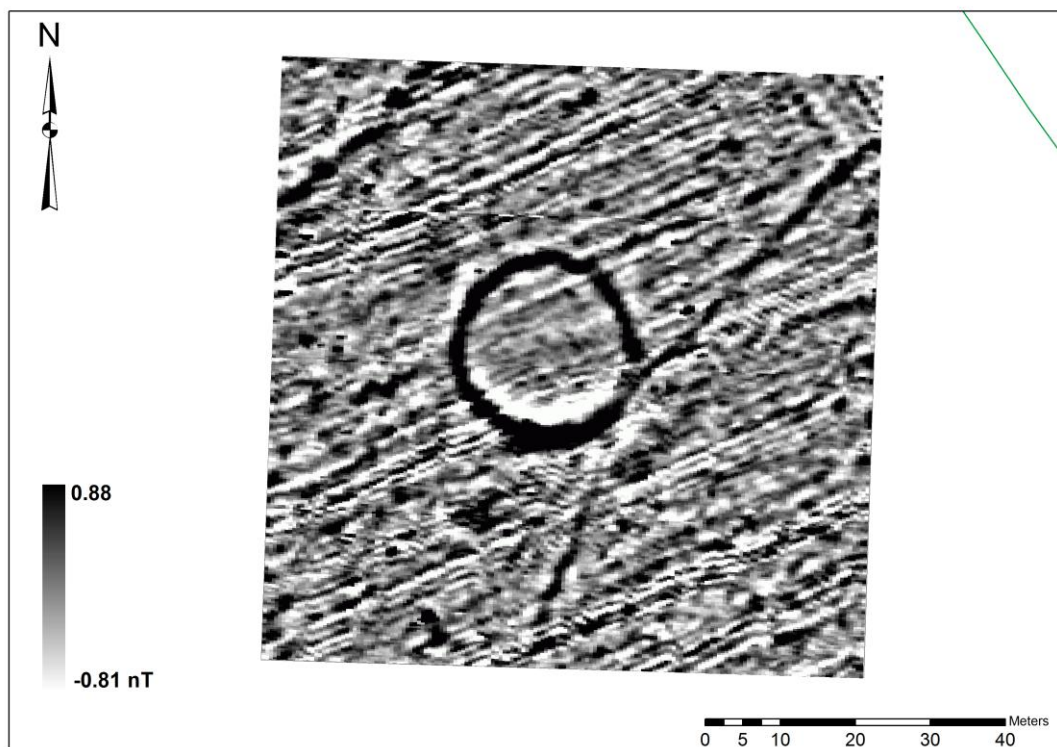
Figure A.18   Bartington dual sensor Grad 601 gradiometer data (processed).
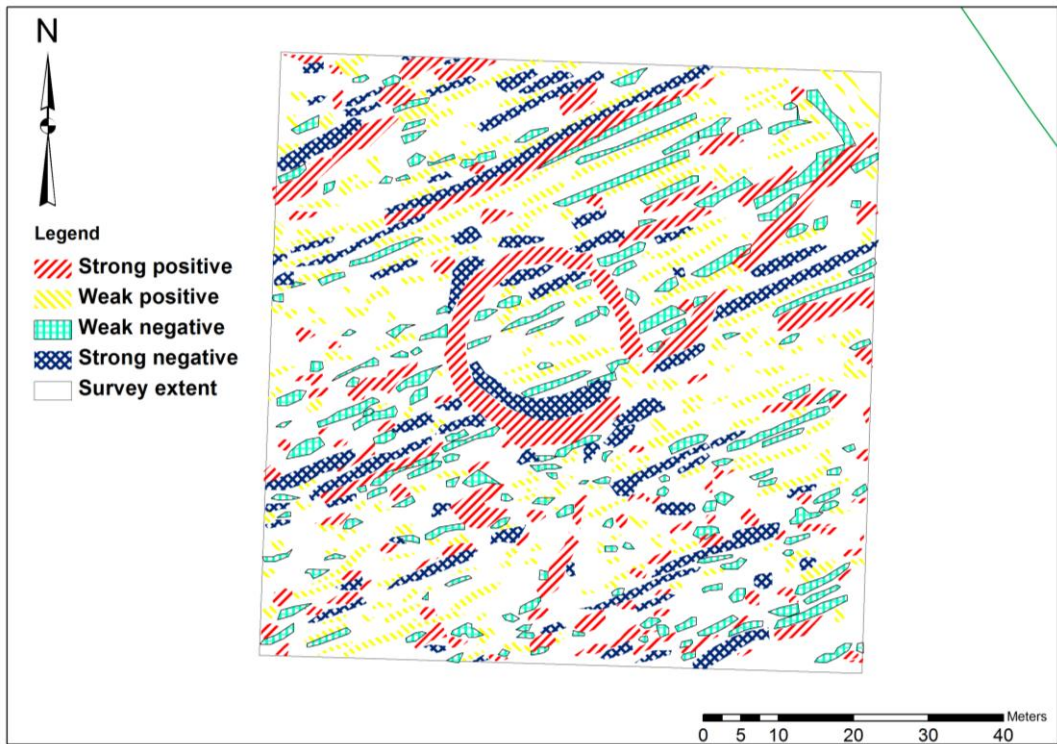
Figure A.19   Bartington dual sensor Grad 601 gradiometer data (geophysical interpretations).

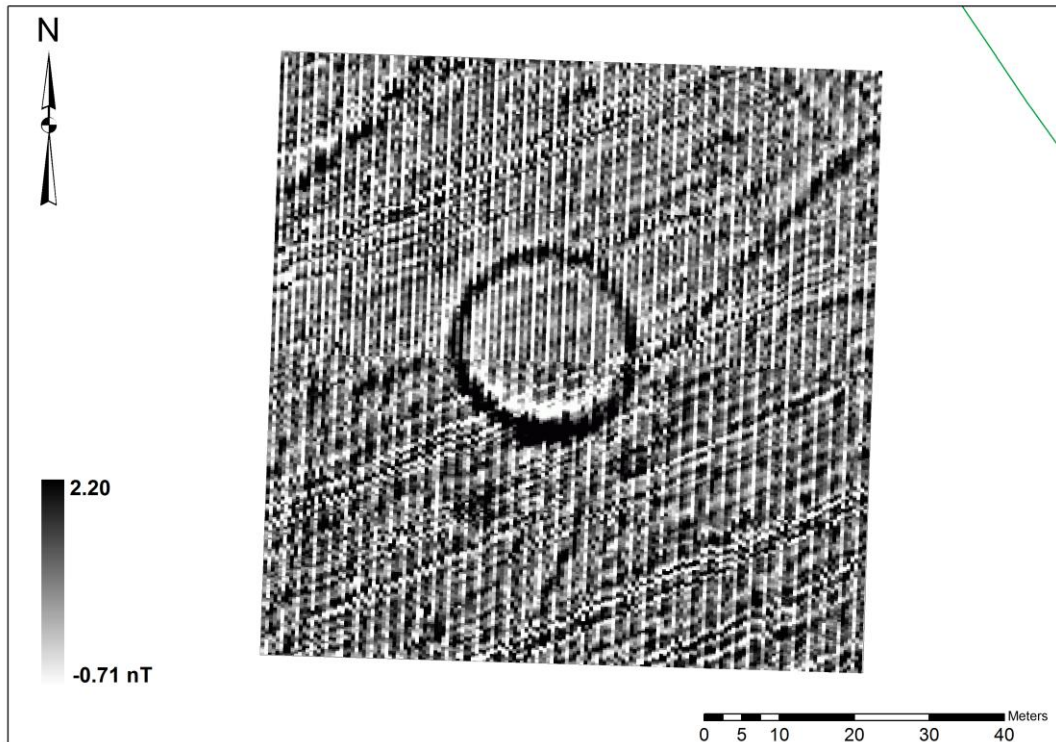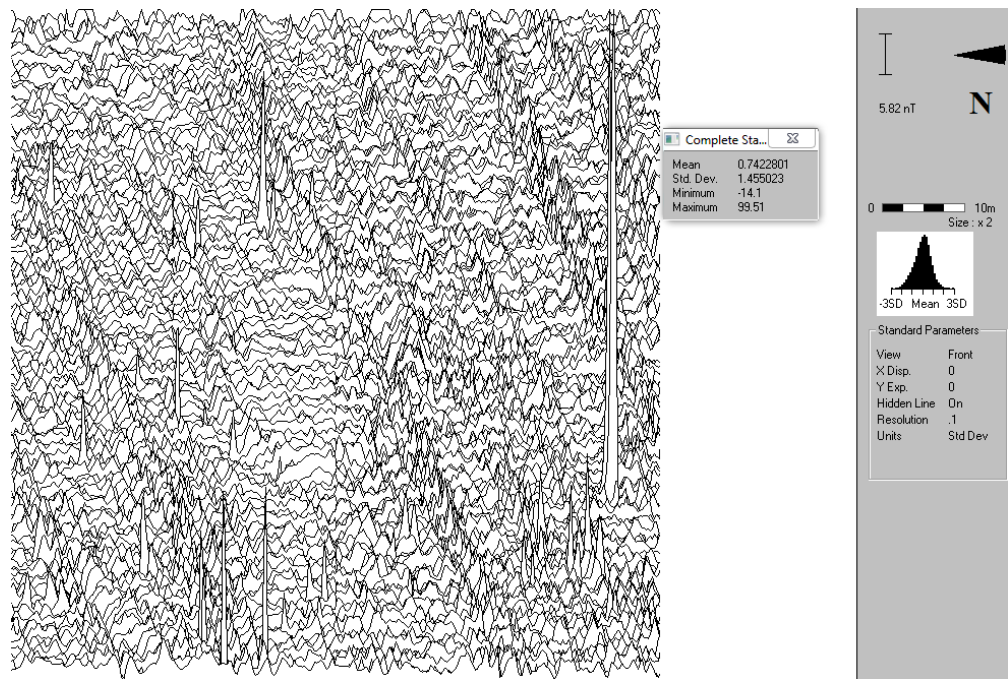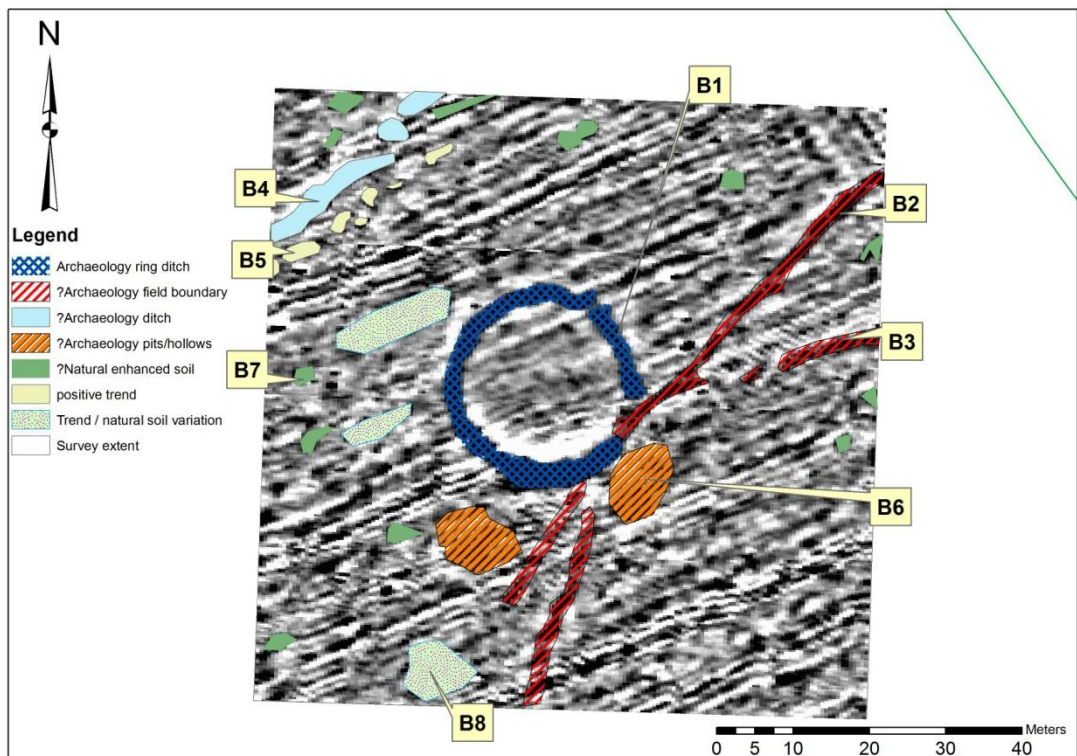Figure A.20   Bartington dual sensor Grad 601 gradiometer data (archaeological interpretations).
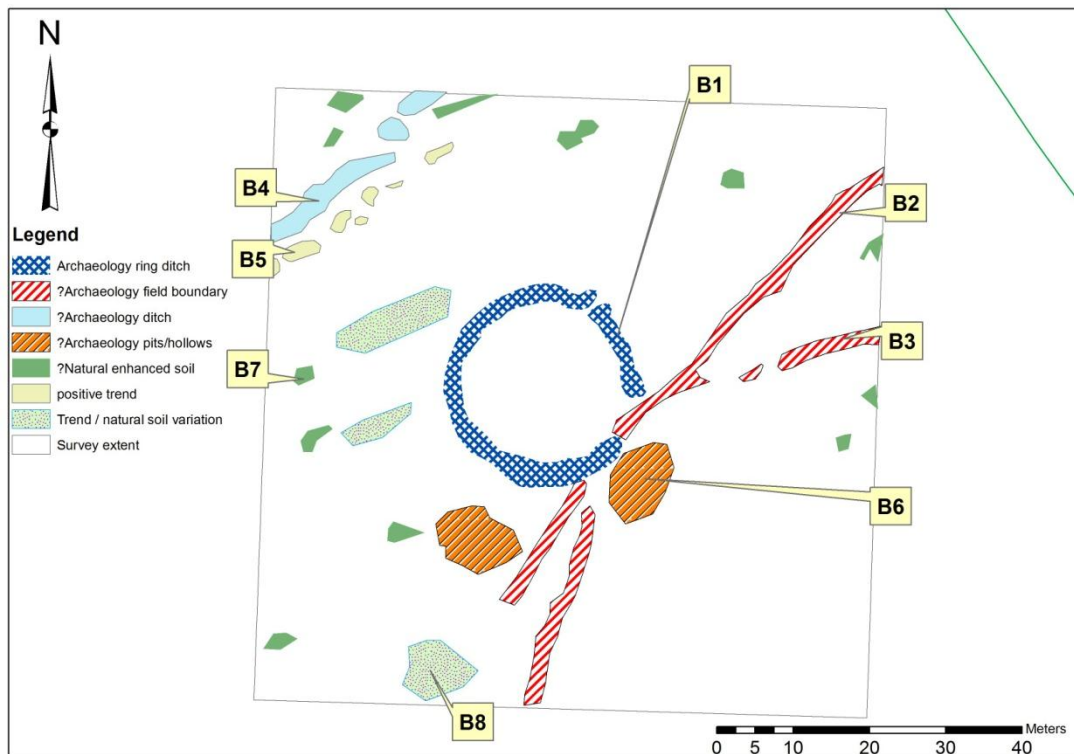
Figure A.21   Bartington dual sensor Grad 601 gradiometer data (archaeological interpretations).

Gradiometer survey results

B1 – Archaeology, strong positive anomaly approximately +1 - +4 nT. forming the circular ring ditch around the barrow. Correlating with the low resistance feature A1.

B2 – Archaeology, strong positive anomaly +0.3 - +1.5 nT. The anomaly is likely to form a previous field boundary ditch. The data correlates with earth resistance anomaly A3. However, a second anomaly is located to the south of B2 with a gradual curve to the south-west (again the anomaly appears to respect the position of the mound) see B3.

B3 - Archaeology, weak positive anomaly + 0.1 - +0.3 nT. The anomaly may form part of a previous field boundary ditch. The anomaly does not correlate with any earth resistance anomaly. However, the anomaly which is located to the south of B2 has a gradual curve to the south-west and once again the anomaly appears to respect the position of the mound.

382

B4 – Archaeology? Strong positive anomaly +1.0 - +2.66 nT. The fragmented anomalies make it difficult to interpret as a small area was surveyed. This makes it difficult to assign an archaeological interpretation but may be a ditch feature as it correlates to the earth resistance anomaly A4. An expansion of the survey area would identify the extent of the anomaly and would aid confidence in the archaeological interpretations.

B5 – Trend, weak positive anomalies +0.3 – +0.9 nT. The anomalies are fragmented into small discrete anomalies but follow a trend line that runs parallel to B4 and may be part of A4 as the trend line correlates with the low resistance anomaly position.

B6 – Archaeology? Weak positive anomalies + 0.3 - + 1.2 nT. The sub circular anomalies may be an archaeological pit or natural soil filled hollow. The close proximity to the round barrow may indicate places were the local soil was used with the Kimmeridge clay from 'Low Mowthorpe' (Mortimer 1905) to construct the barrow.

Alternatively the anomalies may just be soil variation or filled hollows that have a weak positive magnetic susceptibility compared to background responses.

B7 – Natural? Weak positive anomalies +0.3 - +1.2 nT, the anomalies are small sub circular features that are likely caused by natural variations in the soil. However, the size and response of the anomalies may also indicate pit features or enhanced soil filled hollows. Excavation of a few of the anomalies would confirm the cause of the geophysical responses.

B8 – Trend, weak positive trend probably caused by local soil variation and the ploughing across the site as the anomalies run parallel to the plough ridges recorded in the DEM recorded by the RTK GPS mounted on the MSP40.
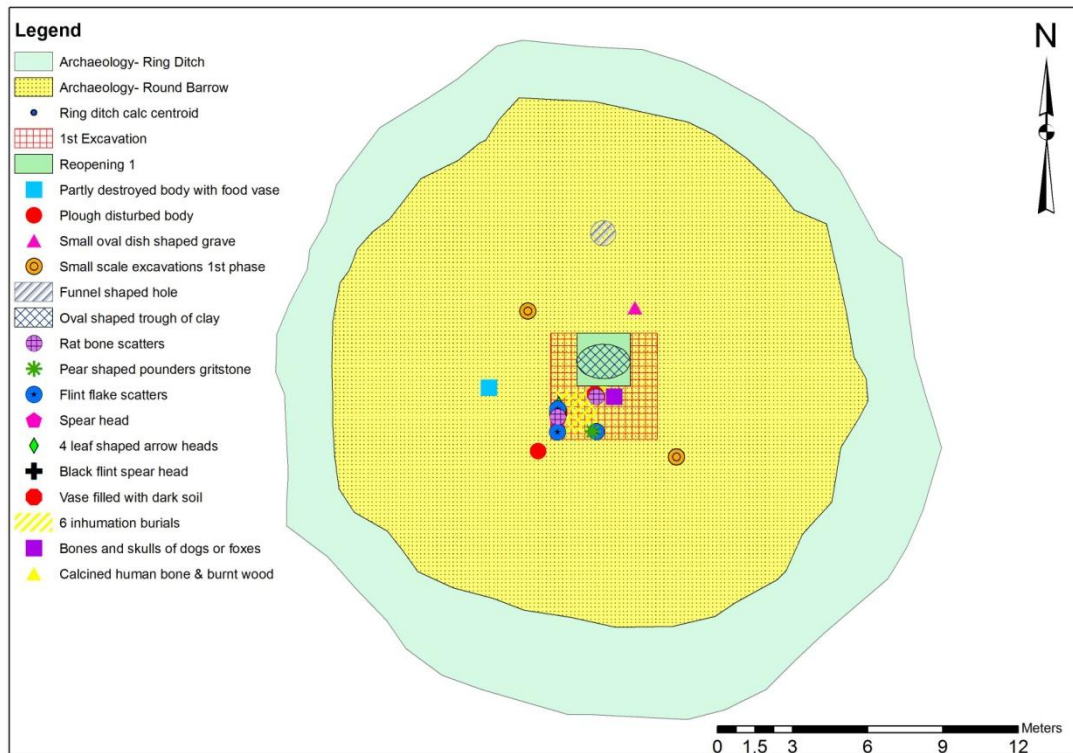
Figure A.22   A reconstruction drawing of the Mortimer excavations based on Mortimer's 1905 account.
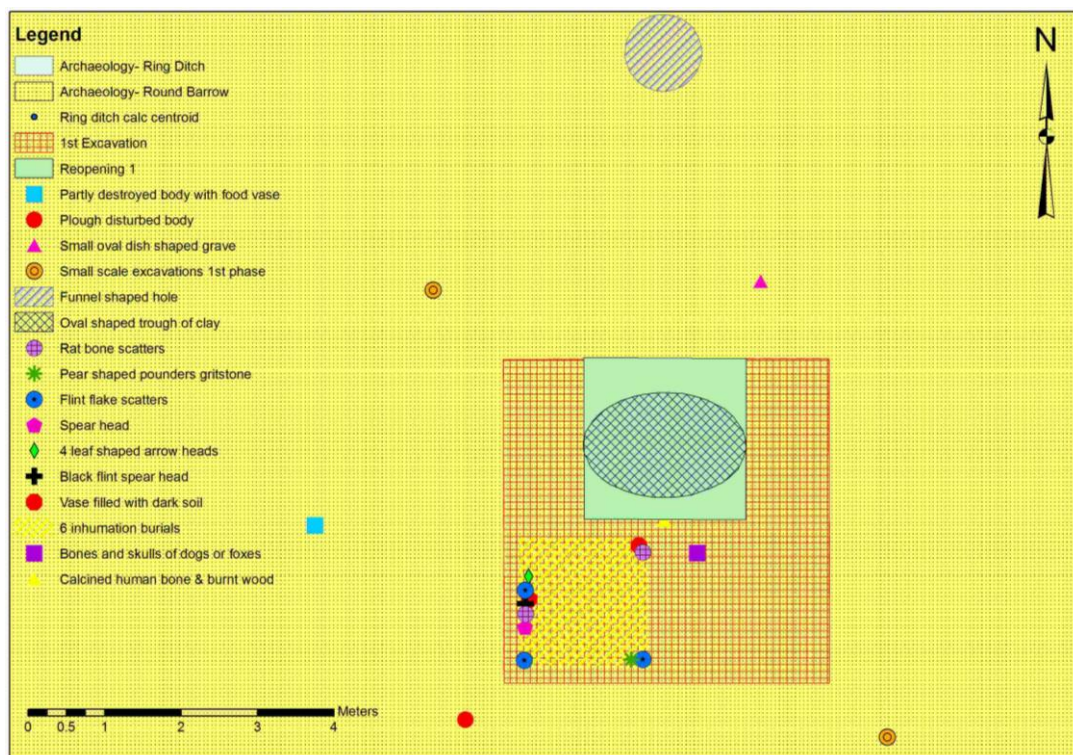
Figure A.23   A reconstruction drawing of the Mortimer excavations.

384

The reconstruction diagrams plotting the position of the archaeological finds showed no correlation with the geophysical anomalies. However, as the round barrow had been excavated by Mortimer before the later removal of the mound and subsequent ploughing then little evidence is likely to have survived. The reconstruction diagram does provide a useful visual aid for the excavation of the site.

A.1.7 Conclusions

The survey results show that the ring ditch surrounding the round barrow excavated by J.R. Mortimer c.1864-1868 is still insitu and only the mound was removed by the tenant farmer c.1887. Evidence of the Mortimer excavations could not be identified in the data, as the reconstruction of the positions of excavations based on the Mortimer accounts do not correlate with geophysical anomalies.

The GPS survey has provided an additional level of information, identifying very faint variations in the topography. These changes correlate to the geophysical data. One clear correlation is the agricultural impact on the ground surface where plough lines running across the field (south-west to north-east) at Towthorpe show up in the earth resistance, gradiometer and GPS data sets. The trials of the simultaneous GPS and earth resistance surveys showed how the extra information aided interpretation and provided location (and height) information for ground surface archaeological features. The powering down of the GPS unit meant the whole of the mound was not recorded in the microtopography survey.

However, sufficient information was recorded to confirm the slight rise visible in the field does relate to the mound location (based on the ring ditch enclosing the mound).

Further survey north, west and south of the round barrow would provide additional evidence for the extent of the site and previous land use, helping to validate the suggested archaeological interpretations. An excavation of the ring ditch may also provide additional information about the site and could provide additional artefactual evidence to further support the C14 dates (Gibson and Bayliss 2008 (published 2010)).

The MSP40 earth resistance survey has shown that the system can be used on heavily ploughed sites even when the field is covered in stubble. The adverse weather conditions prior to the survey (snow and freezing conditions) meant that the ground conditions reduced any potential contact resistance issues.

The MSP40 has also shown it is possible to produce a large scale earth resistance survey in a shorter period of time than traditional equipment (approximately 80m x 80m in a day) with a sampling interval of 0.5m x 1m. This does not factor in time lost through trialling different configurations and time taken to make small repairs on site.

Bibliography

Aaltonen, J (2000) *The applicability of DC resistivity in some geological surroundings in Sweden.* In Sililo, O (ed.) Groundwater: Past achievements and future challenges proceedings of the XXX IAH Congress on Groundwater: 61-66. Cape Town, South Africa: Balkema.

Aaltonen, J (2001) Seasonal resistivity variations in some different Swedish soils. *European Journal of Environmental and Engineering Geophysics* 6(1): 33-45.

Al Chalabi, M & Rees, AI (1962) An experiment on the effect of rainfall on electrical resistivity anomalies in the near surface. *Bonner Jahrbucher* 162: 266-271.

Armit, I, Gaffney, C & Hayes, A (2012) Space and movement in an Iron Age oppidum: integrating geophysical and topographic survey at Entremont, Provence. *Antiquity* 86: 191-206.

Arvidsson, J (1999) Subsoil compaction research in Sweden- a review. *Experiences with the impact and prevention of subsoil compaction in the European community*: 44-49. Wageningen:

Aspinall, A, Gaffney, C & Schmidt, A (2009) *Magnetometry for Archaeologists*. Plymouth: AltaMira Press.

Aspinall, A & Saunders, MK (2005) Experiments with the square array. *Archaeological Prospection* 12(2): 115-129.

Autodesk (2012) *Inventor fusion*. San Rafael: Autodesk.

BADC (2011) *British Atmospheric Data Centre*. Available from *http://badc.nerc.ac.uk/home/* (Accessed 28/06/2010).

Barton, K & Fenwick, J (2005) Geophysical investigations at the Ancient Royal site of Rathcroghan, County Roscommon, Ireland. *Archaeological Prospection* 12: 3-18.

BDLHS (2009) *Photographs and images*. Bingley: Bingley and District Local Historical Society.

Bell, R (2007) *Geology of West Yorkshire*. Available from *http://www.wildyorkshire.co.uk/naturediary/docs/2007/10/31.htm* (Accessed 28/03/2011).

Benderitter, Y & Schott, JJ (1999) Short time variation of the resistivity in an unsaturated soil: The relationship with rainfall. *European Journal of Environmental and Engineering Geophysics* 4: 37-49.

Besson, A, Cousin, I, Samouëlian, A, Boizard, H & Richard, G (2004) Structural heterogeneity of the soil tilled layer as characterized by 2D electrical resistivity surveying. *Soil & Tillage Research* 79: 239-249.

Bonsall, J (2010a) *Method Statement for Seasonality Tests: 2010-2011 Site 1: Kilcloghans Ringfort, adjacent to proposed N17 Tuam Bypass Kilcloghans Townland,Tuam, County Galway*. Earthsound Archaeological Geophysics.

Bonsall, J (2010b) New Research: NRA Review Ten Years of Geophysical Survey Data. *The Newsletter of the Institute of Archaeologists of Ireland* 2(4): 15-16.

Bonsall, J (2011) *pers. comm*. Email exchange, 2011.

Bonsall, J, Gaffney, C & Armit, I (2010) University Of Bradford Awarded Irish Research Fellowship To Review 10 Years Of Geophysical Data

From Road Schemes. *The Newsletter of the International Society for Archaeological Prospection* (25).

Bonsall, J, Gaffney, C & Armit, I (2011) *Long & Winding roads: Reappraising 170 geophysical surveys from 71 road schemes*. In Drahor, MG and Berge, MA (eds) 9th International Conference on Archaeological Prospection 1: 97-98. Izmir, Turkey: Archaeology and Art Publications.

Breeze, DJ & Jilek, S (2009) *'Frontiers of the Roman Empire' World Heritage Site*. Available from *http://www.danube-limes.eu/world_heritage* (Accessed 05/01/2013).

Bruyninx, C, M.C., M, Aerts, W, P., D, Legrand, J, Baire Q. & Pottiaux E. (2011) *Data Acquisition and Analysis* Encyclopedia of Solid Earth Geophysics. Dordrecht: Springer.

Buselli, G, Davis, GB, Barber, C, Height, MI & Howard, SHD (1992) The Application of electromagnetic and electrical methods to groundwater problems in urban environments. *Exploration Geophysics* 23: 543-555.

Campana, S & Dabas, M (2011) Archaeological Impact Assessment: The BREBEMI Project (Italy). *Archaeological Prospection* 18(2): 139-148.

Carpenter, EW & Habberjam, GM (1956) A tripotential method of resistivity prospecting. *Geophysics* 21: 455-469.

Carroll, DM, Hartnup, R & Jarvis, RA (1979) *Soils of South and West Yorkshire*. Hertfordshire: Harpenden.

Chisholm, JI, Waters, CN, Hallsworth, CR, Turner, N, Strong, GE & Jones, NS (1996) Provenance of Lower Coal Measures around Bradford, West Yorkshire. *Proceedings of the Yorkshire Geological Society* 51: 153-166.

Clark, A (1996) *Seeing beneath the soil.* (2 edn). London: B.T. Batsford.

Clark, AJ (1968) A square array for resistivity surveying. *Prospezioni archeologiche* 3: 111 -114.

Clark, AJ (1975) Archaeological Prospecting: A Progress Report. *Journal of Archaeological Science.* 2: 297-314.

Clark, AJ (1980) *Archaeological Detection by Resistivity.* PhD Thesis. Archaeology. Southampton: University of Southampton.

Clark, AJ (1986) Archaeological geophysics in Britain. *Geophysics* 51(7): 1404-1413.

Cott, PJ (1997) *The effect of weather on resistivity measurements over a known archaeological feature.* MPhil. Bradford: University of Bradford.

Cousin, I, Frison, A, Giot, G, Bourennane, H, Guérin, R & Richard, G (2009) *Three-dimensional structure of a highly heterogeneous soil horizon derived by Electrical Resistivity Tomography.* In Marguerie, D and Lanos, P (eds) Mémoire du sol, espace des hommes: 279-281. Paris: Presses Universitaires de Rennes et ArcheoSciences.

Czysz, W, Faber, A, Flügel, C & Sommer, CS (2008) Sites on the Danube Limes in Bavaria. 33.

Dabas, M (2008) *Michel DABAS e l'ARP system* Available from *http://www.youtube.com/watch?v=l4-zsakEjUM&noredirect=1*

Dabas, M (ed.) (2009) *Theory and practice of the new fast electrical imaging system ARP* Seeing the Unseen. Geophysics and Landscape Archaeology. London: Taylor & Francis.

Dabas, M & Gruel, K (2009) *Geophysical Methods of Prospection: ARP©, AMP.* Available from *http://hal.archives-ouvertes.fr/docs/00/59/25/20/PDF/Archeometricresearchesandapplications12mai2011.pdf* (Accessed 11/10/2011).

Dabas, M, Hesse, A & Tabbagh, J (2000) Experimental Resistivity Survey at Wroxeter Archaeological Site with a Fast and Light Recording Device. *Archaeological Prospection* 7(2): 107-118.

Dain-Owens, AP, Hann, MJ, Dresser, ML & Godwin, RJ (2008) Pressure Transfer under Field Going Vehicles relative to Soil Management and Buried Artifact Damage. *2008 Providence, Rhode Island, June 29 – July 2, 2008*: 2201-2217.

Dain-Owens, AP, Kibblewhite, M, Hann, MJ, Godwin, RJ & Spandl, K (2009) Managing Field Operations to Minimize Buried Artifact Damage. *2009 Reno, Nevada, June 21 - June 24, 2009*

David, A, Linford, N, Linford, P, Martin, L & Payne, A (2008) Geophysical
Survey in Archaeological Field Evaluation. Swindon: English Heritage.

Dechezleprêtre, T, Dabas, M & Gruel, K (2009) *Automatic magnetic mapping of
the oppidum of Boviolles (Meuse, France).* In Marguerie, D and Lanos, P
(eds) Mémoire du sol, espace des hommes.: 51-54. Paris: Presses
Universitaires De Rennes.

Directgov (2011) *Quad bikes.* Available from
*http://www.direct.gov.uk/en/Motoring/DriverLicensing/WhatCanYouDrive
AndYourObligations/DG_180318* (Accessed 12.11.2011).

Dotmar (2012) *Nylatron.* Available from *http://www.dotmar.com.au/nylatron-
gsm/nylatron-gsm-mos2-filled-nylon.html* (Accessed 21/06/2012).

Drahor, MG (2011) A Review of Integrated Geophysical Investigations from
Archaeological and Cultural Sites Under Encroaching Urbanisation in
Izmir, Turkey. *Physics and Chemistry of the Earth* 36(16): 1294-1309.

EnglishHeritage (2003) *Ripping up history: archaeology under the plough.*
Swindon: English Heritage.

Ernstson, K & Kirsch, R (2006) *Groundwater Geophysics a tool for
hydrogeology.* Berlin: Springer.

Fassbinder, JWE (2010) Geophysical Prospection of the Frontiers of the Roman
Empire in Southern Germany, UNESCO World Heritage Site.
Archaeological Prospection 17(3): 129-139.

FindTheBest.com (2012) *Find the Best Car safety ratings.* Santa Barbara:
Available from *http://car-safety-
ratings.findthebest.com/q/3682/1038/How-much-does-the-2002-Land-
Rover-Discovery-Series-II-weigh* (Accessed 09/08/2012).

Fisher, BAJ (2004) *Techiques of crime scene investigation.* (7th edn). London: CRC press.

Foerster, ID (2009) *Foerster website.* Available from *http://www.foerstergroup.de/FEREX-DLG.140.0.html* (Accessed 22.10.2009).

FriendsofStIves (2010) *Friends of St Ives.* Bingley: Available from *http://www.friendsofstives.org.uk/index.php* (Accessed 22.10.2010).

Fritton, DD (2008) Evaluation of pedotransfer and measurement approaches to avoid soil compaction. *Soil & Tillage Research* 99: 268-278.

Fry, R, Gaffney, C & Beck, A (2011) *The DART Project: A major new investigation into what lies beneath our soils.* In Drahor, MG and Berge, MA (eds) 9th International Conference on Archaeological Prospection 1: 37-39. Izmir, Turkey: Archaeology and Art Publications.

Gaffney, C (2011) *pers. comm.* Supervisor meeting,

Gaffney, C, Gaffney, V, Cuttler, R & Yorston, R (2008) Initial results using GPS navigation with the Foerster magnetometer system at the World Heritage site of Cyrene, Libya. *Archaeological Prospection* 15(2): 151-156.

Gaffney, C, Gaffney, V, Neubauer, W, Baldwin, E, Chapman, H, Garwood, P, Moulden, H, Sparrow, T, Bat, R, Löcker, K, Hinterleitner, A, Trinks, I, Nau, E, Zitz, T, Floery, S, Verhoeven, G & Doneus, M (2012) Short Report: The Stonehenge Hidden Landscapes Project. *Archaeological Prospection* 19(2): 147-155.

Gaffney, C & Gater, J (2003) *Revealing the Buried Past.* Stroud: Tempus Publishing.

Gardener, RM (2005) *Practical crime scene processing and investigation.* London: CRC Press.

Gebbers, R, Lück, E, Dabas, M & Domsch, H (2009) Comparison of instruments for geoelectrical soil mapping at the field scale. *Near Surface Geophysics* 7: 179-190.

Gibson, A & Bayliss, A (2008 (published 2010)) *Recent work on the Neolithic Round Barrows of the Upper Great Wold Valley, Yorkshire.* In Leary, J, Darvill, T and Field, D (eds) Neolithic Studies Group Seminar papers (Round Mounds and Monumentalitiy in the British Neolithic and Beyond). London: Oxbow Books.

Gifford-Gonzalez, DP, Damrosch, DB, Damrosch, DR, Pryor, J & Thunen, RL (1985a) The Third Dimension in Site Structure: An Experiment in Trampling and Vertical Dispersal. *American Antiquity* 50(4): 803-818.

Gifford-Gonzalez, DP, Damrosch, DB, Damrosch, DR, Pryor, J & Thunen, RL (1985b) The third dimension in site structure: An experiment in trampling and vertical dispersal. *American Antiquity* 50(4): 803-818.

Google (2011) *Google Earth (6.1.0.5001) [Software].* Available from *www.google.com/earth*

Gruel, K, Dabas, M, Gruel, V & Bernollin, V (2009) *Contribution of large scale geophysical survey to analysis of the evolution of the western boundary of the city of Allonnes (Sarthes, France): Integration of Google images, the Napoleonic cadastre and large magnetic surveys.* In Marguerie, D and Lanos, P (eds) Mémoire du sol, espace des hommes: 179-181. Paris: Presses Universitaires de Rennes et ArcheoSciences.

Habberjam, GM (1972) The effects of anisotropy on square array resistivity measurements. *Geophysical Prospecting.* 20: 249-266.

Habberjam, GM (1979) *Apparent resistivity observations and the use of square array techniques.* . In S. Saxov, (ed.) Geoxploration Monographs: 1-9. Berlin: Gerbrüder Borntraeger.

Habberjam, GM & Watkins, GE (1967) The use of square configuration in resistivity prospecting. *Geophysical Prospecting.* 15: 445-467.

Håkansson, I & Medvedev, VW (1995) Protection of soils from mechanical overloading by establishing limits for stresses caused by heavy vehicles. *Soil & Tillage Research* 35: 85-97.

Harris, JC (2011) *Evaluating the Trapezoidal Array's Effectiveness for Archaeological Prospection.* (MSc dissertation). Bradford: University of Bradford.

Hayes, A (2010) *Oppidum d'Entremont: A geophysical survey investigating the organisation of space (MSc dissertation).* Bradford: University of Bradford.

HemisphereGPS (2010) *A100 Smart Antenna.* Calgary: Available from *http://www.hemispheregps.com/Portals/2/literature/A100_Data_Sheet_W EB_11.2010.pdf* (Accessed 03.03.2011).

Hess, T (2010) *DAILYET – Evapotranspiration calculator.* Cranfield University. Available from *http://www.cranfield.ac.uk/sas/naturalresources/research/projects/dailyet. html* (Accessed 07.06.2010).

Hesse, A (1966) The importance of climatologic observations in archaeological prospecting. *Prospezioni Archaeologiche* 1: 11-13.

Hesse, A, Jolivet, A & Tabbagh, A (1986) New prospects in shallow depth electrical surveying for archaeological and pedological applications. *Geophysics* 51(3): 585-594.

Horn, R & Fleige, H (2003) A method for assessing the impact of load on mechanical stability and on physical properties of soils. *Soil & Tillage Research* 73: 89-99.

Horn, R, Way, T & Rostek, J (2003) Effect of repeated tractor wheeling on stress/strain properties and consequences on physical properties in structured arable soils. *Soil & Tillage Research* 73: 101-106.

Keller, GV & Frischknecht, FC (1966) *Electrical Methods in Geophysical Prospection.* Oxford: Pergamon Press.

Kingsley-Hughes, K (2005) *Hacking GPS*. Indianapolis: Wiley Publishing.

Leckebusch, J (1999) *Geophyikalische Untersuchugen* Der römishe Gutshof in Neftenbach. Zürich: Monagraphien der Kantonsarchäologie

Leckebusch, J (2001) Die Anwendung des Bondenradars (GPR) in der archäologischen Prospektion: 3D- Visualisierung und Interpretation. . *Internationale Archäologie, Naturwissenschaft und Technologie*. Verlag Marie Leidorf GmbH, Rahden / Westf:

Leick, A (2004) *GPS satallite surveying* (3rd edn). New Jersey: John Wiley & Sons.

Linford, N (2009) *pers. comm.* Personal communication,

Linford, N, Linford, P, Martin, L & Payne, A (2007) Recent results from the English Heritage Caesium Magnetometer system in comparison with recent Fluxgate Gradiometers. *Archaeological Prospection* 14(3): 151-166.

Loke, MH & Barker, RD (1996) Rapid least-squares inversion of apparent resistivity pseudosections by a quasi-Newton method. *Geophysical Prospecting* 44(1): 131-152.

Lüeck, E & Ruehlmann, J (2011a) *Resistivity mapping with GEOPHILUS ELECTRICUS – information about lateral and vertical soil heterogeneity* The Second Global Workshop on Proximal Soil Sensing. Montreal:

Lüeck, E & Ruehlmann, J (2011b) *Resistivity mapping with Geophilus electricus.* EGU General Assembly 13: 201.

Lynam, JT (1970) *Techniques of Geophysical Prospection as Applied to Near Surface Structure Determination.* PhD Thesis. Postgraduate School of Studies in Physics and Archaeological Sciences. Bradford: The University of Bradford.

Matias, MJS (2002) Square array anisotropy measurements and resistivity sounding interpretation. *Journal of Applied Geophysics* 49(3): 185-194.

Matias, MJS & Habberjam, GM (1986) The effect of structure and anisotropy on resistivity measurements. *Geophysics* 51(4): 964-971.

McBrearty, S, Bishop, L, Plummer, T, Dewar, R & Conrad, N (1998) Tools Underfoot: Human trampling as an agent of lithic artifact edge modification *American Antiquity* 63(1): 108-129.

McBride, RA & Mercer, GD (2011) Assessing damage to Archaeological Artefacts in compacted spoil using Micro-CT scanning. *Archaeological Prospection* 19(1): 7-19.

MetOffice (2012) *Annual weather 2009.* Available from *http://www.metoffice.gov.uk/climate/uk/2009/annual.html* (Accessed 02/02/2012).

Mortimer, JR (1905) *Forty Years' Researches in British and Saxon Burial Mounds of East Yorkshire.* Hull & York: A. Brown & Sons.

Nave, R (2011) *Pressure Calculation.* Atlanta: Available from *http://hyperphysics.phy-astr.gsu.edu/hbase/prcal.html#c1* (Accessed 11.10.2011).

Neubauer, W, Eder-Hinterleitner, A, Seren, S & Melichar, P (2002) Georadar in the Roman Civil Town Carnuntum, Austria: An Approach for Archaeological Interpretation of GPR Data. *Archaeological Prospection* 9(3): 135-156.

Nielsen, AE (1991) Trampling the Archaeological Record: An experimental study. *American Antiquity* 56(3): 483-503.

Oldeman, LR (1992) *Global extent of soil degredation.* Proceedings of the symposium on soil resilience and sustainable land use: 45-56. Budapest:

Pagliai, M, Marsili, A, Servadio, P, Vignozzi, N & Pellegrini, S (2003) Changes in some physical properties of a clay soil in Central Italy following the passage of rubber tracked and wheeled tractors of medium power. *Soil & Tillage Research* 73: 119-129.

Panissod, C, Dabas, M, Florsch, N, Hesse, A, Jolivet, A, A.Tabbagh & Tabbagh, J (1998a) Archaeological Prospecting using Electric and Electrostatic Mobile Arrays. *Archaeological Prospection* 5: 239-251.

Panissod, C, Dabas, M, Hesse, A, Jolivet, A, Tabbagh, J & Tabbagh, A (1998b) Recent developments in shallow-depth electrical and electrostatic prospecting using mobile arrays. *Geophysics* 63(5): 1542-1550.

Panissod, C, Dabas, M, Jolivet, A & Tabbagh, A (1997a) A novel mobile multipole system (MUCEP) for shallow (0-3m) geoelectrical investigation: the 'Vol-de-canards' array. *Geophysical Prospecting.* 45: 983-1002.

Panissod, C, Lajarthe, M & Tabbagh, A (1997b) Potential focusing: a new multielectrode array concept, simulation study and field tests in archaeological prospecting. *Applied Geophysics* 38: 1-23.

Papadopoulos, NG, Tsokas, GN, Dabas, M, Jong Yi, M, Ho Kim, J & Tsourlos, PI (2009a) Three-Dimensional Inversion of Automatic Resistivity Profiling Data. *Archaeological Prospection* 16(4): 267–278.

Papadopoulos, NG, Tsokas, GN, Dabas, M, Jong Yi, M & Tsourlos, PI (2009b) *3D Inversion of Automated Resistivity Profiling (ARP) Data* In Marguerie, D and Lanos, P (eds) Mémoire du sol, espace des hommes 1: 329-332. Paris: Presses Universitaires de Rennes et ArcheoSciences.

Parasnis, DS (1986) *Principles of applied geophysics.* London: Chapman & Hall.

Parkyn, AK (2010) A survey in the park: Methodological and practical problems associated with geophysical investigation in a late Victorian municipal park. *Archaeological Prospection* 17(3): 161-174.

Parkyn, AK, Schmidt, A, Gaffney, C & Walker, R (2011) *It never rains but it pours. Earth resistance seasonality testing in Bradford.* In Drahor, MG and Berge, MA (eds) 9th International Conference on Archaeological Prospection 1: 33-36. Izmir, Turkey: Archaeology and Art Publications.

Parkyn, AK, Sparrow, T & Gaffney, C (2010) *Geophysical Survey Report: Two surveys along the Raetian Limes at Eining and Pförring, Bavaria, Germany.* Bradford: The University of Bradford.

Rasool Mari, G & Changying, J (2008) Effect of small wheel tractor and crawler tractor on soil physical properties. *Journal of Food, Agriculture & Environment* 6(1): 190-194.

Roy, A & Apparao, A (1971) Depth of Investigation in Direct Current methods. *Geophysics* 36(5): 943- 959.

Samouëlian, A, Cousin, I, Tabbagh, A, Bruand, A & Richard, G (2005) Electrical Resistivity Survey in Soil Science: A Review. *Soil & Tillage Research* 83: 173-193.

Saunders, MK (2002) *The square array: potential application in modern British archaeological geophysics.* (MSc dissertation). Bradford: University of Bradford.

Scollar, I, Tabbagh, A, Hesse, A & Herzog, I (1990) *Archaeological Prospecting and Remote Sensing.Topics in Remote Sensing.* Cambridge: Cambridge University Press.

Seger, M, Cousin, I, Frison, A, Boizard, H & Richard, G (2009a) Characterisation of the structural heterogeneity of the soil tilled layer by using in situ 2D and 3D electrical resistivity measurements. *Soil & Tillage Research* 103: 387-398.

Seger, M, Cousin, I, Giot, G, Boizard, H, Mahu, F & Richard, G (2009b) *Characterisation of the structural heterogenity of the soil layer by using in situ 2D and 3D electrical resistivity measurements*. In Marguerie, D and Lanos, P (eds) Mémoire du sol, espace des hommes: 349-351. Paris: Presses Universitaires de Rennes.

Simpson, D (2009) *Geoarchaeological prospection with multi-coil electromagnetic induction sensors.* PhD Thesis. Faculteit Bio-Ingenieurswetenschappen. Gent: Universiteit Gent.

Simpson, D, Meirvenne, MV, Lüc, E, Bourgeois, J & Rühlmann, J (2010) Prospection of two circular Bronze Age ditches with multi-reciever electrical conductivity sensors (North Belgium). *Journal of Archaeological Science* 37: 2198-2206.

Smith, LP (1967) *Potential transpiration.* London:

Smith, LP (1976) *The Agricultural Climate of England and Wales.* London:

Soing & Geocarta (2008) *The ARP Technique:Specialised services for viticulture*. Available from *http://www.soing.eu/pdf/ARP_inglese.pdf* (Accessed 04/02/2012).

Somers, L (2006) *Resistivity Survey* Remote Sensing in Archaeology: An Explicitly North American Perspective. Tuscaloosa: The University of Alabama Press.

Somers, L (2010) *MSP40 photographs*. Durango: Geoscan Research USA.

Sørensen, K (1996) Pulled Array Continuous Electrical Profiling. *First Break* 14(3): 85-90.

Sparrow, T (2004) *The use of the square array in investigating feature orientation in archaeological prospection.* (MSc dissertation). Bradford: University of Bradford.

Sparrow, T (2010) *pers. comm*. Wheel configurations,

Sparrow, T (2011) *What is GPS (Global Positioning Systems)?* Bradford: Geoscan Research and the Universty of Bradford.

Sparrow, T (2013) *MSP40 photographs.*

Tabbagh, A, Dabas, M, Hesse, A & Panissod, C (2000) Soil resistivity: a non-invasive tool to map soil structure horizonation. *Geoderma* 97: 393-404.

Termotex (2006) *Termotex corner system*. Termotex. Available from *http://www.termotex.dk/Termotex3.htm* (Accessed 09/12/2009).

Topcon (2004) *Topcon HiPer Pro brochure*. USA:

Topcon (2010a) Available from *http://www.topconpositioning.com/products/gps/geodetic-receivers/integrated/hiper-pro.html* (Accessed 03/11/2010).

Topcon (2010b) *PC-CDU MS*. Available from *http://www.topconpositioning.com/products/software/updaters-and-utilities/pc-cdu-ms* (Accessed 03/11/2010).

Tsokas, GN, Tsourlos, PI & Szymanski, JE (1997) Square array resistivity anomalies and inhomogeneity ratio calculated by the finite element method. *Geophysics* 62(2): 426-435.

TufnolcompositesLtd (2008) *Engineering Plastics and Composites.* Available from *htttp://www.tufnol.com/tufnol/default.asp?id=60* (Accessed 20/06/2010).

Tymon, B (2011) *West Yorkshire Geology.* Available from *http://www.wyorksgeologytrust.org/westyorksgeology.html*

Unknown (2005) *Landscape Character Type 13: Open High Rolling Farmland* East Riding of Yorkshire Council. Available from *http://www.eastriding.gov.uk/corp-docs/forwardplanning/docs/lca/final/type13.pdf* (Accessed 14/07/2011).

Unknown (2013) *Upper-Germanic Roman Limes.* Available from *http://www.bavaria.by/upper-germanic-roman-limes-unesco-bavaria* (Accessed 05/01/2013).

Van den Akker, JJH, Arvidsson, J & Horn, R (2003) Introduction to the special issue on experiences with the impact and prevention of subsoil compaction in the European Union. *Soil & Tillage Research* 73: 1-8.

Villa, P (1982) Conjoinable pieces and site formation processes. *American Archaeology* 47(2): 276-288.

VISUALGPS (2010) *VISUAL GPS.* Available from *http://www.visualgps.net/VisualGPS/default.htm* (Accessed 01/06/2010).

Waddell, J, Fenwick, J & Barton, K (2009) *Archaeological and geophysical survey in a ritual landscape.* Dublin: Worwell Ltd.

Walker, R (2000) Multiplexed resistivity survey at the roman town of Wroxeter. *Archaeological Prospection* 7(2): 119-132.

Walker, R (2004) *FM256 Instruction manual,* Bradford:Geoscan Research.

Walker, R (2005) *MSP40 Mobile Sensor Platform*. Bradford: Geoscan Research.

Walker, R (2006) Instruction Manual Mobile Sensor Platform MSP40. Bradford: Geoscan Research.

Walker, R (2011a) *pers. comm*. Alpha & Beta discussion (email exchange), 15.07.2011.

Walker, R (2011b) *pers. comm*. Developments email, 2011.

Walker, R (2012a) *MSP40 MOBILE SENSOR PLATFORM*. Bradford: Geoscan Research. Available from *http://www.geoscan-research.co.uk/page23.html* (Accessed 10/05/2012).

Walker, R (2012b) *RM85 Resistance Meter System*. Bradford: Geoscan Research.

Walker, R (2012c) *pers. comm*. Sampling collection rates and general information, 2012.

Walker, R, Gaffney, C, Gater, J & Wood, E (2005) Short report, Fluxgate Gradiometry and square array resistance survey at Drumlanrig, Dumfries and Galloway, Scotland. *Archaeological Prospection* 12: 131-136.

Yorkshire Dales, NPA (2009) *The Yorkshire Dales*. Available from *www.yorkshiredales.org.uk/yorkshire_moors_and_fells_character_areas. htm* (Accessed 13.10.2009).